Methods in Molecular Biology 1213

Springer Protocols

Bruno Christ
Jana Oerlecke
Peggy Stock *Editors*

Animal Models for Stem Cell Therapy

Humana Press

METHODS IN MOLECULAR BIOLOGY

Series Editor
John M. Walker
School of Life Sciences
University of Hertfordshire
Hatfield, Hertfordshire, AL10 9AB, UK

For further volumes:
http://www.springer.com/series/7651

Animal Models for Stem Cell Therapy

Edited by

Bruno Christ, Jana Oerlecke, and Peggy Stock

Department of Surgery, University of Leipzig, Leipzig, Germany

Humana Press

Editors
Bruno Christ
Department of Surgery
University of Leipzig
Leipzig, Germany

Jana Oerlecke
Department of Surgery
University of Leipzig
Leipzig, Germany

Peggy Stock
Department of Surgery
University of Leipzig
Leipzig, Germany

ISSN 1064-3745 ISSN 1940-6029 (electronic)
ISBN 978-1-4939-1452-4 ISBN 978-1-4939-1453-1 (eBook)
DOI 10.1007/978-1-4939-1453-1
Springer New York Heidelberg Dordrecht London

Library of Congress Control Number: 2014946352

Printed on acid-free paper

Humana Press is a brand of Springer
Springer is part of Springer Science+Business Media (www.springer.com)

Preface

Initially, it was the biology of the embryonic stem cell and its unique features to develop into multiple lineages that gave us insight into the molecular nature of developmental processes leading to specified tissues and organs. Yet, soon we understood that there was a much broader spectrum of applicability of stem cells in basic and applied sciences but increasingly also in clinical use. This is today of high medicinal and socioeconomic interest facing an increasing shortage of organs for transplantation, which is very often the only remaining therapeutic option. In recent years the therapeutic potential of both embryonic and adult stem cells has been investigated intensively in animal models of human diseases giving hope for clinical feasibility of stem cell therapy in the near future. However, there is a mandatory need to understand the way stem cells work under specified disease conditions, which is as diverse as the diversity of the diseases itself. Therefore, it is evident that stem cells from their nature as multi- or pluripotent cells may respond in a different way depending on the microenvironment of a specific disease and the affected tissue. This way of response may comprise direct impact on tissue regeneration by differentiation of a stem cell into the healthy cell of the tissue targeted but also paracrine effects such as secretion of growth factors and/or cytokines affecting the diseased tissue to support its self-regenerative capacity just to mention two major routes of action. This, however, implies that before clinical translation of stem cell therapy it is warranted to study effects but as well side effects of transplanted stem cells such as their fate, tumorigenic potential, tissue persistence, systemic impact, and biodistribution etc. in animal models of human diseases.

This book addresses exemplified disease models of hepatic, cardiovascular, and neurological diseases as well as diseases of the connective and contractile tissue. We included also a part describing the impact of stem cells on immunological diseases but also their potential to modulate the host immunological response, which particularly makes mesenchymal stem cells an attractive tool to avoid or at least reduce conventional immunosuppression in allogeneic stem cell transplantation settings or even to use them as immunosuppressant in, e.g., solid organ transplantation. The contents of the book are prepared to cover a wide range of diseases and application of different kinds of stem cells such as embryonic and adult stem cells but also reprogrammed tissue cells (iPS), which are the types of cells most frequently discussed in the context of applied sciences and medicine. Hence, the description of the animal disease models and their use in stem cell transplantation in this book covers interest of basic scientists and clinicians to assess the biological as well as the therapeutic potential of stem cell therapy. The standardization of protocols and assays is mandatory for future implementation into regulatory documents presenting the results from different individual cell types in different animal models in order to prepare a preclinical study in vivo as required for later approval by regulatory bodies.

Leipzig, Germany

Bruno Christ
Jana Oerlecke
Peggy Stock

Contents

Contributors

Reeva Aggarwal • *Cardiovascular Stem Cell Laboratories, The Dorothy M. Davis Heart and Lung Research Institute, Wexner Medical Center at The Ohio State University, Columbus, OH, USA*

Andreas Androutsellis-Theotokis • *Department of Medicine, University of Dresden, Dresden, Germany; Center for Regenerative Therapies Dresden, Dresden, Germany*

Greg Asatrian • *Department of Pathology and Laboratory Medicine, David Geffen School of Medicine, University of California, Los Angeles, Los Angeles, CA, USA*

Agnieszka Banas • *Division of Molecular and Cellular Medicine, National Cancer Center Research Institute, Tokyo, Japan*

Zwi Berneman • *Laboratory of Experimental Hematology, University of Antwerp, Antwerp, Belgium; Vaccine and Infectious Disease Institute (Vaxinfectio), University of Antwerp, Antwerp, Belgium*

Gail E. Besner • *Department of Pediatric Surgery, Center for Perinatal Research, The Research Institute at Nationwide Children's Hospital, Nationwide Children's Hospital, Ohio State University College of Medicine, Columbus, OH, USA*

Moses T. Bility • *Lineberger Comprehensive Cancer Center, University of North Carolina at Chapel Hill, Chapel Hill, NC, USA*

Debbie Le Blon • *Laboratory of Experimental Hematology, University of Antwerp, Antwerp, Belgium; Vaccine and Infectious Disease Institute (Vaxinfectio), University of Antwerp, Antwerp, Belgium*

Annie C. Bowles • *Department of Cell and Molecular Biology, Tulane University School of Medicine, New Orleans, LA, USA; Center for Stem Cell Research and Regenerative Medicine, Tulane University School of Medicine, New Orleans, LA, USA*

Thomas Braun • *Department of Cardiac Development and Remodelling, Max Planck Institute for Heart and Lung Research, Bad Nauheim, Germany*

Walter Brehm • *Large Animal Clinic for Surgery, Faculty of Veterinary Medicine, University of Leipzig, Leipzig, Germany; Translational Centre for Regenerative Medicine, University of Leipzig, Leipzig, Germany*

Stefania Bruno • *Department of Molecular Biotechnology and Healthy Science, Molecular Biotechnology Center, University of Torino, Torino, Italy*

Nicolas Buchon • *Department of Entomology, Cornell University, Ithaca, NY, USA*

Bruce A. Bunnell • *Department of Pharmacology, Tulane University School of Medicine, New Orleans, LA, USA; Center for Stem Cell Research and Regenerative Medicine, Tulane University School of Medicine, New Orleans, LA, USA*

Janina Burk • *Large Animal Clinic for Surgery, Faculty of Veterinary Medicine, University of Leipzig, Leipzig, Germany; Translational Centre for Regenerative Medicine, University of Leipzig, Leipzig, Germany*

Giovanni Camussi • *Department of Medical Sciences; Department of Molecular Biotechnology and Healthy Science, University of Torino, Torino, Italy*

Federica Casiraghi • *Department of Clinical Immunology and Transplantation, Centro Ricerche Trapianti "Chiara Cucchi de Alessandri e Gilberto Crespi", Azienda Ospedaliera Papa Giovanni XXIII, IRCCS-Istituto di Ricerche Farmacologiche Mario Negri, Ranica-Bergamo, Italy*

Chawnshang Chang • *George Whipple Lab for Cancer Research, Departments of Pathology, Urology, Radiation Oncology, The Wilmot Cancer Center, University of Rochester Medical Center, Rochester, NY, USA; Sex Hormone Research Center, China Medical University/Hospital, Taiwan, China*

Le Chang • *Department of Pathology and Laboratory Medicine, David Geffen School of Medicine, University of California, Los Angeles, Los Angeles, CA, USA*

Ji-Mei Chen • *Guangdong Cardiovascular Institute, Guangdong General Hospital, Guangdong Academic of Medical Sciences, Guangzhou, China*

Bruno Christ • *Department of Surgery, University of Leipzig, Leipzig, Germany*

Hans Christiansen • *Department of Radiotherapy and Radiation Oncology, University Medical Centre, Georg-August-University Goettingen, Goettingen, Germany*

Sangmi Chung • *Harvard Medical School, Harvard Stem Cell Institute, McLean Hospital/Harvard Medical School, Belmont, MA, USA*

Emmanuelle Cornali • *Aurigon Life Science GmbH, Tutzing, Germany*

Anthony Curtis • *Lineberger Comprehensive Cancer Center, University of North Carolina at Chapel Hill, Chapel Hill, NC, USA*

Jasmijn Daans • *Laboratory of Experimental Hematology, University of Antwerp, Antwerp, Belgium; Vaccine and Infectious Disease Institute (Vaxinfectio), University of Antwerp, Antwerp, Belgium*

Qiang Dang • *George Whipple Lab for Cancer Research, Departments of Pathology, Urology, Radiation Oncology, The Wilmot Cancer Center, University of Rochester Medical Center, Rochester, NY, USA*

Sylvie Darche • *Innate Immunity Unit, Institut Pasteur, Inserm U668, Paris, France*

Hiranmoy Das • *Cardiovascular Stem Cell Laboratories, The Dorothy M. Davis Heart and Lung Research Institute, Wexner Medical Center at The Ohio State University, Columbus, OH, USA*

Mario Delgado • *Institute of Parasitology and Biomedicine "Lopez-Neyra", CSIC, Granada, Spain*

Uta Delling • *Large Animal Clinic for Surgery, Faculty of Veterinary Medicine, University of Leipzig, Leipzig, Germany*

Peter ten Dijke • *Department of Molecular Cell Biology, Cancer Genomics Centre, Leiden University Medical Center, Leiden, The Netherlands*

Yvette Drabsch • *Department of Molecular Cell Biology, Cancer Genomics Centre, Leiden University Medical Center, Leiden, The Netherlands*

Mathilde Dusséaux • *Innate Immunity Unit, Institut Pasteur, Inserm U668, Paris, France*

Suomi M.G. Fouraschen • *Department of Surgery, Laboratory of Experimental Transplantation and Intestinal Surgery (LETIS), Erasmus MC-University Medical Center, Rotterdam, The Netherlands*

Rachelle Franzen • *Groupe Interdisciplinaire de Génoprotéomique appliquée (GIGA), Neurosciences Unit, University of Liège, Liège, Belgium*

Masayuki Fujino • *Division of Transplantation Immunology, National Research Institute for Child Health and Development, Tokyo, Japan; AIDS Research Center, National Institute of Infectious Diseases, Tokyo, Japan*

Elena Gonzalez-Rey • *Institute of Parasitology and Biomedicine "Lopez-Neyra", CSIC, Granada, Spain*

Herman Goossens • *Vaccine and Infectious Disease Institute (Vaxinfectio), University of Antwerp, Antwerp, Belgium*

Sean R.R. Hall • *Division of Thoracic Surgery, University Hospital Bern, Bern, Switzerland*
Sang Won Han • *Department of Biophysics, Universidade Federal de Sao Paulo, Sao Paulo, SP, Brazil*
Rizwanul Haque • *Department of Microbiology and Immunology, The Pennsylvania State University College of Medicine, Hershey, PA, USA*
Niel Hens • *Vaccine and Infectious Disease Institute (Vaxinfectio), University of Antwerp, Antwerp, Belgium; Center for Statistics, I-Biostat, Hasselt University, Hasselt, Belgium; Centre for Health Economic Research and Modeling Infectious Diseases (Chermid), University of Antwerp, Antwerp, Belgium*
Chloé Hoornaert • *Laboratory of Experimental Hematology, University of Antwerp, Antwerp, Belgium, Germany; Vaccine and Infectious Disease Institute (Vaxinfectio), University of Antwerp, Antwerp, Belgium*
Philip L. Houtz • *Department of Entomology, Cornell University, Comstock Hall, Ithaca, NY, USA*
Chiung-Kuei Huang • *George Whipple Lab for Cancer Research, Departments of Pathology, Urology, Radiation Oncology, The Wilmot Cancer Center, University of Rochester Medical Center, Rochester, NY, USA*
Tsuyoshi Ishii • *Regenerative Medicine Research and Planning Division, Rohto Pharmaceutical Co. Ltd., Minato-ku, Tokyo, Japan*
Shumpei Ishikawa • *Department of Genomic Pathology, Tokyo Medical and Dental University, Bunkyo-ku, Tokyo, Japan*
Aaron W. James • *Department of Pathology and Laboratory Medicine, University of California, Los Angeles, Los Angeles, CA, USA; David Geffen School of Medicine, Los Angeles, CA, USA*
Jeroen de Jonge • *Department of Surgery, Laboratory of Experimental Transplantation and Intestinal Surgery (LETIS), Erasmus MC-University Medical Center, Rotterdam, The Netherlands*
Fumiya Kano • *Department of Oral and Maxillofacial Surgery, Nagoya University Graduate School of Medicine, Showa-ku, Nagoya, Japan*
Takeshi Katsuda • *Division of Molecular and Cellular Medicine, National Cancer Center Research Institute, Chuo-ku, Tokyo, Japan*
Kwang-Soo Kim • *Department of Cardiac Development and Remodelling, McLean Hospital/Harvard Medical School, Belmont, MA, USA*
Johnny Kim • *Department of Cardiac Development and Remodelling, Max Planck Institute for Heart and Lung Research, Bad Nauheim, Germany*
Yusuke Kitazawa • *Division of Transplantation Immunology, National Research Institute for Child Health and Development, Tokyo, Japan*
Sarah Koenig • *Department of General, Visceral, and Pediatric Surgery, University Medical Centre, Georg-August-University Goettingen, Goettingen, Germany*
Petra Krause • *Department of General, Visceral, and Pediatric Surgery, University Medical Centre, Georg-August-University Goettingen, Goettingen, Germany*
Sanjay Kumar • *Center for Stem Cell Research, Christian Medical College, Vellore, Tamilnadu, India*
Hayato Kurata • *Division of Molecular and Cellular Medicine, National Cancer Center Research, Chuo-ku, Tokyo, Japan; Regenerative Medicine Research and Planning Division, Rohto Pharmaceutical Co. Ltd., Minato-ku, Tokyo, Japan*

Luc J.W. van der Laan • *Department of Surgery, Laboratory of Experimental Transplantation and Intestinal Surgery (LETIS), Erasmus MC-University Medical Center, Rotterdam, The Netherlands*
Anne-Marie Lau • *Research Group Adipocyte Development, German Institute of Human Nutrition, Nuthetal, Germany*
Soo Ok Lee • *George Whipple Lab for Cancer Research, Departments of Pathology, Urology, Radiation Oncology, The Wilmot Cancer Center, University of Rochester Medical Center, Rochester, NY, USA*
Fengyang Lei • *Department of Microbiology and Immunology, The Pennsylvania State University College of Medicine, Hershey, PA, USA*
Xiao-Kang Li • *Division of Transplantation Immunology, National Research Institute for Child Health and Development, Setagaya-ku, Tokyo, Japan*
Annemie Van der Linden • *Bio-Imaging Laboratory, University of Antwerp, Antwerp, Belgium*
Jie Luo • *George Whipple Lab for Cancer Research, Departments of Pathology, Urology, Radiation Oncology; The Wilmot Cancer Center, University of Rochester Medical Center, Rochester, NY, USA*
Priscila Keiko Matsumoto Martin • *Department of Biophysics, Universidade Federal de São Paulo, São Paulo, Brazil; Research Center for Gene Therapy, Universidade Federal de São Paulo, São Paulo, Brazil*
Leonardo Martins • *Department of Biophysics, Universidade Federal de São Paulo, São Paulo, Brazil; Research Center for Gene Therapy, Universidade Federal de São Paulo, São Paulo, Brazil*
Kohki Matsubara • *Department of Oral and Maxillofacial Surgery, Nagoya University Graduate School of Medicine, Showa-ku, Nagoya, Japan*
Jisook Moon • *Molecular Neurobiology Laboratory, Department of Psychiatry and Program in Neuroscience, CHA University/CHA Stem Cell Institute, Seoul, South Korea; Department of Bioengineering, CHA University/CHA Stem Cell Institute, Seoul, South Korea*
Christine Mummery • *Department of Anatomy and Embryology, Leiden University Medical Center, Leiden, The Netherlands*
Virginie Neirinckx • *Groupe Interdisciplinaire de Génoprotéomique appliquée (GIGA), Neurosciences Unit, University of Liège, Liège, Belgium*
Takahiro Ochiya • *Division of Molecular and Cellular Medicine, National Cancer Center Research Institute, Chuo-ku, Tokyo, Japan*
Valeria V. Orlova • *Department of Anatomy and Embryology, Leiden University Medical Center, Leiden, The Netherlands*
Vincent J. Pompili • *Cardiovascular Stem Cell Laboratories, The Dorothy M. Davis Heart and Lung Research Institute, Wexner Medical Center at The Ohio State University, Columbus, OH, USA*
Peter Ponsaerts • *Laboratory of Experimental Hematology, University of Antwerp, Antwerp, Belgium; Vaccine and Infectious Disease Institute (Vaxinfectio), University of Antwerp, Antwerp, Belgium*
Steven W. Poser • *Department of Medicine, University of Dresden, Dresden, Germany*
Jelle Praet • *Laboratory of Experimental Hematology, University of Antwerp, Antwerp, Belgium; Vaccine and Infectious Disease Institute (Vaxinfectio), University of Antwerp, Antwerp, Belgium; Bio-Imaging Laboratory, University of Antwerp, Antwerp, Belgium*

Aruna Rakha • *Department of Translational and Regenerative Medicine, Postgraduate Institute of Medical Education and Research, Chandigarh, India*
Margret Rave-Frank • *Department of Radiotherapy and Radiation Oncology, University Medical Centre, Georg-August-University Goettingen, Goettingen, Germany*
Kristien Reekmans • *Laboratory of Experimental Hematology, University of Antwerp, Antwerp, Belgium; Vaccine and Infectious Disease Institute (Vaxinfectio), University of Antwerp, Antwerp, Belgium*
Bernard Rogister • *Groupe Interdisciplinaire de Génoprotéomique appliquée (GIGA), Neurosciences Unit, University of Liège, Liège, Belgium; GIGA, Development, Stem Cells and Regenerative Medicine Unit, University of Liège, Liège, Belgium; Neurology Department, Centre Hospitalier Universitaire de Liège, Liège, Belgium*
Maria Adele Rueger • *Department of Neurology, University of Cologne, Cologne, Germany*
Kiyoshi Sakai • *Department of Oral and Maxillofacial Surgery, Nagoya University Graduate School of Medicine, Showa-ku, Nagoya, Japan*
Eva Santermans • *Vaccine and Infectious Disease Institute (Vaxinfectio), University of Antwerp, Antwerp, Belgium; Center for Statistics, I-Biostat, Hasselt University, Hasselt, Belgium*
Insa S. Schroeder • *Department of Biophysics, GSI Helmholtz Center for Heavy Ion Research, Department of Biophysics, Darmstadt, Germany*
Tim J. Schulz • *Research Group Adipocyte Development, German Institute of Human Nutrition, Nuthetal, Germany*
Brittni A. Scruggs • *Center for Stem Cell Research and Regenerative Medicine and Department of Pharmacology, Tulane University School of Medicine, New Orleans, LA, USA*
Jianxun Song • *Department of Microbiology and Immunology, The Pennsylvania State University College of Medicine, Hershey, PA, USA*
Peggy Stock • *Department of Surgery, University of Leipzig, Leipzig, Germany*
Helene Strick-Marchand • *Innate Immunity Unit, Institut Pasteur, Inserm U668, Paris, France*
Lishan Su • *Lineberger Comprehensive Cancer Center, University of North Carolina at Chapel Hill, Chapel Hill, NC, USA; Center for Infection and Immunity, Institute of Biophysics, Chinese Academy of Sciences, Beijing, China*
Yanwei Su • *Department of Cardiovascular and Respiratory Medicine, Tongji Medical College, Wuhan Puai Hospital, Huazhong University of Science and Technology, Wuhan, Hubei, China*
Rie Tamai • *Division of Molecular and Cellular Medicine, National Cancer Center Research Institute, Chuo-ku, Tokyo, Japan; Regenerative Medicine Research and Planning Division, Rohto Pharmaceutical Co. Ltd., Minato-ku, Tokyo, Japan*
Marta Todeschini • *Department of Clinical Immunology and Transplantation, Centro Ricerche Trapianti "Chiara Cucchi de Alessandri e Gilberto Crespi," Azienda Ospedaliera Papa Giovanni XXIII, IRCCS- Istituto di Ricerche Farmacologiche Mario Negri, Ranica-Bergamo, Italy*
Yu-Hua Tseng • *Integrative Physiology and Metabolism, Joslin Diabetes Center, Harvard Medical School, Boston, MA, USA*
Nathalie de Vocht • *Laboratory of Experimental Hematology, University of Antwerp, Antwerp, Belgium; Vaccine and Infectious Disease Institute (Vaxinfectio), University of Antwerp, Antwerp, Belgium; Bio-Imaging Laboratory, University of Antwerp, Antwerp, Belgium*

RongHao Wang • *George Whipple Lab for Cancer Research, Departments of Pathology, Urology, Radiation Oncology; The Wilmot Cancer Center, University of Rochester Medical Center, Rochester, NY, USA*
Sandra Winkler • *Department of Surgery, University of Leipzig, Leipzig, Germany*
Sabine Wislet-Gendebien • *Groupe Interdisciplinaire de Génoprotéomique appliquée (GIGA), Neurosciences Unit, University of Liège, Liège, Belgium*
Xiaofang Xiong • *Department of Microbiology and Immunology, The Pennsylvania State University College of Medicine, Hershey, PA, USA*
Akihito Yamamoto • *Department of Oral and Maxillofacial Surgery, Nagoya University Graduate School of Medicine, Showa-ku, Nagoya, Japan*
Jixin Yang • *Department of Pediatric Surgery, Tongji Medical College, Tongji Hospital, Huazhong University of Science and Technology, Wuhan, China*
Ping Zhu • *Division of Transplantation Immunology, National Research Institute for Child Health and Development, Tokyo, Japan; Guangdong Cardiovascular Institute, Guangdong General Hospital, Guangdong Academy of Medical Sciences, Guangzhou, China*
Jian Zhuang • *Guangdong Cardiovascular Institute, Guangdong General Hospital, Guangdong Academic of Medical Sciences, Guangzhou, China*

Part I

Introduction

Chapter 1

Stem Cells: Are We Ready for Therapy?

Insa S. Schroeder

Abstract

Cell therapy as a replacement for diseased or destroyed endogenous cells is a major component of regenerative medicine. Various types of stem cells are or will be used in clinical settings as autologous or allogeneic products. In this chapter, the progress that has been made to translate basic stem cell research into pharmaceutical manufacturing processes will be reviewed. Even if in public perception, embryonic stem (ES) cells and more recently induced pluripotent stem (iPS) cells dominate the field of regenerative medicine and will be discussed in great detail, it is the adult stem cells that are used for decades as therapeutics. Hence, these cells will be compared to ES and iPS cells. Finally, special emphasis will be placed on the scientific, technical, and economic challenges of developing stem cell-based in vitro model systems and cell therapies that can be commercialized.

Key words Multipotent stem cells, Pluripotent stem cells, Disease modeling, Stem cell therapy, Translation

1 Introduction

Over the last century, healthcare has advanced significantly enhancing life expectancy and/or quality of life of many patients. Yet there are still a number of degenerative diseases that cannot be treated adequately leading to organ dysfunction and tissue degeneration. Moreover, extended life expectancy comes at a price of higher incidence of diseases such as diabetes mellitus, myocardial infarction, and stroke that eventually may require intervention by cell-based therapies as well. However, due to the shortage of transplantable organs, tissues, or cells, sourcing for replacement therapies is difficult. Therefore, cells of ample supply that can satisfy the medical demands regarding functionality, long-term survival, and safety are badly needed. Embryonic, induced as well as adult stem cells may serve as such sources for the alleviation or cure of a given disease. To date, hematopoietic stem cell transplantation is the most successful stem cell therapy used in genetic blood disorders, immune deficiencies, or malignancies like leukemia. Other stem cells are

Bruno Christ et al. (eds.), *Animal Models for Stem Cell Therapy*, Methods in Molecular Biology, vol. 1213,
DOI 10.1007/978-1-4939-1453-1_1,

tested in clinical trials or are on the cusp of reaching this translational gate. Outside such peer-reviewed, well-controlled clinical trials, unproven stem cell therapies are widely performed without any legitimate investigation of efficacy or safety, misleading patients and their families and trivializing possible adverse effects. Therefore, blinded randomized trials are the minimum requirement for stem cell therapies to reach clinical translation. However, before reaching preclinical or clinical levels, protocols for the isolation, expansion, or differentiation of stem cells that are established in a research laboratory have to be adapted to mass production. Not all laboratory protocols may be easily translated and scaled up one to one into a pharmaceutical manufacturing procedure under GMP conditions. Therefore, already early on in the process of developing cell-based proof-of-concept studies, which are supposed to be used in a clinical setting later on, one should consider designs that allow the implementation of GMP guidelines. Also, thorough cell characterization and functional assays that will be applicable in a high-throughput setting need to be designed as soon as possible. Thus, this review is intended to report about the progress that has been made to translate basic stem cell research into pharmaceutical manufacturing processes and the challenges that still need to be considered.

2 Adult Stem Cells in Regenerative Medicine

2.1 Hematopoietic Stem Cells (HSCs)

Hematopoietic stem cells were first postulated by Alexander A. Maximow [1] and eventually identified in the 1960s [2]. Since then, they have been used excessively in stem cell therapy. As progenitor cells residing in the bone marrow, they will form all blood and immune cells (myeloid and lymphoid cells). Therefore, they are successfully used to cure blood disorders like thalassemia, Fanconi's anemia, immune deficiency, and blood cancers such as leukemia and lymphomas [3]. HSCs are positive for the cell surface markers CD34/CD90/CD59/Thy1 and negative for CD38/CD45Ra or mature blood lineage markers (lin^-). In the bone marrow, 1 out of 10,000–15,000 cells is thought to be a bona fide HSC. In the peripheral blood, this number drops to 1 in 100,000 cells. However, HSCs can also be found in umbilical cord blood that gains increasing importance as a HSC cell source [4, 5]. In a quiescent state, HSCs reside in a stem cell niche consisting of spindle-shaped N-cadherin$^+$ osteoblasts embedded in stromal fibroblasts [6], but they are easily mobilized and migrate into the blood stream when patients are treated with granulocyte colony-stimulating factor. HSCs are a very heterogenic population that can be divided into subpopulations according to their repopulating or differentiation behavior: short-term repopulating HSCs versus long-term repopulating HSCs or lymphoid-biased,

myeloid-biased, and balanced HSCs. As HSCs age, the myeloid-biased HSC subpopulation accumulates at the expense of the lymphoid one [7]. Propagation of HSCs is challenging as they readily undergo differentiation, but factors such as stem cell factor, Flk2/Flt3 ligand, thrombopoietin, and IL-6/sIL-6R can be used for ex vivo expansion of human transplantable HSCs [8]. Currently, there are 1,795 open clinical studies using hematopoietic stem cells (www.clinicaltrials.gov, accessed Oct. 28, 2013) demonstrating the importance of this stem cell source. Based on single HSC transplantation, HSCs show certain plasticity as cell types such as fibroblasts, myofibroblasts, adipocytes, and osteo-chondrocytes were derived from HSCs (reviewed in [9]). However, whether they are able to generate cell types outside the mesodermal lineage is still debated.

2.2 Mesenchymal Stem or Stromal Cells (MSCs)

A second stem cell population that can be found in the bone marrow consists of mesenchymal stem cells, originally discovered by Friedenstein [10] that since then have been found in a number of other tissues [11]. These cells were initially identified by their ability to adhere to plastic surfaces, and for many years findings regarding MSCs were difficult to compare as laboratories used different standards to characterize the MSCs. Finally, in 2006, the International Society for Cellular Therapy defined the minimal criteria MSCs have to fulfill: (1) adherence to plastic under standard tissue culture conditions; (2) the expression of the surface markers CD73, CD90, and CD105 and lack of expression of CD45, CD34, CD14, CD11b, CD79a, and CD19 and HLA-DR surface molecules; and (3) the capacity to differentiate into osteoblasts, adipocytes, and chondrocytes in vitro [12]. Later, CD271 was found to be a unique marker of MSCs [13]. Like HSCs, MSCs are used in a vast number ($n = 221$, www.clinicaltrials.gov, accessed Oct 28, 2013) of clinical studies that are currently pursued for a variety of diseases, among them 19 phase III trials (studies that gather more information about safety and effectiveness by studying different populations and different dosages) related to stroke, myocardial infarction, type 1 and 2 diabetes, chronic graft-versus-host disease, articular cartilage defects, Crohn's disease, and others. However, currently no phase IV trial (studies occurring after FDA has approved a drug/procedure for marketing. These include postmarket requirement and commitment studies that are required of or agreed to by the sponsor. These studies gather additional information about a drug's/procedure's safety, efficacy, or optimal use) using MSCs is performed. As MSCs are able to home to sites of inflammation, may differentiate into other cell types, secrete bioactive substances that may initiate, improve, or accelerate regenerative processes, and are immunomodulatory, they are ideal candidates of clinical applications. The most acknowledged feature of MSCs is their immunomodulatory ability that makes them

useful in diseases such as acute graft-versus-host disease, which may occur after allogeneic HSC transplantation. A recent study though indicates that this ability varies based on MSC isolation techniques [14]. In a small Dutch trial applying MSCs after myocardial infarction (www.trialregister.nl, no. NTR1553), MSC treatment was shown to be feasible and safe at short term and up to 5 years of follow-up. However, the 5-year event-free survival was not different from the control group, and even though global left ventricular function assessed by echocardiography showed continuous improvements in left ventricular systolic function after MSC injection during the first 12 months, these results were comparable to the control group [15]. Therefore, even though beneficial effects have been seen in animal models after MSC transplantation and so far no adverse side effects have been correlated to MSCs, evidence for their usefulness is questioned [16], and more insight has to be gained regarding their efficacy in humans.

MSCs have also been reported to differentiate into other cell types like hepatocytes [17, 18], cardiomyocytes [19], or neuronal cells [20] showing some plasticity even though the degree of differentiation may not reach that of fully functional, mature cell types [16, 21].

In general, even though the underlying molecular mechanism of HSC- or MSC-mediated effects may not always be fully understood, novel stem cell-based therapies will benefit from the experiences acquired during adult stem cell-based transplantations.

3 Embryonic Stem Cells in Regenerative Medicine: Possibilities

Unlike multipotent adult stem cells, pluripotent human embryonic stem (hES) cells can be propagated indefinitely in vitro and can differentiate into any cell type of the human body if given the right stimulus. These characteristics make them suitable for regenerative medicine, drug discovery, but more importantly for disease modeling, and developmental studies, which can only be examined in a limited way using adult stem cells. Ever since embryonic stem cells have been generated first from the inner cell mass of mice in 1981 [22] and a few years later from human blastocysts [23], hundreds of lines were generated including disease-specific hES lines, and every endeavor has been made to establish in vitro protocols leading to functional cells of various organs via the stepwise recapitulation of embryonic development. This has led to the establishment of a number of hES cell-based toxicology assays [24], the screening of teratogenous compounds [25], and neuro- and cardiotoxicity tests [26].

Clinical applications, however, require animal-free isolation, culture, and differentiation of hES cells. Yet early methods of isolating and maintaining hES cells required xenogeneic components such

as enzymes, the coculture with irradiated mouse embryonic fibroblasts (MEF), and enriched culture media containing fetal bovine serum. MEF support the self-renewal of hES cells by secreting essential growth factors, cytokines, and extracellular matrices (e.g., transforming growth factor beta, activin A, laminin 511, or vitronectin). Over the last decade, these procedures have been adapted to xenogeneic-free GMP-compliant isolation and culture methods that now allow using hES cells in clinical applications [27]. The group of O. Hovatta greatly contributed to the development of animal-free substrates and culture media to isolate, maintain, and cryopreserve hES cells [28]. This included the development of a method to mechanically isolate the inner cell mass replacing the use of immunosurgery, which involves animal components and enzymes [29], and the substitution of MEF by human recombinant laminin 511 allowing a feeder-free culture of hES cells [30]. However, the most common approach still is the culture of hES cells on culture plates coated with Matrigel, which is composed of laminin, collagen IV, heparan sulfate proteoglycans, entactin, and growth factors. Yet Matrigel is derived from Engelbreth-Holm-Swarm mouse sarcomas and exhibits lot-to-lot variability and also may induce xenogeneic contaminants [31]. It is increasingly replaced by vitronectin coating, which supports undifferentiated proliferation of pluripotent stem cells [32]. Of great concern is the establishment of culture conditions that will allow large-scale expansion of hES cells for clinical applications. To date, hES cells are commonly grown as adherent colonies requiring elimination of differentiated clones every now and then by manual passage. Upon detachment, hES cells form embryoid bodies and differentiate. However, mass production of hES cells will require suspension culture in bioreactors. Indeed, such suspension culture of hES cells is possible using proper culture media [33, 34], which has helped on bringing hES cell-based cell technology from bench to bedside.

With the progress made in the development of GMP procedures regarding the culture and differentiation of hES cells and extensive preclinical testing, three hES cell-based clinical trials have been approved: Geron launched a study using oligodendrocytes (GRNOPC1) derived from hES cells to treat patients with spinal cord injuries. Even though no adverse effects were reported, Geron surprisingly stopped recruiting patients in November 2011 due to financial reasons. This leaves two phase I/II clinical trials for the treatment of dry age-related macular degeneration and Stargardt's macular dystrophy, which are currently carried out by Advanced Cell Technology. In these studies, hES cell-derived retinal pigment epithelial cells are injected subretinally. Four months after implantation, survival and engraftment of cells as well as visual improvement could be shown, whereas no tumorigenicity was observed [35].

4 Embryonic Stem Cells in Regenerative Medicine: Challenges

One of the most challenging issues regarding hES cell-based therapies is the possible tumorigenicity of residual ES cells that have escaped differentiation. Therefore, thorough characterization and purification of the hES cell derivatives are mandatory. However, such homogeneous, well-defined cell populations can be obtained by double selection as reported, e.g., by Kahan et al. [36]. In a mouse ES cell model based on embryoid body formation, they generated pancreatic cells. Negative selection of pluripotent stem cells using an SSEA1 antibody followed by positive selection of EpCAM-positive pancreatic progenitors resulted in no tumor formation after transplantation ($n=31$), while transplantation of the unsorted progeny led to tumorigenicity in seven out of eight cases. This proves the efficiency of double selection and may be used also in clinical settings.

Another issue raised is the genomic instability of ES cells that may prevent the use of their progeny due to the risk of oncogenic transformation. Lund et al. [37] found that in karyotypically abnormal hES cells, the histone deacetylase proteins, HDAC1 and HDAC2, are increased. Inhibition of these markers resulted in reduced proliferation, induction of the proliferation inhibitor cyclin-dependent kinase inhibitor 1A (CDKN1A), and altered regulation of the tumor suppressor protein retinoblastoma 1 (RB1). Genome-wide analyses revealed altered expression of genes linked to severe developmental and neurological diseases and cancers. Thus, genetic instability in hES cells and their progeny is a parameter that has to be closely monitored.

A third safety issue is the possible immunogenicity of ES cells and their derivatives [38]. This issue has been circumvented in the abovementioned clinical studies by transplanting cells into immune-privileged sites, which was shown to require only mild transient immunosuppression [35]. However, more insight into the immune response of hES cells and their derivatives need to be gained to completely abolish the danger of cell rejection and subsequent failure of cell therapy strategies.

A still remaining technical challenge is the development of simple, scalable differentiation protocols that give rise to mature, functional cell types or to progenitors that are able to mature in vivo in a reasonable time. This goal has not been achieved for several cell types including insulin-producing beta cells [39, 40] requiring more basic research.

5 Induced Pluripotent Stem Cells in Regenerative Medicine

The idea of reprogramming adult somatic cells has been pursued for several decades. Already in 1952, Briggs and King showed that transferring nuclei of blastocysts into an enucleated frog egg

resulted in tadpole clones [41]. However, as the experiment was difficult to reproduce, the authors concluded that cell plasticity declines with differentiation. Ten years later, Sir John Gurdon repeated these experiments succeeding in generating frogs even though such reprogramming process through somatic cell nuclear transfer (SCNT) was inefficient [42]. In contrast to Briggs and King, he concluded that differentiation of cells is not accompanied by irreversible nuclear changes, but that instead cell specialization is reversible. However, apart from cloning the sheep Dolly by Ian Wilmut some 30 years later [43], little public attention was given to the potential of reprogramming cells. This changed dramatically in 2006, when Takahashi and Yamanaka reported the successful reprogramming of mouse embryonic and adult fibroblasts to a pluripotent ES cell-like stage generating the so-called induced pluripotent stem (iPS) cells by only four factors: Oct3/4, Sox2, c-Myc, and Klf4 [44]. In honor of these hallmark discoveries, Gurdon and Yamanaka were awarded the Nobel Prize in medicine in 2012. Indeed, the generation of iPS cells opens up completely new avenues in regenerative medicine. As acquisition of patient samples generally is challenging, analyzing the cause and progression of many diseases was exacerbated in the past. However, as now fibroblasts or other cells from patients suffering from any given disease theoretically can be reprogrammed and differentiated in vitro into almost any cell type desired, it is possible to investigate the underlying mechanisms leading to the disease. This is especially interesting with respect to those diseases, which are correlated with genetic alterations or genetic predispositions. Thus, the iPS technology not only allows establishing in vitro test systems and drug screening methods but also offers the possibility of autologous cell therapy.

5.1 Reprogramming Methods

There are several viral and nonviral methods of iPS generation, each harboring its own advantages and disadvantages in respect to their use in a clinical setting. Viral methods use inducible or non-inducible integrating retro- or (polycistronic) lentiviruses and non-integrative adenoviruses or more recently Sendai viruses. Excisable integrating vectors such as loxP (polycistronic) lentiviruses or (inducible) PiggyBac or Sleeping Beauty transposons are successfully used as well. Nonviral methods employ nonintegrative vectors such as polycistronic plasmids, Epstein-Barr nuclear antigen-1-based vectors or minicircles, proteins, small molecules, mRNA, and microRNA.

In the original method, pluripotency markers were introduced in somatic cells by a replication-defective gammaretroviral Moloney murine leukemia virus (Mo-MLV)-based vector [45]. This approach is very efficient in actively dividing cells but fails to transduce slow- or nondividing cells [46]. In contrast, lentiviral vectors such as HIV or SIV derivatives also transduce nondividing cells as

long as they are metabolically active. However, while retrovirally introduced transgenes are silenced through methylation and epigenetic modifications, lentiviral vectors may lead to prolonged and thus unwanted transgene expression and the generation of only partially reprogrammed progeny [47]. Yet the lentiviral approach is the most robust and most commonly used reprogramming method. Of the nonintegrating systems, the Sendai virus system is becoming increasingly important in the generation of clinically relevant iPS cells. In contrast to other nonintegrating vectors that are still based on DNA intermediates, which in theory may be introduced accidentally into the host genome by DNA repair mechanisms, the Sendai virus possesses an RNA genome, which will never be incorporated into host chromosomes. It efficiently transduces a plethora of host cells, shows no human pathogenicity [48], and is diluted out of the host cells by 5–8 passages [49]. Reprogramming strategies using proteins have been explored using mouse somatic cells [50], and recombinant proteins can be used in a combination with viral systems [51], but to date no stable human iPS line has been generated using proteins, even if combined with epigenetic modifiers [52]. Nonetheless, small molecules that maintain pluripotency/self-renewal or modulate the epigenetic status of the host genome such as the DNA methyltransferase inhibitor 5-azacytidine or the histone deacetylase inhibitors trichostatin A or valproic acid induce chromatin remodeling and may complement other reprogramming methods improving their efficiency (reviewed in [53]). Usage of RNA for reprogramming purposes has been shown to be successful, too [54, 55], but it requires multiple transfections. As pluripotency is regulated and fine-tuned by microRNAs such as the miR-302, miR294, and miR-181 family [56], these noncoding RNAs were also used to reprogram somatic cells [57, 58]. They may also be used to distinguish human ES cells from iPS cells and to judge about reprogramming efficacy [59].

Finally, because reprogramming efficiency largely depends on cell cycle progression, synchronizing cells in GO/G1 by serum starvation increased reprogramming efficiency, since the cells when released went through mitosis when the transgenes expressed the reprogramming factors [60]. Modulating cell cycle regulators such as mitogen-activated protein kinase kinase (MEKK) [61] or using such regulators in combination with other small molecules [62] increased reprogramming efficiency up to 200-fold.

5.2 Reprogramming Factors

The original factors used by the Yamanaka group comprise of Oct4, Sox2, Klf4, and c-Myc (OSKM) and are not only efficient in combination with viral delivery systems but also with nonintegrating approaches such as adenoviruses, Sendai viruses, mRNA, episomal vectors, or proteins albeit with low efficiency (for review *see* [63]). The Thomson group used a slightly different cocktail

substituting KLF4 and c-MYC by NANOG and LIN28 (OSNL) [64]. Besides using cocktails with up to six pluripotency markers to enhance or facilitate reprogramming [65], many more factors that substitute the abovementioned pluripotency factors and are known to be lineage specifiers (reviewed in [66]) have been established such as Nr5a2, which replaces Oct4 [67], or Esrrb that can substitute Klf4 and c-Myc [68].

5.3 Donor Cells

Choosing the right donor material starts with the question of young versus old cells. As cellular aging may be correlated with irreversible cell cycle arrest, accumulation of mutations, and DNA damage or altered signaling pathways and epigenetic alterations, cell reprogramming could be hampered. Whether embryonic cells are more easily reprogrammable than adult tissue cells that would be the most interesting for disease modeling is still debated. Similarly, it also remains to be seen whether the differentiation capacity of iPS cells generated from elderly equals that of younger donors. In a recent work, Wen et al. neither found difference in the reprogramming efficiency of vaginal fibroblast obtained from young and old women nor differences in the expression of senescence or apoptosis markers [69]. There was also no difference in the differentiation capacity of iPS cells produced from young and old donors [69]. The same was shown by Ohmine et al. [70], who successfully differentiated iPS cells from patients into islet-like cells. However, aging cells express higher levels of Ink4/Arf [71], which is a barrier to reprogramming [72]. Nonetheless, the limited capacity to be reprogrammed may be overcome by factors such as sirtuin 6, which was shown to improve reprogramming efficiency in human dermal fibroblast of elderly subjects [73]. As important as the age of donor cells is the right choice of the cell type. Even though most iPS protocols use fibroblasts as a starting material, other cells such as keratinocytes [74] or, more attractive for regenerative medicine, blood cells, which are easily accessible from routine sampling, have been proven to be suitable for iPS cell generation (reviewed in [75]).

6 Human iPS Cells as Models of Human Diseases: Potentials

So far, animal models have been used to investigate the onset and progression of human diseases. Yet, because of genetic and developmental differences between human and animals, it is questionable whether human diseases can be properly simulated using animal models alone. Having the iPS technology at our disposal, especially those diseases that are caused by genetic mutations can be analyzed by producing iPS from patients with genetic disorders and their healthy relatives. This way, the impact of genetic mutations or predispositions in disease initiation and progression can be

investigated, even though this requires not only the bona fide production of iPS cells but also the establishment of differentiation protocols that closely mimic the in vivo development.

Numerous efforts have been undertaken to establish patient-specific pluripotent cells from almost all organs affected by hereditary diseases. Using dermal fibroblasts, Rashid et al. generated iPS lines from patients with inherited metabolic disorders (IMD) of the liver such as alpha-1-antitrypsin deficiency, familial hypercholesterolemia, and glycogen storage disease type 1a [76]. In this study, dermal fibroblasts from seven individuals suffering from five hepatic metabolic disorders were reprogrammed using the Yamanaka factors and compared to iPS lines derived from three healthy individuals. All iPS lines showed endogenous expression of pluripotency markers and were able to differentiate into the three germ layers. However, as these lines showed karyotypic abnormalities after prolonged culture (passages ≥40), differentiation experiments, using among others activin A, oncostatin M, and hepatocyte growth factor [77], were performed only up to passage 30. Differentiated cells showed functional maturity based on albumin secretion and cytochrome P450 metabolic activity. More importantly, iPS cells derived from patients with IMD recapitulated key pathological features of the diseases affecting the patients from which they were derived such as aggregation of misfolded alpha-1-antitrypsin in the endoplasmic reticulum, deficient LDL receptor-mediated cholesterol uptake, and elevated lipid and glycogen accumulation. Advancing the idea of examining and modulating disease-causing genes further, Eggenschwiler et al. [78] used disease-specific iPS cells to target severe α-1-antitrypsin (A1AT) deficiency by overexpressing a human microRNA 30 (miR30)-styled shRNA directed against the PiZ variant of A1AT, which is known to cause chronic liver damage in affected patients. In this study, a functional relevant reduction (-66 %) of intracellular PiZ protein in hepatic cells after differentiation of patient-specific iPS cells could be shown, demonstrating that not only mimicking the disease but also modeling it is possible using patient-specific iPS cells. Likewise, mutation-based congenital heart diseases such as the arrhythmogenic long QT syndrome (LQTS) can be recapitulated using iPS cells from patients affected [79]. When differentiated into cardiomyocytes, these cells revealed significant prolongation of the action potential duration when compared to healthy control cells. Voltage-clamp studies confirmed that QT prolongation originated from a significant reduction of the cardiac potassium current I(Kr). Importantly, LQTS-derived cells also showed marked arrhythmia [79]. Patient-specific iPS cells have also been established from patients suffering from diseases such as type 2 diabetes mellitus that are not correlated with a monogenetic modification [80, 70]. However, genome-wide association studies robustly revealed a number of single nucleotide polymorphisms (SNPs) that

contribute or predispose to diabetes mellitus type 2 (reviewed in [81]). Analyzing these SNPs may broaden our insight into disease pathogenesis leading to new pathways for therapeutic intervention, strategies for patient stratification, and biomarkers for identifying those at greatest risk of developing diabetes. Predicting the risk of type 2 diabetes mellitus with genetic risk models on the basis of established genome-wide association markers even when combined with conventional risk models has been limited [82]. Here, integration-free iPS cell technology could greatly facilitate such risk assessment as it is possible to create isogenic stem cell lines that differ only in the mutation under study followed by differentiation into relevant cell types. This approach is possible thanks to genome editing technologies using zinc finger nucleases (ZFNs) or transcription activator-like effector nuclease (TALEN) [83, 84]. These techniques can also be used for gene correction of autologous human iPS cells intended for cell therapy. Even if currently such therapies are prohibitive due to the enormous costs, it has been suggested to generate human iPS cell banks created from a limited number of homozygous HLA-haplotyped donors that would cover a large proportion of the population [85, 86]. For example, even in an ethnically very heterogeneous population like the United States, it has been calculated that only 100 iPS lines would cover the majority of ethnics [87]. Recently, it has been shown that not only monogenetic disorders but even more complex genetic abnormalities may be targeted in the future as well: Li et al. reported the ablation of the extra chromosome 21 in iPS cells derived from Down syndrome patients [88].

7 Human iPS Cells as Models of Human Diseases: Challenges

Even if looking at the abovementioned possibilities, the iPS cells appear to offer several advantages over ES cells or adult stem cells and the first iPS-based clinical study started recruiting patients with exudative (wet-type) age-related macular degeneration in August 2013 (http://www.riken.jp/en/pr/press/2013/20130730_1/, accessed Oct. 27, 2013), several caveats of the iPS technology need to be addressed before iPS cell-derived progeny can be broadly applied in disease modeling or clinical applications. As discussed for hES cell-based strategies, the genetic stability of iPS cells has to be proven, tumor formation must be prevented without doubts, and it has to be ensured that iPS cell differentiation produces only the cell type of interest with the required functionality. Unique for pluripotent iPS cells, however, are hurdles regarding the reprogramming process itself: (1) genetic and epigenetic differences such as copy number variations and (insertional) mutations, (2) incomplete demethylation and remethylation, or (3) aberrant X-chromosome or imprinting and repeat instability (reviewed in [89]), all of which may be

caused by the reprogramming technique alone or by prolonged culture. Besides raising safety concerns, these changes may lead to partially reprogrammed cells, alter the differentiation potential of fully reprogrammed iPS cells, or mask the impact of genetic variations observed in many diseases rendering them even unsuitable for in vitro disease modeling.

A major concern regarding therapeutic applications is the possible immunogenicity of iPS cells. Even though patient-derived iPS cells for autologous therapeutic reasons have the same genetic background and express the same major histocompatibility complex molecules as the recipient, therefore not requiring immune suppression, a study by Zhao et al. [90] raised concerns as it revealed that autologous iPS cells, but not autologous, strain-matched ES cells triggered a T cell-mediated immunogenicity after transplantation. However, in another study by Guha et al., no evidence of increased T cell proliferation in vitro, rejection of syngeneic iPS cell-derived EBs/tissue-specific cells after transplantation, or an antigen-specific secondary immune response was found [91]. In addition, differentiated cells derived from syngeneic iPS cells were not rejected after transplantation. The authors also found little evidence of an immune response to undifferentiated, syngeneic iPS cells. It has to be seen whether immunogenicity may be correlated with certain reprogramming methods or donor cells.

8 Direct Lineage Reprogramming

Reprogramming cells to the pluripotent "ground state" newly sparked the interest in transforming mature cells from one lineage to another without going through pluripotent intermediates via overexpression of key transcription factors required for the development of the cell type of interest. Meanwhile a range of cells were generated that way, e.g., neurons [92], cardiomyocytes [93], blood cell progenitors [94], hepatic stem cells [95], retinal pigment epithelium-like cells [96], or insulin-producing cells [97]. However, as the mature starting material may be as scarce as the cells they are supposed to be turned into, it needs to be seen if such strategies will enter translation into clinical strategies that would require large quantities of donor cells. Direct reprogramming has also been achieved in vivo converting pancreatic exocrine acinar cells to endocrine insulin-producing cells [98]. Likewise, cardiac fibroblasts were reprogrammed in vivo to cardiomyocytes with an efficiency of about 6 % [99]. However, if such a procedure after myocardial infarction would be beneficial is debatable. Due to massive infiltration of cardiac fibroblasts that may prevent proper alignment of cardiomyocytes, there is the danger of incomplete coupling of cardiomyocytes leading to the induction of arrhythmias.

9 General Criteria and Challenges for Stem Cell-Based Therapies

Regardless of the cell type used, all stem cell-based therapies have to fulfill four major criteria that will rule over clinical or commercial outcome: safety, identity, purity, and potency. Thus, the International Society for Stem Cell Research (ISSCR) composed "The ISSCR Guidelines for the Clinical Translation of Stem Cells" (http://www.isscr.org/home/publications/ClinTransGuide, accessed Oct 27th, 2013). Currently, many approaches that have been published as a proof of principle by basic researchers do not fulfill one or more of the abovementioned requirements. However, only if cell therapy products comprise solely of the intended cell type that shows the desired function, without adverse residual cells or adventitious components or adverse side effects such as tumorigenicity, all requirements for successful approval by regulatory agencies and clinical application will be met. Conversely, some diseases will require the replacement of complex tissues involving the assembly of several cell types within a three-dimensional matrix. Whether such complex tissue replacements will ever reach market authorization is questionable. However, such systems may still be beneficial in drug screening, toxicity testing, or disease modeling and should be pursued regardless of their marketability. The benefits of stem cell therapies and standard pharmaceutical approaches will have to be weighed up against each other taking into account the efficiency, feasibility, and cost-effectiveness. One will also have to take into account whether autologous or allogeneic therapies will be more favorable. Allogeneic products derived from one donor may be administered to a large number of recipients that share the expenditures for research and development and quality control [100], while this is not the case for autologous therapies possibly making this strategy too expensive even though additional lifelong immunosuppression will not be required. A "concise review on guidance in developing commercializable autologous/patient-specific cell therapy manufacturing" has recently been published by Eaker et al. and may serve as an advice for basic researchers [101].

10 Conclusions

Stem cell-based disease modeling or cell therapies may be challenging and cost intensive. However, if combined with meaningful animal models, they can give invaluable insights into the onset and progression of various diseases and alleviate or cure a number of ailments. None of the stem cell sources whether adult or embryonic/pluripotent are dispensable; rather all of them advance our knowledge in terms of disease development and cure. Even if the establishment of such stem cell-based tools and therapeutics will take

decades and be accompanied by many failures, the knowledge gained will vindicate the endeavor. Nevertheless, it has to be ensured that stem cell-based interventions are not applied prematurely or outside of well-controlled clinical trials as otherwise legitimate studies and the public trust in regenerative medicine could be jeopardized. Such unproven interventions already led to the death of a child that received intracranial injections of cord blood and to the formation of a brain tumor following neural stem cell transplantation in an ataxia telangiectasia patient [102]. Nevertheless, taken the progress into account that has been made in the last years, stem cell-based disease modeling or cell therapies may be feasible when preceded with caution.

References

1. Maximow A (1909) Der Lymphozyt als gemeinsame Stammzelle der verschiedenen Blutelemente in der embryonalen Entwicklung und im postfetalen Leben der Säugetiere. Folia Haematol 8:125–134
2. Till JE, McCulloch EA (1961) A direct measurement of the radiation sensitivity of normal mouse bone marrow cells. Radiat Res 14: 213–222
3. Daley GQ (2012) The promise and perils of stem cell therapeutics. Cell Stem Cell 10: 740–749
4. Iafolla MA, Tay J, Allan DS (2013) Transplantation of umbilical cord blood-derived cells for novel indications in regenerative therapy or immune modulation: a scoping review of clinical studies. Biol Blood Marrow Transplant 20(1):20–25
5. Metheny L, Caimi P, de Lima M (2013) Cord blood transplantation: can we make it better? Front Oncol 3:238
6. Zhang J, Niu C, Ye L, Huang H, He X, Tong WG, Ross J, Haug J, Johnson T, Feng JQ, Harris S, Wiedemann LM, Mishina Y, Li L (2003) Identification of the haematopoietic stem cell niche and control of the niche size. Nature 425:836–841
7. Muller-Sieburg CE, Cho RH, Karlsson L, Huang JF, Sieburg HB (2004) Myeloid-biased hematopoietic stem cells have extensive self-renewal capacity but generate diminished lymphoid progeny with impaired IL-7 responsiveness. Blood 103:4111–4118
8. Nakahata T (2001) Ex vivo expansion of human hematopoietic stem cells. Int J Hematol 73:6–13
9. Ogawa M, LaRue AC, Mehrotra M (2013) Hematopoietic stem cells are pluripotent and not just "hematopoietic". Blood Cells Mol Dis 51:3–8
10. Afanasyev BV (2010) A. J. Friedenstein, founder of the mesenchymal stem cell concept. Transplantation 1:35–38
11. Young HE, Mancini ML, Wright RP, Smith JC, Black AC Jr, Reagan CR, Lucas PA (1995) Mesenchymal stem cells reside within the connective tissues of many organs. Dev Dyn 202:137–144
12. Dominici M, Le BK, Mueller I, Slaper-Cortenbach I, Marini F, Krause D, Deans R, Keating A, Prockop D, Horwitz E (2006) Minimal criteria for defining multipotent mesenchymal stromal cells. The International Society for Cellular Therapy position statement. Cytotherapy 8:315–317
13. Jones E, English A, Churchman SM, Kouroupis D, Boxall SA, Kinsey S, Giannoudis PG, Emery P, McGonagle D (2010) Large-scale extraction and characterization of CD271+ multipotential stromal cells from trabecular bone in health and osteoarthritis: implications for bone regeneration strategies based on uncultured or minimally cultured multipotential stromal cells. Arthritis Rheum 62:1944–1954
14. Yoo HS, Yi T, Cho YK, Kim WC, Song SU, Jeon MS (2013) Mesenchymal stem cell lines isolated by different isolation methods show variations in the regulation of graft-versus-host disease. Immune Netw 13:133–140
15. Rodrigo SF, van Ramshorst J, Hoogslag GE, Boden H, Velders MA, Cannegieter SC, Roelofs H, Al Younis I, Dibbets-Schneider P, Fibbe WE, Zwaginga JJ, Bax JJ, Schalij MJ, Beeres SL, Atsma DE (2013) Intramyocardial injection of autologous bone marrow-derived

ex vivo expanded mesenchymal stem cells in acute myocardial infarction patients is feasible and safe up to 5 years of follow-up. J Cardiovasc Transl Res 6:816–825

16. Meier RP, Muller YD, Morel P, Gonelle-Gispert C, Buhler LH (2013) Transplantation of mesenchymal stem cells for the treatment of liver diseases, is there enough evidence? Stem Cell Res 11:1348–1364
17. Aurich H, Sgodda M, Kaltwasser P, Vetter M, Weise A, Liehr T, Brulport M, Hengstler JG, Dollinger MM, Fleig WE, Christ B (2009) Hepatocyte differentiation of mesenchymal stem cells from human adipose tissue in vitro promotes hepatic integration in vivo. Gut 58:570–581
18. Aurich I, Mueller LP, Aurich H, Luetzkendorf J, Tisljar K, Dollinger MM, Schormann W, Walldorf J, Hengstler JG, Fleig WE, Christ B (2007) Functional integration of hepatocytes derived from human mesenchymal stem cells into mouse livers. Gut 56:405–415
19. Hou J, Lu AL, Liu BW, Xing YJ, Da J, Hou ZL, Ai SY (2013) Combination of BMP-2 and 5-AZA is advantageous in rat bone marrow-derived mesenchymal stem cells differentiation into cardiomyocytes. Cell Biol Int 37(12):1291–1299
20. Wang K, Long Q, Jia C, Liu Y, Yi X, Yang H, Fei Z, Liu W (2013) Over-expression of Mash1 improves the GABAergic differentiation of bone marrow mesenchymal stem cells in vitro. Brain Res Bull 99:84–94
21. Pasquinelli G, Valente S (2013) Ultrastructural assessment of the differentiation potential of human multipotent mesenchymal stromal cells. Ultrastruct Pathol 37:318–327
22. Evans MJ, Kaufman MH (1981) Establishment in culture of pluripotential cells from mouse embryos. Nature 292:154–156
23. Thomson JA, Itskovitz-Eldor J, Shapiro SS, Waknitz MA, Swiergiel JJ, Marshall VS, Jones JM (1998) Embryonic stem cell lines derived from human blastocysts. Science 282: 1145–1147
24. Laustriat D, Gide J, Peschanski M (2010) Human pluripotent stem cells in drug discovery and predictive toxicology. Biochem Soc Trans 38:1051–1057
25. Mayshar Y, Ben-David U, Lavon N, Biancotti JC, Yakir B, Clark AT, Plath K, Lowry WE, Benvenisty N (2010) Identification and classification of chromosomal aberrations in human induced pluripotent stem cells. Cell Stem Cell 7:521–531
26. Mandenius CF, Steel D, Noor F, Meyer T, Heinzle E, Asp J, Arain S, Kraushaar U, Bremer S, Class R, Sartipy P (2011) Cardiotoxicity testing using pluripotent stem cell-derived human cardiomyocytes and state-of-the-art bioanalytics: a review. J Appl Toxicol 31:191–205
27. Stephenson E, Jacquet L, Miere C, Wood V, Kadeva N, Cornwell G, Codognotto S, Dajani Y, Braude P, Ilic D (2012) Derivation and propagation of human embryonic stem cell lines from frozen embryos in an animal product-free environment. Nat Protoc 7: 1366–1381
28. Strom S, Holm F, Bergstrom R, Stromberg AM, Hovatta O (2010) Derivation of 30 human embryonic stem cell lines – improving the quality. In Vitro Cell Dev Biol Anim 46:337–344
29. Strom S, Inzunza J, Grinnemo KH, Holmberg K, Matilainen E, Stromberg AM, Blennow E, Hovatta O (2007) Mechanical isolation of the inner cell mass is effective in derivation of new human embryonic stem cell lines. Hum Reprod 22:3051–3058
30. Rodin S, Domogatskaya A, Strom S, Hansson EM, Chien KR, Inzunza J, Hovatta O, Tryggvason K (2010) Long-term self-renewal of human pluripotent stem cells on human recombinant laminin-511. Nat Biotechnol 28:611–615
31. Villa-Diaz LG, Ross AM, Lahann J, Krebsbach PH (2013) Concise review: the evolution of human pluripotent stem cell culture: from feeder cells to synthetic coatings. Stem Cells 31:1–7
32. Chen G, Gulbranson DR, Hou Z, Bolin JM, Ruotti V, Probasco MD, Smuga-Otto K, Howden SE, Diol NR, Propson NE, Wagner R, Lee GO, Antosiewicz-Bourget J, Teng JM, Thomson JA (2011) Chemically defined conditions for human iPSC derivation and culture. Nat Methods 8:424–429
33. Chen VC, Couture SM, Ye J, Lin Z, Hua G, Huang HI, Wu J, Hsu D, Carpenter MK, Couture LA (2012) Scalable GMP compliant suspension culture system for human ES cells. Stem Cell Res 8:388–402
34. Olmer R, Lange A, Selzer S, Kasper C, Haverich A, Martin U, Zweigerdt R (2012) Suspension culture of human pluripotent stem cells in controlled, stirred bioreactors. Tissue Eng Part C Methods 18:772–784
35. Schwartz SD, Hubschman JP, Heilwell G, Franco-Cardenas V, Pan CK, Ostrick RM, Mickunas E, Gay R, Klimanskaya I, Lanza R (2012) Embryonic stem cell trials for macular degeneration: a preliminary report. Lancet 379:713–720

36. Kahan B, Magliocca J, Merriam F, Treff N, Budde M, Nelson J, Browning V, Ziehr B, Odorico J (2011) Elimination of tumorigenic stem cells from differentiated progeny and selection of definitive endoderm reveals a Pdx1+ foregut endoderm stem cell lineage. Stem Cell Res 6:143–157
37. Lund RJ, Emani MR, Barbaric I, Kivinen V, Jones M, Baker D, Gokhale P, Nykter M, Lahesmaa R, Andrews PW (2013) Karyotypically abnormal human ESCs are sensitive to HDAC inhibitors and show altered regulation of genes linked to cancers and neurological diseases. Stem Cell Res 11: 1022–1036
38. Kadereit S, Trounson A (2011) In vitro immunogenicity of undifferentiated pluripotent stem cells (PSC) and derived lineages. Semin Immunopathol 33:551–562
39. D'Amour KA, Bang AG, Eliazer S, Kelly OG, Agulnick AD, Smart NG, Moorman MA, Kroon E, Carpenter MK, Baetge EE (2006) Production of pancreatic hormone-expressing endocrine cells from human embryonic stem cells. Nat Biotechnol 24:1392–1401
40. Kroon E, Martinson LA, Kadoya K, Bang AG, Kelly OG, Eliazer S, Young H, Richardson M, Smart NG, Cunningham J, Agulnick AD, D'Amour KA, Carpenter MK, Baetge EE (2008) Pancreatic endoderm derived from human embryonic stem cells generates glucose-responsive insulin-secreting cells in vivo. Nat Biotechnol 26:443–452
41. Briggs R, KING TJ (1952) Transplantation of living nuclei from blastula cells into enucleated frogs' eggs. Proc Natl Acad Sci U S A 38:455–463
42. Gurdon JB (1962) The developmental capacity of nuclei taken from intestinal epithelium cells of feeding tadpoles. J Embryol Exp Morphol 10:622–640
43. Campbell KH, McWhir J, Ritchie WA, Wilmut I (1996) Sheep cloned by nuclear transfer from a cultured cell line. Nature 380:64–66
44. Takahashi K, Yamanaka S (2006) Induction of pluripotent stem cells from mouse embryonic and adult fibroblast cultures by defined factors. Cell 126:663–676
45. Takahashi K, Tanabe K, Ohnuki M, Narita M, Ichisaka T, Tomoda K, Yamanaka S (2007) Induction of pluripotent stem cells from adult human fibroblasts by defined factors. Cell 131:861–872
46. Bayart E, Cohen-Haguenauer O (2013) Technological overview of iPS induction from human adult somatic cells. Curr Gene Ther 13:73–92
47. Hotta A, Ellis J (2008) Retroviral vector silencing during iPS cell induction: an epigenetic beacon that signals distinct pluripotent states. J Cell Biochem 105:940–948
48. Nishimura K, Sano M, Ohtaka M, Furuta B, Umemura Y, Nakajima Y, Ikehara Y, Kobayashi T, Segawa H, Takayasu S, Sato H, Motomura K, Uchida E, Kanayasu-Toyoda T, Asashima M, Nakauchi H, Yamaguchi T, Nakanishi M (2011) Development of defective and persistent Sendai virus vector: a unique gene delivery/expression system ideal for cell reprogramming. J Biol Chem 286:4760–4771
49. Ye L, Muench MO, Fusaki N, Beyer AI, Wang J, Qi Z, Yu J, Kan YW (2013) Blood cell-derived induced pluripotent stem cells free of reprogramming factors generated by Sendai viral vectors. Stem Cells Transl Med 2:558–566
50. Zhou H, Wu S, Joo JY, Zhu S, Han DW, Lin T, Trauger S, Bien G, Yao S, Zhu Y, Siuzdak G, Scholer HR, Duan L, Ding S (2009) Generation of induced pluripotent stem cells using recombinant proteins. Cell Stem Cell 4:381–384
51. Thier M, Munst B, Mielke S, Edenhofer F (2012) Cellular reprogramming employing recombinant sox2 protein. Stem Cells Int 2012:549846
52. Han J, Sachdev PS, Sidhu KS (2010) A combined epigenetic and non-genetic approach for reprogramming human somatic cells. PLoS One 5:e12297
53. Zhang Y, Li W, Laurent T, Ding S (2012) Small molecules, big roles – the chemical manipulation of stem cell fate and somatic cell reprogramming. J Cell Sci 125:5609–5620
54. Warren L, Manos PD, Ahfeldt T, Loh YH, Li H, Lau F, Ebina W, Mandal PK, Smith ZD, Meissner A, Daley GQ, Brack AS, Collins JJ, Cowan C, Schlaeger TM, Rossi DJ (2010) Highly efficient reprogramming to pluripotency and directed differentiation of human cells with synthetic modified mRNA. Cell Stem Cell 7:618–630
55. Warren L, Ni Y, Wang J, Guo X (2012) Feeder-free derivation of human induced pluripotent stem cells with messenger RNA. Sci Rep 2:657
56. Judson RL, Greve TS, Parchem RJ, Blelloch R (2013) MicroRNA-based discovery of barriers to dedifferentiation of fibroblasts to pluripotent stem cells. Nat Struct Mol Biol 20:1227–1235
57. Anokye-Danso F, Trivedi CM, Juhr D, Gupta M, Cui Z, Tian Y, Zhang Y, Yang W, Gruber PJ, Epstein JA, Morrisey EE (2011) Highly efficient miRNA-mediated reprogramming of mouse and human somatic cells to pluripotency. Cell Stem Cell 8:376–388

58. Miyoshi N, Ishii H, Nagano H, Haraguchi N, Dewi DL, Kano Y, Nishikawa S, Tanemura M, Mimori K, Tanaka F, Saito T, Nishimura J, Takemasa I, Mizushima T, Ikeda M, Yamamoto H, Sekimoto M, Doki Y, Mori M (2011) Reprogramming of mouse and human cells to pluripotency using mature microRNAs. Cell Stem Cell 8:633–638
59. Sharma A, Wu JC (2013) MicroRNA expression profiling of human-induced pluripotent and embryonic stem cells. Methods Mol Biol 936:247–256
60. Chen M, Huang J, Yang X, Liu B, Zhang W, Huang L, Deng F, Ma J, Bai Y, Lu R, Huang B, Gao Q, Zhuo Y, Ge J (2012) Serum starvation induced cell cycle synchronization facilitates human somatic cells reprogramming. PLoS One 7:e28203
61. Si-Tayeb K, Noto FK, Sepac A, Sedlic F, Bosnjak ZJ, Lough JW, Duncan SA (2010) Generation of human induced pluripotent stem cells by simple transient transfection of plasmid DNA encoding reprogramming factors. BMC Dev Biol 10:81
62. Li W, Ding S (2010) Small molecules that modulate embryonic stem cell fate and somatic cell reprogramming. Trends Pharmacol Sci 31:36–45
63. Gonzalez F, Boue S, Izpisua Belmonte JC (2011) Methods for making induced pluripotent stem cells: reprogramming a la carte. Nat Rev Genet 12:231–242
64. Yu J, Vodyanik MA, Smuga-Otto K, Antosiewicz-Bourget J, Frane JL, Tian S, Nie J, Jonsdottir GA, Ruotti V, Stewart R, Slukvin II, Thomson JA (2007) Induced pluripotent stem cell lines derived from human somatic cells. Science 318:1917–1920
65. Liao J, Wu Z, Wang Y, Cheng L, Cui C, Gao Y, Chen T, Rao L, Chen S, Jia N, Dai H, Xin S, Kang J, Pei G, Xiao L (2008) Enhanced efficiency of generating induced pluripotent stem (iPS) cells from human somatic cells by a combination of six transcription factors. Cell Res 18:600–603
66. Shu J, Deng H (2013) Lineage specifiers: new players in the induction of pluripotency. Genomics Proteomics Bioinformatics 11: 259–263
67. Heng JC, Feng B, Han J, Jiang J, Kraus P, Ng JH, Orlov YL, Huss M, Yang L, Lufkin T, Lim B, Ng HH (2010) The nuclear receptor Nr5a2 can replace Oct4 in the reprogramming of murine somatic cells to pluripotent cells. Cell Stem Cell 6:167–174
68. Feng B, Jiang J, Kraus P, Ng JH, Heng JC, Chan YS, Yaw LP, Zhang W, Loh YH, Han J, Vega VB, Cacheux-Rataboul V, Lim B, Lufkin T, Ng HH (2009) Reprogramming of fibroblasts into induced pluripotent stem cells with orphan nuclear receptor Esrrb. Nat Cell Biol 11:197–203
69. Wen Y, Wani P, Zhou L, Baer T, Phadnis SM, Reijo Pera RA, Chen B (2013) Reprogramming of fibroblasts from older women with pelvic floor disorders alters cellular behavior associated with donor age. Stem Cells Transl Med 2:118–128
70. Ohmine S, Squillace KA, Hartjes KA, Deeds MC, Armstrong AS, Thatava T, Sakuma T, Terzic A, Kudva Y, Ikeda Y (2012) Reprogrammed keratinocytes from elderly type 2 diabetes patients suppress senescence genes to acquire induced pluripotency. Aging (Albany NY) 4:60–73
71. Sherr CJ (2012) Ink4-Arf locus in cancer and aging. Wiley Interdiscip Rev Dev Biol 1:731–741
72. Li H, Collado M, Villasante A, Strati K, Ortega S, Canamero M, Blasco MA, Serrano M (2009) The Ink4/Arf locus is a barrier for iPS cell reprogramming. Nature 460:1136–1139
73. Sharma A, Diecke S, Zhang WY, Lan F, He C, Mordwinkin NM, Chua KF, Wu JC (2013) The role of SIRT6 protein in aging and reprogramming of human induced pluripotent stem cells. J Biol Chem 288:18439–18447
74. Aasen T, Raya A, Barrero MJ, Garreta E, Consiglio A, Gonzalez F, Vassena R, Bilic J, Pekarik V, Tiscornia G, Edel M, Boue S, Izpisua Belmonte JC (2008) Efficient and rapid generation of induced pluripotent stem cells from human keratinocytes. Nat Biotechnol 26:1276–1284
75. Zhang XB (2013) Cellular reprogramming of human peripheral blood cells. Genomics Proteomics Bioinformatics 11:264–274
76. Rashid ST, Corbineau S, Hannan N, Marciniak SJ, Miranda E, Alexander G, Huang-Doran I, Griffin J, Ahrlund-Richter L, Skepper J, Semple R, Weber A, Lomas DA, Vallier L (2010) Modeling inherited metabolic disorders of the liver using human induced pluripotent stem cells. J Clin Invest 120:3127–3136
77. Touboul T, Hannan NR, Corbineau S, Martinez A, Martinet C, Branchereau S, Mainot S, Strick-Marchand H, Pedersen R, Di SJ, Weber A, Vallier L (2010) Generation of functional hepatocytes from human embryonic stem cells under chemically defined conditions that recapitulate liver development. Hepatology 51:1754–1765

78. Eggenschwiler R, Loya K, Wu G, Sharma AD, Sgodda M, Zychlinski D, Herr C, Steinemann D, Teckman J, Bals R, Ott M, Schambach A, Scholer HR, Cantz T (2013) Sustained knockdown of a disease-causing gene in patient-specific induced pluripotent stem cells using lentiviral vector-based gene therapy. Stem Cells Transl Med 2: 641–654
79. Itzhaki I, Maizels L, Huber I, Zwi-Dantsis L, Caspi O, Winterstern A, Feldman O, Gepstein A, Arbel G, Hammerman H, Boulos M, Gepstein L (2011) Modelling the long QT syndrome with induced pluripotent stem cells. Nature 471:225–229
80. Kudva YC, Ohmine S, Greder LV, Dutton JR, Armstrong A, De Lamo JG, Khan YK, Thatava T, Hasegawa M, Fusaki N, Slack JM, Ikeda Y (2012) Transgene-free disease-specific induced pluripotent stem cells from patients with type 1 and type 2 diabetes. Stem Cells Transl Med 1:451–461
81. Torres JM, Cox NJ, Philipson LH (2013) Genome wide association studies for diabetes: perspective on results and challenges. Pediatr Diabetes 14:90–96
82. Bao W, Hu FB, Rong S, Rong Y, Bowers K, Schisterman EF, Liu L, Zhang C (2013) Predicting risk of type 2 diabetes mellitus with genetic risk models on the basis of established genome-wide association markers: a systematic review. Am J Epidemiol 178: 1197–1207
83. Gaj T, Gersbach CA, Barbas CF III (2013) ZFN, TALEN, and CRISPR/Cas-based methods for genome engineering. Trends Biotechnol 31:397–405
84. Sanjana NE, Cong L, Zhou Y, Cunniff MM, Feng G, Zhang F (2012) A transcription activator-like effector toolbox for genome engineering. Nat Protoc 7:171–192
85. Taylor CJ, Peacock S, Chaudhry AN, Bradley JA, Bolton EM (2012) Generating an iPSC bank for HLA-matched tissue transplantation based on known donor and recipient HLA types. Cell Stem Cell 11:147–152
86. Yamanaka S (2012) Induced pluripotent stem cells: past, present, and future. Cell Stem Cell 10:678–684
87. Gourraud PA, Gilson L, Girard M, Peschanski M (2012) The role of human leukocyte antigen matching in the development of multi-ethnic "haplobank" of induced pluripotent stem cell lines. Stem Cells 30:180–186
88. Li LB, Chang KH, Wang PR, Hirata RK, Papayannopoulou T, Russell DW (2012) Trisomy correction in Down syndrome induced pluripotent stem cells. Cell Stem Cell 11:615–619
89. Liang G, Zhang Y (2013) Genetic and epigenetic variations in iPSCs: potential causes and implications for application. Cell Stem Cell 13:149–159
90. Zhao T, Zhang ZN, Rong Z, Xu Y (2011) Immunogenicity of induced pluripotent stem cells. Nature 474:212–215
91. Guha P, Morgan JW, Mostoslavsky G, Rodrigues NP, Boyd AS (2013) Lack of immune response to differentiated cells derived from syngeneic induced pluripotent stem cells. Cell Stem Cell 12:407–412
92. Vierbuchen T, Ostermeier A, Pang ZP, Kokubu Y, Sudhof TC, Wernig M (2010) Direct conversion of fibroblasts to functional neurons by defined factors. Nature 463: 1035–1041
93. Ieda M, Fu JD, Delgado-Olguin P, Vedantham V, Hayashi Y, Bruneau BG, Srivastava D (2010) Direct reprogramming of fibroblasts into functional cardiomyocytes by defined factors. Cell 142:375–386
94. Szabo E, Rampalli S, Risueno RM, Schnerch A, Mitchell R, Fiebig-Comyn A, Levadoux-Martin M, Bhatia M (2010) Direct conversion of human fibroblasts to multilineage blood progenitors. Nature 468:521–526
95. Yu B, He ZY, You P, Han QW, Xiang D, Chen F, Wang MJ, Liu CC, Lin XW, Borjigin U, Zi XY, Li JX, Zhu HY, Li WL, Han CS, Wangensteen KJ, Shi Y, Hui LJ, Wang X, Hu YP (2013) Reprogramming fibroblasts into bipotential hepatic stem cells by defined factors. Cell Stem Cell 13:328–340
96. Zhang K, Liu GH, Yi F, Montserrat N, Hishida T, Rodriguez EC, Izpisua Belmonte JC (2014) Direct conversion of human fibroblasts into retinal pigment epithelium-like cells by defined factors. Protein Cell 5:48–58
97. Furuya F, Shimura H, Asami K, Ichijo S, Takahashi K, Kaneshige M, Oikawa Y, Aida K, Endo T, Kobayashi T (2013) Ligand-bound thyroid hormone receptor contributes to reprogramming of pancreatic acinar cells into insulin-producing cells. J Biol Chem 288:16155–16166
98. Zhou Q, Brown J, Kanarek A, Rajagopal J, Melton DA (2008) In vivo reprogramming of adult pancreatic exocrine cells to beta-cells. Nature 455:627–632
99. Qian L, Huang Y, Spencer CI, Foley A, Vedantham V, Liu L, Conway SJ, Fu JD,

Srivastava D (2012) In vivo reprogramming of murine cardiac fibroblasts into induced cardiomyocytes. Nature 485:593–598

100. van den Bos C, Keefe R, Schirmaier C, McCaman M (2014) Therapeutic human cells: manufacture for cell therapy/regenerative medicine. Adv Biochem Eng Biotechnol 138:61–97

101. Eaker S, Armant M, Brandwein H, Burger S, Campbell A, Carpenito C, Clarke D, Fong T, Karnieli O, Niss K, Van't Hof W, Wagey R (2013) Concise review: guidance in developing commercializable autologous/patient-specific cell therapy manufacturing. Stem Cells Transl Med 2(11):871–883

102. Amariglio N, Hirshberg A, Scheithauer BW, Cohen Y, Loewenthal R, Trakhtenbrot L, Paz N, Koren-Michowitz M, Waldman D, Leider-Trejo L, Toren A, Constantini S, Rechavi G (2009) Donor-derived brain tumor following neural stem cell transplantation in an ataxia telangiectasia patient. PLoS Med 6:e1000029

Chapter 2

Aurigon's Point of View on the Safety Assessment of Cell-Based Therapies: An Experience Based on the Participation in 15 ATMPs Projects

Emmanuelle Cornali

Abstract

Cell-based medicinal products (CBMP) require the use of a case-by-case, risk-based, and scientifically justified nonclinical safety testing approach. The challenge is to translate regulatory requirements into concrete testing designs while overcoming technical limitations inherent to animal models and the CBMP and assaying combination strategies to reduce animal use and save time and budget.

Key words Cell-based medicinal products, CBMP, Safety testing

1 Introduction

Although cell-based medicinal products (CBMPs) have been clinically used for more than a decade, robust nonclinical scientific and regulatory provisions for these products have only recently been adopted. Safety assessment of CBMPs has not been performed systematically. Either health benefits were greater compared to any risk (e.g., bone marrow cell transplantation) or side effects were socially accepted (e.g., plastic surgery).

Since the first description of human pluripotent stem cells (1998), a lot of development has been made in new innovative cell-based therapies for diseases and tissue defects, for which traditional therapies and medicinal products have not provided satisfactory outcomes. Developments include induction of adult somatic pluripotent stem cells (iPSCs), 2D or 3D tissue engineering, genetic manipulation of cells, and combination of cells with medical device products.

This wide variety and high complexity of Advanced Therapy Medicinal Products (ATMPs), their foreseen technical limitations (human origin, limited amount, and viability), and their particular risks (identity/variability, plasticity, immunogenicity, tumorigenicity,

Bruno Christ et al. (eds.), *Animal Models for Stem Cell Therapy*, Methods in Molecular Biology, vol. 1213,
DOI 10.1007/978-1-4939-1453-1_2,

migration/persistence) rendered the conventional nonclinical safety testing requirements not adequate.

Consequently, a case-by-case, risk-based, and scientifically justified approach has been developed to evaluate the type of studies required for the Marketing Authorization Application (MAA) of CBMPs. The approach often requires the use of molecular biology methods, well known in most laboratories but rarely used under GLP for safety assessment of medicinal products and for which method validation challenged more than one investigator.

What is needed? The risk-based approach considers the origin (autologous/allogeneic); the ability to proliferate, to differentiate, or to initiate an immune response; the level of ex vivo manipulation; the administration (route and site); the duration of exposure or life span of cells; the combination of products; and finally the availability of clinical data or experience with similar products. Depending on the evaluation of the abovementioned factors, the nonclinical testing program might include the assessment of the following:

- Pharmacologic efficacy/POC (proof of concept)
- Biodistribution (migration, trafficking, persistence)
- In vivo tumorigenic potential
- Toxicity/immunogenicity potential
- Biocompatibility of the medical device product—if applicable

2 Biodistribution: Evaluation of Migration, Trafficking, and Persistence

The most common evaluation strategy of biodistribution is to inoculate the human cell product in immunodeficient small animals (e.g., nude mice or rats; Scid, Scid-beige, NOD-Scid, NOG, or NSG mice) and to trace the target cells at different time points, usually up to 6 months. Cell dose, study duration, and cell-tracing method need careful evaluation when designing biodistribution studies.

Small animals allow meticulous cell detection in whole organs/tissues, while using an appropriate specific detection method. Besides cell-labeling techniques, which might influence the fate of the cells, the method most commonly used is a quantitative real-time PCR for human-specific (e.g., Alu, Chr. 17 α1/α2) and mouse-specific (e.g., PTGER2) gene sequences.

When using PCR, it is very important to avoid any contamination with human DNA from operators during the necropsy and the subsequent extraction and amplification steps and to reach a validated sensitivity of about 10 human cells per mg mouse tissues.

One further challenge for this kind of study often lies in the administration route. This should mimic the clinical one, which might be a technical issue in small immunodeficient animals.

3 Tumorigenic Potential

One of the greatest concerns in cell-based products, especially PSC-based, is their potential to form tumors. The quite standardized assessment of the tumorigenic potential of CBMPs is derived from the method used for cell substrate for production of vaccines (ICHQ5 and Ph. Eur. Monograph 5.2.3.). Basically, the cells are inoculated in immunodeficient mice (e.g., nude, Scid, Scid-beige, NOD-Scid, NOG, NSG) and injection sites, as well as selected potential target tissues are histologically evaluated at 3 or up to 6 months after cell administration for the potential presence of tumors. The procedure is quite simple, but one of the challenges is that immunodeficient animals tend to develop spontaneous tumors, most of the time lymphomas. Based on our experience, depending on the mouse strains, tumors already appear in up to 10 % of the animals at 5 months of age (which corresponds to a 3 months tumorigenicity study). Therefore, it is strongly advised to set up a confirmatory method that can be used on paraformaldehyde-fixed paraffin-embedded tissues, such as ISH (in situ hybridization), to be able to clarify—when needed—the mouse vs. human origin of the tumor.

4 Toxicological Potential

This is one of the most difficult assessments for CBMPs. There are basically two strategies. The first one is an autologous or allogeneic strategy in a large animal model, and the second one—the most commonly used so far—is the xenogeneic testing of the human product in immunodeficient animals. The first strategy may be preferred by complex administration procedures and for long-term toxicity evaluation. The second approach tests the clinical human product in only one species, usually the mouse (no satisfactory chemically induced immunocompromised large animals), and has the disadvantage in overseeing any immunotoxicity aspect.

To add an additional level of complexity and possibilities, as most of the cell-based medicinal products are intended to be used in Phase I studies in diseased/injured patients, animal models of injury/disease may often be the most relevant model in which to assess toxicity. In this case, when the rationale for using diseased/injured animals has been justified, combination of toxicity evaluation within a POC study may be considered to reduce animal use.

Moreover, if application site/route, cell number, and time points are matching, considering that the readout of the tumorigenicity is focused on the histopathology of the application site and selected target organs, the tumorigenicity testing might also be included into the combined POC-toxicity study.

In conclusion, everyone who develops new innovative cell-based therapies faces the challenge of pioneering the safety assessment of such complex products, and it is more than highly recommended to submit the nonclinical testing strategy to the regulatory authorities before starting any experimental studies.

Part II

Liver Diseases

Chapter 3

Preconditioning of the Liver for Efficient Repopulation by Primary Hepatocyte Transplants

Petra Krause, Margret Rave-Frank, Hans Christiansen, and Sarah Koenig

Abstract

The therapeutic potential of liver cell transplantation has been demonstrated in multiple clinical studies to correct hereditary metabolic or chronic liver diseases. However, there are several outstanding issues, which need to be investigated: most notably donor cell engraftment and the subsequent selective expansion of transplanted cells.

This protocol describes the preconditioning of the liver in a dipeptidyl peptidase-IV ($DPPIV^-$)-deficient rat model of efficient repopulation utilizing a selective external beam irradiation technique combined with regional transient portal ischemia (RTPI). Irradiation of the host liver impairs endogenous cell division, and the subsequent RTPI constitutes a strongly proliferative stimulus. Transplanted cells benefit from this stimulus, whereas endogenous cells have no ability to respond, due to a reduction in the mitotic capacity of the host liver. As described here, an effective preparative regime for liver repopulation is external beam liver irradiation in the form of a single dose of 25 Gy applied to the whole organ followed (4 days later) by RTPI of the right liver lobes lasting 90 min. After 1 h of reperfusion, the donor hepatocytes may be transplanted directly into the spleen as implantation site for further redistribution into the portal system and liver. This preparative regime certainly has the potential to be implemented in the clinic, since neither toxins nor highly potent carcinogens are used.

Key words Preconditioning, Liver irradiation, Liver repopulation, Ischemia

1 Introduction

Liver cell transplantation remains a promising alternative to whole organ transplantation in the treatment of hereditary metabolic disorders or chronic liver disease. Acceptable methods for clinical application are needed to promote the proliferation of donor cells in the recipient liver. In therapeutic cell transplantation, the cells are administered slowly during repeated infusions via intraportal injection into the recipient liver, either by catheterization or percutaneous puncture of the portal vein. However, up to 70 % of transplanted cells do not survive and will be destroyed within 24 h, mainly by Kupffer cells. Following this initial phase, many more

Bruno Christ et al. (eds.), *Animal Models for Stem Cell Therapy*, Methods in Molecular Biology, vol. 1213,
DOI 10.1007/978-1-4939-1453-1_3,

transplanted cells appear to lose their way, and no more than 3 % of the transplanted cells will succeed in integrating into the host liver. Protocols are needed to increase the therapeutic efficiency by supporting the selective expansion of transplanted cells.

Experimental protocols in animal models have demonstrated an effective strategy of priming the host liver by using DNA-damaging toxins or even carcinogens to inhibit endogenous cell proliferation [1, 2]. This preconditioning in combination with some strong mitogenic stimulus such as partial hepatectomy leads to massive repopulation by transplanted cells in the recipient liver [3]. Unfortunately, the clinical translation of toxin- or carcinogen-based procedures is not appropriate. Furthermore, partial liver resection is a large surgical procedure and is associated with risks such as liver failure or biliary leakage [4, 5]. Therefore, clinically acceptable methods have to be developed to promote the proliferation of transplanted cells through some more appropriate minimally invasive intervention. Two techniques have been developed in experimental settings: [1] irradiation to impair the endogenous mitotic capacity by blocking the cell cycle and [2] RTPI as mitotic stimulus.

Thus, we combined external beam liver irradiation with RTPI in an experimental rat animal model to achieve ideal conditions for liver repopulation by transplanted hepatocytes. The protocol presented here is suitable for the design of a more noninvasive preparative regime and to optimize cell transplantation. This may provide us with an effective preparative regime with positive prospects for future clinical application.

2 Materials

Prepare all buffers and solutions using deionized water with an electrical resistivity of 18 MΩ cm at 25 °C. Unless otherwise specified, all chemicals should be of analytical grade. Sterilize solutions using 0.22 μm cartridge filters. All buffers and solutions should be stored between +2 and +8 °C and all chemicals at room temperature unless otherwise indicated.

2.1 Hepatocyte Preparation

1. Male DPPIV$^+$ Fischer 344 rats, 180–220 g body mass (Charles River, Sulzfeld, Germany) (*see* **Note 1**).
2. Xylariem® (20 mg xylazine) (Ecuphar NV/SA, Oostkamp, Belgium).
3. Ketamine 10 % (Medistar, Hanover, Germany).
4. 70 % alcohol.
5. Collagenase (Type CLS, 340 U/mg; Biochrom, Berlin, Germany).

6. Carbogen gas (95 % oxygen and 5 % carbon dioxide; Linde Gases Division, Pullach, Germany).
7. Peristaltic pump (Ismatec® SA. Langenfeld, Germany).
8. Heating immersion circulator with water bath (model ED; Julabo, Seelbach, Germany).
9. Indwelling cannula (14 or 16 G; B. Braun, Melsungen, Germany).
10. Extension linetype Heidelberger (B. Braun, Melsungen, Germany).
11. Glass frit (Rettberg, Goettingen, Germany).
12. Bubble trap (Rettberg, Goettingen, Germany) (*see* **Note 2**).
13. Vicryl® 2/0 (Ethicon, Johnson and Johnson, Norderstedt, Germany).
14. Cartridge filter (0.22 μm PVDF membrane; Millipore Cooperation, Billerica, MA, USA).
15. Hemocytometer (Neubauer improved; Brand GmbH, Wertheim a. M., Germany).
16. Percoll® (Sigma Aldrich, St. Louis, MO, USA).
17. 10× Buffer A, Preperfusion—bicarbonate buffer without Ca^{2+} and Mg^{2+}: 67.21 g NaCl, 4.39 g KCl, 0.276 g NaH_2PO_4, 1.7 g Na_2SO_4, 21 g $NaHCO_3$, 11.9 g HEPES, 9.9 g D-glucose, 1.9 g EGTA, adjust pH to 7.38 with HCl or NaOH, respectively. Store at 4 °C.
18. 10× Buffer B, Perfusion—bicarbonate buffer with Ca^{2+} and Mg^{2+}: 67.21 g NaCl, 4.39 g KCl, 0.276 g NaH_2PO_4, 1.7 g Na_2SO_4, 21.0 g $NaHCO_3$, 11.9 g HEPES, 9.9 g D-glucose, 3.68 g $CaCl_2 \times 2H_2O$, 2.4 g $MgCl_2 \times 6H_2O$, adjust pH to 7.38 with HCl or NaOH, respectively. Store at 4 °C.
19. 10× PBS for Percoll® solution preparation: 80.0 g NaCl, 2.0 g KCl, 1.0 g $MgCl_2 \times 6H_2O$, 21.6 g $Na_2HPO_4 \times 7H_2O$, 2.0 g KH_2PO_4. Store at 4 °C.

2.2 Irradiation

1. Male DPPIV$^-$ Fischer 344 rats, 180–220 g body mass (Charles River, Sulzfeld, Germany) (*see* **Note 3**).
2. Xylariem® (20 mg xylazine; Ecuphar NV/SA, Oostkamp, Belgium) (*see* **Note 4**).
3. Ketamine 10 % (Medistar, Hanover, Germany) (*see* **Note 4**).
4. Computed tomography scanner (Somatom Balance, Siemens, Erlangen, Germany).
5. Perspex plate (1 cm).
6. Linear accelerator or X-ray machine (Varian Clinac 600 C, Varian Medical Systems, Inc. Palo Alto, USA; RS 225, Xstrahl Ltd, Camberley, England).

2.3 Regional Transient Portal Ischemia (RTPI) and Hepatocyte Transplantation

1. Male DPPIV$^-$ Fischer 344 rats, 180–220 g body mass (Charles River, Sulzfeld, Germany) (*see* **Note 3**).
2. Sevorane® (sevoflurane 100 % v/v, Abbott GmbH, Wiesbaden, Germany).
3. Physiological saline solution.
4. Rimadyl® (carprofen 50 mg/1 mL, Pfizer, Berlin, Germany).
5. Hair trimmer type GH204 (Aesculap AG, Tuttlingen, Germany).
6. Eye cream (Bayer Healthcare, Leverkusen, Germany).
7. Yasargil clip (Aesculap AG, Tuttlingen, Germany) (*see* **Note 5**).
8. Syringe with 27 G injection needle.
9. MATRISTYPT® (collagen matrix; MedSkin Solutions, Billerbeck, Germany).
10. Vicryl® 4/0 SH (Ethicon, Johnson and Johnson, Norderstedt, Germany).

3 Methods

3.1 Preparation of Hepatocytes

3.1.1 Initial Steps

1. Dilute buffer A with water 1:10 under sterile conditions to a volume of 500 mL. Final concentration: 115 mM NaCl, 5.9 mM KCl, 0.23 mM NaH_2PO_4, 1.2 mM Na_2SO_4, 25 mM $NaHCO_3$, 5 mM HEPES, 5.5 mM D-glucose, 0.5 mM EGTA. Adjust pH to 7.38 with HCl or NaOH, respectively.
2. Dilute buffer B with water 1:10 under sterile conditions to a volume of 500 mL. Final concentration: 115 mM NaCl, 5.9 mM KCl, 0.23 mM NaH_2PO_4, 1.2 mM Na_2SO_4, 25 mM $NaHCO_3$, 5 mM HEPES, 5.5 mM D-glucose, 2.5 mM $CaCl_2 \times 2H_2O$, 1.18 mM $MgCl_2 \times 6H_2O$. Adjust pH to 7.38 with HCl or NaOH, respectively.
3. Weigh 40 mg collagenase in a sterile glass bottle.
4. Prepare fresh Percoll® solution under sterile conditions: 45 mL Percoll, 45 mL deionized water, 10 mL 10× PBS for Percoll® solution.
5. Adjust the water bath at 37 °C and heat the buffers A and B (for collagenase solution).
6. Saturate buffer A with carbogen using a glass frit.
7. Connect the tube of the pump with the extension line Heidelberger and integrate the bubble trap. Recirculate buffer A in the system until liver perfusion begins (*see* **Note 6**).

3.1.2 Hepatocyte Preparation

Isolate the hepatocytes in a 2-step in situ collagenase digestion of the liver according to Seglen [6]. Take care to maintain sterile conditions throughout the whole preparation procedure.

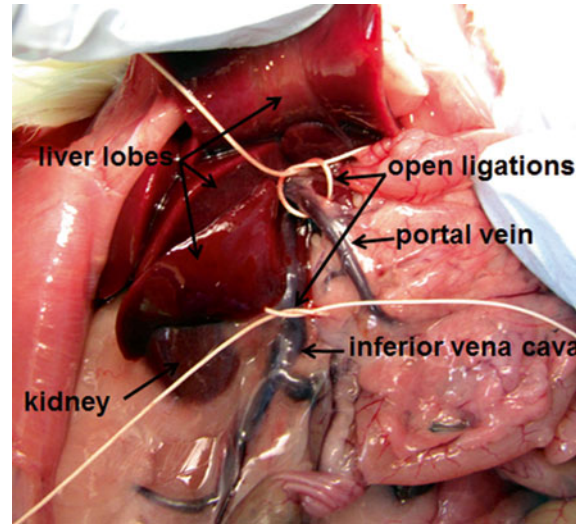

Fig. 1 Situs abdominalis before cannulating the portal vein. The open ligations are placed around the portal vein beneath the liver hilus, and the second ligation is placed around the inferior vena cava above the right renal vein. The indwelling cannula should be placed at around the position of the *arrow* marking the portal vein

1. Anesthetize a male DPPIV$^+$ Fischer 344 rat intraperitoneally (ip) with xylazine (7.5 mg/kg body mass (BM)) and ketamine (90 mg/kg BM).
2. Disinfect its whole chest and abdomen with 70 % alcohol.
3. Perform a large median laparotomy and expose the portal vein by repositioning the intestine on the left side of the animal (*see* **Note 7**).
4. Place an open ligation (2/0 Vicryl®) around the vena portae (Fig. 1).
5. Then, place a second open ligation around the inferior vena cava (IVC) above the right renal vein (Fig. 1).
6. Cannulize the portal vein with an indwelling cannula (size 14 G).
7. Fix the cannula with the ligation placed previously.
8. Connect the cannula to the perfusion tube (Heidelberger type extension line) to initiate perfusion via the portal vein using buffer A (10 mL/min).
9. Immediately sever the IVC below the open ligature.
10. Increase the buffer flow rate to 20 mL/min for 10 min to rinse out the liver blood.
11. Dissolve the collagenase in 100 mL buffer B (37 °C) prior to use.
12. Meanwhile, open the thorax and place a third open ligature around the IVC below the heart.

13. Open the right atrium with scissors and place a cannula (16 G) caudally.
14. Fix the cannula with the ligation placed previously.
15. Connect the cannula with a perfusion tube.
16. Change preperfusion buffer A after 10 min to collagenase solution (0.03–0.05 %) (*see* **Note 8**).
17. Continue perfusion in a recirculating system for 4–8 min (20 mL/min).
18. End perfusion when liver becomes malleable (*see* **Note 9**).
19. Excise the liver and gently separate the liver capsule from the cells in bicarbonate buffer B at room temperature.
20. Filter the cells through a nylon mesh (80 μm) and adjust the volume to 100 mL cell suspension in buffer B.

Continue the work at 4 °C on ice and work in a laminar flow hood.

21. Centrifuge the suspension in 2 × 50 mL tubes for 5 min at 50 × *g*.
22. Resuspend the pellets and add bicarbonate buffer B to a volume of 40 mL.
23. Prepare 4 × 50 mL tubes each with 8 mL Percoll® solution.
24. Layer 10 mL cell suspension gently onto the Percoll® solution.
25. Centrifuge the tubes at 800 × *g* for 10 min beginning with slow acceleration.
26. Resuspend the pellets in 100 mL bicarbonate buffer.
27. Centrifuge the cell suspension (2 × 50 mL tubes) for 5 min at 60 × *g*.
28. Resuspend the pellet and determine the viability using trypan blue exclusion in a counting chamber.
29. Adjust the cell number to the required volume of 200 μL for 12 million cells.

3.2 Preconditioning with Radiation

1. Anesthetize the animal (DPPIV$^-$) ip with xylazine (7.5 mg/kg BM) and ketamine (90 mg/kg BM) (*see* **Note 10**).
2. Place the animal in the prone position on a perspex plate (1 cm) for the planning CT scan.
3. Delineate the upper and lower margins of the liver with a permanent marker on the skin of the animal (Fig. 2a).
4. Subsequently, determine the irradiation plan with suitable software, for example, CadPlan (Varian Medical Systems) for accelerators, or make use of appropriate tables (X-ray machines).
5. Subsequently, place the animal in the chosen irradiation device (accelerator or X-ray machine).

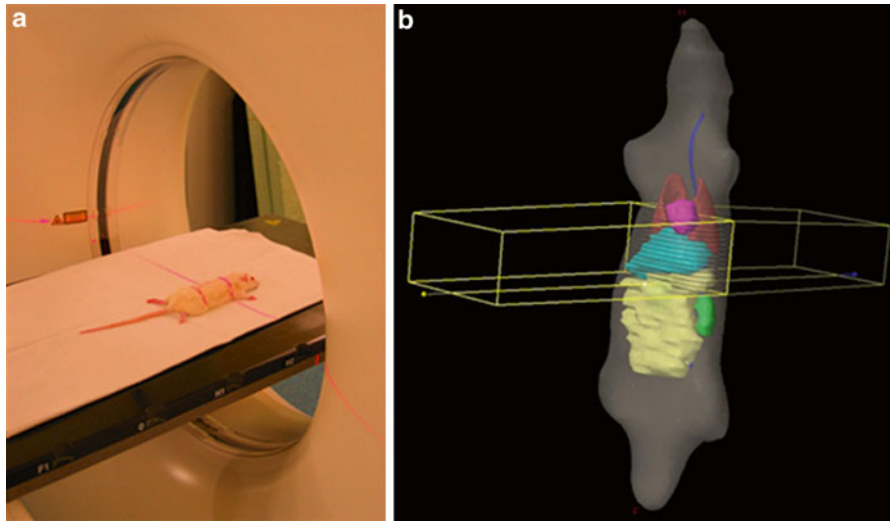

Fig. 2 (**a**) An anesthetized rat in prone position for a planning CT scan. The *red laser beam* delineates the upper and lower margins of the liver for irradiation. (**b**) Exemplified radiation device for rat liver irradiation. The liver and adjacent organs are depicted in different colors (*light blue*, liver; *blue*, spinal cord; *red-brown*, lung; *purple*, heart; *beige-yellow*, gastrointestinal region; *green*, kidney). Radiation is applied successively from two directions, dorsally and ventrally, which is indicated by the two fields marked as *yellow boxes*. To avoid the gastrointestinal region, a so-called half-beam technique was used, in which the isocenter is placed at the lower border of the liver instead of the center of the irradiated region (indicated by the *yellow line* in the *middle* of the (*yellow box*) radiation fields). The region to receive the planned radiation dose of 25 Gy is marked by the *dark parallel lines*

6. Irradiate with a dose of 25 Gy using 6–20 MV photons or 200–250 kV X-rays at a dose rate of 2–3 Gy/min using an ap/pa treatment technique (*see* **Notes 11** and **12**) (Fig. 2b).
7. Replace the animal in the cage (it should recover from anesthesia approximately 1 h after narcotic application).

3.3 Preconditioning of the Liver by RTPI and Hepatocyte Transplantation

Take care to maintain sterile conditions throughout the whole surgical procedure.

1. Initiate anesthesia of an irradiated rat with a sevoflurane concentration of 5–7 vol.% and—once deep unconsciousness has been achieved—reduce the sevoflurane volume to 3–3.5 vol.% (*see* **Note 13**).
2. For pain control, administer carprofen (30 mg/kg BM ip) prior to surgery (Note: continue pain medication daily, up to 3 days when needed).
3. Disinfect the chest and abdomen after shaving off the fur.
4. Perform a limited median laparotomy to the upper abdomen and expose the IVC and then identify the portal vein and its branches to the right superior anterior and right liver lobes.
5. Take the first Yasargil clip to occlude the branch to lobe 1 (Fig. 3).

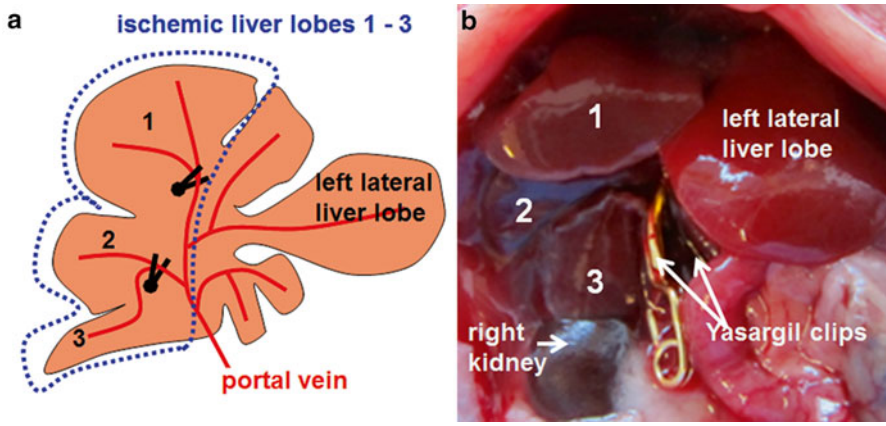

Fig. 3 RTPI due to clamping of the right portal branches. (**a**) Schematic illustration of the Yasargil clip position in the liver to induce transient ischemia. (**b**) In situ view after clamping the right liver lobes with Yasargil clips. Following clamping of the portal vein branches, lobes 1, 2, and 3 (45 % of the liver mass) turn darker in color as ischemia is established when compared with the unaffected lobes

6. Place the second Yasargil clip to occlude the branch to lobes 2 and 3 (Fig. 3).
7. Start recording the duration of ischemia and thereafter reposition the liver lobes in their anatomically correct positions.
8. Administer 1–2 mL physiological saline solution intraperitoneally to prevent perioperative dehydration of the animal.
9. Adapt the wound margins with 4/0 Vicryl® sutures.
10. Continue the anesthesia during the whole ischemia period and place the animal in a cage on a warming plate (37 °C).
11. Just before the designated ischemia time lapses, open the wound suture and cautiously loosen the clips.
12. Reposition the liver and administer 1–2 mL of physiological saline solution again.
13. Adapt the wound margins again with 4/0 SH Vicryl® and put the animal in a cage on a warming plate (37 °C).
14. Continue the anesthesia for 1 h.
15. Following 1 h of reperfusion, open the adapted wound again and mobilize the spleen.
16. Slowly inject 200 μL of cell suspension over 2 min using a 27 G injection needle into the spleen parenchyma (*see* **Note 14**).
17. Remove the needle carefully and stop the bleeding with a small piece of MATRISTYPT®.
18. Reposition the spleen.
19. Close the wound continuously with 3/0 SH Vicryl® in two layers.

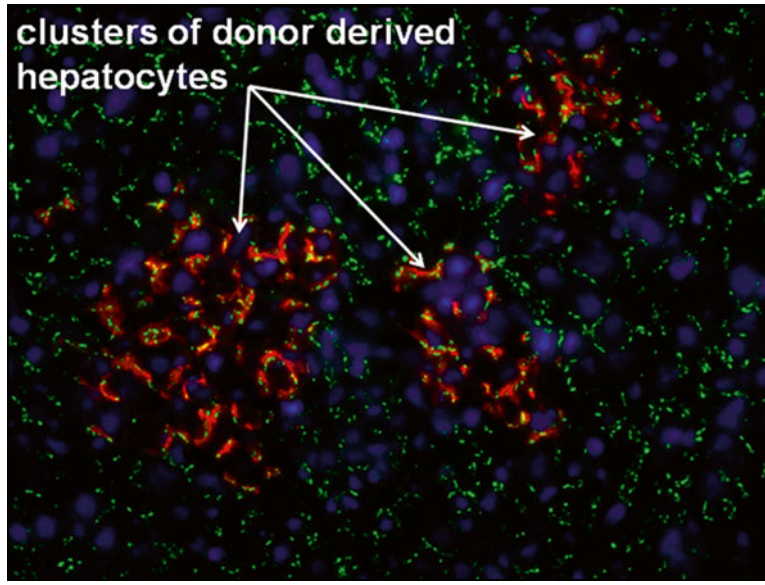

Fig. 4 Transplanted DPPIV-positive hepatocytes 12 weeks after transplantation. The image displays the repopulation of the host liver after preconditioning with external beam liver irradiation (25 Gy) prior to RTPI for 90 min and a subsequent reperfusion interval lasting 1 h. Clusters of transplanted cells are easily identified using immunofluorescence staining of donor-specific DPPIV (*red*) and colocalized with the gap junction marker connexin 32 (*green*). Nuclear counterstaining with DAPI (*blue*). Original magnification 200×

20. First close the muscle and fascia followed by closing the skin to perform complete wound closure.
21. Administer pure oxygen until the animal awakens.
22. Feed the animals with mash for 2 days.

Repopulation of the host liver by DPPIV-positive cells can be confirmed using immunofluorescence staining (Fig. 4).

4 Notes

1. All animals were housed under 12/12 h light/dark cycles with standard rodent diet (Ssniff, Soest, Germany) and water available ad libitum. All animal breeding, care, and experimentation were carried out in accordance with German national and regional legislation on animal protection.
2. We use a specially designed bubble trap manufactured out of glass, but failing that the bubble trap of a perfusion system would be sufficient.
3. A colony of DPPIV$^-$ Fischer rats was established in our animal care facilities with parent animals kindly provided by Prof.

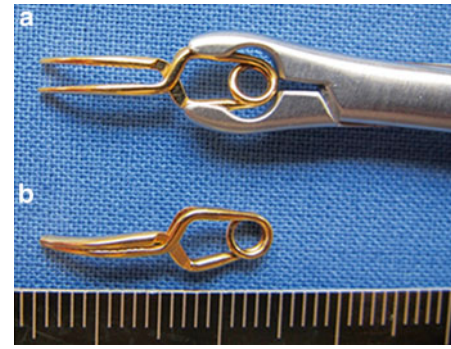

Fig. 5 Yasargil clips: (**a**) A Yasargil clip inserted in a clip applier. (**b**) We use curved clips (approx. 2 cm) for portal vein occlusion

E. Laconi from the Istituto di Patologia Sperimentale, University of Cagliari, Italy.

4. Mix xylazine and ketamine in a single syringe for application.
5. In order to achieve temporary occlusion of the portal branches (right superior and right liver lobes), use Yasargil clips (Fig. 5). The curved clips have a blade length of 10.2 mm and a maximum opening of 7.5 mm.
6. The end of the Heidelberger extension line should fit to the indwelling cannula.
7. The laparotomy should be broadly conceived caudally along the costal arch.
8. The collagenase concentration depends on the quality of different batches and varies from 0.03 to 0.06 %. The appropriate concentration has to be verified by previous cell preparation experiments.
9. Test the plasticity of the liver tissue by tapping lightly with forceps. After 4–6 min of collagenase perfusion, a pitting of the tissue should remain.
10. To follow the fate of transplanted hepatocytes in the host liver, we used the $DPPIV^-$ rat model [7]. Hepatocytes harvested from positive ($DPPIV^+$) wild-type Fischer 344 rats were transplanted into these syngeneic $DPPIV^-$ recipients. This constellation allows us to detect donor cells easily within the host liver using simple immunohistochemical techniques.
11. It is important to ensure that the liver is irradiated homogeneously and to avoid adjacent organs as best as possible.
12. With respect to clinical application, a fractionated irradiation regimen with 5×5 Gy (given on five consecutive days) is also feasible.

13. During anesthesia, apply an eye cream to protect the eyes from dehydrating.
14. A number of 12 million cells is appropriate but may be modified.

Acknowledgements

The authors would like to thank Andrew Entwistle for his critical review of this manuscript.

References

1. Laconi E, Oren R, Mukhopadhyay DK, Hurston E, Laconi S, Pani P, Dabeva MD, Shafritz DA (1998) Long-term, near-total liver replacement by transplantation of isolated hepatocytes in rats treated with retrorsine. Am J Pathol 153: 319–329
2. Joseph B, Kumaran V, Berishvili E, Bhargava KK, Palestro CJ, Gupta S (2006) Monocrotaline promotes transplanted cell engraftment and advances liver repopulation in rats via liver conditioning. Hepatology 44:1411–1420
3. Guha C, Deb NJ, Sappal BS, Ghosh SS, Roy-Chowdhury N, Roy-Chowdhury J (2001) Amplification of engrafted hepatocytes by preparative manipulation of the host liver. Artif Organs 25:522–528
4. van den Broek MA, Olde Damink SW, Dejong CH, Lang H, Malago M, Jalan R, Saner FH (2008) Liver failure after partial hepatic resection: definition, pathophysiology, risk factors and treatment. Liver Int 28:767–780
5. Erdogan D, Busch OR, van Delden OM, Rauws EA, Gouma DJ, van Gulik TM (2008) Incidence and management of bile leakage after partial liver resection. Dig Surg 25: 60–66
6. Seglen PO (1976) Preparation of isolated rat liver cells. Methods Cell Biol 13:29–83
7. Thompson NL, Hixson DC, Callanan H, Panzica M, Flanagan D, Faris RA, Hong WJ, Hartel-Schenk S, Doyle D (1991) A Fischer rat substrain deficient in dipeptidyl peptidase IV activity makes normal steady-state RNA levels and an altered protein. Use as a liver-cell transplantation model. Biochem J 273(Pt 3): 497–502

Chapter 4

Age-Dependent Hepatocyte Transplantation for Functional Liver Tissue Reconstitution

Peggy Stock

Abstract

The transplantation of hepatocytes could be an alternative therapeutic option to the whole organ transplantation for the treatment of end-stage liver diseases. However, this cell-based therapy needs the understanding of the molecular mechanisms to improve efficacy. This chapter includes a detailed method of a rat model for liver regeneration studies after age-dependent hepatocyte transplantation.

Key words Hepatocyte transplantation, Liver regeneration, Cell-based therapy

1 Introduction

End-stage liver diseases are associated with poor prognosis, and the transplantation of the whole organ is still the only curative treatment. Worldwide the amount of patients suffering from end-stage liver diseases is increasing. One major cause is cirrhotic alteration in the liver based on nonalcoholic and alcoholic fatty liver diseases or virus-induced hepatitis. Additionally, the incidence of hepatocellular cancer is higher in cirrhotic livers. For several years now, the clinical transplantation of hepatocytes as an alternative to the organ transplantation has been performed in a nonroutine small number of cases. Yet, provided the maintenance of the functionality of the isolated hepatocytes to be transplanted, this therapeutic option is a versatile novel treatment [1].

The hepatocyte transplantation for the treatment of the terminal Crigler-Najjar syndrome type I was published in 1998 by Ira Fox and colleagues [2]. Since then, various publications have described the method in humans [3, 4] as well as in animal models: in nonhuman primates [5], in rats using adult hepatocytes [6] and fetal liver cells [7], or in mice [8, 9]. However, the transplantation of hepatocytes is still associated with a poor outcome: the transplanted cells will be eliminated in the host liver tissue if they are not

Bruno Christ et al. (eds.), *Animal Models for Stem Cell Therapy*, Methods in Molecular Biology, vol. 1213,
DOI 10.1007/978-1-4939-1453-1_4,

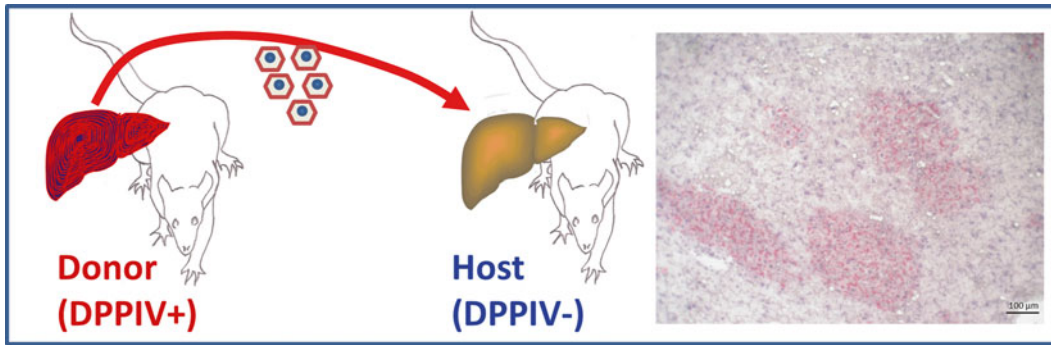

Fig. 1 Principle of hepatocyte transplantation for functional liver tissue reconstitution. DPPIV+ donor rat hepatocytes are transplanted into DPPIV– host rat livers. The microscopic picture shows integrated DPPIV+ cells (red) in the DPPIV– host liver 6 weeks after cell transplantation

supplied with a growth advantage. Unfavorable conditions could be the marginal quality of the donor organs as the source of the hepatocytes, the age of the donors and/or the hosts, or finally, difficulties related to logistic problems like insufficient preservation, storage, and transport conditions. In 2013, Hoyer et al. described [10] the prediction of early allograft dysfunction of whole liver transplants only based on the evaluation of donor data. Taking these facts into account, the transplantation of hepatocytes and their capacity of liver tissue reconstitution might be improved significantly by further understanding of the cellular and molecular mechanisms involved. Certainly, it is important to define the influence of the age of the host (liver) as well as of the donor hepatocytes in animal models before translation into the clinics.

One of the animal models technically well suited to study hepatocyte transplantation was published by Thompson et al. in 1991 [11] utilizing Fischer F344 rats (Fig. 1). A side strain of Fischer F344 rats expresses a nonfunctional protein (DPPIV-) due to a natural modification. Cell transplants from the strain expressing active DPPIV enzyme (DPPIV+) are simply traceable histochemically in the host liver of DPPIV– Fischer F344 rats and may be quantified to determine the reconstitution of the organ by the transplanted hepatocytes.

In this model, which is also described in this chapter, a proliferation advantage is given by hepatectomy and pretreatment of the host animal with the phytotoxin retrorsine preventing host hepatocyte proliferation [12].

Briefly, this chapter describes a rat model for liver tissue reconstitution after age-dependent hepatocyte transplantation including the analysis of functional integration of the cells. The hepatocytes were isolated from 4 weeks old and 35 weeks old DPPIV+ Fischer F344 rats by the two-step perfusion. The cells were then transplanted via portal vein injection into a 1/3 hepatectomized and

retrorsine-pretreated DPPIV– Fischer F344 rat at the age of 10 weeks and 41 weeks, respectively. The transplanted, integrated cells were traced by DPPIV staining, and the functionality of the integrated hepatocytes was assured by co-staining of intracellular glycogen stores.

Thereby, an in vivo method to investigate the influence of age on the integration of transplanted cells and the reconstitution of liver tissue is provided.

2 Materials

2.1 Laboratory Requirements

All methods have to be carried out in class I security level laboratories. The cell separation procedure has to be done under sterile conditions in a class II laminar flow box. Disposable plastic ware has to be used. For the handling of narcotic substances, the regulatory approval is warranted.

2.2 Animals

The animals are kept under a 12/12 h day/night rhythm with open access to standard diet and drinking water in a certified animal facility. The procedures have to be conducted according to national law and only after governmental approval.

The rat strains applied include wild-type (DPPIV+) Fischer F344 and DPPIV– Fischer F344 rats. The donor hepatocytes are isolated from wild-type Fischer rats. These can be obtained from commercial providers. The DPPIV– Fischer F344 rats serve as host animals. These animals are not commercially available but were grown in animal facilities at the University of Leipzig [6]. DPPIV– Fischer rats were described by Watanabe et al. and Hartel-Schenk et al. [13, 14]. Since the modification of the DPPIV enzyme is natural, no gene technology permission is required in Germany.

2.3 Preconditioning of Juvenile and Senescent DPPIV– Fischer F344 Rats

1. 22 G needle.
2. 1 mL syringe.
3. Retrorsine (Sigma-Aldrich, Steinheim, Germany).
4. Scale.

2.4 Isolation of Hepatocytes from Livers of Juvenile and Senescent Wild-Type Fischer F344 Rats

1. Surgical instruments: set of scissors, surgical and curved forceps.
2. Permanent venous catheter.
3. Peristaltic pump.
4. Perfusion tubings.
5. Bubble trap.
6. Glass heat exchanger.
7. Water bath.

8. Surgical suture material (2/0).
9. Pentobarbital (Narcoren; Merial GmbH, Hallbergmoos, Germany): intraperitoneal (i.p.) at a dose of 700 μL/kg body weight.
10. Heparin 25,000 I.E./5 mL, i.p. at a dose of 1,000 μL/kg body weight (ROTEXMEDICA, Trittau, Germany).
11. Sterile gauze compress.
12. Glass funnel.
13. Krebs-Ringer Buffer (KRP): 120 mM NaCl, 4.8 mM KCl, 1.2 mM $MgSO_4 \times 7\ H_2O$, 1.2 mM KH_2PO_4, 24.4 mM $NaHCO_3$.
14. Perfusion buffer I (PPP): 30 mg EGTA, ad 300 mL KRP, equilibrate with carbogen for 30 min, adjust pH to 7.35, and pass the buffer through a sterile filter into a bottle. Before use, prewarm in a water bath at 37 °C.
15. Perfusion buffer II (CPP): 892.5 mg Hepes, 147.5 mg $CaCl_2 \times 2H_2O$, ad 250 mL KRP, equilibrate with carbogen for 30 min, adjust pH to 7.5, and pass the buffer through a sterile filter into a bottle. Before use, prewarm in a water bath at 37 °C, add 0.12 U/mL collagenase NB 4G (Serva, Heidelberg, Germany).
16. Washing buffer: 20 mM Hepes, 120 mM NaCl, 4.8 mM KCl, 1.2 mM $MgSO_4 \times 7H_2O$, 1.2 mM KH_2PO_4, 4 % bovine serum albumin (BSA), 50 mg/L DNase (*see* **Note 1** for **steps 13–16**).

2.5 Hepatocyte Transplantation into Juvenile and Senescent DPPIV– Fischer F344 Rat Livers

1. Phosphate-buffered saline (PBS).
2. Syringe and 25 G needle.
3. Sterile swab.
4. Surgical instruments: set of scissors, tissue retractor 5 cm, surgical forceps, needle holder.
5. Sterile gauze compress.
6. Iodine solution for disinfection.
7. Electric shaver.
8. Surgical suture material (3/0).
9. Ethyl alcohol (70 %).
10. Sterile absorbable gelatin sponge (Chauvin ankerpharm GmbH, Berlin, Germany).
11. Tabotamp (Ethicon, Johnson & Johnson Medical GmbH, Norderstedt, Germany).
12. Isoflurane.
13. Oxygen.
14. Anesthetics inhalator.

15. Electric heating pad.
16. Cold light illumination.

2.6 Liver Resection and Preparation of Samples

1. Surgical instruments (*see* Subheading 2.5).
2. Pentobarbital (Narcoren): i.p. at a dose of 700 μL/kg body weight.
3. Mr. Frosty™ Cryo Freezing Container (Nalgene, Roskilde, Denmark).
4. Cryo vials (TPP, Trasadingen, Switzerland).
5. Cryostat (SLEE Technical GmbH, Mainz, Germany).
6. 3-Aminopropyltriethoxy-silan-coated glass slides.

2.7 Histochemical Detection of Transplanted Cells by DPPIV Staining

1. Acetone.
2. Ethyl alcohol (96 %).
3. Substrate solution: 58 mg NaCl in 10 mL of 100 mmol/L Tris maleate buffer (pH 6.5), in 1 mL of this buffered saline dissolve 0.5 mg gly-pro-methoxy-β-naphthylamide and 1 mg Fast Blue.
4. PBS.
5. Hemalaun (Merck, Darmstadt, Germany).
6. 10 % formalin.
7. Glycerol-gelatin (Merck, Darmstadt, Germany).
8. Brightfield microscope.

2.8 Histochemical Detection of Glycogen by Periodic Acid-Schiff (PAS) Staining

In addition to the materials used for DPPIV staining as listed in Subheading 2.7:

1. 1 % periodic acid (Carl Roth GmbH + Co. KG, Karlsruhe, Germany).
2. Schiff's reagent (Merck, Darmstadt, Germany).

3 Methods

3.1 Preconditioning of Juvenile and Senescent DPPIV– Fischer F344 Rats

Juvenile and senescent DPPIV– Fischer F344 rats serve as hosts for DPPIV+ donor hepatocytes and have to be preconditioned to provide a growth advantage for the transplanted cells. By the treatment with the phytotoxin retrorsine, the proliferative capacity but not the functionality of the host hepatocytes will be altered. The injection of retrorsine has to be carried out twice: 6 and 4 weeks prior to the cell transplantation. Juvenile hosts will receive the first injection at the age of 4 weeks (*see* **Note 2**) and senescent host animals at the age of 35 weeks.

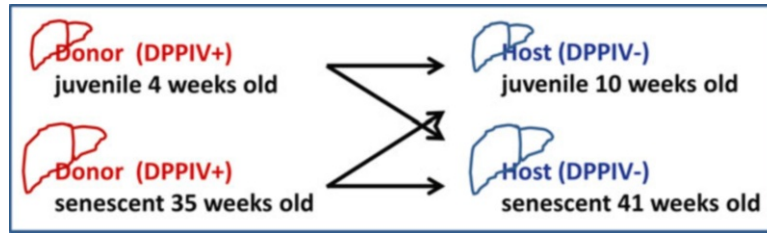

Fig. 2 Schematic illustration of a possible transplantation regimen using hepatocyte donor and host animals of different ages, respectively

1. Dissolve retrorsine in acidified PBS and readjust pH to 7.4 after solving (*see* **Note 3**).
2. Weigh the animals.
3. Administer a dose of 30 mg/kg body weight retrorsine by i.p. injection.
4. Repeat the administration after 2 weeks.

3.2 Isolation of Juvenile and Senescent Rat Hepatocytes for Cell Transplantation

The rat model used in this chapter allows the study of age-dependent hepatocyte transplantation in the host liver. At the time of hepatocyte transplantation, the juvenile and the senescent host animals will be 10 weeks and 41 weeks old, respectively (Fig. 2).

1. Inject the animal i.p. heparin and a lethal dose of pentobarbital (*see* **Note 4**).
2. Open the peritoneal cavity and dislocate the intestinal loop to prepare the portal vein.
3. Open the thorax above the diaphragm, ligate the abdominal aorta tightly using curved forceps.
4. Ligate the portal vein and insert the permanent venous catheter, fix the catheter with the ligature.
5. Attach the perfusion tubing to the catheter and start perfusion with PPP (20–25 mL/min) using a peristaltic pump. Immediately perforate the vena cava inferior to allow blood and buffer outflow (*see* **Note 4**).
6. Flush blood off the liver, stop the pump, exchange PPP for CPP, and continue perfusion until the liver appears spongy.
7. Stop the perfusion and remove the liver carefully without violation of the liver capsule.
8. Transfer the liver into washing buffer. All following steps are carried out under sterile conditions: open the liver capsule by gentle scratching with a needle. Shake the liver to wash out the hepatocytes. Pass the cell suspension through a sterile gauze compress, lined in a glass funnel, and spin the resulting cell

suspension for 5 min at 70 × *g* and 4 °C. Discard the supernatant and wash the cells twice again.

9. Resuspend the cells in PBS, count the cells, and prepare aliquots of 4×10^6 cells/500 µL. Store the cells on ice until infusion into the portal vein.

3.3 Transplantation of Juvenile or Senescent Hepatocytes into Juvenile and Senescent Rats via Portal Vein Injection

1. Place the animal under an anesthetic inhalator and perform the anesthesia with isoflurane inhalation and oxygen at 2 L/min. Shave the abdomen and disinfect with ethyl alcohol (70 %) and iodine solution. Except the abdomen, completely cover the animal with sterile gauze compresses.
2. Open the skin by a 6 cm ventral incision. Prepare the abdominal musculature with the stump ends of surgical forceps and scissors. Open the peritoneal cavity by a 5 cm long incision. Fix with a small retractor in an optimal position.
3. Draw up the cell suspension stored on ice into the syringe immediately before the transplantation.
4. For the 1/3 hepatectomy, perform a proximal ligature of the left lateral liver lobe followed by resection of this lobe (*see* **Note 5**). Dislocate the omentum majus and the intestine to expose the portal vein. Puncture the vein and slowly inject the cells using a syringe with a 25 G needle. After injection is completed, place a 5 × 5 mm piece of Tabotamp gauze onto the puncture site before retraction and stop bleeding after retraction of the needle with an absorbable gelatin sponge (*see* **Note 6**).
5. Put the intestinal loop back into the peritoneal cavity and suture the abdominal musculature and the skin.
6. Place the animals on an electric heating pad to recover from anesthesia (*see* **Note 7**).

3.4 Monitoring of Functional Liver Tissue Reconstitution after Hepatocyte Transplantation

Donor hepatocytes expressing active DPPIV are visualized by histochemical staining of cryosections. Their functionality might be monitored by co-staining with the PAS reaction to detect glycogen storage in the cell transplants within the parenchyma of the reconstituted host liver.

3.4.1 Liver Resection and Preparation of Cryosections of Rat Livers

1. Inject heparin and pentobarbital as described in Subheading 3.2, **Step 1**, then open the peritoneal cavity and explant the whole liver.
2. Split the liver into pieces and place them in cryovials. Use Mr. Frosty™ Cryo Freezing Container to allow a continuous freezing rate.
3. Use a cryostat to prepare 5 µm tissue slices and place them on 3-aminopropyltriethoxy-silan-coated glass slides. Store the slides at −80 °C until histochemical detection of DPPIV.

3.4.2 Histochemical Detection of DPPIV in the Rat Liver and Co-staining of Glycogen Storage by the PAS (Periodic Acid-Schiff) Reaction

1. Fix the slices with acetone for 5 min at –20 °C.
2. Wash the slices with 96 % ethyl alcohol and air-dry.
3. Incubate the slices with substrate solution for 20 min.
4. Rinse the slides shortly with PBS.
5. Incubate the slices with freshly prepared 1 % periodic acid for 5 min.
6. Wash slides with aqua dest. for 5 min and incubate with Schiff's reagent for 10 min.
7. After washing with PBS, stain with hemalaun (*see* **Note 8**) and fix with formalin (10 %).
8. Finally, cover the slices with glycerol-gelatin.
9. Analyze the slices by brightfield microscopy (Fig. 3).

4 Notes

1. For each single substance, stock solutions at appropriate concentrations are prepared and stored in aliquots at –20 °C. Aliquots are used only once and discarded after thawing.
2. The treatment with the phytotoxin retrorsine will halt the proliferation capacity of the hepatocytes. Juvenile animals should have a body weight of at least 80 g at the age of 4 weeks. Otherwise, the treatment will be lethal.
3. Solved retrorsine cannot be stored because it precipitates in neutral solution 2 h after preparation.
4. Pentobarbital eventually triggers respiratory depression at a lethal dose of 100 mg/kg body weight. However, in order to prevent blood coagulation in the sinusoids, the very first step of perfusion with PPP to disintegrate the liver for the isolation of hepatocytes should be performed as soon as the animal is anesthetized and respiratory repression has not occurred, yet.
5. The 1/3 hepatectomy is required to provide the transplanted hepatocytes with a proliferation advantage in the host liver.
6. The infusion of hepatocytes from DPPIV+ Fischer F344 rats into livers of DPPIV– Fischer F344 rats is an autologous cell transplantation model. Hence, the application of an immunosuppressant is not necessary.
7. Usually, we monitor integration of transplanted hepatocytes for a period of 6 weeks. The follow-up of traceable DPPIV+ cells integrated in the parenchyma of the host liver might start 1 week after transplantation. This time frame is required to allow penetration of the hepatocytes through the endothelia. Before 1 week, DPPIV+ cells are mainly found residing in the sinusoids. The observation period can be extended up to

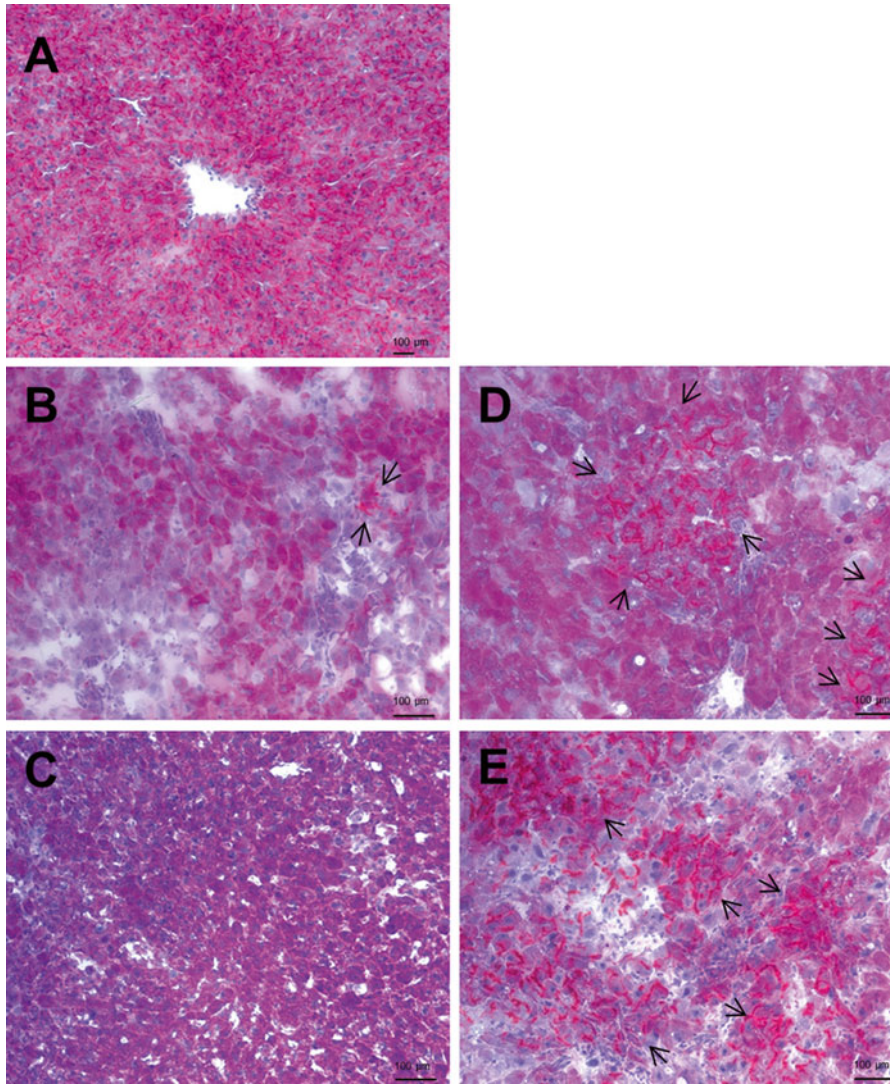

Fig. 3 In vivo DPPIV co-staining (*red*) with the PAS reaction (*purple*), a functional marker of glycogen storage (**a**–**e**). For visualization of equal glycogen storage in host and transplanted hepatocytes after 6 weeks, PAS staining was performed: (**a**) positive control—co-staining of DPPIV enzyme activity and glycogen storage in the liver of wild-type Wistar rats; (**b**) senescent hepatocytes transplanted into senescent host livers; (**c**) juvenile hepatocytes transplanted into senescent host livers; (**d**) juvenile hepatocytes transplanted into juvenile host livers; (**e**) senescent hepatocytes transplanted into juvenile host livers. The *black arrows* indicate double-positive cell clusters of transplanted, integrated, and expanded DPPIV+ hepatocytes. In (**b**) and (**c**), practically no DPPIV+ cell clusters are detectable

1 year. Integrated cells or clusters of cells are usually found in the periportal region of the liver lobule.

8. Color intensity has to be checked carefully during the staining process to avoid overexposure of the section.

Acknowledgement

The author would like to thank Madlen Hempel for her excellent technical assistance.

References

1. Runge D, Runge DM, Jäger D, Lubecki KA, Beer Stolz D, Karathanasis S, Kietzmann T, Strom SC, Jungermann K, Fleig WE, Michalopoulos GK (2000) Serum-free, long-term cultures of human hepatocytes: maintenance of cell morphology, transcription factors, and liver-specific functions. Biochem Biophys Res Commun 269(1):46–53
2. Fox IJ, Chowdhury JR, Kaufman SS, Goertzen TC, Chowdhury NR, Warkentin PI, Dorko K, Sauter BV, Strom SC (1998) Treatment of the Crigler-Najjar syndrome type I with hepatocyte transplantation. N Engl J Med 338(20): 1422–1426
3. Ribes-Koninckx C, Ibars EP, Calzado Agrasot MÁ, Bonora-Centelles A, Miquel BP, Vila Carbó JJ, Aliaga ED, Pallardó JM, Gómez-Lechón MJ, Castell JV (2012) Clinical outcome of hepatocyte transplantation in four pediatric patients with inherited metabolic diseases. Cell Transplant 21(10):2267–2282. doi: 10.3727/096368912X637505
4. Puppi J, Strom SC, Hughes RD, Bansal S, Castell JV, Dagher I, Ellis EC, Nowak G, Ericzon BG, Fox IJ, Gómez-Lechón MJ, Guha C, Gupta S, Mitry RR, Ohashi K, Ott M, Reid LM, Roy-Chowdhury J, Sokal E, Weber A, Dhawan A (2012) Improving the techniques for human hepatocyte transplantation: report from a consensus meeting in London. Cell Transplant 21(1):1–10. doi:10.3727/096368911X566208
5. Yannam GR, Han B, Setoyama K, Yamamoto T, Ito R, Brooks JM, Guzman-Lepe J, Galambos C, Fong JV, Deutsch M, Quader MA, Yamanouchi K, Kabarriti R, Mehta K, Soto-Gutierrez A, Roy-Chowdhury J, Locker J, Abe M, Enke CA, Baranowska-Kortylewicz J, Solberg TD, Guha C, Fox IJ (2014) A nonhuman primate model of human radiation-induced venocclusive liver disease and hepatocyte injury. Int J Radiat Oncol Biol Phys 88(2):404–411. doi:10.1016/j.ijrobp.2013.10.037
6. Laconi E, Oren R, Mukhopadhyay DK, Hurston E, Laconi S, Pani P, Dabeva MD, Shafritz DA (1998) Long-term, near-total liver replacement by transplantation of isolated hepatocytes in rats treated with retrorsine. Am J Pathol 153:319–329
7. Oertel M (2011) Fetal liver cell transplantation as a potential alternative to whole liver transplantation? J Gastroenterol 46(8):953–965. doi:10.1007/s00535-011-0427-5
8. Petersen J, Dandri M, Gupta S, Rogler CE (1998) Liver repopulation with xenogenic hepatocytes in B and T cell-deficient mice leads to chronic hepadnavirus infection and clonal growth of hepatocellular carcinoma. Proc Natl Acad Sci U S A 95(1):310–315
9. Overturf K, Al-Dhalimy M, Tanguay R, Brantly M, Ou CN, Finegold M, Grompe M (1996) Hepatocytes corrected by gene therapy are selected in vivo in a murine model of hereditary tyrosinaemia type I. Nat Genet 12(3):266–273
10. Hoyer DP, Paul A, Gallinat A, Molmenti EP, Reinhardt R, Minor T, Saner FH, Canbay A, Treckmann JW, Sotiropoulos GC, Mathé Z (2013) Donor information based prediction of early allograft dysfunction and outcome in liver transplantation. Liver Int. doi: 10.1111/liv.12443
11. Thompson NL, Hixson DC, Callanan H, Panzica M, Flanagan D, Faris RA, Hong WJ, Hartel-Schenk S, Doyle D (1991) A Fischer rat substrain deficient in dipeptidyl peptidase IV activity makes normal steady-state RNA levels and an altered protein. Use as a liver-cell transplantation model. Biochem J 273(Pt 3): 497–502
12. Laconi S, Curreli F, Diana S, Pasciu D, Filippo GD, Sarma DSR, Pani P, Laconi E (1999) Liver regeneration in response to partial hepatectomy in rats treated with retrorsine: a kinetic study. J Hepatol 31:1069–1074
13. Watanabe Y, Kojima T, Fujimoto Y (1987) Deficiency of membrane-bound dipeptidyl aminopeptidase IV in a certain rat strain. Experientia 43(4):400–401
14. Hartel-Schenk S, Gossrau R, Reutter W (1990) Comparative immunohistochemistry and histochemistry of dipeptidyl peptidase IV in rat organs during development. Histochem J 22(10):567–578

Chapter 5

Treatment of NASH with Human Mesenchymal Stem Cells in the Immunodeficient Mouse

Sandra Winkler and Bruno Christ

Abstract

Nonalcoholic steatohepatitis (NASH) as a severe form of nonalcoholic liver diseases (NAFLD) is one of the prominent liver diseases worldwide. Under favoring conditions it may progress into liver cirrhosis and hepatocellular carcinoma (HCC), which in its end stage strongly requires organ transplantation. Due to the shortage of donor organs, alternative therapeutic approaches like cell therapy treatment are necessary. In this article, an auspicious method of cell therapy with hepatocytic differentiated human mesenchymal stem cells to treat NASH in an immunodeficient mouse model is presented.

Key words Liver disease, NASH, Human mesenchymal stem cells, Immunodeficient mouse, Xenogeneic transplantation, Methionine-choline-deficient diet, Cell differentiation

1 Introduction

In Germany, the incidence of liver diseases has progressed over the last decade from 79,351 cases in 2000 up to 84,003 cases in 2011 [1]. The prevalence of nonalcoholic fatty liver disease (NAFLD) is estimated 20–30 % of the adult population of Western countries [2]. This type of liver diseases includes benign hepatic steatosis and more severe steatohepatitis followed by fibrosis, cirrhosis, and finally hepatocellular cancer [3]. Nonalcoholic steatohepatitis (NASH) is characterized by lipid accumulation, inflammation, and fibrogenesis in the liver parenchyma [4] with a prevalence of 3–16 % of the healthy population [2]. Frequently, NASH requires liver transplantation as the only therapeutic strategy. In the United States, NASH became the third most common reason for liver transplantation and increased up to 9.7 % in 2009 [5]. On the other hand, donor livers for whole organ and hepatocyte transplantation are rare, and alternative therapeutic approaches are needed. One possible option for the treatment of NASH are mesenchymal stem cells (MSCs), which have the potential to differentiate into hepatocyte-like cells and may integrate into the host parenchyma

Bruno Christ et al. (eds.), *Animal Models for Stem Cell Therapy*, Methods in Molecular Biology, vol. 1213,
DOI 10.1007/978-1-4939-1453-1_5,

after transplantation into the mouse liver [4, 6]. To study the impact of transplanted differentiated MSCs, we developed an immunodeficient mouse model of nonalcoholic steatohepatitis. NASH is induced by a methionine-choline-deficient diet (MCD-diet). Animals develop steatosis, inflammation, and fibrogenesis indicated by increased liver triglycerides and serum transaminase levels and collagen type I deposition [4]. Therapeutic treatment with mesenchymal stem cells derived from human bone marrow and differentiated into hepatocyte-like cells reduced these parameters after 1 week posttransplantation. The model seems to be useful to study the impact of transplanted MSCs on NASH and to infer therapeutic strategies as alternative treatment option.

2 Materials

2.1 Animal Experiment

1. Methionine-choline-deficient diet (MCD-diet; MP-Biochemicals Europe, Illkirch Cedex, France).
2. 12–14 weeks old male Pfp/Rag $2^{-/-}$ mice (Taconic, Ejby, Denmark).
3. Small animal anesthesia apparatus (isoflurane inhalation rate, 1.5 vol.%; oxygen rate, 2 L/min).
4. Heating operating table.
5. Surgical forceps and scissors.
6. Sterile swabs.
7. Surgical suture material: Marlin violet DS16 3-0 USP absorbable (Catgut GmbH, Markneukirchen, Germany).
8. 1 mL syringe with 25 G needle (BD, Heidelberg, Germany).
9. Microscales.

2.2 Analysis

Centrifuge, photometer, microtome, microscope, and polarization microscope of any supplier are required for the analysis.

2.2.1 Mouse Serum

Dilute serum for measurement with 0.9 % NaCl in a 2:1 ratio. Store undiluted serum at –20 °C.

2.2.2 Liver Triglycerides

1. Liquid nitrogen to pulverize liver tissue in a ceramic mortar with a pestle.
2. Chloroform/methanol solution (2:1).
3. Ultrasound homogenizer.
4. Qualitative filter paper: 5–13 μm pore size.
5. 0.05 % H_2SO_4.
6. Triglyceride FS* (DiaSys Diagnostic System International, Holzheim, Germany) and a photometer for measuring enzyme activity at 500 nm wavelength.

2.2.3 Histology

1. 1 μm paraffin slices for histological analysis (microtome).
2. Descending graded alcohol: xylene, 96 % ethanol, 80 % ethanol, 70 % ethanol, 50 % ethanol, deionized water.
3. Mayer's hemalum solution and eosin Y solution 0.5 % aqueous.
4. Sirius Red solution: 0.5 g direct red (Alfa Aesar, Karlsruhe, Germany) in 500 mL picrinic acid solution 1.2 %.
5. 0.5 % acetic acid.
6. Tap water.
7. Ascending graded alcohol: deionized water, 50 % ethanol, 70 % ethanol, 80 % ethanol, 96 % ethanol, 2-propanol, xylene.
8. Entellan.

3 Methods

For all animal experiments standard conditions are required. Animals are kept under a 12/12 h day/night rhythm with free access to food and drinking water. Animal experiments have to be performed according to national laws. For feeding and transplantation experiments use 12–14 weeks old male Pfp/Rag $2^{-/-}$ mice.

The MCD-diet is deficient in the essential amino acid methionine and the phospholipid component choline. Caused by depletion of phosphatidylcholine and the downregulation of the microsomal triglyceride transfer protein accompanied by apoB misfolding, very low density lipoprotein (VLDL) assembly in the liver is disturbed leading to massive steatosis.

3.1 Mouse Model

1. Within the first week of the feeding experiments, diet adaption by intermixing the methionine-choline-deficient diet and the standard diet is required. After 1 week, feed the MCD-diet exclusively for another 5 weeks (Fig. 1).
2. Document animal body weight at least once a week (*see* **Note 1**).
3. After 5 weeks of feeding the MCD-diet, transplant hepatocytic differentiated human mesenchymal stem cells. MSCs were enriched from the mononuclear cell fraction purified by density gradient centrifugation and subsequent plastic adherence. For transplantation details, *see* [7].
4. Keep continuing MCD-diet feeding until harvesting the organ after another week (Fig. 1; *see* **Notes 2–4**).
5. Blood and snap-frozen, paraffin-embedded, and cryopreserved liver tissue will be required for further analysis.

3.2 Analysis

3.2.1 Mouse Serum

1. Centrifuge the blood sample for 5 min at 4 °C at 1.5 × *g*.
2. Take the serum supernatant and discard the pellet. Dilute serum with 0.9 % NaCl (*see* **Note 5**).

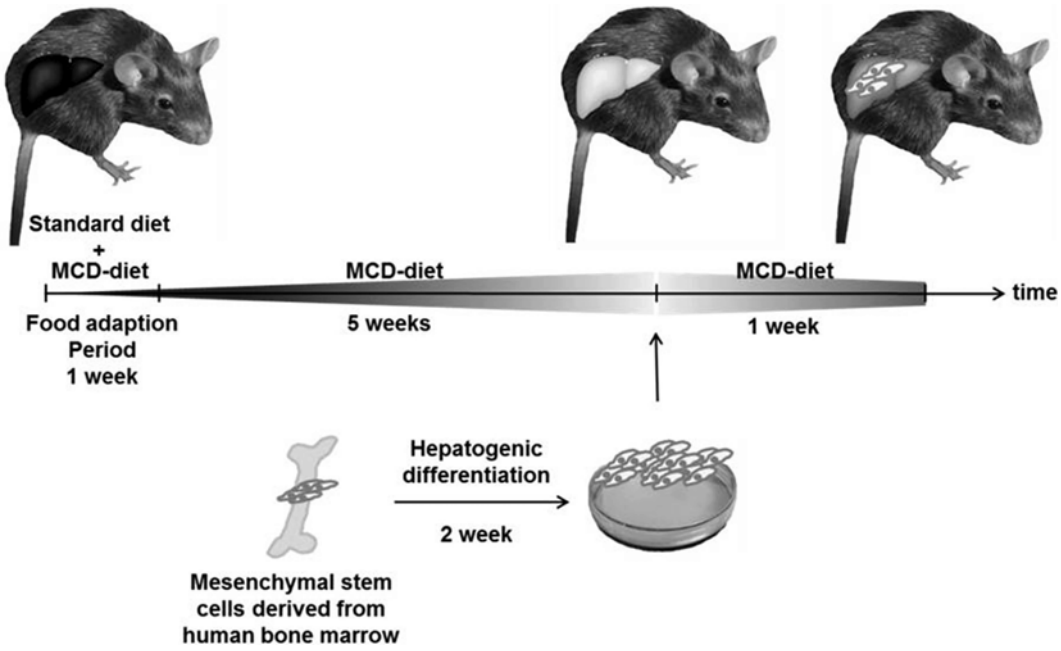

Fig. 1 Experimental design of the NASH model suitable for hepatic cell transplantation. After an adaption period of 1 week, 10–12 weeks old male Pfp/Rag $2^{-/-}$ mice received the methionine-choline-deficient (MCD) diet for 5 weeks. 1.5×10^6 differentiated human mesenchymal stem cells were transplanted (via the spleen) into mice suffering from NASH. The MCD-diet was continued until sacrifice 1 week posttransplantation

3. Serum triglycerides and alanine aminotransferase (ALT) may be determined by any hospital central laboratory according to automatized procedures.

3.2.2 Liver Triglycerides

1. Pulverize 30 mg of liver tissue with liquid nitrogen in a mortar with a pestle.
2. Add 3 mL chloroform/methanol and homogenize the suspension with an ultrasound homogenizer for 5 min at healthy room temperature.
3. Filter the homogenate through a fat-free filter and add 0.6 mL 0.05 % H_2SO_4 to the filtrate to separate phases.
4. Pipet the supernatant mainly consisting of methanol carefully and discard it (*see* **Note 6**).
5. Dry the remaining phase containing triglycerides overnight at 32 °C (*see* **Note 7**).
6. Solve the pellet in 0.3 mL 0.9 % NaCl for 20 min at 45 °C.
7. Measure the triglycerides following the instructions of the Triglyceride FS* test kit.

3.2.3 Histology

1. Use the descending graded alcohol series to deparaffinize the liver tissue; run each ethanol step for 2 min.
2. For hemalum-eosin staining, incubate the slices for 30 s in Mayer's hemalum, followed by 10 min bluing in tap water. Incubate the slices for 5 min in eosin Y solution 0.5 % aqueous. Use the ascending graded alcohol series to dehydrate the slices. Perform the steps quickly until incubation in 96 % ethanol, followed by 2 min incubation for subsequent steps (*see* **Note 8**).
3. For the Sirius red staining incubate the slices for 60 min in direct red solution. Briefly rinse with 0.5 % acetic acid and perform the ascending graded alcohol series.
4. Slices may be embedded with the water-free mounting medium Entellan.
5. For the detection of collagen type I, slices stained with Sirius red may be analyzed using a polarization microscope. For visualization follow the instructions of the microscope manufacturer.

4 Notes

1. Feeding the MCD-diet causes body weight reduction (27.43 % ± 1.46) after 5 weeks of application, an increase in liver triglycerides, and a decrease of blood triglycerides.
2. An interruption of MCD-diet feeding or the change to sole standard diet during the experiments would implicate a complete reversion of the clinical picture of nonalcoholic steatohepatitis. Body weight and, e.g., liver triglyceride content will normalize and liver histology will hardly show any abnormality.
3. MCD-diet application for more than 5 weeks still shows a distinctive picture of NASH, but cell transplantation is not possible because of the massive body weight loss and resulting lethal handling stress.
4. The model creates NASH similar to the human situation, but it is limited because of the reduction of the body weight, adipose tissue, and insulin sensitivity, which is different in human beings. Thus, the model does not display the human pathology one to one.
5. Avoid lysis of erythrocytes during the procedure. Hemolytic serum sophisticates alanine aminotransferase (ALT) pretending higher activity.
6. Be careful pipetting methanol phase; avoid dropping. Dropping leads to intermixing of the phases and the experiment can be canceled.

7. Dry the pellets thoroughly; avoid chloroform residuum. Chloroform may damage measuring equipment made of plastics.
8. The ascending graded ethanol series needs to be performed quickly until incubation in 96 % ethanol. Otherwise the eosin stain will be washed out.

Acknowledgement

This work was supported by funding from the German Research Foundation (Ch 109/15-2) as well as the German Federal Ministry of Education and Research (BMBF, PtJ-Bio, 0315883). The careful assistance of Madlen Hempel and Antje Thonig is greatly acknowledged.

References

1. G.d.B. (2013) K70-K77 Krankheiten der Leber; Diagnosedaten der Krankenhäuser ab 2000 (Fälle/Sterbefälle, Fälle je 100000 Einwohner (altersstandardisiert), Berechnungs- und Belegungstage, durchschnittliche Verweildauer). Gliederungsmerkmale: Jahre, Wohnsitz, Alter, Geschlecht, Verweildauer, ICD10, Art der Standardisierung (04.12.2013). http://www.gbe-bund.de
2. Day CP (2012) Clinical spectrum and therapy of non-alcoholic steatohepatitis. Dig Dis 30(Suppl 1):69–73
3. Yu J, Shen J, Sun TT, Zhang X, Wong N (2013) Obesity, insulin resistance, NASH and hepatocellular carcinoma. Semin Cancer Biol 23:483–491
4. Pelz S, Stock P, Bruckner S, Christ B (2012) A methionine-choline-deficient diet elicits NASH in the immunodeficient mouse featuring a model for hepatic cell transplantation. Exp Cell Res 318:276–287
5. Agopian VG, Kaldas FM, Hong JC, Whittaker M, Holt C, Rana A, Zarrinpar A, Petrowsky H, Farmer D, Yersiz H, Xia V, Hiatt JR, Busuttil RW (2012) Liver transplantation for nonalcoholic steatohepatitis: the new epidemic. Ann Surg 256:624–633
6. Aurich I, Mueller LP, Aurich H, Luetzkendorf J, Tisljar K, Dollinger MM, Schormann W, Walldorf J, Hengstler JG, Fleig WE, Christ B (2007) Functional integration of hepatocytes derived from human mesenchymal stem cells into mouse livers. Gut 56:405–415
7. Stock P, Bruckner S, Ebensing S, Hempel M, Dollinger MM, Christ B (2010) The generation of hepatocytes from mesenchymal stem cells and engraftment into murine liver. Nat Protoc 5: 617–627

Chapter 6

The In Vivo Evaluation of the Therapeutic Potential of Human Adipose Tissue-Derived Mesenchymal Stem Cells for Acute Liver Disease

Takeshi Katsuda, Hayato Kurata, Rie Tamai, Agnieszka Banas, Tsuyoshi Ishii, Shumpei Ishikawa, and Takahiro Ochiya

Abstract

Mesenchymal stem cells (MSCs) have emerged as an attractive candidate for cell therapy applications. In the prior decade, many animal studies have demonstrated that MSCs are therapeutically beneficial for the treatment of liver disease. The carbon tetrachloride (CCl_4)-induced acute hepatitis model has been the most widely used model in these studies. Our group has utilized the CCl_4-induced mouse hepatitis model to study the therapeutic potential of human adipose tissue-derived MSCs (hADSCs). We have demonstrated that systemically administered hADSCs engrafted into the damaged liver and promoted tissue repair. This phenomenon likely reflected the paracrine effects of the administered hADSCs. In this chapter, we describe a method to evaluate the therapeutic efficacy of the systemic administration of hADSCs in the CCl_4-induced mouse model of acute hepatitis.

Key words Acute hepatitis, Carbon tetrachloride (CCl_4), Mesenchymal stem cell (MSC), Adipose-tissue derived MSC (ADSC), Intravenous transplantation

1 Introduction

Mesenchymal stem cell (MSC) transplantation has attracted a great deal of attention as a novel therapeutic option for liver diseases. At present, the only treatment for serious liver diseases is liver transplantation, and the application of this treatment has been limited by the shortage of donors. To compensate for this donor shortage, researchers have intensively studied hepatocyte transplantation as a potential treatment approach. However, the hepatocyte transplantation procedure is hampered by the low liver engraftment rate of transplanted hepatocytes and the low availability of transplantable hepatocytes [1]. Moreover, recent studies have not only examined approaches in which MSCs are used to repopulate a damaged liver, but also demonstrated that MSCs act via paracrine

Bruno Christ et al. (eds.), *Animal Models for Stem Cell Therapy*, Methods in Molecular Biology, vol. 1213,
DOI 10.1007/978-1-4939-1453-1_6,

effects that significantly contribute to tissue repair in injured livers [2]. MSCs can be isolated from various adult connective tissues, including bone marrow and adipose tissues, the placenta, amniotic fluid, and umbilical cord blood [3, 4]. MSCs initially attracted research interest due to their ability to differentiate into cells of the mesodermal lineage. However, in recent years, greater attention has been devoted to exploring their capacity to secrete cytokines and growth factors [2, 5–7]. To date, numerous animal studies have demonstrated that MSCs are therapeutically beneficial for the treatment of liver diseases.

Several animal models for acute liver disease have been proposed, and these models have provided a great deal of insight with respect to evaluating the therapeutic efficacy of MSCs for these diseases. The most widely used model of acute liver disease is the carbon tetrachloride (CCl_4) treatment model [8–13]. In this model, hepatitis is induced by reactive metabolic trichloromethyl radicals ($\cdot CCl_3$) and peroxytrichloromethyl radicals ($\cdot OOCCl_3$), which are mainly metabolized from CCl_4 by cytochrome P450 2E1 (CYP2E1) [14]. Because CYP2E1 is preferentially localized in the pericentral zone of the liver acinus, the main sites of liver injury in the CCl_4-induced model are these pericentral regions. Similarly, acetaminophen (AAP) can also be used to generate an acute hepatitis model in rodents [15]. An overdose of AAP results in the generation of *N*-acetyl-*p*-benzoquinoneimine by CYP2E1 [16] and thereby produces hepatocyte necrosis. In contrast, concanavalin A (ConA) causes acute hepatitis through an excessive auto-immune reaction induced by the overproduction of various cytokines, such as tumor necrosis factor-α and interferon-γ [17]. It has been reported that the immunosuppressive effects of MSCs can improve ConA-induced acute hepatitis [18, 19]. The co-administration of lipopolysaccharide, a component of gram-negative cell walls, and D-galactosamine, another hepatotoxin, has also been used for the induction of acute hepatitis in mice [20].

Using the CCl_4-induced hepatitis model, we have demonstrated that human adipose tissue-derived MSCs (hADSCs) significantly contribute to tissue repair in acute hepatitis. Our research group has previously reported that hADSC-derived hepatocyte-like cells (hADSC-Heps) could be generated from hADSCs [9, 11] stimulated with growth factors that induce the differentiation of embryonic stem (ES) cells into hepatocyte-like cells [21]. Importantly, we confirmed that transplanted hADSC-Heps ameliorated liver injury in the CCl_4-induced mouse hepatitis model [9, 11]. Interestingly, however, we observed that in this model, undifferentiated hADSCs produced greater therapeutic effects than hADSC-Heps [10]. This finding has provided support for the notion that the therapeutic effects of hADSCs are mainly produced by the paracrine factors secreted by these cells rather than MSC

functions related to the repopulation of the liver mass. In this chapter, we describe a method to evaluate the therapeutic efficacy of the systemic administration of hADSCs in the CCl_4-induced acute hepatitis mouse model [10].

2 Materials

2.1 Animals

Six-week-old female BALB/c nude mice (CLEA Japan Inc., Tokyo, Japan) were used in this study (*see* **Note 1**).

2.2 Isolation and Culturing of hADSCs

1. 0.15 % type I collagenase in Dulbecco's phosphate-buffered saline without calcium and magnesium (PBS(−)) (*see* **Note 2**).
2. Sterilized surgical scissors.
3. Water bath equipped with a heating circulator.
4. Dulbecco's modified Eagle's medium (DMEM; high glucose, Invitrogen).
5. Fetal bovine serum (FBS).
6. 160 mM NH_4Cl.
7. 40 μm cell strainer (BD).
8. Hemocytometer.
9. MesenPRO RS™ Medium (Invitrogen).
10. Antibiotic-Antimycotic (Invitrogen).
11. GlutaMAX (Invitrogen).
12. CellBIND™ Surface 100 mm dish (Corning).

2.3 Routine Culturing of hADSCs

1. MesenPRO RS™ Medium (Invitrogen).
2. Antibiotic-Antimycotic (Invitrogen).
3. GlutaMAX (Invitrogen).
4. CellBIND™ Surface 100 mm dish (Corning).
5. Accutase.
6. PBS(−).

2.4 Systemic Administration of hADSCs in the CCl_4-Induced Mouse Model of Acute Liver Disease

1. Carbon tetrachloride (CCl_4).
2. Olive oil.
3. 26-G needle.
4. 1 mL syringe.
5. 27-G needle.
6. Mouse holder for intravenous injections.
7. 40 μm cell strainer.

2.5 Sampling of Serum and Liver Tissue

1. Isoflurane.
2. 24-G needle.
3. 1.5 mL tube.
4. PBS(−) containing 10 % formalin.

2.6 Histological Analyses of Mouse Liver Sections After Cell Transplantation

1. Hematoxylin.
2. Eosin.
3. Anti-human leukocyte antigen (HLA) class I antibody (clone W6/32; Sigma, 1:250).
4. Alexa Fluor 594 (Invitrogen).

3 Methods

3.1 Isolation and Culturing of hADSCs

This portion of the methods section is based on a protocol that was previously published by our laboratory [22].

1. Use surgical scissors to mince adipose tissue into pieces that are less than 3 mm in size. Collect these tissue pieces into a tube, add an equal volume of PBS(−), and mix vigorously at room temperature.
2. Let the mixture stand at room temperature until it separates into two phases.
3. Collect the upper phase, which contains stem cells, adipocytes, blood, and PBS(−), into a new tube, and wash this phase three times with fresh PBS(−). Discard the lower phase.
4. Add an equal volume of PBS(−) containing 0.15 % type I collagenase (thus achieving a final collagenase concentration of 0.075 %), and shake the resulting mixture for 30 min in a 37 °C water bath.
5. Add an equal volume of DMEM containing 10 % FBS, shake the resulting mixture well, and allow this mixture to incubate for 10 min. The mixture will separate into two phases during this incubation.
6. Discard the upper phase. Centrifuge the lower phase at 280 × *g* for 5 min at room temperature.
7. Resuspend the cellular pellet in 5 mL of 160 mM NH_4Cl over the course of 3 min. Filter the resulting mixture through a 40 μm cell strainer into a new tube containing 5 mL DMEM with 10 % FBS.
8. Centrifuge at 280 × *g* for 5 min at room temperature.
9. Dissolve the cell pellet in MesenPRO RS™ complete medium (*see* **Note 3**), and seed the cells onto CellBIND™ Surface 100 mm dishes at 1.0–5.0 × 10^4 cells/cm^2 (*see* **Note 4**).

3.2 Routine Culturing of hADSCs

When cells reach 70–90 % confluence, passage them as follows.

1. Wash the cells twice in PBS(−).
2. Add 1 mL accutase to each 100 mm dish. Incubate each dish for 5 min at 37 °C.
3. Tap the dish, use 5 mL/dish of MesenPRO RS™ complete medium to collect cells into a tube, and centrifuge cells at $220 \times g$ for 5 min at room temperature.
4. Resuspend the cells in MesenPRO RS™ complete medium, count the cell number, and seed the cells into new CellBIND™ dishes at a concentration of 5×10^3 cells/cm^2.

3.3 Intravenous Administration of hADSCs in the CCl_4-Induced Mouse Model of Acute Liver Disease

1. To ensure the acquisition of sufficient numbers of cells, plate hADSCs 2–5 days prior to the intravenous injection of these cells into mice.
2. Prepare diluted CCl_4 solution by mixing one volume CCl_4 with nine volumes olive oil.
3. Intraperitoneally inject mice with 100 μL diluted CCl_4 solution/20 g body weight (10 μL CCl_4/20 g body weight).
4. To establish a sham operation, intraperitoneally inject mice with 100 μL olive oil/20 g body weight.
5. Twenty-four hours after CCl_4 injection, perform the intravenous injection of hADSCs as follows.
6. Wash the cells twice in PBS(−).
7. Add 1 mL accutase per 100 mm dish, and incubate dishes at 37 °C for 5 min.
8. After tapping the dishes, use 5 mL/dish of MesenPRO RS™ complete medium to collect cells into a tube.
9. Remove cell aggregates by filtering the cell suspension through a 40 μm cell strainer into a new tube.
10. Centrifuge the cells at $220 \times g$ for 5 min at room temperature.
11. Resuspend these cells in 0.5–1 mL PBS(−), and count the number of cells obtained.
12. Use PBS(−) to dilute the cell suspension to 7.5×10^6 cells/mL, and store the suspension on ice until it is injected into mice (*see* **Note 5**).
13. Load the hADSC suspension into a 1 mL syringe and equip this syringe with a 27-G needle (*see* **Note 6**).
14. Slowly inject 200 μL ADSC suspension/mouse (1.5×10^6 cells/mouse) into the tail veins of the mice (*see* **Notes 7** and **8**).

3.4 Blood and Tissue Sampling

1. Use isoflurane to anesthetize mice 24 h after the injection of hADSCs.
2. Open the chest of each mouse with surgical scissors to expose the heart.

3. Insert a syringe with a 24-G needle into the left ventricle. Slowly collect blood into the syringe (*see* **Note 9**).
4. After collecting this blood sample, extract the liver of the mouse. Wash the liver once in PBS(−), and fix the extracted liver by soaking it in 10 % formalin.
5. Collect blood into a 1.5 mL tube and incubate this tube at room temperature for 30 min.
6. Incubate the tube at 4 °C for 1 h.
7. Centrifuge the tube at 2,200 × *g* for 20 min at 4 °C.
8. Transfer the supernatant into a new tube.
9. Centrifuge this tube at 2,200 × *g* for 5 min at 4 °C.
10. Carefully collect the supernatant (serum) and transfer it into a new tube (*see* **Note 10**).
11. Use serum samples for blood tests, or store these samples at −20 °C until use (*see* **Note 11**).

3.5 Histological Analyses of Liver Tissue

1. Fix the collected liver tissue in PBS(−) containing 10 % formalin, and prepare a paraffin block. Use a general sectioning procedure to obtain 3–5 μm sections.
2. Utilize a generally accepted procedure to perform hematoxylin and eosin (HE) staining (*see* **Note 12**).
3. To detect human hADSCs in the livers of immunodeficient mice, perform immunofluorescent staining of mouse liver tissue using an anti-HLA-1 antibody (*see* **Note 13**).

4 Notes

1. Animals are maintained in an isolator unit at a constant temperature of 20 °C and subjected to a 12 h light–dark cycle. Mice receive a standard sterilized diet and water ad libitum. All experiments were performed in accordance with national laws and institutional regulations.
2. Dissolve 0.015 g collagenase in 10 mL PBS(−) by layering the powder on the surface of the liquid to avoid clumping. After the powder has completely dissolved, sterilize the solution by filtration through a 0.22 μm filter.
3. Prepare MesenPRO RS™ complete medium by supplementing 500 mL of basal medium with 10 mL growth supplement, 5 mL Antibiotic-Antimycotic, and 5 mL GlutaMAX.
4. The cells exhibit a spindle-shaped morphology that is characteristic of MSCs (Fig. 1a) and express CD105 (endoglin) (Fig. 1b). CD105, which is a component of the receptor complex of transforming growth factor (TGF)-β, is involved in various cellular

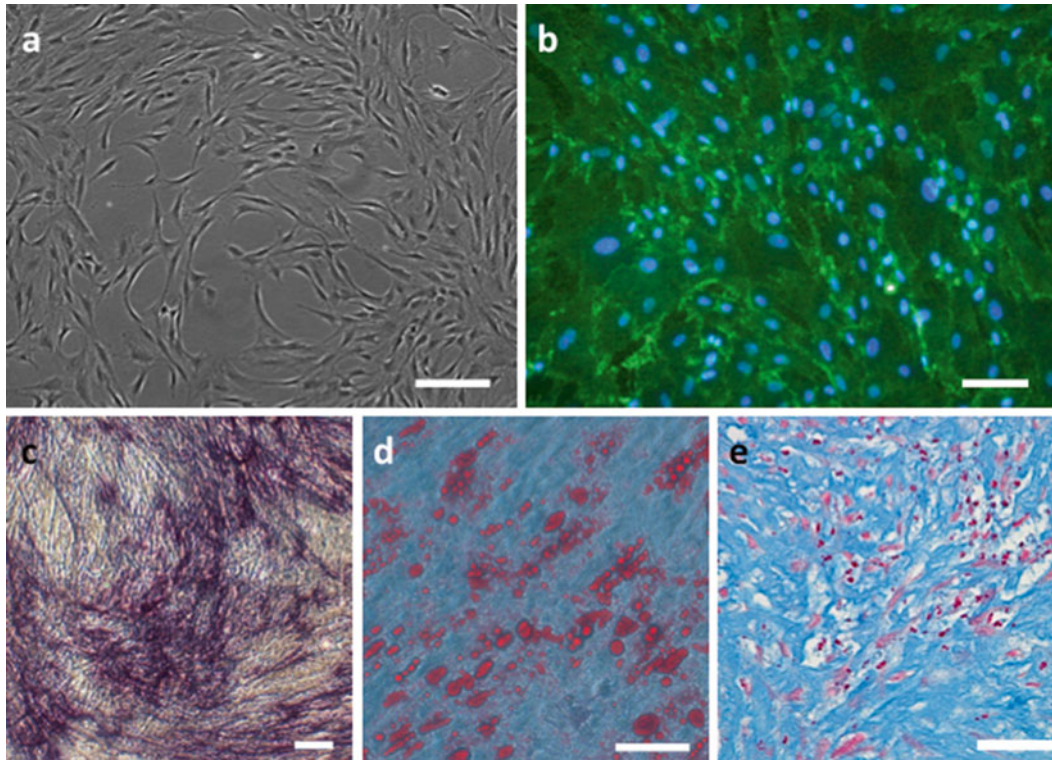

Fig. 1 Characterization of isolated hADSCs. (**a**) Phase contrast images of isolated hADSCs indicate the spindle-shaped morphology of these cells, which is a characteristic feature of MSCs. Scale bar: 200 μm. (**b**) hADSCs are positive for CD105 (*green*), an important molecule for maintaining MSC characteristics [9]. Nuclei are counterstained with Hoechst 33342 (*blue*). Scale bar: 100 μm. (**c**) Alkaline phosphatase staining reveals the osteogenic differentiation of hADSCs. Scale bar: 100 μm. (**d**) Oil red O staining reveals the adipogenic differentiation of hADSCs. Scale bar: 100 μm. (**e**) Alcian blue staining reveals the chondrogenic differentiation of hADSCs. Scale bar: 50 μm

events, including proliferation, differentiation and migration. The cultured cells are also multipotent. In particular, these cells can differentiate into adipocytes, osteoblasts, and chondrocytes (Fig. 1c–e). In accordance with the manufacturer's instructions the following commercial kits are used for the differentiation of hADSCs into three mesodermal lineages: hMSC Mesenchymal Stem Cell Adipogenic Differentiation Medium (Lonza), hMSC Mesenchymal Stem Cell Chondrocyte Differentiation Medium (Lonza), and hMSC Mesenchymal Stem Cell Osteogenic Differentiation Medium (Lonza). Surface marker characterization by flow cytometry indicates that these cells are positive for CD105, CD73, CD90, and CD44 but negative for CD45, CD31, and CD34 [23].

5. hADSCs are likely to aggregate at room temperature. This aggregation may cause pulmonary embolisms in mice injected with these cells.

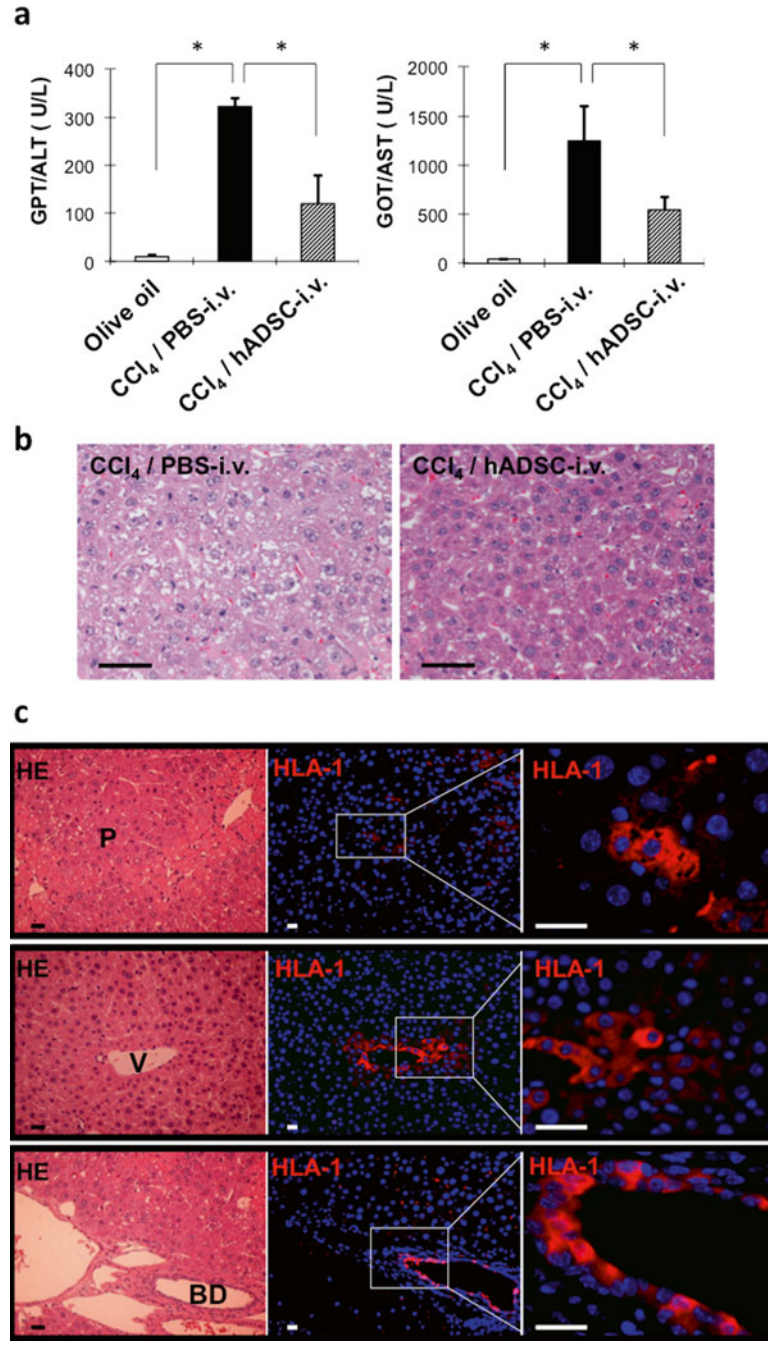

Fig. 2 Therapeutic efficacy of systemically transplanted hADSCs in the CCl4-induced acute hepatitis mouse model. (**a**) Biochemical analysis of mouse blood serum samples for the liver injury markers GPT/ALT (*left*) and GOT/AST (*right*). Immunodeficient mice received an intraperitoneal injection of either olive oil (a control for the CCl_4 injection) or 10 μL CCl_4/20 g body weight. At 24 h after this injection, the CCl_4-injected mice received an intravenous injection of either PBS(–) (a control for hADSC administration) or 1.5×10^6 hADSCs/mouse. Data are expressed as means ± S.D. and subjected to analysis using the Bonferroni

6. When loading cells into a 1 mL syringe, thoroughly mix the cell suspension by pipetting because the cells will tend to fall to the bottom wall of the tube. Do not attach a needle to the syringe prior to loading the cells because the use of a syringe with an attached needle may damage the cells.
7. In our experience, a tail vein injection of more than 2×10^6 cells/mouse is associated with an increased risk of pulmonary embolism.
8. If more than 5 min are required to complete an injection, reloading of the cell suspension is recommended to avoid precipitation of cells.
9. Rapid drawing of the syringe may cause hemolysis.
10. Leave a small portion of the supernatant in the tube to ensure that the serum samples are not contaminated by the pellet.
11. In our laboratory, we use the DRI-CHEM system (Fuji) to measure blood markers of liver injury, such as serum levels of GPT/ALT, GOT/AST, ammonia, uric acid, and blood urea nitrogen. We have observed significant improvement in liver injury markers, particularly with respect to GPT/ALT and GOT/AST levels (Fig. 2a).
12. This staining reveals that hADSC administration produces significant morphological changes in hepatocytes in non-necrotic regions (Fig. 2b). Relative to injured livers from control mice, injured livers from mice that received hADSCs exhibit lower levels of vacuolar degeneration caused by the dilatation of mitochondria and the rough endoplasmic reticulum.
13. We detected hADSCs within the injured mouse liver 24 h after these cells were injected into the mice. HLA-1 positive cells were found in various areas of the examined mouse livers, including the parenchyma, vessels, and bile ducts (Fig. 2c).

Fig. 2 (continued) correction; $n = 3$. (*$p < 0.05$). (**b**) Histological analysis of CCl_4-injured liver sections. This figure presents HE-stained images of mouse livers 24 h after an intravenous injection of either PBS(–) (*left*) or 1.5×10^6 hADSCs/mouse (*right*). These mice received an intraperitoneal injection of CCl_4 24 h prior to the administration of hADSCs. Scale bars: 100 μm. (**c**) Immunohistochemical analyses for human leukocyte antigen 1 (HLA-1)-positive cells in mouse liver sections after the administration of hADSCs. HLA-1-positive cells are present in different areas of the liver, including the parenchyma (P), vessels (V), and bile duct (BD). The left side of this figure presents the results of HE staining for these areas of the examined liver sections. Scale bars: 500 μm. This figure is reproduced from ref. 10

Acknowledgements

We would like to thank Dr. Nobuyoshi Kosaka for his valuable advice. This work was supported in part by a Grant-in-Aid for the Third-Term Comprehensive 10-Year Strategy for Cancer Control, a Grant-in-Aid for Scientific Research on Priority Areas Cancer from the Ministry of Education, Culture, Sports, Science, and Technology, and the Program for Promotion of Fundamental Studies in Health Sciences of the National Institute of Biomedical Innovation (NiBio), and the Japan Society for the Promotion of Science (JSPS) through the "Funding Program for World-Leading Innovative R&D on Science and Technology (FIRST Program)" initiated by the Council for Science and Technology Policy (CSTP), and Grant-in-Aid for Scientific Research on Innovative Areas ("functional machinery for non-coding RNAs") from the Japanese Ministry of Education, Culture, Sports, Science, and Technology.

References

1. Weber A, Groyer-Picard MT, Franco D et al (2009) Hepatocyte transplantation in animal models. Liver Transpl 15:7–14
2. Ochiya T, Yamamoto Y, Banas A (2010) Commitment of stem cells into functional hepatocytes. Differentiation 79:65–73
3. Chamberlain G, Fox J, Ashton B et al (2007) Concise review: mesenchymal stem cells: their phenotype, differentiation capacity, immunological features, and potential for homing. Stem Cells 25:2739–2749
4. Banas A, Yamamoto Y, Teratani T et al (2007) Stem cell plasticity: learning from hepatogenic differentiation strategies. Dev Dyn 236: 3228–3241
5. Salem HK, Thiemermann C (2010) Mesenchymal stromal cells: current understanding and clinical status. Stem Cells 28:585–596
6. Djouad F, Bouffi C, Ghannam S et al (2009) Mesenchymal stem cells: innovative therapeutic tools for rheumatic diseases. Nat Rev Rheumatol 5:392–399
7. Uccelli A, Laroni A, Freedman MS (2011) Mesenchymal stem cells for the treatment of multiple sclerosis and other neurological diseases. Lancet Neurol 10:649–656
8. Seo MJ, Suh SY, Bae YC et al (2005) Differentiation of human adipose stromal cells into hepatic lineage in vitro and in vivo. Biochem Biophys Res Commun 328:258–264
9. Banas A, Teratani T, Yamamoto Y et al (2007) Adipose tissue-derived mesenchymal stem cells as a source of human hepatocytes. Hepatology 46:219–228
10. Banas A, Teratani T, Yamamoto Y et al (2008) IFATS collection: in vivo therapeutic potential of human adipose tissue mesenchymal stem cells after transplantation into mice with liver injury. Stem Cells 26:2705–2712
11. Banas A, Teratani T, Yamamoto Y et al (2009) Rapid hepatic fate specification of adipose-derived stem cells and their therapeutic potential for liver failure. J Gastroenterol Hepatol 24:70–77
12. Kuo TK, Hung SP, Chuang CH et al (2008) Stem cell therapy for liver disease: parameters governing the success of using bone marrow mesenchymal stem cells. Gastroenterology 134:2111–2121
13. Zhang S, Chen L, Liu T et al (2012) Human umbilical cord matrix stem cells efficiently rescue acute liver failure through paracrine effects rather than hepatic differentiation. Tissue Eng Part A 18:1352–1364
14. Weber LWD, Boll M, Stampfl A (2003) Hepatotoxicity and mechanism of action of haloalkanes: carbon tetrachloride as a toxicological model. Crit Rev Toxicol 33:105–136
15. Salomone F, Barbagallo I, Puzzo L et al (2013) Efficacy of adipose tissue-mesenchymal stem cell transplantation in rats with acetaminophen liver injury. Stem Cell Res 11:1037–1044
16. Gonzalez FJ (2007) The 2006 Bernard B. Brodie Award lecture. Cyp2e1. Drug Metab Dispos 35:1–8

17. Dong Z, Wei H, Sun R et al (2007) The roles of innate immune cells in liver injury and regeneration. Cell Mol Immunol 4:241–252
18. Kubo N, Narumi S, Kijima H et al (2012) Efficacy of adipose tissue-derived mesenchymal stem cells for fulminant hepatitis in mice induced by concanavalin A. J Gastroenterol Hepatol 27:165–172
19. Higashimoto M, Sakai Y, Takamura M et al (2013) Adipose tissue derived stromal stem cell therapy in murine ConA-derived hepatitis is dependent on myeloid-lineage and CD4+ T-cell suppression. Eur J Immunol 43: 2956–2968
20. Yu J, Cao H, Yang J et al (2012) In vivo hepatic differentiation of mesenchymal stem cells from human umbilical cord blood after transplantation into mice with liver injury. Biochem Biophys Res Commun 422:539–545
21. Teratani T, Yamamoto H, Aoyagi K et al (2005) Direct hepatic fate specification from mouse embryonic stem cells. Hepatology 41: 836–846
22. Banas A (2012) Purification of adipose tissue mesenchymal stem cells and differentiation toward hepatic-like cells. Methods Mol Biol 826:61–72
23. Katsuda T, Tsuchiya R, Kosaka N et al (2013) Human adipose tissue-derived mesenchymal stem cells secrete functional neprilysin-bound exosomes. Sci Rep 3:1197. doi:10.1038/srep01197

Chapter 7

A Mouse Model of Liver Injury to Evaluate Paracrine and Endocrine Effects of Bone Marrow Mesenchymal Stem Cells

Chiung-Kuei Huang, Soo Ok Lee, Jie Luo, RongHao Wang, Qiang Dang, and Chawnshang Chang

Abstract

Liver fibrosis is the result of chronic liver disease, which is caused by sustaining multiple damage or injury to the liver. While the liver continues to receive injuries, it suffers from the wound healing process and this eventually leads to the derangement of the liver architecture. Recently, bone marrow-derived mesenchymal stem cells (BM-MSCs) have been suggested to have therapeutic effects in treating liver fibrosis. Here, we describe the isolation, purification, culture, and transplantation of BM-MSCs in the liver fibrosis mouse model, and the assessment of paracrine and endocrine (including androgens and/or estrogens) effects of BM-MSCs in the in vitro cell culture system.

Key words Liver fibrosis, Bone marrow mesenchymal stem cells, Transplantation, Androgen receptor, Paracrine or endocrine effects

1 Introduction

Liver fibrosis is the result of chronic liver disease and will eventually become liver cirrhosis [1]. Current treatment for liver cirrhosis is to prevent further damage to the liver with medication [2, 3]. The gold standard treatment for the liver cirrhosis is liver transplantation [4]. However, cirrhotic patients barely have a chance to wait for a liver match for transplantation before death. Therefore, scientists have tried to develop alternative approaches to treat liver cirrhosis. Since hepatocyte apoptosis and loss of hepatocyte functions are the major reasons to cause the consequential death threats for humans, researchers have aimed to determine the functionality of hepatocytes that can be used for transplantation in order to restore liver function. Currently, there are several proposed potential cell types for transplantation therapy in treating liver cirrhosis, including hepatocytes, endothelial progenitor cells, embryonic stem cells,

Bruno Christ et al. (eds.), *Animal Models for Stem Cell Therapy*, Methods in Molecular Biology, vol. 1213,
DOI 10.1007/978-1-4939-1453-1_7,

and bone marrow mesenchymal stem cells (BM-MSCs) [5–10]. Among those proposed cell types, BM-MSCs have been extensively studied recently in preclinical mouse models and human clinical trials [11–16]. Although it has been shown that BM-MSCs exert their therapeutic effects through direct differentiation to replace malfunctioning hepatocytes [17], accumulating evidence indicates that the cytokines and chemokines secreted by BM-MSCs might be the major factors to restore the function of a damaged liver [18–20]. Similar observations have also been shown in other diseases, which adopted BM-MSCs transplantation therapy, including myocardial infarction, lung fibrosis, and sepsis [21–23]. Therefore, developing an in vivo mouse model to evaluate the therapeutic effects of BM-MSCs transplantation through examining their paracrine or endocrine (including androgens and/or estrogens) modulation was needed to study the optimal therapeutic value of BM-MSCs transplantation. Herein, this chapter describes a mouse model of liver injury to evaluate the paracrine and endocrine effects of BM-MSCs.

2 Materials

Prepare all solutions with distilled deionized water (ddH_2O). The ddH_2O is prepared with a MilliQ water purification system and the deionized water attains the sensitivity of 18.2 MΩ cm at room temperature. Store all prepared solutions at 4 °C unless mentioned otherwise below. All waste must be disposed following the Laboratory Biosafety Manual according to the World Health Organization.

2.1 Liver Fibrosis Mouse Model

1. Carbon tetrachloride (CCl_4).
2. Olive oil.
3. Experimental mouse at the age of 8 weeks.
4. Thioacetamide (TAA) solution (Sigma-Aldrich): 300 mg/L in drinking water.
5. Sodium pentobarbital.
6. Surgical scissors and forceps.
7. Dulbecco's Phosphate-Buffered Saline (DPBS) buffer.
8. 4 % paraformaldehyde stored at −80 °C.

2.2 Isolation of BM-MSCs and BM-MSCs Transplantation

1. BM-MSCs cell culture medium: 15 % fetal bovine serum, 2 mM L-glutamine, 1 % Penicillin–Streptomycin (10,000 U penicillin, 10,000 μg streptomycin), 1 % nonessential amino acids, 10 mM HEPES buffer in Dulbecco's Modified Eagle Medium (DMEM).

2. BM-MSCs isolation medium: 10 % fetal bovine serum, 2 mM L-glutamine, 1 % Penicillin–Streptomycin, 1 % nonessential amino acids, 10 mM HEPES buffer in Dulbecco's Modified Eagle Medium (DMEM).
3. RIPA protein lysis buffer: 5 mL 1 M Tris–HCl/pH 7.4, 30 mL 5 M NaCl, 5 mL 20 % NP-40, 5 mL 10 % sodium deoxycholate, 0.5 mL 20 % SDS, 50 mL ddH_2O.
4. 5 mL syringes and 23G needle.
5. 70 μm cell strainers.
6. 50 mL centrifuge tubes.
7. Sterile pipettes.
8. DPBS.
9. 100 mm tissue culture dishes.
10. Surgical scissors and forceps.
11. Experimental mouse expressing green fluorescenc protein (GFP) at the age of 8 weeks.
12. 75 % alcohol.
13. 0.25 % trypsin–EDTA solution.
14. 0.4 % trypan blue solution.
15. Proteinase inhibitor cocktail (Roche). Store at −20 °C.

2.3 Evaluation of Paracrine Effects of BM-MSCs

1. Sterile 6.5 mm Transwell® (Corning) with 8.0 μm pore size polyester membrane inserts.
2. Hepatic stellate cells (HSCs) culture medium: 10 % fetal bovine serum, 2 mM L-glutamine, 1 % Penicillin–Streptomycin in DMEM.
3. Mouse inflammatory cytokine antibody array (R&D Systems).
4. Inflammatory cell lines, such as Raw 264.7 (ATCC).
5. Isolated primary macrophages.
6. Red blood cell (RBC) lysis buffer: 0.8 % NH_4Cl, 0.1 mM EDTA in ddH_2O, 20 ng/mL mouse recombinant granulocyte macrophage colony-stimulating factor (GM-CSF) protein.
7. Hepatic stellate cell lines, such as LX2 and HSC-T6 (*see* **Note 1**), isolated primary hepatic stellate cells (HSCs *see* **Note 2**) [24].
8. Collagenase.
9. Giemsa stain stock solution.
10. Methanol.
11. Cotton swabs.

3 Methods

3.1 Liver Fibrosis Mouse Model I

1. Breed/purchase mice and use at the age of 8 weeks (*see* **Note 3**).
2. Mix CCl_4 with olive oil at the ratio of 1:1 and use the mixed solution within 30 min.
3. Administer mixed CCl_4 solution by intraperitoneal (IP) injection at a dose of 1 mL/kg mouse body weight twice per week.
4. Continue injecting mice with CCl_4 for 8 weeks (*see* **Note 4**).
5. Euthanize mice at 16 weeks with sodium pentobarbital at a dose of ≥100 mg/kg mouse body weight.
6. Collect mouse blood from cardiac puncture (*see* **Note 5**).
7. Use venous blood collection tubes to separate serum following the instruction manual (*see* **Note 6**).
8. Open mouse abdominal cavity.
9. Perfuse liver tissue with DPBS buffer.
10. Dissect liver tissue with surgical forceps and scissors.
11. Fix liver tissue with 4 % paraformaldehyde for 72 h.
12. Freeze liver tissue with liquid nitrogen or dry ice for cytokine analysis (*see* **Note 7**).

3.2 Liver Fibrosis Mouse Model II

1. Breed/purchase mice and use at the age of 8 weeks (*see* **Note 3**).
2. Prepare TAA solution (0.3 % TAA) in sterile drinking water.
3. Give mice free access to the TAA solution in drinking water for a total of 8 weeks.
4. Euthanize mice at the age of 16 weeks with sodium pentobarbital at a dose of ≥100 mg/kg mouse body weight.
5. Collect blood from cardiac puncture (*see* **Note 5**).
6. Use venous blood collection tubes to separate serum following the instruction manual (*see* **Note 6**).
7. Open mouse abdominal cavity.
8. Perfuse liver tissue with DPBS buffer.
9. Dissect liver tissue with surgical forceps and scissors.
10. Fix liver tissue with 4 % paraformaldehyde for 72 h.
11. Freeze liver tissue with liquid nitrogen or dry ice for cytokine analysis (*see* **Note 7**).

3.3 BM-MSCs Isolation and Transplantation

1. Breed mice that ubiquitously express GFP and allow to reach the age of 8 weeks.
2. Euthanize mice with sodium pentobarbital at dose of ≥100 mg/kg mouse body weight (*see* **Note 8**).
3. Use 75 % alcohol to clean the mouse body.

4. Remove the skin from the lower part of the mouse body.
5. Remove legs from the mouse with forceps and scissors.
6. Dissect and remove remaining tissue from pelvic and femoral bones, and separate at knee joint.
7. Immerse the bones in DPBS on ice until next step.
8. Prepare the 5 mL syringe with the 23G needle and fill it with BM-MSCs isolation medium ready to flush the bone marrow out.
9. Cut both ends of the bones.
10. Flush the bone marrow out with the 5 mL syringe/23G needle filled with BM-MSC isolation media into 50 mL tubes.
11. Pipet up and down to dissociate the bone marrow to as many single cells as possible (*see* **Note 9**).
12. Filter BM-MSCs isolation media containing bone marrow through a 70 μm cell strainer to remove tissue debris (*see* **Note 10**).
13. Spin down the cell pellet at 1,000 × *g* for 5 min.
14. Discard the supernatant, resuspend the cell pellet in 10 mL BM-MSCs culture media and plate the cells in 100 mm treated tissue culture dishes.
15. Culture cells for 24 h.
16. Remove unattached cells by changing BM-MSCs culture media.
17. Culture cells for 21 days and change culture media every 2–3 days.
18. Trypsinize BM-MSCs with 1 mL trypsin solution for 5 min.
19. Neutralize trypsin with 5 mL BM-MSCs culture media and collect the cell suspension.
20. Centrifuge at 1,000 × *g* for 5 min to spin down the cell pellets.
21. Discard the supernatant and wash the cells with 5 mL DPBS.
22. Centrifuge at 1,000 × *g* for 5 min.
23. Discard the supernatant and resuspend cells in 1 mL DPBS.
24. Mix 50 μL of the cell suspension with 10 μL trypan blue solution, and let stand for 5 min.
25. Place 10 μL of the incubated cell–trypan blue mixture into a hemocytometer.
26. Under a microscope, count non-stained cells (viable cells cannot be penetrated by trypan blue, since the intact cell membrane is impermeable to the dye).
27. Calculate the cell density and adjust stock suspension to a density of 3×10^5 cells/mL.

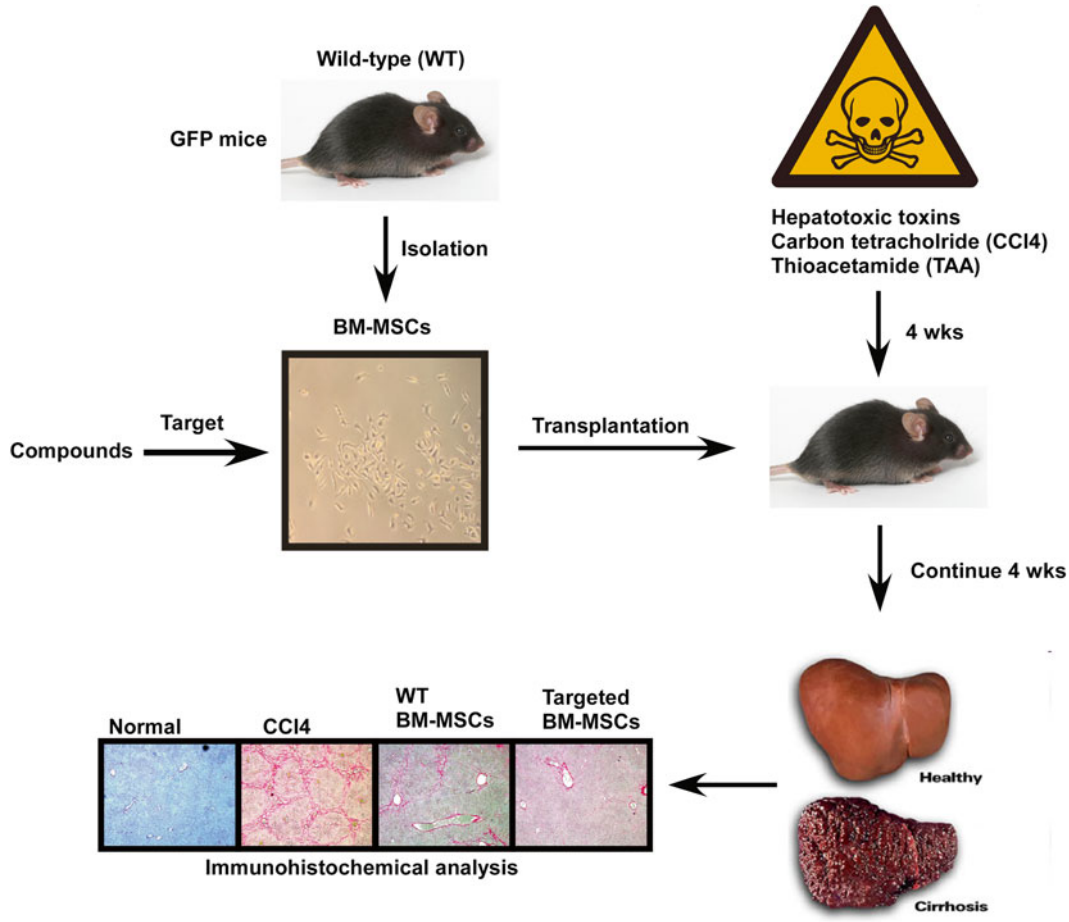

Fig. 1 Experimental flowchart development of the mouse liver fibrosis model and BM-MSCs transplantation time schedule

28. Inject 333 μL (10^5) of cells into the mouse via tail vein injection, after mice received the eighth injection of CCl_4 or after 4 weeks of TAA treatment (Fig. 1 for the experimental flowchart).
29. Continue CCl_4 or TAA treatment for another 4 weeks.
30. Euthanize mice at the age of 16 weeks with sodium pentobarbital at a dose of ≥100 mg/kg mouse body weight (*see* **Note 8**).
31. Collect blood from cardiac puncture (*see* **Note 5**).
32. Use venous blood collection tubes to separate serum following the instruction manual (*see* **Note 6**).
33. Open mouse abdominal cavity.
34. Perfuse liver tissue with DPBS buffer.
35. Dissect liver tissue with surgical forceps and scissors.
36. Fix liver tissue with 4 % paraformaldehyde for 72 h.
37. Freeze liver tissue with liquid nitrogen or dry ice for cytokine analysis (*see* **Note 7**).

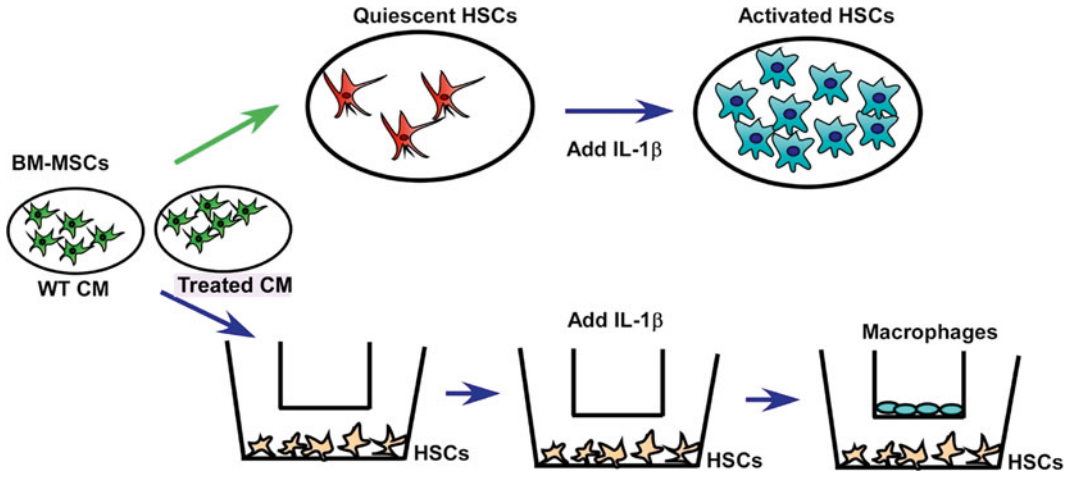

Fig. 2 Schematic representation of anti-inflammation and anti-fibrosis assays. Conditioned medium (CM) will be collected from cultured wild-type (WT) BM-MSCs and treated BM-MSCs. CM will be added to primary isolated hepatic stellate cells (HSCs) or established HSCs cell lines and incubated for 24 h. IL-1β will be used to activate HSCs either in HSCs activation or in macrophage migration assays

38. Homogenize liver tissues from normal, CCl_4- or TAA-treated, CCl_4- or TAA-treated plus wild-type (WT) BM-MSCs transplantation, and CCl_4- or TAA-treated plus manipulated BM-MSCs (*see* **Note 11**) transplantation mice in 500 μL RIPA buffer containing proteinase inhibitor cocktail (*see* **Note 12**).
39. Measure the protein concentrations and load equal total protein amounts to perform mouse inflammatory cytokine array according to the instruction manual (*see* **Note 13**).
40. Compare the array results among the four different groups to pick up candidate cytokines for the anti-inflammation and anti-fibrosis assay (*see* **Note 14**).

3.4 Macrophage Migration

1. On day 0, seed 2×10^4 HSCs in the lower chamber and 2×10^6 BM-MSCs in 12-well plates (*see* **Note 15** and Fig. 2 for experimental settings).
2. On day 1, treat BM-MSCs with vehicle or compounds to target BM-MSCs, and treat HSCs with pro-inflammatory compounds, such as IL-1β and LPS, to induce chemoattractant protein expression.
3. On day 2, collect conditioned media (CM) from BM-MSCs and filter through 0.45 μm pore size filter (*see* **Note 16**).
4. Mix CM and culture medium for HSCs at a 1:1 ratio.
5. Use neutralizing antibodies identified in mouse inflammatory cytokine array to treat CM for 0, 2, and 4 h.
6. Treat the HSCs with the antibody-treated CM for 24 h (*see* **Note 17**).

7. On day 3, seed 2×10^5 macrophages onto the upper chamber of transwell plates (*see* **Note 18**).
8. On day 4, fix the migrated macrophages with methanol for 15 min.
9. Stain the cells with 10 % Giemsa stain for 15 min.
10. Use a cotton swab to clean the upper side of the membrane, and count only cells that migrated to the lower side (*see* **Note 19**).
11. Migrated immune cells can be used as an indication for the anti-inflammatory response.

3.5 Hepatic Stellate Cell Activation

1. Isolate and culture primary HSCs (*see* **Note 3**).
2. On day 0, seed 2×10^6 HSCs in a 10 cm cell culture dish and 2×10^6 BM-MSCs in a 12-well plate (Fig. 2 for the experimental settings).
3. On day 1, treat BM-MSCs with vehicle or compounds, which are used to test for the anti-fibrotic effects of BM-MSCs.
4. On day 2, collect CM from BM-MSCs and filter through a 0.45 μm pore size filter (*see* **Note 16**).
5. Mix CM and HSCs culture media at a 1:1 ratio.
6. Use neutralizing antibodies identified in the mouse inflammatory cytokine array to treat CM for 0, 2, and 4 h.
7. Treat HSCs with treated CM for 24 h.
8. On day 3, treat HSCs with IL-1β and TGFβ1 to activate HSCs.
9. Collect protein lysates from samples with RIPA buffer containing the proteinase cocktail.
10. Use the Western blot procedure to examine α-smooth muscle actin expression to determine the HSCs activation (*see* **Note 20**).
11. α-Smooth muscle actin can be used as HSCs activation marker, and therefore serve as an indicator of liver fibrosis.

4 Notes

1. The LX2 and HSC-T6 cells can be requested from Dr. Scott L. Friedman (Mount Sinai Hospital NY).
2. For the isolation of primary HSC, see reference [24].
3. When breeding mice, use pure genetic background mice to perform experiments, such as C57BL/6. Using pure genetic background mice to perform liver fibrosis studies will prevent huge variations caused by genetic background differences.
4. The location of the injection site should rotate between left and right sides of the abdomen, since the CCl_4 injection will render the skin difficult to penetrate.

5. For blood collection from cardiac puncture, blood should be collected immediately after mouse loses consciousness; otherwise blood will be difficult to aspirate.
6. Let blood stand in the venous collection tube for 30 min and then centrifuge for 30 min at 3,000 × *g*. Aspirate serum and store samples at −80 °C.
7. For long-term storage, the liver tissue should be stored at a temperature less than −75 °C, preferably at −150 °C.
8. Perform cervical dislocation to ensure complete euthanization.
9. After pipetting up and down to separate cells, the red clump should no longer be visible. If cell aggregates are present, continue pipetting until aggregates disappear.
10. In order to maximize the cell recovery rate, rinse the cell strainer with 2 mL of BM-MSCs culture medium before passing the cell suspension through the cell strainer.
11. The definition of manipulated BM-MSCs depends on study targets. Scientists can use compounds, medication, miRNA, or virus systems to deliver the target of interest to BM-MSCs and study therapeutic effects of manipulated BM-MSCs.
12. For assaying the phosphorylated protein, the phosphatase inhibitor must be added to the RIPA buffer.
13. In order to prevent variation, the protein concentration for each sample should be adjusted as close as possible. Do not prepare the total protein loading amount based on the measured protein concentration. Since the protein concentration measurement is calculated using the correlative correction curve, it is the relative but not absolute amount. The closer the protein concentrations are, the less variations will appear in the protein cytokine array.
14. The Quantity One software published by Bio-Rad Inc. is free to use for analyzing the protein array results in the basic mode.
15. The cell density should be adjusted dependent on primary culture of HSCs or HSCs cell lines.
16. Filtering CM through a 0.45 μm pore size filter will remove the remaining BM-MSCs in order to obtain pure CM.
17. For the migration assay, the volume of culture medium in the lower chamber should not be more than 600 μL.
18. For the migration assay, the seeding medium in the upper well must be 200–250 μL.
19. When cleaning the membrane, use cotton swab to gently wipe out the stained cells on the upper side taking care not to break the membrane or even make the membrane uneven causing variations when taking pictures.
20. For the detailed western blot procedure, reference the standard protocol [25].

References

1. Rubin E, Lieber CS (1974) Fatty liver, alcoholic hepatitis and cirrhosis produced by alcohol in primates. N Engl J Med 290:128–135
2. Losowsky MS, Davidson CS (1962) Current concepts in therapy. The treatment of cirrhosis of the liver. N Engl J Med 267:87–90
3. Kershenobich D, Vargas F, Garcia-Tsao G, Perez Tamayo R, Gent M, Rojkind M (1988) Colchicine in the treatment of cirrhosis of the liver. N Engl J Med 318:1709–1713
4. Mazzaferro V, Regalia E, Doci R, Andreola S, Pulvirenti A, Bozzetti F, Montalto F, Ammatuna M, Morabito A, Gennari L (1996) Liver transplantation for the treatment of small hepatocellular carcinomas in patients with cirrhosis. N Engl J Med 334:693–699
5. Cai J, Ito M, Nagata H, Westerman KA, Lafleur D, Chowdhury JR, Leboulch P, Fox IJ (2002) Treatment of liver failure in rats with end-stage cirrhosis by transplantation of immortalized hepatocytes. Hepatology 36:386–394
6. Nakamura T, Torimura T, Sakamoto M, Hashimoto O, Taniguchi E, Inoue K, Sakata R, Kumashiro R, Murohara T, Ueno T, Sata M (2007) Significance and therapeutic potential of endothelial progenitor cell transplantation in a cirrhotic liver rat model. Gastroenterology 133(91–107):e101
7. Oyagi S, Hirose M, Kojima M, Okuyama M, Kawase M, Nakamura T, Ohgushi H, Yagi K (2006) Therapeutic effect of transplanting HGF-treated bone marrow mesenchymal cells into CCl4-injured rats. J Hepatol 44:742–748
8. Kuo TK, Hung SP, Chuang CH, Chen CT, Shih YR, Fang SC, Yang VW, Lee OK (2008) Stem cell therapy for liver disease: parameters governing the success of using bone marrow mesenchymal stem cells. Gastroenterology 134:2111–2121, 2121 e2111–2113
9. Huang CK, Lee SO, Lai KP, Ma WL, Lin TH, Tsai MY, Luo J, Chang C (2013) Targeting androgen receptor in bone marrow mesenchymal stem cells leads to better transplantation therapy efficacy in liver cirrhosis. Hepatology 57:1550–1563
10. Moriya K, Yoshikawa M, Ouji Y, Saito K, Nishiofuku M, Matsuda R, Ishizaka S, Fukui H (2008) Embryonic stem cells reduce liver fibrosis in CCl4-treated mice. Int J Exp Pathol 89:401–409
11. Nikeghbalian S, Pournasr B, Aghdami N, Rasekhi A, Geramizadeh B, Hosseini Asl SM, Ramzi M, Kakaei F, Namiri M, Malekzadeh R, Vosough Dizaj A, Malek-Hosseini SA, Baharvand H (2011) Autologous transplantation of bone marrow-derived mononuclear and CD133(+) cells in patients with decompensated cirrhosis. Arch Iran Med 14:12–17
12. Kim JK, Park YN, Kim JS, Park MS, Paik YH, Seok JY, Chung YE, Kim HO, Kim KS, Ahn SH, Kim do Y, Kim MJ, Lee KS, Chon CY, Kim SJ, Terai S, Sakaida I, Han KH (2010) Autologous bone marrow infusion activates the progenitor cell compartment in patients with advanced liver cirrhosis. Cell Transpl 19:1237–1246
13. Salama H, Zekri AR, Zern M, Bahnassy A, Loutfy S, Shalaby S, Vigen C, Burke W, Mostafa M, Medhat E, Alfi O, Huttinger E (2010) Autologous hematopoietic stem cell transplantation in 48 patients with end-stage chronic liver diseases. Cell Transplant 19:1475–1486
14. Peng L, Xie DY, Lin BL, Liu J, Zhu HP, Xie C, Zheng YB, Gao ZL (2011) Autologous bone marrow mesenchymal stem cell transplantation in liver failure patients caused by hepatitis B: short-term and long-term outcomes. Hepatology 54:820–828
15. Terai S, Ishikawa T, Omori K, Aoyama K, Marumoto Y, Urata Y, Yokoyama Y, Uchida K, Yamasaki T, Fujii Y, Okita K, Sakaida I (2006) Improved liver function in patients with liver cirrhosis after autologous bone marrow cell infusion therapy. Stem Cells 24: 2292–2298
16. Kharaziha P, Hellstrom PM, Noorinayer B, Farzaneh F, Aghajani K, Jafari F, Telkabadi M, Atashi A, Honardoost M, Zali MR, Soleimani M (2009) Improvement of liver function in liver cirrhosis patients after autologous mesenchymal stem cell injection: a phase I-II clinical trial. Eur J Gastroenterol Hepatol 21: 1199–1205
17. Alison MR, Poulsom R, Jeffery R, Dhillon AP, Quaglia A, Jacob J, Novelli M, Prentice G, Williamson J, Wright NA (2000) Hepatocytes from non-hepatic adult stem cells. Nature 406:257
18. Lin H, Xu R, Zhang Z, Chen L, Shi M, Wang FS (2011) Implications of the immunoregulatory functions of mesenchymal stem cells in the treatment of human liver diseases. Cell Mol Immunol 8:19–22
19. Gilchrist ES, Plevris JN (2010) Bone marrow-derived stem cells in liver repair: 10 years down the line. Liver Transpl 16:118–129
20. Houlihan DD, Newsome PN (2008) Critical review of clinical trials of bone marrow stem cells in liver disease. Gastroenterology 135: 438–450
21. Ortiz LA, Dutreil M, Fattman C, Pandey AC, Torres G, Go K, Phinney DG (2007)

Interleukin 1 receptor antagonist mediates the antiinflammatory and antifibrotic effect of mesenchymal stem cells during lung injury. Proc Natl Acad Sci U S A 104:11002–11007

22. Nemeth K, Leelahavanichkul A, Yuen PS, Mayer B, Parmelee A, Doi K, Robey PG, Leelahavanichkul K, Koller BH, Brown JM, Hu X, Jelinek I, Star RA, Mezey E (2009) Bone marrow stromal cells attenuate sepsis via prostaglandin E(2)-dependent reprogramming of host macrophages to increase their interleukin-10 production. Nat Med 15: 42–49
23. Gnecchi M, He H, Liang OD, Melo LG, Morello F, Mu H, Noiseux N, Zhang L, Pratt RE, Ingwall JS, Dzau VJ (2005) Paracrine action accounts for marked protection of ischemic heart by Akt-modified mesenchymal stem cells. Nat Med 11:367–368
24. Weiskirchen R, Gressner AM (2005) Isolation and culture of hepatic stellate cells. Methods Mol Med 117:99–113
25. (1989) Molecular Cloning: A Laboratory Manual (Fourth Edition) © 2012 • 2,028 pp. illus, appendices, index Paperback (three-volume set) • ISBN 978-1-936113-42-2

Chapter 8

Animal Models to Test hiPS-Derived Hepatocytes in the Context of Inherited Metabolic Liver Diseases

Mathilde Dusséaux, Sylvie Darche, and Helene Strick-Marchand

Abstract

Human induced pluripotent stem (hiPS) cells are established following reprogramming of somatic cells from a wide variety of tissues. Given the scarcity of adult human hepatocytes, hiPS-derived hepatocytes would be a valuable source of cells to study differentiation programs, model patient-specific diseases, test drug toxicities, and cell transplantation therapies. Although hiPS-derived hepatocytes are extensively characterized in cell culture assays, testing these cells in animal models is necessary to fully evaluate their differentiation profile and their lack of tumorigenicity. Immunodeficient mouse models harboring liver damage are effective hosts in which xenogeneic hepatocytes can engraft, proliferate, and participate in liver regeneration, thus constituting a stringent test of hepatocyte functionality. The in vivo evaluation of disease-specific hiPS-derived hepatocytes should broaden our understanding of the cellular and molecular processes involved in inherited metabolic liver disease phenotypes. Herein, we detail our methods to test the functions of hiPS-derived hepatocytes in the context of the immunodeficient Rag2$^{-/-}$IL2Rγc$^{-/-}$Alb-uPA^{tg} mouse model.

Key words Human induced pluripotent stem cells (hiPS), Immunodeficient mouse models, Liver repopulation, Stem cell therapy, Hepatocyte

1 Introduction

The phenotypes of inherited metabolic liver diseases are the result of impaired or absent protein functions leading to disrupted cellular pathways specifically in mature hepatocytes. The complexity of maintaining fully differentiated hepatocytes in culture has been a roadblock for many studies aimed at deciphering the molecular mechanisms underlying disease phenotypes. For patients who progress to end stage liver disease, orthotopic liver transplantation is required to restore proper liver metabolism. Alternatively, infusion of healthy primary hepatocytes may be used as a bridge before organ transplantation. However, the lack of sufficient high quality donor tissue restricts the number of patients that are treated with these methods. Thus, mature human hepatocytes are a precious cell type needed to advance our understanding of hepatocyte functions and disease mechanisms, as well as for potential clinical applications.

Bruno Christ et al. (eds.), *Animal Models for Stem Cell Therapy*, Methods in Molecular Biology, vol. 1213,
DOI 10.1007/978-1-4939-1453-1_8,

An alternative source of cells was established by making use of the intrinsic cellular plasticity. Human induced pluripotent stem (hiPS) cells are established from readily accessible somatic cells (e.g., fibroblasts) following reprogramming to a pluripotent state through the overexpression of pluripotency factors (Oct3/4, Sox2, Klf4, and c-Myc) [1]. These hiPS cells may be specifically induced to differentiate into numerous cell types including hepatocytes, constituting a potentially renewable and reproducible source of cells to model liver diseases [2, 3]. With this aim, hiPS cells were derived from patients affected by inherited metabolic liver diseases including α1-antitrypsin (α1-AT) deficiency, type I glycogen storage disease, familial hypercholesterolemia, tyrosinemia, progressive familial hereditary cholestasis, and Crigler–Najjar syndrome [2, 4, 5]. In these studies, the patient-derived hiPS hepatocytes phenocopied key cellular abnormalities, validating the use of these cells for deciphering the molecular mechanisms of disease onset or as a platform for drug screening.

Although an in depth in vitro analysis of differentiated hiPS cells is required at first to screen culture conditions, in vivo testing of stem cell-derived hepatocytes brings complementary information related to the differentiation profile, tumorigenicity, and potential use of these cells in therapeutic settings. Sustained engraftment of xenogeneic cells in an animal model depends on several criteria: inhibition of the host's immune response against the donor cells, creation of a niche in which the cells can home, and maintenance of a selective advantage of the transplanted cells over the host's.

Immune suppression of the host is achieved by injecting myeloablating compounds (e.g., clodronate encapsulated liposomes) and by inactivating key genes in T, B, and NK lymphocyte development to generate immunodeficient animal models (e.g., $Rag1^{-/-}$, $Rag2^{-/-}$, Scid, $IL2R\gamma c^{-/-}$ mice) [6, 7]. The recruitment of the injected cells to the proper target organ can be achieved by inducing toxic damage to the tissue. In the case of the liver, the most permissive models described for testing stem cell-derived hepatocytes have been the $Rag2^{-/-}IL2R\gamma c^{-/-}$Alb-$uPA^{tg}$ mice (in which the liver-specific expression of the uPA^{tg} is cytotoxic) and the NOD/Scid/$IL2R\gamma c^{-/-}$ mice treated with hepatotoxic compounds (e.g., DMN, CCl_4, retrorsine) [8–11]. Although a number of studies show initial engraftment of stem cell-derived hepatocytes by immunohistochemical analysis of liver sections, mature human hepatocyte functions should be evaluated over several weeks by more stringent tests such as the secretion of human proteins in the serum by ELISAs [8–11]. In order to obtain long-term engraftment, continuous liver damage may be necessary to provide the required stress and growth signals.

To determine whether genetically corrected hiPS cells could execute hepatocyte functions in vivo, we compared hiPS-derived

hepatocytes isolated from "normal" donors or isolated from α1-AT-deficient patients, in whom the Z mutation of *α1-AT* had been previously corrected in vitro in the hiPS patient-derived cells. Both of these cell lines demonstrated similar engraftment and production of functional hepatocytes in vivo after transplantation into the Rag2$^{-/-}$IL2Rγc$^{-/-}$Alb-uPA^{tg} mice [9]. These results constituted an important proof-of-principle establishing that gene therapy combined with cell therapy could be successfully applied using hiPS cells.

To improve the engraftment and function of donor cells in the host, future work could aim to improve both the host's permissiveness and the grafted cells' differentiation profile. In the host, certain mouse-derived growth factors may not cross-react with human cells, thus the correct cues for human cells to fully participate in the liver's regeneration may be lacking. As an example, the addition of human cytokines to mouse models has led to substantial improvements in generating robust humanization of the immune system in vivo following human hematopoietic stem cell engraftment [12, 13]. Additionally, novel methods to induce more fully differentiated hepatocytes in vitro could ameliorate engraftment efficiencies in vivo. In our hands, a side-by-side comparison of liver repopulation by human adult hepatocytes and by human embryonic stem (hES)- or hiPS-derived hepatocytes in the same animal model showed that the former engrafted and regenerated the liver most efficiency. In the serum of mice injected with human adult hepatocytes or with hES and hiPS cells the measured human albumin levels were 10–2,000 μg/mL and 2–50 ng/mL, respectively. These observations suggest that optimization of differentiation protocols could lead to substantially higher levels of liver humanization and thus more efficient participation in liver regeneration in future clinical settings of cell therapy. As an important precaution, hiPS cells should be systematically screened for tumorigenicity with in vivo tests before being considered for therapeutic applications.

In this chapter, we describe our methods to test the capacity of hiPS-derived hepatocytes to participate in liver regeneration in the Rag2$^{-/-}$IL2Rγc$^{-/-}$Alb-uPA^{tg} mouse model. The use of this animal model will help to evaluate future applications combining gene and cell therapy methodologies with hiPS cells to treat patients afflicted by inherited metabolic liver diseases.

2 Materials

2.1 Mouse Model and Solutions for hiPS Cell Dissociation

1. 3–5 weeks old BALB/c Rag2$^{-/-}$IL2Rg$^{-/-}$NOD.*sirpa* uPA$^{tg/tg}$ mice.
2. HepatoZYME serum-free medium (Invitrogen).
3. Dulbecco's modified Eagle medium (DMEM): 1× streptomycin and penicillin, no fetal calf serum (FCS) (Gibco).

4. Trypsin-EDTA solution 1×, cell culture tested (Sigma).
5. Cell dissociation buffer (Gibco).
6. Phosphate-buffered saline (PBS).
7. Trypan blue.
8. T25 flask.
9. 15 mL centrifuge tube.
10. 40 μm cell strainer.

2.2 Injection of Stem Cells

1. 70 % ethanol.
2. Sterile cotton swabs.
3. Sterilized surgical instruments: dressing toothless straight and curved forceps, ophthalmic straight scissors, needle holder.
4. Syringe with 29 G×1/2″ needle (Myjector, Terumo).
5. Anesthetic solution: 9 mg/mL Ketamine (Imalgene®), 1,2 mg/mL Xylazine (Rompun®) in sterile PBS.
6. Polyamide monofilament surgical suture with surgical needle (6-0 12 mm FILAPEAU or OPTIME).
7. Surgical dressing (e.g., Band Aid® or Urgo®).
8. Ophthalmological ointment with antibiotics (chloramphenicol 10 mg/g, Ophtalon)
9. Heating pad, such as a Thermo Mat with control panel (Lucky Reptile), to maintain the mice at a warm temperature (30 °C) in the post-operative period prior to their awakening.

2.3 Analysis of Liver Engraftment

1. Dry ice.
2. 2-Methylbutane.
3. Microhematocrit heparinized capillary tubes (Fisherbrand).
4. Human albumin ELISA kit (Bethyl Laboratories).
5. 5 % sucrose in PBS solution, prepared the day of the experiment.
6. Tissue-Tek® O.C.T. compound and cryomolds (Sakura).
7. SuperFrost® microscope slides (Thermo Scientific).
8. Paraformaldehyde: 4 % in PBS, prepared from a 16 % liquid stock solution the day of the experiment.
9. PBS-TS: PBS containing 0.1 % Triton and 1 % fetal calf serum (FCS).
10. Primary antibodies: rabbit anti-human albumin (Dako), goat anti-human albumin (Bethyl Laboratories), rabbit anti-human a1-antitrypsin (Dako).
11. Secondary antibodies: donkey anti-rabbit Alexa Fluor, donkey anti-goat Alexa Fluor (Molecular Probes).

12. ProLong® Gold antifade reagent with DAPI (Life Technologies).
13. Glass coverslips.

3 Methods

Carry out all procedures involving cells and mice in a sterile environment under a biosafety level (BSL) cabinet (*see* **Note 1**).

3.1 Preparation of hiPS Cells for Transplantation

1. Plate cells in a T25 flask following previously described protocols [2, 9, 14]. Remove culture medium, wash cells with 4 mL PBS pre-warmed at 37 °C, add 4 mL cell dissociation buffer pre-warmed at 37 °C, and return the flask to the incubator at 37 °C for 15 min.
2. Tap the flask every 5 min to help the cells' dissociation from the culture dish (*see* **Note 2**).
3. Using a 5 mL serological pipette, flush cells up and down ten times in cell dissociation buffer.
4. Add 5 mL HepatoZYME medium. Using a 10 mL serological pipette, flush the cells up and down 10-times. Collect the cells in a 15 mL centrifuge tube.
5. Centrifuge cells at $470 \times g$ for 3 min at 20 °C.
6. Discard the supernatant and resuspend the cell pellet in 10 mL HepatoZYME medium. Filter the cell suspension through a 40 μm cell strainer (*see* **Note 3**).
7. Count viable cells by trypan blue exclusion.
8. Centrifuge cells at $470 \times g$ for 3 min at 20 °C.
9. Discard the supernatant and resuspend the cell pellet to 5×10^5 cells in 50 μL DMEM.

3.2 Cell Infusion into Mouse Model

1. Anesthetize the mouse with the solution of Ketamine–Xylazine: inject intraperitoneally 0.1 mL for 10 g of mouse weight (final concentration = 90 μg Ketamine and 12 μg Xylazine per gram of mouse). Wait 15–20 min for complete anesthesia.
2. Place the mouse on its back, check for stimulus response by pinching the foot pad. Disinfect the abdomen with 70 % ethanol and wipe clean.
3. Using sterile scissors, make a small 1 cm long incision anterior to posterior through the skin and abdominal wall of the left lateral side under the thoracic cavity.
4. Expose the spleen and hold it in place with curved forceps.

5. Inject 50 μL cell suspension into the spleen using a syringe with a 29 G × 1/2″ needle (*see* **Note 4**). After removing the needle, quickly apply pressure with a sterile cotton swab to stop splenic hemorrhaging (*see* **Note 5**).
6. Suture the peritoneal wall and abdominal cavity. Wipe clean and protect the wound with surgical dressing.
7. Place the mouse in a cage with a heated pad under the bedding until it fully awakes (*see* **Note 6**).

3.3 Evaluation of Liver Repopulation by Human Cells

1. Two weeks after cell infusion, sample the blood of the mouse in heparinized capillaries.
2. Centrifuge at 2,400 × *g* for 5 min. Aliquot plasma to new tube, store at −20 °C or use immediately.
3. Quantify human albumin content in the plasma by ELISA according to manufacturer's protocols (Bethyl Laboratories) (*see* **Note 7**).
4. Starting at 2 weeks post cell infusion, the liver can be immunohistologically analyzed.
5. After sacrificing the mouse, remove the liver, rinse it with PBS, and place it in the 5 % sucrose solution for 1–2 h at 4 °C. Place the liver in a cryomold with Tissue-Tek® O.C.T. compound, wait 30 min at room temperature (RT) before freezing.
6. Prepare a large plastic beaker of dry ice with 100 % ethanol and place in it a smaller glass beaker containing 2-methylbutane. Allow to chill for 20 min. Snap freeze liver tissue in O.C.T. in the prechilled 2-methylbutane for 20–30 s and store at −20 or −80 °C until use (*see* **Note 8**).
7. Cut 10 μm cryosections of frozen liver tissue and transfer onto SuperFrost® slides. Air-dry the cryosections for 15 min at RT. Store at −20 or −80 °C until use (*see* **Note 9**).
8. Air-dry the slides for 5 min at RT before fixing the cryosections with 4 % paraformaldehyde at 4 °C for 15 min. Rinse the slides with PBS.
9. Permeabilize and block the cryosections by incubating in 10 % FCS in PBS-TS for 30 min at RT in a humid chamber.
10. Incubate cryosections with primary antibody diluted in PBS-TS for 2 h at RT or overnight at 4 °C in a humid chamber (*see* **Note 10**).
11. Wash the slides three times with PBS-TS for 5 min in a jar with a rotational movement.
12. Incubate cryosections with secondary antibodies diluted in PBS-TS for 1 h at RT in a humid chamber (*see* **Note 11**).
13. Wash the slides three times with PBS-TS for 5 min in a jar with a rotational movement.

14. Mount cryosections with one drop of ProLong® Gold antifade reagent with DAPI and cover with glass coverslips. Allow to solidify for 30 min at RT, and then store in the dark at 4 °C until microscopic observation.

4 Notes

1. The health and welfare of the immunodeficient animals is essential to their survival. The SOPF (specific and opportunistic pathogen-free) status of the animals must be maintained by housing them either in individually ventilated cages or in isolators. Everything that comes into contact with the mice must be sterilized (by autoclaving or vaporized hydrogen peroxide) and all cage changes should be done under a laminar flow hood in a sterile environment.
2. The cells should be completely detached from the culture surface, and then returned to the incubator for further cell dissociation.
3. Cells must be well dissociated and resuspended for injections. Only single cell suspensions should be infused to avoid venous thrombosis.
4. The intrasplenic injection must be done slowly: 50 μL are injected in approximately 30 s.
5. Applying light pressure with a cotton swab for 5 min effectively stops splenic bleeding.
6. Monitor injected mice daily for 5 days following surgery. Surgical dressing should be removed 3–5 days after surgery.
7. To ensure proper reading of the ELISA, three dilutions are tested for each sample.
8. Do not freeze the tissue sample more than 30 s in the chilled 2-methylbutane as this may cause the O.C.T. to crack.
9. Do not freeze-thaw cryosections more than once, as this severely damages the tissue architecture.
10. Antibody dilutions depend on each lot's concentration and must be tested individually. As an indication, we use the following antibody concentrations: rabbit anti-human albumin (Dako) 1/2,000, goat anti-human albumin (Bethyl Laboratories) 1/1,000, rabbit anti-human a1-antitrypsin (Dako) 1/500.
11. Antibody dilutions depend on each lot's concentration and must be tested individually. As an indication, we use the following antibody concentrations: donkey anti-rabbit Alexa Fluor 1/1,000 and donkey anti-goat Alexa Fluor 1/1,000 (Molecular Probes).

Acknowledgements

The authors thank James Di Santo, Anne Weber, and Ludovic Vallier for helpful and stimulating discussions, and the following funding sources for their support: Agence Nationale de la Recherche (ANR programme Emergence), Agence Nationale de Recherches sur le sida et les hépatites virales (ANRS), Institut Pasteur, and Institut National de la Santé et de la Recherche Médicale (INSERM).

References

1. Takahashi K, Tanabe K, Ohnuki M, Narita M, Ichisaka T, Tomoda K, Yamanaka S (2007) Induction of pluripotent stem cells from adult human fibroblasts by defined factors. Cell 131:861–872
2. Rashid ST, Corbineau S, Hannan N, Marciniak SJ, Miranda E, Alexander G, Huang-Doran I, Griffin J, Ahrlund-Richter L, Skepper J, Semple R, Weber A, Lomas DA, Vallier L (2010) Modeling inherited metabolic disorders of the liver using human induced pluripotent stem cells. J Clin Invest 120:3127–3136
3. Si-Tayeb K, Noto FK, Nagaoka M, Li J, Battle MA, Duris C, North PE, Dalton S, Duncan SA (2010) Highly efficient generation of human hepatocyte-like cells from induced pluripotent stem cells. Hepatology 51:297–305
4. Ghodsizadeh A, Taei A, Totonchi M, Seifinejad A, Gourabi H, Pournasr B, Aghdami N, Malekzadeh R, Almadani N, Salekdeh GH, Baharvand H (2010) Generation of liver disease-specific induced pluripotent stem cells along with efficient differentiation to functional hepatocyte-like cells. Stem Cell Rev 6: 622–632
5. Cayo MA, Cai J, DeLaForest A, Noto FK, Nagaoka M, Clark BS, Collery RF, Si-Tayeb K, Duncan SA (2012) JD induced pluripotent stem cell-derived hepatocytes faithfully recapitulate the pathophysiology of familial hypercholesterolemia. Hepatology 56:2163–2171
6. Shultz LD, Ishikawa F, Greiner DL (2007) Humanized mice in translational biomedical research. Nat Rev 7:118–130
7. Legrand N, Ploss A, Balling R, Becker PD, Borsotti C, Brezillon N, Debarry J, de Jong Y, Deng H, Di Santo JP, Eisenbarth S, Eynon E, Flavell RA, Guzman CA, Huntington ND, Kremsdorf D, Manns MP, Manz MG, Mention JJ, Ott M, Rathinam C, Rice CM, Rongvaux A, Stevens S, Spits H, Strick-Marchand H, Takizawa H, van Lent AU, Wang C, Weijer K, Willinger T, Ziegler P (2009) Humanized mice for modeling human infectious disease: challenges, progress, and outlook. Cell Host Microbe 6:5–9
8. Touboul T, Hannan NR, Corbineau S, Martinez A, Martinet C, Branchereau S, Mainot S, Strick-Marchand H, Pedersen R, Di Santo J, Weber A, Vallier L (2010) Generation of functional hepatocytes from human embryonic stem cells under chemically defined conditions that recapitulate liver development. Hepatology 51:1754–1765
9. Yusa K, Rashid ST, Strick-Marchand H, Varela I, Liu PQ, Paschon DE, Miranda E, Ordonez A, Hannan NR, Rouhani FJ, Darche S, Alexander G, Marciniak SJ, Fusaki N, Hasegawa M, Holmes MC, Di Santo JP, Lomas DA, Bradley A, Vallier L (2011) Targeted gene correction of alpha1-antitrypsin deficiency in induced pluripotent stem cells. Nature 478:391–394
10. Liu H, Kim Y, Sharkis S, Marchionni L, Jang YY (2011) In vivo liver regeneration potential of human induced pluripotent stem cells from diverse origins. Sci Transl Med 3:82
11. Ma X, Duan Y, Tschudy-Seney B, Roll G, Behbahan IS, Ahuja TP, Tolstikov V, Wang C, McGee J, Khoobyari S, Nolta JA, Willenbring H, Zern MA (2013) Highly efficient differentiation of functional hepatocytes from human induced pluripotent stem cells. Stem Cells Transl Med 2:409–419
12. Huntington ND, Legrand N, Alves NL, Jaron B, Weijer K, Plet A, Corcuff E, Mortier E, Jacques Y, Spits H, Di Santo JP (2009) IL-15 trans-presentation promotes human NK cell development and differentiation in vivo. J Exp Med 206:25–34
13. Rongvaux A, Takizawa H, Strowig T, Willinger T, Eynon EE, Flavell RA, Manz MG (2013) Human hemato-lymphoid system mice: current use and future potential for medicine. Annu Rev Immunol 31:635–674
14. Hannan NR, Segeritz CP, Touboul T, Vallier L (2013) Production of hepatocyte-like cells from human pluripotent stem cells. Nat Protoc 8:430–437

Chapter 9

Support of Hepatic Regeneration by Trophic Factors from Liver-Derived Mesenchymal Stromal/Stem Cells

Suomi M.G. Fouraschen, Sean R.R. Hall, Jeroen de Jonge, and Luc J.W. van der Laan

Abstract

Mesenchymal stromal/stem cells (MSCs) have multilineage differentiation potential and as such are known to promote regeneration in response to tissue injury. However, accumulating evidence indicates that the regenerative capacity of MSCs is not via transdifferentiation but mediated by their production of trophic and other factors that promote endogenous regeneration pathways of the tissue cells. In this chapter, we provide a detailed description on how to obtain trophic factors secreted by cultured MSCs and how they can be used in small animal models. More specific, in vivo models to study the paracrine effects of MSCs on regeneration of the liver after surgical resection and/or ischemia and reperfusion injury are described.

Key words MSCs, Trophic factors, Mouse model, Liver regeneration, Partial hepatectomy, Ischemia and reperfusion injury

1 Introduction

The potential role of stem and progenitor cells as a therapeutic strategy for tissue injury or disease is widely being investigated. In recent years, stem/progenitor cells have been successfully applied in experimental models to treat several inflammatory and autoimmune diseases, including graft-versus-host disease, systemic lupus erythematosus, multiple sclerosis, type I diabetes, and inflammatory bowel disease [1–5]. Treatment with stem/progenitor cells resulted in decreased immune cell infiltration, reduced production of auto-antibodies and improvement of survival. Furthermore, multiple studies have shown that stem/progenitor cells are also effective in mediating tissue repair. Beneficial effects have been reported in cases of myocardial infarction, cornea damage as well as spinal cord, lung, and skin injury [6–10].

Bruno Christ et al. (eds.), *Animal Models for Stem Cell Therapy*, Methods in Molecular Biology, vol. 1213,
DOI 10.1007/978-1-4939-1453-1_9,

Another research area in which stem cell-based treatment strategies have been brought forward as a promising new therapeutic intervention is the field of liver regeneration. The liver has the remarkable capacity to regenerate in order to compensate for lost or damaged liver tissue after injury, a process that enables large (oncologic) liver resections and living-donor liver transplantation. However, after surgery for malignancies, regeneration is often compromised due to neoadjuvant chemotherapy, poor nutritional status, and increasing age of the patient population, thereby restricting surgical treatment options [11–14]. In the setting of living-donor liver transplantation, on the other hand, both donor and recipient end up with a small-for-size liver, associated with significant morbidity and mortality [15–17]. In this situation, both loss of a substantial part of the liver mass as well as oxidative stress after ischemia and reperfusion are major mechanisms of hepatic injury [18, 19]. Potential therapeutic strategies to improve liver regeneration and stimulate recovery are therefore most welcome.

Several studies describe the ability of stem cells, especially MSCs, to promote liver regeneration after toxic injury and protect against fulminant hepatic failure [20–23]. MSCs have the ability to differentiate into hepatocytes and cholangiocytes and induce immunomodulatory and anti-inflammatory responses [9, 24–27]. Furthermore, they are described to promote angiogenesis by up-regulating the expression of pro-angiogenic factors [28, 29].

MSCs can be obtained from multiple different sources [30, 31]. The first described and most widely used source of MSCs for regenerative purposes is bone marrow. Alternative and more accessible sources include cord blood and adipose tissue. Our group has shown that the adult human liver harbors a population of MSCs, which is mobilized from liver grafts at time of transplantation [32]. These liver-derived MSCs (L-MSCs) can be retrieved from the organ preservation solution and, similar to bone=marrow MSCs, appear to have immunosuppressive capacities as well as multilineage differentiation potential. Furthermore, we have reported that the trophic factors secreted by these L-MSCs stimulate liver regeneration after surgical resection, mainly by promoting hepatocyte proliferation and altering expression levels of regeneration-related genes [33].

Beneficial effects of MSC-secreted factors have also been reported in the setting of toxic liver injury and hepatic failure [34, 35]. In a clinical setting, the use of MSC-derived factors may have several advantages over the use of MSCs, since there is no risk of rejection or possible malignant transformation and the factors can be produced in large clinical grade quantities. In this chapter, we describe the technical aspects to produce MSC-conditioned culture medium (MSC-CM) to obtain these factors, including serum free culturing and the concentration of MSC-CM. Furthermore, we outline several procedures to study the effects of MSC-derived factors in vivo on liver regeneration, using partial hepatectomy and/or ischemia and reperfusion injury models in mice.

2 Materials

The materials listed do not include standard equipment used in cell culture labs or animal facilities. Tubes, vials and reagents used for cell culture should be sterile. Reagents should be stored according to the manufacturers' description, unless otherwise described.

2.1 Isolation of MSCs for Primary Cultures

1. 50 mL conical tubes.
2. DMEM medium, high glucose (Lonza).
3. Ficoll-Paque Plus.
4. Trypan Blue.
5. 1 mL cryovials.
6. Freezing container for cryovials.
7. Medium A: 80 % DMEM and 20 % fetal bovine serum (FBS; Sigma-Aldrich); store at 4 °C (*see* **Note 1**).
8. Medium B: 60 % DMEM, 20 % FBS, and 20 % dimethylsulfoxide (DMSO; Sigma-Aldrich); store at 4 °C (*see* **Note 1**).

2.2 Culturing System for MSCs

1. Serum-containing culture medium: DMEM, 10–15 % FBS, 1 % L-Glutamine (Lonza), and 1 % penicillin/streptomycin solution (Invitrogen); store at 4 °C (*see* **Note 2**).
2. T25 and T75 culture flasks.
3. Trypsin–EDTA.
4. 15 mL conical tubes.
5. FBS.
6. Phosphate-buffered saline (PBS).
7. Trypan Blue.

2.3 Concentration of MSC-Secreted Factors

1. PBS.
2. Serum-free culture medium: MEM-alpha (Invitrogen), 0.05 % bovine serum albumin (Sigma-Aldrich), 1 % L-Glutamine, 1 % penicillin/streptomycin solution; store at 4 °C.
3. 50 mL syringes.
4. 0.45 μm syringe filters (Corning).
5. 50 mL conical tubes.
6. Amicon Ultra-15 centrifugal filter units with 3 kDa molecular weight cutoff (Millipore).
7. 2 mL vials.

2.4 In Vivo Liver Injury and Regeneration Models

1. Male C57Bl/6 mice (preferably young adults, age around 8–14 weeks) maintained in the animal facility on a 12–12 h light–dark schedule with free access to food and drinking water.
2. Isoflurane vaporizer with induction chamber and suitable mouth piece for mice.
3. Isoflurane.
4. Heating pad (to keep mice at body temperature during the procedure).
5. Thin polystyrene foam or cork pad.
6. Shaver.
7. Tape.
8. 70 % ethanol.
9. Microsurgery instruments: curved blunt forceps, straight dissecting forceps, curved needle holder, half-curved scissors, microvascular clamps, microvascular clamp holder.
10. Other surgical instruments: operating scissors, two paper clips (partly unfolded to be used as retractors), two needles.
11. PBS or 0.9 % NaCl.
12. Cotton tips.
13. Cotton gauzes (5 × 5 cm).
14. Silk sutures: 4-0 for liver lobe resections, 5-0 for abdominal wall closure.
15. 1 mL syringes with injection needles (25 G).
16. Heparin (LEO Pharma).

3 Methods

Culture procedures should be performed in a culture grade flow cabinet to keep reagents and cultures sterile. Reagents should be stored according to the manufacturers' description, unless otherwise described. Animal experiments should be performed according to national laws and with approval of the institutional animal welfare committee.

3.1 Primary Cultures of MSCs from Human Tissue

MSCs can be obtained from various tissue samples, including bone marrow, dental marrow, adipose tissue and organs like lung, liver, and heart. The different methods for processing these tissues for primary cell cultures depend on the tissue type and have been described elsewhere. As an alternative for invasive techniques to obtain healthy tissue for the isolation of MSCs, organs and tissues

used for transplantation are an attractive source. In this setting, not only tissue biopsies but also the graft preservation solution can be used as a source of cells. This section describes the procedure for primary MSC cultures from liver graft preservation solution.

1. Collect the organ preservation solution of human liver grafts for transplantation (UW solution; Viaspan, Bristol-Myers Squibb) in sterile tubes or cups at the end of the cold storage period and store at 4 °C until further processing in the laboratory (*see* **Note 3**).
2. Put the freezing container and cryovials at 4 °C to cool down before use.
3. Distribute the organ preservation solution in 50 mL conical tubes, centrifuge (at 450 × *g*) for 5 min at 4 °C; and aspirate the supernatant.
4. Pool the cell pellets in one 50 mL conical tube using ice-cold DMEM up to a final volume of 30 mL (*see* **Note 4**).
5. Fill another 50 mL conical tube with 15 mL Ficoll, pipet the cell suspension gently onto the Ficoll and centrifuge (400 × *g*; 20 °C; 20 min; acceleration 9; brake off).
6. Gently collect the buffy coat/mononuclear cell layer, transfer into a new 50 ml conical tube and wash the collected fraction two times: add DMEM, centrifuge (450 × *g*; 4 °C; 10 min.) and aspirate the supernatant (*see* **Note 5**).
7. Resuspend the pellet in 10 mL DMEM and remove an aliquot of cells to perform a cell count with Trypan Blue (vital and dead cells; standard protocol).
   If at this point cells will be frozen and placed in storage prior to use, continue to the next step; otherwise continue with the culture expansion protocol.
8. Freeze the cells at a concentration of 10×10^6 cells per cryovial as follows:
   (a) Centrifuge (450 × *g*; 4 °C; 5 min.) and aspirate the supernatant.
   (b) Add the desirable amount of medium A (0.5 mL per cryovial) and store the cells on ice for 30 min.
   (c) Slowly add the desirable amount of medium B (0.5 mL per cryovial) and distribute the cells into the cryovials (1 mL per cryovial) (*see* **Note 6**).
   (d) Put the cryovials directly in the freezing container and store at −80 °C. The next day, the cells can be transferred to regular −135 °C storage boxes until further use (*see* **Notes 7** and **8**).

3.2 Culture Expansion of MSCs

If starting with cryofrozen cells, begin with the first step; otherwise continue to **step 2**.

1. Thawing cryofrozen cells for culture:
   (a) Fill 15 mL conical tubes with 3 mL ice-cold FBS per tube (one tube per cryovial frozen cells).
   (b) Thaw cryovials in a 37 °C water bath till a small piece of ice is left (*see* **Note 9**).
   (c) Transfer the thawed cell suspensions to the 15 mL conical tubes with ice-cold FBS.
   (d) Wash the cryovials with 2 mL ice-cold PBS and add to the 15 mL conical tubes with ice-cold FBS.
   (e) Centrifuge (450×*g*; 4 °C; 7 min) and aspirate the supernatant.
   (f) Resuspend the pellets using ice-cold serum-containing culture medium, centrifuge (450×*g*; 4 °C; 7 min), and aspirate the supernatant.
   (g) Pool the pellets in one 15 mL conical tube with serum-containing culture medium up to a final volume of 10 mL (if frozen cells are obtained from different liver grafts, the cells can be cultured separately) and remove an aliquot of cells to perform a cell count with Trypan Blue (vital and dead cells; standard protocol).
2. Centrifuge (450×*g*; 4 °C; 7 min.) and aspirate the supernatant.
3. Resuspend the pellet in serum-containing culture medium and transfer the cell suspension into T75 culture flasks (approximately 10×10^6 cells per flask). Add up to 12 mL serum-containing culture medium per flask and store them in a 37 °C cell culture incubator (*see* **Notes 10** and **11**).
4. Change the culture medium every 3 days:
   (a) Pre-warm the serum-containing medium in a 37 °C water bath.
   (b) Gently rinse the cell layer with serum-containing medium to get rid of debris (*see* **Note 12**).
   (c) Put 12 mL of fresh serum-containing medium in the culture flasks and place them in the incubator.
5. After approximately 7–10 days, fibroblast-like colonies should be scattered throughout the culture plate (Fig. 1). For expansion, wash the plate with pre-warmed PBS, aspirate and add Trypsin–EDTA to cover the bottom of the flask. After the cells have lifted from the culture plate, transfer them with serum-containing medium into a 15 mL conical tube and centrifuge (450×*g*; 4 °C; 7 min) (*see* **Note 13**).

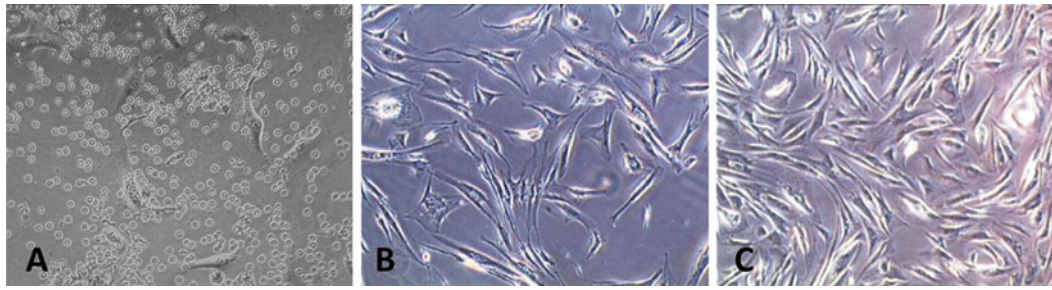

Fig. 1 MSC cultures (**a**) In the majority of cultures, cells with a fibroblast-like morphology appear within 10 days. (**b**) Fibroblast-like cells, e.g., MSCs rapidly proliferate and can be subcultured and expanded for up to 10–20 passages. (**c**) MSC cultures with 70–80 % confluence are optimal for collecting MSC-CM

6. Reseed cells at a density of 1,000 cells/cm^2 in a T25 culture flask (or 10 cm culture dish) overlayed with fresh medium. Afterwards, make fresh medium changes every 3 days. When cell density reaches 70–80 % confluence, harvest the cells, count, and reseed (*see* **Notes 14–16**).

3.3 Collection and Concentration of MSC-Secreted Factors

1. Expand the cultures until the desired amount of concentrated MSC-conditioned culture medium (MSC-CM) for in vivo use of MSC-secreted factors can be prepared (preferably passage 5–10). One T75 culture flask with at least 70–80 % MSC confluence will result in approximately 400 μL MSC-CM (in our experiments 100 μL per mouse per treatment were used) (*see* **Note 17**).
2. Three days before collection, remove the serum-containing culture medium, gently rinse the culture flasks with pre-warmed PBS and change to 10 mL pre-warmed serum-free culture medium per T75 culture flask (*see* **Notes 18** and **19**).
3. After 3 days of culture, collect the conditioned culture medium in a 50 mL syringe, connected to a 0.45 μm syringe filter and placed on a 50 mL conical tube (*see* **Note 20**).
4. Filter the conditioned culture medium to remove any cells and cell debris possibly present.
5. Transfer the filtered conditioned culture medium to the 3 kDa molecular weight cutoff centrifugal filters and centrifuge (3,200 × *g*; 4 °C; 60 min; brake off; this will concentrate the conditioned culture medium approximately 25-fold) (*see* **Note 21**).
6. Transfer the concentrated MSC-CM above the filter to 2 ml vials and put on ice until further use (*see* **Note 22**).

3.4 In Vivo Models to Study Paracrine Effects of MSC-CM

3.4.1 Partial Hepatectomy Model

1. Place the mouse into the induction chamber of the isoflurane vaporizer and use 2–3 L/min oxygen flow until anesthesia is induced.
2. Shave the abdominal skin, transfer the mouse onto the heating plate covered with the foam/cork pad (preheated at 37 °C) and continue the anesthesia by using the mouth piece connected to the vaporizer.
3. Fixate the mouse with the abdominal wall upward by taping the stretched legs to the plate and disinfect the abdominal skin with 70 % ethanol (*see* **Note 23**).
4. Make a midline incision (2.5–3 cm) using the curved blunt forceps and operating scissors: gently lift the skin resp. the peritoneum when cutting to avoid damaging the intestines; start in the lower abdominal area and work your way up until the xyphoid is exposed.
5. Place the two unfolded paperclips in the midline incision in such a position that they retract the abdominal wall lateral and upward, thereby exposing the liver, and fixate them to the pad with the needles.
6. Gently lift up the left lateral lobe using saline-moistened cotton tips, cut the membrane connecting this lobe to the caudate lobe with the half-curved scissors, and hold the left lobe in this upward position (if needed by retracting it with the tip of a saline-moistened gauze) (*see* **Note 24**).
7. Use the blunt forceps to place a 4-0 silk thread close to the hilum under the left lateral lobe and flip the lobe back to its original position, thereby wrapping the silk thread around the base of the lobe.
8. Use the curved needle holder and forceps to tie the ends of the silk thread close to the hilum (the color of the lobe will darken due to interruption of the blood flow) and cut the lobe close to the knot. Make sure there's no bleeding from the remnant (*see* **Note 25**).
9. Place a second silk thread underneath the median lobe, gently pull down this lobe and cut the falciform ligament.
10. Pull one end of the thread in the groove on the right side of the gall bladder and the other end around the back of the right part of the median lobe, tie the ends together (which will cut across the liver tissue) and remove the right part of the median lobe by cutting close to the knot.
11. Perform the same procedure for the left part of the median lobe, which is smaller than the right part, and shorten the ends of all remnant silk threads (*see* **Note 26**).
12. Close the peritoneum and skin separately with 5-0 silk sutures, clean the abdominal skin from blood remnants, and place the animals in a warm environment to recover (*see* **Notes 27** and **28**).

13. If chosen to treat the animals at time of surgery, inject the MSC-CM/treatment solution when the animals are still anesthetized (*see* **Notes 29** and **30**).
14. Sacrifice the animals at the preferred time point and collect blood and/or tissue for further analysis (*see* **Note 31**).

3.4.2 Ischemia–Reperfusion Model with or Without Partial Hepatectomy

1. Inject the mouse approximately 15 min prior to surgery intraperitoneally with heparin (100 U/kg; solution of 10 U/mL in PBS) to prevent intravascular thrombus formation.
2. Follow steps 1-5 as described in the partial hepatectomy protocol. For the ischemia–reperfusion model, it is best to perform the surgical procedures using a microscope (especially the vascular clamping).
3. Lift the intestines from the abdominal cavity and wrap them in a saline-moistened gauze to protect them from dehydrating.
4. Gently lift the median and left lateral lobes using saline-moistened cotton tips, cut the membrane connecting the left lateral lobe to the caudate lobe with the half-curved scissors, and hold the lobes in this upward position by retracting it with a moistened gauze (*see* **Note 24**).
5. Use another moistened gauze to gently retract the right lateral and caudate lobes in the caudal direction to expose the portal triad.
6. Using the straight dissecting forceps, carefully dissect the space behind the portal triad without puncturing the aorta.
7. After creating a sufficiently large opening behind the portal triad, place a microvascular clamp just above the branch of the right lateral lobe using the clamp holder (*see* **Note 32**).
8. Reposition the liver lobes and the intestines in their anatomic position, inject 0.5 mL of saline in the abdominal cavity, and cover the animal with a moistened gauze.
9. Keep the animals anesthetized and on the heating plate during the ischemic time and make sure the gauze stays moist (*see* **Note 33**).
10. At the end of the ischemic period, gently remove the microvascular clamp to reperfuse the median and left lateral lobes.
11. Follow **steps 12–14** of the partial hepatectomy protocol to finish the procedure, unless chosen to combine ischemia and reperfusion injury with a (approximately) 50 % partial hepatectomy, leaving only ischemic liver tissue.
12. Gently remove the intestines and lift the median and left lateral liver lobes as described in **steps 3** and **4** of this protocol.
13. Using moistened cotton tips, the blunt forceps, and the half-curved scissors, carefully dissect the right lateral and caudate lobes from their surroundings so that they can be lifted.

14. Place a 4-0 silk thread underneath the right lateral lobe, close to the base and flip the lobe back to its original position, thereby wrapping the silk thread around the base of the lobe.
15. Use the curved needle holder and forceps to tie the ends of the silk thread close to the base and cut the lobe close to the knot. Make sure there's no bleeding from the remnant (*see* **Note 25**).
16. Perform the same procedure for the caudate lobes as well as the right part of the median lobe (**steps 9** and **10** of the partial hepatectomy protocol) and shorten the ends of all remnant silk threads (*see* **Note 34**).
17. Close the peritoneum and skin separately with 5-0 silk sutures, clean the abdominal skin from blood remnants, and place the animals in a warm environment to recover (*see* **Notes 27** and **28**).
18. If chosen to treat the animals at time of surgery, inject the MSC-CM/treatment solution when the animals are still anesthetized (*see* **Notes 29** and **30**).
19. Sacrifice the animals at the preferred time point and collect blood and/or tissue for further analysis (*see* **Note 31**).

4 Notes

1. Do not use medium A and B older than 2 weeks.
2. Between research laboratories, the composition of stem cell culture medium may differ. Another well defined medium for MSC cultures is MEM-alpha supplemented with 2 % FBS, 20 ng/mL fibroblast growth factor 2 (FGF2), and 20 ng/mL epidermal growth factor (EGF).
3. In our institution, liver grafts are flushed twice before implantation into the recipient: prior to preparation at the backbench and between backbench preparation and implantation. Both batches of preservation solution can be used, however, the first batch contains most of the cells.
4. If preferred, RPMI or MEM-alpha can also be used.
5. Plastic pipettes are convenient for controlled collection of the buffy coat/mononuclear cell fraction. To avoid taking up the underlying Ficoll, it is advisable to use a circular motion when collecting the buffy coat.
6. Slowly drip the medium along the side of the tube while rotating the tube, to evenly distribute medium B over the cell suspension. If added too quickly the DMSO will damage the cells.
7. Transfer the cryovials to a −80 °C environment as soon as possible, as DMSO (especially if not kept cold) damages cells.

8. If planning to store cells for a longer period of time, transfer them to a −135 or −150 °C freezer to conserve optimal cell condition.
9. Leaving a small piece of ice ensures a relatively low temperature. If the temperature gets too high, the DMSO in the cell freezing suspension damages too many cells. Perform the thawing steps b–d therefore as quickly as possible.
10. The seeding density is critical for selecting adherent fibroblast-like cell colonies. Data on bone marrow MSCs reveal an optimal seeding density for these cells of 10^5 cells/cm^2. Most investigators use between 10^5 and 10^6 cells/cm^2. Plating at a higher density overcrowds the well or plate; the first cells to plate down will be monocytes/macrophages, as they easily adhere to plastic and the MSCs might still be floating in the non-adherent fraction, which unfortunately will be discarded. Some researchers furthermore prefer to use 10 cm dishes for primary cultures, because it allows to pick the individual colonies using cloning rings. This is a proper way to expand colonies and avoid expanding, as much as possible, the adherent monocytes.
11. Serum-free culture medium usually causes insufficient growth stimulation of cells in the initial phase of the culture.
12. One needs to find a balance between rinsing too gentle (thereby not removing the debris) and rinsing too rough (thereby removing adherent living cells from the culture flask).
13. In the primary cultures, fibroblast-like cells/L-MSCs can be easily distinguished, as they are phase bright using phase contrast microscopy and they develop from an oval shape into long, sprouted cells with a fibroblast-like morphology.
14. Cell cultures can often best be split 1:2 or 1:3 (up to 1:4) to keep the seeding density sufficiently high and prevent senescence.
15. Cells can be maintained in culture up to passage 20. Below passage 5, MSC numbers are usually too low to perform in vivo experiments. At high passages, cells can show signs of senescence due to a high number of cell doublings (cells stopped replicating and are very large). Cultures can be tested for senescence by staining for beta-gal or looking at telomeres or aneuploidy.
16. At higher passages, always be aware of possible spontaneous transformation of cells. Our group has identified, though rare, spontaneous malignant transformation in MSC cultures after long-term culturing [36].
17. Factors like MSC batch, passage number, differences in cell density and amount of proliferating and resting cells in a culture can influence the quality of the MSC-CM. It is therefore very

important to standardize the cultures, culture conditions and MSC-CM preparations as much as possible. Conditioned medium from different culture flasks (from the same batch) can also be combined before concentrating the MSC-CM, to prevent differences in the quality of the MSC-CM used for an experiment. In addition, quality control can be performed by protein content/cell number detection, ELISA, mass spectrometry, or gel electrophoresis.

18. The fetal bovine serum in serum-containing culture medium contains several growth factors that stimulate survival, growth and proliferation of cultured cells. Rinsing the culture flasks with PBS will remove remnants of the serum-containing culture medium, thereby preventing these factors to influence the experiment results.
19. If feasible, plan the collection and concentration of MSC-CM on the same day as the experiments to prevent possible brake down of MSC-secreted factors.
20. Filter units can be used for large volumes.
21. If a lower concentration factor is preferred, shorten the spinning time accordingly.
22. Determining the overall protein concentration using a Pierce Protein assay kit is recommended to control for protein content during the in vivo studies. Include unconditioned medium, which contains bovine serum albumin, as baseline control. After determining protein content, it is possible to store aliquots of the MSC-CM at known protein concentration at −80 °C for long-term storage. Also, this avoids the issue of repeated thaw–freeze cycles when using the MSC-CM in future experiments.
23. The forelegs can also be fixated "embracing" the mouth piece. The advantage is that the rib cage and diaphragm are positioned a bit more cranial, thereby exposing the liver slightly better.
24. The liver tissue is very delicate and easily damaged. Using moistened cotton tips and gauzes will reduce the chance of damaging the tissue.
25. If the remnant is bleeding, tighten the knot to stop the bleeding.
26. The right and left part of the median lobe can also be removed together, using one silk thread and thereby also removing the gall bladder. However, if the knot is placed too close to the hilum/supra-hepatic caval vein, the resection will cause venous obstruction resulting in congestion, necrosis and failure of regeneration. On the other hand, the further away the knot is

placed, the more functional liver tissue is left in situ. By removing the right and left part of the median lobe separately, leaving the gall bladder in situ, the risk of causing venous obstruction or leaving too much liver tissue is reduced.

27. Mice tend to bite the sutures. If the abdomen is closed in one layer, knots are too easily accessible (the lower, the easier) or not properly tied, this will result in evisceration.
28. A warm recovery environment can be created using an incubator designed for animals (keep at 37 °C) or heating lamps. Be careful if using heating lamps, they tend to get very hot and dehydrate/overheat the animals.
29. The site and time of MSC-CM administration possibly affect its therapeutic effects. Stem cell-derived factors have been injected intravenously as well as intraperitoneally and at time points prior to, during or after the induction of injury. The best time and route of administration still need to be elucidated. However in our study on liver regeneration after partial hepatectomy, pretreatment 4 h prior to surgery seemed beneficial over treatment at time of resection [33]. A possible explanation could be that the liver is already primed in those 4 h and can therefore immediately respond to the loss of liver mass (Fig. 2).
30. Always look for strategies/alternatives that least harm the animals.

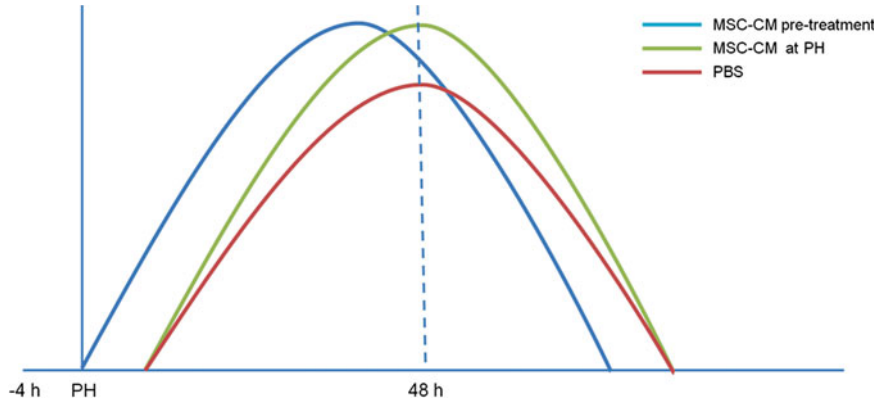

Fig. 2 Postulated kinetics of hepatocyte proliferation after MSC-CM treatment. In our study on the paracrine effects of MSC-derived factors on liver regeneration after partial hepatectomy, treatment 4 h prior to surgery was compared with treatment at time of resection. Based on the hepatocyte proliferation and gene expression data, treatment at time of resection seemed most effective in stimulating liver regeneration. Interestingly, however, a significant increase in liver to body weight ratio was found after pretreatment, whereas no significant difference compared to control treated animals was found if animals were treated at time of resection. We hypothesize that MSC-CM pretreatment shifts the regenerative response of the liver after surgical injury forward and thus accelerates liver regeneration

31. Depending on the field of interest, multiple readouts for regeneration can be used, for instance:
    (a) Immunohistochemical staining for BrdU (5-bromo-2′-deoxyuridine), PCNA (proliferating cell nuclear antigen), or Ki67 to determine the percentage of proliferating cells. In case of using BrdU, the animals have to be injected at least 30 min prior to sacrifice with 50 mg/kg dissolved BrdU, as this compound needs to be incorporated into the DNA of proliferating cells.
    (b) qRT-PCR to investigate cell cycle related, inflammatory, and pro-angiogenic gene expression levels.
    (c) Western blotting or ELISA techniques to detect levels of relevant proteins in tissue or blood (for example serum transaminases and bilirubin).
32. Only the median and left lateral lobes should show a change in color. If the right lateral lobe shows any signs of ischemia, the clamp is placed too close to its branch.
33. The duration of the ischemic time period depends on the preferred amount of injury. Most studies describe an ischemic time in rodents between 60 and 90 min. Below 60 min, the injury inflicted is often not severe enough to show clear beneficial effects of a treatment. Above 90 min, the survival rate of the animals drops, which is often only preferred in survival studies. While developing our model, we noticed that ischemia and reperfusion injury combined with a 50 % partial hepatectomy allowed ischemic times up to 60 min before the survival rates went down.
34. Part of the caudate lobes can best be approached by flipping the intestines to the right.

References

1. Polchert D, Sobinsky J, Douglas G et al (2008) IFN-gamma activation of mesenchymal stem cells for treatment and prevention of graft versus host disease. Eur J Immunol 38(6): 1745–1755
2. Sun L, Akiyama K, Zhang H et al (2009) Mesenchymal stem cell transplantation reverses multiorgan dysfunction in systemic lupus erythematosus mice and humans. Stem Cells 27(6):1421–1432
3. Fiorina P, Jurewicz M, Augello A et al (2009) Immunomodulatory function of bone marrow-derived mesenchymal stem cells in experimental autoimmune type 1 diabetes. J Immunol 183(2):993–1004
4. Hawkey CJ (2012) Stem cells as treatment in inflammatory bowel disease. Dig Dis 30(Suppl): 3134–139
5. Uccelli A, Laroni A, Freedman MS (2011) Mesenchymal stem cells for the treatment of multiple sclerosis and other neurological diseases. Lancet Neurol 10(7):649–656
6. Lim GB (2012) Stem cells: myocardial regeneration after infarction-promising phase I trial results. Nat Rev Cardiol 9(4):187
7. Roddy GW, Oh JY, Lee RH et al (2011) Action at a distance: systemically administered adult stem/progenitor cells (MSCs) reduce inflammatory damage to the cornea without engraftment and primarily by secretion of TNF-alpha

stimulated gene/protein 6. Stem Cells 29(10): 1572–1579
8. Liu WG, Wang ZY, Huang ZS (2011) Bone marrow-derived mesenchymal stem cells expressing the bFGF transgene promote axon regeneration and functional recovery after spinal cord injury in rats. Neurol Res 33(7): 686–693
9. Ortiz LA, Dutreil M, Fattman C et al (2007) Interleukin 1 receptor antagonist mediates the antiinflammatory and antifibrotic effect of mesenchymal stem cells during lung injury. Proc Natl Acad Sci U S A 104(26):11002–11007
10. Huang S, Lu G, Wu Y et al (2012) Mesenchymal stem cells delivered in a microsphere-based engineered skin contribute to cutaneous wound healing and sweat gland repair. J Dermatol Sci 66(1):29–36
11. Karoui M, Penna C, Amin-Hashem M et al (2006) Influence of preoperative chemotherapy on the risk of major hepatectomy for colorectal liver metastases. Ann Surg 243(1):1–7
12. Kandutsch S, Klinger M, Hacker S et al (2008) Patterns of hepatotoxicity after chemotherapy for colorectal cancer liver metastases. Eur J Surg Oncol 34(11):1231–1236
13. Skullman S, Ihse I, Larsson J (1990) Influence of malnutrition on regeneration and composition of the liver in rats. Acta Chir Scand 156(10):717–722
14. Timchenko NA (2009) Aging and liver regeneration. Trends Endocrinol Metab 20(4): 171–176
15. Shiffman ML, Brown RS Jr, Olthoff KM et al (2002) Living donor liver transplantation: summary of a conference at The National Institutes of Health. Liver Transpl 8(2):174–188
16. Marsh JW, Gray E, Ness R et al (2009) Complications of right lobe living donor liver transplantation. J Hepatol 51(4):715–724
17. Dahm F, Georgiev P, Clavien PA (2005) Small-for-size syndrome after partial liver transplantation: definition, mechanisms of disease and clinical implications. Am J Transplant 5(11): 2605–2610
18. Wu C, Wang P, Rao J et al (2011) Triptolide alleviates hepatic ischemia/reperfusion injury by attenuating oxidative stress and inhibiting NF-kappaB activity in mice. J Surg Res 166(2): e205–213
19. Selzner N, Rudiger H, Graf R et al (2003) Protective strategies against ischemic injury of the liver. Gastroenterology 125(3):917–936
20. Cho KA, Ju SY, Cho SJ et al (2009) Mesenchymal stem cells showed the highest potential for the regeneration of injured liver tissue compared with other subpopulations of the bone marrow. Cell Biol Int 33(7): 772–777
21. Abdel Aziz MT, Atta HM, Mahfouz S et al (2007) Therapeutic potential of bone marrow-derived mesenchymal stem cells on experimental liver fibrosis. Clin Biochem 40(12): 893–899
22. Forbes SJ, Vig P, Poulsom R et al (2002) Bone marrow-derived liver stem cells: their therapeutic potential. Gastroenterology 123(2): 654–655
23. Oertel M, Shafritz DA (2008) Stem cells, cell transplantation and liver repopulation. Biochim Biophys Acta 1782(2):61–74
24. Duncan AW, Dorrell C, Grompe M (2009) Stem cells and liver regeneration. Gastroenterology 137(2):466–481
25. Fausto N (2004) Liver regeneration and repair: hepatocytes, progenitor cells, and stem cells. Hepatology 39(6):1477–1487
26. Kaplan JM, Youd ME, Lodie TA (2010) Immunomodulatory activity of mesenchymal stem cells. Curr Stem Cell Res Ther 6:297–316
27. Crop M, Baan C, Weimar W et al (2009) Potential of mesenchymal stem cells as immune therapy in solid-organ transplantation. Transpl Int 22(4):365–376
28. Aguirre A, Planell JA, Engel E (2010) Dynamics of bone marrow-derived endothelial progenitor cell/mesenchymal stem cell interaction in co-culture and its implications in angiogenesis. Biochem Biophys Res Commun 400(2):284–291
29. Zacharek A, Chen J, Cui X et al (2007) Angiopoietin1/Tie2 and VEGF/Flk1 induced by MSC treatment amplifies angiogenesis and vascular stabilization after stroke. J Cereb Blood Flow Metab 27(10):1684–1691
30. da Silva Meirelles L, Chagastelles PC, Nardi NB (2006) Mesenchymal stem cells reside in virtually all post-natal organs and tissues. J Cell Sci 119(Pt 11):2204–2213
31. Bieback K, Kern S, Kocaomer A et al (2008) Comparing mesenchymal stromal cells from different human tissues: bone marrow, adipose tissue and umbilical cord blood. Biomed Mater Eng 18(1 Suppl):S71–76
32. Pan Q, Fouraschen SM, Kaya FS et al (2011) Mobilization of hepatic mesenchymal stem cells from human liver grafts. Liver Transpl 17(5):596–609
33. Fouraschen SM, Pan Q, de Ruiter PE et al (2012) Secreted factors of human liver-derived mesenchymal stem cells promote liver regeneration early after partial hepatectomy. Stem Cells Dev 21(13):2410–2419
34. van Poll D, Parekkadan B, Cho CH et al (2008) Mesenchymal stem cell-derived molecules

directly modulate hepatocellular death and regeneration in vitro and in vivo. Hepatology 47(5):1634–1643

35. Parekkadan B, van Poll D, Suganuma K et al (2007) Mesenchymal stem cell-derived molecules reverse fulminant hepatic failure. PLoS One 2(9):e941

36. Pan Q, Fouraschen SM, de Ruiter PE et al (2014) Detection of spontaneous tumorigenic transformation during culture expansion of human mesenchymal stromal cells. Exp Biol Med (Maywood) 239(1):105–115 doi: 10.1177/1535370213506802. Epub 2013 Nov 13. PMID: 24227633

Part III

Cardiovascular Diseases

Chapter 10

Assessment of Functional Competence of Endothelial Cells from Human Pluripotent Stem Cells in Zebrafish Embryos

Valeria V. Orlova, Yvette Drabsch, Peter ten Dijke, and Christine L. Mummery

Abstract

Human pluripotent stem cells (hPSCs) are proving to be a valuable source of endothelial cells (ECs), pericytes, and vascular smooth muscle cells (vSMCs). Although an increasing number of phenotypic markers are becoming available to determine the phenotypes of these cells in vitro, the ability to integrate and form functional vessels in the host organism, typically mouse, remains critical for the assessment of EC functional competence. However, current mouse models require relatively large numbers of cells that might be difficult to derive simultaneously from multiple hPSCs lines. Therefore, there is an urgent need for new functional assays that are robust and can be performed with small numbers of cells. Here we describe a novel zebrafish xenograft model to test functionality of hPSC-derived ECs. The assay can be performed in 10 days and requires only ~100–400 human cells per embryo. Thus, the zebrafish xenograft model can be useful for the accurate and rapid assessment of functionality of hPSC-derived ECs in a lower vertebrate model that is widely viewed by regulatory authorities as a more acceptable alternative to adult mice.

Key words Human pluripotent stem cells (hPSCs), Endothelial cells (ECs), Zebrafish xenograft

1 Introduction

Zebrafish (*Danio rerio*), a tropical fish originating in fresh waters of East India and Burma, has fast become an invaluable tool for both basic biology research and biomedical sciences in many laboratories all over the globe. Since the early 1970s, zebrafish have been widely used in developmental and genetic studies. However, in the past decade their application has extended into other fields of biology, including drug screening, modeling of human diseases and cancer [1–4]. Vascular biologists have been using the zebrafish extensively as a model to study vasculogenesis, angiogenesis, and lymphangiogenesis, as well as for modeling tumor angiogenesis [5, 6]. A major advantage of zebrafish is the large number of embryos that can be generated (approximately 100–200 embryos/day/adult zebrafish). Development occurs relatively fast and can

Bruno Christ et al. (eds.), *Animal Models for Stem Cell Therapy*, Methods in Molecular Biology, vol. 1213,
DOI 10.1007/978-1-4939-1453-1_10,

be easily staged. Furthermore, there are many transgenic strains that are readily available with fluorescent proteins under regulatory elements of cell specific promoters that simplify visualization of different cell types and processes and allow live imaging since the embryos are transparent. Importantly, the adaptive immune system develops at approximately 4 days post fertilization (dpf); therefore, transplantation of heterologous cells can be tolerated by the host and does not require immunosuppression [7]. Moreover, zebrafish xenografts require very few human cells for injection (~100-400 cells per embryo) [8, 9].

The recent discovery of human pluripotent stem cells (hPSCs) is already another major breakthrough in the field of regenerative medicine. These stem cells include both embryonic stem cells (ESCs) that are derived from the inner cell mass of pre-implantation blastocyst-stage human embryos and induced pluripotent stem cells (iPSCs) that are derived from adult somatic cells upon reprogramming with a defined cocktail of transcription factors [10–12]. hPSCs give rise to all the cells of the body in vivo, and can be differentiated into many cell types in vitro. In particular, hPSCs can be a very useful source of different vascular subtypes, such as endothelial cells (ECs), pericytes, and vascular smooth muscle cells (vSMCs) [8, 13, 14]. However, the need for robust, accessible, and easy to use in vivo models for functional assessment of hPSC-derived cells that are also reasonably priced remains high. Despite the availability of mouse models for vascular integration and function studies, they are expensive, require large numbers of cells ($>2 \times 10^6$ per mouse), and produce highly variable results. In addition, hPSC-derived cells and ECs are quite often immature and exhibit embryonic-like cell features [8, 15]. The acquisition of the tissue specific or mature cellular characteristics is highly dependent on the local cellular microenvironment. Therefore, the local host microenvironment might be crucial for further maturation of hPSC-derived cells, particularly ECs.

Recently, zebrafish xenografts have been used for cell fate assessment of cord blood-derived CD34+ progenitors [16]. Since the zebrafish model has been a very useful tool to study vascular development, and can tolerate transplantation of cells from other species, we thought this would be a suitable model for robust screening applications of control and disease hPSC-derived cells, as well as future drug discovery examining the effects of compounds on human vasculature in a surrogate in vivo environment. Strikingly, hPSC-derived ECs were capable of integrating into developing zebrafish vasculature upon implantation at the blastula stage, or in developing embryos 48 h post fertilization (hpf) [8]. Furthermore, the percentage of vessels with human cells, as well as the length of chimeric vessels can be assessed relatively easily. Interestingly, hPSC-derived ECs had much higher integration rates, compared to primary human umbilical vein-derived ECs (HUVECs) which

are much more commonly used in biomedical research on vasculature [8]. This would indicate that hPSC-derived ECs are more plastic and capable of adapting to different environments compared to more mature postnatal or adult ECs. Therefore, hPSC-derived ECs are likely to be a good candidate for future regenerative medicine applications. In addition, zebrafish can be used to study functionality of hPSC derivatives, and possibly future studies on cell maturation and disease modeling.

In this chapter, we describe a method for the assessment of hPSC-derived EC functionality in zebrafish xenograft models. This includes a basic description of hPSC culture, differentiation, and isolation of hPSC-derived ECs. Moreover, grafting of ECs into zebrafish at the blastula stage and 48 hpf, and whole mount zebrafish immunofluorescent staining are described.

2 Materials

2.1 hPSC Culture

1. BD Matrigel Matrix GFR (BD Biosciences): Thaw Matrigel on ice and prepare small aliquots, store at −20 °C.
2. Matrigel-coated 6-well plates: Prepare a 1:10 dilution of Matrigel in cold DMEM/F-12 (see below) on ice. Add 2 mL of Matrigel per 6-well plate. Incubate the plates for 1 h at room (RT) temperature. Plates can be stored at 4 °C for up to 2 weeks. Pre-warm the plates for 30 min at RT before use.
3. mTeSR™1 (Stemcell Technologies).
4. Dispase II, powder (Gibco).
5. Dulbecco's Modified Eagle's Medium (DMEM)/F-12, 1:1 (Gibco).
6. Dispase solution: 5 mg/mL in DMEM/F-12, pass through sterile filter and make 1 or 2 mL aliquots, store at −20 °C.
7. Dispase working solution: 1 mg/mL in DMEM/F-12. The solution can be stored for up to 2 weeks at 4 °C.
8. Cell scraper.
9. 15 mL conical tube.

2.2 Differentiation of ECs from hPSCs

1. BEL differentiation medium (250 mL) [17]: 108 mL Iscove's Modified Dulbecco's Medium (IMDM, Gibco), 114.25 mL Ham's F-12 Nutrient Mix (Gibco), 12.5 mL Protein-free Hybridoma Medium (PFHM-II, Gibco), 6.25 mL 10 % bovine serum albumin (BovoStar BSA, Bovogen Biologicals) in IMDM, 2.5 mL Chemically Defined Lipid Concentrate (Gibco), 250 µL Insulin-Transferrin-Selenium-Ethanolamine (ITS-X, Gibco), 750 µL 1-thioglycerol (Sigma Aldrich; stock 13 µL in 1 mL IMDM), 2.5 mL L-Ascorbic acid 2-phosphate

sesquimagnesium salt hydrate (AA2P, Sigma Aldrich), 2.5 mL of 200 mM GlutaMAX™ Supplement (Gibco), 1.25 mL of 5,000 U ml^{-1} Pen/Strep (Gibco).

2. Growth factors: bone morphogenetic protein (BMP) 4 (Miltenyi Biotech), vascular endothelial growth factor (VEGF, R&D Systems), ActivinA (Miltenyi Biotech).
3. Small molecule inhibitors: CHIR99021 (Tocris Bioscience), SB431542 (Tocris Bioscience).

2.3 Isolation and Expansion of ECs from hPSCs

1. CD31 Dynabeads® (Life Technologies).
2. Bovine serum albumin (BSA, BioXtra, Sigma-Aldrich).
3. Dulbecco's Modified Eagle's Medium (DMEM, Gibco).
4. Phosphate-buffered saline (PBS, Gibco).
5. Fetal bovine serum (FBS, Gibco).
6. DMEM-0.1 % BSA: dissolve 0.25 g BSA (BioXtra, Sigma) in 250 mL DMEM, pass through a sterile filter and store at 4 °C.
7. 1x TrypLE (Gibco).
8. FACsB: 2.5 g BSA in 500 mL PBS, add 2 mL of 0.5 M EDTA (pH 8.0). Pass through a sterile filter and store at 4 °C.
9. FACsB-10 % FBS: 5 mL FBS, 45 mL FACsB, pass through a sterile filter and store at 4 °C.
10. CellTrics 100 μm filter, sterile (CellTrics).
11. DynaMag™-5 (Life Technologies).
12. Human endothelial serum-free medium (EC-SFM, Gibco).
13. Growth factors: VEGF (R&D Systems), basic fibroblast growth factor (bFGF, Miltenyi Biotec).
14. Platelet poor bovine serum (BTI).
15. 0.1 % gelatin from porcine skin, type A (Sigma-Aldrich).
16. 0.1 % gelatin-coated plates: Add 0.1 % gelatin to the plate, leave for at least 30 min at 37 °C, aspirate gelatin prior to adding cell culture media.

2.4 Preparation of ECs for the Injection

1. Endothelial cell growth medium; basal serum-free medium EBM-2 (Lonza).
2. CellTracker™ Cm Dil (Life Technologies).
3. T25 culture flask.
4. 15 mL conical falcon tube.

2.5 Zebrafish Egg Laying and Embryo Production

Transgenic zebrafish with expression of green fluorescent protein (GFP) (Tg(fli1:GFP)) in blood vessels is used for generation of embryos [18].

2.6 Integration of ECs into Zebrafish (Blastula Stage)

1. Pneumatic Picopump (World Precision Instruments).
2. Borosilicate glass capillary (1 mm O.D. × 0.78 mm I.D.) (Harvard Apparatus).
3. Egg water: Add 1.5 mL of stock salt solution (40 g Instant Ocean Sea Salts™ in 1 L distilled water) to 1 L distilled water with a small amount of methylene blue.
4. Microinjection mold (Adaptive Science Tools).
5. 3 % agarose plate with microinjection groves: Dissolve 3 g agarose in 100 mL egg water and microwave until fully dissolved; cool the solution until safe to handle and pour in into a petri dish to make ~5 mm thick gel; lay the mold on the top of the liquid; allow agarose to solidify at room temperature; once solidified remove the mold; store at 4 °C.

2.7 Integration of ECs into Zebrafish (48 hpf Stage)

1. 3 % agarose plate: Dissolve 3 g agarose in 100 mL egg water and microwave until fully dissolved; cool the solution until safe to handle and pour in into a petri dish to make ~5 mm thick gel; store at 4 °C.
2. 10x Tricaine: 400 mg tricaine powder (Ethyl 3-aminobenzoate methanesulfonate salt, Sigma) in 97.9 mL deionized water, add ~2.1 mL of 1 M Tris (pH 9); adjust pH to ~7; store at −20 °C.
3. Fine forceps.
4. Stereomicroscope.
5. For other materials *see* Subheading 2.6.

2.8 Zebrafish Embryos Fixation and Whole Mount Staining Protocol

1. 4 % Paraformaldehyde (PFA): mix one part 16 % formaldehyde aqueous solution (PFA, Electron Microscopy Sciences) with three parts distilled water, store at 4 °C.
2. Methanol (Sigma-Aldrich).
3. PBS-0.1 % Tween®20 (PBS-T): 500 mL PBS, 500 μL Tween®20 (Sigma-Aldrich).
4. Proteinase K (10 μg/mL): 1 mg Proteinase K (Sigma-Aldrich) in 1 mL water (stock solution 1 mg/ml), store at −20 °C. Prepare working solution of Proteinase K (10 μg/ml) in PBS.
5. Primary antibodies: anti-Ki67 (Millipore), anti-Caspase-3 (Cell Signaling, 1:200), anti-PECAM1 (Scbt; M-20, 1:200).
6. Secondary antibodies: donkey anti-mouse and anti-rabbit Alexa568 (Life Technologies).

3 Methods

3.1 hPSC Culture

1. Culture hPSCs on Matrigel-coated 6-well plates in mTeSR™1 stem cell culture medium. Refresh cells with 2 mL of new mTeSR™1 daily (*see* **Note 1**).
2. Passage hPSCs once per week. Remove differentiated parts of hPSC colonies by scraping with a 10 μL pipet tip prior to passaging. Aspirate mTeSR™1 from the cells and add 1 mL of dispase solution in DMEM/F-12 (1 mg/mL). Incubate cells with dispase at 37 °C for 3–5 min. Aspirate dispase solution and wash cells three times with 2 mL of DMEM/F-12. Scrape hPSC colonies in DMEM/F-12 medium with a cell scraper and transfer them to a new 15 mL conical tube. Break colonies into small pieces with a 1 mL pipet tip.
3. Distribute 15–20 pieces to a new Matrigel-coated 6-well plate. Next day, and every day after, refresh the cells with 2 mL of new mTeSR™1 (*see* **Note 1**).

3.2 Differentiation of ECs from hPSCs

1. For the differentiation, distribute up to eight pieces (from Subheading 3.1**, step 3**) into a new Matrigel-coated 6-well plate. Next day, refresh the cells with 4 mL of new mTeSR™1 (for the schematic of differentiation *see* Fig. 1).
2. Induce mesoderm differentiation 3–4 days after passaging (day (0)) by replacing mTeSR™1 with 2 mL of BEL supplemented with 30 ng/mL BMP4, 50 ng/mL VEGF, 25 ng/mL ActivinA, and 1.5 μM CHIR99021 (BVAC).
3. Induce vascular specification at day (3) by replacing BVAC with 2 mL BEL supplemented with 50 ng/mL VEGF and 10 μM SB431542. Refresh vascular specification medium additionally on day (7) and day (9).

3.3 Isolation and Expansion of ECs from hPSCs

1. To isolate ECs, wash cells (from Subheading 3.2**, step 3**) twice with 2 mL PBS, and add 2 mL DMEM-0.1 % BSA. Add CD31 Dynabeads®. Seal the plate with Parafilm, and put on rotating platform for 20 min at room temperature.
2. Aspirate CD31 Dynabeads® and wash cells once with 2 mL PBS.
3. Add 0.5 mL 1× TrypLE and incubate for 3–5 min at room temperature.
4. Add 2 mL FACsB-10 %FBS and resuspend cells thoroughly. Filter cell suspension through CellTrics filter. Wash cell suspension additionally with 1 mL of FACsB-10 %.
5. Place cell suspension on DynaMag™-5 magnet. Aspirate the supernatant.
6. Resuspend cells in 2 mL FACsB (Subheading 2.3, **item 8**) Repeat **step 5**. Repeat **step 6** one more time.

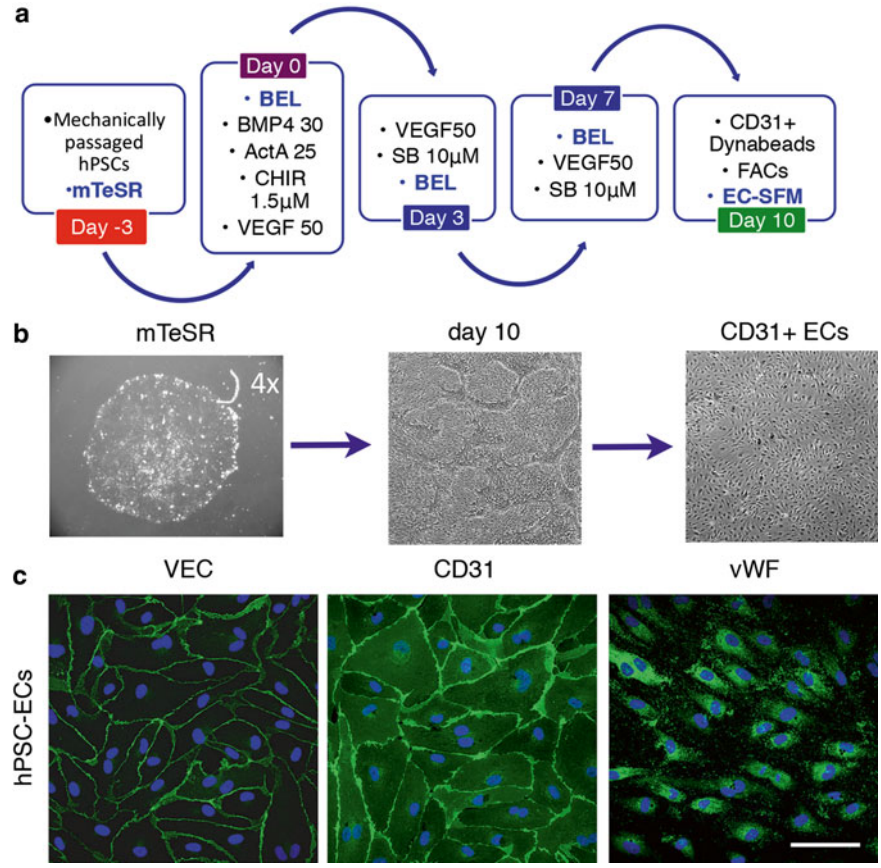

Fig. 1 Derivation of ECs from hPSCs. (**a**) Schematic of differentiation of ECs from hPSCs. (**b**) Representative phase-contrast images of undifferentiated hPSCs in mTeSR medium, EC islands at day 10 and isolated CD31+ ECs. (**c**) Representative immunofluorescent images of ECs derived from hPSCs stained for endothelial specific VE-Cadherin (VEC), CD31, von Willebrand factor (vWF, in *green*), and DAPI (in *blue*). Scale bar 100 μm. Adapted from: Orlova et al. (2014) *ATVB* **34**, 177–186

7. Resuspend cells in 2 mL DMEM-0.1 % BSA. Repeat **step 5**. Repeat **step 7** once more.
8. Resuspend cells in EC-SFM supplemented with 20 ng/mL bFGF, 30 ng/mL VEGF and 1 % platelet poor bovine serum (complete EC-SFM). Plate approximately 5,000 cells/cm^2 in EC-SFM complete medium into 0.1 % gelatin-coated plates.
9. Passage ECs until reaching 80–90 % confluence.

3.4 Preparation of ECs for the Injection

1. Prepare one T25 culture flask of the sub-confluent (80–90 %) ECs.
2. Wash ECs once with PBS.
3. Incubate ECs with 1 mL 1× TrypLE for 3–5 min at room temperature. Inactivate TrypLE with 4 mL EC-SFM.

Transfer cells to the 15 mL conical falcon tube. Centrifuge cells at 300 × *g* for 3 min.

4. Label ECs with general cytoplasmic labeling agent (Cm Dil) according to the manufacturer's instructions.
5. Resuspend ECs in basal serum-free medium (EBM-2) (*see* **Note 2)** and place cells on ice.

3.5 Zebrafish Egg Laying and Embryo Production

1. Zebrafish are maintained according to the institutional animal good practice regulations.
2. For egg production, set up a single cross breeding of Tg(fli1:GFP) at the end of the light cycle or in the afternoon. Upon the beginning of the next light cycle, female zebrafish will initiate egg production that will be fertilized by males (*see* **Note 3**).
3. Collect fertilized eggs about 1 h after the beginning of the light cycle. Wash zebrafish embryos in the clean egg water. Distribute approximately 60 eggs per petri dish and store eggs at 28 °C until zebrafish are roughly 2 hpf (for the blastula stage implantation) or 48 hpf (for the 48 hpf implantation).

3.6 Integration of EC into Zebrafish (Blastula Stage)

1. For the implantation ECs should be ready for the injection before the embryos are 2 hpf (*see* Subheading 3.4). Ideally implantation of ECs should be performed on the embryos of the same stage and not later than 4 hpf (*see* **Note 4**). On average 80–100 embryos are injected.
2. For the implantation procedure, five to ten embryos are positioned on a 10 cm petri dish coated with 3 % agarose with appropriate molded groves. Molds are used to help place the embryos into the correct position prior to injection. If the embryo needs to be moved, use a fine tipped paintbrush and gently push the embryo into place. During the injection procedure it is important to keep the embryos moist.
3. Inject approximately 100 cells through the blastula into an area slightly above the margin (of cells and yolk) and on the ventral side (Fig. 2a). For the injection of cells up to 10 μL of the single cell suspension are loaded into the borosilicate glass capillary. Cells are injected with the Pneumatic PicoPump (*see* **Note 2**).
4. Transfer embryos to the petri dish filled with the fresh egg water. The survival and development of the injected embryos should be monitored by comparing with a control, uninjected group. The correctly injected embryos are maintained at 33 °C (*see* **Note 4**). The egg water should be refreshed every second day. Embryo survival is monitored every day. In case the survival rate is lower than 50 % the experiment should be terminated.

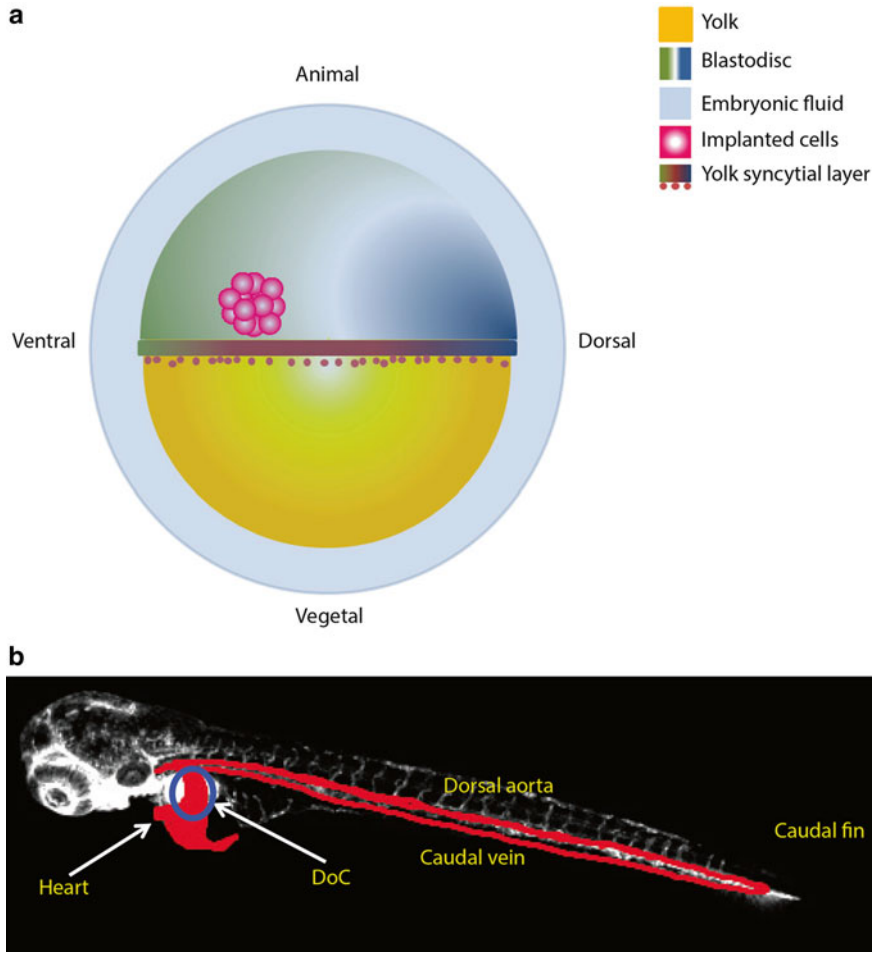

Fig. 2 Schematic of ECs injection in blastula stage (**a**) and 48 hpf (**b**). The injection site of cells into 48 hpf embryos is shown in the *blue circle*

3.7 Integration of ECs into Zebrafish (48 hpf Stage)

1. For the implantation of ECs into 48 hpf embryos, prior to the injection of cells (~47 hfp) embryos should be dechorionized (special procedure for the chorion removal) (*see* **Note 5**). The chorion removal is performed with fine forceps under a stereomicroscope. Approximately 50–100 embryos per group should be dechorionized for the implantation. Upon dechorionization, return the embryos to the 28 °C incubator.
2. Anesthetize dechorionized embryos by placing them into egg water with the 1x Tricaine solution. For the implantation procedure, place five to ten anesthetized embryos on 3 % agarose-coated 10 cm petri dish. During the injection procedure, embryos should be kept moist.
3. Inject about 400 cells ± 60 μm above the ventral end of the Duct of Cuvier (DoC), where the duct opens into the heart (Fig. 2b). For the injection of cells up to 20 μL of the single

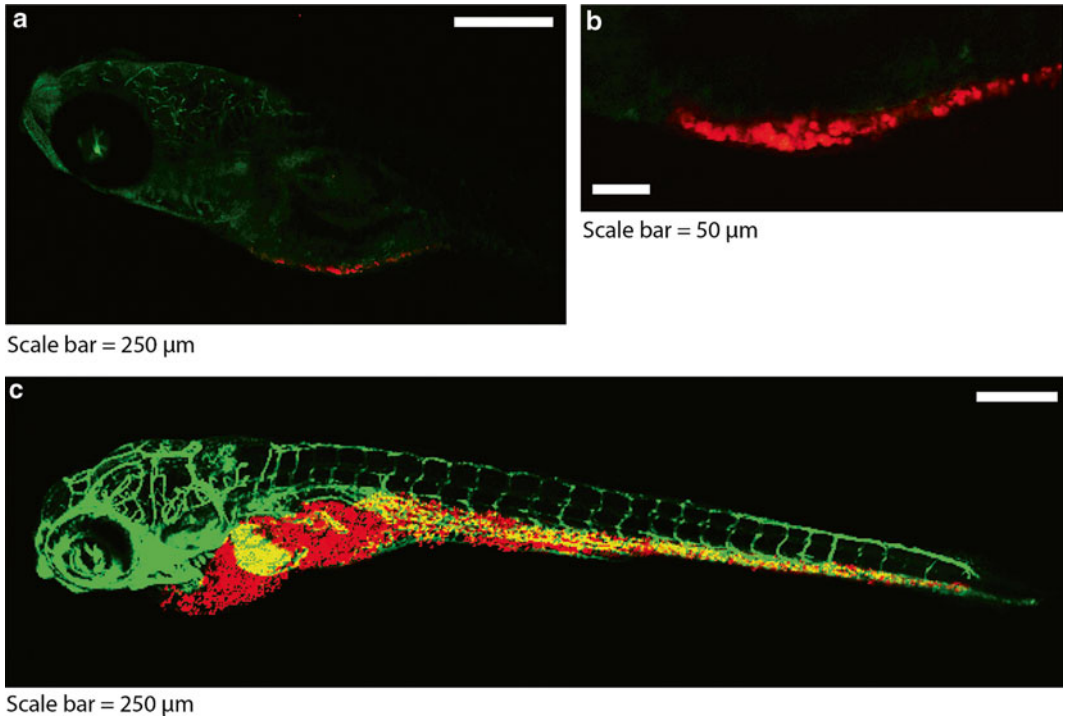

Fig. 3 Integration of ECs into zebrafish vessels. Representative images of blastula stage injected hPSC-ECs (**a**, **b**) and 48 hpf injected hPSC-ECs (**c**). Scale bar 250 μm (**a**, **c**) and 50 μm (**b**)

cell suspension are loaded into the borosilicate glass capillary. Cells are injected with the Pneumatic PicoPump (*see* **Note 2**).

4. Transfer embryos to the petri dish filled with the fresh egg water. The survival of the injected embryos should be monitored daily. The correctly injected embryos are maintained at 33 °C (*see* **Note 4**). The egg water should be refreshed every other day. If the survival rate is lower than 80 % the experiment should be terminated.

3.8 Zebrafish Embryos Fixation and Whole Mount Staining Protocol

1. Fix zebrafish embryos by incubation in 4 % PFA overnight at 6 or 5 days post implantation (dpi) for the blastula stage or 48 hpf injection of cells, respectively. The fixed embryos can be stored in PBS at 4 °C for the subsequent confocal analysis (Fig. 3) or the immunofluorescent staining procedure (Fig. 4).
2. Dehydrate fixed zebrafish embryos in 100 % methanol for 15 min at room temperature. Place 100 % methanol-immersed embryos at −20 °C for additional 2 h.
3. Rehydrate embryos by immersing them subsequently into a methanol gradient: 75 % methanol, 50 % methanol, and 25 % methanol in PBS-0.1 % Tween-20 (PBS-T) for 5 min at room temperature. Wash embryos additionally four times in PBS-T for 5 min per wash.

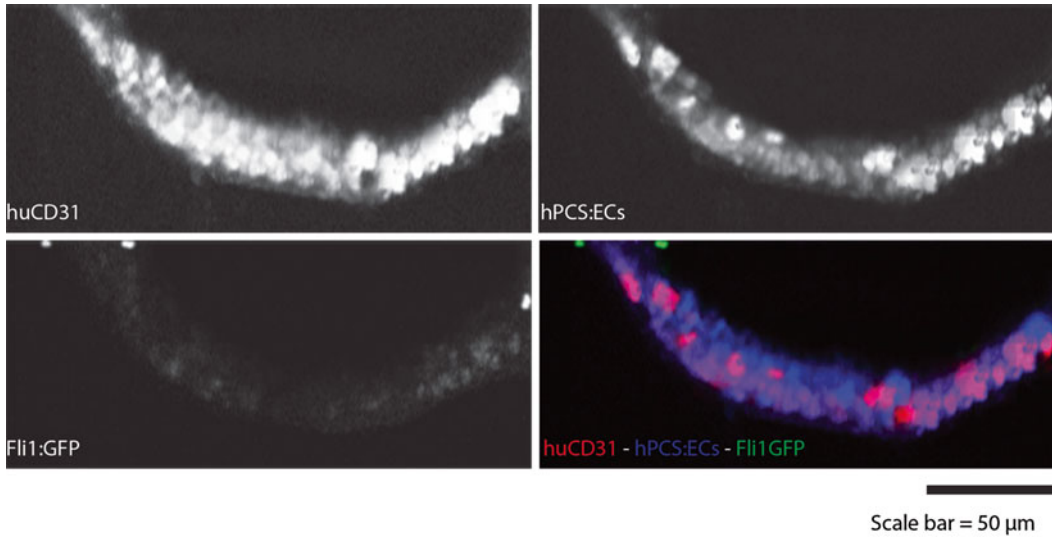

Fig. 4 Zebrafish whole mount staining. Immunofluorescent staining of zebrafish embryos at 6 dpf with hPSC-ECs injected at blastula stage for human specific CD31 (huCD31), hPSC-ECs, and zebrafish vasculature Tg(fli1:GFP) and overlay image. Scale bar 50 µm

4. Permeabilize embryos with proteinase K (10 µg/mL) for 30 min at room temperature. Wash embryos with PBS-T and block with 1 % BSA in PBS-T for 2 h at room temperature.
5. Incubate embryos with the primary antibody in PBS-T at 4 °C overnight.
6. Rinse embryos three times with PBS-T, and wash additionally four times in PBS-T for 10 min per wash.
7. Block embryos in 1 % BSA in PBS-T for 1 h at room temperature.
8. Incubate embryos with secondary antibodies (far red labeled) in PBS-T at room temperature for 2 h.
9. Rinse embryos three times with PBS-T, and wash additionally three times in PBS-T for 10 min per wash.
10. Embryos can be stored in PBS at 4 °C for subsequent confocal analysis.

4 Notes

1. The medium is refreshed daily except the weekends when it is possible to add 6 mL mTeSR™1 from Friday until Monday to the cells.
2. Cell concentration should be optimized prior to injection in zebrafish. We advise starting with ~5×10^7 cells/mL. The number of cells can be estimated by the size of the cell droplet injected onto the agarose plate, and by counting.

3. Zebrafish breeding behavior depends on the light cycle that is typically divided into 14 h of light and 10 h of dark. On average single cross breeding pair one male and one female can produce up to 100 eggs per day.
4. It is possible to slow the development of the embryo down by keeping them at a temperature lower than 28 °C. Although this is not recommended for long periods of time, it can be useful for extending the development time to ensure that the most embryos are injected correctly. As such, the embryos may be kept between 18 and 22 °C while the cells are being prepared and during the implantation procedure. Zebrafish embryos develop normally at 28 °C, and mammalian cells grow at 37 °C; therefore, upon injection of mammalian cells, it is advisable to place zebrafish embryos at 33 °C. It has been noticed that placing embryos at 33 °C upon injection does not significantly affect behavior or development.
5. It is advisable to perform dechorionization prior to injection of cells and not earlier than 40 hpf, since dechorionized embryos can easily be damaged.

Acknowledgments

The authors would like to thank Francijna E. van den Hil for technical assistance.

We are grateful for financial support from LUMC (Gisela Thier Fellowship, V.V.O); the Netherlands Institute of Regenerative Medicine and the Netherlands Heart Foundation (2008B106) (C.L.M.); Cancer Genomics Centre and LeDucq Foundation (P.D.).

References

1. Santoriello C, Zon LI (2012) Hooked! Modeling human disease in zebrafish. J Clin Invest 122:2337–2343. doi:10.1172/JCI60434
2. Lawson ND, Wolfe SA (2011) Perspective. Dev Cell 21:48–64. doi:10.1016/j.devcel.2011.06.007
3. Stoletov K, Klemke R (2008) Catch of the day: zebrafish as a human cancer model. Oncogene 27:4509–4520. doi:10.1038/onc.2008.95
4. Zon LI, Peterson RT (2005) In vivo drug discovery in the zebrafish. Nat Rev Drug Discov 4:35–44. doi:10.1038/nrd1606
5. Gore AV, Monzo K, Cha YR et al (2012) Vascular development in the zebrafish. Cold Spring Harb Perspect Med 2:a006684–a006684. doi:10.1101/cshperspect.a006684
6. Nicoli S, Ribatti D, Cotelli F, Presta M (2007) Mammalian tumor xenografts induce neovascularization in zebrafish embryos. Cancer Res 67:2927–2931. doi:10.1158/0008-5472.CAN-06-4268
7. Traver D, Herbomel P, Patton EE et al (2003) The Zebrafish as a model organism to study development of the immune system. Adv Immunol 81:254–330
8. Orlova VV, Drabsch Y, Freund C et al (2013) Functionality of endothelial cells and pericytes from human pluripotent stem cells demonstrated in cultured vascular plexus and zebrafish xenografts. Arterioscler Thromb Vasc Biol 34:177–186. doi:10.1161/ATVBAHA.113.302598

9. Drabsch Y, He S, Zhang L et al (2013) Transforming growth factor-β signalling controls human breast cancer metastasis in a zebrafish xenograft model. Breast Cancer Res 15:1–1. doi:10.1186/bcr3573
10. Thomson JA, Itskovitz-Eldor J, Shapiro SS et al (1998) Embryonic stem cell lines derived from human blastocysts. Science 282:1145–1147
11. Yu J, Vodyanik MA, Smuga-Otto K et al (2007) Induced pluripotent stem cell lines derived from human somatic cells. Science 318:1917–1920. doi:10.1126/science.1151526
12. Takahashi K, Tanabe K, Ohnuki M et al (2007) Induction of pluripotent stem cells from adult human fibroblasts by defined factors. Cell 131:861–872. doi:10.1016/j.cell.2007.11.019
13. Kusuma S, Shen Y-I, Hanjaya-Putra D et al (2013) Self-organized vascular networks from human pluripotent stem cells in a synthetic matrix. Proc Natl Acad Sci. doi:10.1073/pnas.1306562110
14. Cheung C, Bernardo AS, Trotter MWB et al (2012) Generation of human vascular smooth muscle subtypes provides insight into embryological origin–dependent disease susceptibility. Nat Biotechnol 30:165–173. doi:10.1038/nbt.2107
15. White MP, Rufaihah AJ, Liu L et al (2012) Limited Gene Expression Variation in Human Embryonic Stem Cell and Induced Pluripotent Stem Cell-Derived Endothelial Cells. Stem Cells 31:92–103. doi:10.1002/stem.1267
16. Pozzoli O, Vella P, Iaffaldano G et al (2011) Endothelial Fate and Angiogenic Properties of Human CD34+ Progenitor Cells in Zebrafish. Arterioscler Thromb Vasc Biol 31:1589–1597. doi:10.1161/ATVBAHA.111.226969
17. Ng ES, Davis R, Stanley EG, Elefanty AG (2008) A protocol describing the use of a recombinant protein-based, animal product-free medium (APEL) for human embryonic stem cell differentiation as spin embryoid bodies. Nat Protoc 3:768–776. doi:10.1038/nprot.2008.42
18. Lawson ND, Weinstein BM (2002) In Vivo Imaging of Embryonic Vascular Development Using Transgenic Zebrafish. Dev Biol 248:307–318. doi:10.1006/dbio.2002.0711

Chapter 11

Stem Cell Therapy for Necrotizing Enterocolitis: Innovative Techniques and Procedures for Pediatric Translational Research

Jixin Yang, Yanwei Su, and Gail E. Besner

Abstract

Necrotizing enterocolitis (NEC) is the most common gastrointestinal emergency of newborns, especially those born prematurely. Mesenchymal stem cell (MSC) therapy has shown efficacy in protection against various forms of tissue injury, and we have demonstrated efficacy in experimental NEC. However, few studies have been performed to establish a safe and effective method of intravenous MSC infusion for newborns. Here we described a safe, non-traumatic, and effective technique for systemic MSC transplantation in newborn rats.

Key words Necrotizing enterocolitis, Mesenchymal stem cells, Transplantation, Intravenous injection

1 Introduction

Necrotizing enterocolitis (NEC) is the most common gastrointestinal emergency of newborns, occurs most frequently in premature babies, and has an associated mortality ranging from 20 to 50 % [1]. Mesenchymal stem cells (MSC) have been shown to protect various tissues including the intestines from injury [2, 3]. Local stem cell (SC) delivery may result in increased risk of bleeding and tissue injury when administered by intralesional injection, and occlusion when administered intra-arterially [4–6]. Intravenous (IV) infusion has been used for systemic SC delivery in preclinical studies and in clinical trials. However, it has been noted that a large fraction of systemically infused MSC become trapped in the lungs, and pulmonary sequestration after MSC intravascular infusion causes mortality ranging from 25 to 40 % [7].

One of the goals of our laboratory is to devise novel therapeutic strategies to prevent or treat neonatal NEC. For neonatal studies, the small size of the vascular system creates considerable challenges for IV stem cell administration. The ability to successfully perform

Bruno Christ et al. (eds.), *Animal Models for Stem Cell Therapy*, Methods in Molecular Biology, vol. 1213,
DOI 10.1007/978-1-4939-1453-1_11,

neonatal rat IV injections should prove useful in studies of many neonatal diseases due to premature delivery, including NEC, respiratory distress syndrome, retinopathy of prematurity, and others. Here we introduce an innovative, non-traumatic, and effective technique for systemic MSC transplantation in newborn rat pups immediately after birth. This technique allows good visualization to confirm successful injection, is easy to perform, has a short operating time, a high success rate, high efficiency of systemic MSC delivery, and a low mortality rate. Administration of MSC using this technique, combined with administration of growth factors, specifically heparin-binding EGF-like growth factor (HB-EGF), is highly effective in protecting the intestines from experimental NEC [8].

2 Materials

2.1 Animals

1. Homozygous 129-Tg(CAG-eYFP)7AC5Nagy/J mice are used as a source of YFP-labeled bone marrow-derived mesenchymal stem cells (BM-MSC) [9]. Initially, a transgenic construct (pCX::EYFP) containing an enhanced YFP gene under the control of a chicken beta actin promoter, coupled with the cytomegalovirus (CMV) immediate early enhancer, was introduced into (129X1/SvJ x 129S1/Sv) F1-derived R1 mouse embryonic stem (ES) cells (http://jaxmice.jax.org/strain/005483.html). The YFP-labeled BM-MSC line can be used for eight to ten passages after cell isolation (*see* **Note 1**).
2. Time pregnant Sprague–Dawley rats (Harlan, Indianapolis, IN) are used for delivery of premature rat pups by Cesarean section (C-section) at gestational day 21 (E21).
3. After delivery by C-section, the premature newborn rat pups (average weight 5.2 g) are placed in a neonatal incubator for temperature control. The placentas of the pups are kept moist and warm, and the integrity of the umbilical cords maintained for injection.
4. All animals are bred in a specific pathogen free environment with exposure to normal diet and water.

2.2 Culture Reagents for Bone Marrow-Derived Mesenchymal Stem Cells (BM-MSC)

1. Culture medium: Dulbecco's Modified Eagle Medium (D-MEM) Nutrient Mixture F-12/GlutaMAX-ITM medium (GIBCO Invitrogen; Carlsbad, CA).
2. Medium supplements: 10 % MSC-qualified fetal bovine serum (FBS) (GIBCO, Grand Island, NY) and 0.01 % gentamicin (GIBCO, Grand Island, NY).
3. Phosphate Buffer Solution (PBS) for tissue/cell rinse (GIBCO, Grand Island, NY).
4. Trypsin for cell/tissue digestion: 0.25 % (Cellgro, Manassas, VA).

5. 70 μm nylon mesh (Becton Dickinson; Franklin Lakes, NJ).
6. Hemocytometer.

2.3 Identification and Differentiation Assays

1. Anti-vimentin monoclonal antibody at a 1:50 dilution (Thermo Scientific; IL, USA) for identification of the MSC marker Vimentin and Cy3-labeled donkey anti-mouse antibody at a 1:500 dilution (Jackson ImmunoResearch, West Grove, PA) as the secondary antibody.
2. 4′,6-Diamidino-2-Phenylindole Dihydrochloride (DAPI) (Vector Laboratories, Burlingame, CA) for counterstaining of nuclei.
3. Adipogenic and Osteogenic Differentiation kits (GIBCO Invitrogen, Grand Island, NY) to confirm differentiation of MSC.
4. Alizarin Red S solution (pH 4.2).
5. Oil Red O staining.
6. Paraformaldehyde for cell fixation (Santa Cruz Biotechnology, Dallas, TX).
7. Tissue embedding reagent: Tissue-Tek Optimal Cutting Temperature (OCT) (Sakura Finetek, Torrance, CA).
8. Tissue fixation reagent: 1 % paraformaldehyde, 15 % picric acid, and 0.1 M sodium phosphate buffer (pH 7.0)
9. Vectashield mounting medium (Vector Laboratories, Burlingame, CA).
10. Fluorescent microscope (Axioscope, Carl Zeiss; Jena, Germany) for observation of fluorescent signals.

2.4 Detection of Intra-Umbilical Vein Injection

1. Ultrasound machine (VisualSonics Vevo 2100) with a 40 MHz transducer (Visualsonics, Toronto, Ontario) for in vivo cardiac structure identification.
2. Methylene blue (10 %) (Thermo Scientific, Hudson, NH) to confirm intravascular injection, and for tracking the route of the dye after intra-umbilical vein injection.
3. Ultrasound gel (Aquasonic, Parker Labs, Fairfield, New Jersey).

2.5 BM-MSC Intravenous Administration

1. Polyethylene-10 (PE-10) tubing (Becton Dickinson, Sparks, MD) for umbilical vein catheterization.
2. Atraumatic micro vessel clips (Roboz Surgical Instrument, Gaithersburg, MD) to secure PE-10 tubing.
3. Low-dose U-100 insulin syringes with 29 G needles (200 μL, Becton Dickinson; Franklin Lakes, NJ) for MSC administration.
4. A three-dimension laboratory shaker (Labnet International, Edison, NJ) with a container holding crushed ice to keep the MSC in syringes cool prior to injection.

2.6 NEC Induction

1. Hypertonic formula containing 15 g of Similac 60/40 (Ross Pediatrics, Columbus, OH) in 75 mL of Esbilac (Pet-Ag, New Hampshire, IL).
2. Intragastric lipopolysaccharide derived from Salmonella (LPS, 2 mg/kg, Sigma-Aldrich, St. Louis, MO).
3. Nitrogen.

2.7 NEC Evaluation

1. 10 % formalin.
2. Paraffin.
3. Hematoxylin and eosin (H and E).

3 Methods

3.1 Culture of BM-MSC and Preparation for Injection

1. For initial isolation of BM-MSC, harvest bone marrow from the femurs and tibias of hind limbs (*see* **Note 2**) and suspend the bone marrow in D-MEM Nutrient Mixture F-12/GlutaMAX-ITM medium.
2. Pipet and filter the cell mixture through a cell strainer with 70 μm nylon mesh.
3. Seed cells in D-MEM Nutrient Mixture F-12/GlutaMAX-ITM medium supplemented with 10 % MSC-qualified FBS and 0.01 % gentamicin at 37 °C in 5 % CO_2.
4. Change culture medium every 4 days and remove non-adherent cells.
5. Prior to MSC injection, trypsinize adherent cells for 3 min and then neutralize the trypsin with D-MEM/F-12/GlutaMAX-ITM medium supplemented with 10 % MSC-qualified FBS.
6. Quantify cells using a hemocytometer and centrifuge the cells at $350 \times g$ for 5 min at 4 °C.
7. Discard supernatants and resuspend the cell pellets in sterile PBS.
8. Filter the suspended MSC through a cell strainer with 70 μm nylon mesh before injection.
9. Adjust the concentration of MSC to 7.5×10^6 cells/mL for injection.
10. Load MSC suspensions into 0.3 mL low-dose U-100 insulin syringes with 29 G needles.
11. Prior to IV infusion, maintain syringes at 4 °C with continuous shaking and resuspend MSC gently to ensure they are not aggregated prior to infusion.

3.2 Identification of MSC

1. To confirm that the cultured cells are MSC, fix the cells in 4 % paraformaldehyde at 4 °C for 20 min and rinse the cells in PBS three times.

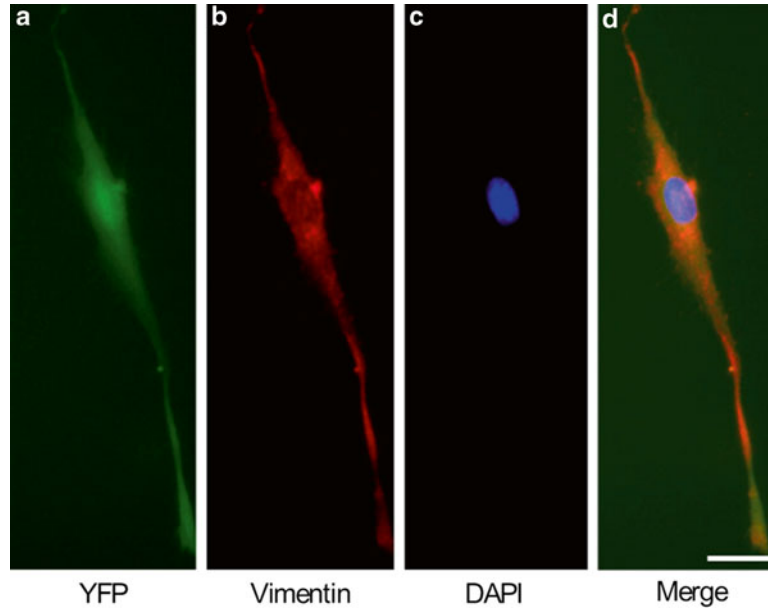

Fig. 1 MSC immunocytochemistry. (**a**) YFP, green fluorescence; (**b**) vimentin, red fluorescence; (**c**) DAPI nuclear staining; (**d**) merged images. 400× magnification, scale bar = 15 μm. *MSC* mesenchymal stem cells, *YFP* yellow fluorescent protein, *DAPI* 4′,6-Diamidino-2-Phenylindole Dihydrochloride

2. Perform immunocytochemistry by incubation with primary mouse anti-Vimentin monoclonal antibodies (to detect the MSC marker Vimentin) at a 1:50 dilution for 2 h at room temperature.
3. Rinse the cells with PBS three times, and incubate the cells with Cy3-labeled donkey anti-mouse secondary antibody at a 1:500 dilution for 1 h at room temperature. Rinse the cells with PBS three times.
4. Counterstain nuclei using DAPI.
5. Observe fluorescent signals using a fluorescent microscope using green fluorescence protein (GFP), Cy3 and DAPI channels (Fig. 1).
6. To confirm the ability of MSC to differentiate, grow cells in adipogenic or osteogenic differentiation media for 15 days using Adipogenic and Osteogenic Differentiation kits.
7. Use MSC cultured without adipogenic or osteogenic differentiation media as undifferentiated controls (*see* **Note 3**).
8. For osteogenic differentiation, use a 60–80 % subconfluent culture of MSC from passages 2–4, and replace osteogenic differentiation medium twice a week.
9. After 15 days in differentiation medium, add Alizarin Red S solution (pH 4.2) to the cultures for 3 min and remove the solution.

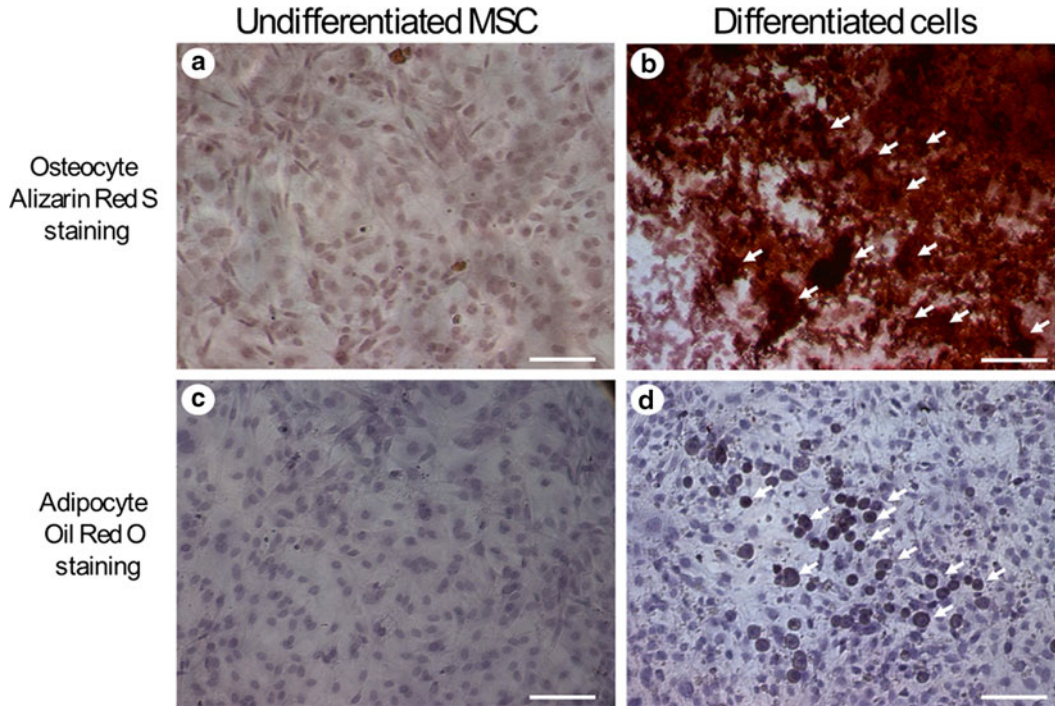

Fig. 2 In vitro MSC differentiation assay. (**a**) and (**c**) undifferentiated MSC; (**b**) differentiated MSC grown in osteogenic medium had extracellular calcium deposits and stained positively with Alizarin Red S (*white arrows*); (**d**) differentiated MSC grown in adipogenic medium had accumulation of lipid droplets and stained positively with Oil Red O (*white arrows*). 100× magnification, scale bar = 50 μm

10. For adipogenic differentiation, grow MSC in adipogenic differentiation medium and replace the medium twice a week. Perform Oil Red O staining 15 days later (Fig. 2).

3.3 C-Section Rat Pup Delivery

1. Perform C-section on time pregnant Sprague–Dawley rats under CO_2 anesthesia on day 21 of gestation (*see* **Note 4**).
2. After delivery, keep placentas moist and warm, and maintain the integrity of the umbilical cords for injection (*see* **Note 5**). Place the premature newborn rats in a neonatal incubator for temperature control (*see* **Notes 6** and **7**).

3.4 Intravenous Injection of Methylene Blue into Cannulated Umbilical Veins

1. Inject rat pups with methylene blue dye to confirm that the injected fluid enters the systemic circulation after injection.
2. Inject a volume of 40 μL of methylene blue via the PE-10 tubing used to cannulate the umbilical vein.
3. Open the abdominal wall in order to track the methylene blue in the organs inside the abdominal cavity (Fig. 3) (*see* **Note 8**).

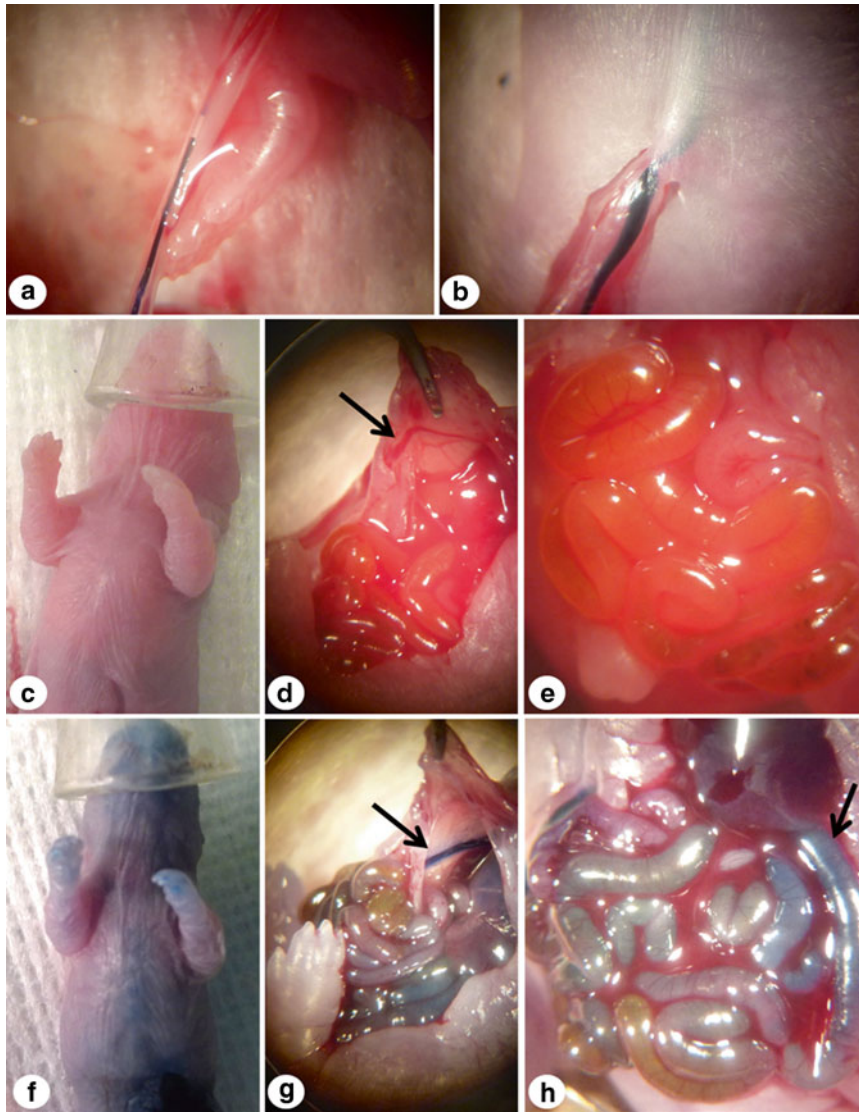

Fig. 3 Tracking of methylene blue dye in the systemic circulation. (**a**) Prior to injection, showing the catheter in the umbilical vein; (**b**) after injection, showing blue dye entering the umbilical vein; (**c**) pink skin prior to dye injection; (**d**) the internal umbilical vein (*black arrow*) prior to dye injection; (**e**) intestines prior to dye injection; (**f**) blue discoloration of the skin immediately after dye injection; (**g**) internal aspect of the umbilical vein (*black arrow*) after dye injection; (**h**) blue discoloration of the intestines several seconds after dye injection (*black arrow*)

3.5 Ultrasonographic Scanning of Right-to-Left Shunt in Newborn Rat Pups

1. Identify the cardiac structures using a VisualSonics Vevo 2100 ultrasound machine with a 40 MHz transducer.
2. After umbilical vein cannulation, move rat pups to a heated procedure board.

3. Place pre-warmed ultrasound gel on the chest and place a 15 MHz probe (optimized and dedicated to rodent studies) in a subcostal orientation and obtain a four chamber apical view.
4. After obtaining the four chamber view, visualize and locate the patent foramen ovale (PFO) (*see* **Note 9**).
5. Subsequently, inject the sample volume to the level of the PFO and capture baseline shunt flow by using pulsed wave Doppler channel (*see* **Note 10**).
6. When injecting MSC suspensions, record extra waves and changes of wave shapes (Fig. 4).

3.6 Monitoring of Animals After Intravenous MSC Infusion

1. Transfer prematurely delivered newborn rats to surrogate rat mothers and monitor for 96 h.
2. Record immediate deaths and deaths within 24 h of MSC injection.

3.7 Quantification of MSC Engraftment

1. Ninety-six hours after MSC administration, euthanize rat pups that received systemic MSC and control rat pups that received an equal volume of PBS injection, by carbon dioxide asphyxiation followed by exsanguination.
2. Harvest lungs, hearts, and intestines and fix the organs in fixation solution shaken gently at 4 °C overnight.
3. Embed samples in Tissue-Tek Optimal Cutting Temperature (OCT) compound and make frozen sections (10 μm).
4. Wash slides with PBS three times and mount the slides with VECTASHIELD mounting medium for fluorescence with DAPI.
5. Observe fluorescence under a fluorescence microscope using GFP and DAPI channels.
6. Perform quantification of MSC by counting YFP-positive cells per visual field at 100× magnification (Fig. 5).

3.8 Vimentin Staining of MSC in the Mucosa of Intestinal Villi

1. Prepare frozen sections of OCT-embedded intestines and rinse sections in PBS three times.
2. Incubate slides with mouse anti-Vimentin monoclonal antibody overnight at 4 °C.
3. Rinse slides with PBS three times and incubate the slides with Cy3-labeled donkey anti-mouse antibody for 1 h at room temperature.
4. Observe fluorescence under a fluorescent microscope using GFP and Cy3 channels at 400x magnification (Fig. 6).

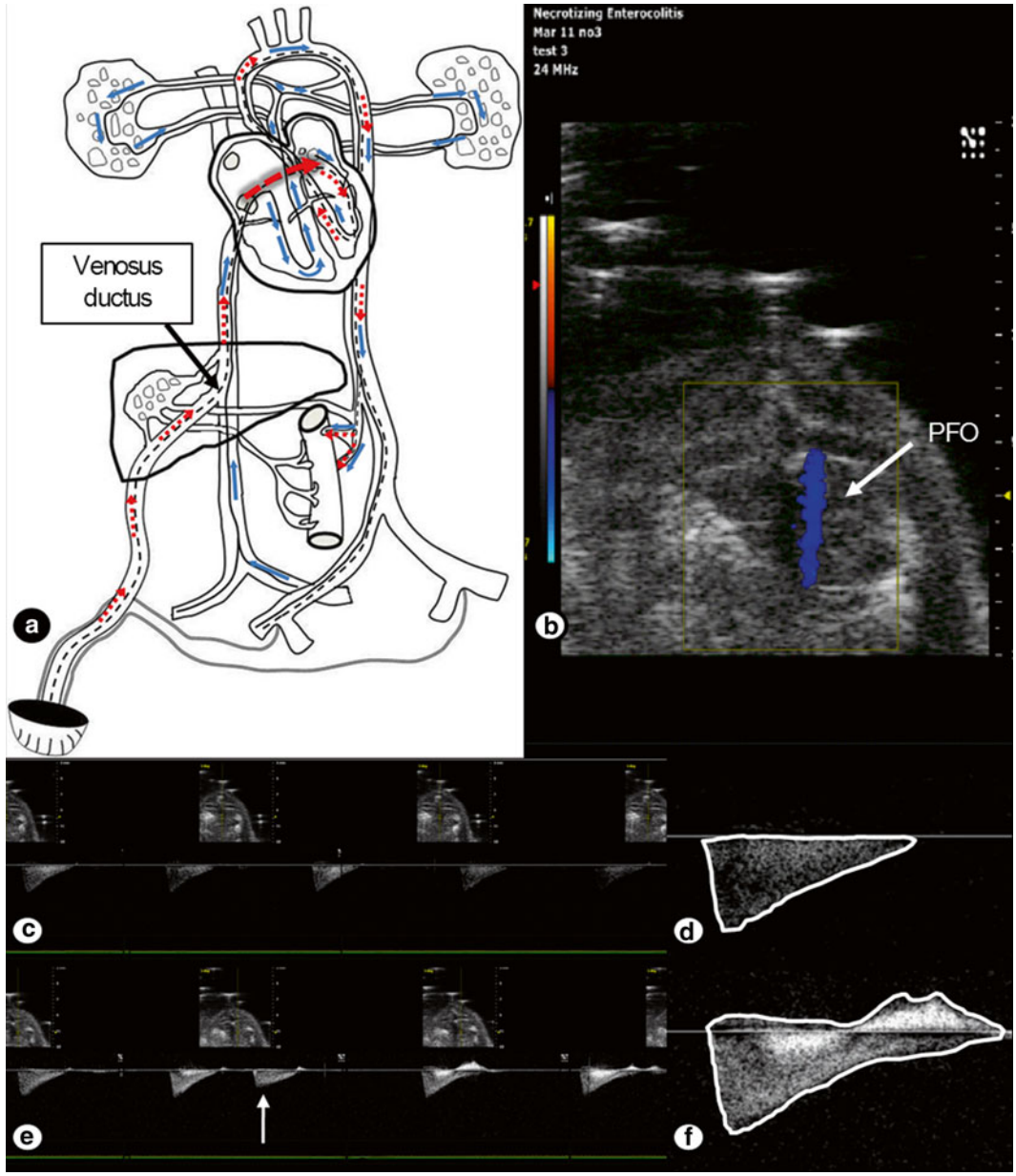

Fig. 4 Right-to-left shunt in newborn premature rat pups. (**a**) Diagram illustrating a right-to-left shunt in a newborn rat pup. Small red dashed arrows show the route of the mesenchymal stem cells (MSC) delivered via the umbilical vein through the ductus venosus (*black arrow*) into the systemic circulation and the peripheral organs. *Blue arrows* show the blood circulation. The shunt is through the patent foramen ovale (PFO) from the right to the left atrium (*large red dashed arrow*); (**b**) Doppler ultrasound imaging demonstrating PFO with right-to-left shunt between the atria (*white arrow*); (**c**) Pulse wave ultrasound scanning showing the right-to-left shunt prior to injection. The pulse waves are regular; (**d**) The wave shape of the shunt detected at the site of the PFO of a premature rat pup; (**e**) Extra wave detected after the normal wave at the time of injection of stem cells (*white arrow*); (**f**) Several following waves had a longer wavelength and higher wave peak

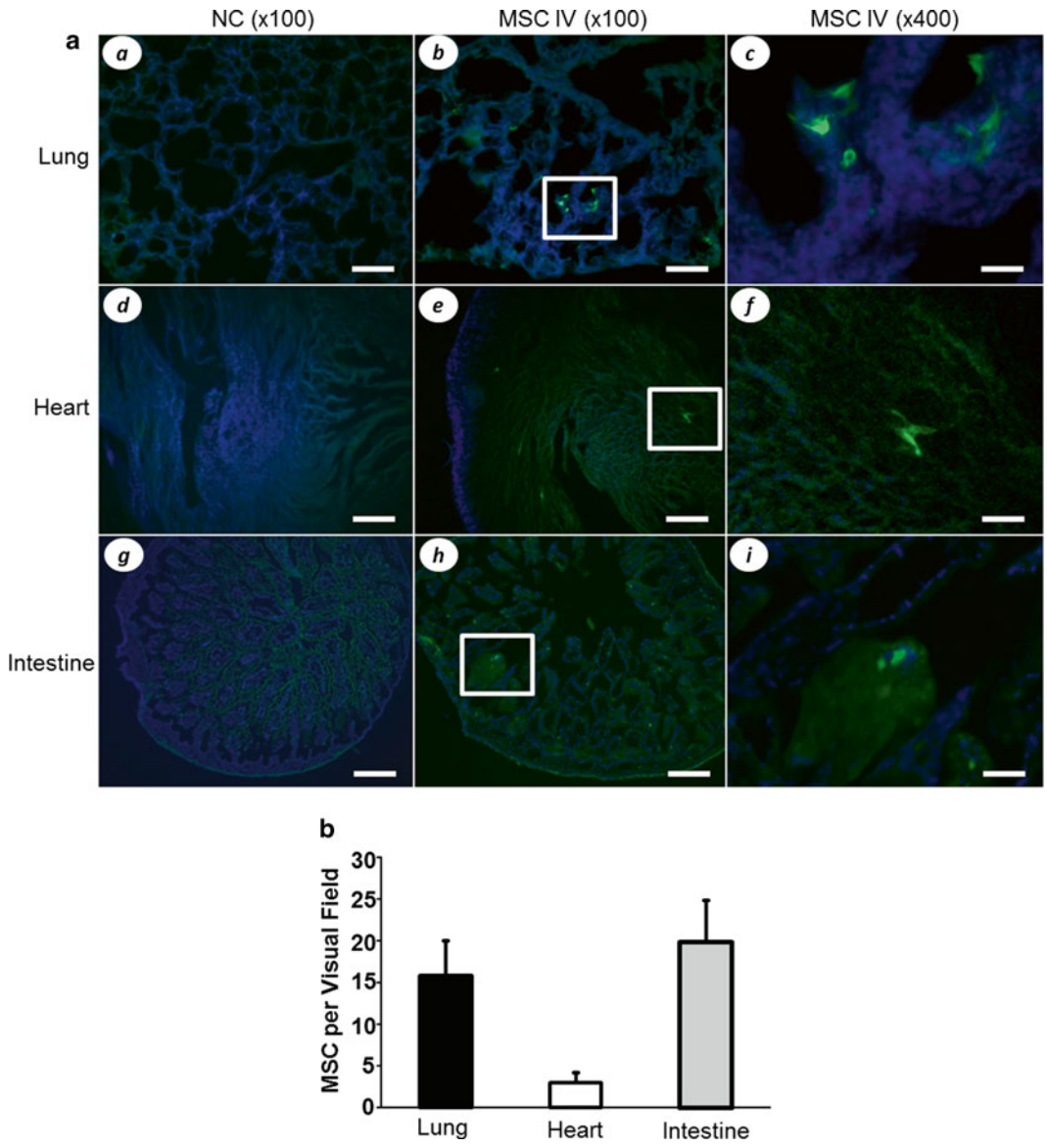

Fig. 5 Distribution and quantification of MSC after systemic infusion. (**a**) Distribution of MSC in the lung, heart and intestine after IV injection in newborn rat pups. Nuclei are stained with DAPI. YFP-positive cells are demonstrated by green fluorescence. (**a, d, g**) Control pups that received PBS injection only, 100× magnification. Scale bar = 50 μm; (**b, e, h**) Pups received 300×10^3 MSC IV, 100× magnification. Scale bar = 50 μm; (**c, f, i**) High power view of the areas contained within the white rectangles in panels **b**, **e**, **h**. 400× magnification. Scale bar = 12.5 μm; (**b**) Quantification of YPF-positive cells in the lung, heart and intestine

3.9 Rat Model of NEC

1. After MSC administration, subject pups to experimental NEC using a modification of the methods initially described by Barlow et al. [10] (*see* **Note 11**).
2. Keep pups in an incubator at 35 °C and feed the pups with hypertonic formula containing 15 g of Similac 60/40 in 75 mL of Esbilac, which provides 836.8 kJ/kg per day.

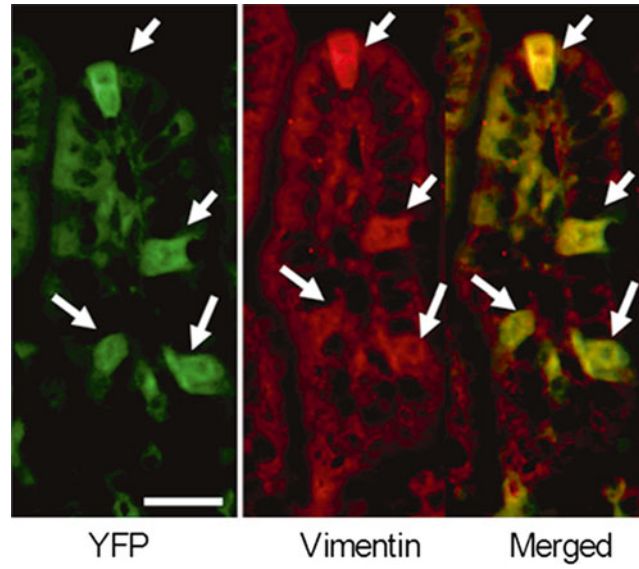

Fig. 6 Vimentin immunofluorescence in engrafted MSC. Immunofluorescence of vimentin in the cytoplasm of engrafted MSC in the mucosa of the intestine 96 h after systemic MSC administration. *White arrows* indicate the YFP-MSC which have engrafted into the villi. Scale bar = 12.5 μm

3. Starting with 0.1 mL of formula every 4 h, advance the volume of formula to a maximum of 0.4 mL per feed by the fourth day of life.
4. Give intragastric lipopolysaccharide (LPS) (2 mg/kg) prior to the first feed.
5. Immediately after feeding, expose pups to hypoxia (100 % nitrogen for 1 min), followed by hypothermia (4 °C for 10 min) twice a day until the end of the experiment (Fig. 7).
6. Upon the development of clinical signs of NEC, euthanize pups immediately by cervical dislocation.
7. Euthanize all surviving animals after 96 h.
8. Record survival of all pups daily.

3.10 NEC Evaluation

1. Immediately upon sacrifice, remove intestines carefully and inspect visually for typical signs of NEC including intestinal dilation (diameter ≥2.5 mm at the ileum), intestinal narrowing (diameter ≤1.0 mm at the ileum), perforation, intraluminal bleeding, and subserosal collections of gas (pneumatosis) (Fig. 8) (*see* **Note 12**).
2. Record findings using the template shown in Table 1.
3. Fix the terminal ileum in 10 % formalin for 24 h and make paraffin-embedded sections. Perform hematoxylin and eosin (H and E) staining to evaluate the grade of histologic injury using a standard histological scoring system [11] (*see* **Note 13**).

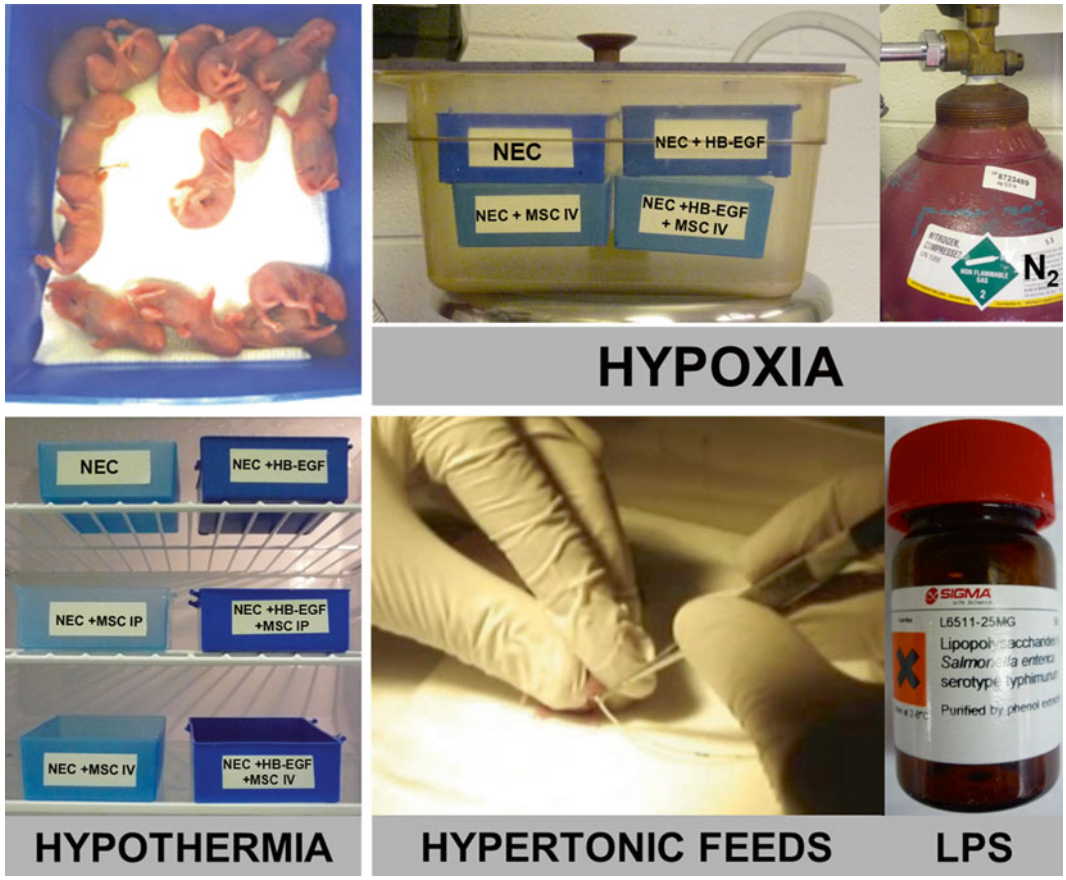

Fig. 7 Rat experimental NEC model. Pups were kept in an incubator at 35 °C and fed with hypertonic formula every 4 h. The volume of formula was advanced to a maximum of 0.4 mL per feed by the fourth day of life. Immediately after feeding, the pups were exposed to hypoxia (100 % nitrogen for 1 min), followed by hypothermia (4 °C for 10 min) twice a day until the end of the experiment

Fig. 8 Gross view of the small intestine subjected to experimental NEC. The proximal small intestine is to the left and the cecum is to the right. (*1*) pneumatosis; (*2*) intestinal narrowing; (*3*) perforation; (*4*) intraluminal bleeding; (*5*) intestinal dilation

4 Notes

1. The benefit of using YFP-labeled BM-MSC, rather than non-labeled BM-MSC, is that it allows for tracking of the labeled cells by fluorescence microscopy in any organ of interest after MSC infusion.

Table 1
The table used to record the incidence of pathological changes in experimental NEC

Groups	Total number of animals	Intestinal dilation	Perforation	Intraluminal bleeding	Intestinal narrowing	Pneumatosis
1						
2						
3						
…						

2. Principles of sterilization should be strictly obeyed during the protocol of harvesting BM-MSC. Sterilized surgical tools should be used. After the femurs and tibias of hind limbs are dissected from the body, the limbs should be soaked in ethanol for 10 min before separating the bone marrow from the bones.
3. MSC differentiation should be assessed after the cells are grown in adipogenic or osteogenic differentiation media for at least 15 days.
4. The age of time pregnant rats should be strictly between E21 and E21.5. C-section earlier than E21 leads to high mortality of the delivered premature pups. Waiting past E21.5 usually leads to natural delivery of the pups. During natural delivery, the dam ingests the umbilical vessels and placentas, causing the operator to miss the chance to catheterize the umbilical veins.
5. Prior to C-section, the duration of CO_2 anesthesia for time pregnant rats should be 3-5 min, depending on the level of consciousness. Importantly, twitches in the abdomen of pregnant rats reflect the movement of rat pups in the uterus caused by hypoxia. As soon as these signs are observed, the pregnant rats should be transferred immediately to the operating table for C-section.
6. When performing C-section and delivering rat pups, the operator and assistants should cooperate closely. Immediately after transferring the pregnant rats to the operating table, a longitudinal incision is made from the xiphoid to the pubic bone. After exposure of the uterus, a longitudinal incision is made to expose the pups and their amniotic membranes. The operator should squeeze the pups out of the amniotic membranes and pass the pups to the assistants. The assistant, holding a gauze pad in the left hand, should place the pup on the gauze. By using the right index finger to rub the chest and back of the pups, the assistant helps the pups to clear the lungs. A Q-tip is used to remove any discharge from the mouth and nose of the pups.

7. The signs of successful viability are "crying" of pups, pink coloration of the skin, and movement of the pups. The process of stimulating the delivered pups viable should persist for at least 5 min. During this time, the placentas must be kept moist and warm and the integrity of the umbilical cords maintained for injection.
8. The skin of rat pups is pink prior to methylene blue injection. Blue discoloration of the skin was noted immediately after injection in the order of chest, head, abdomen, and paws. The internal aspect of the umbilical vein stains blue upon injection of the dye. Bluish discoloration of the intestines is noted ~5 s after dye injection. The methylene blue dye injection was used only to confirm the experimental technique, so that subsequent experiments using MSC administration could be confidently performed.
9. A method to confirm that injected MSC could "detour" the pulmonary barrier involved the use of ultrasonographic scanning of the PFO. The intra-umbilical vein tubing should be placed prior to scanning. The ultrasound gel must be pre-warmed so that the pups will not lose heat. The detection probe should be placed in a subcostal orientation and a four chamber apical view used for detection of the PFO. Continuous recording of the waves is gained using the Pulse wave Doppler channel.
10. When cannulating the umbilical veins, the placenta is placed on a gauze pad and the umbilical cord straightened for exposure. Under a surgical dissecting microscope, the membrane covering the umbilical vein and arteries is dissected and the vein separated from the arteries. A fine toothed forceps is placed beneath the exposed umbilical vein. An oblique incision (~1.5 mm) is made in the umbilical vein and the vein is flushed with PBS. One end of the tip of the PE-10 tubing is slightly stretched to make it thinner, and the other end of the tubing is fitted onto the needle of the syringe holding the MSC suspension. Using sterile technique, the stretched end of the tube is cannulated into the umbilical vein and the tube fixed with an atraumatic vessel clip. A total volume of 40 μL containing 300×10^3 MSC is infused through the umbilical vein of the pups. MSC suspensions are injected within 1 min of cannulation. Rat pups receiving the same volume of IV PBS injection are used as control animals. Injections that drive blood in the umbilical vein back to the circulation are considered to be successful (Fig. 9). Fluid extravasation, umbilical vein rupture, resistance while injecting or obstruction of umbilical veins were signs of injection failure.
11. In the experimental rat NEC model, we use pipet tip boxes as containers to hold pups. Ten to 16 pups can be placed in one box.

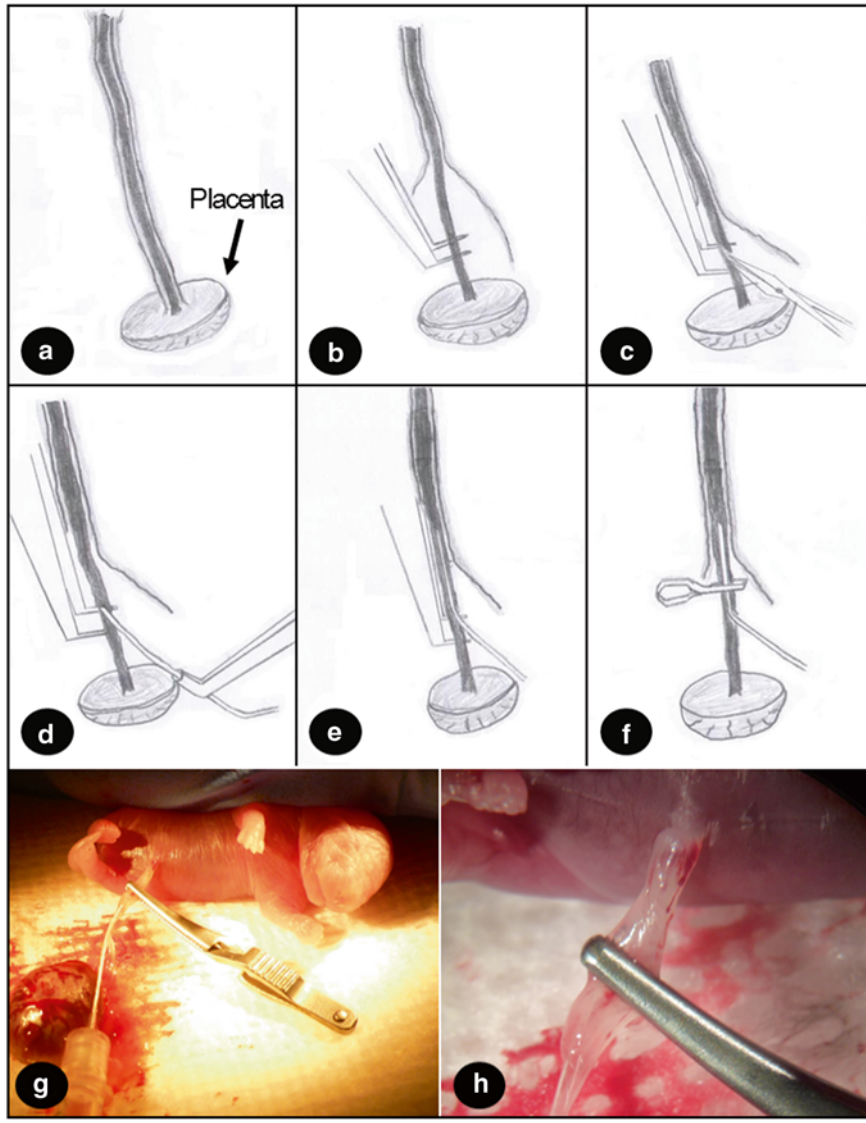

Fig. 9 Technique of cannulation of the umbilical vein of newborn rat pups. (**a**) The placenta (*black arrow*) is placed on a gauze pad and the umbilical cord straightened for exposure; (**b**) The membrane covering the umbilical vein and arteries is dissected and the vein is separated from the arteries. A fine toothed forceps is placed beneath the exposed umbilical vein; (**c**) An oblique incision (~1.5 mm) is made in the umbilical vein which is then flushed with PBS for visualization; (**d**) After slightly stretching the tip of the PE-10 tubing to make it thinner, the tube is held with vessel cannulation forceps at an angle of 30° to the umbilical vein and the vein cannulated; (**e**) The tubing is gently advanced into the vein for ~1.5 cm; (**f**) The tubing is fixed in the umbilical vein with an atraumatic vessel clip; (**g**, **h**) Images showing the completed cannulation

12. When evaluating for NEC, the gross view should be first evaluated before the intestines are fixed in 4 % paraformaldehyde. The intestinal mesentery is removed, and the stool in the intestine should be flushed gently using a 5 mL syringe with PBS. The intestines are straightened for further evaluation.

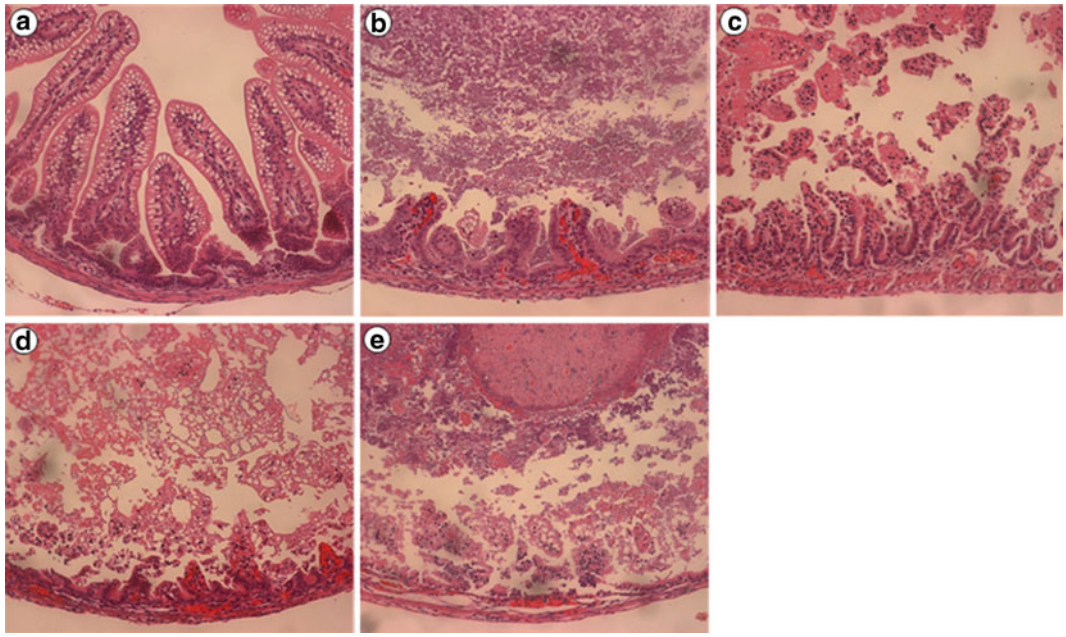

Fig. 10 Histologic grading of intestines from neonatal rats. (**a**) Grade 0: uninjured intestines; (**b**) Grade 1: epithelial cell lifting or separation; (**c**) Grade 2: epithelial cell sloughing to mid villus level; (**d**) Grade 3: necrosis of entire villus; (**e**) Grade 4: transmural necrosis. Grade 2 or higher injury is defined as being consistent with NEC. 100× Magnification

13. NEC is graded using an intestinal injury scoring system. H and E stained sections should be evaluated blindly by two independent observers, and graded as follows: Grade 0, no damage; Grade 1, epithelial cell lifting or separation; Grade 2, sloughing of epithelial cells to the mid villus level; Grade 3, necrosis of the entire villus; or Grade 4, transmural necrosis. Grade 2, 3, or 4 injury was defined as being consistent with NEC (Fig. 10).

Acknowledgements

This work was supported by NIH R01 DK74611 and NIH R01 GM61193 (GEB).

References

1. Kliegman RM, Fanaroff AA (1984) Necrotizing enterocolitis. N Engl J Med 310:1093–1103
2. Semont A, Mouiseddine M, Francois A, Demarquay C, Mathieu N, Chapel A, Sache A, Thierry D, Laloi P, Gourmelon P (2010) Mesenchymal stem cells improve small intestinal integrity through regulation of endogenous epithelial cell homeostasis. Cell Death Differ 17:952–961
3. Kudo K, Liu Y, Takahashi K, Tarusawa K, Osanai M, Hu DL, Kashiwakura I, Kijima H, Nakane A (2010) Transplantation of mesenchymal stem cells to prevent radiation-induced intestinal injury in mice. J Radiat Res 51:73–79

4. Dimmeler S, Burchfield J, Zeiher AM (2008) Cell-based therapy of myocardial infarction. Arterioscler Thromb Vasc Biol 28:208–216
5. Ott HC, McCue J, Taylor DA (2005) Cell-based cardiovascular repair—the hurdles and the opportunities. Basic Res Cardiol 100:504–517
6. Sherman W, Martens TP, Viles-Gonzalez JF, Siminiak T (2006) Catheter-based delivery of cells to the heart. Nat Clin Pract Cardiovasc Med 3(Suppl 1):S57–S64
7. Furlani D, Ugurlucan M, Ong L, Bieback K, Pittermann E, Westien I, Wang W, Yerebakan C, Li W, Gaebel R et al (2009) Is the intravascular administration of mesenchymal stem cells safe? Mesenchymal stem cells and intravital microscopy. Microvasc Res 77:370–376
8. Yang J, Watkins D, Chen CL, Bhushan B, Zhou Y, Besner GE (2012) Heparin-binding epidermal growth factor-like growth factor and mesenchymal stem cells act synergistically to prevent experimental necrotizing enterocolitis. J Am Coll Surg 215:534–545
9. Hall B, Andreeff M, Marini F (2007) The participation of mesenchymal stem cells in tumor stroma formation and their application as targeted-gene delivery vehicles. Handb Exp Pharmacol 180:263–283
10. Barlow B, Santulli TV, Heird WC, Pitt J, Blanc WA, Schullinger JN (1974) An experimental study of acute neonatal enterocolitis—the importance of breast milk. J Pediatr Surg 9: 587–595
11. Caplan MS, Hedlund E, Adler L, Hsueh W (1994) Role of asphyxia and feeding in a neonatal rat model of necrotizing enterocolitis. Pediatr Pathol 14:1017–1028

Chapter 12

Exploring Mesenchymal Stem Cell-Derived Extracellular Vesicles in Acute Kidney Injury

Stefania Bruno and Giovanni Camussi

Abstract

Several experimental animal models have been set up to study the characteristics of acute kidney injury (AKI) and to develop possible new treatments for clinical applications. Herein, we review the experimental procedures used to induce AKI to test the therapeutic potential of extracellular vesicles (EV) produced by stem cells. In particular, we focused on AKI models induced by rhabdomyolysis, by cisplatin treatment, and by renal ischemia–reperfusion injury.

Key words Glycerol, Cisplatin, Ischemia–reperfusion injury, Mouse model, Kidney injury, Renal regeneration

1 Introduction

Acute kidney injury (AKI) is a syndrome characterized by the acute loss of kidney function that leads to increased serum creatinine or oliguria. In clinical setting, AKI recognizes many promoting events including disorders causing rhabdomyolysis, drug nephrotoxicity, environmental poisons, urinary tract obstructions, bacterial toxins, ischemic episodes, etc.

AKI is classically divided into pre-renal, renal (or intrinsic), and post-renal failure. Pre-renal AKI is a consequence of decreased renal perfusion, due to hypovolemia or ischemia. Intrinsic AKI happens when there is a damage of renal tubules, vessels, or interstitium. The major cause of intrinsic AKI is acute tubular necrosis that results from ischemic or nephrotoxic injury. Post-renal AKI follows obstruction of the urinary system with an increase in pressure within the renal collecting system.

Several experimental animal models have been developed to mimic the different clinical settings of AKI and to set up and/or improve possible new treatments. Herein, we present a review of the experimental procedures to obtain AKI used in our laboratory to test whether mesenchymal stem cells (MSCs) or MSC-derived

Bruno Christ et al. (eds.), *Animal Models for Stem Cell Therapy*, Methods in Molecular Biology, vol. 1213,
DOI 10.1007/978-1-4939-1453-1_12,

extracellular vesicles (MSC-EVs) may promote renal regeneration. In particular, we focused on AKI induced by rhabdomyolysis, by cisplatin treatment, and by renal ischemia–reperfusion injury (IRI).

EVs derived from MSCs are spherical membrane fragments with heterogeneous size (from 60 to 250 nm in diameter) that are involved in cell-to-cell communication and are capable to modify the fate and phenotype of recipient cells after delivery of their content [1]. MSC-derived EVs express several adhesion molecules of MSCs such as CD44, CD29 (β1-integrin), α4- and α5 integrins, and CD73 [2]. Human MSC-derived EVs stimulated proliferation and apoptosis resistance of tubular epithelial cells in vitro [2, 3]. In vivo MSC-derived EV treatment accelerates the morphological and functional recovery of different experimental animal models of renal injury in a manner comparable to that of MSCs, suggesting that they may mediate, at least in part, the MSC-regenerative potential [2–5].

2 Materials

1. Sterile saline solution.
2. Pure and sterile water.
3. Anesthetic: a solution of Xylazine and Tiletamine/Zolazepam at a concentration of 0.016 mg/kg and 0.05 mg/kg, respectively, in sterile saline solution.
4. Glycerol solution: 50 % solution in pure water.
5. Syringes with 26-G needles.
6. Syringes with 29-G needles.
7. Cisplatin: suspend the powder in pure water at a concentration of 2 mg/mL.
8. Ventilator cages.
9. Heating pad.
10. Surgical scissors.
11. Dressing forceps.
12. Micro aneurysm clips.
13. Sterile cotton swabs.
14. Surgical suture: braided silk/virgin silk, sterile, non-adsorbable (7-0).

3 Methods

MSC-EVs were tested in the following AKI models:

– Glycerol-induced AKI (Subheading 3.1) as a model of rhabdomyolysis;

– Cisplatin-induced AKI (Subheading 3.2) as a model of drug-induced injury;
– Ischemia and reperfusion-induced AKI (Subheading 3.3) (IRI-AKI).

We describe below the basic experimental procedures and methodologies for each of these murine models of AKI. During the experimental procedures, mice were housed in ventilated cage system at 22 °C, 55 ± 5 % humidity, on a 12–12 h dark–light cycle and allowed free access to chow and water ab libitum.

3.1 Glycerol-Induced AKI

The different disorders that may cause rhabdomyolysis in human include muscle dysfunctions (trauma, burns, intrinsic muscle disease, excessive muscular activity), medications, infections, metabolic and idiopathic disorders. About 10–40 % of the cases of rhabdomyolysis develop AKI. The model for studying this form of AKI can be obtained in rats or mice by intramuscular injection of glycerol that mimics the rhabdomyolysis-induced AKI in humans [6]. Glycerol-induced AKI is characterized by myoglobinuria, tubular necrosis and vasoconstriction [7], and the pathogenic mechanisms involved in this kind of AKI include ischemic injury, tubular nephrotoxicity caused by myoglobin, and the renal actions of cytokines released after rhabdomyolysis [8, 9]. Marked tubular epithelial injury is evident starting from day 1 after glycerol injection. The morphological alterations included vacuolization and widespread necrosis of tubular epithelial cells and tubular hyaline cast formation (Fig. 1). Proximal tubules showed loss of brush border, cytoplasmic vacuolization and flattening of epithelial cells. Distal tubules showed areas of loss of the epithelial layer with aspect of apparent denudation of tubular basal membrane [10]. This model has been extensively used to evaluate the capacity of stem cells [11, 12] or of EVs (2) to contribute to the renal regeneration. The standard method to induce AKI-glycerol is by intramuscular administration of a hypertonic solution of 50 % glycerol.

1. After anesthesia (*see* **Note 1**), administer glycerol solution by intramuscular injection (*see* **Note 2**). The required amount of glycerol is equally distributed to both hind legs, as a deep intramuscular injection with a syringe with a 26-G needle. Intramuscular injection of glycerol induces significant increases in serum creatinine and blood urea nitrogen, which usually peaks at 1–4 days after glycerol administration, declined and normalized at different time points, depending on the murine strain.
2. Depending on protocols, inject MSCs or EVs 1–3 days after glycerol administration (*see* **Note 3**). These can be administered either by intravenous (i.v.) or intraperitoneal (i.p.) injection (*see* **Note 4**) with a syringe with a 29-G needle.
3. Sacrifice mice 1–8 days after cell or EV administration to determine the extent of damage by histological and functional analyses.

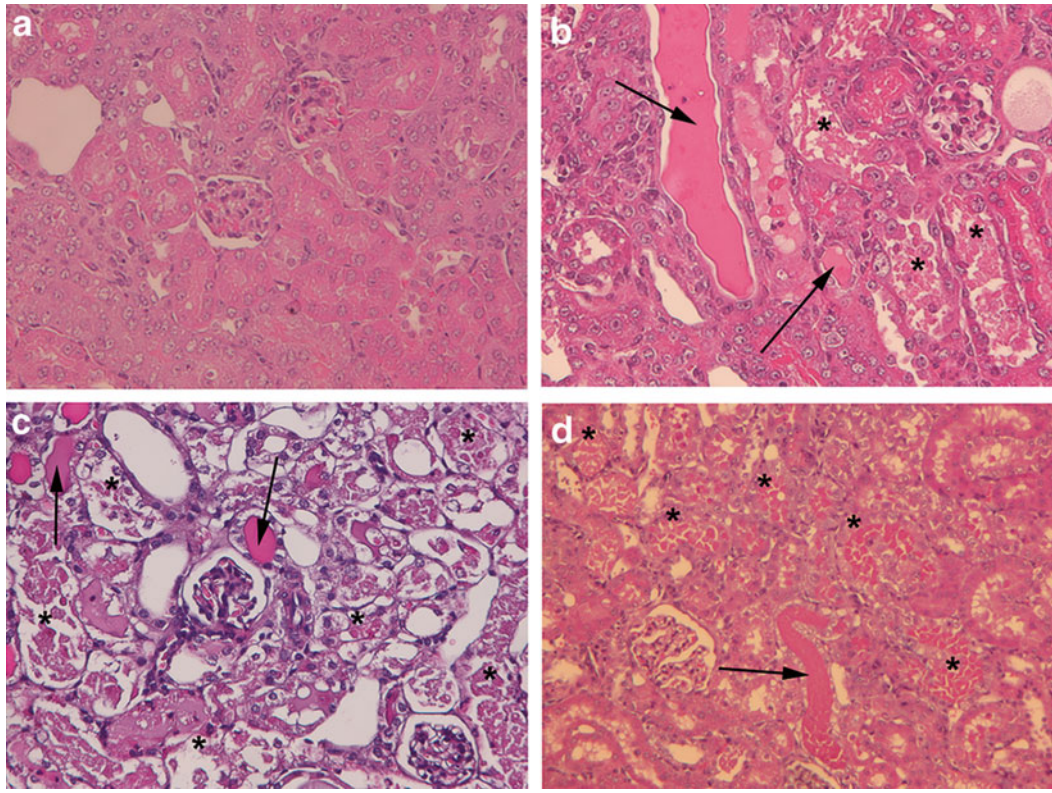

Fig. 1 Representative micrographs of renal histology of a healthy SCID mouse (**a**), of a SCID mouse injected with glycerol and sacrificed at day 5 after treatment (**b**), of a SCID mouse injected with cisplatin and sacrificed at day 4 (**c**) and of a SCID mouse with IRI and sacrificed at day 2 (**d**). Original magnification: ×200. The typical aspect of intra-tubular cast and tubular necrosis are shown by *arrows* and *asterisks*, respectively

3.2 Cisplatin-Induced AKI

Cisplatinum [*cis*-diaminedichloroplatinum(II)] is an anticancer drug widely used for the therapy of different types of cancer. Nephrotoxicity is frequent, and it is the major limitation in cisplatin-based chemotherapy [13]. Several mechanisms contribute to renal dysfunction after cisplatin treatment, including direct tubular toxicity, production of reactive oxygen species, calcium overload, inhibition of mitochondrial respiratory chain, and ATP depletion. The model for studying this form of AKI is obtained in rats or mice by intraperitoneal injection of cisplatin [14, 15]. In mice, cisplatin-induced injury is usually associated with tubular necrosis, revealed by cast formation, loss of tubular brush border, and dilatation of tubules (Fig. 1). Usually kidney failure is evident at day 2 and reaches a maximum at day 3 or 4, depending on the doses. The tubular dysfunction is comparable to that found in humans. Moreover, in some mouse strain, this type of AKI is lethal, and it is useful to evaluate the effect of stem cells or EVs from stem cells in improving survival [3, 16].

1. Inject the cisplatin solution in the abdominal cavity (*see* **Note 5**) with a syringe with a 29-G needle.
2. At different time points after cisplatin injection (8–24 h or 2 days), proceed with cell or EV administration. These might be administered by i.v. or i.p. injection (*see* **Note 4**).
3. Sacrificed mice 4–21 days after cisplatin administration to determine the extent of damage by histological and functional analyses.

3.3 Ischemia and Reperfusion-Induced AKI

In the kidney, ischemia–reperfusion injury is associated with death of tubular epithelial cells, localized in the stripe between the cortex and medulla, by necrosis or apoptosis depending on the severity of the ischemic insult. Experimentally, ischemia and reperfusion AKI is induced by clamping the renal artery, followed by reperfusion in anesthetized uninephrectomized mice or rats. Renal dysfunction develops within 24 h [17]. The kidneys exhibit tubular atrophy and dilatation, cast formation accompanied by interstitial inflammation (Fig. 1) [18].

1. After anesthesia, place the mouse on a heating pad to maintain its body temperature during surgery (*see* **Notes 1**, **6** and **7**).
2. Cut open the skin and muscle on the right flank side along the back to expose the right kidney.
3. Push out the kidney from the cut with sterile cotton swabs to expose the renal pedicle.
4. Place a single thread ligature around the renal blood vessels and the ureter. The thread ligature is tied securely with a double knot and the blood vessels are transected next to the kidney, which is removed.
5. Close the incision.
6. Cut open the skin and muscle on the left flank side along the back to expose the left kidney.
7. Push out the kidney from the cut with sterile cotton swabs to expose the renal pedicle. The duration of kidney ischemia starts from the time of clamping. Complete ischemia is indicated by color change of the kidney from red to white in a few seconds (*see* **Note 8**). After the ischemia, the micro aneurysm clips are released at desired time, which is indicated by the change of kidney color to red.
8. Immediately after the wound closure, give 0.5 mL warm sterile saline intraperitoneally to each mouse (*see* **Note 9**).
9. Keep the animal on a heating pad until it gains full consciousness before being returned to its housing cage.
10. Immediately after reflow, proceed with cell or EV i.v. administration.
11. Sacrifice mice at day 2–3 post surgery.

4 Notes

1. Anesthesia is induced by intramuscular injection of 30 μL of a solution of Xylazine (0.016 mg/kg) and Tiletamine/Zolazepam (0.05 mg/kg). Animal manipulation will not be started until the mouse is in deep anesthesia and thus does not respond to pain induced by toe pinch.
2. The amount of glycerol depends on the mouse strain, varying from 7.5 to 8 mL/kg. Usually male are more susceptible to glycerol injury compared to female animals.
3. To determine whether MSCs or MSC-derived EVs were capable to favor renal regeneration, usually we inject i.v. the cells or the EVs 3 days after glycerol administration to evaluate the potential therapeutic effect on AKI reversal. If the researcher would explore the possible preventive effect on AKI development, it is recommended to inject the cells or the EVs at day 1 after glycerol administration, when the AKI is not yet fully established.
4. Don't exceed the volume of 150 μL for i.v. injection and 500 μL for i.p. injection.
5. The amount of cisplatin necessary to cause AKI is different in different mouse strains.
6. It is important to minimize trauma associated with the surgery. The surgeon is the key factor to the establishment of a consistent and reproducible mouse model of ischemic AKI. A well-trained surgeon can reduce surgical trauma and can also complete the procedure within the anesthesia time. Sham operated animals should be used as control.
7. The body temperature during ischemia is one of the most critical factors that may affect the severity of AKI. It is of crucial importance to do surgery with a heating pad to keep mice warm during the operation.
8. The duration of ischemia in mice varied from 20 to 30 min. Since there are marked differences in the susceptibility to ischemic AKI among different mouse strains it is mandatory to set up the model with preliminary experiments to define the time of ischemia needed. Moreover, males are more susceptible to I/R injury compared to females.
9. AKI is greatly affected by the dehydration status of the body.

References

1. Camussi G, Deregibus MC, Bruno S et al (2010) Exosomes/microvesicles as a mechanism of cell-to-cell communication. Kidney Int 789:838–848
2. Bruno S, Grange C, Deregibus MC et al (2009) Mesenchymal stem cell-derived microvesicles protect against acute tubular injury. J Am Soc Nephrol 20:1053–1067
3. Bruno S, Grange C, Collino F et al (2012) Microvesicles derived from mesenchymal stem cells enhance survival in a lethal model of acute kidney injury. PLoS One 7:e33115
4. Gatti S, Bruno S, Deregibus MC et al (2011) Microvesicles derived from human adult mesenchymal stem cells protect against ischaemia-reperfusion-induced acute and chronic kidney injury. Nephrol Dial Transplant 26:1474–1483
5. He J, Wang Y, Sun S et al (2012) Bone marrow stem cells-derived microvesicles protect against renal injury in the mouse remnant kidney model. Nephrology (Carlton) 17:493–500
6. Thiel G, Wilson DR, Arce ML et al (1967) Glycerol induced hemoglobinuric acute renal failure in the rat. Nephron 4:276–297
7. Karam H, Bruneval P, Cloze JP et al (1995) Role of endothelin in ARF due to rhabdomyolysis in rats. J Pharmacol Exp Ther 274: 481–486
8. Curry SC, Chang D, Connor D (2002) Drug- and toxin-induced rhabdomyolysis. Ann Emerg Med 18:1068–1084
9. Dai RP, Dheen ST, Tay SS (2002) Induction of cytokine expression in rat post-ischemic sinoatrial node (SAN). Cell Tissue Res 310:59–66
10. Zager RA, Burkhart KM, Conrad DS et al (1995) Iron, heme oxygenase, and glutathione: effects on myohemoglobinuric proximal tubular injury. Kidney Int 48:1624–1634
11. Herrera MB, Bussolati B, Bruno S et al (2004) Mesenchymal stem cells contribute to the renal repair of acute tubular epithelial injury. Int J Mol Med 14:1035–1041
12. Herrera MB, Bussolati B, Bruno S et al (2007) Exogenous mesenchymal stem cells localize to the kidney by means of CD44 following acute tubular injury. Kidney Int 72:430–441
13. dos Santos NA, Carvalho Rodrigues MA, Martins NM et al (2012) Cisplatin-induced nephrotoxicity and targets of nephroprotection: an update. Arch Toxicol 86:1233–1250
14. Fillastre JP, Raguenez-Viotte G (1989) Cisplatin nephrotoxicity. Toxicol Lett 46:163–175
15. Bi B, Schmitt R, Israilova M et al (2007) Stromal cells protect against acute tubular injury via an endocrine effect. J Am Soc Nephrol 18:2486–2496
16. Morigi M, Introna M, Imberti B et al (2008) Human bone marrow mesenchymal stem cells accelerate recovery of acute renal injury and prolong survival in mice. Stem Cells 26:2075–2082
17. Lieberthal W, Levine JS (1996) Mechanisms of apoptosis and its potential role in renal tubular epithelial cell injury. Am J Physiol 271: F477–F488
18. Mohaupt M, Kramer HJ (1989) Acute ischemic renal failure: review of experimental studies on pathophysiology and potential protective interventions. Ren Fail 11:177–185

Chapter 13

Angiogenic Properties of Mesenchymal Stem Cells in a Mouse Model of Limb Ischemia

Leonardo Martins, Priscila Keiko Matsumoto Martin, and Sang Won Han

Abstract

Mesenchymal stem cells (MSCs) can be obtained from adult bone marrow and adipose tissue in large quantities and are the main cell types that contribute to recovery from ischemia because, among their biological activities, they produce several proangiogenic paracrine factors and differentiate into endothelial cells. Mouse hind limb ischemia induced by surgery is a useful animal model to study the angiogenic properties of MSCs, but it requires several precautions to be reproducible. The preparation of MSCs, the ischemic surgery, and the physiological and histological analyses are described in detail.

Key words Mesenchymal stem cell, Angiogenesis, Limb ischemia, Peripheral artery disease, Stem cell therapy

1 Introduction

Peripheral arterial disease (PAD) is mainly caused by atherosclerosis, which narrows the arteries and reduces the oxygen supply to the limbs, resulting in severe pain, non-healing ulcers, and the possible loss of the affected limb. The incidence of PAD is approximately 1,000 affected per million individuals, and this incidence increases in individuals over 70 years of age and in diabetic individuals [1]. According to the Transatlantic Inter-Society Consensus, approximately 25 % of patients with advanced PAD will suffer amputation because conventional medical and revascularization treatments are limited in such cases. The prognosis for these patients is poor; after 1 year, approximately 25 % of them will die and 20 % will still have PAD [1]. Therefore, it is necessary to continue the search for new therapies.

Mesenchymal stem cells (MSCs) are adult stem cells that can be obtained in large quantities from bone marrow and adipose tissue and in limited quantities from other tissues. These cells have the capacity to differentiate into cell types including osteoblasts, chondrocytes, adipocytes, endothelial cells, and vascular smooth

Bruno Christ et al. (eds.), *Animal Models for Stem Cell Therapy*, Methods in Molecular Biology, vol. 1213,
DOI 10.1007/978-1-4939-1453-1_13,

muscle cells, but their destinies are mainly determined by the local microenvironment [2]. In addition to multipotency, MSCs are capable of suppressing the immune system by secreted mediators that include nitric oxide, prostaglandins, indoleamine 2,3-dioxygenase, and IL-6, which modulate T cells, natural killer cells, dendritic cells, and macrophages [3]. MSCs also secrete several proangiogenic growth factors, especially in a microenvironment of low oxygen concentration [4].

These properties have made MSCs the favorite stem cells to treat several diseases, especially ischemic diseases such as PAD. Although MSCs have already been used to treat patients with critical limb ischemia, the outcomes of these clinical studies have not been satisfactory, and more basic and preclinical studies are required. The procedures used for MSC preparation, the induction of limb ischemia in mice, and the forms of therapeutic analysis from different papers show significant variations. Here, we detail the procedures routinely used in our laboratory, which we established, adopted, or modified from other authors' papers.

2 Materials

2.1 Extraction and Culture of Mesenchymal Stem Cells from Mouse Bone Marrow

1. Culture medium for the extraction and maintenance of mouse bone marrow MSCs: Dulbecco's Modified Eagle's Medium (DMEM), low glucose, 3.7 g/L sodium bicarbonate, 15 mM (acid free) HEPES, pH approximately 7.4; the complete culture medium further includes 10 % (v/v) fetal bovine serum (FBS); for preservation, the culture medium should be stored at 4 °C.
2. 1 pair of sterile tweezers and one pair of sterile sharpened scissors.
3. 2 sterile 15 mL conical tubes.
4. 4 sterile 24 G needles.
5. 4 sterile 5 mL syringes.
6. 5, 10, and 25 mL sterile serological pipettes.
7. 70 % (v/v) alcohol.
8. Animal fixation system for surgical procedures (e.g., styrofoam and needles).
9. C57BL/6 mice aged up to 8 weeks. Transgenic animals of the same strain may also be used, e.g., green fluorescent protein (GFP) mice.
10. Freezing medium: 90 % (v/v) FBS, 10 % (v/v) dimethyl sulfoxide (DMSO). Store at −20 °C.

11. Phosphate-buffered saline (PBS): 8 g NaCl, 0.2 g KCl, 1.44 g Na_2HPO_4, 0.24 g KH_2PO_4, add water to a total volume of 1 L, pH 7.4, filter the solution using a 0.22 μm pore membrane filter, store at 4 °C.
12. 0.25 % (v/v) trypsin solution in PBS: 5 mL 2.5 % trypsin (Life Technologies, São Paulo, Brazil), 45 mL PBS, store at 4 °C.
13. 0.03 % (w/v) PBS-EDTA solution: 0.3 g EDTA dissolved in 1 L PBS, pH 7.4, autoclave the solution and store at 4 °C.
14. Medium used for MSC subculturing: DMEM, high glucose, 3.7 g/L sodium bicarbonate, 15 mM (acid free) HEPES, pH 7.4; the complete culture medium further includes 10 % (v/v) FBS.
15. Neubauer Chamber.
16. 6-well plates.

2.2 MSC Osteogenic Differentiation

1. Ascorbic acid 2-phosphate (AsAP), 5 mg/mL: 50 mg AsAP (L-ascorbic acid 2-phosphate magnesium salt hydrate) in 10 mL DMEM, sterilize by filtration through a 0.22 μm pore membrane, store the solution at 4 °C; this solution remains stable for several months.
2. ß-glycerophosphate, 31.5 mg/mL: 630 mg ß-glycerophosphate (glycerol 2-phosphate disodium salt hydrate) in 20 mL DMEM, sterilize by filtration through a 0.22 μm pore membrane, store the solution at 4 °C; this solution remains stable for 2 months.
3. Dexamethasone, 1,000×: Under a laminar flow hood, dissolve 1.2 mg of dexamethasone in 1.223 mL of ethanol to obtain a 2.5×10^{-3} M stock solution; this solution may be stored at −20 °C for future use. Transfer 10 μL of the stock solution to 2.5 mL of sterile culture medium to obtain a 1×10^{-5} M solution for use as a supplement (Dexamethasone 1,000×), sterilize by filtration through a 0.22 μm pore membrane, prepare 10 μL aliquots for single use and store at −20 °C.
4. Osteogenic base medium: 10 mL 31.5 mg/mL ß-glycerophosphate solution, 10 mL FBS, 100 μL 5 mg/mL AsAP solution, add DMEM to obtain a total volume of 100 mL, store the solution at 4 °C.
5. 4 % (w/v) paraformaldehyde: 4 g paraformaldehyde, 100 mL PBS, shake at 60 °C until dissolved (approx. 4 h); to avoid paraformaldehyde degradation, store the solution at 4 °C.
6. Alizarin Red S: 2 g Alizarin Red S, 90 mL deionized water, adjust pH to 4.1 by adding ammonium hydroxide, add deionized water to obtain a total volume of 100 mL, filter through a paper filter to remove precipitates.

2.3 MSC Adipogenic Differentiation

1. Dexamethasone, 1,000×: *see* Subheading 2.2, **step 3**.
2. Insulin from bovine pancreas, 1 mg/mL (stock solution): 1 mg insulin (use a high-precision scale) in 1 mL DMEM, sterilize by filtration through a 0.22 μm pore membrane, aliquot in 10 μL, and store at −20 °C.
3. 1 mM rosiglitazone: 1 mg rosiglitazone (use a high-precision scale) in 4 mL DMEM, sterilize by filtration through a 0.22 μm pore membrane, aliquot in 10 μL, and store at −20 °C.
4. Adipogenic medium: DMEM, high or low glucose plus FBS 10 % (v/v), prepare this solution, which can be stored at 4 °C for several months; upon replacing the medium, add 1×10^{-8} M dexamethasone, insulin from bovine pancreas (2.5 μg/mL), and rosiglitazone (5 μM).
5. Oil Red O: 3.75 g Oil Red O in 100 mL isopropanol, filter this solution through filter paper and store at room temperature; for use, mix this solution with 2 volumes of deionized water and filter again with filter paper.
6. Sudan Black B: 2 g of Sudan Black B in 100 mL isopropanol, filter this solution through filter paper and store at room temperature; for use, mix this solution with 2 volumes of deionized water and filter again with filter paper.

2.4 MSC Chondrogenic Differentiation

1. Insulin from bovine pancreas, 1 mg/mL (stock solution): *see* Subheading 2.3, **step 2**.
2. AsAP, 1 μg/mL: 1 mg AsAP (use a high-precision scale), in 1 mL DMEM; to prepare a 1 μg/mL solution, dilute 1 μL of the 1 mg/mL AsAP solution in 999 μL DMEM, sterilize by filtration through a 0.22 μm pore membrane, store the solution at 4 °C.
3. TGF-β1, 1 μg/mL: 1 mg TGF-β1 (use a high-precision scale), in 1 mL PBS or sterile water; to prepare a 1 μg/mL solution, dilute 1 μL of the 1 mg/mL TGF-β1 solution in 999 μL PBS or sterile water, sterilize by filtration through a 0.22 μm pore membrane, separate 10 μL aliquots, and store at −20 °C.
4. Chondrogenic medium: DMEM, high or low glucose, 15 mM HEPES, 10 % (v/v) FBS, this solution may be stored at 4 °C for several months; upon replacing the medium, add 6.25 μg/mL insulin, 10 ng/mL TGF-β1, and 8.8 μg/L AsAP.

2.5 Flow Cytometry of MSCs

1. Mouse Mesenchymal Stem Cell Marker Antibody Panel (R&D Systems, Minneapolis, MN, USA).
2. 5 mL flow cytometry tubes.
3. 15 mL conical tube.
4. PBS.

2.6 Injection of MSCs

1. DMEM without FBS.
2. 24 G needle.
3. Insulin syringe.

2.7 Ischemia Induction Surgery

1. Male Balb/c mice (age 10–12 weeks).
2. Sterile surgical gloves.
3. 1 sterile insulin syringe (1 mL).
4. 1 sterile 29 G × ½″ needle.
5. Ketamine hydrochloride.
6. Xylazine hydrochloride.
7. Sterile saline (0.9 % sodium chloride).
8. 1 surgical clipper.
9. 1 roll of adhesive tape.
10. 0.2 % chlorhexidine digluconate.
11. 5 % Bepanthen.
12. 5 % polyvinylpyrrolidone.
13. 1 1.5 × 1.5 cm fenestrated surgical drape.
14. 1 portable surgical microscope.
15. 2 scalpels blade no. 15 and 11.
16. 1 pair of curved tweezers.
17. 1 pair of Westcott conjunctival scissors.
18. Nylon suture #4-0.

2.8 Assessment of Muscle Strength and Mass

1. 1 table with temperature control.
2. 1 pair of 12 cm straight Iris scissors.
3. 1 pair of curved tweezers.
4. 1 pulse stimulator (Grass S88′, Grass Instruments, Quince, MA, USA).
5. 1 force transducer (iWorx/CB Science, Inc., Dover, NH, USA).
6. Nylon suture #3-0.
7. 1 unit of 10 mm hoop.
8. Computer with Powerlab® 8/30 software (ADinstruments Pty Ltd, Colorado Springs, CO, USA).
9. PBS.
10. 1 analytical balance.

2.9 Histology Processing

1. 10 % buffered formaldehyde solution (pH 7.3–7.4).
2. Histological cassettes.
3. Absolute ethanol.

4. Xylol P.A. (98.5 %).
5. Paraffin for histology.
6. 1 rotary microtome (RM2255 Leica®, Wetzlar, Germany, or similar).
7. 1 tissue flotation bath at 35 °C.
8. Clean microscope slides.
9. Silanized (adhesive) microscope slides.
10. 1 pair of precision tweezers—broad tip.
11. 1 pair of precision tweezers—fine tip.
12. Alcian Blue solution.

2.10 Hematoxylin-Eosin (HE) and Picro-Sirius Red Staining

1. Absolute ethanol.
2. 70 % ethanol.
3. Xylol P.A. (98.5 %).
4. Harris's hematoxylin: Dissolve 1 g of crystalline hematoxylin in 10 mL of slightly warmed absolute ethanol. In parallel, dissolve 20 g of potassium alum in warmed distilled water. Mix the solutions together and heat until boiling. Remove from heat, and immediately but gradually add 0.5 g of mercury oxide (while stirring). Cool the solution, and store it in an amber glass bottle. Filter before use.
5. 2 % alcohol-acid solution (v/v): 20 mL HCl in 940 mL absolute ethanol, add distilled water to a total volume of 1,000 mL, store at room temperature.
6. Eosin yellow: 0.25 g eosin yellow in 100 mL distilled water, store at room temperature.
7. 0.2 % phosphomolybdic acid.
8. Picro-Sirius Red: 0.5 g Sirius Red F3B in 500 mL 1.3 % picric acid in water (w/v), store at room temperature.
9. Acid water (adjust with 0.01 N HCl).
10. Microscope cover slips (20 × 20 mm to 24 × 60 mm).
11. Entellan® mounting medium.

2.11 Immunohistochemistry

1. Absolute ethanol.
2. 70 % ethanol.
3. Xylol p.a. (98.5 %).
4. 3 % hydrogen peroxide in methanol.
5. Sodium citrate buffer: 18 mL 100 mM citric acid and 82 mL 100 mM sodium citrate, add distilled water to a total volume of 1 L, adjust pH to 6.0.
6. 1 steamer.

7. PBS.
8. Avidin/biotin blocking kit (Vector Laboratories, Burlingame, CA).
9. Lectin I—isolectin B4 from *Griffonia simplicifolia* (*Bandeiraea simplicifolia*) (BSI-B4—Vector Laboratories, Burlingame, CA, USA).
10. Anti-alpha-smooth muscle actin (α-SMA) antibody (clone 1A4 Dako A/S, Glostrup, Denmark).
11. 1 humid chamber.
12. Diaminobenzidine (DAB): 0.06 g diaminobenzidine in 2 mL 3 % hydrogen peroxide, add 1 mL DMSO and 100 mL PBS.
13. Harris's hematoxylin diluted in distilled water 1:3 (*see* Subheading 2.10, **step 4**).

2.12 Histological Quantification

1. Light microscope coupled to a camera.
2. Computer with Image-Pro Plus® software (v6.0, Media Cybernetics, Rockville, USA) or open-access equivalent, e.g., ImageJ (v1.48k NIH, Bethesda, MA, USA).

3 Methods

3.1 Extraction of Mesenchymal Stem Cells from Mouse Bone Marrow

1. Sacrifice the animal.
2. Soak the animal in 70 % alcohol, and transfer it to a laminar flow hood. Secure the animal in a supine position to a rectangular piece of Styrofoam or similar material by fastening the limbs with needles.
3. Using sterile tweezers and scissors, remove the femur, and dissect the connective tissue around it. The tibia may also be used as a bone marrow source, though with greater difficulty. Cut the bone epiphyses.
4. Fill a 5 mL syringe with the complete culture medium. Insert the needle into one end of the bone, press the syringe, and collect the bone marrow fluid in an appropriate container (e.g., 15 mL conical tube).
5. Use the syringe to separate the bone marrow until no visible particles remain (successive aspirations and disposals). *See* **Note 1**.
6. Transfer the cell suspension to a clean 15 mL tube, centrifuge at $400 \times g$ for 10 min, and discard the supernatant.
7. Resuspend the cells in 5–7 mL of complete culture medium, and separate one aliquot for counting in a Neubauer Chamber.
8. Centrifuge again, and resuspend the cells in an appropriate volume of complete culture medium to achieve a concentration of 5×10^6 viable cells per mL.

9. Plate 3 mL of cell suspension per well in 6-well plates.
10. Incubate in a humidified oven at 37 °C and 5 % CO_2 in air.
11. At 72 h after plating, aspirate the full culture medium (together with the non-adherent cells), and add 3 mL of fresh culture medium to each well.
12. Under such conditions, the cells must become confluent in 6–7 days, at which time subculturing should be performed.

3.2 MSC Cryopreservation

1. Centrifuge the cells at $400 \times g$ for 10 min.
2. Remove the supernatant, and resuspend the cells in freezing medium at a concentration of 1×10^6–5×10^6 cells/mL.
3. Place the cell suspension in a cryotube previously kept on ice, and keep it on ice (or in a refrigerator) for 1 h. Then, transfer the tube to a freezer at −80 °C, and leave it for 1–5 days. Finally, transfer the tube to liquid nitrogen for permanent storage.
4. Cell freezing may also be performed using specialized equipment that controls the temperature reduction.

3.3 MSC Subculturing

1. Heat the complete culture medium, 0.25 % trypsin and 0.03 % PBS-EDTA to 37 °C.
2. Remove the old culture medium, and wash the cell monolayer with at least 5 mL of 0.03 % PBS-EDTA.
3. Add trypsin (1–2 mL) to cover the cell layer, and incubate at 37 °C for 5 min.
4. Resuspend the cells in complete culture medium (twice the original volume); to inactivate trypsin, centrifuge at $400 \times g$ for 10 min, and discard the supernatant.
5. Resuspend the cells in an appropriate volume of complete culture medium for plating.
6. For passage 1 (or the first subculture), plate the cells in a culture plate or flask twice as large as the original area (1:2 passage). *See* **Note 2**.
7. Repeat **steps 1–4** whenever the cells attain confluence. From passage 2 onwards, the culture appearance becomes increasingly homogeneous (Fig. 1a). The passage ratio (e.g., 1:2, 1:3, 1:4) is determined by the culture kinetics; that is, the faster the cells expand, the lower the passage ratio (*see* **Notes 3–5**).

3.4 Characterization of MSCs

Osteogenic, adipogenic, and chondrogenic differentiation make up one of the most widely used approaches to characterize MSCs (*see* **Note 5**). Although exclusive markers specific for mouse MSC characterization are not yet available, investigating the presence of certain positive markers, such as CD44, CD105, CD90, and Sca-1,

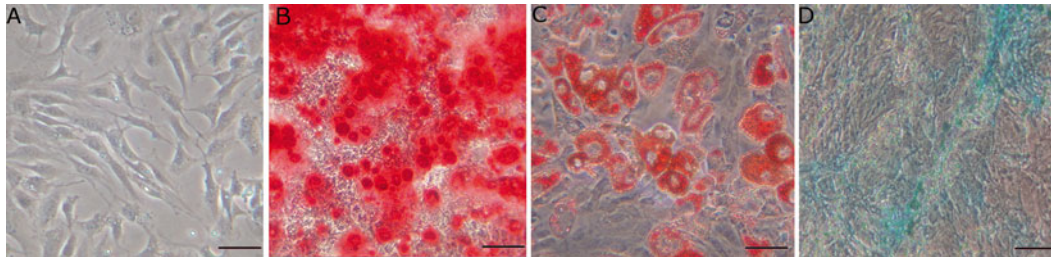

Fig. 1 Photomicrographs of mesenchymal stem cells. Mesenchymal stem cell passage 2 (**a**). Osteogenic differentiation after Alizarin red staining (**b**). Adipogenic differentiation after Oil Red staining (**c**). Chondrogenic differentiation after Alcian blue staining (**d**). Bar = 50 μm

and the absence of CD45 by flow cytometry is recommended by the International Society of Cellular Therapy [5]. More extensive panels are commercially available, or alternatively, can be set up at a laboratory using individual antibodies.

3.5 Osteogenic Differentiation

1. Plate the cells in 6-well plates so as to attain 100 % confluence on the day differentiation is induced.
2. Remove all the culture medium, and replace it with 2 mL of osteogenic base medium to each well. Upon replacement, add 10 μL of the 1,000× dexamethasone solution.
3. The culture medium should be replaced twice per week for 3–4 weeks.
4. As a rule, the deposition of mineralized extracellular matrix can be detected about 1 week after the induction of differentiation and becomes increasingly patent over time.

3.6 Osteogenic Staining Procedure

1. Wash the cell monolayer with PBS.
2. Fixate with 4 % paraformaldehyde for approximately 20 min at room temperature. Use 1 mL per well in the 6-well plate.
3. Remove paraformaldehyde, and wash once with deionized water.
4. Cover the cell monolayer with 1 mL of Alizarin Red S solution, and wait 5 min.
5. Remove the dye, and wash several times with deionized water.
6. The calcium-rich extracellular matrix will be stained red and may be macroscopically or microscopically visible, depending on the deposit amount (Fig. 1b).

3.7 Adipogenic Induction Procedure

1. Plate the cells in 6-well plates so as to attain 100 % confluence on the day differentiation is induced.
2. Remove all the complete culture medium, and replace it with adipogenic medium to induce differentiation. In each well, place

2 mL of adipogenic medium, 5 μL of insulin stock solution, 2 μL of dexamethasone (adipogenic induction medium) (*see* Subheading 2.2, **step 3**), and 10 μL of 1 mM rosiglitazone.

3. Keep the culture in adipogenic induction medium, replacing it twice per week, until a satisfactory degree of differentiation is attained (*see* **Note 6**).

3.8 Adipogenic Staining Procedure

1. Wash the cell monolayer with PBS.
2. Fixate with 4 % paraformaldehyde for 1 h at room temperature. Use 1 mL per well in the 6-well plate.
3. Remove paraformaldehyde, and wash once with deionized water.
4. Cover the cell monolayer with 1 mL of Oil Red O or Sudan Black B, and wait 5 min.
5. Remove the dye, and wash several times with deionized water until no precipitate is visible.
6. Observe under inverted microscope. The fat vacuoles stained by Oil Red O or Sudan Black B will have a reddish or black hue, respectively (Fig. 1c).

3.9 Chondrogenic Induction Procedure

1. Plate the cells in 6-well plates so as to attain 100 % confluence on the day differentiation is induced.
2. Remove all the complete culture medium and replace it with 2 mL of chondrogenic medium and add 20 μL of 1 μg/mL TGF-β1, 17.6 μL of 1 μg/mL AsAP, and 12.5 μL of 1 mg/mL insulin.
3. The culture medium should be replaced twice per week over 3–4 weeks (*see* **Note 7**).

3.10 Chondrogenic Staining Procedure

1. Wash the cell monolayer with PBS.
2. Fixate with 1 mL of 4 % paraformaldehyde per well for 20 min at room temperature.
3. Remove paraformaldehyde, and wash once with deionized water.
4. Cover the cell monolayer with 2 mL of Alcian Blue solution, and wait 5 min.
5. Remove the dye, and wash several times with deionized water.
6. The glycosaminoglycan-rich extracellular matrix will be stained blue and may be macroscopically or microscopically visible as a function of the deposit amount (Fig. 1d).

3.11 MSC Flow Cytometry

1. Repeat the procedure described in Subheading 3.3, **steps 1–5**.
2. Count the cells in a Neubauer Chamber. A minimum of 1×10^5 cells is needed for antibody labeling. The protocol described below is for the use of the "Mouse Mesenchymal Stem Cell

Marker Antibody Panel," which contains Sca-1, CD106, CD105, CD73, CD29, CD44 (positive MSC markers), CD11b, and CD45 (negative MSC markers).

3. Reconstitute each antibody-containing vial with 250 μL of sterile PBS, which provides reagents sufficient to process 25 samples.
4. Resuspend the cells in Flow Cytometry Staining Buffer at a concentration of 1×10^6 cells/mL.
5. For each marker, transfer 90 μL of the cell suspension into a separate 5 mL tube. Add 10 μL of antibody. Incubate for 30 min at room temperature.
6. Following incubation, centrifuge the cells at $300 \times g$ for 5 min and decant the buffer. Resuspend the cells in 2 mL of Flow Cytometry Staining Buffer, and repeat centrifugation. Repeat the resuspension and centrifugation steps.
7. Resuspend the cells in 100 μL of Flow Cytometry Staining Buffer, and add the appropriate secondary developing reagent, such as anti-rat IgG or anti-sheep IgG conjugated to a fluorochrome, according to the manufacturer's instructions.
8. Incubate for 30 min at room temperature in the dark.
9. Following incubation, centrifuge the cells at $300 \times g$ for 5 min and decant the buffer. Resuspend the cells in 2 mL of Flow Cytometry Staining Buffer, and repeat centrifugation. Repeat the resuspension and centrifugation steps.
10. Resuspend the cells in 200 μL of Flow Cytometry Staining Buffer for flow cytometric analysis. As a control for analysis, cells in a separate tube should be treated with the isotype control.

3.12 MSC Injection

1. Repeat the procedure described in Subheading 3.3, **steps 1–5** (*see* **Note 8**).
2. Count the cells in a Neubauer Chamber. A minimum of 1×10^6 cells per injection site (usually in the quadriceps) is needed.
3. Centrifuge the cells at $400 \times g$ for 10 min.
4. Wash with 1 mL of PBS. Repeat **step 3**.
5. Resuspend 1×10^6 cells in 50 μL of DMEM without FBS.
6. To inject, use an insulin syringe with a 24 G needle. Inject the cells into the quadriceps a few days after ischemia induction surgery (*see* Subheading 3.14). The ideal site for injection is the center of the muscle. Place the needle at 90° to the direction of the muscle fiber (*see* **Note 9**).
7. Following the injection of cells, wait 30 s, and then, remove the needle slowly to avoid leaking.

3.13 In Vivo Cell Monitoring

MSCs labeled with a fluorescent reagent may be localized in vivo without having to sacrifice the animal as reported [6]. This technique allows monitoring of the cell survival duration at the site of injection to choose the ideal moment to sacrifice the animal and perform the histological assays. The observation of luciferase-labeled cell spots is more appropriate for this method than the GFP-labeled cells [7].

3.14 Ischemia Induction Surgery

1. Use male Balb/c mice aged 10–12 weeks and weighing 25–29 g (*see* **Note 10**).
2. Immobilize the animal by pressing it onto a microinsulator grid. For anesthesia and sedation, administer ketamine (40 mg/kg body weight) and xylazine (10 mg/kg body weight) diluted in saline solution, respectively, to a maximum of 1 mL/animal intraperitoneally (right lower lateral quadrant) using a 29 G × ½″ needle (*see* **Note 11**).
3. Before surgery, remove the hair at the site of incision with a surgical clipper, and perform local asepsis with a solution containing 0.2 % chlorhexidine digluconate and 5 % polyvinylpyrrolidone (povidone) (*see* **Note 12**).
4. Place the animal on the dorsal decubitus, secure the limbs to a rigid platform with adhesive tape, and apply 5 % Bepanthen® over the animal's eyes. The use of 1.5 × 1.5 cm fenestrated surgical drapes is recommended. The full surgical procedure should be performed under a portable surgical microscope.
5. Using a scalpel blade no. 15, make a 0.5 cm longitudinal incision on the inguinal area (Fig. 2a, b) to expose the neurovascular bundle that is immediately below. With a pair of curved tweezers and a pair of Westcott conjunctival scissors, sever the connective tissue that covers the bundle and separate the arteries, veins, and nerves.
6. Use nylon suture #4-0 to ligate the femoral artery at the level of the inguinal ligament and its proximal branches (deep femoral, epigastric, saphenous, and popliteal arteries). Next, excise the full length of the femoral artery from the epigastric artery to the bifurcation of the saphenous and popliteal arteries (Fig. 2c, d).
7. Suture the skin using nylon suture (#4-0), repeat the sterilization, and transfer the animal to a warm surface, where it will remain until total recovery from anesthesia. Place the animal in a microisolator (maximum five animals/box) with ventilated shelves, and supply water and food ad libitum.

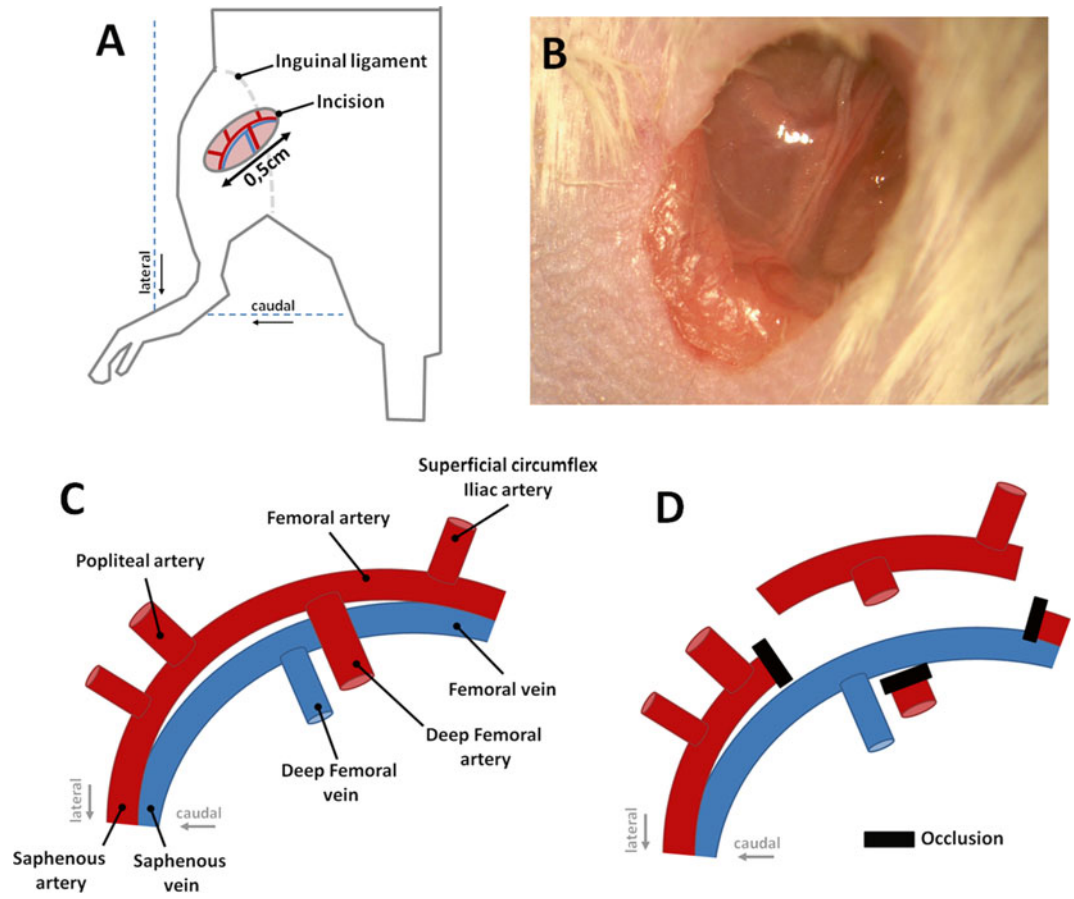

Fig. 2 Representation of the ischemia model. Schematic representation of a mouse hind limb indicating the site for the 0.5 cm incision at the level of the inguinal ligament (**a**) and the image of the incision (**b**). Representation of the vessels at the hind limb proximal area indicating the main vessels (**c**) and the standard ischemia induction model used in our laboratory [12], including occlusion of the proximal region of the femoral artery, deep femoral artery and bifurcation of the saphenous and popliteal artery, and excision of the full segment (**d**)

3.15 Assessment Parameters

3.15.1 Visual Assessment of the Ischemic Limb

1. Perform visual assessment of the ischemic limb according to Table 1 and Fig. 3 on a weekly basis for at least 4 weeks.
2. Grade II ischemia is defined as when one or more nails become black with or without changes in the limb color.
3. Grade III ischemia is defined by the presence of necrosis in one or more toes with or without changes in the limb color (reddening or blackening).

Table 1
Visual assessment of ischemic limbs

Ischemia grade	Macroscopic limb appearance
I	No necrosis
II	Blackened nails
III	Necrosis of toes
IV	Necrosis below the heel

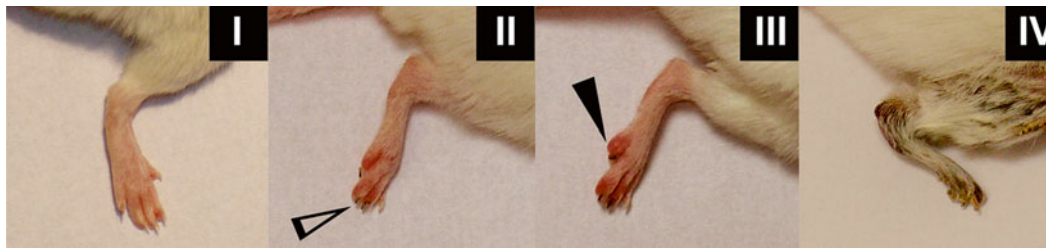

Fig. 3 Visual assessment of limb quality according to degree of ischemia. Blackened nails in grade II (*unfilled arrow*); necrosis of fingers in grade III (*filled arrow*) [12]

3.15.2 Muscle Strength In Situ Assessment

1. Anesthetize the animal, place it on the ventral decubitus, and secure the front and hind limbs to a table with the temperature set to 30 °C (Fig. 4a).
2. Make an incision on the calcaneal region, and retract the skin covering the gastrocnemius muscle (Fig. 4b, c).
3. Expose the distal portion of the sciatic nerve, and connect it to bipolar electrodes that are in turn connected to a pulse stimulator (Fig. 4d–f). Check that the electrodes are in contact only with the sciatic nerve and do not also contact muscles and/or connective tissue.
4. Isolate the gastrocnemius muscle completely while keeping the vascular connections and muscle origins in the femoral lateral and medial epicondyles intact; at the insertion site, isolate the calcaneal tendon from the calcaneal tubercle, and attach it to the force transducer using suture and a 10 mm loop (Fig. 4g).
5. Assess the muscle function by measuring the isometric contraction response with adjustment for the tension at rest to achieve the maximum muscle tension (tetanus). Use the peak of the tension curve generated by the pulse stimulator (frequency of 60 Hz, duration of 1 ms, and amplitude of 5 V) to calculate the difference between the maximum and minimum tension.

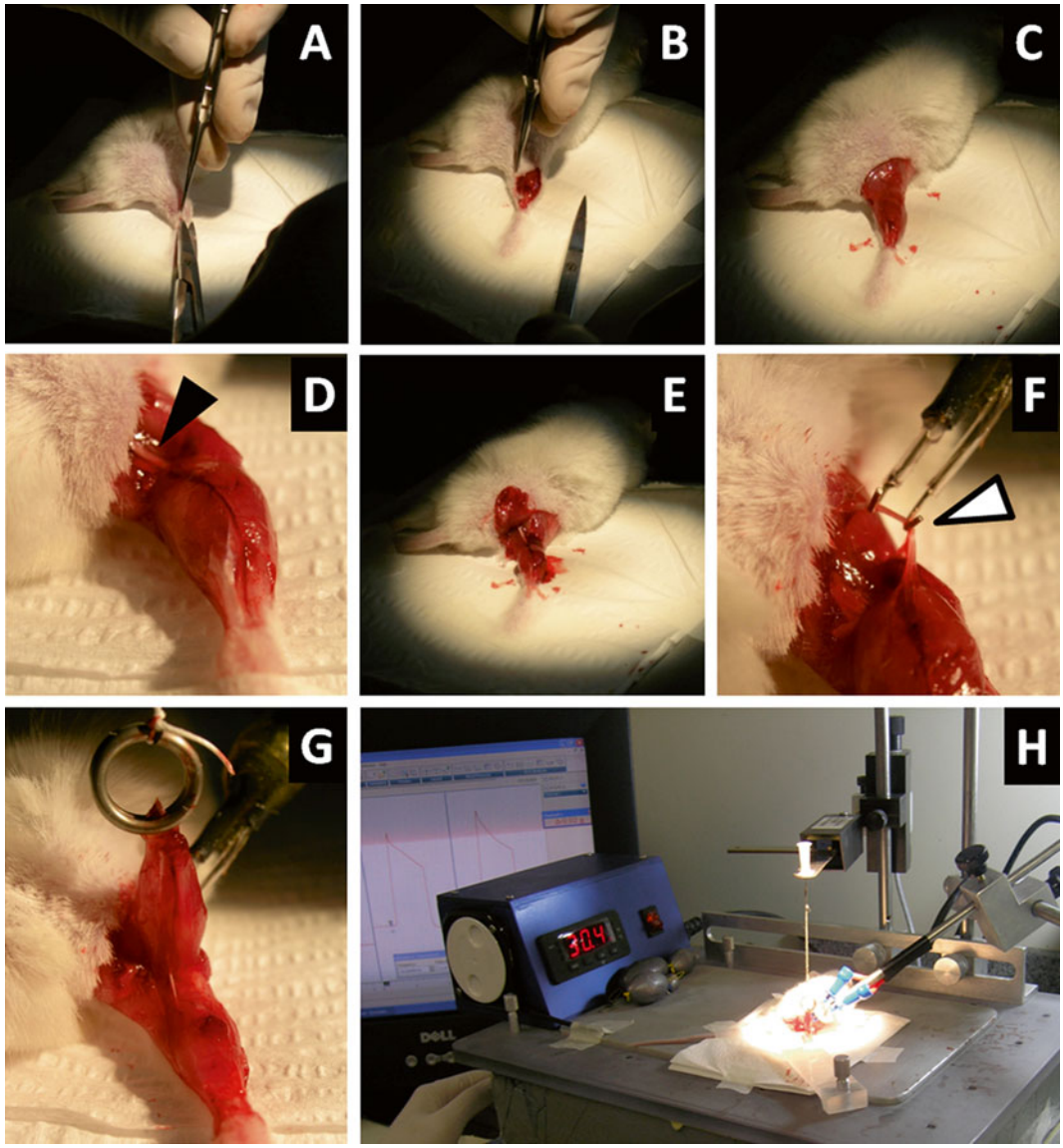

Fig. 4 Steps for in situ assessment of muscle strength. Proper position of the surgical instruments used for preparation (**a**); incision on the calcaneal area and retraction of the skin covering the gastrocnemius muscle (**b**); full excision of hind limb skin (optional) (**c**); exposure of the sciatic nerve (*filled arrow*) (**d**, **e**); coupling of the sciatic nerve to electrodes (*unfilled arrow*) (**f**); coupling of the calcaneal tendon to the force transducer with suture and loop (**g**); overview of the preparation (**h**)

Record the tension peaks at 1-min intervals while adding 10 g of tension at 1-min intervals (Fig. 4h). Use the software for data recording and analysis (*see* **Note 13**).

6. Next, euthanize the animal with an anesthetic dose approximately three times higher than the one used for anesthesia (*see* **Note 14**).

3.15.3 Muscle Mass Assessment

1. Following euthanasia, secure the animal to a flat rigid surface using adhesive tape for muscle excision.
2. Excise each muscle starting from their origins and insertions.
3. Isolate the origins of the gastrocnemius muscle at the medial and lateral epicondyles using anatomical tweezers and a pair of small curved Iris scissors (*see* **Note 15**).
4. Wash the muscle quickly and gently with PBS, and weigh it using an analytical balance.

3.15.4 Histopathology

Histological Processing

1. Fixate the muscle specimens immediately in 10 % buffered formaldehyde solution for at least 48 h. The volume of formaldehyde must be approximately 15 % of the specimen volume. Cleave the specimen within this period of time to preserve the internal structures of the tissue. Use a scalpel blade no. 11 to achieve precise and homogenous cleavage in all the specimens.
2. Place the specimens in histological cassettes and label them. This step and the next should be performed under the fume hood.
3. Dehydrate the specimens in descending ethanol baths (5 baths lasting 20 min each) and clarify with xylol (2 baths lasting 20 min each). Impregnate the samples with paraffin in an oven at 56 °C (2 baths lasting 45 min each), and place them in a paraffin mold with the surface to be sectioned turned down (muscle transverse section) (*see* **Note 16**).
4. Cut the paraffin blocks into 4–8 μm thick sections using the rotary microtome (*see* **Note 17**).
5. Transfer the samples to a tissue flotation bath at 35 °C, and place them on clean slides for routine staining or on silanized slides for immunohistochemical analysis. Next, dry the slides in an oven at 50 °C (*see* **Note 18**).

Hematoxylin-Eosin (HE) and Picro-Sirius Red Staining

1. All the samples for histopathological analysis must have been harvested within the boundaries of the ischemic area. Assess the HE-stained sections according to the criteria described in Table 2 (*see* **Note 19**).
2. Before staining: Remove all paraffin remnants from the histological sections with xylol (three baths lasting 10 min each), and rehydrate in decreasing concentrations of alcohol in pure distilled water (100, 100, 70 %, H_2O—5 min each). This procedure is common to most routine stainings. From this point onwards, the stains specific to the various histomorphometric assays are used.
3. HE staining: Immerse the histological sections in filtered Harris's hematoxylin for 5 min, then immerse them quickly (maximum 2 s) in the differentiator (3 % alcohol-acid solution), wash in running tap water for 5 min, and immerse in eosin yellow solution.

Table 2
Steps for morphological analysis

	Histopathological parameters assessed by HE staining
1	Changes in the myocyte size (hypertrophy; atrophy)
2	Changes in nuclei (hyperchromasia; hypochromasia)
3	Changes in the fiber architecture and sarcolemma integrity
4	Degenerative changes (nucleus fragmentation)
5	Regenerative changes (myocytes/myoblasts with central nuclei)
6	Cell reaction (endomysial and/or perivascular inflammatory infiltration with or without invasion of non-necrotic fibers by inflammatory mononuclear cells and presence of adipose cells characteristic of metaplasia)

4. Sirius Red staining: Immerse the histological sections in 0.2 % phosphomolybdic acid for 1 min, then in Picro-Sirius Red solution for 90 min, and wash once in an acid water (0.01 N HCl) bath.
5. After staining: The final processing is common to all stains. Dehydrate the histological section in increasing concentrations of ethanol (70, 100, and 100, 5 min each) and three xylol baths (5 min each) and mount on (20 × 20 mm to 24 × 60 mm) microscope slides using Entellan®. Once the slides are dried, analyze them under a microscope.

Immunohistochemistry

1. Several vessel markers used in studies on angiogenesis may also be used in tumorigenic assays, as well as in studies on ischemia-reperfusion injury, ranging from relatively unspecific markers, such as CD31 (PECAM-1), to markers of newly formed vessels, such as CD105 (endoglin). We recommend two procedures to assess vessels in ischemic tissue. The first consists of capillary labeling using lectin I—isolectin B4 from *Griffonia simplicifolia* (*Bandeiraea simplicifolia*) (in a 1:200 dilution) to assess small residual capillaries or vessel collateralization. Next, perform vessel-specific labeling using components of developed vessels, such as alpha-smooth muscle actin (α-SMA) (dilute 1:50). Those two markers suffice to assess the density of capillaries and larger vessels; however, testing other vessel markers might also be useful, such as the von Willebrand factor (vWF) and the vascular endothelial growth factor (VEGF) receptors.
2. Use the above markers according to the manufacturers' instructions. The assays might be performed using paraffin sections. Prioritize monoclonal primary antibodies to increase the reaction specificity as follows:

3. Deparaffinize sections with xylol and rehydrate in a series of increasing alcohol concentrations (see previous section).
4. Inhibit the endogenous peroxidase using 3 % hydrogen peroxide in methanol.
5. Wash the sections with distilled water or PBS and heat in a steamer for 15–30 min for antigen recovery in sodium citrate buffer. Block avidin and biotin using a blocking kit.
6. Incubate with the primary antibody in a humid chamber overnight. Dilute the antibody with PBS at 4 °C (this procedure might vary among manufacturers).
7. Wash the sections and incubate with the conjugated secondary antibodies (follow the manufacturer's instructions). Develop the reaction using H_2O_2 as a substrate and DAB as a chromogen.
8. Counterstain with hematoxylin diluted 1:3 in distilled water.

Measurement

1. Acquire digitized images of tissues at 50, 200, and 400× magnification. The images acquired with less magnification are recommended for the overall assessment of the muscle tissue, whereas the ones with greater magnification are recommended for assessment at the cellular level.
2. For histomorphometric assessment, measurement is performed using the Image-Pro Plus® software or an open-access equivalent [8].
3. Before analysis, calibrate the software by indicating the standard unit of measurement based on the micrometer bar available in the previously digitized photomicrographs.
4. Using 20–40 photomicrographs with 400× magnification of the muscle injury area of each animal, measure the area of collagen fiber deposition in the extracellular matrix surrounding myocytes, which indicates the replacement of muscle tissue.
5. Adjust the sensitivity to a higher level (e.g., to level 4 when using Image-Pro Plus®) for monochromatic stains, while maintaining a ratio of 1:1 pixel in the recognition window.
6. Apply the color standard differentiation tool, and select the areas stained with Sirius Red only (Fig. 5a).
7. Individually record only the number of each area around the red-stained myocytes ("count/size" option when using Image-Pro Plus®) (Fig. 5b).
8. The results will appear in a table at the right side of the software interface (Fig. 5c). Apply the "Total" tool, and the sum of all the areas will appear in the table of statistical tools in micrometers (or in the unit selected in the calibration step) (Fig. 5d).
9. Express the total values of the areas with fibrosis as percentages relative to the total area of the analyzed muscle histological section.

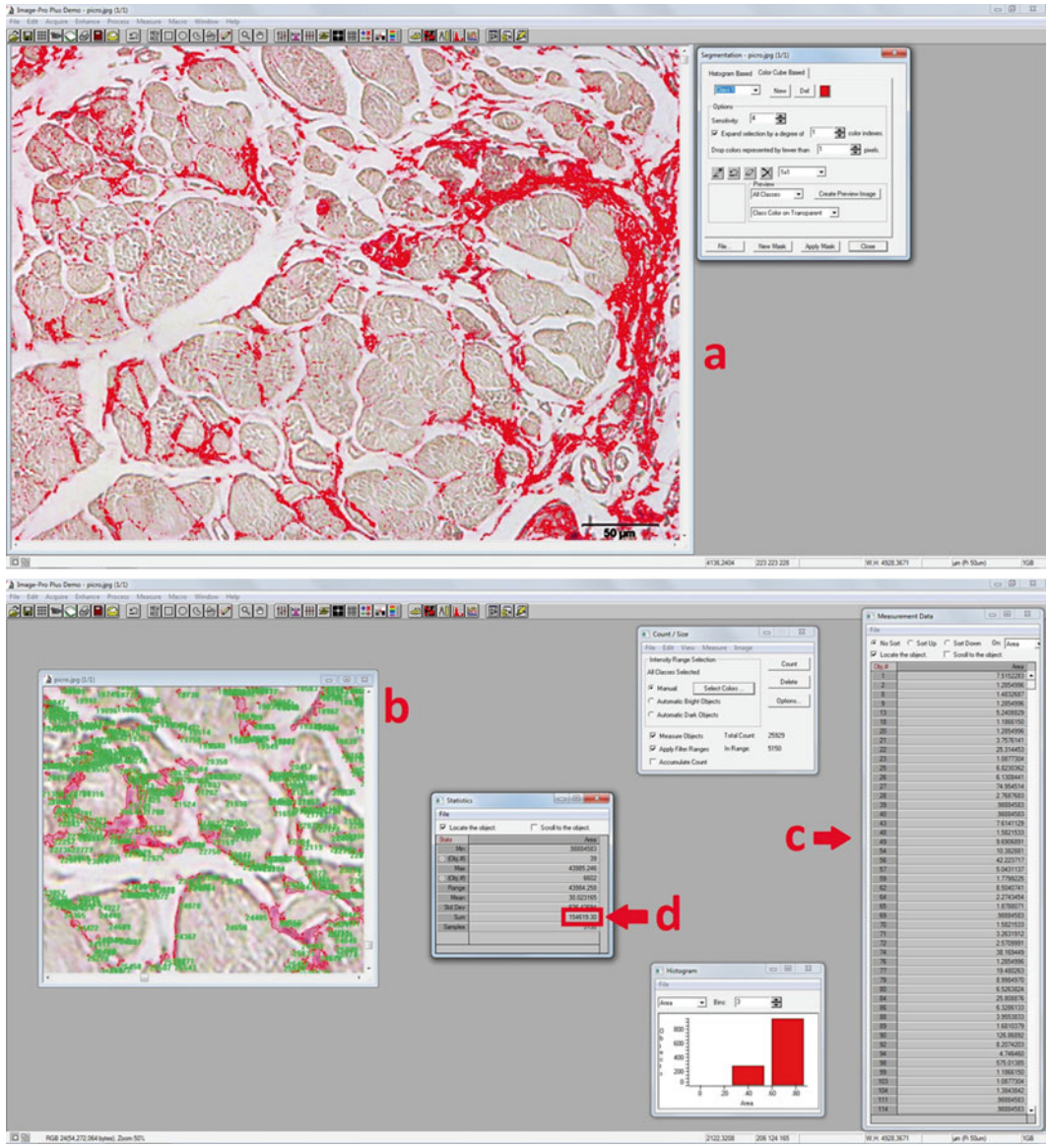

Fig. 5 ImagePro Plus® v6.0 software interface used for measurement. Photomicrograph of muscle tissue stained using the Picro-Sirius Red, showing monochromatically selected fibrous connective tissue (*red area*); bar = 50 µm (**a**); individual values of the selected areas (**b**); table of individual values (**c**); and table of the statistical values corresponding to the areas selected for analysis (**d**)

4 Notes

1. Although the murine MSCs are quite resistant to adverse conditions, they should be treated gently. All media and solutions should be preincubated at 37 °C in a water bath.
2. In the earlier passages, cell growth to confluence might require approximately 45 days until achieve great cell number for experiments.

3. Cells should be transferred every 3–4 days; when there is not enough expansion for the passage, change the culture medium.
4. In the later passages, confluence occurs faster. Passage the cells as soon as they exhibit confluence. When the long-term maintenance of a culture demands more than two passages per week, the passage ratio should be increased until the transfers are reduced to twice weekly.
5. Long-term maintenance of confluent cultures might result in unwanted differentiation. Spontaneous differentiation is different from induced differentiation and should not be used as a criterion for cell characterization.
6. Although differentiation usually occurs within 1–3 weeks, it may not occur for up to 2 months in cell populations with low adipogenic differentiation potential.
7. Deposition of chondrogenic extracellular matrix is slower and thus becomes visible only 3 weeks after inducing differentiation.
8. After several passages, the cultures may no longer represent the original cell population because selection may occur throughout the establishment and maintenance of cultures. In turn, the cells in passages 1 and 2 may still be too heterogeneous and contaminated by other somatic cells. The ideal number of passages before injection is 3–5.
9. The day of injection for therapy is variable and should be determined experimentally; in our experiments, 5 days after ischemia have brought the best outcome. To improve the quality of the cells, they should be well suspended in the syringe during injection. Do not inject the cells when precipitates are visible in the syringe or tube. To make injection easier, it is recommended to anesthetize the animals using inhalational (isoflurane) or injectable (ketamine and xylazine) agents (see description in ischemia induction surgery).
10. The mice strains BALB/c and C57BL/6 are the most widely used in animal experiments, but only BALB/c should be used in studies on severe ischemia that reproduce human critical limb ischemia (CLI) due to the presence of a smaller capillary network. Strain C57BL/6 is more suitable for studies on milder peripheral artery disease, such as intermittent claudication. In addition, age, weight, and the presence of diabetes are factors to be taken into consideration by investigators when selecting the most appropriate animal model for a given study.
11. Anesthesia demands appropriate knowledge of the mechanisms of action and routes of administration of the various anesthetic agents. The cost, feasibility, and potential interference of the agents used with the parameters assessed in a study should be taken into consideration. First, investigators should master

the procedures for animal immobilization. Then, the absence of signs of pain should be established as an indication of the attainment of general anesthesia, and the animal temperature should be kept at 37 °C. Pay attention to the duration of anesthetic induction to avoid the occurrence of pain signs during surgery. Use of an ophthalmic ointment (5 % Bepanthen®) is indicated to avoid drying of the eye mucosa.

12. (a) A hair removal cream (Veet cream, Reckitt Benckiser, Berkshire, UK) may be used for hair removal. In that case, completely remove any remnants with water and a piece of gauze before performing the incision. (b) Depending on the surgeon's skills, the bevel of a 30 G × ½″ needle may be used to break the connective tissue and carefully separate the elements of the neurovascular bundle when it is not possible to use Westcott conjunctival scissors. (c) This procedure is extremely delicate, and capillary bleeding, vein obliteration, or nerve rupture may occur. Avoid any bleeding by removing excess fluid in the surgical field with a cotton swab. The innervation of the incision site should be fully preserved because any rupture of the local nerve network may cause clinical immobility or hypotension, which will interfere with the results of the later physical-clinical assessment. (d) This ischemia model is an adaptation of the model from [9]. Six different models of induced ischemia were assessed in that study: ligation of the femoral vein alone; distal ligation of the femoral artery alone; ligation of the femoral artery and vein; ligation and excision of the femoral artery alone; ligation and excision of the femoral artery and vein; and proximal ligation of the femoral artery alone. Ours is an adaptation of the model involving proximal ligation of the femoral artery alone because we also ligated the artery branches up to its bifurcation into the saphenous and popliteal arteries, and its full length was excised (Fig. 2d).
13. The values of the in situ muscle strength of the gastrocnemius muscle in ischemic animals 30 days after induction are approximately 10–12 % of the values of normal animals.
14. As ketamine has dissociative properties, it cannot be used as a general anesthetic. The higher dose used for euthanasia may induce strong muscle contractions and even seizures. For that reason, it must be associated with a centrally acting muscle relaxant, such as xylazine. Cervical dislocation is an acceptable physical method of euthanasia. The method selected for euthanasia must follow regulatory demands and apply techniques that ensure the animal's death; such methods may be chemical, exsanguination, or decapitation. Physical methods followed by exsanguination and perfusion are ideal when the muscle tissue should be preserved for morphometric analysis.

15. All excisions must be performed by a single trained professional to avoid variations associated with the technical-surgical procedure and to make the assessment of mass more precise.
16. To optimize the time allotted to the dehydration and clarification baths, the passages may be performed with warmed solutions on a heating plate at 56 °C. In that case, the passage duration should be halved. To optimize the paraffin block, one part beeswax may be added to nine parts paraffin. This addition makes the microtomy easier.
17. To optimize the quality of the sections, it is recommended to cool the paraffin blocks in a freezer at –20 °C before microtomy.
18. Placement of the sections to float on a 50 % ethanol solution at room temperature before transfer to a water bath at 35 °C is indicated to avoid the occurrence of folds and cracks in the sections.
19. Ischemia induces chronic muscle injury with signs of tissue damage, including the presence of necrotic fibers, irregular diameter of myocytes, fissures in myocytes, and defragmented central nuclei. The endomysium is a thin layer of reticular fibers mostly composed of type III collagen that covers the muscle fibers. Post-injury tissue repair is associated with increased collagen deposition, especially in the endomysial areas of the ischemic muscle, which increases the thickness of the collagen layer between fibers (endomysium), resulting in loss of the tissue function. These parameters have been extensively reviewed in the literature [10, 11]. HE staining allows the identification of general tissue or cell features. As hematoxylin stains the cell nucleus and eosin stains the cytoplasm, several histopathological findings may be inferred. One such histopathological finding is the presence of fibrosis, which, among other things, consists of the excessive deposition of collagen matrix in the muscle endomysium and perimysium. To detect the occurrence of fibrosis, Sirius Red staining is indicated, as it makes the tissue deposits of collagen matrix apparent. In the analysis of collagen matrix deposition, the collagen found in the muscle epimysium and aponeurosis should be excluded because they are typically found in those tissues.

Acknowledgments

L.M. and P.K.M.M. are recipients of FAPESP scholarships. This work was supported by the Fundação de Amparo à Pesquisa do Estado de São Paulo (FAPESP 2011/00859-6 and 2012/21861-1).

References

1. Norgren L, Hiatt WR, Dormandy JA, Nehler MR, Harris KA et al (2007) Inter-society consensus for the management of peripheral arterial disease (TASC II). Eur J Vasc Endovasc Surg 33(Suppl 1):S1–S75
2. Pittenger MF, Mackay AM, Beck SC, Jaiswal RK, Douglas R, Mosca JD et al (1999) Multilineage potential of adult human mesenchymal stem cells. Science 284:143–147
3. Nauta AJ, Fibbe WE (2007) Immunomodulatory properties of mesenchymal stromal cells. Blood 110:3499–3506
4. Annabi B, Lee YT, Turcotte S, Naud E, Desrosiers RR, Champagne M et al (2003) Hypoxia promotes murine bone- marrow-derived stromal cell migration and tube formation. Stem Cells 21:337–347
5. Dominici M, Le Blanc K, Mueller I, Slaper-Cortenbach I, Marini F, Krause D et al (2006) Minimal criteria for defining multipotent mesenchymal stromal cells. The International Society for Cellular Therapy position statement. Cytotherapy 8(4):315–317
6. Boddington S, Henning TD, Sutton EJ, Daldrup-Link HE (2008) Labeling stem cells with fluorescent dyes for non-invasive detection with optical imaging. J Vis Exp 14:e686
7. Wilson K, Yu J, Lee A, Wu JC (2008) In vitro and in vivo bioluminescence reporter gene imaging of human embryonic stem cells. J Vis Exp 14:e740
8. Schneider CA, Rasband WS, Eliceiri KW (2012) NIH image to ImageJ: 25 years of image analysis. Nat Methods 9:671–675
9. Goto T, Fukuyama N, Aki A, Kanabuchi K, Kimura K, Taira H et al (2006) Search for appropriate experimental methods to create stable hind-limb ischemia in mouse. Tokai J Exp Clin Med 3:128–132
10. Andres-Mateos E, Mejias R, Soleimani A, Lin BM, Burks TN, Marx R et al (2012) Impaired skeletal muscle regeneration in the absence of fibrosis during hibernation in 13-lined ground squirrels. PLoS One 7:e48884
11. Mann CJ, Perdiguero E, Kharraz Y, Aguilar SP, Serrano AL, Muñoz-Cánoves P (2011) Aberrant repair and fibrosis development in skeletal muscle. Skelet Muscle 1:21
12. Cunha FF, Martins L, Martin PK, Stilhano RS, Paredes Gamero EJ, Han SW (2013) Comparison of treatments of peripheral arterial disease with mesenchymal stromal cells and mesenchymal stromal cells modified with granulocyte and macrophage colony-stimulating factor. Cytotherapy 7:820–829

Chapter 14

Methods to Assess Intestinal Stem Cell Activity in Response to Microbes in *Drosophila melanogaster*

Philip L. Houtz and Nicolas Buchon

Abstract

Drosophila melanogaster presents itself as a powerful model for studying the somatic stem cells of the gut and how bacteria affect intestinal homeostasis. The *Gal4/UAS/Gal80^{ts}* system allows for temporally controlled expression of fluorescent proteins, RNAi knock-down, and other genetic constructs targeted to specific cell populations in the midgut. Similarly, FLP/FRT-mediated somatic recombinations in intestinal stem cells (ISCs) are utilized to visualize and analyze the clonal lineages of individual or populations of stem cells. Live imaging microscopy and immunofluorescence allow both qualitative and quantitative characterization of stem cell shape, proliferation, and differentiation. Here, we detail the use of these tools and techniques for studying gut performance during and following a bacterial infection in the adult fruit fly.

Key words *Drosophila*, Intestinal stem cell, Epithelium renewal, Bacterial infection, Midgut homeostasis, Lineage analysis, Immunostaining

1 Introduction

The gut of *Drosophila melanogaster* is composed of a monolayer of epithelial cells, surrounded by two layers of visceral muscles and arranged into a tube with three distinct compartments: the foregut, the midgut, and the hindgut (Fig. 1) [1, 2]. The foregut and hindgut are derived from the ectoderm and their epithelium is covered by chitin, while the midgut is derived from the endoderm, covered by a chitinous matrix (the peritrophic matrix), and serves as the primary site of nutrient processing and absorption [1]. Three types of cells compose the epithelia of the midgut: large, nutrient absorbing enterocytes (ECs), small, secretory enteroendocrine (EE) cells, and pluripotent intestinal stem cells (ISCs).

ISCs in *Drosophila*, like those in mammals, maintain the gut by self-renewing division, yielding one new ISC and one nondividing progenitor cell called an enteroblast (EB) [3, 4]. EB cells undergo further fate decision and ultimately differentiate to become new ECs or EE cells, replacing the old intestinal cell population [5].

Bruno Christ et al. (eds.), *Animal Models for Stem Cell Therapy*, Methods in Molecular Biology, vol. 1213,
DOI 10.1007/978-1-4939-1453-1_14,

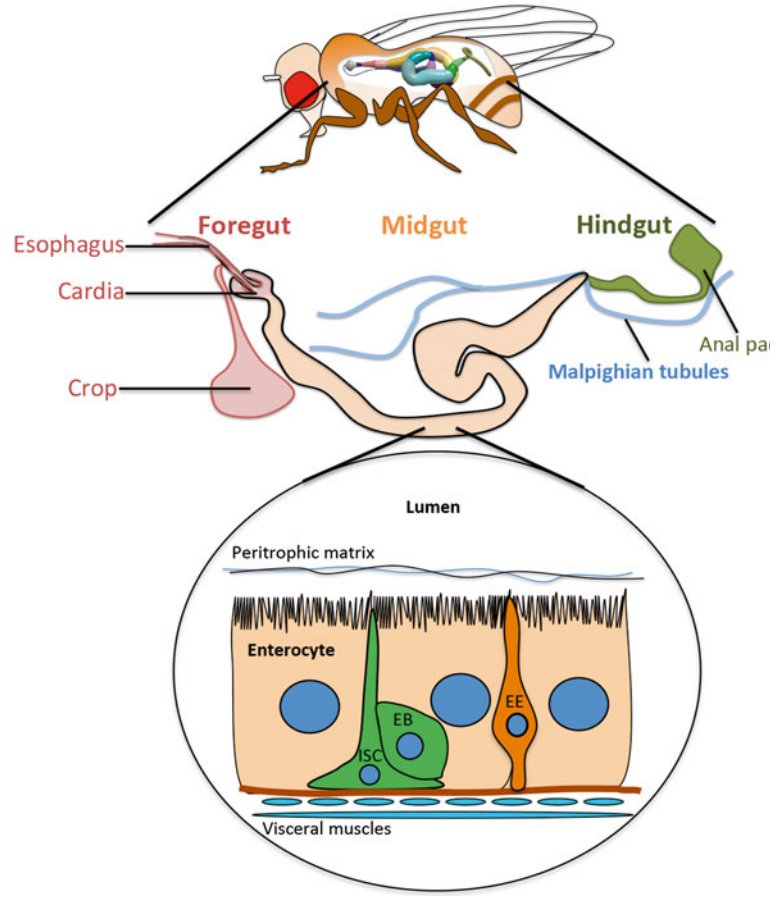

Fig. 1 The *Drosophila* gut. The gut of an adult fruit fly is organized into three distinctive regions: the foregut, the midgut, and the hindgut. The foregut comprises the esophagus and the crop, which acts as a storage organ and initiates nutrient processing. Food is then passed on to the midgut where the majority of nutrient digestion and absorption occurs. Finally, the hindgut functions to reabsorb water from waste material before its removal. The midgut epithelium is surrounded by visceral muscles and is composed of four primary cell types: Enterocytes (ECs), Enteroendocrine (EE) cells, Intestinal Stem Cells (ISCs), and Enteroblasts (EBs). ECs and EEs are differentiated and carry out absorptive and neurosecretory functions, respectively. ISCs replenish old or destroyed cells through self-renewing division, yielding a new ISC and an EB, which is dedicated to differentiate into either an EC or an EE cell

Complete turnover of the midgut is accomplished by this process in 10–15 days under basal conditions, but is greatly accelerated in response to intestinal damage and microbial pathogens [2, 6, 7]. The discovery of ISCs in the midgut of *Drosophila*, and the wealth of genetic tools established in the fruit fly, make it an ideal and exciting model for studying the behavior of ISCs during infection.

In this chapter, we describe techniques for performing oral infections in *Drosophila* and monitoring ISC proliferation and

subsequent lineage. The *Gal4/UAS/Gal80^{ts}* system allows for fluorescence and lacZ labeling of particular intestinal cell types by making expression of a reporter gene dependent upon the expression of cell-specific enhancers. In addition, immunostaining allows cell types to be labeled according to cell-specific, targetable antigens. Furthermore, visualization of progenitor lineages, stem cell division rates, and global tissue renewal can be accomplished with diverse genetic systems such as *esg-Gal4^{ts}*, *tub-FRT-lacZ clones*, *esg$^{F/O}$*, *MARCM*, and *Twin-spot MARCM* (*see* Subheading 2.3).

2 Materials

2.1 Fly Rearing and Husbandry

1. *Drosophila* diet: 50 g baker's yeast, 40 g sucrose, 60 g cornmeal, 7 g agar, 16 mL Moldex (10 %), 8 mL acid mix (*see* **Notes 1** and **2**), 1,000 mL deionized water.
2. Standard fly vials (~22 mm in diameter) with *Drosophila* diet.
3. Facilities to maintain flies at 18 and 29 °C.

2.2 Bacterial Cultures

1. Sterile Luria Bertani Broth (LB).
2. LB agar plates: 1.5 % agar in LB, poured into sterile culture plates.
3. Sterile, disposable inoculation loops.
4. Autoclaved Erlenmeyer flasks.
5. Pathogenic bacteria stocks: *Erwinia carotovora* subsp. *carotovora* 15 (*Ecc15*), *Pseudomonas entomophila*, *Serratia marcescens* str. Db11, or *Pseudomonas aeruginosa* (*see* **Note 3**).
6. Shaking incubator thermostated at 29 °C.

2.3 Fly Genetics

1. *Gal4/UAS/Gal80^{ts}* system (Fig. 2a): Allows labeling of specific cells in the gut (*see* **Note 4**). We can induce the *Gal4/UAS* system to visualize different cell populations in the gut by expressing fluorescent proteins in specific cell types. For instance, the *esg-Gal4^{ts}* system (*esg-Gal4*, *Gal80^{ts} UAS-GFP* flies) allows for visualization of progenitors to monitor ISC shape, number, and proliferation [4, 6].
2. *tub-FRT-lacZ* clones: Randomly labels individual stem cells and their progeny in a heat shock-inducible manner (*see* **Note 5**) [8]. Used to study ISC proliferation and ISC lineage.
3. *esg$^{F/O}$* system: Systematically labels all ISCs and their progeny with GFP in an inducible manner (Fig. 2b) [7]. Used to study proliferation of progenitors, ISC lineage, and tissue renewal over time (*see* **Note 6**).
4. MARCM (Mosaic Analysis with a Repressible Cell Marker) clones: Randomly labels individual stem cells and the progeny of one of the two daughter cells [9, 10]. For its application to ISC lineage, see Singh et al. [11].

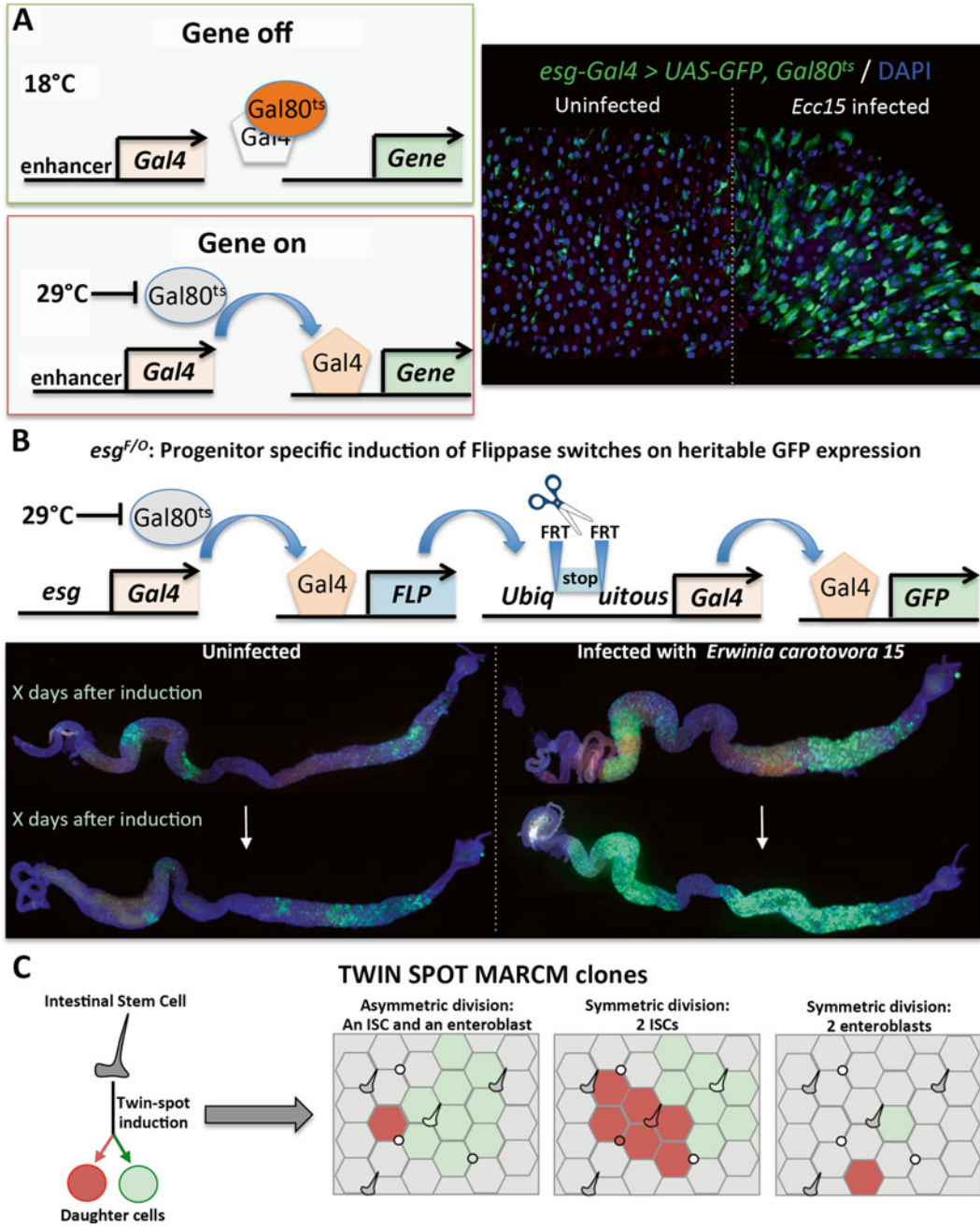

Fig. 2 Fly genetic tools for studying intestinal stem cell activity. (**a**) *Left*: The *Gal4/UAS/Gal80ts* system allows the expression of *UAS-GFP*, and other *UAS*-regulated transgenes, to be induced by Gal4 in a temperature-dependent manner in only the cells where the promoter of the *Gal4* transgene is active. Gal80ts inhibits Gal4 at 18 °C, preventing GFP expression controlled by *UAS*, but becomes inactivated at 29 °C. *Right*: Choosing a promoter expressed in progenitors (*esg*) allows us to visualize the activation of progenitor cells during infection, as illustrated by the diffuse GFP signal in infected guts (*right panel*). (**b**) The *esgF/O* system drives the temperature-dependent expression of FLP recombinase in progenitors (when moved to 29 °C). This triggers the FLP out of the CD2 cassette and the activation of the *act-Gal4* ubiquitous driver in subsequent ISC progeny that therefore expresses GFP. The proportion of GFP positive cells in the midgut reflects turnover rates. Infection with *Ecc15* induces an acceleration of epithelium renewal (see microscopy examples in *lower panel*). (**c**) The *Twin-spot MARCM* system induces the expression of different heritable markers (GFP and RFP) in the two daughter cells of an ISC. This allows establishment of the symmetrical or asymmetrical behavior of ISC divisions, discernible through the analysis of the subsequent lineage of the two daughter cells

5. Twin-spot MARCM system: Randomly labels dividing ISCs and progeny in a heat shock-inducible manner [12, 13]. After mitosis of the parent cell, the two daughter cells are tagged with a different fluorescent reporter. This allows observing the fate of the two daughter cells of an ISC division, monitoring both proliferation and the proportion of symmetric versus asymmetric division (*see* **Note 7**) (Fig. 2c).
6. Additional molecular markers to study ISC in the gut of *Drosophila* can be found in Singh et al. [11].
7. 37 °C water bath.

2.4 Oral Infection

1. Absorbent pads (e.g., Whatman filter paper), cut to the diameter of the fly vials (usually 22 mm).
2. Empty fly vials.
3. Fly vials with *Drosophila* diet.
4. Concentrated sucrose solution in sterilized water (*see* **Note 8**).
5. Bacterial pellet: The infectious dose varies for different bacteria species (i.e., *Ecc15* pellet should have an $OD_{600} = 200$).

2.5 Gut Dissection

1. Multi-well glass dish.
2. Source of CO_2 for anesthetization (Fig. 3a).
3. Forceps (*x*2).

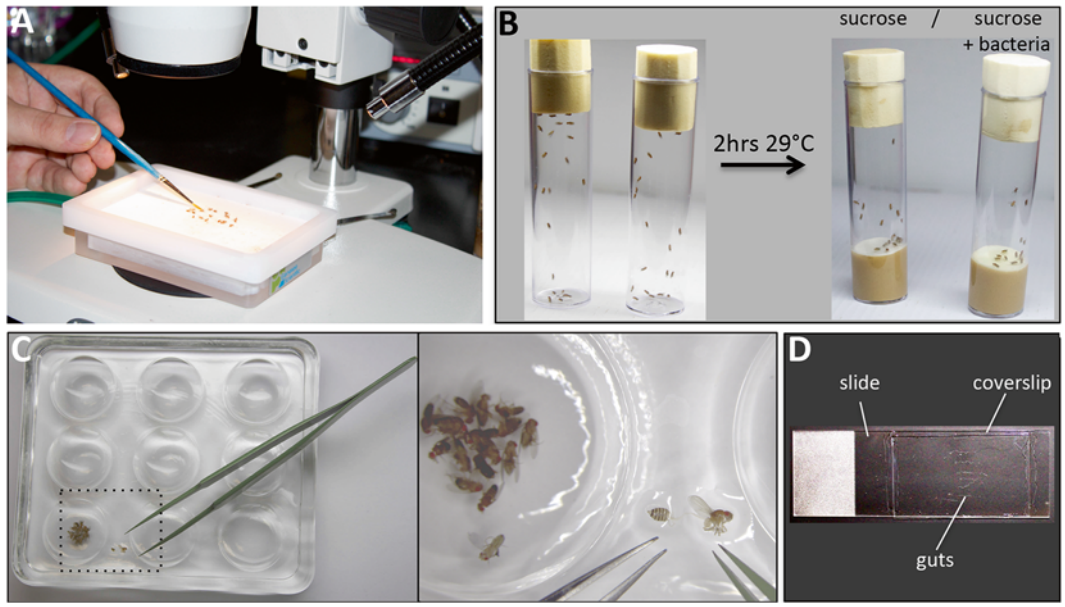

Fig. 3 Steps in studying intestinal stem cells using *Drosophila*. (**a**) Fly pushing and sorting on a CO_2 pad to obtain the desired genotype/phenotype. (**b**) Flies are starved at 29 °C for 2 h in empty tubes before being transferred onto filter pads with sucrose (control) or bacteria and sucrose mixes. (**c**) Dissection of midguts from anesthetized flies in PBS, on a spot plate. (**d**) Guts positioned on a slide with mounting solution under a coverslip

4. 70 % EtOH.
5. Sterile 1× PBS (Phosphate Buffer Saline).

2.6 Live Imaging

1. Sterile, 1.5 or 2 mL centrifuge tubes.
2. PBT solution (0.05 % Tween 20): Add 25 μL of Tween 20–50 mL 1× PBS and mix.
3. DAPI staining solution: Add 1 μL of 20 mg/mL DAPI dilactate in sterile water to 50 mL PBT. Store at 4 °C.
4. PBS/glycerol (1:1) or antifadent mounting medium (Citifluor AF1 or Vectashield).
5. Glass microscope slides.
6. Glass coverslips.
7. Nail polish (to seal coverslips on slides).

2.7 Immunostaining

1. Sterile, 1.5 or 2 mL centrifuge tubes.
2. PBT solution (0.1 % Tween 20): Add 50 μL of Tween 20–50 mL 1× PBS and mix.
3. 4 % paraformaldehyde (PFA) fixative in PBT (0.1 % Tween 20). Store solution at −20 °C or at 4 °C not more than 2 days.
4. PBTA: PBT solution (0.1 % Tween 20) with 1 % bovine serum albumin (BSA).
5. Primary antibody stocks: mouse anti-GFP (Roche), mouse anti-RFP (Clontech), rabbit anti-PH3 (Millipore) for cells undergoing mitosis, mouse anti-Prospero (Developmental Studies Hybridoma Bank) for EE cells, anti-PDM1 for ECs [14]. Additional primary antibodies used to study ISC in the gut of *Drosophila* can be found in Singh et al. [11].
6. Secondary antibody stocks: Alexa-488 anti-mouse (Invitrogen), Alexa-594 anti-rabbit (Invitrogen).
7. PBS/glycerol (1:1) or antifadent mounting medium (Citifluor AF1 or Vectashield).
8. Glass microscope slides.
9. Glass coverslips.
10. Nail polish (to seal coverslips on slides).

3 Methods

3.1 Fly Rearing and Husbandry

1. *Drosophila* stocks: Maintain flies by transferring adults to new vials every 2–3 days at room temperature or in a 25 °C incubator, or every 7 days in an 18 °C incubator (stocks with a Gal80^{ts} system). Maintain at a ~12/12 h light/dark cycle.

3.2 Bacterial Cultures

1. Pour 500 mL of sterile LB medium into a sterile, autoclaved Erlenmeyer flask with foil cover (*see* **Note 9**).
2. Locate a single colony on an LB bacterial stock plate and gently scrape it onto a sterile, disposable inoculation loop.
3. Transfer the colony to the Erlenmeyer flask with LB medium and seal the flask with a sterile cover (for aerobic bacteria, it should not be air tight).
4. Secure the Erlenmeyer flask in a shaking incubator at 29 or 37 °C, depending on the growth requirements of the bacteria, and incubate for 16 h while shaking at 200 rpm (*see* **Note 10**) to reach stationary growth phase.
5. Pour the liquid culture into a sterile centrifuge flask and centrifuge at 4 °C and 3,220 × *g* for 15 min.
6. Empty most of the LB medium from the centrifuge flask.
7. Use a pipette and sterile tips to resuspend the bacterial pellet in the remaining LB medium. Transfer the liquid, concentrated bacterial pellet into a sterile 15 mL tube.
8. Make a 1:1,000 dilution of the pellet in sterile water in a separate test tube. Measure the OD_{600} absorbance of the dilution and subsequently calculate the concentration of the bacterial pellet. Adjust the bacterial concentration ($OD_{600} = 200$ for *Ecc15*).
9. Store bacterial pellet at 4 °C for up to 1 week.

3.3 Fly Genetics

1. Raise Gal80^{ts} stocks (*esg-Gal4^{ts}* and *esg$^{F/O}$*) at 18 °C and shift to 29 °C 2 days prior to infection for activation of Gal4-mediated expression.
2. For flies using FLP/FRT-mediated recombination and *hsFLP* (*tub-FRT-lacZ*, *MARCM*, and *Twin-spot MARCM* systems), cross stocks appropriately for the F1 progeny to carry all required transgenes [8, 11, 12]. Raise the F1 progenies at 18 °C, then heat shock for 40 min at 38 °C, and use 2 days post-clonal induction.
3. Sort flies of the proper genotype on a CO_2 pad prior to infection (Fig. 3a).

3.4 Oral Infection

1. Flip experimental flies into empty fly tubes and put at 29 °C for 2 h (*see* **Note 11**).
2. Prepare 2.5 % and 5 % sucrose dilutions in sterile water. Mix the 5 % sucrose solution with an equal volume of the bacterial pellet (at $OD_{600} = 200$ for *Ecc15*) to create the infection mix.
3. Set up labeled standard fly tubes with diet. Place an absorbent pad into a tube and push it down until it contacts the diet.

The pad should completely cover the diet. Immediately add 150 μL of either 2.5 % sucrose, for controls, or sucrose and bacteria mix, for infections. Repeat for all tubes.

4. Flip flies into appropriate tubes for infection and controls (sucrose). Incubate flies at proper infection temperature for required infection time (*see* **Note 12**).

3.5 Gut Dissection

1. Prepare a clean multi-well glass spot plate and place under a dissection scope (*see* **Note 13**).
2. Anesthetize flies using CO_2 source.
3. Transfer flies to a spot plate well containing 70 % ethanol and briefly submerge (*see* **Note 14**).
4. Remove ethanol and replace with 1× PBS.
5. Use forceps to create a drop of PBS on a flat portion of the spot plate and transfer a fly into the droplet. There should be enough PBS covering the fly that the gut remains submerged during dissection.
6. Using two pairs of forceps, decapitate the fly with a clean stroke across the "neck." Ensure that the esophagus is completely severed.
7. Carefully separate the thorax from the abdomen by bracing one pair of forceps against the thorax while using the other to hold the first abdominal segment, and pull it away from the thorax. Stop once the two are separated and the gut is visible between them.
8. Sever the last two abdominal segments by pinning the end of the abdomen down with one pair of forceps and slicing across it with the other. Carefully pull the remainder of the abdomen away from the thorax and off of the gut. If the gut remains attached, either in the thorax or the abdomen, locate the crop and use it to gently pull the gut away from these segments.
9. Use the forceps to puncture the crop without removing it (*see* **Note 15**).
10. Store the gut in 1× PBS and proceed to Subheadings 3.6 or 3.7.

3.6 Live Imaging

1. Dissect guts for live imaging (*see* Subheading 3.5).
2. Transfer 3–6 guts into a 1.5 mL centrifuge tube with 0.5–1 mL of DAPI staining solution. Incubate guts at room temperature for 10–15 min.
3. Rinse three times with 1× PBS. First and second washes are quick (1 min). The last wash is 5 min.
4. Mount guts on microscope slides in mounting solution or PBS/glycerol.

5. Carefully lay a coverslip over the sample in mounting solution. Carefully remove any excess that oozes from between the slide and coverslip with a Kimwipe.
6. Seal the slide with nail polish.
7. Analyze guts using fluorescent or laser confocal microscopy (Fig. 3d).

3.7 Immunostaining

1. Dissect guts to be stained (*see* Subheading 3.5).
2. Transfer 3–6 guts into a 1.5 mL centrifuge tube with 1 mL of 4 % PFA fixative in PBT. Fix guts at room temperature for 30 min in PFA/PBT.
3. Wash 2–3 times in PBT. First and second washes are quick (1 min). Last wash is 5–10 min.
4. Tissues may be stored in the dark and at 4 °C at this stage before continuing with staining, but only for 1–2 days.
5. Block the epitopes by incubation with PBTA for 1 h.
6. Remove PBTA and incubate in primary antibody hybridization solution overnight in the dark at 4 °C. The hybridization solution is made by diluting the antibody to the proper concentration in PBTA (*see* **Note 16**).
7. Rinse in PBTA, three times 10 min each.
8. Incubate guts with the secondary antibody in PBTA and counterstain. Typical nucleus counterstain is DAPI or TO-PRO-3 (Invitrogen). Depending on the type of staining, this step may occur from 2 h of incubation to a new overnight treatment.
9. Wash three times in PBT, 10–30 min each.
10. Mount and image guts (*see* Subheading 3.6, **steps 4–6**).

4 Notes

1. Acid mix is made by combining a solution of 8.3 mL phosphoric acid in 91.7 mL dH_2O and a solution of 83.6 mL propionic acid in 16.4 mL dH_2O.
2. Mix yeast, sucrose, cornmeal, and agar into the water and autoclave on a liquid cycle to dissolve. Add Moldex and acid mix to the diet once it is cool enough to handle with bare hands. Dispense the diet rapidly into empty fly tubes.
3. *Ecc15* is used to induce nonlethal oral infections, in which flies are able to repair and recover from damage [6, 15]. Oral infections with *P. entomophila* are nonlethal at low doses but ultimately lethal at high doses and associated with high levels of Reactive Oxygen Species (ROS) and pore-forming bacterial toxins [15–18]. Oral infections with *S. marcescens* are lethal

due to the ability of the bacteria to cross the epithelial barrier of the gut and establish a systemic infection [19–21]. *Pseudomonas aeruginosa* induces cell death in the gut and promotes ISC proliferation [22].

4. The basis of the *Gal4/UAS* transgenic system is the generation of transgenic flies that bear either Gal4 expressing transgenes that express the Gal4 yeast transcription factor in a cell-specific manner (dependent of the promoter cloned in front of *Gal4*) or inducible transgenes that are controlled by Gal4 target sites: Upstream Activation Sequence (*UAS*) enhancers. The *UAS* transgene can induce the expression of a fluorescent reporter such as *GFP* or *RFP*. Flies with *UAS* and *Gal4* transgenes are crossed together and, in the F1 progeny, the *UAS* transgene is bound and transactivated by Gal4 only in cells with active *Gal4* expression. This system is further implemented by incorporation of $Gal80^{ts}$, encoding a thermosensitive form of Gal80, which acts as a Gal4 antagonist. The addition of ubiquitously expressed $Gal80^{ts}$ to the *Gal4/UAS* constructs allows the expression of the transgene in flies to be induced by incubation at 29 °C, a temperature at which $Gal80^{ts}$ is inactivated (Fig. 2a). The promoter of *delta* is used to drive expression in ISCs (*delta-Gal4*), the promoter of *Su(H)* is used for EBs (*Su(H)-Gal4*), *Myo1A* for ECs (*Myo1A-Gal4*) [23], *prospero* for EE cells (*prospero-Gal4*), and *escargot* for expression in both ISCs and EBs (*esg-Gal4*) [4].
5. The *tub-FRT-lacZ* clone system makes use of a heat shock-induced, FLP recombinase-dependent, chromosome recombination that results in a heritable expression of *tub-lacZ* in the progeny of a cell [8]. Two homologous chromosomes bear FRT sites (FLP recombination targets), one containing the ubiquitous promoter of *tubulin* (*tub-FRT*) and one containing the gene encoding β-galactosidase (*FRT-lacZ*). The two stocks are crossed and the F1 progeny is collected. Upon heat shock at 38 °C, *hsFLP* is expressed in the F1 progeny, triggering *FRT*-mediated recombination and reactivation of *lacZ* expression by joining the *tubulin* promoter to *lacZ* (*tub-lacZ*), thereby inducing *lacZ* expression in all daughter cells.
6. The $esg^{F/O}$ system (*esg-Gal4*, $Gal80^{ts}$, *UAS-FLP*, *act>CD2>Gal4*, *UAS-GFP*) uses a temperature-sensitive inducible *Gal4*, driven in progenitor cells (*esg-Gal4*, $Gal80^{ts}$) to express FLP recombinase (*UAS-FLP*) in all intestinal progenitors. In this line, FLP removes an FRT-flanked CD2 cassette, allowing *Gal4* to be heritably expressed under the control of a ubiquitous promoter (*actin*). Expression of *Gal4* transactivates the expression of *UAS-GFP*, thereby causing all progenitor cells and their progeny to inherit GFP expression. This system allows for monitoring of midgut renewal in varying conditions (Fig. 2b).

7. Under basal conditions, about 90 % of *Drosophila* ISC divisions occur asymmetrically, resulting in one daughter cell committed to differentiation and a second daughter cell that retains pluripotency [12, 13, 24]. The remaining 10 % are symmetric divisions, yielding either two differentiating cells or two ISCs, leading to the loss or expansion of stem cell clones in the gut. Twin-spot MARCM (Mosaic Analysis with a Repressible Cell Marker) allows labeling of the two daughter cells of an ISC with distinct fluorescent markers (GFP or RFP) (Fig. 2c). In the case of asymmetrical division, one daughter will differentiate and give rise to a single differentiated cell, whereas the other daughter will have ISC fate, and generate a clonal population. In the case of symmetrical division, either two single differentiated cells will be generated, or two ISCs that will generate two clones labeled in GFP and RFP.
8. Sucrose can be stored at 25 % concentration and at −20 °C in 1–2 mL aliquots.
9. **Steps 1–3** should always be performed using sterile techniques.
10. *Ecc15*, *P. entomophila*, and *S. marcescens* are grown at 29 °C; *P. aeruginosa* is grown at 37 °C.
11. Two hours of starvation at 29 °C are required to ensure that the flies will rapidly feed on the prepared sucrose and infection mix.
12. Flies infected by *Ecc15* are damaged in the first 4 h, which triggers ISC proliferation (massive from 8 to 16 h) and gut repair (up to 5 days).
13. Special care should be taken in each step to ensure that the midgut is never handled directly by the forceps. Pinching or even holding the guts with metal forceps will puncture or tear the tissue.
14. This removes cuticular hydrocarbons that will otherwise cause flies to float on PBS and not mix. This also further anesthetizes the flies.
15. The crop is often filled with bacteria prior to oral infection and this step is often necessary to prevent guts from floating during further processing, and to reduce the presence of free-floating bacteria during imaging.
16. Usual antibody dilutions in PBTA found in the literature: anti-GFP = 1:1,000, anti-RFP = 1:250, anti-PH3 = 1:1,000, anti-Prospero = 1:500,anti-PDM1 = 1:500,Alexa-anti-mouse = 1:500, Alexa-anti-rabbit = 1:500.

Acknowledgements

Photography for figures was performed by lab technician Aurélien Guillou. We thank our colleagues Peter Newell, David Duneau, Katia Sotelo-Troha, and Robert Houtz for comments on the chapter.

References

1. Demerec M (1994) Biology of Drosophila. Cold Spring Harbor Laboratory Press, New York, NY
2. Buchon N, Broderick NA, Lemaitre B (2013) Gut homeostasis in a microbial world: insights from Drosophila melanogaster. Nat Rev Microbiol 11:615–626
3. Ohlstein B, Spradling A (2006) The adult Drosophila posterior midgut is maintained by pluripotent stem cells. Nature 439:470–474
4. Micchelli CA, Perrimon N (2006) Evidence that stem cells reside in the adult Drosophila midgut epithelium. Nature 439:475–479
5. Ohlstein B, Spradling A (2007) Multipotent Drosophila intestinal stem cells specify daughter cell fates by differential notch signaling. Science 315:988–992
6. Buchon N, Broderick NA, Poidevin M et al (2009) Drosophila intestinal response to bacterial infection: activation of host defense and stem cell proliferation. Cell Host Microbe 5:200–211
7. Jiang H, Patel PH, Kohlmaier A et al (2009) Cytokine/Jak/Stat signaling mediates regeneration and homeostasis in the Drosophila midgut. Cell 137:1343–1355
8. Harrison DA, Perrimon N (1993) Simple and efficient generation of marked clones in Drosophila. Curr Biol 3:424–433
9. Lee T, Luo L (1999) Mosaic analysis with a repressible cell marker for studies of gene function in neuronal morphogenesis. Neuron 22: 451–461
10. Wu JS, Luo L (2006) A protocol for mosaic analysis with a repressible cell marker (MARCM) in Drosophila. Nat Protoc 1:2583–2589
11. Singh SR, Mishra MK, Kango-Singh M et al (2012) Generation and staining of intestinal stem cell lineage in adult midgut. Methods Mol Biol 879:47–69
12. Yu HH, Chen CH, Shi L et al (2009) Twin-spot MARCM to reveal the developmental origin and identity of neurons. Nat Neurosci 12:947–953
13. de Navascués J, Perdigoto CN, Bian Y et al (2012) Drosophila midgut homeostasis involves neutral competition between symmetrically dividing intestinal stem cells. EMBO J 31: 2473–2485
14. Beebe K, Lee WC, Micchelli CA (2010) JAK/STAT signaling coordinates stem cell proliferation and multilineage differentiation in the Drosophila intestinal stem cell lineage. Dev Biol 338:28–37
15. Buchon N, Broderick NA, Chakrabarti S et al (2009) Invasive and indigenous microbiota impact intestinal stem cell activity through multiple pathways in Drosophila. Genes Dev 23:2333–2344
16. Vodovar N, Vinals M, Liehl P et al (2005) Drosophila host defense after oral infection by an entomopathogenic Pseudomonas species. Proc Natl Acad Sci U S A 102:11414–11419
17. Liehl P, Blight M, Vodovar N et al (2006) Prevalence of local immune response against oral infection in a Drosophila/Pseudomonas infection model. PLoS Pathog 2:e56
18. Opota O, Vallet-Gely I, Vincentelli R et al (2011) Monalysin, a novel ß-pore-forming toxin from the Drosophila pathogen Pseudomonas entomophila, contributes to host intestinal damage and lethality. PLoS Pathog 7:e1002259
19. Nehme NT, Liégeois S, Kele B et al (2007) A model of bacterial intestinal infections in Drosophila melanogaster. PLoS Pathog 3:e173
20. Cronin SJF, Nehme NT, Limmer S et al (2009) Genome-wide RNAi screen identifies genes involved in intestinal pathogenic bacterial infection. Science 325:340–343
21. Chatterjee M, Ip YT (2009) Pathogenic stimulation of intestinal stem cell response in Drosophila. J Cell Physiol 220:664–671
22. Apidianakis Y, Pitsouli C, Perrimon N et al (2009) Synergy between bacterial infection and genetic predisposition in intestinal dysplasia. Proc Natl Acad Sci U S A 106:20883–20888
23. Zeng X, Chauhan C, Hou SX (2010) Characterization of midgut stem cell- and enteroblast-specific Gal4 lines in drosophila. Genesis 48:607–611
24. O'Brien LE, Soliman SS, Li X et al (2011) Altered modes of stem cell division drive adaptive intestinal growth. Cell 147:603–614

Part IV

Connective and Contractile Tissue

Chapter 15

Muscle Pouch Implantation: An Ectopic Bone Formation Model

Greg Asatrian, Le Chang, and Aaron W. James

Abstract

Ectopic bone formation refers to the ossification of tissue outside of its typical microenvironment. Numerous animal models exist to experimentally induce ectopic bone formation in order to examine the process of osteogenesis or to evaluate the "osteogenic potential" of a given implant. The most widely employed methods in the rodent include subcutaneous, intramuscular, and renal capsule implantation. This chapter will outline the (1) clinical correlates to ectopic ossification, (2) a brief history of experimental models of ectopic ossification, (3) advantages and disadvantages of various models (with a focus on rodent models), and (4) detailed methods and explanation of a mouse intramuscular implantation procedure.

Key words Ectopic, Bone, Model, Graft, Muscle pouch implantation, Heterotopic

1 Introduction

Ectopic bone or heterotopic ossification (HO) formation refers to the ossification of tissue outside of its typical microenvironment [1] such as soft tissues, which include fat, muscle, and other tissue types [2, 3]. Etiologies that result in HO include the clinical consequences of spinal cord injury [4], acute burns [5], and traumatic injury [2, 6]. HO can occur in 10–20 % of patients who undergo invasive surgery, and is considered attributable to the up-regulation of local inflammatory signals and recruitment of pro-osteogenic, skeletal progenitor cells [3, 7]. Additionally, ectopic bone formation may be observed in congenital defects and inherited malformations [8, 9]. HO can be seen in genetic disorders, including fibrodysplasia ossificans progressiva (FOP) and progressive osseous heteroplasia (POH) [10, 11].

Ectopic bone formation has been frequently studied in a research setting, both to examine the process of osteogenesis outside its native environment, and also to understand the clinical entity of HO. Various models have been developed and employed in the field of tissue engineering to study the osteogenic potential

Bruno Christ et al. (eds.), *Animal Models for Stem Cell Therapy*, Methods in Molecular Biology, vol. 1213,
DOI 10.1007/978-1-4939-1453-1_15,

of growth factors, bone graft substitutes, as well as osteoprogenitor and stem cell populations. Typically, rodents are used because of their low cost and the wide availability of immunodeficient strains. However, studies have also been conducted in larger animal models including, but not limited to, leporine [12], ovine [13], and canine [14] species.

In small animal models, several locations have been used to perform ectopic bone formation procedures, each with significant advantages and drawbacks (reviewed in ref. Scott et al. [6]). The most simplistic model for ectopic bone formation is subcutaneous implantation, which involves the implantation of graft material under the dermis [15–17]. The microenvironment of this model is advantageous due to the theoretical lack of local host bone-forming cells. Therefore, virtually all bone formation at the implantation site is attributable to the graft material. In addition, numerous implants may be used per animal—allowing for cost efficiency. However, this model poses minor technical disadvantages, including the risk of implant migration due to the lax skin of rodents [6]. A second model for ectopic bone formation is the "kidney capsule implantation" model, which generally requires a more experienced technician. In this procedure, the graft is placed between the renal parenchyma and the overlying fibrous capsule. This allows for supra-physiological levels of blood and nutrient supply, which have been observed to promote more robust bone formation than in other ectopic sites [6, 18–21]. However, the renal capsule model requires a higher level of surgical precision and only accommodates a relatively small implant size [21]. Lastly, the "intramuscular" or "muscle pouch" implantation model (MPI) is a frequently utilized model to study ectopic bone formation [22–24]. Intramuscular implantation procedures typically are performed in rodent models (~50 % of publications in our recent review [6]); however, larger animal models may be used [6, 25]. In brief, this procedure involves the implantation of graft material into skeletal muscle and can accommodate relatively large volumes of implant material; in the rodent model this is generally located in the hind limbs.

Here, we explain the procedure for implantation of graft material intramuscularly to assess ectopic bone formation in a mouse model. Some common pitfalls of the procedure are highlighted and suggestions for postoperative analysis are briefly discussed.

2 Materials

1. Immunocompromised mice, such as SCID (severe combined immunodeficient) or athymic mice, are required for all xenograft procedures (to circumvent immunologic response) (*see* **Note 1**). For implantation of syngeneic or allograft material, immunocompetent (wild type) mice may be used.

2. Anesthesia is required. We recommend isoflurane anesthesia apparatus (isoflurane vaporizer, oxygen supply, supply gas regulator, flowmeter, induction chamber, connective tubing, and scavenger), equipped with a nose cone for continuous intraoperative sedation. Intraperitoneal administration of anesthetic is also a valid option. Additionally, analgesia is recommended (*see* **Note 2**).
3. Surgical preparation material: shaving device, Betadine and ethanol scrubs.
4. Blade holder and 15 blade, thumb forceps, iris scissors, 5-0 Vicryl sutures, and needle holder.

3 Methods

3.1 Surgical Procedure

1. Anesthetize animal. For example, use isoflurane gas (3 % for induction, 2 % for maintenance).
2. Prepare mouse aseptically for surgery by shaving hind limb and performing three scrubs of Betadine/ethanol (Fig. 1a).
3. Create a 2 mm longitudinal incision along the hind limb using a 15 blade (Fig. 1b).
4. Using blunt dissection (tips of iris scissors) to prevent muscle damage (*see* **Note 3**), create 4 mm deep pockets by separating

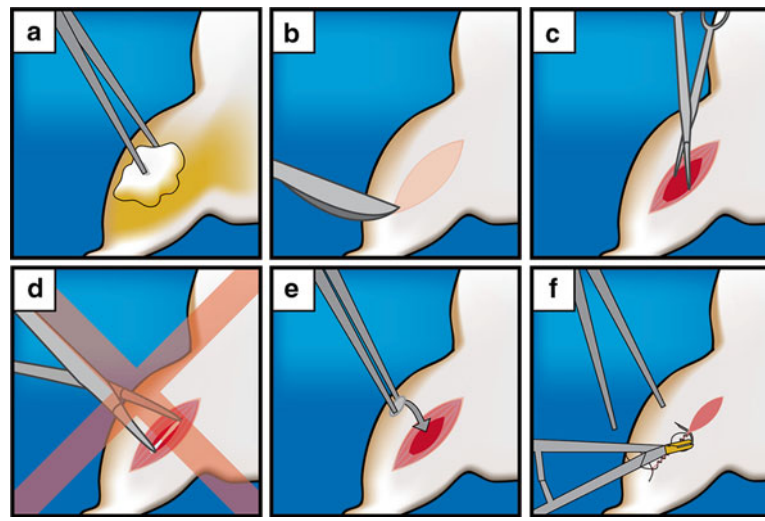

Fig. 1 Illustrated Procedure of Muscle Pouch Implantation. Dorsal view of mouse left hind limb. (**a**) After ascetically preparing animal with three alternating scrubs of Betadine/ethanol, (**b**) create a longitudinal incision. (**c**) Bluntly dissect biceps femoris (or muscle of interest), (**d**) being cautious to not go so deep as to expose the periosteum. (**e**) Place graft material into the created muscle pouch, and (**f**) suture the overlying fascia and skin

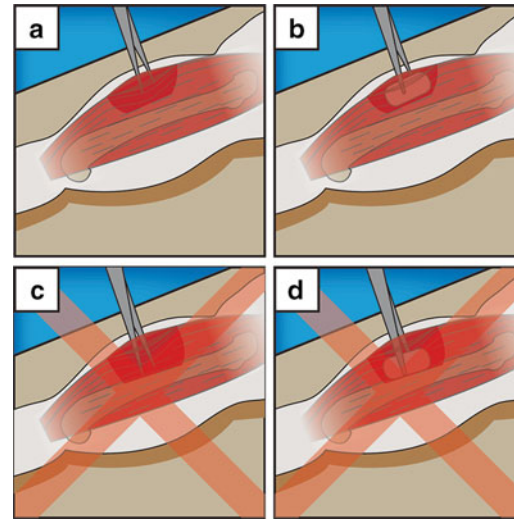

Fig. 2 Illustrated Depth of Muscle Pouch Creation. Axial view of mouse left hind limb. (**a**) Proper surgical creation of muscle pouch and (**b**) implantation of graft material. (**c**) One must be mindful as to not create a pocket so deep as to expose the periosteum. (**d**) Graft placed too close to the periosteum will render new bone indistinguishable from the femur

muscle fibers within biceps femoris (or muscle of interest, *see* **Note 4**) (Figs. 1c and 2a). Minimal bleeding should be observed. The surgeon should be careful to not go so deep as to dissect down to the periosteum (*see* **Note 5**, Figs. 1d and 2c, d).

5. Insert graft material into the created muscle pouch (Figs. 1e and 2b) (*see* **Note 6**) and suture the fascia overlying the muscle using a 5-0 Vicryl in a simple continuous pattern (*see* **Note 7**).
6. Close the skin using a 5-0 Vicryl suture in a subcuticular pattern (Fig. 1f).
7. Normal walking should be observed on postoperative day 1 (*see* **Note 8**).

3.2 Suggested Assays

Although numerous techniques and procedures may be used to analyze bone formation, we have highlighted some of the common techniques, both antemortem and postmortem.

Antemortem: To assess bone formation during the study period, high-resolution X-ray (XR), live computed tomography (live CT), or combined CT/positron emission tomography (PET) may be performed. Live CT/PET scans can be quantified to assess bone formation, including quantification of bone mineral density (BMD), fractional bone volume (BV/TV), and Fludeoxyglucose F18, or FDG (a glucose analog), uptake, useful for the detection of newly forming bone.

Postmortem: After animals are sacrificed and hind limbs (or other region of interest) are harvested, several procedures may be done to evaluate the bone formation of graft material. Radiographic analysis may be performed with high-resolution micro-computed tomography (microCT), which allows for measurement of even fine trabecular bone. Additionally, routine histology with Hematoxylin and Eosin (H&E) staining or other stains helpful in evaluating bone (Mason's Trichrome, Movat's Pentachrome, Aniline Blue) may be performed. Lastly, implanted cells may be identified using various techniques including fluorescent dyes or labels, immunostaining for cell- or species-specific markers, or sex chromosome in situ hybridization in the case of gender mismatch implants (*see* **Note 9**).

4 Notes

1. Generally, the intramuscular implantation procedure is performed in a mouse or rat model; however, it is translatable into large animals, with graft material implanted in the intra-erector spinae of the lumbar region [13, 26].
2. To minimize animal morbidity, analgesics are recommended. Suggested dosages of buprenorphine for mice and rats are 0.05–0.2 mg/kg and 0.01–0.05 mg/kg, respectively, injected subcutaneously, perioperatively, and twice daily for 48 h post-surgery.
3. It has previously been reported that increased bone morphogenetic protein (BMP) as well as other pro-osteogenic cytokines such as fibroblast growth factor (FGF), vascular endothelial growth factor (VEGF), and transforming growth factor (TGF)-β1 are up-regulated after muscle injury [27–29]. To minimize these potentially confounding effects, blunt dissection and minimal muscular injury is suggested.
4. Although the biceps femoris allows for larger volume implantation, the gastrocnemius can alternatively be utilized. Performing such a procedure allows for more efficient monitoring due to ease of palpation and ability for ultrasound imaging.
5. The surgeon must pay careful attention to the placement of implant material, as to not place graft material near, or especially on top of, periosteum. This would result in host periosteal reactive bone formation and confound the result of an experimental design.
6. Although pocket size is dependent upon surgical technique, generally a 100 μL scaffold can be accommodated easily. If using a rat model, a larger volume may be used.

7. A variety of osteoinductive and non-osteoinductive scaffolds may be utilized in muscle pouch implantation studies. Scaffolds previously used include, but are not limited to, collagen sponges [30], demineralized bone matrices [31], and hydroxyapatite scaffolds [32].
8. If normal mobility is not observed on postoperative day 1, nerve damage may have occurred, and depending on institutional animal protocols, euthanizing the animal may be required.
9. To verify that new bone formation is indeed due to graft material, rather than host osteoprogenitor cells, it is recommended that fluorescent labeling is performed prior to implantation [23]. Additionally, species-specific antigen detection can be performed to confirm the origin of bone forming cells [33].

References

1. Kewalramani LS (1977) Ectopic ossification. Am J Phys Med 56:99–121
2. Potter BK, Forsberg JA, Davis TA, Evans KN, Hawksworth JS, Tadaki D, Brown TS, Crane NJ, Burns TC, O'Brien FP, Elster EA (2010) Heterotopic ossification following combat-related trauma. J Bone Joint Surg Am 92(Suppl 2):74–89
3. Shimono K, Tung WE, Macolino C, Chi AH, Didizian JH, Mundy C, Chandraratna RA, Mishina Y, Enomoto-Iwamoto M, Pacifici M, Iwamoto M (2011) Potent inhibition of heterotopic ossification by nuclear retinoic acid receptor-gamma agonists. Nat Med 17:454–460
4. Roche MB, Jostes FA (1948) Ectopic bone deposits; a paraplegic complication. Am J Surg 75:633–636
5. Holavanahalli RK, Helm PA, Parry IS, Dolezal CA, Greenhalgh DG (2011) Select practices in management and rehabilitation of burns: a survey report. J Burn Care Res 32:210–223
6. Scott MA, Levi B, Askarinam A, Nguyen A, Rackohn T, Ting K, Soo C, James AW (2012) Brief review of models of ectopic bone formation. Stem Cells Dev 21:655–667
7. Garland DE (1991) A clinical perspective on common forms of acquired heterotopic ossification. Clin Orthop Relat Res 13–29
8. Singh GK, Verma V (2011) Progressive osseous heteroplasia in a 10-year-old male child. Indian J Orthop 45:280–282
9. Rosborough D (1966) Ectopic bone formation associated with multiple congenital anomalies. J Bone Joint Surg Br 48:499–503
10. Medici D, Olsen BR (2012) The role of endothelial-mesenchymal transition in heterotopic ossification. J Bone Miner Res 27:1619–1622
11. Lebrun M, Richard N, Abeguile G, David A, Coeslier Dieux A, Journel H, Lacombe D, Pinto G, Odent S, Salles JP, Taieb A, Gandon-Laloum S, Kottler ML (2010) Progressive osseous heteroplasia: a model for the imprinting effects of GNAS inactivating mutations in humans. J Clin Endocrinol Metab 95:3028–3038
12. Qu D, Li J, Li Y, Khadka A, Zuo Y, Wang H, Liu Y, Cheng L (2011) Ectopic osteochondral formation of biomimetic porous PVA-n-HA/PA6 bilayered scaffold and BMSCs construct in rabbit. J Biomed Mater Res B Appl Biomater 96:9–15
13. Le Nihouannen D, Daculsi G, Saffarzadeh A, Gauthier O, Delplace S, Pilet P, Layrolle P (2005) Ectopic bone formation by microporous calcium phosphate ceramic particles in sheep muscles. Bone 36:1086–1093
14. Yao J, Li X, Bao C, Zhang C, Chen Z, Fan H, Zhang X (2010) Ectopic bone formation in adipose-derived stromal cell-seeded osteoinductive calcium phosphate scaffolds. J Biomater Appl 24:607–624
15. Ben-David D, Kizhner T, Livne E, Srouji S (2010) A tissue-like construct of human bone marrow MSCs composite scaffold support in vivo ectopic bone formation. J Tissue Eng Regen Med 4:30–37
16. Gammelgaard B, Veien NK (1990) Nickel in nails, hair and plasma from nickel-hypersensitive women. Acta Derm Venereol 70:417–420
17. Chang SC, Tai CL, Chung HY, Lin TM, Jeng LB (2009) Bone marrow mesenchymal stem cells form ectopic woven bone in vivo through

endochondral bone formation. Artif Organs 33:301–308

18. Gurevitch O, Khitrin S, Valitov A, Slavin S (2007) Osteoporosis of hematologic etiology. Exp Hematol 35:128–136
19. Gurevich O, Vexler A, Marx G, Prigozhina T, Levdansky L, Slavin S, Shimeliovich I, Gorodetsky R (2002) Fibrin microbeads for isolating and growing bone marrow-derived progenitor cells capable of forming bone tissue. Tissue Eng 8:661–672
20. Berger E, Bleiberg I, Weisman Y, Lifschitz-Mercer B, Leider-Trejo L, Harel A, Kaye AM, Somjen D (2001) The hormonal milieu in early stages of bone cell differentiation modifies the subsequent sex-specific responsiveness of the developing bone to gonadal steroids. J Bone Miner Res 16:823–831
21. Slater BJ, Lenton KA, James A, Longaker MT (2009) Ex vivo model of cranial suture morphogenesis and fate. Cells Tissues Organs 190: 336–346
22. Zhang X, Peault B, Chen W, Li W, Corselli M, James AW, Lee M, Siu RK, Shen P, Zheng Z, Shen J, Kwak J, Zara JN, Chen F, Zhang H, Yin Z, Wu B, Ting K, Soo C (2011) The Nell-1 growth factor stimulates bone formation by purified human perivascular cells. Tissue Eng Part A 17:2497–2509
23. James AW, Zara JN, Corselli M, Chiang M, Yuan W, Nguyen V, Askarinam A, Goyal R, Siu RK, Scott V, Lee M, Ting K, Peault B, Soo C (2012) Use of human perivascular stem cells for bone regeneration. J Vis Exp 63:e2952
24. Askarinam A, James AW, Zara JN, Goyal R, Corselli M, Pan A, Liang P, Chang L, Rackohn T, Stoker D, Zhang X, Ting K, Peault B, Soo C (2013) Human perivascular stem cells show enhanced osteogenesis and vasculogenesis with NELL-1 protein. Tissue Eng Part A 19: 1386–1397
25. Yuan H, van Blitterswijk CA, de Groot K, de Bruijn JD (2006) Cross-species comparison of ectopic bone formation in biphasic calcium phosphate (BCP) and hydroxyapatite (HA) scaffolds. Tissue Eng 12:1607–1615
26. Le Nihouannen D, Saffarzadeh A, Gauthier O, Moreau F, Pilet P, Spaethe R, Layrolle P, Daculsi G (2008) Bone tissue formation in sheep muscles induced by a biphasic calcium phosphate ceramic and fibrin glue composite. J Mater Sci Mater Med 19:667–675
27. Clever JL, Sakai Y, Wang RA, Schneider DB (2010) Inefficient skeletal muscle repair in inhibitor of differentiation knockout mice suggests a crucial role for BMP signaling during adult muscle regeneration. Am J Physiol Cell Physiol 298:C1087–C1099
28. Ten Broek RW, Grefte S, Von den Hoff JW (2010) Regulatory factors and cell populations involved in skeletal muscle regeneration. J Cell Physiol 224:7–16
29. Huntsman HD, Zachwieja N, Zou K, Ripchik P, Valero MC, De Lisio M, Boppart MD (2013) Mesenchymal stem cells contribute to vascular growth in skeletal muscle in response to eccentric exercise. Am J Physiol Heart Circ Physiol 304:H72–H81
30. Bae HW, Strenge KB, Ashraf N, Badura JM, Peckham SM, McKay WF (2012) Transient soft-tissue edema associated with implantation of increasing doses of rhBMP-2 on an absorbable collagen sponge in an ectopic rat model. J Bone Joint Surg Am 94:1845–1852
31. Lee JH, Lee KM, Baek HR, Jang SJ, Lee JH, Ryu HS (2011) Combined effects of porous hydroxyapatite and demineralized bone matrix on bone induction: in vitro and in vivo study using a nude rat model. Biomed Mater 6: 015008
32. Zhang X, Zara J, Siu RK, Ting K, Soo C (2010) The role of NELL-1, a growth factor associated with craniosynostosis, in promoting bone regeneration. J Dent Res 89:865–878
33. Reichert JC, Quent VM, Noth U, Hutmacher DW (2011) Ovine cortical osteoblasts outperform bone marrow cells in an ectopic bone assay. J Tissue Eng Regen Med 5:831–844

Chapter 16

Bone Defect Repair in Mice by Mesenchymal Stem Cells

Sanjay Kumar

Abstract

Adult bone marrow niche contains rare primitive but highly functional multipotent progenitors (e.g., mesenchymal stem cells; MSCs) capable of differentiating into specific mesenchymal tissues like bone, cartilage, muscle, fat tissues, ligament, dermis, bone marrow stroma, tendon, and other connective tissues. Upon in vivo transplantation, MSCs also secrete a wide range of growth factors, immunomodulatory cytokines, and important bioactive macromolecules including cell-derived exosomes to structure regenerative microenvironments. This protocol describes a mouse model to study bone formation/regeneration from adult mesenchymal stem cells.

Key words Bone marrow, Mesenchymal stem cells, MSCs, Bone defect, Bone repair, Bone formation, Bone fracture regeneration

1 Introduction

Bone is the primary calcified tissue in vertebrates. Bone, a specialized connective tissue, develops by differentiation of osteoprogenitors, mainly osteoblasts, towards gradual ossification by the process called osteogenesis [1]. Osteoblasts produce an amorphous fibrous nano-biomaterial that gradually becomes densely packed to form core bone matrix by adhesion between the secreted extracellular matrices, which are assembled in an osteoid structure followed by calcium phosphate crystal deposition in the process called bone mineralization.

The idea that bone forming progenitor cells coexist in bone marrow (BM) arose from remarkable in vitro expansion potential shown by non-hematopoietic stromal cells isolated from bone marrow [1, 2]. Experiments in these studies rigorously established that suspensions of dispersed BM cells could form fibroblast-like colonies (colony-forming unit fibroblasts, CFU-F) that were derived from single BM-derived progenitor cells. These investigations postulated the fact that clonogenic cells capable of producing CFU-F colonies represent the prominent group of cells in the stem cell

Bruno Christ et al. (eds.), *Animal Models for Stem Cell Therapy*, Methods in Molecular Biology, vol. 1213,
DOI 10.1007/978-1-4939-1453-1_16,

niche capable of mounting recovery from whole-body irradiation [3]. Most importantly, self-renewal and multilineage differentiation potential were demonstrated by in vivo transplantation experiments [2, 4]. These core scientific works established the basis for the bona fide stromal stem cell (mesenchymal stem cells, MSCs) existence in the bone marrow.

Adult MSCs can be isolated from bone marrow or marrow aspirates and because they are culture-dish adherent, they can be expanded in culture while maintaining their multipotency [5]. The MSCs have been used in preclinical models for tissue engineering of bone, cartilage, muscle, marrow stroma, tendon, fat, and other connective tissues. These tissue-engineered materials show considerable promise for use in rebuilding damaged or diseased mesenchymal tissues [6]. MSCs secrete a large spectrum of bioactive molecules and paracrine factors upon in vivo transplantation and create an immunosuppressive microenvironment. These secreted bioactive molecules provide a regenerative microenvironment for a variety of injured adult tissues to limit the area of damage and to mount a self-regulated regenerative response [7]. This regenerative microenvironment is referred to as trophic activity and, therefore, MSCs appear to be valuable mediators for tissue repair and regeneration [8].

Thus, we are describing a complete protocol of a mouse animal model to study bone formation from MSCs.

2 Materials

2.1 Animals

1. 6–8-weeks-old C57BL/6j female mice can be used for transplantation experiments (*see* **Notes 1–6** and **9**).
2. All animals were kept separately in individual cages and provided with routine animal care in the animal house (*see* **Notes 7** and **8**).

2.2 Anesthesia System (See Note 1)

1. Anesthesia system (SURGERY Anesthesia system, Protech International Inc., USA) including oxygen flowmeter and anesthetic vaporizer (SURGERY Anesthesia system Protech International Inc., USA).
2. Isoflurane (Aesica Queen Borough Limited, UK, trade name: FORANE).
3. Oxygen cylinders.

2.3 Bone Flushing Syringes and Needles

1. Insulin syringe.
2. 19 G needle with 10 mL syringe.
3. 21 G needle
4. 23 G needle
5. 25 G needle

2.4 Surgical Tools (from ROBOZ, Gaithersberg, MD, USA)

1. Roboz Ideal micro-drill and saw system.
2. Littauer bone cutting forceps.
3. Surgical instrument cleaning solution.
4. Dry sterilizer.
5. Straight sharp scissors.
6. Reflex wound closure staple and clip.
7. Micro-dissecting forceps.

2.5 External Bone Fracture Fixators

1. A modified 6 mm track distractor (KLS Martin, USA).
2. 0.010-in. ligature wire (3 M Unitek, USA), titanium ligature wire (3 M Unitek).
3. Absorbable and nonabsorbable surgical sutures (EHICON, USA).

2.6 Mouse Bone Marrow-Derived Mesenchymal Stem Cells (MSC) Isolation, In Vitro Culture and Differentiation

1. Mesenchymal stem cell (MSC) culture medium: Stemline medium (Sigma-Aldrich Corp. St Louis, MO, USA) supplemented with 10 % fetal bovine serum (FBS), 4 mmol/L L-glutamine, and 1 % penicillin/streptomycin.
2. Bone marrow (BM) conditioned medium [9], preparation: Flush the total bone marrow cells from femur and tibia bone fragments. Culture the total flushed bone marrow cells in Stemline MSC medium supplemented with 20 % FBS. Collect the medium after 72 h by centrifugation (discard the cell pellet, collect only supernatant medium), dilute with equal volume of Stemline MSC medium to get the 10 % FBS concentration, and filter through disposable 0.22 μm tissue culture filtration unit [9] and store at 4 °C for routine use.
3. Osteoblast induction medium: MSC culture medium containing 10 % FBS, 0.1 μM dexamethasone, 2 mM β-glycerophosphate, and 150 μM ascorbate-2-phosphate.
4. Adipogenic induction medium: Stemline medium with 20 % FBS, 1 μM dexamethasone, 0.35 μM hydrocortisone, 0.5 mM isobutyl-methylxanthine (IBMX), 100 ng/mL insulin, and 60 μM indomethacin.
5. Chondrogenic induction medium: Stemline medium with 0.1 μM dexamethasone, 1 mM sodium pyruvate, 170 μM ascorbic acid-2-phosphate, 350 μM proline, 1x insulin-transferrin-selenium, and 10 ng/mL TGF-β.
6. Myogenic induction medium: Stemline medium with 12.5 % screened horse serum, 12.5 % FBS, 20 μM L-glutamine, 0.8 mM L-serine, 0.15 mM L-asparagine, 1 mM sodium pyruvate, 5 mM sodium bicarbonate, 1 μM hydrocortisone, and 1 % penicillin and streptomycin [9].

7. Neurogenic induction medium: Stemline medium supplemented with 100 μM $CoCl_2$ (Sigma) and 5 ng/mL basic FGF-2.
8. Recombinant fibroblast growth factor (FGF-2, Peprotech, NJ, USA).
9. CO_2 chamber.
10. Ficoll.
11. Trypsin.

2.7 Characterization of In Vitro Expanded MSC by Immunophenotyping

1. Antibodies: CD34, CD45, CD29, CD44, CD106, ScaI, GFP, SMA, or nestin antibodies (all antibodies from e-biosciences, San Diego, CA).
2. CD11b IMAC beads (BD Biosciences, San Diego, CA, USA)
3. Dulbecco's phosphate-buffered saline (DPBS) without calcium and magnesium (Cellgro).
4. Flow cytometer (e.g., FACS Calibur; Becton Dickinson).
5. Smooth muscle actin antibody (e.g., Neomarkers, Fremont, CA, USA) in 5 % BSA
6. Alexa Fluor 594-conjugated goat anti-mouse secondary antibody and Alexa Fluor 488-conjugated donkey anti-mouse secondary antibody (Molecular Probes, Eugene, OR, USA).
7. Leica fluorescence microscope (e.g., Leica Microsystems Wetzlar GmbH, Wetzlar, Germany).

2.8 Scaffold Preparation

1. Allomatrix (HA) scaffold (Wright Medical Technology Inc.).
2. Non-adherent culture dish.

2.9 Histological Stains

1. Hematoxylin and eosin (H&E) or Goldner trichrome stain.
2. Calcein (Sigma): Dissolve 0.219 g NaCl in 25 mL distilled water, add 0.5 g sodium bicarbonate, and stir until dissolved. Add 0.250 g calcein powder slowly while gently heating above solution (be careful—it can foam up). Stir until all calcein is dissolved. Pass through a sterile filter. Dose of calcein used for mouse is 30 mg/kg.
3. 10 % buffered formalin.
4. Von Kossa stain: 5 % (w/v) silver nitrate (Sigma) and 5 % (w/v) sodium thiosulfate (Sigma) solutions.
5. Oil red O (Sigma): prepared in isopropanol and filtered through Whatman filter paper.
6. Toluidine blue-O or Safranin-O staining.
7. Methanol.
8. Xylene.
9. Paraffin.
10. Ethanol.

2.10 Animal Treatment, Noninvasive Whole Body Bioluminescence Imaging, Tissue Processing for in situ Hybridization, μCT Analysis, and Biomechanical Testing

1. X-ray (e.g., Faxitron system, USA).
2. Heating pad.
3. Carprofen.
4. Buprenorphine.
5. Clindamycin-2-dihydrogenphosphate.
6. rAAV2-GFP (Addgene, Cambridge, MA, USA) and rAAV2-α4 integrin (developed in our lab; contact emails pons@uab.edu or skumar@cmcvellore.ac.in).
7. IVIS-100 system (Xenogen, Applied Biosystems, USA).
8. Luciferin substrate: 2.5 mg luciferin potassium salt (Xenogen) in PBS.
9. Living Cell Image data acquisition and analysis software (Xenogen, Applied Biosystems, USA).
10. PBS.
11. Citrate buffer: 0.01 M, pH 6.0.
12. DIG-labeling mixPlus (e.g., Molecular Biochemicals, Mannheim, Germany).
13. ULTRAhyb hybridization solution (e.g., Ambion, Austin, TX, USA).
14. DIG nucleic acid detection kit (Roche Applied Science).
15. Immuno-mount solution (Thermo Shandon, CA, USA).
16. Microscope.
17. DXA equipment for DXA analysis (e.g., PIXImus software, version 1.45; GE-Lunar, Madison, WI, USA).
18. High-resolution micro-CT imaging system (μCT40; Scanco Medical, Bassersdorf, Switzerland).
19. Micro-computed tomography instrument (e.g., μCT40, Scanco Medical AG).
20. 0.5 mol/L EDTA in Ca^{2+}- and Mg^{2+}-free DPBS.
21. Bioquant Image analysis software (R&M Biometrics).
22. 858 MiniBionix Materials Testing System (MTS Systems).
23. Aluminum cylinder (diameter = 8 mm) with SelfCem (e.g., Heraeus Kulzer, Hanau, Germany).

3 Methods

3.1 Bone Marrow Mesenchymal Stem Cell (MSC) Isolation (See Notes 2–6)

1. Sacrifice 6–8 weeks old male C57BL6j mice in a CO_2 chamber.
2. Remove all the muscles and clean long bones, e.g., femur and tibia.

3. Flush bone marrow from femur and tibia using an insulin syringe with Stemline MSC medium without serum.
4. Sequentially pass flushed bone marrow cells through a series of decreasing pore size (19, 21, 23, 25 G) needles to make a single-cell suspension.
5. Purify the bone marrow mononuclear cells on Ficoll gradient.
6. Seed on plastic dishes and grow plastic-adherent bone marrow stromal cells in BM-conditioned medium containing 10 % FBS supplemented with 10^{-9} M FGF-2 to maintain cells in pluripotent, undifferentiated state [10].
7. Periodically remove floating cells, replenish fresh medium every alternate day, and grow MSC culture until 70–80 % confluence.
8. Detach cells by trypsinization (0.05 % trypsin) and make a single-cell suspension, and purify the MSCs by IMAC using anti-mouse CD11b beads.

3.2 Immunophenotypic Characterization of In Vitro Expanded MSCs

1. Trypsinize BM-MSCs and distribute equal aliquots (1×10^5 cells per reaction) into FACS tubes and stain with fluorescently labeled antibodies on live cells. Use unstained cells and cells stained with isotype antibody as controls.
2. Add antibodies to the BM-MSCs in the dark to avoid photobleaching. After addition of the antibody, incubate the sample at room temperature in the dark for 20 min before analyzing by FACS.
3. Wash labeled cells with 1 mL of DPBS without calcium and magnesium followed by centrifugation at $300 \times g$ for 5 min.
4. Resuspend pelleted cells in 300 μL DPBS without calcium and magnesium, then analyze in a flow cytometer.
5. Gate a minimum of 10^4 events acquired from each sample for analysis using cell quest software.
6. Determine phenotype of BM-MSCs isolated and cultured from low-density mononuclear cells from bone marrow of mice by flow cytometry. The MSCs should be negative for CD14, CD34, and CD45 surface markers and positive for CD29, CD44, Sca1, and CD106 cell surface markers [9].

3.3 Multilineage Differentiation Studies of Cultured Mouse BM-MSCs

3.3.1 Osteogenic Lineage Differentiation

1. Osteoblast differentiation of MSCs is induced by osteoblast induction medium [9].
2. Seed 10,000 BM-MSCs/cm^2 and incubate for 28 days at 37 °C.
3. Change osteoblast induction medium every 3 days for 4 weeks before fixing for osteoblast staining.

4. For evaluation of mineralized matrix, fix the cell layer in 10 % buffered formalin, followed by staining with von Kossa stain using 5 % (w/v) silver nitrate under ultraviolet light for 30 min, then wash with 5 % (w/v) sodium thiosulfate for 2 min.

3.3.2 Adipogenic Lineage Differentiation

1. Adipogenic differentiation of MSCs is induced by adipogenic induction medium [9].
2. Seed 20,000 BM-MSCs/cm^2 and incubate in adipogenic induction medium for 21 days at 37 °C.
3. Change adipogenic induction medium every alternate day for 3 consecutive weeks before staining with oil red O.
4. For visualization of adipogenic differentiation by oil red O staining, fix cultured cells in 10 % buffered formalin and stain for 1 h with 5 % oil red O solution.

3.3.3 Chondrogenic Lineage Differentiation

1. Chondrogenic differentiation of MSCs should be obtained in micropellets (*see* **Note 10**) (3×10^6 cells/pellet) incubated at 37 °C for 25 days in chondrogenic induction medium [9].
2. Change chondrogenic induction medium every 3 days for 4 weeks.
3. For toluidine blue-O or safranin-O staining for chondrogenic differentiation, micropellet-cultured cells should be fixed in 10 % buffered formalin for 24 h and cell block can be prepared and mounted in paraffin wax and cut into 5 μm sections.

3.3.4 Myogenic Lineage Differentiation

1. Vascular smooth muscle differentiation is obtained in myogenic differentiation medium.
2. Change myogenic induction medium every 3 days for 2 weeks after the end of the first week of passage.
3. For immunofluorescence detection of myogenic differentiation, fix confluent layers of culture and permeabilize with methanol for 10 min. Incubate slides for 1 h with smooth muscle actin antibody in 5 % BSA followed by Alexa Fluor 594-conjugated goat anti-mouse secondary antibody, and examine with a Leica fluorescence microscope after thorough washing and mounting in antifade fluoromount medium.

3.3.5 Neuronal Differentiation

1. Neurogenic differentiation can be induced by the incubation of sub-confluent MSCs in neurogenic induction medium for 10 days with changing the medium every alternate day [9].
2. For immunofluorescence detection of neuronal differentiation, fix the cells with cold methanol and permeabilize the cells with 1 % triton X-100 in PBS for 10 min. Incubate slides for 1 h with nestin antibody in 5 % BSA for neurogenic differentiation, followed by Alexa Fluor 594-conjugated goat anti-mouse

secondary antibody, and examine with a Leica fluorescence microscope after thorough washing and mounting in antifade fluoromount medium.

3.4 Bone Defect Creation in Mice and X-Ray Confirmation of Bone Defect

1. Get approval from your Institutional Animal Care and Use Committee (IACUC) for all procedures of animal work.
2. Anesthetize each animal with an isoflurane and oxygen mixture and transfer onto a heating pad (maintained at 37 °C) in a sterile operating field (Laminar flow hood fitted with HEPA filters) (*see* **Notes 1** and **12**).
3. Inject mice with analgesic like injectable carprofen (5 mg/kg SQ) to avoid adverse effects, including pain after the surgery.
4. When performing minor or major surgery using isoflurane, use carprofen in combination with buprenorphine (0.05–0.1 mg/kg SQ) pre-incision (as soon as the animal is anesthetized) at the time of surgery.
5. Repeat carprofen (5 mg/kg SQ) injection once at 24 h for major surgeries like fractures.
6. Perform osteotomy in long bones (tibia or femur) of 0.5 mm segmental defect in 10–12 weeks old mice, with a micro-surgery Gigli saw by penetrating the fascia latae between the gluteus superficialis and biceps femoris muscles of the long bones (Fig. 1).
7. Confirm the bone fractures by X-ray examination (Fig. 2).

3.5 Bone Fracture Stabilization by External Fixators

1. Attach a modified 6 mm track distractor to both ends of the segmental defect with 0.010-in. ligature wire to stabilize the fractured bone (Fig. 3).
2. Fit the external fixator in a craniolateral position with bones fully wrapped around with fixators and then titanium ligature wire can be tied with bone and external fixator.

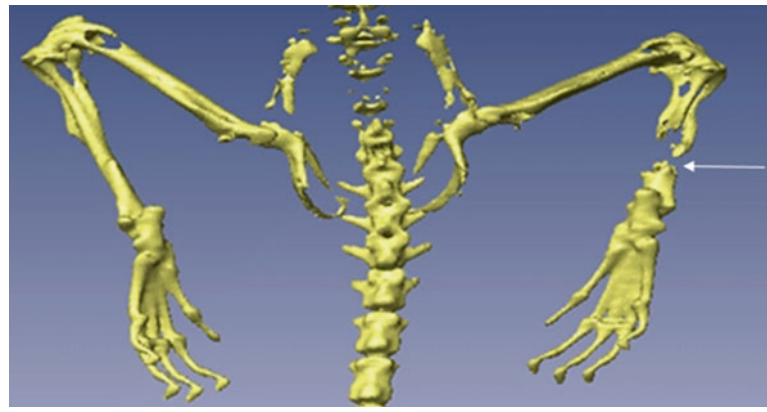

Fig. 1 Whole body X-ray imaging with long-bone fracture is shown by *arrow*

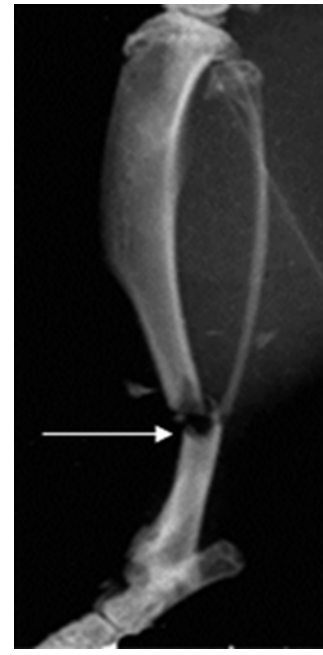

Fig. 2 X-ray imaging of long-bone fracture before stabilization with external fixators; fracture site is shown by an *arrow*

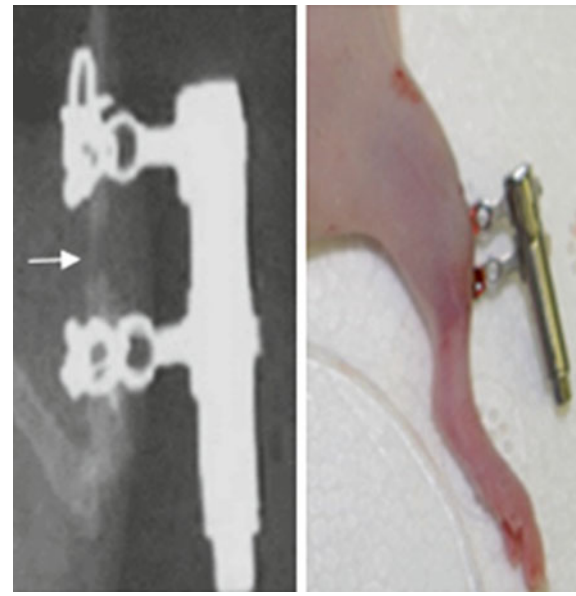

Fig. 3 External fixators to stabilize the long-bone fractures. New bone generation in the fracture area is shown by *arrow*

3. Suture the muscles with absorbable sterile suture threads, and the skin with nonabsorbable sterile suture threads.
4. Inject daily clindamycin-2-dihydrogen phosphate (45 mg/kg) until the third postoperative day to avoid wound infection.
5. Leave animals with free access to food and water and monitor daily in the postoperative phase to look for any discomfort, complications, or abnormal behavior.

3.6 Enhancing Bone-Specific Homing of Systemically Transplanted MSCs by Engineering Integrins on MSCs [9]

1. A total of eight mice can be included in each group.
2. Suspend mock-transduced or rAAV2-GFP (CMV-GFP, control) or rAAV2-α4 integrin-transduced MSCs (bone-specific homing MSCs) in a volume of 100 μL sterile 0.9 % NaCl solution and systemically administer into recipient mice through tail vein injection.
3. Cohorts of mice should receive 1×10^6 cells each of untransduced, rAAV2-GFP-transduced, or rAAV2-α4 integrin-transduced MSCs (*see* **Note 9**).
4. Four weeks after transplantation, animals may be sacrificed [11].

3.6.1 Analysis of Donor Cell Engraftment by Transplantation of Y Chromosome-Marked MSCs into Syngeneic Female Mice

1. Perform in situ hybridization using a Y chromosome-specific probe in order to identify the homed transplanted MSCs from the male donor mice based on the positivity for Y chromosome-specific genes.
2. Generate a digoxigenin (DIG)-labeled mouse Y chromosome-specific probe [9] by polymerase chain reaction (PCR) using DIG-labeling mixPlus following the manufacturer's protocol.
3. Deparaffinize formalin-fixed and decalcified bone tissue sections in xylene and rehydrate through a series of graded ethanol and PBS.
4. Treat slides with 0.01 M citrate buffer, pH 6.0, at 42 °C for 3 h.
5. Perform prehybridization at 65 °C for 2 h in ULTRAhyb hybridization solution.
6. Perform hybridization reaction with 400 ng/mL DIG-labeled, Y chromosome-specific probe in same solution at 65 °C overnight.
7. Wash excess probe thoroughly with series of PBS solution at 42 °C.
8. Detect the hybridized probe signal by using the DIG nucleic acid detection kit.
9. Counterstain the slides with diluted eosin solution for 1–2 min and then mount with Immuno-mount solution and coverslip.
10. Select a region of interest (ROI) just below the growth plate area of mouse decalcified bone marrow section.

11. Enumerate relative percentage of homed MSCs, as evidenced by positive signal by microscopy.
12. Count at least five random fields from each slide under the microscope for quantitation of homed transplanted cells.

3.6.2 Analysis of Donor Cell Engraftment by Transplantation of GFP-Marked MSCs into Syngeneic Female Mice [9]

1. Identify GFP-positive donor MSCs, isolated from syngeneic GFP transgenic mice in the recipient mouse bone sections by performing immunohistochemistry using anti-mouse CD44 and anti-GFP primary antibodies and develop the slide with Alexa Fluor 594-labeled goat anti-mouse and Alexa Fluor 488 donkey anti-mouse secondary antibodies, respectively.
2. To determine the percentage of engrafted MSCs in the recipient bone marrow, isolate stromal cells 2 months after cell implantation and culture for 3 weeks in vitro.
3. Analyze the trypsinized cells by flow cytometry based on GFP fluorescence.

3.7 Mesenchymal Stem Cell Transplantation on Biodegradable Scaffolds

1. Add mouse bone marrow-derived MSCs in a predetermined number (100–200 K) on Allomatrix (HA) scaffold and grow at 37 °C in Stemline medium in a non-adherent dish for 24 h before transplantation into mice.
2. Implant scaffolds with MSCs at long-bone fracture site in mice.

3.8 In Vivo Tracking of MSCs in Transplanted Mice

1. Isolate MSCs from beta-actin promoter-driven luciferase reporter transgenic mice.
2. Perform in vivo bioluminescence image in a cryogenically cooled IVIS-100 system to detect luciferase expression in MSCs after injecting luciferin substrate and using Living Cell Image data acquisition and analysis software.
3. Briefly anesthetize mice with isoflurane and inject 2.5 mg luciferin potassium salt in PBS intraperitoneally.
4. Perform imaging after intravenous injection of luciferase-positive MSCs [12] periodically (1 h after transplantation followed by daily bioluminescence imaging).
5. Image acquisition times should be in the range of 10–240 s. Calibrate the data acquisition software to ensure that pixels remain saturated during image collection.
6. Measure light emission from the tissue regions (relative photons/s) by using Living Cell Image software. The intensity of light emission may be represented with a pseudocolor scaling of bioluminescent images.
7. Superimpose the bioluminescent images on black-and-white images of mice, which are collected at the same time.

3.9 In Vivo New Bone Growth Analysis by Calcein Labeling

Inject 30 mg/kg of filter sterilized calcein for bone labeling in mice to visualize rate of new bone formation.

3.10 Analysis of Regenerated Bone by Dual Energy X-Ray Absorptiometry (DXA)

1. Briefly anesthetize mice with isoflurane (2 %) + Oxygen (4 %) and place in a prostrate position on the imaging plate of the DXA equipment for DXA analysis.
2. Assess BMD, BMC, and other body composition in vivo by DXA periodically.
3. Scan long bones of each mouse using high-resolution micro-CT imaging system to assess bone density, bone mass, bone geometry, and bone trabecular and cortical microarchitecture.
4. Evaluate histomorphometric parameters analysis including bone volume, trabecular connectivity, trabecular thickness, trabecular separation, and degree of anisotropy (DA) from the high resolution micro-CT data.

3.11 Micro-computed Tomography Analysis (Fig. 4)

1. Harvest the long bones from sacrificed mice for the determination of the three-dimensional architecture of the trabecular and cortical bones.
2. Analyze the harvested bones in an advanced micro-computed tomography instrument.

Fig. 4 Micro-CT of the regenerating long bone around the fracture. New trabecular bone growth can be visualized by reconstructed 3D μCT images of harvested fractured bone following MSC transplantation

3. Perform two scans for each long bone, one for whole tibia/femur bone with 16 μm resolution and one for trabecular analysis with a 6 μm resolution [12].
4. For the whole tibia, the scan may be composed of 1,129 slices, with a threshold value of 265.
5. Reconstruct a three-dimensional image with the ROI consisting of trabecular and cortical areas.
6. For trabecular bone analysis perform the micro-CT scanning below the growth plate area.
7. Each scan may be composed of 209 slices, of which 100 should be used for the analysis.
8. Draw ROIs on each of the 100 slices, just inside the cortical bone, to include only the trabecular bone and the marrow.
9. Set to a threshold at 327 for trabecular bone to distinguish it from the marrow.
10. Reconstruct the three-dimensional image on the ROI, which only contains trabecular bone; no cortical bone may be present in these ROIs.

3.12 Histological and Histomorphometric Analysis of Regenerated Bone

1. Decalcify the bone tissues in 0.5 mol/L EDTA in Ca^{2+}- and Mg^{2+}-free DPBS before embedding in paraffin.
2. Cut 6 μm micrometer longitudinal serial sections from the femur and tibia.
3. Stain with hematoxylin and eosin (H&E) or Goldner's trichrome stain to determine the characteristics of bone growth (*see* **Note 11**).
4. Goldner trichrome staining may be done on bone sections to determine osteoblast number and activity.
5. Perform quantitative osteomeasurements of bones using a microscope and Bioquant Image analysis software [13].

3.13 Biomechanical Testing of Quality of Regenerated Bone

1. Sacrifice mice after 4 weeks of the MSCs treatments.
2. Collect long bones and fresh freeze or preserve in 70 % ethanol.
3. Test specimen biomechanical characteristics by three-point bending apparatus on 858 MiniBionix Materials Testing System.
4. Calculate stiffness and peak load from the force displacement data in the attached computer with Bioquant Image Analysis software (R&M Biometrics).
5. Perform a nondestructive 3-point bending test in the materials testing machine to evaluate the flexural rigidity of the healed long bones.

6. Contralateral limbs may serve as controls.
7. Fix the proximal end of the bone in an aluminum cylinder (diameter = 8 mm) with SelfCem.
8. Then fix the cylinder itself in a hinge joint, serving as the proximal support for the bending test.
9. Rest the condyles on the bending support, the distance between both supports being 20 mm.
10. Apply the bending load F on top of the callus tissue and continuously record versus sample deflection (d) up to a maximum force of 1.5 N at a crosshead speed of 2 mm/min.
11. Test each sample three times: the first two test cycles (maximum force 0.5 N) may be conditioned to the sample in order to avoid potential artifacts due to contact settlements.
12. Evaluate the third loading cycle (maximum force 1.5 N) of each sample to define the flexural rigidity (EI) from the slope (k) of the linear region of the load-deflection curve [14].
13. Since the callus may not be always located in the middle of the supports (l/2), the distances between the load vector and the proximal (a) and distal (b) supports should be considered for calculating $EI = k\ (a^2b^2)/3\ l\ (N\ mm^2)$ [14].

4 Notes

1. Inhalation of 2–3 % isoflurane vapors with 4 % oxygen provides safe general anesthesia for small animal surgical processes.
2. Stem cells isolated from syngeneic mice should be used to avoid variability in results.
3. Reporter transgenic mice in the similar background could be used to track the transplanted cells in recipient mice.
4. MSCs should be maintained as low passage cells for efficient engraftment.
5. Split adherent stromal cells before attaining confluence to avoid possible onset of differentiation.
6. Routinely prepare MSCs according to this protocol and maintain as low passage cultures (passage 4–8) for in vitro and in vivo studies.
7. Mice should be fed phytoestrogen-free diet to get the reliable bone density data by DXA analysis.
8. Mice should be pair fed (controls should get same amount of food daily by accurate measuring) in comparison to control animals to avoid increase in standard deviation of data.
9. 1×10^6 MSCs can be transplanted in 2–3 injections to avoid mice death by too many cells injected in one injection.

10. Prepare cell micropellet for chondrogenic differentiation by trypsinizing the two T175 flasks and pelleting the total cells in one 15 mL tube with filtered cap for CO_2 gas exchanges during in vitro differentiation.
11. 10 % buffered formalin-fixed bone should be decalcified with EDTA for antigen preservation.
12. When performing minor or major surgery with ketamine/xylazine, carprofen may be used alone (without buprenorphine).

Acknowledgments

We are grateful to Department of Biotechnology (DBT), Government of India for Ramalingaswami Fellowship and research support grant (DBT Grant #BT/PR15420/MED/31/122/2011) to SK.

References

1. Caplan AI (1991) Mesenchymal stem cells. J Orthop Res 9:641–650
2. Friedenstein AJ, Petrakova KV, Kurolesova AI, Frolova GP (1968) Heterotopic of bonemarrow. Analysis of precursor cells for osteogenic and hematopoietic tissues. Transplantation 6: 230–247
3. Friedenstein AJ, Gorskaja JF, Kulagina NN (1976) Fibroblast precursors in normal and irradiated mouse hematopoietic organs. Exp Hematol 4:267–274
4. Bianco P, Kuznetsov SA, Riminucci M, Gehron RP (2006) Postnatal skeletal stem cells. Methods Enzymol 419:117–148
5. English K, French A, Wood KJ (2010) Mesenchymal stromal cells: facilitators of successful transplantation? Cell Stem Cell 7:431–442
6. Pittenger MF, Mackay AM, Beck SC, Jaiswal RK, Douglas R et al (1999) Multilineage potential of adult human mesenchymal stem cells. Science 284:143–147
7. Karp JM, Leng Teo GS (2009) Mesenchymal stem cell homing: the devil is in the details. Cell Stem Cell 4:206–216
8. Keating A (2012) Mesenchymal stromal cells: new directions. Cell Stem Cell 10:709–716
9. Kumar S, Ponnazhagan S (2007) Bone homing of mesenchymal stem cells by ectopic alpha 4 integrin expression. FASEB J 21(14): 3917–3927
10. Kalajzcic I, Kalajzcic J, Hurley M, Licthler A, Rowe D (2003) Stage specific inhibition of osteoblast lineage differentiation by FGF2 and Noggin. J Cell Biochem 88:1168–1176
11. Kumar S, Nagy TR, Ponnazhagan S (2010) Therapeutic potential of genetically modified adult stem cells for osteopenia. Gene Ther 17(1):105–116
12. Kumar S, Wan C, Ramaswamy G, Clemens TL, Ponnazhagan S (2010) Mesenchymal stem cells expressing osteogenic and angiogenic factors synergistically enhance bone formation in a mouse model of segmental bone defect. Mol Ther 18(5):1026–1034
13. Chanda D, Isayeva T, Kumar S, Hensel JA, Sawant A, Ramaswamy G, Siegal GP, Beatty MS, Ponnazhagan S (2009) Therapeutic potential of adult bone marrow-derived mesenchymal stem cells in prostate cancer bone metastasis. Clin Cancer Res 15(23):7175–7185
14. Röntgen V, Blakytny R, Matthys R, Landauer M, Wehner T, Göckelmann M, Jermendy P, Amling M, Schinke T, Claes L, Ignatius A (2010) Fracture healing in mice under controlled rigid and flexible conditions using an adjustable external fixator. J Orthop Res 28(11):1456–1462

Chapter 17

Generation of Osteoporosis in Immune-Compromised Mice for Stem Cell Therapy

Reeva Aggarwal, Vincent J. Pompili, and Hiranmoy Das

Abstract

To evaluate therapeutic efficacy and to investigate involved molecular mechanisms of cell-based therapy in osteoporosis, the generation of a clinically relevant model is critically important. Herein, we describe detailed methods in generation of an immune-deficient osteoporotic murine model, and application of human umbilical cord blood-derived stem cells to assess their therapeutic efficacy.

Key words Osteoporosis, Stem cells, NOD/SCID mice, Intramyocardial injection

1 Introduction

Maintaining homeostasis and regeneration of damaged tissues are well-known phenomena in animals; however, mechanisms involved in regeneration are very complex, and yet to be established [1]. Understanding homeostasis and regeneration of osteoporosis, a bone degenerative disease, is becoming paramount in today's ever increasing elderly population. Ageing, nutritional/hormonal deficiencies, or side effects of drugs such as glucocorticoids are mainly responsible for osteoporosis [2, 3]. Over a period of time, bones loose their mechanical strength, become frail, and susceptible to fractures, which are major manifestations of osteoporosis [4]. Bone tissue comprises bone forming cells (osteoblasts), bone resorbing cells (osteoclasts), and mature osteocytes; their interplay is critical in maintaining functional bone tissue and bone health [5, 6]. Bone tissue undergoes continual bone formation and degradation cycles called remodeling; however, with time, bone formation slows down either due to reduced number/activity of osteoblast or increased number/activity of osteoclast cells, although other microenvironmental factors are also responsible for bone tissue degeneration. Current therapies such as hormone replacement or nutritional supplement do not offer long-term treatments and may

Bruno Christ et al. (eds.), *Animal Models for Stem Cell Therapy*, Methods in Molecular Biology, vol. 1213,
DOI 10.1007/978-1-4939-1453-1_17,

not specifically address the issue of bone regeneration. Thus recently, curative applications based on stem cells are being considered for the treatment of various degenerative diseases including osteoporosis [7].

Stem cells could be defined as totipotent, pluripotent, or multipotent cells depending on their differentiation potentials [8], and could be derived from bone marrow, peripheral blood, umbilical cord blood, adipose tissues, and from various organs or tissues (tissue-specific) [9]. Additionally, stem cells have the ability to self-renew and give rise to any type of cells in the body endowing them with the unique capacity of regeneration and repair [7, 10–12]. Thus, stem cells are able to maintain and restore homeostasis in degenerative tissues of the body and are believed to be at the verge of revolutionizing the health care industry. In this section, we specifically focus on the step-by-step methodology in generation of an osteoporotic condition in immune-deficient mice and therapeutic applications of adult stem cells derived from human umbilical cord blood to treat those mice. Briefly, $CD133^+$ stem cells were isolated from freshly harvested human umbilical cord blood, and then expanded ex vivo using a novel nanofiber-based expansion technology, and characterized [11]. Cells were then injected into the osteoporotic mouse via the intramyocardial route as described below to assess their therapeutic efficacy. The main advantages of using umbilical cord blood-derived stem cells are their ease of availability, isolation, ex vivo expansion, and reduced chance in immune rejection, and minimal chance in development of host versus graft disease [11, 13].

2 Materials

All experiments should be conducted in a sterile condition in an approved BSL-2 laboratory facility (*see* **Note 1**). Prepare the reagents at room temperature (*see* **Notes 2** and **3**). All procedures performed on human fluids need to be Institutional Review Board (IRB) approved and all protocols performed on rodents need to be Institutional Animal Care and Use Committee (IACUC) approved. Discard all waste materials according to standard regulations of biohazard disposals (*see* **Notes 4** and **5**).

2.1 Generation of Osteoporosis in Mice

1. Nonobese diabetic/severe combined immunodeficient (NOD/SCID) female mice, 7 months old retired breeders (body weight approximately 25 g; Jackson Laboratory, Bar Harbor, ME).
2. Dexamethasone sodium phosphate (American Reagent, Inc. Shirley, NY), stored at room temperature in a dark place. Dexamethasone sodium phosphate solution is fractionated in

aliquots within the sterile biosafety cabinet. Aliquots may be made for the amount (40 μL) needed for each mouse/day (5 mg/kg body weight).

3. Phosphate buffer saline (PBS): 0.9 %, pH 7.4.
4. Alcohol swipes.
5. Sterile BSL-2 cabinet.
6. Sterile pipettes and tips.
7. Sterile microcentrifuge tubes and holding rack.
8. Weighing machine.

2.2 Stem Cell Transplantation

1. Ex vivo nanofiber-expanded human umbilical cord blood-derived $CD34^+$ stem cells.
2. Serum-free medium: supplemented with cytokines and growth factors.
3. Osteoporotic NOD/SCID mice.
4. Sterile biosafety cabinet in animal facility.
5. Pipettes and tips.
6. 50 mL Falcon tubes.
7. Hemocytometer.
8. Microcentrifuge tubes and holding rack.
9. Syringes and needles.
10. Anesthesia machine.

3 Methods

3.1 Generation of Osteoporosis

1. After obtaining mice from commercial vendors, house the mice for acclimatization for a week in a sterile and Institutional Animal Care and Use Committee (IACUC) approved animal facility (*see* **Notes 6** and **7**).
2. Intraperitoneal (i.p.) injections: Inject mice with 5 mg/kg body weight (b.wt.) of dexamethasone (40 μL) for 21 consecutive days or with saline as a control (*see* **Notes 3** and **8**). For i.p. injection, hold the mouse dorsally with its peritoneum facing upwards. Sterilize the area around the peritoneum to be injected with alcohol swipes. Keep the needle at 45° angle to inject dexamethasone into the peritoneum.
3. After injecting, swipe the surrounding areas with the alcohol swab.
4. Place the mice gently back into the cage (*see* **Note 9**).
5. Similar procedure needs to be repeated over a period of 21 + 5 days at the same time of the day (once daily).

6. Weigh the mice once a week to monitor any significant weight loss.
7. Perform similar injection procedure to the control group that receives equal volume of saline solution intraperitoneally.
8. After 21 days of consecutive injection of dexamethasone, inject the mice (6–9 animals/group) with tapering doses of dexamethasone for 5 days followed by stem cell therapy (therapy group), or sacrifice animals as a control (dexamethasone control).
9. Harvest long bones from sacrificed animals, fix, embed, and process for sectioning. Stain with hematoxylin and eosin (H&E), or scan with micro-computed tomography (micro CT) for any bone loss from therapy group compared to its control group.

3.2 CD34⁺ Cell Transplantation

1. Sacrifice mice that received dexamethasone or saline injections after 26 (21 + 5) days as an osteoporotic control or sham control. Mice from other groups that were used for $CD34^+$ cell therapy or media injections (6–9 mice/group) are sacrificed after 4 weeks of $CD34^+$ cells injection or medium injection.
2. Simultaneously, when osteoporotic mice are being developed, expand human umbilical cord blood-derived $CD34^+$ cells in the cell culture laboratory using nanofiber scaffold and serum-free expansion medium supplemented with cytokines and growth factors [11].
3. After 26 days of dexamethasone injections or saline injections, inject mice with stem cells (half a million $CD34^+$ cells/mouse in 300 μL volume) in a serum-free medium via cardioventricular route.

3.3 Preparation of CD34⁺ Cells

1. After 10 days of culture, isolate nanofiber-expanded human umbilical cord blood-derived stem cells by pipetting within the BSL-2 sterile cabinet.
2. Since $CD34^+$ cells are non-adherent to the nanofiber scaffold these cells are easily isolated and detached from nanofiber by simple jet action of repeated pipetting of the medium.
3. Collect stem cells and medium in a 50 mL Falcon tube, and count cells under microscope using a hemocytometer.
4. Centrifuge cells for 5 min at 416 × *g*, discard supernatants, and gently break the pellet.
5. Once the pellet is broken, resuspend the cells in serum-free medium at the ratio of 0.5 million cells/300 μL (*see* **Note 10**).
6. Make aliquots in microcentrifuge tubes (1 mL/tube). Then transport tubes to the mouse facility maintaining sterile conditions at 4 °C.

7. Transport serum-free medium in separate tubes to the mouse facility maintaining sterile conditions at 4 °C to inject control mice.
8. Then in the mouse room, within BSL-2 cabinet, maintaining sterility, fill the syringe with 300 μL volume of cells and remove air bubbles from the syringe by simple tapping.

3.4 Cardioventricular Injections

1. Anesthetize the mouse and scuff at the neck and tail so that chest and rib cage face the ceiling.
2. Locate the apex of the heart near the diaphragm and sterilize the chest area with alcohol swab.
3. Feel the heart beat, and push the needle gently into the left ventricle of the heart and pull the piston of the syringe slowly.
4. Observe the blood back lashing into the needle (*see* **Note 11**). Then gently inject the cells and slowly retrieve the needle out of the heart, and discard the used needle and syringe into the biohazard container (*see* **Note 12**).
5. Place the mouse gently into the cage and observe its movement as it awakens from the anesthesia to ensure its survival and normal activities.
6. Continue injection of cells or medium to all mice following the method as described in **steps 1–5**.
7. After 28 days of injection, sacrifice mice and harvest their bones for further processing as described [7].

4 Notes

1. To perform experiments requires proper training.
2. All the procedures need to be carried out at room temperature and in sterile conditions unless otherwise stated.
3. Always check solutions for contamination with any kind of cellular growth, and precisely observe against light before each use.
4. Always wear gloves and lab coats when performing any tissue culture experiments.
5. Dexamethasone phosphate should be stored in the cabinet within the animal facility to avoid any contamination during daily transport from lab to animal facility.
6. Always wear protective/sterile gears when working with mice.
7. Monitor mice regularly.
8. Before injecting dexamethasone/cell suspension, make needles air bubble-free as bubbles may cause rupture of surrounding blood vessels and inaccurate delivery of solutions.

9. Cages should be transported by keeping lid closed, and only opened under a sterile hood to avoid exposure of mice to the non-sterile environment.
10. Make single cell suspension of the cell pellet; avoid formation of any cell clumps as clumps may block capillaries.
11. Blood back lashing into the needle confirms that the needle was inserted to the right place in the heart (left ventricle).
12. Discard biohazard materials appropriately.

Acknowledgements

This work was supported in part by National Institutes of Health grants, K01 AR054114 (NIAMS), SBIR R44 HL092706-01 (NHLBI), Pelotonia Idea Award (OSUCCC), and The Ohio State University start-up fund. The funders had no role in study design, data collection and analysis, decision to publish, or preparation of the manuscript.

Disclosure

Authors do not have any competing financial interests.

References

1. Forbes SJ, Vig P, Poulsom R, Wright NA, Alison MR (2002) Adult stem cell plasticity: new pathways of tissue regeneration become visible. Clin Sci (Lond) 103:355–369
2. Raisz LG, Rodan GA (2003) Pathogenesis of osteoporosis. Endocrinol Metab Clin North Am 32:15–24
3. South-Paul JE (2001) Osteoporosis: part I. Evaluation and assessment. Am Fam Physician 63(897–904):908
4. Zaidi M (2007) Skeletal remodeling in health and disease. Nat Med 13:791–801
5. Martin TJ, Sims NA (2005) Osteoclast-derived activity in the coupling of bone formation to resorption. Trends Mol Med 11:76–81
6. Karsenty G, Wagner EF (2002) Reaching a genetic and molecular understanding of skeletal development. Dev Cell 2:389–406
7. Aggarwal R, Lu J, Kanji S, Joseph M, Das M, Noble GJ et al (2012) Human umbilical cord blood-derived CD34+ cells reverse osteoporosis in NOD/SCID mice by altering osteoblastic and osteoclastic activities. PLoS One 7:e39365
8. Krause DS (2002) Plasticity of marrow-derived stem cells. Gene Ther 9:754–758
9. Orbay H, Tobita M, Mizuno H (2012) Mesenchymal stem cells isolated from adipose and other tissues: basic biological properties and clinical applications. Stem Cells Int 2012: 461718
10. Das H, George JC, Joseph M, Das M, Abdulhameed N, Blitz A et al (2009) Stem cell therapy with overexpressed VEGF and PDGF genes improves cardiac function in a rat infarct model. PLoS One 4:e7325
11. Das H, Abdulhameed N, Joseph M, Sakthivel R, Mao HQ, Pompili VJ (2009) Ex vivo nanofiber expansion and genetic modification of human cord blood-derived progenitor/stem cells enhances vasculogenesis. Cell Transplant 18:305–318
12. Lu J, Kanji S, Aggarwal R, Das M, Joseph M, Wu LC et al (2013) Hematopoietic stem cells improve dopaminergic neuron in the MPTP-mice. Front Biosci 18:970–981
13. Kita K, Lee JO, Finnerty CC, Herndon DN (2011) Cord blood-derived hematopoietic stem/progenitor cells: current challenges in engraftment, infection, and ex vivo expansion. Stem Cells Int 2011:276193

Chapter 18

Application of Stem Cells for the Treatment of Joint Disease in Horses

Walter Brehm, Janina Burk, and Uta Delling

Abstract

Stem cells in the form of mesenchymal stromal cells derived from various sources have been identified to have the potential of supporting the therapy of joint disease in the horse, and preliminary data has been published about the clinical application of stem cells in horses suffering from clinical joint disease.

Furthermore, the horse is recognized to be the ideal large animal model for the preclinical study of cell therapy in joints. The advantage of this species in this respect is the size of the joints, which makes surgical applications practically feasible in analogy to human surgery. Additionally, the horse is the only model species with a cartilage thickness in the knee joint comparable to that of humans. Especially the fact that horses develop clinical joint disease discerns this species from other large animal models like small ruminants. The therapy of clinical disease in model animal species represents the ideal situation for preclinical studies of novel therapeutic strategies.

Here, we describe the experimental and clinical approaches to joint disease in the horse.

Key words Equine, Osteoarthritis, Cartilage defect, Stem cell therapy, Cell culture

1 Introduction

Stem cell therapy of joint disease in the horse is a novel approach, which to date has yielded encouraging, however preliminary, clinical results when osteoarthritis (OA) was targeted [1]. The application of equine stem cells for the treatment of cartilage defects and aiming at the repair of such substantial defects has been applied in single cases but has not been reported in clinical case studies yet.

The stem cell treatment of both OA and cartilage defects has been tackled experimentally, however.

OA can be induced using a carpal chip fracture model [2, 3]. Stem cells from different sources have been tested with respect to their therapeutic potential in this model. Horses suffering from OA induced by experimental osteochondral fragmentation were treated with bone marrow-derived mesenchymal stromal cells (MSC) or the stromal-vascular fraction from adipose tissue [2].

Bruno Christ et al. (eds.), *Animal Models for Stem Cell Therapy*, Methods in Molecular Biology, vol. 1213,
DOI 10.1007/978-1-4939-1453-1_18,

Cartilage defects, on the other hand, are created in the knee joint, mainly in the trochlea femoris, but also in the condyles [3]. In general, horses are considered more suitable as large animal models than for example small ruminants, because the cartilage thickness in an equine knee joint is similar to that of human beings (1.75 mm and 2.35 mm, respectively) [4]. Stem cells have been applied in various forms with the aim of neocartilage formation at the defect sites.

The stem cells, which have been applied so far, were mainly of mesenchymal origin, the main sources being bone marrow aspirates and adipose tissue. As the characterization of these cells focuses mainly on their mononuclear appearance upon isolation and/or plastic adherence in culture, the term MSC should ideally be translated into mesenchymal stromal cell instead of mesenchymal stem cell.

This chapter describes the methods of joint disease induction as well as isolation, propagation, transport, and application of equine MSC the way they are currently used experimentally and in clinical applications.

2 Materials

Specific instrumentation is needed for the induction of equine joint disease. The most important prerequisite, however, is the availability of a fully equipped equine hospital with the capacity of performing surgery under general anesthesia. This obviously includes the availability of veterinary specialists for equine anesthesia and equine surgery. Instrumentation for general surgery and arthroscopic surgery is necessary and not detailed here.

2.1 Induction of Joint Disease

2.1.1 Induction of the Carpal Chip Fragment Model of Equine Osteoarthritis

1. 8 mm curved osteotome.
2. Surgical hammer.
3. Arthroscopic burr.

2.1.2 Induction of the Cartilage Defect Model in the Equine Femoropatellar Joint

1. Surgical curette and/or
2. Custom made drill guide with sharp cutting edge.
3. Custom made flat drill of critical size (>9 mm diameter).

2.2 Tissue Harvest for Cell Recovery

2.2.1 Bone Marrow Aspiration

1. 11 G bone marrow aspiration trocar with crown cannula and pyramid obturator.
2. #11 or #15 scalpel blade.
3. Heparin-Na^+.
4. Sterile syringes (5, 10, 20 mL).
5. Sterile hypodermic needles (0.6 mm).
6. Sterile surgical gloves.
7. Local anesthetic solution (lidocaine or mepivacaine).

2.2.2 Adipose Tissue Harvest

Surgical Excision of Adipose Tissue

1. #20 scalpel blade.
2. Surgical forceps.
3. Needle holder.
4. Surgical suture (absorbable and nonabsorbable material).

Liposuction

1. #11 or #15 scalpel blade.
2. Sterile isotonic NaCl solution.
3. Sterile syringe 50 mL.
4. Liposuction cannula.

2.3 Cell Isolation and Culture

1. Centrifuge tubes (50 mL).
2. Serological pipettes (5, 10, 25 mL).
3. Ficoll-Paque™ PREMIUM 1.078 g/mL (GE Healthcare Life Sciences) (for cell isolation from bone marrow).
4. Collagenase I solution: 0.8 mg/mL collagenase I (Life Technologies) in Hank's balanced salt solution (HBSS) (for cell isolation from adipose tissue).
5. Phosphate-buffered saline (PBS).
6. Cell culture medium: low-glucose (1 g/L) Dulbecco's modified eagle medium (DMEM) with 10 % fetal bovine serum (FBS), 1 % penicillin-streptomycin, 0.1 % gentamicin.
7. Cell culture flasks (75, 175 cm^2).
8. Trypsin-EDTA.

2.4 Cell Application in an Osteoarthritic Joint and in Cartilage Defects

1. Sterile surgical gloves.
2. Sterile hypodermic needle.
3. Sterile syringe.
4. Fibrin hydrogel as a cell matrix.

3 Methods

3.1 Induction of Joint Disease

3.1.1 Induction of the Carpal Chip Fragment Model of Equine Osteoarthritis (See **Note 1)**

1. Prepare the horse for surgery under general anesthesia. Routinely, induce general anesthesia, position the horse in dorsal recumbency, and prepare the surgical field aseptically.
2. Place the horse on an equine surgery table in dorsal recumbency.
3. Prepare the carpal joint for arthroscopy.
4. Perform arthroscopy of the middle carpal joint to control the induction of the chip fracture model.
5. Introduce the osteotome and place it under arthroscopic control perpendicular to the articular cartilage surface of the distal aspect of the radial carpal bone at the level of the medial synovial plica.
6. Using the surgical hammer, drive the osteotome into the bone in a disto-proximal direction to create the chip. Leave the chip attached or remove the chip.
7. Use the motorized arthroscopic burr to debride the exposed subchondral bone of the parent bone to create a 15 mm wide defect bed for the 8 mm wide fragment (measure visually during each surgery with a 7 mm wide arthroscopic probe).
8. Close the wounds in routine manner.

3.1.2 Induction of the Cartilage Defect Model in the Equine Femoropatellar Joint

1. Prepare the horse for surgery under general anesthesia.
2. Place the horse on an equine surgery table in dorsal recumbency.
3. Prepare the stifle joint for arthroscopy.
4. Perform arthroscopy of the femoropatellar joint to control the induction of the cartilage defect model.
5. Introduce the drill guide and place it under arthroscopic control to create a cartilage defect at the medial or lateral side of the medial or lateral trochlear ridges of the trochlea femoris in critical size (>9 mm).
6. Using the flat drill, excise the cartilage within the drill guide until the surface of the subchondral bone is reached, i.e., until spots of bleeding occur.
7. Close the wounds in routine manner.

3.2 Tissue Harvest for Cell Recovery

3.2.1 Bone Marrow Aspiration

Preparation of the Horse for Bone Marrow Aspiration

The sternebrae and tuber coxae are the preferred sites for bone marrow harvesting in the horse [5]. Within the sternum, the fourth and fifth sternebrae are the ones most often used for bone marrow aspiration (Fig. 1).

1. Sedate the horse.
2. Prepare the puncture sites aseptically.

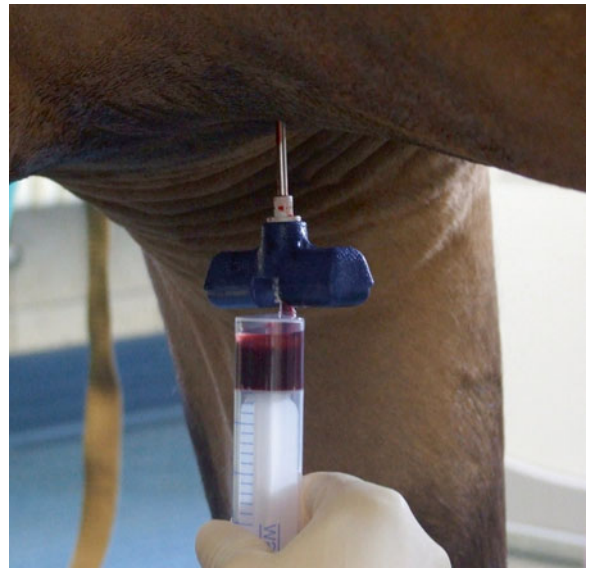

Fig. 1 Bone marrow collection from a sedated horse by sternal puncture: After localizing the puncture site by ultrasonography, the bone marrow aspiration needle is inserted, and the depth of insertion controlled by the finger tip. After insertion, the syringe, preloaded with anticoagulant, is attached to the trocar and bone marrow outflow stimulated through gentle aspiration

Bone Marrow Harvest by Sternal Puncture (*see* **Note 2**)

1. Identify the puncture site by having the horse in parallel position of the front limbs and imagine a line between the caudal edges of the antebrachium or mark the intervertebral space between the fourth and fifth sternebra under ultrasonographic guidance from where you direct the puncture trocar cranially and caudally to reach the respective sternebra.
2. Mark the midline at the level of the sternum, e.g., using a razor blade.
3. Disinfect again.
4. Insert a 0.6 mm hypodermic needle and inject 5 mL of 2 % local anesthetic solution subcutaneously and until the bony surface of the sternum is reached.
5. Create a stab incision using the #11 or #15 scalpel blades.
6. Insert the bone marrow aspiration trocar until the bone surface is touched exactly at the axial midline of the sternum.
7. Having contact, define with the index finger a 2–3 cm distance to the skin.
8. Insert the trocar by pushing and rotating it simultaneously through the cortex of the sternebra until the index finger touches the skin.

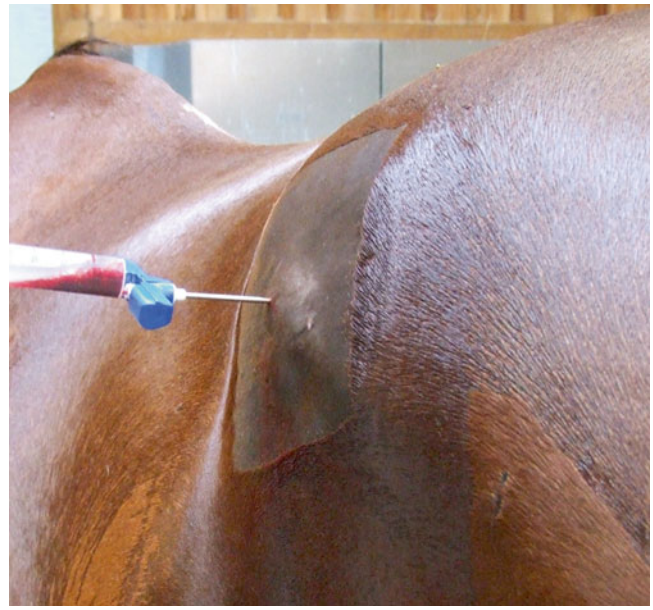

Fig. 2 Bone marrow aspiration at the left tuber coxae of a horse in standing sedated position. The bone marrow aspiration needle is inserted straight and advanced up to 8 cm into the ilium

9. Gently withdraw the trocar by 2 mm and withdraw the obturator from it.
10. Apply the 5, 10, or 20 mL syringe loaded with anticoagulant through the cannula and create gentle aspiration.
11. Observe the marrow running into the syringe (Fig. 1).
12. When reaching the volume desired, stop aspiration.
13. Insert the obturator and gently withdraw the bone marrow aspiration trocar.

Bone Marrow Harvest by Puncture of Tuber Coxae (*see* **Note 3**)

1. Identify the puncture site at the middle of the tuber coxae (*see* Fig. 2).
2. Mark the puncture site using a razor blade.
3. Disinfect again.
4. Insert a 0.6 mm hypodermic needle and inject 5 mL of 2 % local anesthetic solution subcutaneously and until the bony surface of the tube coxae is reached.
5. Create a stab incision using the #11 or #15 scalpel blades.
6. Insert the bone marrow aspiration trocar until the bone surface is touched.

7. Insert the trocar by pushing and rotating it simultaneously through the cortex of the tuber coxae.
8. Gently withdraw the trocar by 2 mm and withdraw the obturator from it.
9. Apply the 5, 10, or 20 mL syringe loaded with anticoagulant through the cannula and create aspiration.
10. Observe the marrow running into the syringe.
11. When reaching the volume desired, stop aspiration.
12. Insert the obturator and gently withdraw the bone marrow aspiration trocar.

Processing of Equine Bone Marrow Aspirates (*see* **Note 4**)
Process bone marrow aspirates immediately, or cool them to 4–6 °C and store them for up to 24 h, or ship them to the processing laboratory within 24 h.

3.2.2 Adipose Tissue Harvest

Adipose tissue is best harvested from a site situated besides the head of the tail, where this tissue is abundant and harvesting is easily performed (Fig. 3).

Fig. 3 Adipose tissue collection from the region paraxial to the tail head in a standing sedated horse. After surgical preparation, an incision is made with a scalpel to expose the adipose tissue for the excision of a piece of the size of a walnut (2.5 g of tissue)

Preparation of the Horse for Adipose Tissue Harvest

1. Sedate the horse, and apply analgesic and antibiotic medication.
2. Prepare the surgical site for aseptic surgery.

Surgical Excision

1. Create an incision of 4–6 cm through the skin using the #20 scalpel blade.
2. Expose the subcutaneous tissue.
3. Excise a piece of adipose tissue 1 cm^3 in size.
4. Close the wounds in routine manner with subcutaneous and skin sutures.

Liposuction (*see* **Note 5**)

1. Create a stab incision using a #11 or #15 scalpel blade at the site of tissue harvest (site analogous to Fig. 3).
2. Insert the liposuction device.
3. Flush with saline/anticoagulant and move the device around while aspirating.
4. Close the wound in routine manner with skin sutures.

Processing of Equine Adipose Tissue

1. Immediately place the tissue sample in a sterile tube containing a buffer solution.
2. Process adipose tissue samples immediately, or cool them to 4–6 °C and store them for up to 24 h, or ship them to the processing laboratory within 24 h.

3.3 Cell Isolation and Culture

Equine MSC culture is an adaptation of routine procedures. Here, the main steps are only briefly presented. Specific details of culture protocols are described in original literature [6].

All procedures are carried out under the clean bench at room temperature.

3.3.1 Cell Isolation from Bone Marrow

1. Mix the recovered bone marrow with PBS (1:1) (*see* **Note 6**).
2. Pipette 15 mL Ficoll-Paque™ PREMIUM into a fresh 50 mL centrifuge tube.
3. Carefully layer 30 mL of the bone marrow/PBS on top of the Ficoll-Paque™ PREMIUM using a 25 mL serological pipette (*see* **Note 7**).
4. Centrifuge at 320 × *g* for 30 min.
5. Collect the buffy coat containing the mononuclear cells, which is located above the Ficoll-Paque™ PREMIUM (*see* **Note 8**), transfer it to a fresh tube, and fill this tube with PBS.

6. Centrifuge at 400 × *g* for 5 min.
7. Carefully remove the supernatant and resuspend the cell pellet in PBS for washing.
8. Remove a small volume (10 μL) of the cell suspension for cell counting.
9. Centrifuge the remaining cell suspension at 400 × *g* for 5 min.
10. Carefully remove the supernatant, resuspend the cell pellet in cell culture medium, and seed the cells into culture flasks (for $>5 \times 10^7$ cells, use 20 mL cell culture medium and a 175 cm^2 flask; for $<5 \times 10^7$ cells, use 10 mL cell culture medium and a 75 cm^2 flask).
11. Incubate at 37 °C, 5 % CO_2 and 95 % rH for 2 days to allow cell attachment before changing the culture medium.

3.3.2 Cell Isolation from Adipose Tissue

1. Place the recovered adipose tissue on a dish, wash it with HBSS, and mince it into 1 mm^3 pieces using scissors.
2. Place the minced tissue into a centrifuge tube and add collagenase I solution (for 1 g of tissue, use approximately 10 mL of collagenase I solution).
3. Incubate at 37 °C under permanent shaking for 2–4 h.
4. When the tissue is disintegrated (*see* **Note 9**), centrifuge at 400 × *g* for 5 min.
5. Penetrate the fat layer with a 5 mL serological pipette and collect the cell pellet in approximately 2 mL of the digestion solution. Transfer the cells into a fresh tube and fill this tube with PBS.
6. Centrifuge at 400 × *g* for 5 min.
7. Carefully remove the supernatant and resuspend the cell pellet in PBS for washing.
8. Remove a small volume (10 μL) of the cell suspension for cell counting.
9. Centrifuge the remaining cell suspension at 400 × *g* for 5 min.
10. Carefully remove the supernatant, resuspend the cell pellet in cell culture medium, and seed the cells into culture flasks (for $>2 \times 10^6$ cells, use 20 mL cell culture medium and a 175 cm^2 flask; for $<2 \times 10^6$ cells, use 10 mL cell culture medium and a 75 cm^2 flask).
11. Incubate at 37 °C, 5 % CO_2 and 95 % rH for 2 days to allow cell attachment before changing the culture medium.

3.3.3 Cell Culture and Expansion

1. Check the cell cultures under the microscope and change the cell culture medium twice weekly. At the first medium change after cell isolation, additionally wash with PBS to remove the non-adherent cells.

2. At confluency of the MSC colonies (*see* **Note 10**), detach the cells after thorough washing with PBS using trypsin-EDTA according to the manufacturer's instructions (*see* **Note 11**).
3. If further expansion is required, seed the cells in fresh culture flasks ($0.5–1 \times 10^6$ cells per 20 mL culture medium and 175 cm^2 flask).

3.3.4 Cell Preparation for Transport and Application

MSC are shipped ideally using the autologous bone marrow supernatant, autologous serum or, less ideally, PBS. Prior to shipment, sterility of the culture is evaluated through rapid bioassays. Transportation is preferably accompanied by cooling the package to 4 °C and delivery should be made within 24 h after cell harvest for best viability of the cells upon application [7].

3.4 Cell Application In Vivo in Experimental and Clinical Joint Disease

1. Prepare the joint for sterile puncture.
2. Inject the cell suspension.
3. Cover the puncture site with sterile bandage.

*3.4.1 Application of Equine MSC in Osteoarthritis (See **Note 12**)*

*3.4.2 Application of Equine MSC in Cartilage Defects (See **Note 13**)*

1. Prepare the joint for sterile surgery.
2. Open the joint through an arthrotomy approach or, if feasible, use arthroscopy to control the application of the material.
3. Apply the cell implant accordingly to its physical properties.

3.5 Expected Outcome of Stem Cell Application in Equine Joint Disease

3.5.1 Results of Stem Cell Therapy of Equine Osteoarthritis

Experimentally, it could be shown that the injection of MSC in suspension intra-articularly yields beneficial effects in terms of anti-inflammatory action and early pain relief [2]. When comparing the adipose-derived stromal vascular fraction with bone marrow-derived MSC, the isolated and propagated marrow-derived MSC reduced inflammation more than the adipose-derived stromal vascular fraction, which tended to produce the pro-inflammatory TNFα. This was not reflected by the clinical development of the horses that had undergone the abovementioned carpal chip fracture model.

Clinically, horses suffering from joint disease (Fig. 4) were treated through intra-articular injection of 30×10^6 bone marrow-derived MSC in suspension [1]. The majority of 40 equine patients suffered from diseased knee joints. Each animal received 30 Mio of bone marrow-derived MSC combined with hyaluronic acid into the afflicted joint. These joints had been refractory to treatment and stem cell therapy was introduced after other standard therapies had failed to improve the clinical situation. The analysis of this series of

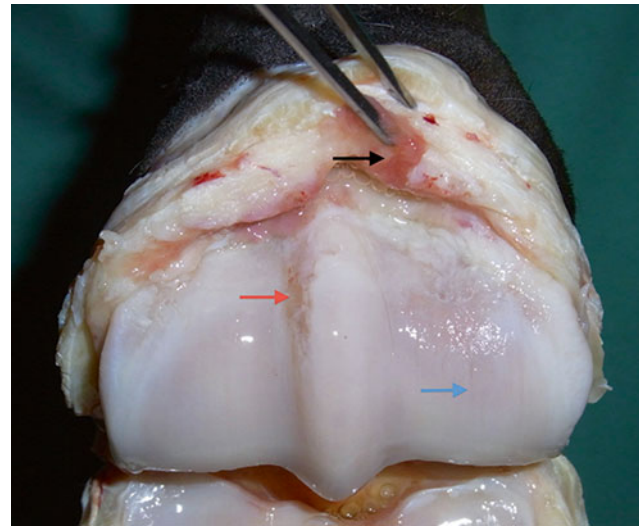

Fig. 4 Example of an equine osteoarthritic joint: macroscopic view of the distal, third metacarpal condyle of a horse with osteoarthritis of the fetlock joint; *red arrow*: full thickness cartilage lesion; *blue arrow*: partial thickness cartilage lesions (wear lines); *black arrow*: synovitis (hyperemic synovial tissue). This type of joints did not benefit from stem cell therapy as much as the more complex knee joint [1] (Color figure online)

cases revealed a beneficial effect of MSC therapy mainly in the more complex joints, particularly the knee joint, whereas the treatment of other diarthrotic joints like the metacarpo-phalangeal joint did not improve as much after stem cell treatment. The beneficial effect of MSC injection did not impose as an immediate clinical improvement but merely after a period of 2–3 months after stem cell application. Twenty-nine of these animals (73 %) were able to return to their intended athletic function. Age, sex, breed, discipline, or severity of the lesion had no influence on the outcome.

3.5.2 Results of Stem Cell Therapy of Equine Cartilage Defects

Any attempt to restore hyaline cartilage using equine MSC so far has failed. As with other strategies, the implantation resulted in improved coverage of the subchondral bone, which would most probably reduce the clinical symptoms of a human patient through reduction of pain derived from the subchondral bone itself. An equine model to examine the impact of MSC implantation on healing of osteochondral defects was studied by Wilke [8]. Undifferentiated MSC embedded in a fibrin gel were filled into the defects and assessed after 30 days and 8 months. Improved early tissue regeneration due to fibrous tissue formation was found when using MSC-fibrin constructs. However, after 8 months, no significant difference between control (cell-free fibrin gel) and MSC implants could be detected with respect to collagen II and proteoglycan content of the tissue regenerate [8].

Clinically, in contrast to treatments for humans, where the approach is standard of care, there are no reports of engineered cartilage applied in equine clinical cases. This might be due to the fact that focal cartilage defects with stable and clean margins are only infrequently encountered in horses. Additionally, postoperative management after implant application in humans entails a period of no or only limited weight bearing on the affected limb. This is of limited practicability, especially in large animals like horses, and might restrict the applicability of such therapeutic strategies.

3.6 Conclusion

The horse is an important preclinical model for the evaluation of stem cell therapy for the treatment of different conditions of diseased joints in both experimental and veterinary clinical applications. Therefore, stem cell treatment of articular problems is an emerging field in veterinary orthopedics, and the future will see more cases treated and strategies to be confirmed or rejected. These observations will be interpreted as being preclinical data for human orthopedics, too.

4 Notes

1. The debris is not actively flushed from the joint. This model causes a consistent level of OA by day 70 after creation. The opposite joint (control joint) receives a sham arthroscopic examination.
2. For sternal puncture, be sure the cannula is positioned exactly axially (the correct position of the cannula must be checked very carefully) and inserted vertically until it reaches the bone surface.

   Be sure not to insert the cannula more than 2–3 cm deep: Penetrating the transcortex might produce puncture of the pericardium and sudden collapse of the horse!

   When it is difficult to obtain marrow easily, flush with some anticoagulant, rotate, and withdraw the trocar a little but do not just push in more!

   Be aware that creating negative pressure by aspiration might cause some reaction of unease for the horse. Lower the aspiration force in this case and wait for some seconds.
3. For puncture of the tuber coxae, be aware that this procedure can be physically hard due to the density and thickness of the ilium at this site. The cannula is to advance well over 4–5 cm under rotating movements and slightly withdrawn before aspiration is started. Other than in the sternebrae, hard aspiration may be necessary especially in older horses to obtain bone marrow, and in some cases, mainly fatty marrow will be obtained.
4. When marrow aspiration is performed, keep in mind that the concentration of colony-forming cells is highest in the first 5 mL fraction of aspirate [3, 8]. Therefore, the aspiration of volumes

greater than 25 mL is not useful when a maximum number of plastic adherent cells is the aim. It is preferable in such cases to puncture more than one sternebra. Furthermore, the aspiration of bone marrow from the tuber coxae may only be practical in young horses. In older horses, aspiration can be difficult and the aspirate may contain mostly fatty marrow [3] and therefore, isolation and propagation of cells might be ineffective.

5. When liposuction is used for adipose tissue harvest, the advantage of this procedure is decreased wound morbidity, while a drawback might be the prolonged time used for harvesting.
6. More than an equal volume of PBS can be used if it is necessary to adjust the volume of the bone marrow/PBS mixture for the further steps.
7. Layering the bone marrow on top of the Ficoll-Paque™ PREMIUM needs to be done with caution, letting the bone marrow flow out of the pipette along the wall of the tube very slowly, to avoid mixing the fluids.
8. In some cases, the buffy coat is not clearly recognizable or there are cloudy clots of bone marrow in the tube. If that happens, we rather collect a larger volume of the buffy coat cell suspension (including the supernatant or the bone marrow clots) than to risk loosing too many cells.
9. Usually, if thoroughly minced before digestion, adipose tissue is completely disintegrated after 2 h. If required, small remaining tissue fibers can be removed by sieving the digestion solution through a 70 μm cell sieve.
10. The first passaging can usually be performed after 2 weeks of primary culture in case of bone marrow-derived MSC, and after 1 week of primary culture in case of adipose-derived MSC.
11. Trypsinization is the most commonly used technique to detach equine MSC. However, if the cells are to be used for characterization assays such as immunophenotyping, we do not recommend enzymatic cell detachment, as it impairs the detection of surface antigens.
12. The postulated effect of MSC therapy of OA lies in its immunemodulating and cell-stimulating effect. Equine MSC have been used mainly as a cell suspension in PBS or in autologous bone marrow supernatant. Cell suspensions are injected intraarticularly into the respective synovial space [1, 6].
13. The treatment of cartilage defects has been trialed in analogy to the Autologous Chondrocyte Transplantation technique injecting cells underneath a membrane, which is sutured onto the margins of the cartilage defect. Another way of keeping the MSC in the cartilage void is their integration in a scaffold. Fibrin hydrogel has been used in experimental trials and single cases this way [7]. Other investigators tested anchoring systems to keep constructs in the defect sites [9].

MSC were also used to produce scaffold-free cartilage constructs [10], which might be implanted directly onto the subchondral bone [11].

The application is performed after surgical opening of the joint through arthrotomy (open approach) or under arthroscopic control with CO_2 distension of the joint (arthroscopic approach). The arthrotomy approach is suitable for implants which need to be sutured onto the cartilaginous margin of the cartilage defect, while the arthroscopic approach is preferred when such implants can be fixed using arthroscopic pins or when the structure of the implant allows its application by injection through a cannula into the void, along with gas distension of the joint and visual control of the placement and aggregation of the material inserted.

Acknowledgements

The work presented in this paper was made possible by funding from the German Federal Ministry of Education and Research (BMBF 1315883).

References

1. Ferris DJ, Frisbie DD, Kisiday JD, McIlwraith CW, Hague BA, Major MD, Schneider RK, Zubrod CJ, Watkins JJ, Kawcak CE, Goodrich LR (2009) Clinical follow-up of horses treated with bone marrow derived mesenchymal stem cells for musculoskeletal lesions. Proc Am Ass Equine Practnrs 55:59–60
2. Frisbie DD, Kisiday JD, Kawcak CE, Werpy NM, McIlwraith CW (2009) Evaluation of adipose-derived stromal vascular fraction or bone marrow-derived mesenchymal stem cells for treatment of osteoarthritis. J Orthop Res 27:1675–1680
3. McIlwraith CW, Fortier LA, Frisbie DD, Nixon AJ (2011) Equine models of articular cartilage repair. Cartilage 2:317–326
4. Ahern BJ, Parvizi J, Boston R, Schaer TP (2009) Preclinical animal models in single site cartilage defect testing: a systematic review. Osteoarthritis Cartilage 17:705–713
5. Delling U, Lindner K, Ribitsch I, Jülke H, Brehm W (2012) Comparison of bone marrow aspiration at the sternum and the tuber coxae in middle-aged horses. Can J Vet Res 76: 52–56
6. Burk J, Ribitsch I, Gittel C, Juelke H, Kasper C, Staszyk C, Brehm W (2012) Growth and differentiation characteristics of equine mesenchymal stromal cells derived from different sources. Vet J. http://dx.doi.org/10.1016/j.tvjl.2012.06.004
7. Espina M, Jülke H, Ribitsch I, Brehm W, Winter K, Delling U (2013) Optimization of transport conditions for autologous bone marrow-derived multipotent stromal cells for therapeutic application in horses. Proceedings of the World Veterinary Congress, Prague, Czech Republic ID: 332
8. Wilke MM, Nydam DV, Nixon AJ (2007) Enhanced early chondrogenesis in articular defects following arthroscopic mesenchymal stem cell implantation in an equine model. J Orthop Res 25:913–925
9. Kasashima Y, Smith RKW, Goodship A (2009) Optimizing the recovery of mesenchymal progenitor cells from bone marrow. Regen Med 4(Suppl 2):19–20
10. Brehm W, Werren C, Mainil-Varlet P (2007) Production of very large sized scaffold-free engineered cartilage constructs from the adult equine donor—a basis for therapeutical and experimental applications in the horse. Pferdeheilkunde 23:111–117
11. Brehm W, Aklin B, Yamashita T, Rieser F, Trüb T, Jakob RP, Mainil-Varlet P (2006) Repair of superficial osteochondral defects with an autologous scaffold-free cartilage construct in a caprine model: implantation method and short-term results. Osteoarthritis Cartilage 14:1214–1226

Chapter 19

Adipogenic Fate Commitment of Muscle-Derived Progenitor Cells: Isolation, Culture, and Differentiation

Anne-Marie Lau, Yu-Hua Tseng, and Tim J. Schulz

Abstract

Skeletal muscle harbors several types of cells, among which a population of progenitors committed to the adipogenic lineage has only recently been identified. Potential sources of white and brown adipocytes, the latter representing a potential target to treat obesity, are of considerable interest to the field. Fluorescence-activated cell sorting (FACS) provides an elegant strategy for prospective isolation of closely defined cell populations. Here we describe a flow cytometric method to isolate muscle-resident adipogenic progenitor cells with a default potential to undergo white adipogenesis. We further describe an approach to induce commitment to a lineage of brown-like adipocytes upon exposure to bone morphogenetic protein 7 (BMP7).

Key words Skeletal muscle, Adipogenic progenitors, Fluorescence-activated cell sorting, Cell surface marker antibodies, Brown adipogenesis, Bone morphogenetic protein 7

1 Introduction

Skeletal muscle contains various populations of progenitor cells from different developmental ancestries. The most noted precursor cells that possess myogenic potential have been termed satellite cells and were originally described by Mauro [1]. Principally, myogenic progenitors are quiescent in adult muscle, but in response to injury represent the major source of regenerating myofibers (reviewed in [2, 3]). In contrast to satellite cells that reside underneath the myofiber basal lamina, adipogenic progenitor cells are predominantly localized in the interstitial space between mature myofibers [4]. Developmental lineage tracing studies using the Cre/loxP recombination system have revealed that myogenic cells commonly arise from an embryonic lineage of stem/progenitor cells that express myogenic transcription factors such as myogenic factor 5 (Myf5). On the other hand, adipogenic progenitors within skeletal muscle derive from a lineage that never expresses these transcription factors (Fig. 1) [5–7]. These muscle-resident adipogenic progenitor cells (MusAPCs) are therefore functionally and

Bruno Christ et al. (eds.), *Animal Models for Stem Cell Therapy*, Methods in Molecular Biology, vol. 1213,
DOI 10.1007/978-1-4939-1453-1_19,

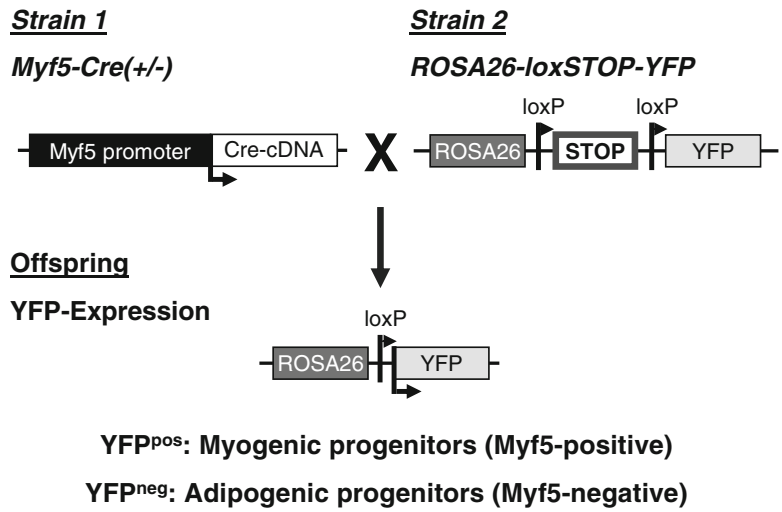

Fig. 1 MusAPCs are not derived from a Myf5-expressing lineage. Animals expressing Cre recombinase under control of the Myf5-promoter are crossed to ROSA26-YFP (yellow fluorescent protein) reporter mice. Transient Myf5-expression during development (that will therefore also lead to expression of Cre) leads to permanent Cre-mediated DNA recombination that removes the loxP-flanked transcriptional stop cassette in the ROSA26 locus. Subsequently, expression of the reporter YFP is detectable in Myf5-expressing cells and, importantly, all their progeny independent of actual Myf5 expression

developmentally distinct from satellite cells and were described in two independent studies by their characteristic expression of the surface markers platelet-derived growth factor receptor (PDGFR)-α [4] and stem cell antigen 1 (Sca1) [5]. Both populations display adipogenic capacity in vivo and in vitro. Additional analysis of Sca1-expressing cells isolated from muscle revealed that these populations of adipogenic cells within skeletal muscle are in fact identical and homogenously express a set of surface markers commonly found in progenitors derived from regular adipose tissues, altogether suggesting functional similarities [6]. Specifically, the adipogenic Sca1$^+$ population is negative for the hematopoietic markers Integrin αM (CD11b), Leukocyte common antigen (CD45), and c-Kit (CD117), and the endothelial marker PECAM-1 (CD31) and expresses typical pre-adipocyte markers such as Integrin β1 (CD29), CD34, PDGFRα (CD140a), and PDGFRβ (CD140b) [6]. Taken together, these studies collectively indicate that MusAPCs are non-myogenic and committed towards an adipogenic lineage and do not require further lineage commitment steps besides a regular adipogenic induction that is commonly used for bone marrow- or adipose-derived progenitor cells. Hence, this unique surface molecule signature can be used for identification and prospective isolation of muscle-resident adipose progenitors.

In healthy muscle tissue, differentiation of adipogenic progenitors is strongly inhibited by direct cell–cell interaction with myofibers suggesting that the local microenvironment (also known as the stem cell niche) triggers their developmental fate [4]. However, in response to muscle damage [4] and absence of functional Interleukin (IL)-4/IL-13 signaling [8], they contribute to ectopic fat infiltration of skeletal muscle. Muscle-resident pre-adipocytes, belonging to a distinct developmental lineage, do not generate myofibers themselves (Fig. 1) [4, 6, 7], but enhance differentiation of adjacent satellite cells in injured muscle [5, 8, 9]. Besides their regulatory function in myogenesis by direct cell–cell interactions, cell fate decisions might be driven by external factors. Schulz et al. were able to demonstrate the capacity of MusAPCs to differentiate into adipocytes with a brown adipocyte-like phenotype, the so-called beige or brite adipocytes, in response to stimulation with bone morphogenetic protein 7 (BMP7) [6]. The notion of muscle-resident brown fat is entirely consistent with previous observations that skeletal muscle of obesity-resistant mouse strains contains large depots of UCP1-expressing brown adipocytes [10]. Consequently, MusAPCs might be not constitutively committed to a white adipogenic lineage, but could indeed give rise to either white or beige/brite adipocytes after exposure to specific inductive cues.

One of the first methods to isolate muscle-derived stem cells (MDSC) is the pre-plate technique [11–13] by separating cells based on adhesion characteristics. In order to dissociate MDSC from their niche, steps of mincing, enzymatic digestion, and repetitive trituration have to be performed. Various protocols for muscle digestion have been frequently described in the literature [14, 15]. Substantial efforts to further improve the pre-plate technique to purify enriched populations of distinct cell fractions, such as satellite cells, were made [16, 17]. A more specific protocol for isolation of satellite cells according to their anatomical localization and subsequent purification by fluorescence-activated cell sorting (FACS) has previously been described [7, 18, 19].

Here, we describe a modified approach based on this method that enables the separation of two distinct muscle cell fractions: Interstitial cells and myofiber-associated cells. An enriched population of progenitor cells with adipogenic potential (MusAPCs) is purified by flow cytometry using antibodies directed against a specific set of surface antigens. Besides pre-adipocytes, this technique provides a promising strategy to isolate different, highly purified cell populations within the general population of mononucleated cells isolated from skeletal muscle by including additional surface markers. We further describe a method to differentiate this highly adipogenic population of cells into bona fide brown adipocytes of the recruitable type under in vitro conditions. While many studies suggest that the default commitment of these cells is white adipogenic, our studies also indicate that mouse strain-specific genetic

differences determine whether these progenitor cells do or do not express a signature of genes that is typical for brown adipocytes, such as UCP1 [6].

2 Materials

2.1 Isolation of Progenitors from Murine Skeletal Muscle

1. 70 % ethanol.
2. 50 mL conical tubes.
3. Water bath.
4. Fetal bovine serum (FBS).
5. Phosphate-buffered saline (PBS).
6. 10 cm petri dish.
7. 37 °C incubator.
8. 10 mL serological pipette.
9. Digestion solution 1: 0.2 % Collagenase type 2 (Life Technologies; *see* **Note 1**) in Dulbecco's modified Eagle's medium (DMEM; high glucose, L-glutamine with sodium pyruvate, Life Technologies). Freshly prepare an appropriate volume; approximately 10 mL per 2 g of muscle wet weight (*see* **Note 2**). Filter the solution through a 0.22 μm filter.
10. Digestion solution 2: 0.1 % Dispase 2, 0.025 % Collagenase 2 in F-10 Nutrient Mixture (all purchased from Life Technologies). Prepare approximately 5–6 mL per mouse. Filter the solution through a 0.22 μm filter. Prepare on day of isolation and keep refrigerated until use.
11. F-10 Nutrient Mixture supplemented with 20 % FBS.
12. ACK lysis buffer: 0.15 M ammonium chloride, 0.01 M potassium bicarbonate, 0.01 M ethylenediaminetetraacetic acid (EDTA) in 1 L distilled deionized water. Pass through a sterile 0.22 μm filter. Solution can be stored at room temperature.
13. Sorting medium: PBS supplemented with 2 % FBS.
14. Glass Pasteur pipette: Use a diamond pen to prepare pipette with desired opening width for trituration of skeletal muscle pieces. Flame with gas burner to blunt sharp edges and sterilize the pipette.
15. Fisherbrand cell strainer 40, 70, and 100 μm (Thermo Fisher Scientific).

2.2 FACS Staining

1. Compensation beads: OneComp eBeads (eBioscience).
2. Calcein blue stock solution (10 mM): 1 mg calcein blue (Life Technologies) in 215 μL dimethylsulfoxide (DMSO).

Table 1
Mouse monoclonal antibodies used for FACS isolation of MusAPCs

Antibody	Fluorochrome	Clone	Isotype	Concentration (μg/mL)
Anti-mouse-Sca1	APC	D7	Rat IgG2a	0.5
Anti-mouse-CD11b	FITC	M1/70	Rat IgG2b	2.5
Anti-mouse-CD45	FITC	30-F11	Rat IgG2b	2.5
Anti-mouseCD31	PE/Cy7	390	Rat IgG2a	1

APC allophycocyanin, *FITC* fluorescein isothiocyanate, *PE-Cy7* phycoerythrin/Cy7

Table 2
Growth medium for culture of MusAPCs

	Stock concentration	Final concentration	Volume (500 mL)
DMEM (low glucose)	–	60 %	300 mL
MCDB201 media	–	40 %	200 mL
FBS	–	2 %	10 mL
Penicillin/streptomycin	100×	1×	5 mL
Dexamethasone	10 μM	1 nM	50 μL
L-Ascorbic acid-2P	50 mM	0.1 mM	1,000 μL
ITS MIX	100×	1×	5 mL
Linoleic acid-albumin	100×	1×	5 mL

3. Propidium iodide (PI, Sigma-Aldrich): Use a final concentration of 1 μg/mL from a 1,000× stock in water.
4. Fluorochromes conjugated to anti-mouse antibodies (eBioscience) at final concentrations indicated in Table 1.

2.3 Cell Culture

1. 24- and 48-well cell culture plates.
2. Matrigel-coated dishes: Thaw a Matrigel aliquot at 4 °C overnight and resuspend in cold F-10 medium to a final concentration of 2 % under sterile conditions (*see* **Note 3**). Pipette an aliquot of the 2 % solution onto culture plate/well and aspirate. Leave coated plates to dry for several hours. To ensure sterility, dried plates can be exposed to UV light in the cell culture hood for 20 min.
3. Growth medium (modified from [20]; (Table 2)): 60 % DMEM with low glucose, 40 % MCDB201 (Sigma-Aldrich), 100 U/mL penicillin and 1,000 U/mL streptomycin (Life Technologies), 2 % FBS, 1× insulin-transferrin-selenium mix,

Table 3
Adipogenic induction medium

	Stock concentration	Final concentration
Insulin (human)	10 mg/mL (water)	5 μg/μL
Indomethacin	30 mM (methanol)	50 μM
IBMX	5 mM (methanol)	0.5 μM
Dexamethasone	2 mg/mL (5 mM, ethanol)	1 μM
T3	10 μM (water)	1 nM

1× linoleic acid conjugated to bovine serum albumin (BSA), 1 nM dexamethasone, and 0.1 mM L-Ascorbic acid 2-phosphate (all purchased from Sigma-Aldrich). Pass through a sterile filter; store at 4 °C. Immediately before use, add the following growth factors to the medium: 10 ng/mL epidermal growth factor (EGF; PeproTech), 10 ng/mL leukemia inhibitory factor (LIF; Millipore), 10 ng/mL platelet-derived growth factor BB (PDGFR-BB; PeproTech), and 5 ng/mL basic fibroblast growth factor (bFGF; Sigma-Aldrich) and pass through a sterile filter.

4. Adipogenic induction medium: Growth medium without growth factors, 5 μg/mL human insulin (Roche Applied Science), 50 μM indomethacin, 1 μM dexamethasone, 0.5 μM isobutylmethylxanthine (IBMX), 1 nM 3,3′,5-triiodo-L-thyronine (T3) (all purchased from Sigma-Aldrich). Prepare stock solutions for all chemicals in the adipogenic induction medium and store at −20 °C (Table 3).
5. Adipogenic differentiation medium: Growth medium without growth factors, 5 μg/mL human insulin and 1 nM T3.
6. Gentamycin.
7. Trizol reagent (or similar).
8. 25 μL Hamilton syringe.

3 Methods

3.1 Isolation of Progenitors from Murine Skeletal Muscle

1. Sacrifice mouse by cervical dislocation.
2. Spray dead animals extensively with 70 % ethanol. Create a transversal incision through the skin in the abdominal region. Peel the flap of skin to completely expose underlying tissue and the abdominal area of the animal. Harvest skeletal muscles of hind limbs (e.g., Soleus, Gastrocnemius, Tibialis anterior, Extensor digitorum longus, Quadriceps femoris). Ensure that

mostly intact muscles are collected; this is critical for the subsequent digestion step.

3. Remove as much contaminating non-muscle tissue as possible (e.g., connective tissue and the small adipose tissue depots). Place intact muscles into a 50 mL conical tube with digestion solution 1, seal tube with Parafilm, and incubate at 37 °C in a water bath with gentle agitation for 90 min (*see* **Note 4**).
4. Stop enzymatic digestion by adding 10 % FBS, incubate for 10 min at room temperature.
5. Carefully discard liquid and floating debris without disturbing muscle pieces. Fill the tube with F-10 supplemented with 20 % FBS. Before decanting, let pieces sink to the bottom (*see* **Note 5**). Repeat washing twice using PBS to remove residual serum.
6. Single myofibers are separated mechanically; add muscle pieces with an appropriate volume of PBS to a 10 cm petri dish. The muscle is triturated/minced with a flamed glass Pasteur pipette by gently pipetting the digest up and down. The pipette tip has been cut further up to increase its opening width to approximately 3 mm (*see* **Note 6**). When PBS becomes turbid with single fibers and debris, collect supernatant into a clean 50 mL conical tube. Ensure that no intact muscle pieces are collected and add more PBS to the dish (approximately 5–10 mL each time). Repeat this step as many times as necessary to completely mince muscle. In the end, only connective tissue should remain.
7. Interstitial cells and myofibers are separated by differential centrifugation (no more than $50 \times g$ for 1 min; all subsequent centrifugations are performed in a cooled centrifuge at 4 °C) leaving interstitial cells in the supernatant and fibers as pellet. Collect approximately 25 mL of the supernatant in another 50 mL conical tube. For preparation of interstitial cells proceed with Part B.
8. Wash single myofibers with PBS and repeat centrifugation (**step 7**).
9. After the second centrifugation step, remove most of the supernatant, but ensure that the myofiber-pellet is not disturbed. Wash myofibers again with PBS, invert two times, and place in a 37 °C incubator for 10–15 min to let fibers settle by sedimentation. Repeat this procedure until supernatant remains more or less clear, i.e., free of interstitial cells and debris. Usually, 3–4 repeats are sufficient.
10. Remove supernatant carefully to less than 5 mL residual volume including the pellet of myofibers (*see* **Note 7**). For preparation of myofiber-associated cells proceed with Part A.

Part A: Preparation of Myofiber-Associated Cells

1. Add 5–6 mL of digestion solution 2, seal cap with Parafilm, and incubate for 30 min in a 37 °C water bath with gentle agitation.
2. To inactivate enzymatic digestion, add FBS to a final concentration of approximately 10 %. Pipette fibers several times with a 10 mL serological pipette to dissociate myofiber-associated cells from myofibers. Use high speed mode on the pipettor to generate mechanical strain to break predigested myofibers. Differential centrifugation (no more than $50 \times g$ for 1 min) sediments most of the larger debris, but leaves myofiber-associated cells in the supernatant.
3. Collect supernatant and filter through a 100 μm cell strainer. Discard leftover debris and wash strainer with an additional volume of sorting medium. Centrifuge at $300 \times g$ for 5 min. Resuspend the pellet and repeat filtration with a 40 μm cell strainer. Spin down the cells and resuspend in sorting medium to transfer suspension to a 5 mL sorting tube for staining (5 min, $300 \times g$).

Part B: Preparation of Interstitial Cells

1. Centrifuge the supernatant containing interstitial cells at $300 \times g$ for 5 min.
2. To remove red blood cells, resuspend pellet in 2–3 mL ACK lysis buffer and incubate on ice for 3 min. Stop lysis by adding 10 mL of sorting medium.
3. After centrifugation at $300 \times g$ for 5 min, resuspend cells in sorting medium and pass through a 100 μm cell strainer, and subsequently through a 40 μm cell strainer (*see* **step 3** of Part A).
4. Spin down as before and resuspend the pellet in sorting medium and transfer the suspension to a 5 mL sorting tube for staining.

3.2 Purification of Adipogenic Progenitors by FACS

For FACS purification of adipogenic progenitors, isolated muscle cells are stained with fluorophore-tagged monoclonal antibodies directed against Sca1, the lineage markers CD11b, CD45, and CD31, and optionally CD29 to enrich myogenic cells (*see* **Note 8**).

1. Sample preparation: Centrifuge myofiber-associated cells and interstitial cells at $300 \times g$ for 5 min. Resuspend pellets in a small defined volume (e.g., 250–150 μL). Take small aliquots of interstitial cells for preparing staining controls as indicated in **steps 2–4**.
2. Use staining controls for voltage adjustments according to specific flow cytometer parameters, depending on the instrument used for sorting (*see* **Note 9**).

3. Compensation controls: Prepare an unstained sample as autofluorescence control as well as single color controls for each fluorochrome used. This includes antibody-coupled fluorochromes as well as live/dead-staining fluorochromes (*see* **Note 10**). To generate each control, use a 100 µL aliquot of a control cell suspension that contains cells that are comparable to the cell types occurring in the regular samples. Since compensation controls with cells are not always completely effective, compensation beads which contain microparticles that bind to mouse isotype antibodies (positive compensation control) and microparticles with no binding capacity (negative compensation control) can be used alternatively. Add individual fluorochromes at concentrations indicated in Table 1.
4. Fluorescence-minus-one (FMO) controls: FMOs are used for setting the threshold of negative and positive signals. In each FMO control, all antibodies (not for other non-antibody fluorochromes) used in the multicolor stain are included except the individual antibody for which the threshold is to be determined. Hence, if four antibodies are being used in a four color stain, four FMOs, each lacking one antibody, need to be generated.
5. Antibody preparation: Add all antibodies at the indicated concentrations (Table 1) to samples and staining controls (*see* **Note 11**).
6. Incubate samples and controls on ice and in the dark for at least 20 min.
7. Wash cells and centrifuge at 300 × *g* for 5 min and resuspend in 200 µL sorting medium.
8. Immediately before sorting, filter cell suspensions through a 70 µm cell strainer to avoid clogging of the tubing of the flow cytometer.
9. Live cells are isolated by positive selection for calcein blue staining and negative selection for propidium iodide staining. The dyes can be added before or after final filtration (*see* **Note 12**).
10. Analyze samples on a flow cytometer that is equipped with sorting capacity. Start data acquisition on flow cytometer by creating a forward scatter (FSC) and sideward scatter (SSC) plot to adjust the settings until the proceeded events are clearly delineated. Set the photomultiplier tube (PMT) voltage of the FITC, APC, PE/Cy7 detectors using the unstained sample and single color controls (*see* **Note 13**).
11. Run the single color sample to correct the potential spectral overlap between color filters and fluorochromes using software compensation.
12. After compensation, run FMO controls for defining negative signal threshold.

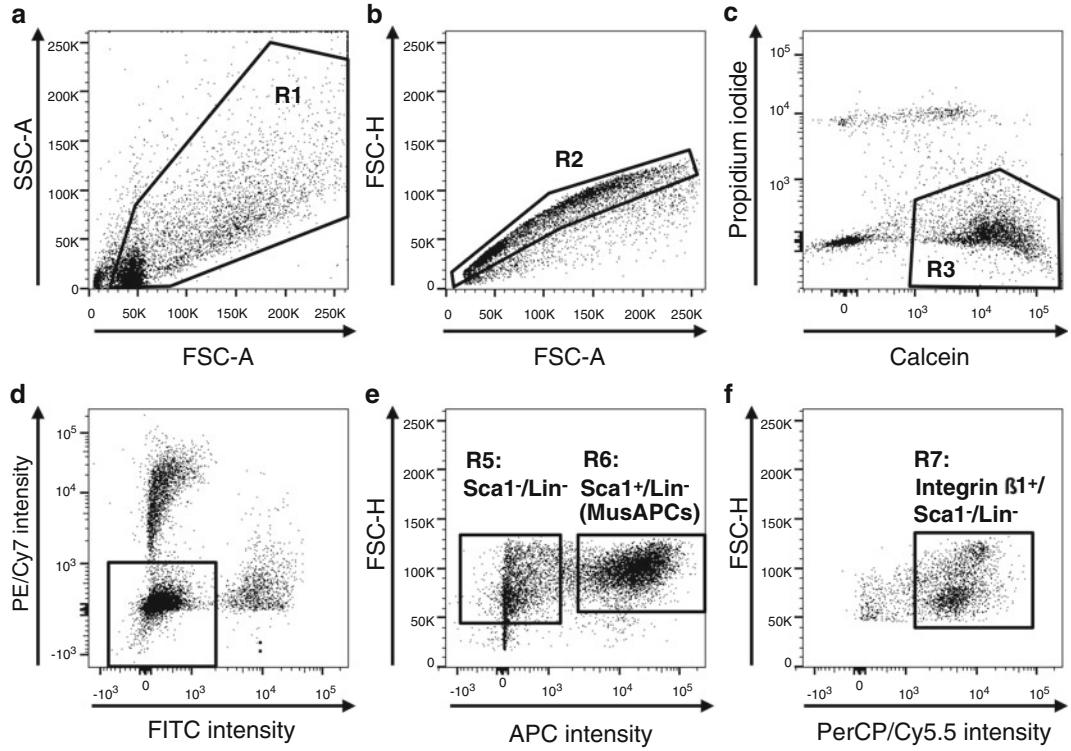

Fig. 2 Gating strategy for FACS purification of adipogenic progenitor cells from a heterogeneous muscle cell population. (**a**) In the FSC vs. SSC plot, draw a polygonal region (R1) around the events that represent intact cells, thereby excluding debris. (**b**) Perform duplet discrimination by gating for single cells (R2) in FSC-H vs. FSC-A plot as indicated. (**c**) Calcein and Propidium iodide (PI) are used to discriminate between live (Calcein$^+$/PI$^-$, R3) and dead cells (Calcein$^-$/PI$^+$). (**d**) Exclude hematopoietic cells and endothelial cells by selecting cells that are CD11b$^-$/CD45$^-$/CD31$^-$ (R4: lineage negative (Lin$^-$) cells) in the PE/Cy7 vs. FITC plot. (**e**) Select MusAPCs marked as the Sca1$^+$/Lin$^-$ population (R6) for sorting. For optional analysis/collection of myogenic progenitors, define a gate for the Sca1$^-$/Lin$^-$ population (R5). (**f**) To enrich satellite cells within the myogenic Sca1$^-$/Lin$^-$ population, select the Integrin ß1 positive population (R7) and apply a specifc selection marker for satellite cells (*see* **Note 8**)

13. Gating strategy (Fig. 2): To select and sort defined populations of cells, a gating strategy to remove debris, cell aggregates, and dead cells will be used before selection of certain cell populations according to surface marker expression.
14. To exclude debris, define a muscle cell population in the FSC versus SSC plot by means of a polygonal region (R1) drawn around the events that represent cells (Fig. 2a).
15. To exclude duplets, the selected population is gated for single cells (R2) in a forward scatter-height (FSC-H) versus forward scatter-area (FSC-A) plot (Fig. 2b).
16. The single cells are further analyzed for their uptake of calcein blue or propidium iodide to determine live (Calcein-positive) versus dead (PI-positive) cells and cellular debris (double negative) (Fig. 2c).

17. Set gates according to Fig. 2d, e to select for MusAPCs. Within the viable population (R3), gate for cells negative for lineage markers CD31, CD11b, and CD45 (R4) in the PE/Cy7 versus FITC plot (*see* Fig. 2d). Finally, select cells residing in Sca1 positive gate (R6) in the FSC-H versus APC plot for sorting and collection (Fig. 2e). For additional analysis of myogenic progenitors *see* **Note 8**.

3.3 Cell Culture and (Brown) Adipogenic Differentiation of MusAPCs

1. Centrifuge the collected Sca1 positive progenitor cells at 4 °C and 50 × *g* for 5 min. Resuspend in an appropriate volume of growth medium to plate approximately 50,000 cells per well on coated 24-well cell culture plates. Wash the tube with growth medium to collect and plate residual cells. Important: Use growth medium supplemented with 50 µg/mL gentamycin to prevent bacterial contamination.
2. After 2 days, add fresh growth medium without gentamycin.
3. Expand cells until they reach 90–95 % confluence. This should take approximately 1 week.
4. For adipogenic differentiation, seed cells into Matrigel-coated 48-well plates and leave to adhere overnight (15,000 cells per well in a 48-well plate).
5. Pretreatment with bone morphogenic protein 7 (BMP7) can be used to induce brown adipogenesis and UCP1 expression in the mature adipocytes [6]. Seeding 15,000–20,000 cells will allow the cells to reach confluence within a 72 h treatment with BMP7. The pretreatment with 3.3 nM BMP7 is for 72 h in basal growth medium with growths factors (termed as day 3 of the time course of differentiation; Fig. 3). BMP7 does not need to be replaced during this period (*see* **Note 14**).
6. For adipogenic induction, cells are treated with adipogenic induction medium without growth factors (Table 3) for 48 h followed by differentiation in growth medium without growth

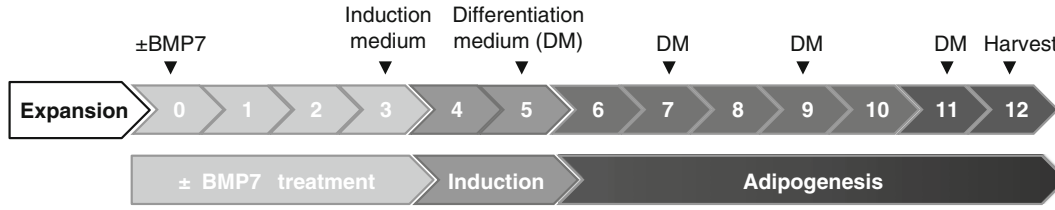

Fig. 3 Time course of adipogenic differentiation of MusAPCs. After expansion of purified MusAPCs, cells are seeded into Matrigel-coated 48-well plates and left to adhere overnight. Before starting the differentiation procedure, a BMP7 pretreatment is performed for 72 h. Start adipogenic differentiation after removal of BMP7 and by treating the cells with adipogenic induction medium for 48 h. On day 5, cells are treated with differentiation medium and re-fed fresh medium containing only insulin and T3 every other day until they are differentiated into mature adipocytes (usually on day 12)

factors, but addition of T3 and insulin only for 7 days (Fig. 3). Cells are re-fed fresh medium every other day until cells are differentiated into mature adipocytes (*see* **Note 15**).

7. To harvest cells for gene expression analysis of brown adipogenic markers, add 0.5 mL Trizol reagent or similar to lyse cells. Pipette up and down several times to fully lyse cells before transferring liquid to reaction tubes.

3.4 Cell Culture and Implantation of Brown Adipogenic Progenitors (See Note 16)

1. Grow and pretreat MusAPCs with BMP7 as described. Harvest cells after a 72 h exposure to 3.3 nM BMP7 by trypsinizing. Be sure not to over-trypsinize since the cells detach very quickly.
2. Count and spin down the cells for resuspension in an appropriate volume of F-10 medium with 2 % Matrigel. Resuspend to a final concentration of one million cells per 25 μL injection volume.
3. Inject cells using a cooled 25 μL Hamilton syringe into gastrocnemius muscle after removing fur from the lower hind legs, or the subcutaneous or epididymal fat pads. While the muscle can be easily reached by intramuscular injections, injection into the fat pad requires a surgical procedure to either depot.
4. Sacrifice animals 10 days after implantation for monitoring engraftment of cells. GFP^+ cells can be identified under a fluorescence microscope prior to embedding for further analysis of the implanted cells.

4 Notes

1. An appropriate collagenase batch has to be determined in pilot studies. Usually, a higher enzyme activity leads to better dissociation of the tissue. However, a lower viability could be an adverse side effect.
2. Use no less than 10 mL of digestion buffer per animal. A lower volume will negatively affect cell viability.
3. To culture MusAPCs, it is recommended to use coated cell culture dishes. To avoid uneven coating by polymerization, keep Matrigel at 4 °C all the time and work quickly as pure Matrigel solidifies at room temperature. It should be kept on ice until diluted in cold media. The ready-to-use Matrigel solution in F-10 can be used for up to 2 weeks if kept cold and sterile. Only discard aliquots that have been used for coating.
4. Less time-consuming protocols for muscle cell isolation performing only one enzymatic digestion have been reported [9, 21, 22]. In previous tests of different methods, one step digestion results in muscle digests containing much more debris and a significantly lower yield of adipogenic progenitors.
5. Be careful not to destroy the muscle pieces, as this will result in loss of intact fibers.

6. Make sure the opening is not too wide in order to generate some mechanical strain while pipetting up and down. This will help to break open the predigested muscle pieces to release individual fibers.
7. Do not touch the fiber pellet as it is only lightly packed.
8. Including additional surface markers in the FACS analysis enables the prospective purification of multiple muscle cell populations, for instance endothelial cells ($CD31^+/Sca1^+/CD45^-$) [22]. Moreover, several protocols for the isolation of satellite cells by FACS with distinct marker configurations have been published. Specifically, satellite cells could be identified by expression of Integrin β1 (CD29) and CXCR4 (C-X-C chemokine receptor type 4; CD184) [7, 19]. Similarly, the selection of Integrin $\alpha7^+/CD34^+$ double positive cells and negative selection for CD45, CD31, CD11b, and Sca1 has been shown before [23]. We successfully incorporated the isolation of myogenic progenitors (Integrin $\beta1^+/Sca1^-/CD11b^-/CD45^-/CD31^-$) in a complex gating strategy (Fig. 2). In the FSC-H versus APC plot, gate for $Sca1^-$, $lineage^-$ (Lin^-) cells (R5, Fig. 2d). Myogenic progenitors are further enriched by gating for Integrin ß1 positive population (R7, *see* Fig. 2f). To discriminate satellite cells more rigorously, specific markers have to be included, like abovementioned CXCR4 [24], CD34 [25], or Integrin α7 [26].
9. The staining controls described here are sufficient for a setup for most FACS-instrument brands.
10. Contrary to calcein, it is not necessary to compensate for propidium iodide as PI^+/dead cells are excluded in the subsequent gating strategy (Fig. 2c).
11. Prior to use in a FACS experiment, the antibody concentrations need to be optimized by titration to avoid unspecific binding (false positive signals). To ensure reliable FACS data acquisition, perform a titration with each antibody lot. Titration protocols have been described elsewhere [27].
12. Keep all the samples on ice and in the dark until FACS analysis is carried out. Vortex and filter all samples before analysis.
13. The strategy for color compensations and subsequent setups strongly depends on the instrument and should be performed by experienced personnel.
14. Other reagents that promote browning of adipogenic cells have been described in the literature and may do so in MusAPCs as well. Typical inducers are Rosiglitazone [28], Irisin [29], or FGF21 [30]. The efficiency of browning through these factors would have to be determined. Our studies indicate that a pretreatment with BMP7 is critical for induction of brown adipogenesis, whereas a full-time exposure to BMP7 throughout differentiation may not promote brown adipogenesis as

efficiently. Our findings suggest that BMP7 indeed acts as a lineage commitment factor that switches an adipogenic cell between a white adipocyte differentiation program and a brown adipocyte-like differentiation program.

15. Importantly, and depending on the mouse strain used, the cells will not normally express high levels of brown adipocyte markers without an inductive cue, such as BMP7. Moreover, high levels of brown adipogenesis are strongly dependent on differentiation time and serum batch. In order to achieve high level of brown adipocyte-marker expression, several batches of FBS may need to be tested. We typically obtain induction of UCP1 expression after pretreatment with BMP7 ranging from 10- to 30-fold.
16. MusAPCs can be transplanted into skeletal muscle or adipose tissue of recipient mice. We typically use cells pretreated with BMP7 to achieve good implantation and subsequent differentiation into adipocytes. To allow identification of the engrafted cells after implantation, we suggest using cells from GFP-transgenic animals or a similar genetic intervention that permanently labels the donor cells. Our studies show that implanted cells do not survive prolonged periods of time in healthy, immunocompetent mice, which is consistent with previous reports showing that adipogenic progenitors expressing our described set of markers do not persist in normal mice, likely due to the presence of a large population of competing adipogenic progenitors already present within the host [31].

Acknowledgments

This work was supported by grants from the German Research Foundation (DFG; grant # SCHU 2445/2-1) and the European Research Council (grant # ERC-StG-2012-311082) to TJS.

References

1. Mauro A (1961) Satellite cell of skeletal muscle fibers. J Biophys Biochem Cytol 9:493–495
2. Hawke TJ, Garry DJ (2001) Myogenic satellite cells: physiology to molecular biology. J Appl Physiol 91:534–551
3. Zammit PS, Partridge TA, Yablonka-Reuveni Z (2006) The skeletal muscle satellite cell: the stem cell that came in from the cold. J Histochem Cytochem 54:1177–1191
4. Uezumi A, Fukada S, Yamamoto N et al (2010) Mesenchymal progenitors distinct from satellite cells contribute to ectopic fat cell formation in skeletal muscle. Nat Cell Biol 12:143–152
5. Joe AWB, Yi L, Natarajan A et al (2010) Muscle injury activates resident fibro/adipogenic progenitors that facilitate myogenesis. Nat Cell Biol 12:153-U144
6. Schulz TJ, Huang TL, Tran TT et al (2011) Identification of inducible brown adipocyte progenitors residing in skeletal muscle and white fat. Proc Natl Acad Sci U S A 108:143–148
7. Cerletti M, Jurga S, Witczak CA et al (2008) Highly efficient, functional engraftment of

skeletal muscle stem cells in dystrophic muscles. Cell 134:37–47
8. Heredia JE, Mukundan L, Chen FM et al (2013) Type 2 innate signals stimulate fibro/adipogenic progenitors to facilitate muscle regeneration. Cell 153:376–388
9. Mozzetta C, Consalvi S, Saccone V et al (2013) Fibroadipogenic progenitors mediate the ability of HDAC inhibitors to promote regeneration in dystrophic muscles of young, but not old Mdx mice. EMBO Mol Med 5:626–639
10. Almind K, Manieri M, Sivitz WI et al (2007) Ectopic brown adipose tissue in muscle provides a mechanism for differences in risk of metabolic syndrome in mice. Proc Natl Acad Sci U S A 104:2366–2371
11. Qu Z, Balkir L, van Deutekom JC et al (1998) Development of approaches to improve cell survival in myoblast transfer therapy. J Cell Biol 142:1257–1267
12. Rando TA, Blau HM (1994) Primary mouse myoblast purification, characterization, and transplantation for cell-mediated gene therapy. J Cell Biol 125:1275–1287
13. Richler C, Yaffe D (1970) The in vitro cultivation and differentiation capacities of myogenic cell lines. Dev Biol 23:1–22
14. Arsic N, Mamaeva D, Lamb NJ et al (2008) Muscle-derived stem cells isolated as nonadherent population give rise to cardiac, skeletal muscle and neural lineages. Exp Cell Res 314:1266–1280
15. Qu-Petersen ZQ, Deasy B, Jankowski R et al (2002) Identification of a novel population of muscle stem cells in mice: potential for muscle regeneration. J Cell Biol 157:851–864
16. Gharaibeh B, Lu A, Tebbets J et al (2008) Isolation of a slowly adhering cell fraction containing stem cells from murine skeletal muscle by the preplate technique. Nat Protoc 3:1501–1509
17. Jankowski RJ, Haluszczak C, Trucco M et al (2001) Flow cytometric characterization of myogenic cell populations obtained via the preplate technique: potential for rapid isolation of muscle-derived stem cells. Hum Gene Ther 12:619–628
18. Conboy IM, Conboy MJ, Smythe GM et al (2003) Notch-mediated restoration of regenerative potential to aged muscle. Science 302:1575–1577
19. Sherwood RI, Christensen JL, Conboy IM et al (2004) Isolation of adult mouse myogenic progenitors: functional heterogeneity of cells within and engrafting skeletal muscle. Cell 119:543–554
20. Steenhuis P, Pettway GJ, Ignelzi MA Jr (2008) Cell surface expression of stem cell antigen-1 (Sca-1) distinguishes osteo-, chondro-, and adipoprogenitors in fetal mouse calvaria. Calcif Tissue Int 82:44–56
21. Pisani DF, Clement N, Loubat A et al (2010) Hierarchization of myogenic and adipogenic progenitors within human skeletal muscle. Stem Cells 28:2182–2194
22. Ieronimakis N, Balasundaram G, Reyes M (2008) Direct isolation, culture and transplant of mouse skeletal muscle derived endothelial cells with angiogenic potential. PLoS One 3. doi:10.1371/journal.pone.0001753
23. Pasut A, Oleynik P, Rudnicki MA (2012) Isolation of muscle stem cells by fluorescence activated cell sorting cytometry. Methods Mol Biol 798:53–64
24. Ratajczak MZ, Majka M, Kucia M et al (2003) Expression of functional CXCR4 by muscle satellite cells and secretion of SDF-1 by muscle-derived fibroblasts is associated with the presence of both muscle progenitors in bone marrow and hematopoietic stem/progenitor cells in muscles. Stem Cells 21:363–371
25. Beauchamp JR, Heslop L, Yu DS et al (2000) Expression of CD34 and Myf5 defines the majority of quiescent adult skeletal muscle satellite cells. J Cell Biol 151:1221–1234
26. Blanco-Bose WE, Yao CC, Kramer RH et al (2001) Purification of mouse primary myoblasts based on alpha 7 integrin expression. Exp Cell Res 265:212–220
27. Hulspas R (2010) Titration of fluorochrome-conjugated antibodies for labeling cell surface markers on live cells. Curr Protoc Cytom 54:6.29.1–6.29.9
28. Petrovic N, Walden TB, Shabalina IG et al (2010) Chronic peroxisome proliferator-activated receptor gamma (PPAR gamma) activation of epididymally derived white adipocyte cultures reveals a population of thermogenically competent, UCP1-containing adipocytes molecularly distinct from classic brown adipocytes. J Biol Chem 285:7153–7164
29. Bostrom P, Wu J, Jedrychowski MP et al (2012) A PGC1-alpha-dependent myokine that drives brown-fat-like development of white fat and thermogenesis. Nature 481:463–468
30. Fisher FM, Kleiner S, Douris N et al (2012) FGF21 regulates PGC-1alpha and browning of white adipose tissues in adaptive thermogenesis. Genes Dev 26:271–281
31. Rodeheffer MS, Birsoy K, Friedman JM (2008) Identification of white adipocyte progenitor cells in vivo. Cell 135:240–249

Chapter 20

Skeletal Muscle Stem Cells for Muscle Regeneration

Johnny Kim and Thomas Braun

Abstract

Adult skeletal muscle possesses remarkable regenerative capacity. Muscle regeneration is mediated by a rare population of muscle stem cells that reside between the basal lamina and sarcolemma of muscle fibers. Due to their anatomical location, muscle stem cells have been coined satellite cells. Here, we describe a method that we routinely use to isolate large and pure populations of satellite cells from skeletal muscles enabling studies on autonomous properties of satellite cells to unravel the role of muscle stem cells in tissue regeneration.

Key words Muscle stem cells, Satellite cells, Pax7, FAC sorting

1 Introduction

Stem cells have profound regenerative capacity because they retain the ability to self-renew and can differentiate into specialized cell types. Skeletal muscle contains a rare population of muscle-specific stem cells called satellite cells [1, 2]. At the molecular level, undifferentiated satellite cells can be robustly identified by the combinatorial exclusion of the hematopoietic lineage markers CD45, Cd11b, and Sca1 and expression of distinct cell surface markers including CD34, m-Cadherin, CXCR4, and α-integrin7 [3–5]. Alternatively, expression of the transcription factor Pax7 is sufficient to unambiguously identify satellite cells in skeletal muscles (Fig. 1) [5–7]. Based on the expression of such markers, we and others have devised techniques that enable isolation of large and highly purified populations of primary muscle satellite cells via FACS from freshly dissociated skeletal muscle tissue [1, 4–6, 8–10]. Importantly, these isolated muscle stem cells express Pax7 and exhibit efficient self-renewal and myogenic differentiation at the single cell level, and do not differentiate into other cell types (Fig. 2). When injected into muscle, freshly isolated Pax7 expressing satellite cells can graft, and repopulate the muscle stem cell pool thus functionally rescuing dystrophic muscle tissue [3].

Bruno Christ et al. (eds.), *Animal Models for Stem Cell Therapy*, Methods in Molecular Biology, vol. 1213,
DOI 10.1007/978-1-4939-1453-1_20,

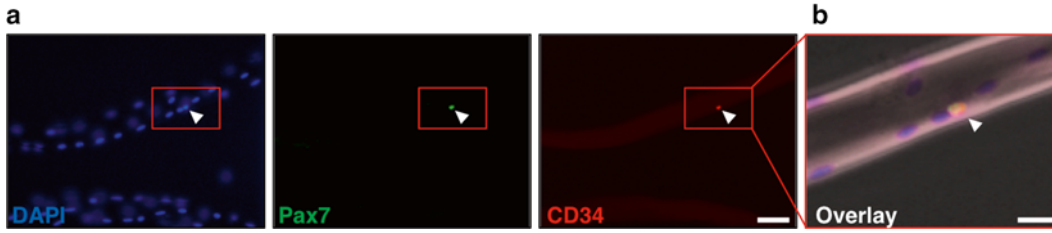

Fig. 1 Immunofluorescent stain of a satellite cell on an isolated myofiber. Satellite cells reside on top of myofibers and express the transcription factor Pax7 and cell surface marker CD34 (**a**, **b**). Scale bars in (**a**, **b**) are 50 and 5 μm, respectively

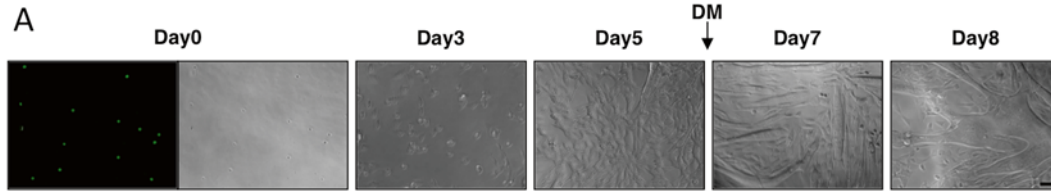

Fig. 2 Culture of primary satellite cells. (**a**) FACS-purified satellite cells from Pax7::ZsGreen reporter mice. On day 5, when the cells have proliferated to confluency, they can be efficiently induced to terminally differentiate upon mitogen depletion into multinucleated myotubes (*DM* differentiation medium. Scale bar = 5 μm)

In contrast, more differentiated myoblasts that do not express Pax7 graft very poorly. Several studies in aged mice indicate a substantial reduction in the overall frequency of myogenic stem cells, and a profound impairment in their functional activity. In addition, it has been suggested that loss of muscle stem cell activity leads to deficient muscle repair not only under pathological conditions such as muscular dystrophy but also in old age [1]. Therefore, strategies to expand muscle stem cells or to restore their function would have a significant benefit for muscle regeneration. Indeed, recent studies suggest that muscle stem cell "rejuvenating" factors exist including Notch, Wnt, or epigenetic modifiers [11–13], reviewed in [14]. It seems likely that many more factors exist orchestrating self-renewal and differentiation of muscle stem cells, which might be identified by functional screening approaches.

With the advent of very sensitive detection methods such as RNAseq or high-resolution mass spectrometry it is now possible to profile expression patterns of self-renewing and differentiating satellite cells at both the transcriptional and translational level, respectively. Likewise, high-throughput technologies such as image-based high-content RNAi or compound screening provide means to identify genes or compounds that may significantly enhance the regenerative capacity of isolated muscle stem cells. Essentially, such

methods allow identification of new factors that regulate muscle stem cell properties provided that sufficient amounts of material can be obtained. Here, we describe a method to isolate a large and pure population of muscle stem cells using transgenic Pax7 reporter mice and FAC sorting. This approach yields sufficient amounts of pure muscle stem cells enabling to investigate autonomous properties of muscle stem cells without contaminating cell types at the cellular and molecular level.

2 Materials

2.1 Satellite Cell Isolation and Culture

1. Dissecting forceps heavy, rounder points with corrugated tips.
2. Dissecting forceps, fine point.
3. Dissecting scissors.
4. 1× phosphate-buffered saline (PBS) without magnesium and calcium.
5. Dulbecco's modified Eagle Medium (DMEM), supplement with penicillin-streptomycin (DMEM/PS).
6. Dispase solution (BD).
7. Collagenase type II (Worthington Biochemicals).
8. 100, 70, and 40 μm cell strainers.
9. Red Blood Cell Lysis Buffer: 0.16 M NH_4Cl, 1 M $KHCO_3$, 0.2 mM EDTA, adjust pH to 7.35 with 0.1 N NaOH, 0.2 μm filter sterilize, store at 4 °C.
10. Cell Sorting Buffer: 1× PBS, 1 mM EDTA, 25 mM HEPES, adjust pH to 7.0, 2 % Fetal bovine serum (FBS), heat-inactivated, 0.2 μm filter sterilize, store a 4 °C.
11. DNase solution: Prepare stock solution of 100 U/mL in 1× PBS.
12. Growth medium: DMEM-Glutamax-I, 20 % FBS, supplement with penicillin-streptomycin, basic fibroblast growth factor (bFGF; 5 ng/mL).
13. Matrigel, growth factor-reduced.

2.2 Discontinuous Percoll Gradient

1. Percoll.
2. 1× PBS without magnesium and calcium.
3. 10× PBS without magnesium and calcium.
4. 15 mL conical tube.
5. 5 mL syringe.

3 Methods

3.1 Isolation of a Heterogeneous Skeletal Muscle-Derived Cell Population

1. Excise skeletal muscle from 8 weeks old mice and place into a 50 mL conical tube containing DMEM/PS using dissecting forceps and scissors. Place on ice (*see* **Note 1**).
2. Wash the muscle pieces with DMEM/PS to remove excess fat and red blood cells. Centrifuge the muscle briefly for 30 s at 1,200 × *g* and pour off the supernatant. Repeat this step three times and discard the supernatant (*see* **Note 2**).
3. Thoroughly mince the muscle in a minimal amount of DMEM/PS to obtain a fine slurry and subsequently transfer the minced muscle to a fresh 50 mL conical tube (*see* **Note 3**).
4. Wash the minced muscle. Centrifuge for 30 s at 1,200 × *g* and pour off the supernatant. Do this several times until the supernatant becomes clear.
5. Add 18 mL DMEM/PS and 2 mL dispase per conical tube. Incubate in a circulating water bath at 37 °C for 30 min. Occasionally mix by vortexing. Additionally, triturate the suspension with a 10 mL pipette or a 30 mL syringe several times (*see* **Note 4**).
6. After initial dispase digestion, add 5 mL of 0.4 % [w/v] type II collagenase to the tube. Mix well and incubate the mixture for additional 30 min in a circulating water bath at 37 °C. Occasionally mix by vortexing. Additionally, triturate the suspension with a 10 mL pipette or a 30 mL syringe several times (*see* **Note 4**).
7. Add 1 mL of FBS to inactivate the dispase/collagenase. Incubate for 1 min at room temperature.
8. Fill the conical tube to the brim with DMEM/PS and centrifuge for 30 s at 500 × *g* (*see* **Note 5**).
9. Pour the supernatant containing cells consecutively over filters of descending pore sizes (100, 70, 40 μm) into 50 mL Falcon tubes. You will need four 50 mL conical tubes per sample.
10. Collect cells by centrifugation at 1,200 × *g* for 10 min. Discard supernatant.
11. Prepare a fresh solution of red blood cell lysis buffer with DNase: add 50 μL of DNase solution per 10 mL red blood cell lysis buffer.
12. Gently resuspend the pellet in a total amount of 3 mL red blood cell lysis buffer with DNase via pipetting up and down and incubate the cell suspension on ice for 3 min.
13. Fill to 6 mL with cell sorting buffer and store cell suspension on ice.

3.2 Enrichment of Satellite Cells

1. Prepare a 90 % Percoll solution by diluting nine parts Percoll with one part 10× PBS. Next, prepare 70 and 30 % Percoll solutions by diluting the 90 % Percoll solution with 1× PBS to the appropriate concentration. Gently underlay 6 mL of 30 % Percoll with 3 mL 70 % Percoll in a 15 mL conical tube with a 5 mL syringe that fits into the 15 mL conical tube mounted with a 21 G needle (*see* **Note 6**).
2. Gently overlay the 6 mL of cell suspension from Subheading 3.1, **step 13** on top of the Percoll gradient using a 2 or 5 mL pipette. For this step gently dip the tip of the pipette into the 30 % phase and pull out the tip along the wall of the conical tube. This will create an attached line of fluid, which can be gently pipetted on top of the 30 % phase together with the cell suspension. We typically employ a pipette boy adjusted to the slowest dispense speed (*see* **Note 7**).
3. Centrifuge the gradient at 1,200 × *g* for 20 min with acceleration and break turned off and set to 4 °C.
4. Isolate cells from the 70/30 interface in a minimal volume (use 1 mL pipette) and transfer to freshly pre-coated FACS tube and fill to the brim with cell sorting buffer (*see* **Note 8**).
5. Perform FAC sorting of Percoll pre-purified cells (*see* **Note 9**).

3.3 Culturing of FACS-Purified Satellite Cells

1. The day before satellite cell isolation, thaw the appropriate amount of Matrigel on ice overnight. Matrigel is liquid at 0–15 °C, but will form a gel at higher temperatures.
2. Dilute Matrigel 1:50 with ice cold growth medium and pre-coat cell culture dishes of your desired format with a volume so that the surface is just covered. Incubate at room temperature for 1 h. It is not necessary to aspirate the residual solution after coating the cell culture dish.
3. Subsequently, incubate plates at 37 °C in a humidified incubator until cells are ready to be plated.
4. After sorting, directly resuspend cells in the desired volume of growth medium and plate onto desired cell culture dishes (*see* **Note 10**).

4 Notes

1. Isolation of satellite cells from younger animals typically results in higher yields. Typically, we isolate satellite cells from 8 weeks old mice. The use of female animals also results in a higher yield relative to male animals. This yield difference is most likely due to the fact that female muscles are less fibrous and therefore more easily minced and digested compared to male muscles.

2. It is recommended to remove any fat, bones, tendons, and fascia under a dissecting microscope as thoroughly and reasonably as possible, since the removal of these structures will enhance the yield and facilitate subsequent steps of the isolation procedure. We also employ washing steps prior to enzymatic digestion to remove excess blood and to equilibrate the minced muscle in isotonic medium since destruction of fibers will release calcium from the sarcoplasmic reticulum and cytoplasm.
3. It is critical that the muscle is thoroughly minced. Extensive mincing gives the digestive enzymes a larger surface area and facilitates digestion. Therefore, it is important to spend a decent amount of time on this step. We employ a tissue chopper (McIwain Tissue Chopper, H-Saur, Reutlingen, Germany); however alternatively, one can use a pair of curved mincing scissors and forceps.
4. A thorough digestion is the key to a good yield. Therefore, the suspension should be vortexed every 10 min during the enzymatic incubation. The addition of Collagenase type II after the initial dispase digestion boosts the digestion dramatically. Use only freshly prepared dispase and collagenase solutions.
5. After the enzymatic digestion it is critical to centrifuge the sample only very briefly. The trick here is to get rid of most of the large particles that would clog the nylon filters. The bulk debris will be at the bottom of the tube while mononuclear cells are still in suspension. This centrifugation step facilitates passage of the sample through the nylon filters. After this step there will be a very thin layer of fat on top. Eventually, one will also see residual tendons or fibrous tissue floating on the surface of the supernatant, which should be removed carefully with a pipette.
6. Underlaying the 30 % Percoll phase with the 70 % Percoll phase will require some practice. We prefer this approach over overlaying the 70 % phase with the 30 % phase because this results in a sharp "cut-off" between the two phases. As such, the collection volume of the desired cells will be minimal.
7. Do not overlay more than two animals worth of muscle-derived cell suspension per Percoll gradient. If the starting sample is too dense the separation will not be efficient as the separation resolution of the gradient becomes over-capacitated. In fact, if maximum yield is desired, we distribute the sample over two Percoll gradients.
8. Pre-coating means to fill the tube with the cell sorting buffer and emptying it before transferring the cell suspension to the tube. Satellite cells are inherently "sticky." Hence, to avoid cell loss, any plastic (e.g., tips, tubes) that potentially comes into immediate contact with the cells should be pre-coated.

We set aside a 15 mL Falcon tube filled with cell sorting buffer to pre-coat tips whenever necessary.

9. The usage of a discontinuous Percoll gradient enables the isolation of a heterogeneous cell population that is well suited for antibody staining and FAC sorting. This prepurification step gets rid of debris and dead cells in one step. In addition, the sample volume is greatly reduced and hence dramatically decreases the time needed for sorting. Most often, we employ genetically labeled cells [6] to isolate satellite cells. In this case, the pre-purified cells from the Percoll gradient can be immediately FAC sorted without the need for antibody staining which results in relatively large yields. From Pax7::ZsGreen reporter mice [6], 10–15 % the cells of the Percoll pre-purified sample are satellite cells based on ZsGreen expression and we typically isolate 300k–500k satellite cells per 8 weeks old mouse. In contrast, only 0.86 % of the input sample are positive for ZsGreen without a Percoll prepurification [6]. If antibody staining is necessary, several washing steps will be required and one can expect a 10–20 % loss of cells per washing step. In our hands, we typically isolate 100k–200k cells from wild-type mice when using antibodies for sorting. A detailed protocol for antibody-based sorting has been described [15]. In Fig. 3 the FACS-gating procedure that we typically employ using genetically labeled satellite cells is depicted. This approach is not only

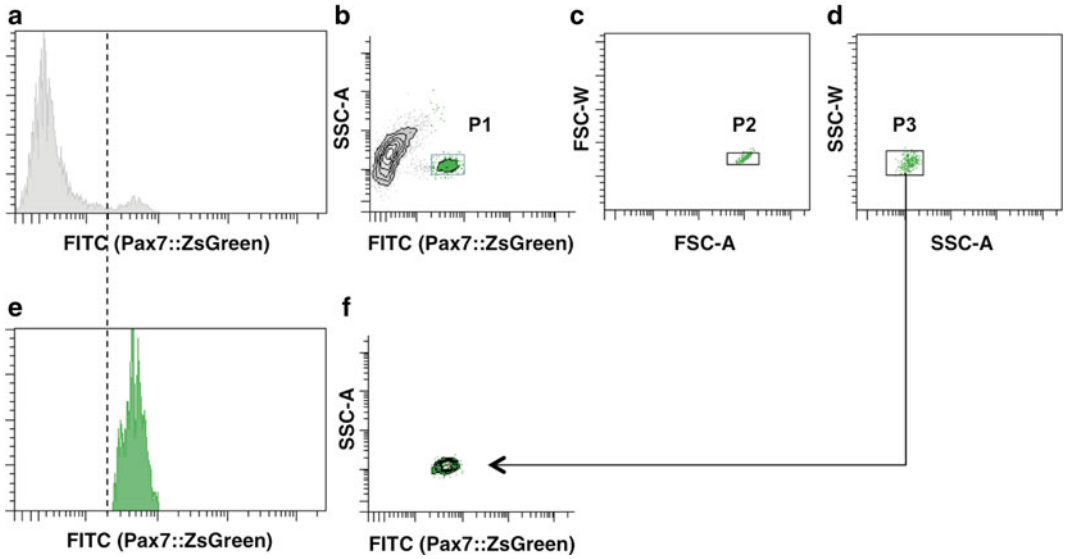

Fig. 3 Gating strategy for FAC sorting of ZsGreen labeled satellite cells. (*A*) Histogram of FITC fluorescence of all events of the input sample. (*B*) Density plot of the gated satellite cells that are low in granularity and ZsGreen positive (P1). P1 is further gated for doublet discrimination in forward and side scatter (P2 and P3, respectively) to obtain a pure population of satellite cells (*C*, *D*). (*E*, *F*) show the resulting population that is sorted after gating. *Dotted line* between (*A*) and (*E*) depicts purity of sorted Pax7::ZsGreen satellite cells

much simpler than antibody-based FAC sorting, but is more cost-effective, in particular when isolation of satellite cells is routinely required. We have successfully sorted satellite cells with a Beckman Coulter EPICS Altra FAC sorter and currently use a FACSAriaIII high-speed cell sorter equipped with an 85 or 100 μm nozzle. Of course, other high-speed cell sorters can be used as well.

10. When plating the cells onto Matrigel-coated dishes, prewarm the growth medium, in which the cells will be taken up. Do not use cold medium as this will resolubilize the Matrigel. In addition, for subsequent culturing of FAC sorted cells, do not wash cells as centrifugation of the cells will make the cells stick together.

Acknowledgements

We are indebted to Dr. Michael Kyba for contribution of the Pax7::ZsGreen mouse strain. This work was supported by the DFG (Excellence Cluster Cardio-Pulmonary System (ECCPS), Br1416, and SFB TR81), the German-Israeli Fund, the LOEWE Center for Cell and Gene Therapy, the German Center for Cardiovascular Research, and the Universities of Giessen and Marburg Lung Center (UGMLC).

References

1. Carlson ME, Suetta C, Conboy MJ, Aagaard P, Mackey A, Kjaer M, Conboy I (2009) Molecular aging and rejuvenation of human muscle stem cells. EMBO Mol Med 1:381–391
2. Braun T, Gautel M (2011) Transcriptional mechanisms regulating skeletal muscle differentiation, growth and homeostasis. Nat Rev Mol Cell Biol 12:349–361
3. Cerletti M, Jurga S, Witczak CA, Hirshman MF, Shadrach JL, Goodyear LJ, Wagers AJ (2008) Highly efficient, functional engraftment of skeletal muscle stem cells in dystrophic muscles. Cell 134:37–47
4. Sacco A, Doyonnas R, Kraft P, Vitorovic S, Blau HM (2008) Self-renewal and expansion of single transplanted muscle stem cells. Nature 456:502–506
5. Günther S, Kim J, Kostin S, Lepper C, Fan C-M, Braun T (2013) Myf5-positive satellite cells contribute to Pax7-dependent long-term maintenance of adult muscle stem cells. Cell Stem Cell 13:590–601
6. Bosnakovski D, Xu Z, Li W, Thet S, Cleaver O, Perlingeiro RC, Kyba M (2008) Prospective isolation of skeletal muscle stem cells with a Pax7 reporter. Stem Cells 26:3194–3204
7. Seale P, Sabourin LA, Girgis-Gabardo A, Mansouri A, Gruss P, Rudnicki MA (2000) Pax7 is required for the specification of myogenic satellite cells. Cell 102:777–786
8. Montarras D, Morgan J, Collins C, Relaix F, Zaffran S, Cumano A, Partridge T, Buckingham M (2005) Direct isolation of satellite cells for skeletal muscle regeneration. Science 309:2064–2067
9. Sherwood RI, Christensen JL, Conboy IM, Conboy MJ, Rando TA, Weissman IL, Wagers AJ (2004) Isolation of adult mouse myogenic progenitors: functional heterogeneity of cells within and engrafting skeletal muscle. Cell 119:543–554
10. Conboy MJ, Conboy IM (2010) Preparation of adult muscle fiber-associated stem/precursor cells. Methods Mol Biol 621:149–163

11. Carlson ME, Conboy MJ, Hsu M, Barchas L, Jeong J, Agrawal A, Mikels AJ, Agrawal S, Schaffer DV, Conboy IM (2009) Relative roles of TGF-beta1 and Wnt in the systemic regulation and aging of satellite cell responses. Aging Cell 8:676–689
12. Conboy IM, Conboy MJ, Smythe GM, Rando TA (2003) Notch-mediated restoration of regenerative potential to aged muscle. Science 302:1575–1577
13. Liu L, Cheung TH, Charville GW, Hurgo BM, Leavitt T, Shih J, Brunet A, Rando TA (2013) Chromatin modifications as determinants of muscle stem cell quiescence and chronological aging. Cell Reports 4: 189–204
14. Rando TA, Chang HY (2012) Aging, rejuvenation, and epigenetic reprogramming: resetting the aging clock. Cell 148:46–57
15. Conboy MJ, Cerletti M, Wagers AJ, Conboy IM (2010) Immuno-analysis and FACS sorting of adult muscle fiber-associated stem/precursor cells. Methods Mol Biol 621: 165–173

Part V

Neurological Diseases

Chapter 21

Bone Marrow Stromal Stem Cells Transplantation in Mice with Acute Spinal Cord Injury

Virginie Neirinckx, Bernard Rogister, Rachelle Franzen, and Sabine Wislet-Gendebien

Abstract

Spinal cord injured experimental animals are widely used for studying pathophysiological processes after central nervous system acute traumatic lesion and elaborating therapeutic solutions, some of them based on stem cell transplantation. Here, we describe a protocol of spinal cord contusion in C57BL/6J mice, directly followed by bone marrow stromal stem cells transplantation. This model allows for the characterization of neuroprotective and neurorestorative abilities of these stem cells in a context of spinal cord trauma.

Key words Spinal cord contusion, Impactor, Bone marrow stromal stem cells

1 Introduction

The global incidence of traumatic spinal cord injuries was estimated in 2007 at ~23 cases per million worldwide, as stipulated by the last report of Lee et al. published in 2013 [1, 2]. In the last decade, although numerous reports have shown significant improvements in medical management and clinical recuperation after spinal cord injury (SCI), etc. (e.g., methylprednisolone treatment [3]), there is still no effective surgical and/or medical treatment that completely allows functional recovery.

Mesenchymal stem cells (MSCs) in the adult bone marrow stroma (bone marrow stromal cells, BMSCs) were first identified in the late 1970s by Friedenstein et al. [4, 5] as colony-forming unit fibroblast-like cells. Those mesoderm-derived cells were subsequently described to be self-renewable and highly multipotent, giving rise to different cells of mesodermal origin such as adipocytes, chondrocytes, and osteocytes [6, 7]. In the following years, MSCs were isolated from other adult tissues (fat tissue [8], muscle [9], synovium [10], peripheral blood and circulatory system [11], etc.), where they contribute and regulate organ physiology and homeostasis.

Bruno Christ et al. (eds.), *Animal Models for Stem Cell Therapy*, Methods in Molecular Biology, vol. 1213,
DOI 10.1007/978-1-4939-1453-1_21,

BMSCs were especially considered for cell therapy in neurological lesions regarding their capacity to give rise to neural-like cells [12–14]. However, in vivo neural differentiation is currently a matter of debate and it seems that adult BMSCs would rather help lesion recovery through many other mechanisms than in-host differentiation [15, 16]. Indeed, those cells have anti-inflammatory and immunomodulatory effects and secrete several neurotrophic factors (reviewed in details by Uccelli et al. [17], Prockop et al. [18], and Singer and Caplan [19]), making them attractive candidates for SCI therapy.

Different animal models of SCI have been developed in order to study physiopathological events after trauma, and to set up cell-based therapies and pharmacological treatments [20, 21]. Among those models, the spinal cord contusion is one of the most relevant models, nicely mimicking the SCI pathology. Diverse recent reviews focus on different aspects of spinal cord injuries and on the way stem cells could help in such lesions (Neirinckx et al. [22]). A wide range of protocols can be followed in terms of lesion type, cell transplantation timing, route of administration, etc. In this chapter, we detail a protocol for acute spinal cord contusion in mice at low thoracic level, directly followed by an intraspinal bone marrow stem cell graft.

2 Materials

2.1 Mice

10- to 15-week old female C57Bl/6 J mice, body weight 20–30 g.

2.2 Anesthesia

1. Xylazine (Rompun®, Bayer).
2. Ketamine (Ketalar®, Pfizer).
3. 1 mL syringe coupled with 26 G needle.
4. Warming pad.
5. NaCl.

2.3 Surgical Material

1. Bone chisel.
2. Laminectomy forceps.
3. Scissors and miniscissors.
4. Graefe forceps.
5. Addson forceps.
6. Halsted-Mosquito Hemostat.
7. Coated Vicryl* Plus, Antibacterial (polyglactin 910) braided suture (Ethicon).

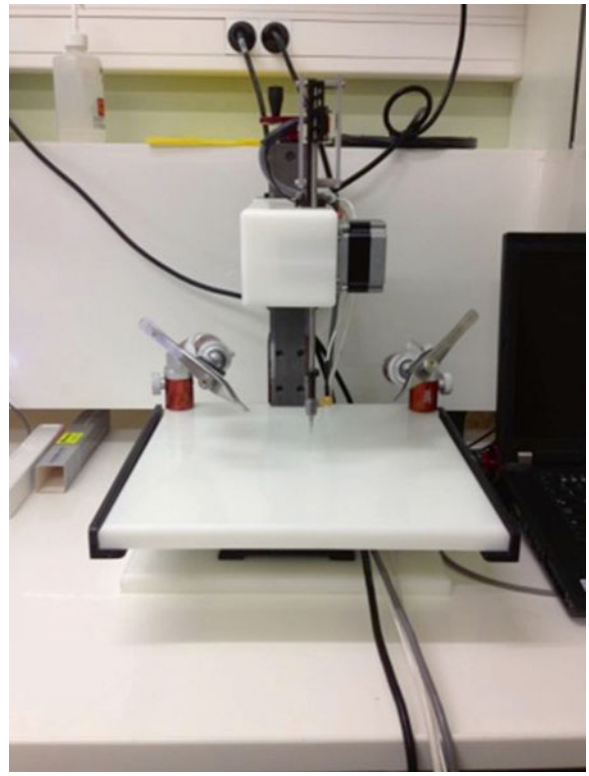

Fig. 1 Infinite Horizon [IH-0400] Impactor (Precision Systems and Instrumentations, LLC)

2.4 Spinal Cord Contusion

1. Infinite Horizon [IH-0400] Impactor (Precision Systems and Instrumentations, LLC) and software (Fig. 1).
2. Use mouse impact tip (1.3 mm).

2.5 Cell Culture

1. MesenCult Proliferation Kit (Stem Cell Technologies).
2. Phosphate-buffered saline (PBS) (GIBCO®, Life Technologies).
3. 0.05 % Trypsin-EDTA (1×), Phenol Red (GIBCO®, Life Technologies).
4. Thoma counting chamber and Trypan blue.
5. Standard material (Pipettes, micropipettes, tips, culture flasks, etc.).

2.6 Cell Transplantation

1. Hamilton syringe (5 μL, Model 75 RN SYR) coupled with a 33 G needle.
2. Stereotaxic frame.

2.7 Monitoring and Behavioral Scoring

Open field zone.

3 Methods

All culture experiments must be carried out under sterile conditions, under laminar flow hood, with totally sterile material.

Animals must be kept under normal day/night conditions, with ad libitum water and food. All procedures must be in accordance with the local ethical committee rules.

3.1 Bone Marrow Stromal Stem Cells Harvest and Culture

1. Euthanize mice by cervical dislocation.
2. Directly after death, dissect and harvest the left and right femurs. Clean the bones by scrubbing all muscle tissues.
3. Cut femurs in two mains pieces. Use a 5 mL syringe coupled with a 22 G needle (previously rinsed and partially filled with reconstituted MesenCult culture medium) to harvest bone marrow tissue. Enter the needle inside the bone, and aspirate bone marrow inside the syringe. Rinse the inside of the bone and then re-aspirate several times.
4. After dissociating tissue and homogenizing the cell suspension, place the collected bone marrow cells in reconstituted MesenCult culture medium.
5. Incubate cells under adherent conditions (in a plastic flask), at 37 °C, humidity atmosphere, 95 % air, 5 % CO_2 (Fig. 2).
6. After 24 h, remove the supernatant containing non-adherent hematopoietic cells. Rinse three times with warmed PBS and refill the flask with fresh reconstituted MesenCult medium.

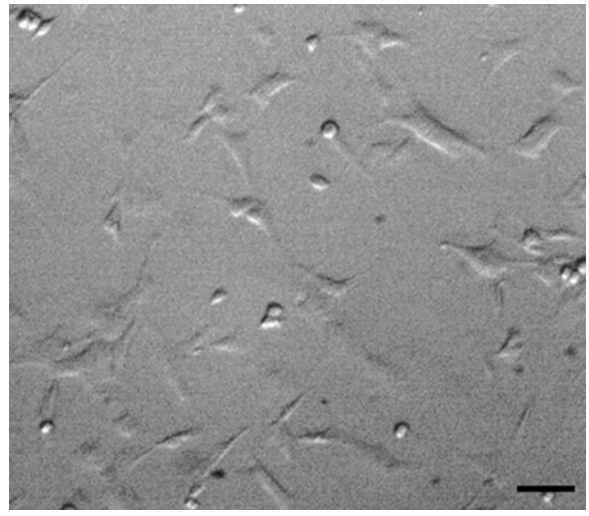

Fig. 2 Bone marrow stromal cells under adherent conditions (in a plastic flask), at 37 °C, humidity atmosphere, 95 % air, 5 % CO_2 (scale bar = 20 μm)

7. Let the cells proliferate until they reach 80 % confluence.
8. After PBS rinse and trypsin-EDTA incubation, subculture cells at a density of 5,000 cells/cm^2.

3.2 Anesthesia

1. Anesthetize mice with i.p. injection of a solution combining xylazine (Rompun®, 10 mg/kg) and ketamine (Ketalar®, 100 mg/kg).
2. Keep mice under warm light until they recover a regular heart rate, and check for the absence of hindlimb reflexes.

3.3 Dissection and Laminectomy

1. Once mice are deeply anesthetized, shave their backs and apply alcohol on the zone in order to get a sterile work area.
2. Place mice on a warming pad and stabilize them by sticking their four paws on the pad with light adhesive paper.
3. Cut back skin from the neck to the bottom using forceps and scissors, on approximately 2 cm. By maintaining the backbone with Addson forceps, separate skin from muscles, and dissect tissues to free the backbone and expose vertebrae (Fig. 3a).
4. Identify 13th thoracic vertebra (T13), from which spinous process is flatter, and which is associated with 13th floating rib (then slightly moving under a light pressure). With T13 as landmark, you can identify T12 just above.
5. Using laminectomy forceps, progressively break the top part of T12, while paying huge attention not causing damage to the spinal cord below. Free a sufficiently wide space (from left to right) to avoid the impact to be deviated by remaining bone pieces and ensure the rest of the procedure to be executed in the right conditions (Fig. 3b, c).

3.4 Spinal Cord Contusion

1. If possible, keep the mice attached on the warming pad and only displace it under the impactor.
2. Using the two Addson forceps present on the impactor, attach both the top and bottom of rachis, in order to rightly expose

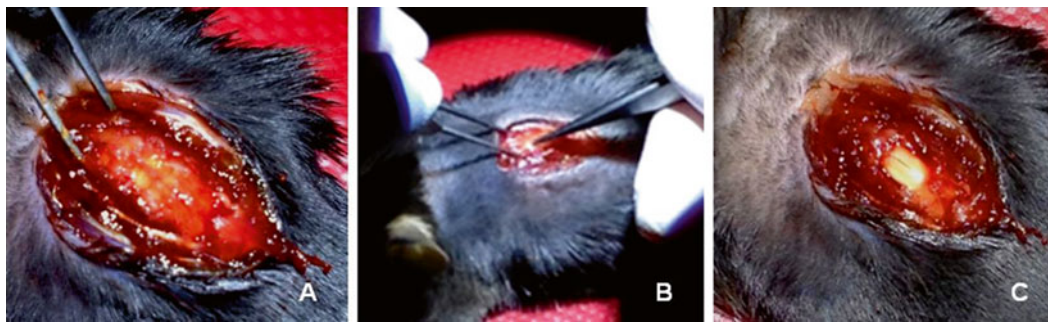

Fig. 3 Laminectomy procedure. (**a**) Free the backbone and expose vertebrae. (**b**) Identify T12 vertebrae and remove the upper part by laminectomy. (**c**) Expose the spinal cord segment

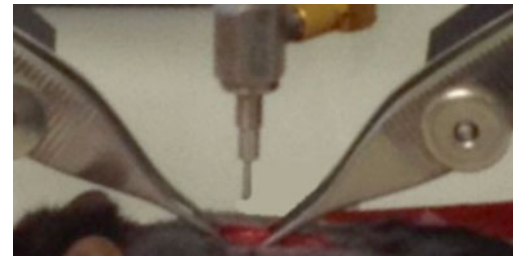

Fig. 4 Impact procedure

horizontally the nude spinal cord segment. Be careful not to stretch it or to damage it with the forceps (Fig. 4).

3. Use the *X* and *Z* axis to position the spinal cord segment under the impact tip.
4. Get the impact tip closest possible from the spinal cord using the Υ axis, without touching it properly. Afterwards, pull the tip up for desired height.
5. After defining the parameters of impact, concerning applied force or displacement, press the "Start the experiment" button (*see* **Note 1**).
6. After the impact is done, detach the forceps and remove the mice from the fixation plate.

3.5 Bone Marrow Stromal Stem Cells Transplantation

1. When bone marrow stromal stem cells have reached the desired confluence and number of passages, remove culture medium and rinse with PBS. Incubate cells with 0.05 % trypsin-EDTA.
2. Collect the cells in MesenCult culture medium, homogenize the cell suspension, and count the number of cells (using Thoma counting chamber and Trypan blue).
3. Centrifuge the cell suspension for 5 min at 200 × *g*.
4. After removing the supernatant, suspend the cell pellet in sterile PBS at a concentration of 10,000 cells/μL PBS (*see* **Note 2**).
5. Use a 5 μL Hamilton syringe (coupled with a 33 G needle) previously moistened with PBS, and aspirate 3 μL of the cell suspension (30,000 cells). Fix it on the arm of a stereotaxic apparatus.
6. After fixing the mice in the stereotaxic frame (coupled with spinal adaptor) and maintaining the backbone at the upper and lower part, insert the needle 0.5 mm deep inside the epicenter of the lesion.
7. Slowly inject 1 μL of the cell solution (10,000 cells). Leave the needle in place for some minutes before retracting it to avoid reflux along the injection track.

8. Displace the syringe 1 mm rostrally and repeat the injection of 10,000 cells.
9. Displace the syringe 2 mm caudally (1 mm from epicenter) and repeat the injection of 10,000 cells.
10. After injection, free the mice from stereotaxic apparatus.

3.6 End of the Surgery

1. Use Vicryl-Plus resorbable suture for suturing the muscle layer first, then the skin layer.
2. Inject sterile NaCl (around 10 mL/kg) subcutaneously (e.g., under head skin, between the ears) in order to compensate for blood loss and to prevent dehydration.
3. Detach mice from warming pad. Keep the mice under a warm lamp until their complete awakening.

3.7 Monitoring and Behavioral Scoring

1. Keep mice in individual cages. Watch if they have easy access to water and food (*see* **Note 3**).
2. During the next weeks after surgery, bladders of the mice have to be emptied manually twice a day until animals recover normal urinary function.
3. Monitor the weight of the mice every 2 days after the surgery.
4. At the first day following surgery (and at desired time points thereafter), place the mice in an open-field area for 4 min. Assign them a score according to the criteria of the Basso Mouse Scale [23].

4 Notes

1. Mice included in the SCI experiment should be of equal (or at least similar) weight, in order to minimize variability in the impact displacement. Indeed, it seems that weight is negatively correlated with impact displacement.
2. In order to minimize surgery time, the cell suspension that will be transplanted in the impacted spinal cord should be prepared just before spinal cord contusion procedure (or concomitantly by a second experimenter).
3. Before the experiment starts, mice should be accommodated in the environment at least a week before the surgery. For behavioral testing, place mice in the open field for 4 min twice a day, during a week before the surgery, then they could become familiar with the surroundings before being tested.

Acknowledgements

This work was supported by a grant from the Fonds National de la Recherche Scientifique (FNRS) of Belgium, by the Belgian League against Multiple Sclerosis associated with the Leon Frédericq Foundation, and by the Fonds Spéciaux à la Recherche of the University of Liège.

References

1. Lee BB et al (2014) The global map for traumatic spinal cord injury epidemiology: update 2011, global incidence rate. Spinal Cord (52):110–116
2. National Spinal Cord Injury Statistical Center (2012) Spinal cord injury: facts and figures at a glance. J Spinal Cord Med 35(6):480–481
3. Bracken MB (1990) Methylprednisolone in the management of acute spinal cord injuries. Med J Aust 153(6):368
4. Friedenstein AJ (1980) Stromal mechanisms of bone marrow: cloning in vitro and retransplantation in vivo. Haematol Blood Transfus 25: 19–29
5. Friedenstein AJ et al (1974) Precursors for fibroblasts in different populations of hematopoietic cells as detected by the in vitro colony assay method. Exp Hematol 2(2):83–92
6. Bianco P et al (2001) Bone marrow stromal stem cells: nature, biology, and potential applications. Stem Cells 19(3):180–192
7. Pittenger MF et al (1999) Multilineage potential of adult human mesenchymal stem cells. Science 284(5411):143–147
8. Zuk PA et al (2002) Human adipose tissue is a source of multipotent stem cells. Mol Biol Cell 13(12):4279–4295
9. Dellavalle A et al (2007) Pericytes of human skeletal muscle are myogenic precursors distinct from satellite cells. Nat Cell Biol 9(3): 255–267
10. Fan J et al (2009) Synovium-derived mesenchymal stem cells: a new cell source for musculoskeletal regeneration. Tissue Eng B Rev 15(1):75–86
11. Caplan AI, Correa D (2011) The MSC: an injury drugstore. Cell Stem Cell 9(1):11–15
12. Sanchez-Ramos J et al (2000) Adult bone marrow stromal cells differentiate into neural cells in vitro. Exp Neurol 164(2):247–256
13. Wislet-Gendebien S et al (2005) Plasticity of cultured mesenchymal stem cells: switch from nestin-positive to excitable neuron-like phenotype. Stem Cells 23(3):392–402
14. Morikawa S et al (2009) Development of mesenchymal stem cells partially originate from the neural crest. Biochem Biophys Res Commun 379(4):1114–1119
15. Prockop DJ, Oh JY (2012) Medical therapies with adult stem/progenitor cells (MSCs): a backward journey from dramatic results in vivo to the cellular and molecular explanations. J Cell Biochem 113(5):1460–1469
16. Neirinckx V et al (2013) Concise review: adult mesenchymal stem cells, adult neural crest stem cells, and therapy of neurological pathologies: a state of play. Stem Cells Transl Med 2(4): 284–296
17. Uccelli A, Moretta L, Pistoia V (2008) Mesenchymal stem cells in health and disease. Nat Rev Immunol 8(9):726–736
18. Prockop DJ, Oh JY (2012) Mesenchymal stem/stromal cells (MSCs): role as guardians of inflammation. Mol Ther 20(1):14–20
19. Singer NG, Caplan AI (2011) Mesenchymal stem cells: mechanisms of inflammation. Annu Rev Pathol 6:457–478
20. Rosenzweig ES, McDonald JW (2004) Rodent models for treatment of spinal cord injury: research trends and progress toward useful repair. Curr Opin Neurol 17(2):121–131
21. Steuer I, Guertin PA (2009) Spinal cord injury research in mice: 2008 review. ScientificWorldJ 9:490–498
22. Neirinckx V, Cantinieaux D, Coste C, Rogister B, Franzen R, Wislet S (2014) Spinal cord injuries: how could adult mesenchymal and neural crest stem cells take up the challenge. Stem Cells 32(4):829–843
23. Basso DM et al (2006) Basso mouse scale for locomotion detects differences in recovery after spinal cord injury in five common mouse strains. J Neurotrauma 23(5):635–659

Chapter 22

Histological Characterization and Quantification of Cellular Events Following Neural and Fibroblast(-Like) Stem Cell Grafting in Healthy and Demyelinated CNS Tissue

Jelle Praet, Eva Santermans, Kristien Reekmans, Nathalie de Vocht, Debbie Le Blon, Chloé Hoornaert, Jasmijn Daans, Herman Goossens, Zwi Berneman, Niel Hens, Annemie Van der Linden, and Peter Ponsaerts

Abstract

Preclinical animal studies involving intracerebral (stem) cell grafting are gaining popularity in many laboratories due to the reported beneficial effects of cell grafting on various diseases or traumata of the central nervous system (CNS). In this chapter, we describe a histological workflow to characterize and quantify cellular events following neural and fibroblast(-like) stem cell grafting in healthy and demyelinated CNS tissue. First, we provide standardized protocols to isolate and culture eGFP$^+$ neural and fibroblast(-like) stem cells from embryonic mouse tissue. Second, we describe flow cytometric procedures to determine cell viability, eGFP transgene expression, and the expression of different stem cell lineage markers. Third, we explain how to induce reproducible demyelination in the CNS of mice by means of cuprizone administration, a validated mouse model for human multiple sclerosis. Fourth, the technical procedures for cell grafting in the CNS are explained in detail. Finally, an optimized and validated workflow for the quantitative histological analysis of cell graft survival and endogenous astroglial and microglial responses is provided.

Key words Neural stem cells, Mouse embryonic fibroblasts, Cell grafting, Cuprizone, Quantitative histology, Inflammation

1 Introduction

Multiple sclerosis (MS) is a chronic neurodegenerative disease of the central nervous system (CNS), in which myelin-specific T cells are generally considered as the driving force behind the detrimental autoimmune inflammatory reaction. While pathological events

Electronic supplementary material The online version of this chapter (doi:10.1007/978-1-4939-1453-1_22) contains supplementary material, which is available to authorized users.

Bruno Christ et al. (eds.), *Animal Models for Stem Cell Therapy*, Methods in Molecular Biology, vol. 1213,
DOI 10.1007/978-1-4939-1453-1_22, © Springer Science+Business Media New York 2014

in MS are heterogeneous between patients, eventually all patients show a loss of oligodendrocytes, demyelination, axonal damage, and loss of brain function [1–3]. MS is most often studied using the experimental autoimmune encephalomyelitis (EAE) model, in which active or passive immunization against myelin-specific proteins results in T cell-driven demyelination of the CNS [4]. Currently, most of the novel MS treatments are being developed using the EAE model, and many of these strategies focus on halting the autoimmune inflammatory reaction. However, despite being successful in the EAE mouse model, some of these therapies fail to show any clinical therapeutic benefit upon application in human MS patients. For example, while anti TNF-α treatment showed mixed results in the EAE model, it was shown to be deleterious in human MS [5]. Therefore, alternative MS models are gaining interest to study several aspects of MS, for which the EAE model fails to mimic them. As such, the cuprizone mouse model reproducibly induces demyelination and remyelination following the ingestion of a cuprizone supplemented diet. As this is a toxin-induced model, it allows elucidation of factors contributing to demyelination and remyelination, as well as the evaluation of novel therapeutic approaches, without interference of an ongoing autoimmune inflammatory attack [6].

Recently, intracerebral grafting of stem cells has gained tremendous interest as a possible MS treatment, as stem cells have the potential to repair/replace lost brain tissue. As such, neural stem cells (NSCs) are an obvious candidate as these cells have the potential to differentiate into the three major cell types of the brain: neurons, astrocytes and oligodendrocytes [7]. While efficacy of NSC grafting has been shown in different animal models of MS, NSCs are hard to obtain in a clinical setting as they are isolated from neural tissue [8]. As such, fibroblast-like (stem) cells, e.g., mesenchymal stromal cells or adult/embryonic fibroblasts, are gaining interest due to the observation that these cells were also able to exert therapeutic effects in animal models of MS. While fibroblast-like (stem) cells were shown to be able to differentiate into neurons in vitro, therapeutic efficacy has mostly been linked to their intrinsic neuro-immune modulatory properties [9–11].

In this chapter, we describe validated protocols to [12–15]: (1) isolate, culture, and characterize NSCs and mouse embryonic fibroblasts (mEFs) from embryonic tissue, (2) induce and characterize demyelination in the CNS of mice by means of cuprizone administration, (3) stereotactically graft NSCs or mEFs in the CNS of mice, (4) histologically quantify survival and migration of the grafted cell populations, and (5) quantify histologically the cell graft-induced microglial and astroglial cell responses.

2 Materials

2.1 Animals

1. C57BL/6J eGFP$^+$ transgenic mice (Jackson Laboratories; strain code 003291).
2. C57BL/6J wild type (wt) mice (Jackson Laboratories; strain code 000664).

2.2 Cell Isolation, Culture, and Characterization

2.2.1 Products

1. 15 mL tube.
2. 5 mL FACS tube.
3. Accutase (Sigma-Aldrich).
4. Amphotericin B (Life Technologies).
5. Apo-Transferrin (Sigma-Aldrich).
6. Collagenase A (Roche).
7. Dulbecco's modified Eagle medium (DMEM; +L-glutamine, Life Technologies).
8. DMEM/F12 medium (Life Technologies).
9. DNase I (Sigma-Aldrich).
10. Epidermal growth factor (EGF; ImmunoTools).
11. Ethanol, 70 %.
12. Fetal calf serum (FCS; Life Technologies).
13. Gelred (1× final concentration; Biotum).
14. Human fibroblast growth factor-2 (hFGF-2; ImmunoTools).
15. Bovine fibronectin (R&D Systems).
16. Insulin (Sigma-Aldrich).
17. Isoflurane (Isoflo).
18. L-glutamine (Life Technologies).
19. Neurobasal A medium (Life Technologies).
20. Nitrogen and oxygen gas.
21. Penicillin and streptomycin (Life Technologies).
22. Petri dish.
23. Phosphate-buffered saline (PBS; Life Technologies): 10× PBS diluted to 1× in demineralized water.
24. Progesterone (Sigma-Aldrich).
25. Putrescine (Sigma-Aldrich).
26. Bovine serum albumin (BSA; Life Technologies).
27. Sodium selenite (Sigma-Aldrich).
28. T25 culture flask.
29. Trypsin–EDTA (Life Technologies).

2.2.2 Media Preparation

1. Isolation medium: PBS containing 100 U/mL penicillin and 100 mg/mL streptomycin.
2. Dissociation medium: PBS containing 0.2 % collagenase A and DNase I (2,000 Kunitz units/50 mL).
3. Neural expansion medium (NE medium): Neurobasal A medium containing 100 U/mL penicillin, 100 mg/mL streptomycin, 0.5 μg/mL amphotericin B, 10 μL L-glutamine (200 mM), and 1 % modified N2 supplement.
4. Modified N2 supplement: DMEM/F12 medium containing 7.5 mg/mL BSA, 2.5 mg/mL insulin, 2 mg/mL apo-Transferrin, 0.518 μg/mL sodium selenite, 1.6 mg/mL putrescine, and 2 μg/mL progesterone.
5. Fibronectin-coated T25 culture flasks: Prepared by incubating T25 culture flasks overnight with a solution containing 5 μg bovine fibronectin/mL PBS (4 mL/T25 culture flask). Remove the fibronectin solution before plating cells. Fibronectin-coated culture flasks can be stored at 4 °C and used up to 2 weeks after preparation.
6. mEF medium: DMEM containing L-glutamine, 10 % FCS, 100 U/mL penicillin, and 100 mg/mL streptomycin.

2.3 Antibodies

1. For flow cytometric characterization of NSCs and mEFs: All primary antibodies (AB) are reactive to mouse antigens unless stated otherwise and are diluted to a final concentration of 1 μg/100 mL (Table 1).
2. For histological analysis of cell grafted brains: All primary antibodies (AB) are reactive to mouse antigens unless stated otherwise and are diluted to the indicated concentration (Table 2).

2.4 Induction of Demyelination Using the Cuprizone Mouse Model

1. Cuprizone (Sigma-Aldrich).
2. Standard rodent lab chow (Carfil).
3. Sterile water.

Table 1
Overview of antibodies used for flow cytometric analysis

Primary AB	Label	Company
α-Sca-1	PE	eBioscience (12-5981-82)
α-A2B5	PE	Miltenyi Biotec (130-093-581)
α-CD45	PE	eBioscience (12-0451-82)

PE phycoerythrine

Table 2
Overview of antibodies used for immunofluorescence histological analysis

Primary AB	Dilution	Company	Secondary AB	Dilution	Company
α-IBA1	1,25 μg/mL	Wako (019-19714)	Donkey α-rabbit AF555	2 μg/mL	Life Technologies (A31572)
α-GFAP	1 μL/mL	Abcam (ab7260)	Donkey α-rabbit AF555	2 μg/mL	Life Technologies (A31572)
Fluoromyelin	5 μL/mL	Life Technologies (F34652)			

2.5 Cell Grafting

1. 0.9 % NaCl solution.
2. 10 μL Hamilton syringe.
3. 30 G needle (Hamilton).
4. Chlorohexidinedigluconate 0.3 % mv (Certa).
5. Ethanol, 70 %.
6. Iso-Betadine (MundiPharma).
7. Ketamine (Pfizer; Ketalar, 50 mg/mL).
8. Microinjection pump (Kd Scientific).
9. Vidisic (Bausch + Lomb).
10. PBS (Life Technologies): 10× PBS diluted to 1× in demineralized water.
11. Stereotactic frame (Stoelting).
12. Ethilon II sutures.
13. Xylazine (Bayer Health care; Rompun, 2 %).
14. Dental drill burr + 1 mm drill bit (Stoelting Co).

2.6 Quantitative Histological Analysis

2.6.1 Products

1. 1 and 12 N HCl.
2. 23 G needle (BD Microlance).
3. BX51 fluorescence microscope with an Olympus DP71 digital camera.
4. Dako pen.
5. DAPI (1 mg/mL).
6. Donkey serum (Jackson Immunoresearch).
7. Glass slides.
8. Goat serum (Jackson Immunoresearch).
9. Liquid nitrogen.
10. Micron HM5000 cryostat (Prosan).

11. Milk powder—Any store-bought lyophilized bovine milk powder will suffice.
12. Nembutal, 60 mg/mL (Ceva Sante Animale; pentobarbital).
13. Paraformaldehyde.
14. PBS (Life Technologies): 10× PBS diluted to 1× in demineralized water.
15. Prolong Gold antifade (Life Technologies).
16. Triton-X.

2.6.2 Software

1. Adobe Photoshop CS6.
2. ImageJ software (NIH ImageJ; v1.47).
3. TissueQuest software (TissueGnostics GmbH; v3.00).
4. R statistical software (v2.153).

2.6.3 Buffer Preparation

1. TRIS solution: Demineralized water containing 0.124 g/mL TRIS and 0.74 mL/mL of 1 N HCl.
2. Tris-buffered saline (TBS): Demineralized water containing 7.65 g/L of NaCl, 100 mL/L TRIS solution, and two drops/L 12 N HCl.
3. Antibody dilution buffer: TBS containing 10 % milk powder (weight/volume).

3 Methods

3.1 Isolation and Culture of Mouse NSCs

3.1.1 Neural Stem Cell Isolation

1. Deeply anesthetize a pregnant female eGFP transgenic C57BL/6J mouse (E14.5 embryos) by inhalation of 4 % isoflurane in a 30 % oxygen–70 % nitrogen mixture for 2 min. Sacrifice the mouse by cervical dislocation and disinfect the abdomen with 70 % ethanol.
2. Pull back the skin to expose the peritoneum and cut open the peritoneal wall to expose the uterine horns. Remove the uterine horns containing the embryos, and place them in a petri dish containing ice-cold isolation medium.
3. Open each embryonic sac and place the individual embryos into separate new petri dishes containing ice-cold isolation medium (*see* **Note 1**). Dissect the embryonic forebrain from each embryo and place them in separate 15 mL tubes containing 5 mL of ice-cold isolation medium (*see* **Note 2**).
4. Place each embryonic forebrain in a clean petri dish containing 5 mL of ice-cold isolation medium. Mince the forebrain tissues with two scissors for 5 min and then place the minced tissues in 15 mL tubes.

5. Centrifuge for 5 min at 129 × *g* and remove the supernatant. Add 2 mL of dissociation medium to each tube and incubate for 1.5 h at 37 °C in a shaking water bath.
6. After incubation, add 8 mL of NE medium and centrifuge for 5 min at 129 × *g*. Remove the supernatant and suspend the pellets in 10 mL of NE medium supplemented with 10 ng/mL EGF and FGF-2.
7. Plate out the obtained cell populations in uncoated T25 culture flasks and keep T25 culture flasks inside an incubator at 5 % CO_2 and at 37 °C. Add 10 ng/mL EGF and FGF-2 every 2–3 days until neurospheres are formed.
8. Following neurosphere formation, remove the 10 mL culture medium from the T25 culture flask and place in a 15 mL tube. Centrifuge for 5 min at 129 × *g* and remove the supernatant. Add 5 mL of accutase to the pellet and incubate for 5 min at 37 °C.
9. Add 5 mL of NE medium to the 15 mL tube and centrifuge for 5 min at 129 × *g*. Remove the supernatant and add 10 mL of NE medium to the pellet supplemented with 10 ng/mL EGF and FGF-2. Plate out the cells in fibronectin-coated T25 culture flasks and keep T25 culture flasks inside an incubator at 5 % CO_2 and at 37 °C.
10. Following 24 h of culture, remove non-adherent cells by replacing medium with 10 mL fresh NE medium and add 10 ng/mL EGF and FGF-2. Refresh NE medium and add 10 ng/mL EGF and FGF-2 every 2–3 days thereafter, until 90 % confluence is reached.

3.1.2 Neural Stem Cell Culture

For routine cell culture, NSC cultures are kept inside an incubator at 5 % CO_2 and at 37 °C. NE medium is replaced every 3–4 days and 10 ng/mL EGF and FGF-2 is added every 2–3 days. NSC cultures are split 1:5 every 7 days according to the following procedure:

1. Remove the culture medium from the T25 culture flasks and add 3 mL of accutase to the culture flasks and incubate for 5 min at 37 °C.
2. Add 7 mL of NE medium to the culture flasks and place the medium in a 15 mL tube and centrifuge for 5 min at 129 × *g*.
3. Remove the supernatant and suspend the pellet in 5 mL of fresh NE medium. Plate 1 mL cell suspension per new fibronectin-coated T25 flask and add 9 mL NE medium to obtain a final volume of 10 mL culture medium. Add 10 ng/mL EGF and FGF-2.

3.2 Isolation and Culture of mEFs

3.2.1 Mouse Embryonic Fibroblast Isolation

1. Deeply anesthetize a pregnant female eGFP$^+$ transgenic C57BL/6J mouse (E14.5 embryos) by inhalation of 4 % isoflurane in a 30 % oxygen–70 % nitrogen mixture for 2 min. Sacrifice the mouse by cervical dislocation and disinfect the abdomen with 70 % ethanol.
2. Pull back the skin to expose the peritoneum and cut open the peritoneal wall to expose the uterine horns. Remove the uterine horns containing the embryos, and place them in a petri dish containing ice-cold isolation medium.
3. Open each embryonic sac and place the individual embryos into separate new petri dishes containing ice-cold isolation medium (*see* **Notes 1** and **2**). Remove the embryonic forebrain, the liver, and spleen from each embryo and place the remainder of the embryo in separate 15 mL tubes containing 5 mL of ice-cold isolation medium (*see* **Note 3**).
4. Place each embryo in a clean petri dish containing 5 mL of ice-cold isolation medium. Mince the embryonic tissues with two scissors for 5 min and then place the minced tissue suspensions in 15 mL tubes.
5. Centrifuge the 15 mL tubes for 5 min at 100 × *g* and remove the supernatant. Enzymatically digest the pellet by adding 3 mL of Trypsin–EDTA and 15 μL DNAse I (2,000 Kunitz units/50 mL) for 15 min at 37 °C.
6. Halt Trypsin activity by adding 7 mL of mEF medium. Stir the solution and let it rest for 3 min to allow any remaining tissue chunks to sink. Very gently pipet up the supernatant and transfer it to a 15 mL tube. Centrifuge the 15 mL tubes for 5 min at 100 × *g*.
7. Remove the supernatant and add 10 mL mEF medium. Plate the obtained cell suspension in a T25 culture flask (one flask per embryo) and keep cultures inside an incubator at 5 % CO_2 and at 37 °C. One day after plating the cells, remove all non-adherent cells by replacing culture medium with 10 mL of fresh mEF medium.

3.2.2 Mouse Embryonic Fibroblast Culture

For routine cell culture, mEF cultures are kept inside an incubator at 5 % CO_2 and at 37 °C. mEF medium is replaced every 2–3 days and mEF cultures are split 1:3 every 4–5 days according to the following procedure:

1. Remove the culture medium from the T25 culture flasks and add 3 mL of Trypsin–EDTA to the culture flasks and incubate for 5 min at 37 °C.
2. Add 7 mL of mEF medium to the culture flasks and place the culture medium in a 15 mL tube. Centrifuge for 5 min at 100 × *g*.

3. Remove the supernatant and suspend the pellet in 3 mL of fresh mEF medium. Plate 1 mL cell suspension per T25 flask and add 9 mL mEF medium to obtain a final volume of 10 mL culture medium.

3.3 Flow Cytometric Characterization of NSCs and mEFs

For all flow cytometric measurements, cell viability is assessed through the addition of 1 μL GelRed to the cell suspension immediately before flow cytometric analysis using an Epics XL-MCL analytical flow cytometer. At least 5,000 cells are analyzed per sample and flow cytometry data are analyzed using the FlowJo software package (v7.2.2).

3.3.1 Flow Cytometric Analysis of eGFP Transgene Expression in NSC and mEF

1. Harvest eGFP$^-$ and eGFP$^+$ NSCs and mEFs according to the procedures used for routine cell culture (use PBS instead of culture medium) and transfer cell suspension to a 5 mL FACS tube (*see* **Note 4**).
2. Wash the cells once by adding PBS and centrifuging at 100 or 129 × *g* for mEFs and NSCs, respectively.
3. Suspend the cells in 1 mL PBS and analyze directly by flow cytometry.

3.3.2 Flow Cytometric Analysis Using Directly Labeled Primary Antibodies

1. Harvest eGFP$^+$ NSC and mEF according to the procedures used for routine cell culture (use PBS instead of culture medium).
2. Wash the cells twice by adding PBS and centrifuging at 100 or 129 × *g* for mEFs and NSCs, respectively.
3. Suspend the cells in PBS at a concentration of 1×10^6 cells/mL and transfer 100 μL of this cell suspension to a 5 mL FACS tube (one tube per staining).
4. Add 1 μg of each directly labeled primary antibody to the 5 mL FACS tubes containing the cell suspension and incubate for 30 min at 4 °C. Wash the cells twice by adding PBS and centrifuging at 100 or 129 × *g* for mEFs and NSCs, respectively.
5. Suspend the cells in 1 mL PBS and analyze directly by flow cytometry.

3.3.3 Expected Outcome

The quality and progression of eGFP$^+$ NSC and mEF cell cultures can be determined directly by means of both fluorescence and bright-field microscopy as shown in Fig. 1a. The level of eGFP expression relative to eGFP$^-$ cell cultures can be determined by means of FACS analysis as is shown in Fig. 1b. Additionally, cell cultures can be further characterized by means of FACS analysis following an immunofluorescent staining. Shown in Fig. 1c is the FACS analysis of NSCs and mEFs immunofluorescently stained for A2B5 (a marker for neuronal cells), SCA1 (a marker for mesenchymal cells) and CD45 (a marker for hematopoietic cells).

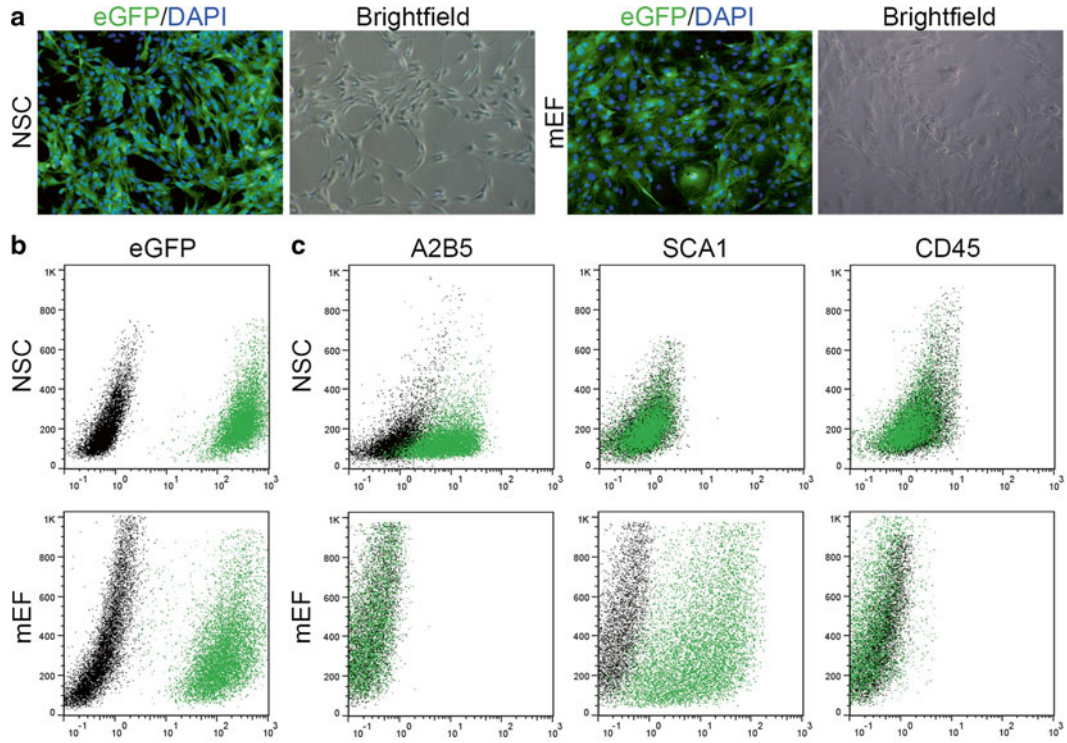

Fig. 1 (**a**) Fluorescence and bright-field images of NSC and mEF cell cultures. Fluorescence images show each time the eGFP$^+$ NSCs or mEFs (*green*) and the cell nuclei by means of DAPI staining (*blue*). (**b**) FACS plots of eGFP$^-$ (*black*) and eGFP$^+$ (*green*) NSC or mEF cell cultures. (**c**) Immunofluorescent characterization of NSC and mEF cell cultures by means of A2B5 (neuronal marker), SCA1 (mesenchymal marker), and CD45 staining (hematopoietic marker). Unstained cell populations are shown in *black* while immunofluorescently stained cell populations are shown in *green*

3.4 Induction of Demyelination Using the Cuprizone Mouse Model

To induce demyelination of the main white matter tracts (in particular the corpus callosum) of 8 weeks old female wild type C57BL6/J mice (*see* **Note 5**), mice are given ad libitum access to a 0.2 % cuprizone supplemented diet prepared as follows.

1. Weigh 500 g of standard rodent chow and put this in a bowl.
2. Weigh 1 g of cuprizone powder (0.01 g accurate).
3. Very gently spray a little sterile water over the 500 g of standard rodent chow so that the pellets become damp (pellets should look damp but no signs of water droplets should be present).
4. Thoroughly mix the 1 g of cuprizone powder with the 500 g of damp standard rodent chow. The moist on the pellets helps the cuprizone powder to adhere to the pellets.

5. Make fresh 0.2 % cuprizone supplemented rodent chow every week as deterioration of the cuprizone compound might otherwise affect reproducibility.

3.5 Intracerebral Grafting of Stem Cells in the Healthy and Demyelinated Mouse Brain

3.5.1 Cell Preparation for Grafting Experiments

1. Harvest eGFP$^+$ NSCs or mEFs according to the procedures used for routine cell culture.
2. Wash the cells twice by adding PBS and centrifuging at 100 or $129 \times g$ for mEFs and NSCs, respectively.
3. Suspend the cells in PBS at the desired concentration (here 5×10^5 cells in 2 μL PBS). Cell preparations are kept on ice until grafting experiments.

3.6 Cell Grafting of eGFP-Expressing NSC and mEF

Cell implantation was reproducibly targeted in the right hemisphere according to the below described procedure and at following coordinates relative to bregma: 0 mm anterior, 2 mm lateral (right side of the brain) and 2.5 mm ventral.

1. Anesthetize the mouse by an intraperitoneal injection of an 80 mg/kg body weight (BW) ketamine–16 mg/kg BW xylazine in PBS mixture.
2. Shave the mouse head and fix the head in a stereotactic frame. Wet the eyes using Vidisic to prevent dehydration.
3. Gently disinfect the skin using 0.3 % m/v chlorohexidinedigluconate and make a midline scalp incision to expose the skull. Adjust the mouse head position to obtain a flat-skull position (*see* **Note 6**).
4. Drill a hole in the skull using a dental drill burr at the respective coordinates.
5. Vortex the cell suspension briefly and aspirate the cell suspension in a 10 μL Hamilton Syringe to which a 30 G needle is attached. Attach the syringe to an automatic micro-injector pump and position the syringe above the exposed dura.
6. Stereotactically place the 30 G needle attached to the syringe through the intact dura to a depth of 2.5 mm. Wait 1 min to allow pressure equilibration.
7. Inject 5×10^5 eGFP$^+$ NSCs or mEFs (2 μL) at a speed of 0.7 μL/min using an automatic micro-injector pump. Wait 3 min after injection to allow pressure equilibration and to prevent backflow of the injected cell suspension, and then slowly retract the needle.
8. Disinfect the skin borders using Iso-Betadine and suture the skin using Ethilon II sutures. Administer a 0.9 % NaCl solution subcutaneously in order to prevent dehydration and place mice under a heating lamp to recover.

3.7 Histological Analysis of Cell Graft Survival and Endogenous Glial Cell Responses

3.7.1 Mouse Perfusion-Fixation and Brain Dissection

Prior to starting the perfusion-fixation protocol, prepare the perfusion setup. Perfusion-fixation can then be performed as follows.

1. Euthanize the mouse using Nembutal (150 mg/kg BW) via an intraperitoneal injection.
2. Once breathing halts and the mouse is unresponsive (*see* **Note 7**), open the skin starting at the abdomen and up to the diaphragm. Sufficiently open the rib cage by making an incision on the bottom, left and right side of the rib cage. This will fully expose the heart and allow blood to escape the thoracic cavity.
3. Allow ice-cold PBS to flow out of the needle attached to the rubber tubing of a perfusion pump at a speed of ±20 mL/min. Insert the needle in the left ventricle of the heart and take care not to pierce through the heart. Make a cut in the left atrium to allow blood to flow out.
4. After approximately 3 min, the fluid coming out of the atrium should no longer be colored red and the liver should have changed color from dark red to a more brownish color. At this moment, switch from perfusing with ice-cold PBS to fixating with 4 % paraformaldehyde.
5. Fixation is complete when spontaneous movement of the mouse tail can be observed (*see* **Note 8**). Dissect the whole mouse brain from the skull.
6. Post-fixate the brain in 4 % paraformaldehyde for 1 h. Then freeze-protect the brain tissue by placing it subsequently in different gradients of sucrose (2 h in 5 %, 4 h in 10 % and overnight in 20 %).
7. Snap freeze the brain tissue in liquid nitrogen and store at −80 °C until sectioning (*see* **Note 9**).

3.7.2 Sectioning of Mouse Brains for Histological Analysis

1. Allow the frozen brain to acclimatize the temperature of the cryostat before sectioning.
2. Section the entire implant region in serial 10 μm thick cryosections using a cryostat, hereby noting consecutively marked and missing slides. Collect every tissue section on a separate glass slide. Keep slides at −20 °C as much as possible.
3. Screen unstained cryosections directly using a fluorescence microscope to locate eGFP$^+$ NSCs and mEFs.
4. Store slides at −20 °C until histological analysis.

3.7.3 Histological Analysis: Immunofluorescence Staining

Histological analysis was performed to determine microglia (IBA1), astrocytes (S100β) astrogliosis (GFAP) and the severity of tissue damage by assessing the myelination status (MBP). All experimental procedures are performed at room temperature in the dark unless stated otherwise.

1. Use a Dako pen to delineate the tissue section.
2. Rinse the slide for 5 min with TBS.

3. For intracellular staining, permeabilize the slide by incubating for 30 min with a 0.1 % Triton-X in TBS solution.
4. Incubate the slide for 1 h with a blocking solution consisting of 20 % serum in TBS. Serum should originate from the animal species in which the secondary antibody was raised. Place the slide on a horizontal rotary shaker at a low speed.
5. Incubate the slide overnight at 4 °C with the primary antibody at the appropriate dilution in antibody dilution buffer.
6. The following day, wash the slide three times 5 min with TBS.
7. Incubate the slide for 1 h at room temperature with secondary antibody at the appropriate dilution in antibody dilution buffer. Place the slide on a horizontal rotary shaker at a low speed.
8. Wash the slide three times 5 min with TBS.
9. Counterstain the slide by incubating with the nuclear stain DAPI for 20 min at a concentration of 1/1,000 in TBS.
10. Wash the slide two times 5 min with TBS, followed by washing two times 5 min with distilled water.
11. Mount the slide using cover glass and Prolong Gold antifade reagent. Let the mounting medium dry for 5 min and visualize immediately with a fluorescence microscope.

3.7.4 *Expected Outcome*

Cuprizone, as a copper chelator, imposes a severe metabolic stress resulting in a selective loss of oligodendrocytes and severe demyelination of the main white matter tracts [6]. Following the administration of a 0.2 % cuprizone diet to 8 weeks old female wild type C57BL6/J mice during a period of 4 weeks, we observed severe demyelination and inflammation in the corpus callosum as is shown in Fig. 2. Compared to the healthy control group (Healthy), the cuprizone-treated group (Cuprizone) shows: (1) an accumulation

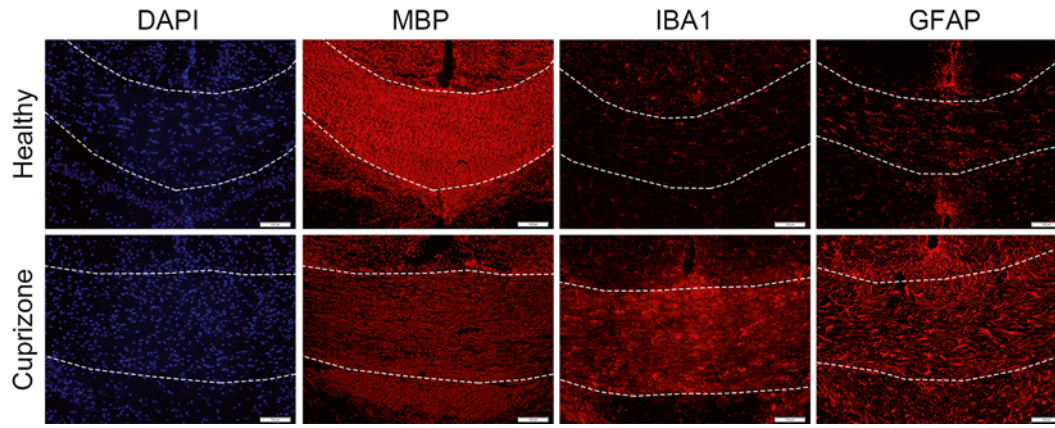

Fig. 2 Immunofluorescent characterization of demyelination and inflammation in healthy mice (Healthy) and in mice following a 4-week 0.2 % cuprizone treatment (Cuprizone). For both groups we show images of cell nuclei (DAPI), myelin (MBP), microglia (IBA1), and astrogliosis (GFAP). *Dotted white lines* indicate the corpus callosum

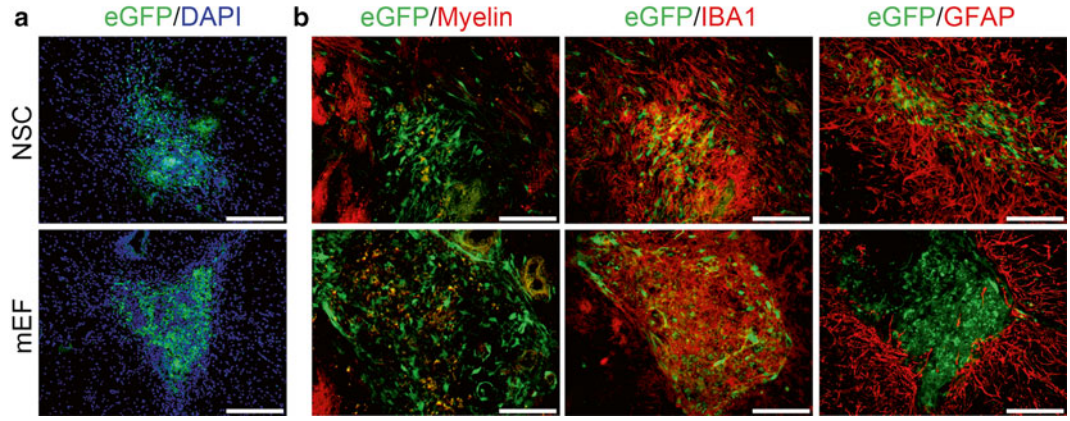

Fig. 3 (**a**) Fluorescence images of NSC or mEF grafts at 2 weeks postgrafting. Shown in *green* is each time the eGFP$^+$ cell graft (GFP) while cell nuclei are shown in *blue* (DAPI, scale bars = 200 μm). (**b**) Immunofluorescent characterization of eGFP$^+$ NSC or mEF graft-induced damage to the endogenous brain structure as visualized by means of fluoromyelin staining (Myelin, shown in *red*). Additionally shown is the degree of microgliosis (IBA1, shown in *red*) and astrogliosis (GFAP, shown in *red*, scale bars = 100 μm)

of cells as observed by the increase of DAPI$^+$ nuclei, (2) severe demyelination as indicated by the reduced MBP staining intensity, (3) an accumulation of IBA1$^+$ microglia, and (4) severe astrogliosis as shown by GFAP staining.

To allow identification of NSC or mEF grafts in the CNS, we isolated these cell populations from transgenic mice constitutively expressing eGFP in all cell types. At two weeks post-grafting of eGFP$^+$ NSCs or mEFs in the CNS of syngeneic mice, cell grafts could be identified by means of eGFP expression using direct fluorescence microscopy as shown in Fig. 3a. In addition, the presence of a large number of DAPI$^+$ eGFP$^-$ cell nuclei was noted inside both the NSC and mEF graft, indicative of the accumulation of inflammatory cells. Indeed, as is shown in Fig. 3b, we could observe: (1) severe graft-induced tissue damage as MBP$^+$ myelin tracts were disrupted in the graft area, (2) an accumulation of IBA1$^+$ microglia inside the graft area and (3), severe astrogliosis as visualized by GFAP staining. Concerning the latter, it is of interest that while NSC grafts become highly invaded by GFAP$^+$ astrocytes, mEF grafts become surrounded by GFAP$^+$ astrocytes.

3.7.5 Quantitative Analysis of Cell Graft Volume, Survival, and Migration

1. Using a fluorescence microscope, obtain an image of every consecutive brain slide containing eGFP$^+$ cells.
2. Using the ImageJ software package, determine the surface area (XY plane provided as mm^2) of the NSC or mEF cell grafts based on eGFP expression.
3. Linearly extrapolate data from missing slides based on the acquired data. This allows calculation of the total graft site

volume, provided as graft site volume in mm^3 (=sum of each individual graft volume per slide in $mm^2 \times 10$ μm).

4. To determine the degree of lateral migration, first identify the midline of the mouse brain separating the left and right hemisphere. Using ImageJ, measure the distance from the midline to the outer left and right side of the graft as well as the injection tract.
5. Linearly extrapolate data from missing slides based on the acquired data. This allows calculation of the maximal graft site migration in both lateral directions, provided in mm.

3.7.6 Quantitative Analysis of Immunofluorescence Stainings

The quantitative analysis of the endogenous glial cell response is performed using image analysis software (TissueQuest, Adobe Photoshop and ImageJ) according to the following procedure.

1. On each of the stained tissue slides, manually delineate the graft site based on eGFP expression and the graft border using Adobe Photoshop. The graft border can be defined as the area extending 100 μm outwards from the graft site.
2. For each of the delineated regions determine the surface area in XY plane provided as mm^2 (ImageJ).
3. Within both delineated regions, quantify the number of $DAPI^+$ cell nuclei and the number of $eGFP^+$ cells for each stained slide (TissueQuest). Per mouse, multiply the average $eGFP^+$ cell density with the total graft site volume to obtain the total amount of surviving $eGFP^+$ cells.
4. Quantify the number of $IBA1^+$ microglia or $S100\beta^+$ astrocytes within both delineated regions (TissueQuest) and divide by the surface area of the respective regions to obtain the microglial or astroglial cell density.
5. The degree of myelination and astrogliosis is determined by calculating the optical density of MBP and GFAP expression in both delineated regions (ImageJ), and dividing this by the surface area of the respective regions.

3.7.7 Schematic Representation of the Analysis Pipeline to Determine Cell Graft Survival, Migration and Inflammatory Response

A schematic overview of the quantitative histological analysis pipeline is shown in Fig. 4. First, consecutive 10 μm thick coronal cryosections of the cell graft were made while keeping track of missing slides. Direct fluorescence images of the $eGFP^+$ cell grafts are acquired, and an image stack is made. Using Photoshop and ImageJ, it is then possible to calculate the total graft site volume as described. Using the same image stack, it is also possible to determine the degree of cell migration outwards from the injection tract. This allows a top-down view reconstruction of the cell migration in the XY-plane using the statistical package R. To determine the degree of microgliosis or astrogliosis, slides can be immunofluorescently stained with IBA1 or GFAP, respectively. Next, the graft site and

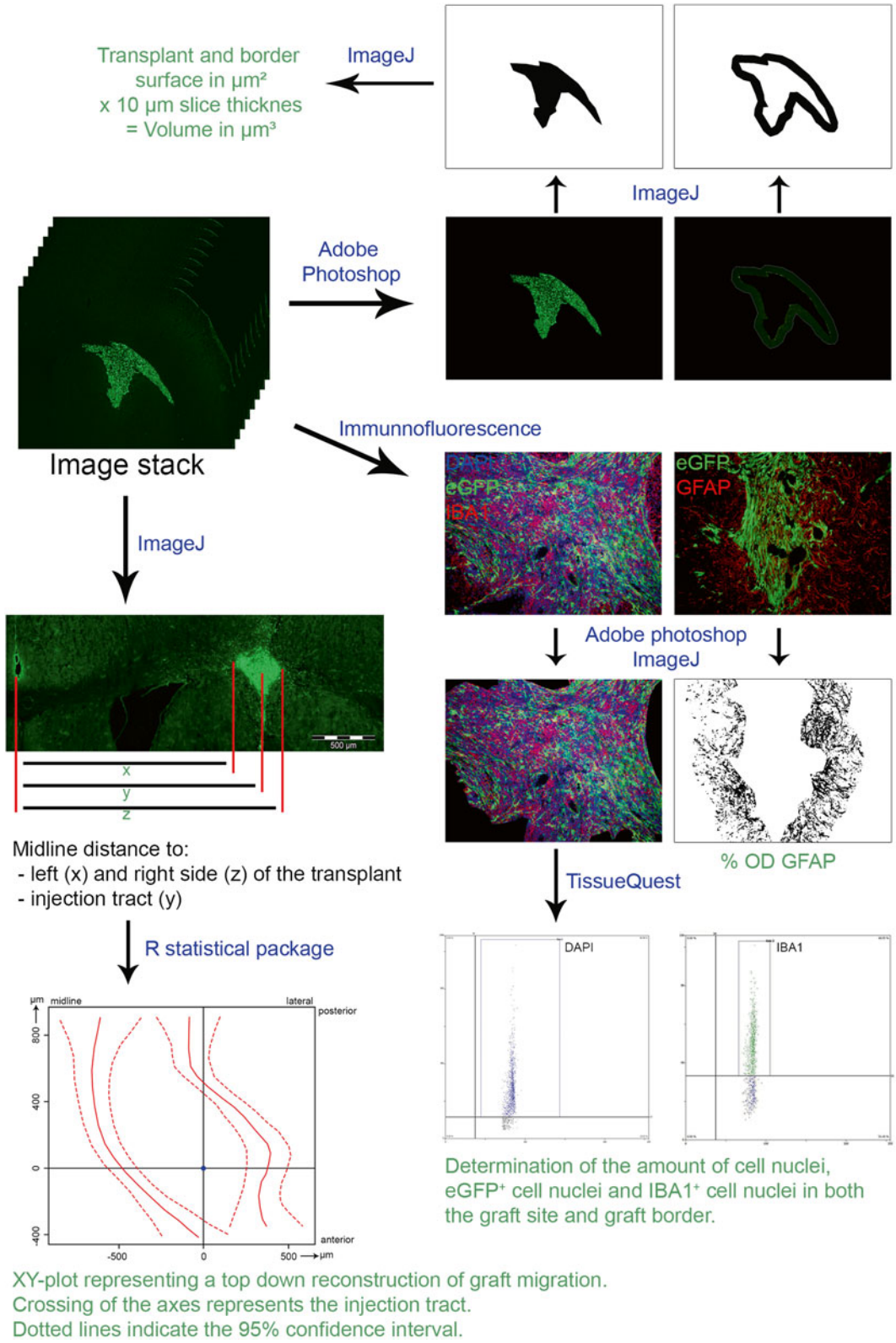

Fig. 4 Schematic overview of the complete workflow for histological quantification of cell graft survival (eGFP⁺ cell nuclei) and migration (*XY* plot) as well as the graft-induced inflammatory reaction (IBA1⁺ cell nuclei and % OD GFAP). The program/technique used for each step is indicated in *blue* while the expected results are indicated in *green*

graft border is delineated using Adobe Photoshop. The amount of surviving grafted cells can then be calculated from the graft site volume combined with the average eGFP$^+$ cell density within the graft site (determined using TissueQuest). The percentage optical density of GFAP (determined using ImageJ) is a measure for the degree of astrogliosis while the number of IBA1$^+$ cell nuclei (determined using TissueQuest) is a measure for the degree of microgliosis.

3.8 Statistical Analysis of the Obtained Results

All statistical analyses are performed using the statistical software R and all used R codes are provided in the Online Supplementary File 1.

3.8.1 Migration Analysis

Cell migration can be visualized by construction of two-dimensional top-down views of cell graft localization for both cell populations.

1. Data are specified in the following format: Two columns contain the migration to the left and right of the injection spot for each consecutive slide in both directions along the *x*-axis (this can be calculated from the values obtained in Subheading 3.6.5), and one column contains the position of the slide with respect to the injection spot in both directions along the *y*-axis. In addition, two columns contain the animal ID and the cell type grafted. An example of this data format is shown in the Online Supplementary File 2.
2. To obtain a smooth function of the cell migration for each population, the penalized smoothing splines technique, which is a flexible semi-parametric method to smooth the response of interest over space, is used. This can be fitted as a mixed effects model using the "lme"-function in the "nlme"-library.
3. Construct the 95 % point-wise confidence bands for the smoothed curves.

3.8.2 Evaluating Differences Between NSC and mEF Cell Grafts

When assessing the statistical significance of differences in for example the number of microglia between both cell populations, we need to take into account the association structure induced by the multiple measurements per animal. To do so, generalized estimating equations (GEE) will be used. This approach is more flexible than a full likelihood approach, since it is not necessary to specify the full association structure, but instead adopt "working" assumptions.

1. Data need to be specified in long or stacked format, which means that per response variable one column contains all observations. In addition, two columns contain animal ID and cell type. An example of this data format is shown in the Online Supplementary File 2.

2. Fit the GEE model using the "geeglm"-function from the "geepack"-library.
3. Significance of the difference between both groups is indicated by the Wald test statistic, which is included in the result summary.

4 Notes

1. As NSC isolation requires the embryonic forebrain and mEF isolation requires the embryo without liver, spleen and brain, it is possible to isolate both NSCs and mEFs from the same embryo.
2. Keep the embryos separated as soon as possible to avoid contamination of $eGFP^+$ cell cultures with cells from $eGFP^-$ embryos. Additionally, keep the 15 mL tubes with the dissected tissue on ice until all tissues are dissected and the next step can be performed.
3. Both liver and spleen are red in an otherwise transparent embryo.
4. For the initial determination of $eGFP^+$ and $eGFP^-$ cell cultures, perform flow cytometry at the moment of splitting and use 1 volume of the cell suspension for flow cytometry while the other volumes are used to continue cell cultures. Alternatively, discrimination between $eGFP^+$ and $eGFP^-$ cells can already be made while dissecting the embryos, using eGFP fluorescence glasses.
5. Reproducibility of cuprizone-induced demyelination was observed to be the greatest in 8 weeks old female C57BL6/J mice. A dose of 0.2 % cuprizone steadily induces demyelination by week 4 of treatment without the occurrence of adverse side effects.
6. To obtain a flat skull position, position the needle on top of bregma. Mark this point as 0 on the *Z*-axis and then move the needle to lambda. Observe whether the brain is tilted too little or too much (using the needle as a reference point) and adjust accordingly. Repeat this process until bregma and lambda are at an equal height.
7. To test unresponsiveness, gently pinch the toes of the left or right back paw of the mouse. If the mouse shows any reaction, wait another minute and test responsiveness again. Once no more reaction can be observed, proceed with the perfusion-fixation protocol.
8. Tail muscle spasms will occur as paraformaldehyde is neurotoxic and results in muscle contractions.

9. For snap freezing we take the brain tissue out of the 20 % sucrose solution and gently dip it dry using a paper towel to remove most of the fluid. To avoid tissue damage, we put the brain inside a small aluminum can, which is then held in the liquid nitrogen. Take care to avoid direct contact of the brain with the liquid nitrogen as this will cause the brain tissue to split.

References

1. Keegan BM, Noseworthy JH (2002) Multiple sclerosis. Annu Rev Med 53:285–302
2. Noseworthy JH, Lucchinetti C, Rodriguez M, Weinshenker BG (2000) Multiple sclerosis. N Engl J Med 343:938–952
3. Lucchinetti C, Bruck W, Parisi J, Scheithauer B, Rodriguez M, Lassmann H (2000) Heterogeneity of multiple sclerosis lesions: implications for the pathogenesis of demyelination. Ann Neurol 47:707–717
4. Fletcher JM, Lalor SJ, Sweeney CM, Tubridy N, Mills KH (2010) T cells in multiple sclerosis and experimental autoimmune encephalomyelitis. Clin Exp Immunol 162:1–11
5. Lim S-Y (2010) TNF-α: a paradigm of paradox and complexity in multiple sclerosis and its animalmodels~!2009-10-07~!2009-11-23~!2010-07-14~! Open Autoimmun J 2:160–170
6. Kipp M, Clarner T, Dang J, Copray S, Beyer C (2009) The cuprizone animal model: new insights into an old story. Acta Neuropathol 118:723–736
7. Glaser T, Pollard SM, Smith A, Brustle O (2007) Tripotential differentiation of adherently expandable neural stem (NS) cells. PLoS One 2:e298
8. Reekmans K, Praet J, De Vocht N, Daans J, Van der Linden A, Berneman Z, Ponsaerts P (2012) Stem cell therapy for multiple sclerosis: preclinical evidence beyond all doubt? Regen Med 7:245–259
9. Najm FJ, Lager AM, Zaremba A, Wyatt K, Caprariello AV, Factor DC, Karl RT, Maeda T, Miller RH, Tesar PJ (2013) Transcription factor-mediated reprogramming of fibroblasts to expandable, myelinogenic oligodendrocyte progenitor cells. Nat Biotechnol 31: 426–433
10. Yi T, Song SU (2012) Immunomodulatory properties of mesenchymal stem cells and their therapeutic applications. Arch Pharm Res 35: 213–221
11. Krampera M, Marconi S, Pasini A, Galie M, Rigotti G, Mosna F, Tinelli M, Lovato L, Anghileri E, Andreini A, Pizzolo G, Sbarbati A, Bonetti B (2007) Induction of neural-like differentiation in human mesenchymal stem cells derived from bone marrow, fat, spleen and thymus. Bone 40:382–390
12. De Vocht N, Lin D, Praet J, Hoornaert C, Reekmans K, Le Blon D, Daans J, Pauwels P, Goossens H, Hens N, Berneman Z, Van der Linden A, Ponsaerts P (2013) Quantitative and phenotypic analysis of mesenchymal stromal cell graft survival and recognition by microglia and astrocytes in mouse brain. Immunobiology 218:696–705
13. Praet J, Reekmans K, Lin D, De Vocht N, Bergwerf I, Tambuyzer B, Daans J, Hens N, Goossens H, Pauwels P, Berneman Z, Van der Linden A, Ponsaerts P (2012) Cell type-associated differences in migration, survival, and immunogenicity following grafting in CNS tissue. Cell Transplant 21:1867–1881
14. Reekmans K, De Vocht N, Praet J, Fransen E, Le Blon D, Hoornaert C, Daans J, Goossens H, Van der Linden A, Berneman Z, Ponsaerts P (2012) Spatiotemporal evolution of early innate immune responses triggered by neural stem cell grafting. Stem Cell Res Ther 3:56
15. Reekmans K, De Vocht N, Praet J, Le Blon D, Hoornaert C, Daans J, Van der Linden A, Berneman Z, Ponsaerts P (2013) Quantitative evaluation of stem cell grafting in the central nervous system of mice by in vivo bioluminescence imaging and postmortem multicolor histological analysis. Methods Mol Biol 1052:1–17

Chapter 23

Improvement of Neurological Dysfunctions in Aphakia Mice, a Model of Parkinson's Disease, after Transplantation of ES Cell-Derived Dopaminergic Neuronal Precursors

Sangmi Chung, Jisook Moon, and Kwang-Soo Kim

Abstract

Parkinson's disease (PD) is characterized by selective death of the substantia nigra dopaminergic neurons, and previously we have shown that *aphakia* mice, which harbor spontaneous Pitx3 gene mutation, show specific degeneration of the substantia nigra dopaminergic neurons accompanied by behavioral deficits that is reversed by L-DOPA treatment or transplantation of dopaminergic neural precursors. Here, we describe transplantation of dopaminergic neural precursors to a mouse model of PD, an *aphakia* mouse, followed by behavioral analyses of transplanted mice.

Key words Embryonic stem cells, Dopamine, Neuronal precursors, *Aphakia* mice, Parkinson's disease, Transplantation

1 Introduction

There are several animal models of Parkinson's disease (PD), and among these, an *aphakia* mouse is a genetic model [1, 2] that can provide a homogeneous model system compared to the pharmacologically induced models. Unlike many other genetic models of PD [3, 4], *aphakia* mice show selective degeneration of the substantia nigra dopaminergic neurons [1, 5–7] as in the case of human diseases, accompanied by behavioral deficits, which can be reversed by pharmacological treatment [2] or cell transplantation [8, 9]. Here, we describe the generation of dopaminergic neuronal precursors from mouse embryonic stem cells for transplantation, stereotaxic surgery of *aphakia* mice to deliver dopaminergic neuronal precursors into the striatum, and the behavioral analyses of the transplanted *aphakia* mice using various assays such as challenging beam test and pole test.

Bruno Christ et al. (eds.), *Animal Models for Stem Cell Therapy*, Methods in Molecular Biology, vol. 1213,
DOI 10.1007/978-1-4939-1453-1_23,

2 Materials

2.1 In Vitro Differentiation of Embryonic Stem (ES) Cells

1. Gelatin-coated dish: Incubate a 10 cm tissue culture plate with 1 mL of 0.1 % Gelatin solution (STEMCELL Technologies) at room temperature for 30 min (*see* **Note 1**).
2. ES cell medium: Dulbecco's modified Eagle medium (DMEM) supplemented with 2 mM glutamine (Invitrogen), 0.001 % β-mercaptoethanol, 1× nonessential amino acids (Invitrogen), 10 % donor horse serum (Sigma), and 2,000 U/mL human recombinant leukemia inhibitory factor (LIF; R&D Systems).
3. Trypsin–EDTA: diluted to 1× with Ca_2^+-free, Mg_2^+-free phosphate-buffered saline (PBS).
4. Embryoid bodies (EB) medium: DMEM supplemented with 2 mM glutamine, 0.001 % β-mercaptoethanol, 1× nonessential amino acids, 10 % fetal bovine serum (FBS).
5. Non-adherent bacterial dishes (Fisher Scientific).
6. Insulin, transferrin, selenium, and fibronectin (ITSFn) medium: DMEM/F12 (Invitrogen) supplemented with 50 μg/mL transferrin (Sigma), 5 μg/mL insulin (Sigma), 30 nM sodium selenite (Sigma), and 500 ng/mL fibronectin (Sigma).
7. Poly-L-ornithine and fibronectin-coated coverslips: Incubate sterile glass coverslips in Poly-L-ornithine (PLO; 15 μg/mL; Sigma) and fibronectin (FN; 1 μg/mL; Sigma) at room temperature for 30 min (*see* **Note 2**).
8. Neuronal progenitor (NP) medium: DMEM/F12 supplemented with N2 supplement (Invitrogen), 1 μg/mL laminin (Sigma), and 10 ng/mL basic fibroblast growth factor (bFGF; R&D Systems).
9. Neuronal differentiated (ND) cell medium: DMEM/F12 supplemented with N2 supplement and 1 μg/mL laminin.
10. FACS medium: phenol-free, Ca^{2+}-free, Mg^{2+}-free Hank's balanced salt solution (HBSS) supplemented with 1× penicillin/streptomycin, 20 mM D-glucose, and 2 % FBS.
11. Anti-Corin antibody [10]: a kind gift from Bruce A. Morgan, Harvard Medical School/Massachusetts General Hospital, Boston.
12. Alexa Fluor 647-conjugated anti-rabbit antibodies (Invitrogen).
13. FACSAria cell sorter with FACSDiva software (BD Biosciences).

2.2 Stereotaxic Surgery

1. Transplantation medium: phenol-free, Ca^{2+}-free, Mg^{2+}-free HBSS supplemented with 10 ng/mL brain-derived neurotrophic factor (BDNF) and 10 ng/mL glial cell-derived neurotrophic factor (GDNF).

2. Pre-anesthesia: acepromazine (3.3 mg/kg, PromAce) and atropine sulfate (0.2 mg/kg, Phoenix Pharmaceuticals).
3. Anesthesia injection: Mix 0.6 mL ketamine (100 mg/mL; Sigma) and 0.15 mL xylazine (20 mg/mL; Phoenix Pharmaceuticals) with 9.25 mL saline, and use 0.1 mL per 10 g body weight.
4. Kopf stereotaxic frame (Kopf Instruments) with mouse adaptor.
5. Betadine.
6. Disposable scalpel.
7. Micro drill sets (Fine Scientific Tools).
8. 5 μL Hamilton syringe with 2′ 28-gauge needle with beveled end.

2.3 Behavioral Analyses

1. Challenging beam test: 1 m beam that starts at a width of 3.5 cm and gradually narrows to 0.5 cm in 1 cm decrements with wire-grid surface (1 cm square).
2. Pole test: 50 cm length round wooden pole vertically fixed on a styrofoam platform.

3 Methods

3.1 In Vitro Differentiation of ES Cells (ESCs)

1. Culture undifferentiated Otx2GFP KI ESCs [11] on gelatin-coated dishes in ES cell medium.
2. Differentiate ESCs into embryoid bodies (EBs) on non-adherent bacterial dishes for 4 days in EB medium.
3. Transfer EBs onto adhesive tissue culture plate. Twenty-four hours after transfer, initiate selection of neuronal progenitor (NP) cells in serum-free ITSFn medium (*see* **Note 3**).
4. After 10 days of selection, trypsinize cells for FACS isolation of dopaminergic neuronal precursors.
5. Trypsinize differentiated cells at the end of stage 3, gently triturate and label by incubating with an anti-Corin antibody in FACS medium for 30 min at 4 °C, followed by incubation for 15 min with Alexa Fluor 647-conjugated anti-rabbit antibodies in FACS medium. Perform all washing steps in FACS medium. Filter stained cells through cell strainer caps (35 mm mesh) to obtain single-cell suspensions (10^7 cells/mL for sorting).
6. Sort stained cells on a fluorescence-activated cell sorter, FACSAria, using FACSDiva software (*see* **Note 4**). Forward- and side-scatter gating identify the population of interest, excluding debris and dead cells. Corin positivity will be determined according to negative controls consisting of absence of

primary antibody and absence of primary and secondary antibodies, whereas GFP positivity will be determined by comparing J1 ESC-derived cells lacking GFP expression. Before sorting, the nozzle, sheath, and sample lines should be sterilized with 70 % ethanol or 2 % hydrogen peroxide for 15 min, followed by washes with sterile water to remove residual decontaminant.

7. Plate sorted OtxGFP$^+$Corin$^+$ NP cells on PLO/FN-coated tissue culture plate or coverslips in NP medium for transplantation or in vitro analysis, respectively. After 4 days of expansion in NP medium, initiate differentiation by changing medium to ND medium for in vitro analysis.

3.2 Stereotaxic Surgery

1. Trypsinize FACS-purified Otx2GFP$^+$Corin$^+$ cells, expanded for 4 days in NP medium, and suspended to a final concentration of 50,000 cells/μL in transplantation medium (*see* **Note 5**).
2. Anesthetize the mice by administering (i.p.) a mixture of acepromazine and atropine sulfate, as pre-anesthetics followed by intraperitoneal administration of ketamine and xylazine.
3. Test depth of anesthesia by foot pinch. If needed (i.e., animal responding to foot pinch), inject half a dose of anesthetics, followed by retesting the animals by foot pinch after 10 min.
4. Load 2 μL of cell solution into a Hamilton syringe and fasten to the stereotaxic frame (*see* **Note 6**).
5. Remove the hair from the surgery area of anesthetized mice, and then place them on the stereotaxic equipment with the mouse adaptor. Secure the skull with ear bars, and then apply betadine to the surgical area and make an incision using a disposable scalpel (*see* **Note 7**) exposing the skull, which will be wiped with betadine.
6. After identification of the stereotaxic coordinate of bregma, calculate the injection site coordinates and mark the injection site (*see* **Note 8**).
7. Using a micro drill make a burr hole at the injection site.
8. Lower the end of the needle to the surface of the dura, and measure ventral coordinate of dura to calculate the coordinate of injection site based on that. Lower the needle to the injection site and slowly inject 1 μL of cell solution at a rate of 0.5 μL/min (*see* **Note 9**).
9. Upon completion of the injection, leave the needle at the injection site for 2 more min to allow time for the cell solution to diffuse. After 2 min, pull the needle up slowly.
10. Remove the mice from the stereotaxic frame and transfer them to a warm heat pad for suture and recovery. After applying betadine solution to the suture site, also apply

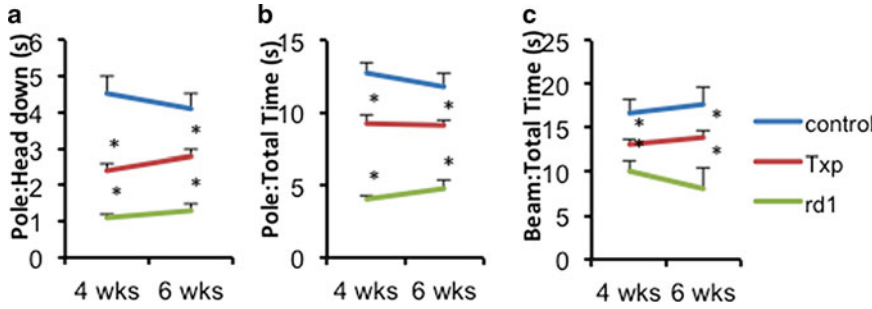

Fig. 1 Otx2GFP + Corin + midbrain dopaminergic neuronal precursors, when transplanted into *aphakia* mice, can ameliorate the behavioral deficit. *Rd1* mice were used as a blind mice control. (**a**, **b**) Pole test. (**c**) Challenging beam test. (Mean ± S.E.M.; $n = 10$)

antibiotic ointment to the area. Also, if needed, ear punch the mice for identification.

11. Upon awakening, transfer the mice to their original cage (*see* **Note 10**).

3.3 Behavioral Analyses

1. Perform nigrostriatal pathway-sensitive motor behavioral tests such as challenging beam and pole tests (*see* **Note 11**) 4 weeks and 6 weeks post transplantation, using mock-transplanted *aphakia* mice and blind retinal degeneration 1 (*rd1*) mutation mice as controls (*see* **Note 12**).
2. For the pole test, place the animals head upward on top of a vertical wooden pole (50 cm in length and 1 cm in diameter) with the base of the pole being placed in the home cage. Once on the pole, the animals orient themselves downward and descend the length of the pole back into their home cage. Train all the animals for 2 days consisting of three trials at each session. On the test day, the animals receive three trials, and the times to orient downward and total travel time are measured (Fig. 1a, b) (Reproduced from ref. 8 with permission from PNAS).
3. For the challenging beam traversal test, measure motor performance with the beam test as described previously [2]. The beam (length, 1 m) starts at a width of 3.5 cm and gradually narrows to 0.5 cm in 1 cm decrements with wire-grid surface (1 cm wire). Train the animals for 2 days to traverse the length of the beam, starting at the widest section and ending at the narrowest section (*see* **Note 13**).
4. While traversing the grid-surfaced beam for a total of three trials, video record the animals and measure times for each animal to traverse as shown in Fig. 1c (Reproduced from ref. 8 with permission from PNAS) (*see* **Note 14**).

4 Notes

1. Gelatin-coated plates can be made in bulk and stored at 4 °C until needed.
2. Poly-L-ornithine and Fibronectin can be mixed together for 30 min coating, or can be incubated for coating serially. Extra coverslips coated with Poly-L-ornithine and Fibronectin can be stored at 4 °C until needed.
3. To increase the proportion of midbrain dopaminergic neuronal precursors, recombinant sonic hedgehog (SHH; 100 ng/mL; R&D systems) or chemical activators of SHH signaling such as Purmorphamine (2 μM; Cayman Chemicals) can be added at the selection stage in ITSFn media [8].
4. In general, we start with approximately 5×10^6 ES cells for in vitro differentiation, resulting in approximately $2–4 \times 10^8$ mixed NP cells at the end of stage 3. Thus, allowing for a certain degree of cell loss during staining and FACS, we usually recover $2–4 \times 10^6$ viable double-positive cells.
5. Adding Boc-Asp(OMe)-fluoromethyl ketone (BAF) to the transplantation medium increases post-transplantation cell viability mildly but significantly [12].
6. Prior to loading the Hamilton syringe with cell solution, make sure to flush the syringe with 70 % ethanol, followed by rinsing with sterile water and then with PBS and make sure that the needle is not clogged. When taking up the cell solution, avoid air bubbles (keep the entire beveled end of the needle in the liquid). Even though 1 μL will be used for injection, taking up 2 μL of cell solution makes it easier to dispense exactly 1 μL of cells.
7. If the animal reacts to the scalpel blade, pause the surgery and inject another half dose of anesthesia, wait 10 min and retest by foot pinch before resuming surgery.
8. We used the following injection site coordinates from bregma: AP + 0.05, L ± 0.18, V –0.30, IB 9.
9. It is important to inject the cell solution slowly to minimize tissue damage caused by the pressure of the sudden injection.
10. If male mice are used, especially make sure to return the mice to their original cage and littermate to avoid fighting.
11. As an additional test for the nigrostriatal pathway-sensitive motor behavioral test, a cylinder test can be performed. Spontaneous movement is measured using a small transparent cylinder (height, 15.5 cm; diameter, 12.7 cm). Mice are placed in the cylinder for 3 min and the number of rears is measured. A rear is defined as an animal's vertical movement with both forelimbs and immediately touching the wall of the cylinder after removing both limbs from the ground. (Reproduced from ref. 8 with permission from Cell Transplant.)

12. Since *aphakia* mice are born blind, we used blind *rd1* mice as control for these behavioral tests, in addition to sham treated *aphakia* mice.
13. Use gentle prodding if necessary during training, until the mice cross the bar readily. Sometimes putting bedding from the home cage at the end point helps.
14. As independent variables, the number of slips and the number of steps taken to traverse could be measured after slow speed playback of the videotape. To measure motor learning, the mean of the slope difference from training day 1 to the testing day (performance on the testing day minus that on the first training day) can be analyzed.

Acknowledgement

This study was supported by NIH grants NS079977, MH048866, MH087903, and NS070577 and a Harvard Stem Cell Institute Seed Grant.

References

1. Hwang DY, Ardayfio P, Kang UJ, Semina EV, Kim KS (2003) Selective loss of dopaminergic neurons in the substantia nigra of Pitx3-deficient aphakia mice. Brain Res Mol Brain Res 114:123–131
2. Hwang DY, Fleming SM, Ardayfio P, Moran-Gates T, Kim H, Tarazi FI, Chesselet MF, Kim KS (2005) 3,4-Dihydroxyphenylalanine reverses the motor deficits in Pitx3-deficient aphakia mice: behavioral characterization of a novel genetic model of Parkinson's disease. J Neurosci 25:2132–2137
3. Dawson T, Mandir A, Lee M (2002) Animal models of PD: pieces of the same puzzle? Neuron 35:219–222
4. Beal MF (2001) Experimental models of Parkinson's disease. Nat Rev Neurosci 2: 325–334
5. Smidt MP, Smits SM, Bouwmeester H, Hamers FPT, van der Linden AJA, Hellemons AJCGM, Graw J, Burbach JP (2004) Early developmental failure of substantia nigra dopamine neurons in mice lacking the homeodomain gene Pitx3. Development 131:1145–1155
6. van den Munckhof P, Luk KC, Ste-Marie L, Montgomery J, Blanchet PJ, Sadikot AF, Drouin J (2003) Pitx3 is required for motor activity and for survival of a subset of midbrain dopaminergic neurons. Development 130:2535–2542
7. Nunes I, Tovmasian LT, Silva RM, Burke RE, Goff SP (2003) Pitx3 is required for development of substantia nigra dopaminergic neurons. Proc Natl Acad Sci U S A 100: 4245–4250
8. Chung S, Moon JI, Leung A, Aldrich D, Lukianov S, Kitayama Y, Park S, Li Y, Bolshakov VY, Lamonerie T, Kim KS (2011) ES cell-derived renewable and functional midbrain dopaminergic progenitors. Proc Natl Acad Sci U S A 108:9703–9708
9. Moon J, Lee HS, Kang JM, Park J, Leung A, Hong S, Chung S, Kim KS (2013) Stem cell grafting improves both motor and cognitive impairments in a genetic model of Parkinson's disease, the aphakia (ak) mouse. Cell Transplant 22:1263–1279
10. Enshell-Seijffers D, Lindon C, Morgan BA (2008) The serine protease Corin is a novel modifier of the Agouti pathway. Development 135:217–225
11. Fossat N, Le Greneur C, Beby F, Vincent S, Godement P, Chatelain G, Lamonerie T (2007) A new GFP-tagged line reveals unexpected Otx2 protein localization in retinal photoreceptors. BMC Dev Biol 7:122
12. Hedlund E, Pruszak J, Lardaro T, Ludwig W, Vinuela A, Kim KS, Isacson O (2008) Embryonic stem cell-derived Pitx3-enhanced green fluorescent protein midbrain dopamine neurons survive enrichment by fluorescence-activated cell sorting and function in an animal model of Parkinson's disease. Stem Cells 26:1526–1536

Chapter 24

Methods for Assessing the Regenerative Responses of Neural Tissue

Steven W. Poser, Maria Adele Rueger, and Andreas Androutsellis-Theotokis

Abstract

In order to establish novel therapeutic paradigms and advance the field of regenerative medicine, methods for their effective implementation as well as rigorous assessment of outcomes are critical. This is especially evident and challenging in the context of treating complex and devastating neurodegenerative disorders, such as Parkinson's disease, multiple sclerosis, and ischemic stroke. Stem cell-based approaches offer great promise in addressing these conditions. Here, we demonstrate an approach for identifying factors that mobilize endogenous neural stem cells in the repair and recovery of the central nervous system of rodents, involving site-specific administration of growth factors that activate particular signal transduction pathways, and that allows for the assessment of outcome utilizing magnetic resonance imaging and immunohistochemistry.

Key words Stem cells, Regenerative medicine, Neurodegeneration, Magnetic resonance imaging, Immunohistochemistry

1 Introduction

The well recognized ability of lower order organisms, such as amphibians, to grow back entire limbs points towards the existence of mechanisms for dramatic regeneration. However, in higher organisms, this level of plasticity is lost. One important consequence of this is seen in the brain and the ability to form long term memories. You can imagine a level of rigidity is required to maintain the neural network necessary for robust information storage and retrieval. However, as often demonstrated following ischemic stroke, the brain retains a reparative capacity that allows for a degree of functional recovery. The ability to augment this capacity represents a holy grail for regenerative medicine in the treatment of traumatic injury, neurodegenerative disorders, and even the natural losses due to aging.

Bruno Christ et al. (eds.), *Animal Models for Stem Cell Therapy*, Methods in Molecular Biology, vol. 1213,
DOI 10.1007/978-1-4939-1453-1_24,

A population of neural stem cells (NSCs) that reside in the adult brain plays an important role in maintaining the central nervous system (CNS) as well as in recovery from damage. These cells were originally identified as the result of experiments demonstrating that new neurons are generated in the adult mammalian brain from a slowly dividing population of cells that incorporate proliferation markers such as BrdU [1, 2]. Subsequent experiments identified markers that established niches where they reside, the subventricular zone and the subgranular zone of the hippocampus [3, 4], where the cells are identified by staining for expression of specific markers, such as nestin or Sox2 [5, 6]. More recently, with the identification of additional markers, the population of stem cells appears to be more widespread than previously thought, being found throughout the cortex as a largely quiescent population of cells [7]. A common characteristic they all share is a tight association with blood vessels; they are also able to respond to signals generated from the vasculature such as Notch ligands and Angiopoietin 2 with increased proliferation and survival [8]. In addition, when placed into culture, cells isolated from these areas demonstrate their multipotent character, being able to differentiate into neurons, astrocytes and oligodendrocytes [9]. This leads to a more detailed understanding of the mechanisms that underlie fate choices, and how they can be manipulated in vitro through specific treatment regiments.

Given these insights, and the observations that stem cells are mobilized following traumatic insults to the brain [10–12], the prospect of employing these cells for therapeutic benefit became a real possibility. Extensive preclinical work in animal models demonstrates this to be the case for neurological diseases such as spinal cord injury, stroke, and amyotrophic lateral sclerosis [13–18]. In some models, neural stem cells harvested from allogeneic sources are expanded in culture, directed to differentiate towards a specific fate, such as dopamine neurons, then implanted into the brain to replace lost neurons in for example Parkinson's disease [19–21]. Neural stem cells isolated from fetal tissue are not the only cellular source that has proven some degree of therapeutic usefulness. Embryonic stem cells as well as induced pluripotent stem (iPS) cells generated from adult somatic tissue both have demonstrated benefit in neurodegenerative models after differentiation into specific fates [22, 23]. Some of these approaches have even moved into early clinical trials in humans [24, 25]. However, issues regarding the number of therapeutically relevant cells that survive implantation, the possibility of tumor formation, the most efficacious route of administration and the potential for host rejection of the allogeneic cells still persist [26]. A promising alternative approach is to stimulate regeneration by mobilizing endogenous NSCs through pharmacological manipulation of specific signal transduction

cascades to affect recovery [27]. In neurodegenerative disorders, these cells likely provide their own trophic support to improve neuronal cell survival, and additionally possess the potential to physically replace lost neurons.

Regardless of the therapeutic avenue taken, means for critically assessing the changes in the CNS that correlate with differences in outcome, measures are essential to predict the therapeutic efficacy of a given treatment and facilitate its translation into clinical studies. Ideally, outcome parameters will be assessed noninvasively, i.e., by imaging and behavioral tests. Here, we present methodologies (1) for the introduction of pharmaceuticals aimed at expanding the NSC niche, as well as (2) to monitor the therapeutic efficacy of these treatments in an animal model of neurodegenerative disease through Magnetic Resonance Imaging (MRI).

2 Materials

2.1 Stereotactic Injection

1. Stereotactic injection frame for rats.
2. Hamilton syringe suitable for injection of 5 μL volumes.
3. Isoflurane liquid for inhalation (Baxter, Deerfield, IL, USA).
4. 10 % betadine solution (Purdue Pharma, Stamford, CT, USA).

2.2 MRI Analysis

1. 120 mM isotonic $MnCl_2$ solution (Sigma-Aldrich Co, MO, USA).
2. 21 cm horizontal bore 7T scanner on an Avance platform.
3. Isoflurane liquid for inhalation (Baxter, Deerfield, IL, USA).
4. Stereotaxic holder for MRI.

2.3 Immunohistochemistry

1. Phosphate-buffered saline (PBS) pH 7.4 (Sigma Aldrich Co., St. Louis, MO, USA).
2. 4 % Formaldehyde solution in PBS pH 7.4 (Affymetrix Inc., Cleveland, OH, USA).
3. 30 % Sucrose solution: Dissolve 150 g of sucrose in water to yield a final volume of 500 mL. Pass through a sterile filter and store at 4 °C.
4. Embedding molds (Polysciences Inc., Warrington, PA, USA).
5. Neg50 freezing medium (Thermo Scientific, Waltham, MA, USA).
6. Cryostat to generate 16–30 μm brain sections.
7. Superfrost Plus glass microscope slides (Thermo Scientific, Waltham, MA, USA).
8. 0.02 M sodium citrate solution: Dissolve 588 mg of sodium citrate dihydrate in 100 mL water. Adjust pH to 6.0.
9. 2 N HCl: Dilute 2 mL of concentrated HCl (37 %) in 22 mL water.

10. Bromodeoxyuridine (BrdU) solution: Dissolve BrdU (Sigma Aldrich Co., St. Louis, MO, USA) at a concentration of 10 mg/mL in sterile PBS. Store at −20 °C.
11. Permeabilization buffer: 0.5 % Triton X-100/PBS. Add 500 μL of 10 % Triton X-100 to 9.5 mL PBS. Mix well. Make fresh for each use (*see* **Note 1**).
12. Blocking buffer: 5 % normal serum/5 % bovine serum albumin (BSA)/PBS. Dissolve 500 mg of BSA in 9.5 mL PBS. Add 500 μL of normal serum (*see* **Note 2**). Store at −20 °C.
13. Antibody dilution buffer: 3 % BSA/0.1 % Tween 20/PBS. Dissolve 300 mg of BSA in 10 mL PBS. Add 100 μL 10 % Tween 20. Mix well.
14. Wash buffer: 0.1 % Tween 20/PBS. Add 1 mL 10 % Tween 20 to 99 mL PBS. Mix well.
15. Hes3 antibody (Santa Cruz Biotechnology, Dallas, TX, USA).
16. BrdU antibody (Accurate Chemical and Scientific Corp, Westbury, NY, USA).
17. RECA-1 antibody (AbD Serotec, Raleigh, NC, USA).
18. CD31 antibody (Dako Inc., Carpentaria, CA, USA).
19. Nestin antibody (EMD Millipore Corp., Billerica, MA, USA).
20. Sox2 antibody (R&D Systems Inc., Minneapolis, MN, USA).
21. Beta tubulin III (TuJ1) antibody (Covance Inc., Princeton, NJ, USA).
22. GFAP antibody (Dako Inc., Carpentaria, CA, USA).
23. CNPase antibody (EMD Millipore Corp., Billerica, MA, USA).
24. 5 mg/mL 4′,6-diamidino-2-phenylindole (DAPI) solution: Dissolve 5 mg of DAPI (Sigma Aldrich Co., St. Louis, MO, USA) in methanol. Store at −20 °C.

3 Methods

Please consult with your institution's veterinary policy (IACUC or other animal welfare board) regarding appropriate animal handling and euthanasia guidelines.

3.1 Stereotactic Injection

1. Place a male Sprague Dawley rat 3–6 months of age, 250–300 g into anesthesia using 1.5 % isoflurane (*see* **Note 3**).
2. Position the rat's head into the stereotactic frame.
3. Place a nosecone attached to an isoflurane source over the rat's snout.

4. To prevent the rat's eyes from drying, cover them with ophthalmic ointment.
5. Sterilize the surface of the head with betadine solution.
6. Make an incision down the midline of the skull, and retract the skin.
7. Place the Hamilton syringe to be used for administration of compounds into the stereotactic frame. Center the tip of the needle at bregma, and lower the needle so that it touches the skull. Take note of the AP, ML, and DV measurements as these represent a zeroing of the coordinates.
8. Raise the tip of the needle slightly, then move it to coordinates bregma AP −0.9 mm, ML −1.4 mm.
9. Move the needle sufficiently out of the way so a small hole can be drilled at these coordinates using a #74 bit.
10. Lower the needle through the hole to DV +3.8 mm.
11. Deliver 5 μL of compounds of interest at a rate of 1 μL/min.
12. After the injection is finished, leave the syringe in place for 5 min, then retract the needle slowly until it is clear of the skull.
13. Suture the incision.
14. Remove the rat from the stereotactic frame and return it to its home cage.
15. Provide postoperative analgesics as per institutional guidelines.

3.2 MRI Analysis

1. Twenty four hours prior to imaging, inject the rat i.p. with 30 mg/kg $MnCl_2$ as a contrast agent.
2. Anesthetize the rat using 1.5 % isoflurane and place it in stereotaxic holder with the brain centered in a 72/25 mm volume transmit/surface receiver coil assembly.
3. Maintain the body core temperature at 37 °C using a warm air flow over the rat, and monitor the respiration cycle using a pressure transducer.
4. Place the rat into the MRI scanner.
5. Generate scout images by making three mutually perpendicular slice images through the brain.
6. Acquire T_2-weighted images with a fast spin echo (FSE) sequence (matrix = 256 × 2, echoes = 8, TR/TE = 3500/14.15 ms, field of view = 3.2 cm), fourteen contiguous 1 mm thick axial images through the area of interest (i.e., the striatum).
7. Capture an identical set of FSE images with T_1 weighting (TR/TE = 355/10.25 ms) (Fig. 1) (*see* **Notes 4** and **5**).

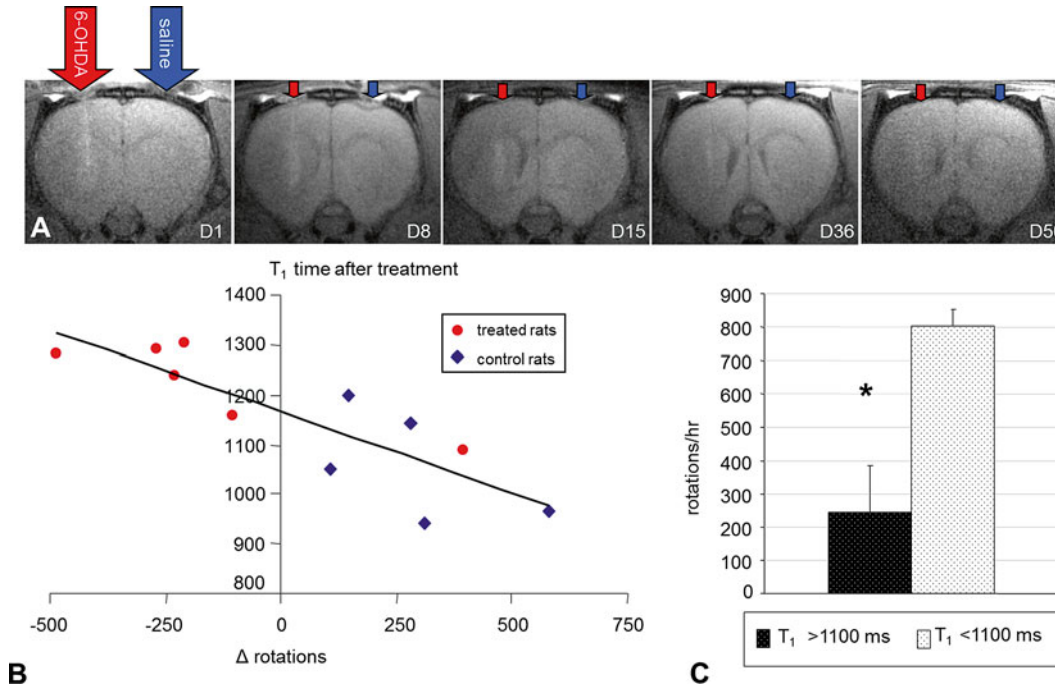

Fig. 1 T_1-weighted MRI to monitor both the severity of 6-OHDA induced lesions as well as treatment effects. (**a**) Injecting 6-OHDA into the striatum of adult rats led to a T_1-hyperintensity in the Manganese-enhanced MRI (MEMRI) for several weeks. (**b**) T_1-weighted MRI to monitor the response to neuroprotective treatments. After a pharmacological treatment to rescue DA neurons, the Mn^{2+}-induced shortening of T_1 correlated with the treatment effect ($R^2 = 0.72$, $p < 0.001$). (**c**) Stratifying the rats based on their T_1 time as assessed by MEMRI 14 days after lesion allowed for predicting the behavioral deficits as assessed by rotometry after 6 weeks (means ± STD, $p < 0.001$)

3.3 Immuno-histochemistry

1. To assess changes in cell proliferation, inject animals with 50 mg/kg BrdU i.p. every 12 h for 5 days beginning on day 1 postoperative to label dividing cells.
2. Place the rat under deep anesthesia using 2.5 % isoflurane.
3. Perfuse the rat via transcardial administration of PBS, followed by 4 % formaldehyde.
4. Decapitate the rat and remove the brain from the skull.
5. Post-fix the brain by placing it in 4 % formaldehyde solution overnight at 4 °C.
6. Cryoprotect the brain using incubation in 30 % sucrose for 3 days at 4 °C.
7. Place a small volume of freezing medium into the bottom of an embedding mold. Set the brain into the embedding mold, then fill the remainder of the volume with freezing medium.

8. Let the embedding mold sit in dry ice until frozen solid (*see* **Note 6**).
9. Generate sequential 16–30 μm sections, starting at approximately bregma +2.20 mm using a cryostat and mount the sections to a glass slide. In the case of examining the subventricular zone, sections can be taken between bregma +1.70 and −0.40 mm. For the substantia nigra, sections between bregma −4.80 and −6.30 mm can be used, while sections between bregma −3.14 and −5.30 mm can be used to evaluate the hippocampus (*see* **Note 7**).
10. Remove any excess mounting medium from the slide.
11. Perform BrdU antigen retrieval by boiling the sections in 0.02 M sodium citrate solution pH 6.0 in a microwave oven for 5 min.
12. Wash the slides with PBS 3 times for 5 min.
13. Incubate the slides in 2 N HCl for 45 min at room temperature.
14. Wash the slides with PBS 3 times for 5 min.
15. Permeabilize the sections by incubating with permeabilization solution for 10 min at room temperature.
16. Block the sections with blocking buffer for 1 h.
17. Add primary antibodies diluted in antibody dilution buffer and incubate overnight at room temperature (*see* **Note 8**). For staining neural stem cells: Hes3, Nestin, Sox2. For staining proliferating cells: BrdU. For assessing changes in blood vessels: RECA-1, CD31. For staining neurons, astrocytes, and/or oligodendrocytes: TuJ1, GFAP, CNPase.
18. Wash the slides three times with wash buffer for 5 min each.
19. Dilute appropriate secondary antibodies in antibody dilution buffer and apply to the sections. Incubate for 1 h at room temperature (*see* **Note 9**).
20. Wash the slides three times with wash buffer for 5 min each.
21. Incubate the slides with DAPI diluted 1:10,000 in PBS solution for 5 min at room temperature.
22. Wash one time for 10 min with PBS.
23. Place a small volume of aqueous mounting medium onto the sections and cover with a coverslip taking care not to trap any bubbles underneath.
24. The slides are now ready for visualization using a fluorescent microscope (Fig. 2) (*see* **Notes 10** and **11**).

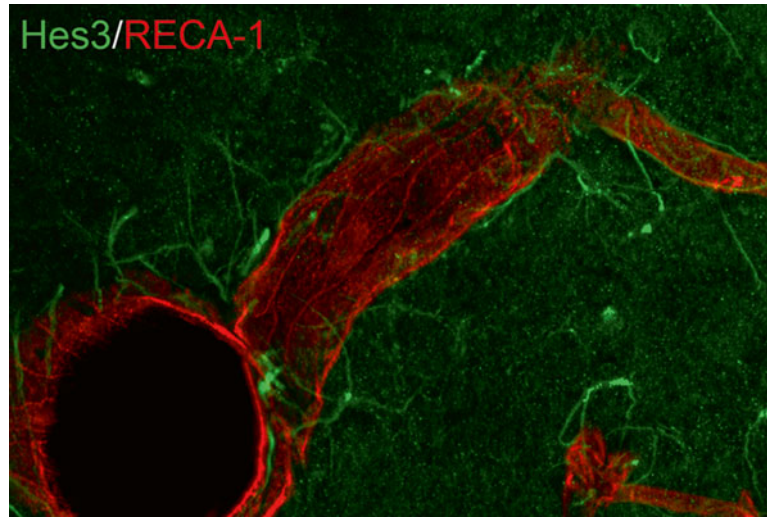

Fig. 2 Immunohistochemistry of NSC and blood vessel architecture in the adult rat midbrain. Hes3 positive cells (*green*) are in close proximity to blood vessels (*red*) in the adult rat midbrain. 5 days prior to imaging, the rat was given a single injection of a mixture of Delta4, Angiopoietin 2, and a JAK inhibitor, a treatment paradigm that increases the number of Hes3 positive cells [31]

4 Notes

1. 0.5 % NP-40 can also be used for permeabilizing the cells.
2. Use normal serum appropriate for the secondary antibody to be utilized for immunofluorescence. For example, goat serum for antibodies generated in goats.
3. Alternative anesthesia protocols suitable for use in the stereotactic injections procedure are discussed in [28].
4. In addition to the cellular changes that occur as a result of a given treatment paradigm, behavioral assessment is often performed as an important measure of successful intervention. These can include, for example, rotometry for Parkinson's disease (Fig. 1c) [29] and limb placement tests for stroke [30].
5. When calculating quantitative T_1 maps, take into account the perturbations caused by the flip angle.
6. Blocks can be stored at −80 °C for later sectioning.
7. The slides can be stored at −80 °C for later immunohistochemical analysis. When removed from the freezer, let the slides dry at room temperature for 20 min prior to staining.
8. The volume of antibodies used can be reduced by drawing a border around the sections using a hydrophobic pen. This allows for as little as 100–200 μL of antibody dilution to be

placed directly onto the section, instead of immersing the entire slide into a slide jar. Be sure to allow the border to dry completely prior to adding antibody solution.

9. Incubation with secondary antibodies should be kept in the dark by placing into a light-tight container. All subsequent steps should be performed under reduced light conditions to avoid diminishing the intensity of the fluorescent signal.
10. The slides can be stored at 4 °C for later analysis.
11. As a supplement to the above procedures, changes in specific cell populations can be assessed. A commonly used example is immunohistochemistry staining for tyrosine hydroxylase to examine the effect of a given treatment on dopamine neurons in models of Parkinson's disease. This can be used in conjunction with FluoroGold labeling for neuronal tract tracing experiments as described in [31].

Acknowledgements

This work was funded (in part) by the Helmholtz Alliance ICEMED—Imaging and Curing Environmental Metabolic Diseases, through the Initiative and Network Fund of the Helmholtz Association, and a grant from the Deutsche Forschungsgemeinschaft (SFB 655: Cells into tissues).

References

1. Altman J, Das GD (1965) Autoradiographic and histological evidence of postnatal hippocampal neurogenesis in rats. J Comp Neurol 124(3):319–335
2. Kaplan MS, Hinds JW (1977) Neurogenesis in the adult rat: electron microscopic analysis of light radioautographs. Science 197(4308): 1092–1094
3. Luskin MB (1993) Restricted proliferation and migration of postnatally generated neurons derived from the forebrain subventricular zone. Neuron 11(1):173–189
4. Reynolds BA, Weiss S (1992) Generation of neurons and astrocytes from isolated cells of the adult mammalian central nervous system. Science 255(5052):1707–1710
5. Lendahl U, Zimmerman LB, McKay RD (1990) CNS stem cells express a new class of intermediate filament protein. Cell 60(4): 585–595
6. Graham V, Khudyakov J, Ellis P, Pevny L (2003) SOX2 functions to maintain neural progenitor identity. Neuron 39(5):749–765
7. Androutsellis-Theotokis A, Rueger MA, Mkhikian H, Korb E, McKay RD (2008) Signaling pathways controlling neural stem cells slow progressive brain disease. Cold Spring Harb Symp Quant Biol 73:403–410
8. Androutsellis-Theotokis A, Rueger MA, Park DM, Boyd JD, Padmanabhan R, Campanati L, Stewart CV, LeFranc Y, Plenz D, Walbridge S, Lonser RR, McKay RD (2010) Angiogenic factors stimulate growth of adult neural stem cells. PLoS One 5(2):e9414
9. Cattaneo E, McKay R (1991) Identifying and manipulating neuronal stem cells. Trends Neurosci 14(8):338–340
10. Jin K, Minami M, Lan JQ, Mao XO, Batteur S, Simon RP, Greenberg DA (2001) Neurogenesis in dentate subgranular zone and rostral subventricular zone after focal cerebral ischemia in the rat. Proc Natl Acad Sci U S A 98(8): 4710–4715
11. Zhang RL, Zhang ZG, Zhang L, Chopp M (2001) Proliferation and differentiation of progenitor cells in the cortex and the subventricular

zone in the adult rat after focal cerebral ischemia. Neuroscience 105(1):33–41

12. Nakatomi H, Kuriu T, Okabe S, Yamamoto S, Hatano O, Kawahara N, Tamura A, Kirino T, Nakafuku M (2002) Regeneration of hippocampal pyramidal neurons after ischemic brain injury by recruitment of endogenous neural progenitors. Cell 110(4):429–441
13. Cummings BJ, Uchida N, Tamaki SJ, Salazar DL, Hooshmand M, Summers R, Gage FH, Anderson AJ (2005) Human neural stem cells differentiate and promote locomotor recovery in spinal cord-injured mice. Proc Natl Acad Sci U S A 102(39):14069–14074
14. Ogawa Y, Sawamoto K, Miyata T, Miyao S, Watanabe M, Nakamura M, Bregman BS, Koike M, Uchiyama Y, Toyama Y, Okano H (2002) Transplantation of in vitro-expanded fetal neural progenitor cells results in neurogenesis and functional recovery after spinal cord contusion injury in adult rats. J Neurosci Res 69(6):925–933
15. Chu K, Kim M, Park KI, Jeong SW, Park HK, Jung KH, Lee ST, Kang L, Lee K, Park DK, Kim SU, Roh JK (2004) Human neural stem cells improve sensorimotor deficits in the adult rat brain with experimental focal ischemia. Brain Res 1016(2):145–153
16. Jeong SW, Chu K, Jung KH, Kim SU, Kim M, Roh JK (2003) Human neural stem cell transplantation promotes functional recovery in rats with experimental intracerebral hemorrhage. Stroke 34(9):2258–2263
17. Klein SM, Behrstock S, McHugh J, Hoffmann K, Wallace K, Suzuki M, Aebischer P, Svendsen CN (2005) GDNF delivery using human neural progenitor cells in a rat model of ALS. Hum Gene Ther 16(4):509–521
18. Kim SU, Lee HJ, Kim YB (2013) Neural stem cell-based treatment for neurodegenerative diseases. Neuropathology 33(5):491–504
19. Studer L, Tabar V, McKay RD (1998) Transplantation of expanded mesencephalic precursors leads to recovery in parkinsonian rats. Nat Neurosci 1(4):290–295
20. O'Keeffe FE, Scott SA, Tyers P, O'Keeffe GW, Dalley JW, Zufferey R, Caldwell MA (2008) Induction of A9 dopaminergic neurons from neural stem cells improves motor function in an animal model of Parkinson's disease. Brain 131(Pt 3):630–641
21. Sanchez-Pernaute R, Studer L, Bankiewicz KS, Major EO, McKay RD (2001) In vitro generation and transplantation of precursor-derived human dopamine neurons. J Neurosci Res 65(4):284–288
22. Sun N, Longaker MT, Wu JC (2010) Human iPS cell-based therapy: considerations before clinical applications. Cell Cycle 9(5):880–885
23. Srivastava AS, Malhotra R, Sharp J, Berggren T (2008) Potentials of ES cell therapy in neurodegenerative diseases. Curr Pharm Des 14(36):3873–3879
24. Lindvall O, Kokaia Z, Martinez-Serrano A (2004) Stem cell therapy for human neurodegenerative disorders-how to make it work. Nat Med 10(Suppl):S42–S50
25. NIH Clinical Trial Database http://clinicaltrials.gov
26. Lindvall O, Kokaia Z (2010) Stem cells in human neurodegenerative disorders-time for clinical translation? J Clin Invest 120(1):29–40
27. Kittappa R, Bornstein SR, Androutsellis-Theotokis A (2012) The role of eNSCs in neurodegenerative disease. Mol Neurobiol 46(3):555–562
28. Flecknell PA (1987) Laboratory animal anaesthesia: an introduction for research workers and technicians. Academic Press, San Diego, London
29. Schwarting RK, Huston JP (1996) The unilateral 6-hydroxydopamine lesion model in behavioral brain research. Analysis of functional deficits, recovery and treatments. Prog Neurobiol 50(2–3):275–331
30. Markgraf CG, Green EJ, Hurwitz BE, Morikawa E, Dietrich WD, McCabe PM, Ginsberg MD, Schneiderman N (1992) Sensorimotor and cognitive consequences of middle cerebral artery occlusion in rats. Brain Res 575(2):238–246
31. Androutsellis-Theotokis A, Rueger MA, Park DM, Mkhikian H, Korb E, Poser SW, Walbridge S, Munasinghe J, Koretsky AP, Lonser RR, McKay RD (2009) Targeting neural precursors in the adult brain rescues injured dopamine neurons. Proc Natl Acad Sci U S A 106(32):13570–13575

Chapter 25

Mesenchymal Stem Cell-Based Therapy in a Mouse Model of Experimental Autoimmune Encephalomyelitis (EAE)

Annie C. Bowles, Brittni A. Scruggs, and Bruce A. Bunnell

Abstract

Multiple sclerosis (MS) is a common neurodegenerative disease that presents after an auto-reactive immune response against constituents of the central nervous system. Demyelination, inflammation, and white matter lesions are all hallmarks of this disease. Clinical research supports the use of mesenchymal stem cells (MSCs) as therapy for MS to ameliorate symptoms and pathology. MSCs can be isolated from multiple tissues, including adipose and bone marrow, and are able to migrate to sites of pathology, release anti-inflammatory factors, and provide immunomodulatory and neuroprotective effects once administered. Numerous studies have demonstrated the beneficial effects of MSCs in experimental autoimmune encephalomyelitis (EAE), an induced model of MS. EAE can be induced in several species; however, the mouse is commonly used for therapeutic testing. In the following chapter, scientists will be able to learn how to prepare reagents and MSCs (e.g., isolate, culture, and expand) as well as skillfully execute induction of EAE in mice and administer stem cell-based treatments. Standard methods used to evaluate the disease progression and analyze postmortem tissues are also included.

Key words Multiple sclerosis, Murine experimental autoimmune encephalomyelitis, EAE, T cell-mediated autoimmune disease, Mesenchymal stem cells, Myelin oligodendrocyte glycoprotein

1 Introduction

Multiple sclerosis (MS) is a neurodegenerative disease affecting over 300,000 people in the USA making it the leading cause of neurological impairment, especially in young adults [1]. More specifically, MS is generated by an autoimmune response against constituents of the central nervous system (CNS) that manifests as various symptoms that distinguishes the four subtypes of the disease: relapsing-remitting, primary progressive, secondary progressive, and progressive relapsing [1, 2]. Evidence suggests that T cells lose self-tolerance and attack their own nervous system due to exposure to a stimulatory molecule that structurally resembles myelin. Once stimulated to attack myelin or myelin-producing

Bruno Christ et al. (eds.), *Animal Models for Stem Cell Therapy*, Methods in Molecular Biology, vol. 1213,
DOI 10.1007/978-1-4939-1453-1_25,

cells, the cytotoxic and pathogenic helper T cells initiate the inflammatory processes characteristic of MS [3]. The induction phase of the disease is associated with an increase in cytotoxic $CD8^+$T cells within the CNS that destroy oligodendrocytes, leading to inflammation, demyelination, and damage to the blood–brain barrier (BBB) [3, 4]. Compromise to the BBB allows infiltration of immune cells, such as $CD4^+$T cells and macrophages, into the CNS. These cells further enhance the pathology to the CNS tissues by producing demyelinating lesions of the white matter, reactive gliosis, and increasing axonal loss [3, 5]. Currently, there are several FDA-approved drugs available for relapsing-remitting MS [1, 6]; however, there is still no cure for MS and no effective treatments available for the progressive forms.

Mesenchymal stem cells (MSCs) have recently been tested in clinical trials as therapy for MS patients, and all trials have demonstrated the safety of MSCs in these patients using autologous MSCs without the use of immunosuppression [6–8]. MSCs are isolated from adipose tissue and bone marrow and are capable of homing to damaged areas [9], providing immunomodulatory effects [10, 11], and inducing neuroregeneration through neuroprotective mechanisms [12]. More specifically for MS, these stem cells have the ability to inhibit the migration of T cells from the periphery to the CNS [13, 14], and multiple animal models of MS have had significant symptomatic alleviation, improved CNS pathology, and decreased inflammation after MSC transplantation [13, 15–17].

MS-like symptoms can be induced in many species (e.g., mouse, rat, guinea pigs, rabbits, and primates); however, the mouse is most commonly used for therapeutic screening for MS. The mouse can be induced with experimental autoimmune encephalomyelitis (EAE) using purified myelin, myelin protein, spinal cord homogenate, or a myelin oligodendrocyte glycoprotein (MOG) peptide in the presence of an adjuvant with *Mycobacterium tuberculosis* and pertussis toxin [13, 18]. EAE results in widespread brain inflammation and demyelination throughout the CNS, making it the prototype for T cell-mediated autoimmune diseases [17], as well as an ideal model for progressive forms of MS. The administration of a myelin product stimulates the animal's T cells to recognize its own myelin as foreign, whereas the adjuvant and pertussis toxin are administered to generate inflammation and increase the permeability of the BBB, respectively [13, 17]. After induction, EAE-induced mice have increased levels of infiltrating immune cells in the CNS and present with lesions similar to those seen in MS patients [17].

Several methods are used to evaluate the efficacy of stem cell-based treatments. Clinical scoring is a widely used method based on assessments of the motor functions of research animals. A concise description of scoring: Score 0—no disease, Score 1—tail atony, Score 2—hind limb weakness, Score 3—partial hind limb paralysis, Score 4—complete hind limb paralysis and incontinence,

Score 5—moribund or dead. A more objective means to assess motor function capabilities is by recording the animals in an arena over a set time period. Videos can then be uploaded and analyzed with Noldus EthoVision XT7 software for quantification of several spatial parameters [19, 20].

Standard techniques exist to quantitatively compare groups of research animals for postmortem histological analyses. Histological staining of CNS tissues can quantify (de)myelination and infiltration of immune cells using Luxol fast blue (LFB) and hematoxylin and eosin (H & E), respectively. Immunohistochemistry (IHC) uses antibody-mediated detection of markers to localize specific cells or tissues prepared on microscope slides. Detection of such antigens on CNS infiltrating immune cells allows identification and quantification of cell populations pertinent to this model.

2 Materials

2.1 Induction of EAE

1. C57BL/6 female mice, 6–8 weeks old.
2. Lyophilized MOG_{35-55} peptide.
3. *Mycobacterium tuberculosis* H37 RA, desiccated.
4. Lyophilized pertussis toxin.
5. Complete Freund's adjuvant (CFA).
6. 5 cc emulsifying glass syringes with metal Luer lock tip.
7. Metal micro-emulsifying needle with reinforcing bar, 13G 2-7/8″.
8. 50 mL polystyrene reagent reservoir.
9. 1 mL Luer lock disposable syringes with 0.1 mL graduations.
10. 27G ½″ needles.
11. Isoflurane.
12. Biosafety laminar flow hood.
13. Anesthesia induction chamber for small animals.
14. Anesthetic vaporizer machine with oxygen tank.

2.2 Bone Marrow-Derived Stem Cell (BMSC) Isolation

1. Femurs and tibias.
2. Scissors.
3. 50 mL conical tube.
4. Phosphate-buffered saline (PBS).
5. Complete expansion medium (CEM).
6. 25G 1″ needle.
7. 5 mL disposable syringe with Luer lock tip.
8. 70 μm mesh strainer.

9. Trypan blue.
10. Microcentrifuge tubes.
11. Hemocytometer.
12. Micropipettes and pipettes with tips.
13. 140 × 20 mm cell culture dishes.
14. Large centrifuge.

2.3 Adipose-Derived Stem Cell (ASC) Isolation

1. Subcutaneous/inguinal fat tissue.
2. Scissors.
3. Scale with measurements in grams.
4. 50 mL conical tubes.
5. PBS.
6. 265 units/mg Collagenase type-1.
7. Bovine serum albumin (BSA).
8. 2 mM calcium chloride in ddH_2O ($CaCl_2$).
9. 70 μm mesh strainer (optional).
10. Parafilm.
11. Complete expansion medium (CEM).
12. 50 mL Steriflip disposable vacuum filtration system with 0.22 μm filter.
13. Vacuum tubing.
14. Timer.
15. Wedge-shaped object.
16. Trypan blue.
17. Microcentrifuge tubes.
18. Hemocytometer.
19. Micropipettes and pipettes with tips.
20. T225 cell culture flasks.
21. Incubator shaker.
22. Large centrifuge.

2.4 Cell Culture, Expansion, and Injection Preparation

1. Phosphate-buffered saline (PBS).
2. Hank's balanced salt solution (HBSS).
3. Dulbecco's Minimum Essential Medium: Nutrient Mixture F-12 (DMEM/F-12 medium).
4. Fetal bovine serum (FBS).
5. 2 mM L-glutamine.

6. 10,000 units/mL penicillin—10,000 μg/mL streptomycin (Pen-Strep).
7. 140 × 20 mm cell culture dishes.
8. T225 cell culture flasks.
9. 0.25 % Trypsin–EDTA.
10. Trypan blue.
11. Microcentrifuge tubes.
12. Cryovials.
13. Dimethylsulfoxide (DMSO).
14. Stericup vacuum-mediated 0.22 μm filter unit.
15. 1 mL Luer lock disposable syringes with 0.1 mL graduations.
16. 27G ½″ needle.
17. Micropipettes and pipettes with tips.
18. Hemocytometer.
19. Aspirator.
20. Water bath.
21. Large centrifuge.
22. CO_2 incubator.
23. Biosafety hood.
24. Liquid nitrogen dewar.

2.5 Motor Function Testing

1. Cylindrical arena.
2. White paper.
3. Ring stand.
4. Webcam, video capture software, and computer.
5. Noldus EthoVision XT7 software.
6. Biosafety hood.

3 Methods

3.1 Induction of EAE

3.1.1 Reagent Preparation

It is important to prepare an overestimated amount of reagents to compensate for loss during emulsification and transfer into syringes. For example, for induction of 20 mice, prepare reagents for 25 mice (Fig. 1).

Preparing MOG/CFA emulsion:

1. Place all materials in a sterilized biosafety hood.
2. Add CFA to sterile reagent reservoir.
3. Reconstitute lyophilized *M. tuberculosis* powder in ddH_2O to make 1 mg/mL bacteria stock.

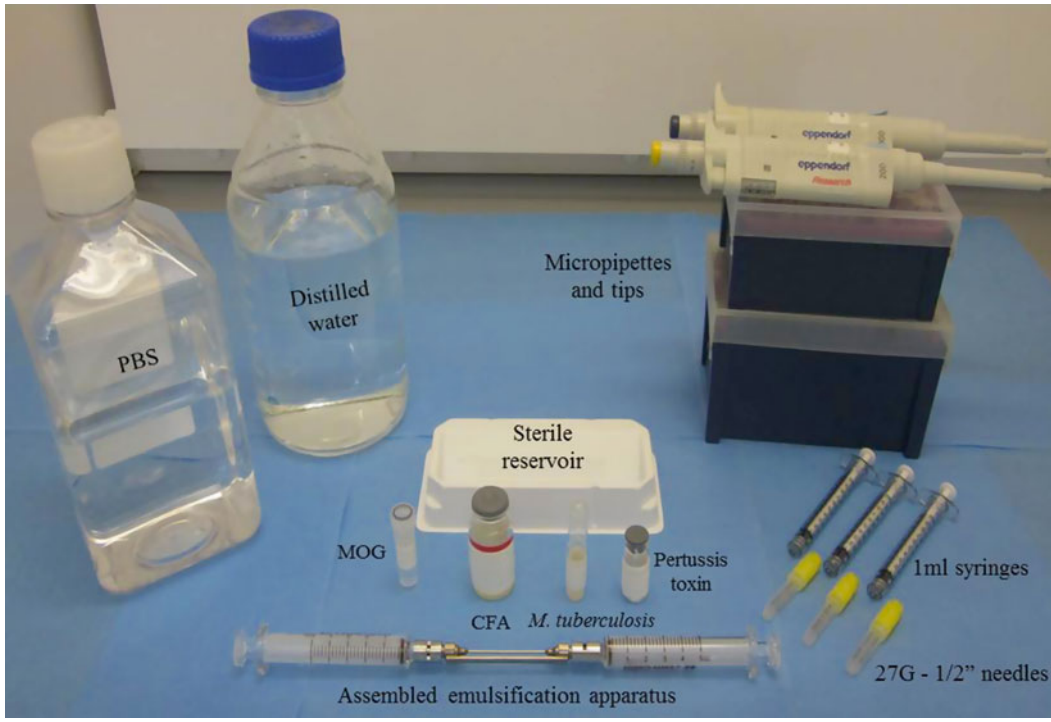

Fig. 1 Materials for induction of EAE. Induction of EAE requires administration of emulsified reagents, i.e., myelin oligodendrocyte glycoprotein (MOG) peptide, complete Freund's adjuvant (CFA), *Mycobacterium tuberculosis*, and pertussis toxin

4. Add appropriate volume of bacteria stock to CFA to make 5 mg/mL CFA/*M. tuberculosis*. Store bacteria stock in 4 °C.
5. Reconstitute lyophilized MOG_{35-55} peptide in PBS to make 2 mg/mL solution.
6. Add (v/v) MOG_{35-55} peptide solution to 5 mg/mL CFA/*M. tuberculosis* in reservoir.
7. Assemble one emulsification syringe with micro-emulsifying needle.
8. Place needle tip into a corner of the reservoir with gathered reagents.
9. Draw reagents into the syringe until completely collected in syringe.
10. Secure second syringe to free tip of the micro-emulsifying needle.
11. Emulsify reagents by pushing reagents into alternating syringes for about 45 min to 1 h to ensure product is fully emulsified (*see* **Note 1**).
12. Collect MOG/CFA emulsion into one syringe.
13. Unscrew empty syringe from emulsifying needle.

14. Screw on 1 mL Luer lock tip disposable syringe to free end of micro-emulsifying needle.
15. Securely fill disposable syringe by pushing glass syringe containing MOG/CFA emulsion (*see* **Note 2**).
16. Screw on 27G ½″ needle.
17. Repeat **steps 14–16** until all MOG/CFA emulsion is transferred to disposable syringes.

Preparing 2 ng/μL pertussis toxin solution:

1. Reconstitute lyophilized powder in ddH_2O to make a 100 ng/μL stock solution.
2. Add appropriate volume of stock solution to PBS to make a 2 ng/μL pertussis toxin solution. Store stock solution at 4 °C.

3.1.2 Induction Procedure

Each animal receives a total of 200 μL of MOG/CFA emulsion. For example, administer two 100 μL injections of MOG/CFA emulsion, one injection per flank. At the time of induction, each animal receives a single 100 μL injection of the 2 ng/μL pertussis toxin solution, and each animal receives a second 100 μL injection of the 2 ng/μL pertussis toxin solution 48 h after induction (Fig. 2).

1. Fill anesthetic vaporizer machine with Isoflurane gas. Open oxygen dial to allow oxygen to combine with Isoflurane gas.
2. Set output to 4 % Isoflurane gas in oxygen.
3. Place mouse in anesthesia induction chamber to induce anesthesia by inhalation.
4. Monitor respiratory rate. Once slowed, relocate the mouse to auxiliary nosepiece.
5. Administer 100 μL of MOG/CFA emulsion via subcutaneous injection into right flank near tail (Fig. 2a).

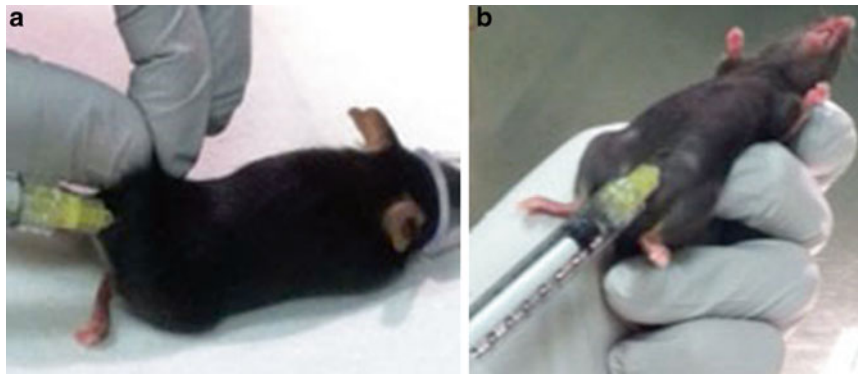

Fig. 2 Administration of induction reagents. The research animal is anesthetized and prepared for the induction procedure. (**a**) MOG/CFA emulsification via subcutaneous injection is administered to the flanks of the tail. (**b**) Pertussis toxin is administered via intraperitoneal injection

6. Repeat **step 5** for injection into left flank near tail.
7. Carefully handle the mouse to secure on its backside.
8. Administer first dose of 100 μL of the 2 ng/μL pertussis toxin solution (i.e., 200 ng total) via intraperitoneal (IP) injection (Fig. 2b).
9. After 48 h, administer second dose of 100 μL of the 2 ng/μL pertussis toxin solution via IP injection.

3.2 Cell Isolation, Culture, Expansion, Cryopreservation, and Injection

3.2.1 Making Complete Expansion Medium (CEM)

1. Sterilize biosafety hood with UV-sterilization for 30 min prior to use.
2. Place all cell culture supplies in sterile hood.
3. Add desired amount of DMEM/F-12 medium to upper chamber of Stericup vacuum-mediated 0.22 μm filter unit.
4. Add supplements to upper chamber: 10 % FBS, 1 % L-glutamine, and 1 % Pen-Strep.
5. Attach vacuum tubing to filter unit and vacuum port.
6. Filter CEM into receiver bottle.
7. Remove filter unit and secure lid to CEM bottle.
8. Store at 4 °C (*see* **Note 3**).

3.2.2 Cell Isolation

BMSC Isolation

1. Securely hold long bone at one end.
2. Carefully cut epiphysis off with scissors to expose the bone marrow in medullary cavity.
3. Assemble a 5 mL disposable syringe with 25G 1″ needle containing PBS.
4. Insert tip of needle into the cavity of the long bone.
5. Flush bone marrow out of the opposite end of the long bone and collect in a 50 mL conical tube.
6. Flush long bone with ample PBS from each end until bone is visibly cleared of bone marrow and collected in conical tube.
7. Break up and resuspend bone marrow in PBS by pipetting up and down several times in a conical tube.
8. Filter through a 70 μm mesh strainer and collect in a new 50 mL conical tube.
9. Centrifuge the capped conical tube at 420×*g* for 5 min at room temperature.
10. Carefully aspirate PBS leaving the cell pellet intact.
11. Resuspend the pellet with a small volume of warm CEM.
12. Determine cell viability and count: Transfer 10 μL sample of the cell suspension to a microcentrifuge tube, stain with (v/v) trypan blue, and count live cells using a hemocytometer. Determine total cell count.

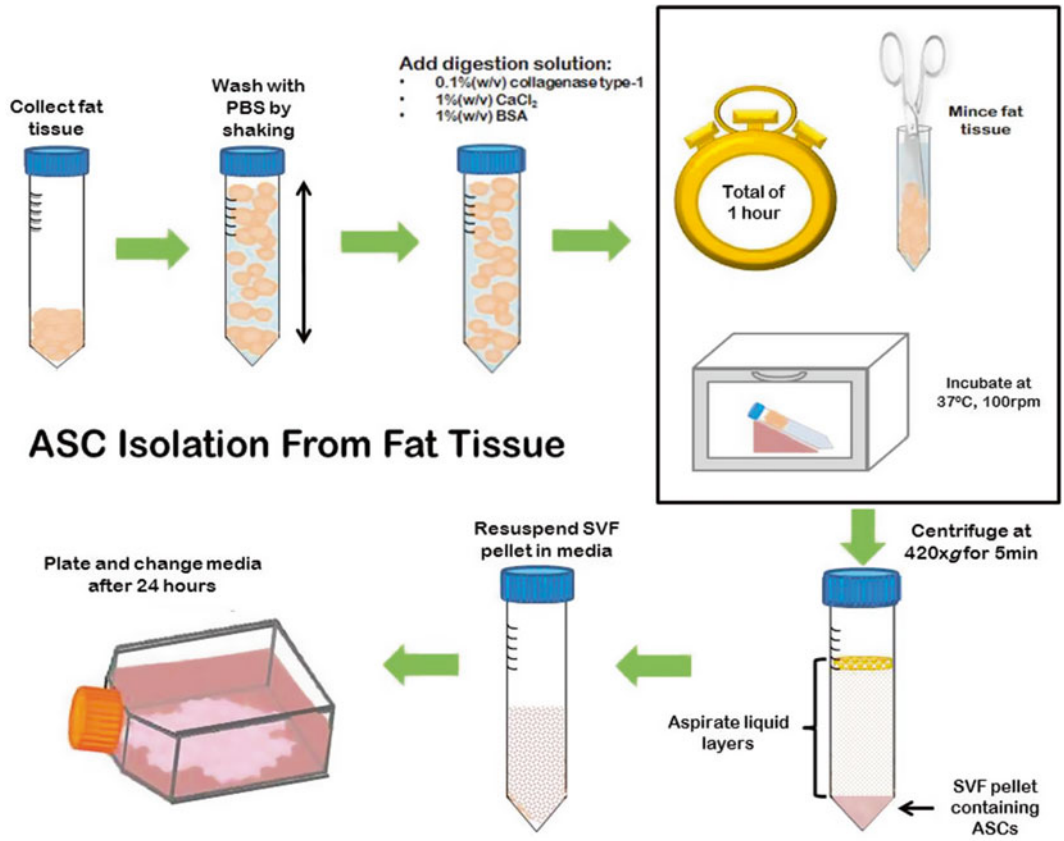

Fig. 3 Adipose-derived stem cell (ASC) isolation from fat tissue. ASCs are isolated from fat tissue after digestion, isolation of stromal vascular fraction (SVF), and plating of SVF. The initial plate will contain a heterogeneous population of cells that will disintegrate leaving ASCs after culturing and passaging

13. Plate cells on 140 × 20 mm cell culture dish with a total volume of 20 mL CEM (*see* **Note 4**).
14. Place culture dish(es) in incubator at 37 °C and 5 % CO_2 (*see* **Note 5**).

ASC Isolation (for an outline of the procedure cf. Fig. 3)

1. Collect fat tissue in 50 mL conical tube.
2. Weigh the fat.
3. Wash the fat by adding ample PBS, vigorously shaking the capped conical tube, removing PBS, and replacing with fresh PBS. Do this 3–4 times.
4. Remove the fat tissue with forceps and transfer to a new conical tube. Put aside a conical tube containing the fat tissue.
5. In a new 50 mL conical tube, make the digestion solution with (w/v) PBS (i.e., 1 g of fat to 1 mL PBS).
6. Add supplements to PBS: 0.1 % (w/v) collagenase type-1, 1 % (w/v) BSA, and 1 % (v/v) $CaCl_2$ (*see* **Note 6**).

7. Gently rock the conical tube to dissolve solutes; do not vortex.
8. Assemble Steriflip 50 mL disposable vacuum filtration system with a 0.22 μm filter to the conical tube with digestion solution.
9. Attach vacuum tubing to the filter unit and vacuum port.
10. Filter the digestion solution into an attached collection tube.
11. Add the filtered digestion solution to the conical tube containing fat tissue. Start timer for 1 h.
12. Quickly mince the fat in digestion solution with scissors by downward motion cutting in the conical tube. Mince until the fat tissue is the size of small pebbles.
13. Add Parafilm around the top of the conical tube to seal.
14. Place conical tube with fat tissue in digestion solution into an incubator shaker (*see* **Note 7**).
15. Incubate the fat in digestion solution at 37 °C in the incubator for the time remaining. Set shaker speed to 100 rpm (*see* **Note 8**).
16. After 1 h incubation, remove the conical tube from the incubator shaker.
17. Neutralize the digestion solution by adding (v/v) complete expansion medium (CEM) to the conical tube.
18. Pipette up and down several times to break up tissue.
19. Centrifuge the conical tube for 5 min at 300 × *g* at room temperature.
20. Remove and shake the conical tube to assist in release of cells from tissue.
21. Centrifuge the conical tube again for 5 min at 300 × *g* at room temperature.
22. Carefully remove the conical tube from the centrifuge. Be sure not to disturb layers.
23. Carefully aspirate the top liquid layers leaving the pellet of stromal vascular fraction (SVF) (Fig. 3) (*see* **Note 9**).
24. Add CEM to the conical tube to resuspend cells of SVF by pipetting up and down several times.
25. (Optional) Filter the cell suspension through a 70 μm filter and collect in a new 50 mL conical tube.
26. Determine cell viability and count: transfer 10 μL sample of cell suspension to a microcentrifuge tube, stain with (v/v) trypan blue, and count live cells using a hemocytometer. Determine total cell count.
27. Plate the cells into a T225 flask at desired density (*see* **Note 10**).

28. Add CEM to the flask and disperse the cells evenly by gently rocking side to side.
29. Place primary cell culture (passage 0) in an incubator for 24 h at 37 °C and 5 % CO_2.
30. After 24 h, remove flask from the incubator and decant CEM.
31. Wash culture with PBS.
32. Replace with fresh CEM (*see* **Note 5**).

3.2.3 Cell Expansion

Replace cell cultures with fresh CEM every 3–4 days until a desired confluence is reached (≤70 % confluence is recommended). Then, lift cells from the plasticware, collect, and re-plate on multiple, new plasticware at a lower density where it is considered the next higher passage. When the desired passage is achieved, cells can either be prepared for injections or frozen in liquid nitrogen until time of use.

1. Sterilize biosafety hood with UV-sterilization for 30 min prior to use.
2. Place all cell culture supplies in the sterile hood.
3. Remove culture dish/flask from the incubator and transfer to the sterile biosafety hood.
4. Carefully aspirate CEM. Be sure not to place the aspirator tip near cell cultures (*see* **Note 11**).
5. Wash plate with PBS.
6. Aspirate PBS using the same method as in **step 4**.
7. Add a minimum volume of 0.25 % trypsin–EDTA sufficient to cover the surface of the culture dish/flask.
8. Transfer the culture dish/flask to the incubator for 4 min at 37 °C and 5 % CO_2.
9. In the hood, neutralize digestion with (v/v) prewarmed CEM.
10. Transfer the cell suspension solution from the culture dish/flask to 50 mL conical tube(s).
11. Centrifuge conical tube(s) at 420 × *g* for 5 min at room temperature.
12. In the hood, carefully aspirate the liquid leaving the cell pellet.
13. Resuspend the cell pellet by adding a minimal volume of CEM and pipette up and down several times (*see* **Note 12**).
14. Determine cell viability and count: Transfer 10 μL sample of the cell suspension to a microcentrifuge tube, stain with (v/v) trypan blue, and count live cells using a hemocytometer. Determine total cell count.
15. Re-plate cells at a desired concentration in a new culture dish/flask containing CEM for further expansion.

*3.2.4 Cryopreservation of Cells (Continue from Subheading 3.2.3, **Step 14**)*

1. In a biosafety hood, prepare cryopreservation medium: CEM with 5–10 % DMSO (*see* **Note 13**).
2. Centrifuge conical tube at 420 × *g* for 5 min.
3. In the hood, carefully aspirate CEM leaving the cell pellet.
4. Add cryopreservation medium and resuspend cells (*see* **Note 14**).
5. Aliquot cryopreserved cells into cryovials.
6. Quickly transfer tubes to a liquid nitrogen dewar.

*3.2.5 Preparation of Cells for Injection into EAE Model (Continue from Subheading 3.2.3, **Step 14**)*

1. Centrifuge conical tube at 420 × *g* for 5 min.
2. In a hood, carefully aspirate liquid leaving the cell pellet.
3. Wash cells by adding prewarmed PBS and resuspend by gently pipetting up and down several times.
4. Centrifuge the conical tube at 420 × *g* for 5 min.
5. In the hood, carefully aspirate PBS leaving the cell pellet.
6. Resuspend the cells in sterile HBSS at the desired concentration (*see* **Note 15**).

3.3 Assessments of Disease

Blinded researchers assess the motor functions of each EAE mouse as a method to quantify the severity of pathology during the disease course. It is important to conduct motor function testing for each animal daily for clinical scoring and weekly for video recordings, ideally at a set time of day for consistency. Clinical scores are based on observations of the animal's gait and hind limb spread while suspended [19, 20] (Fig. 4).

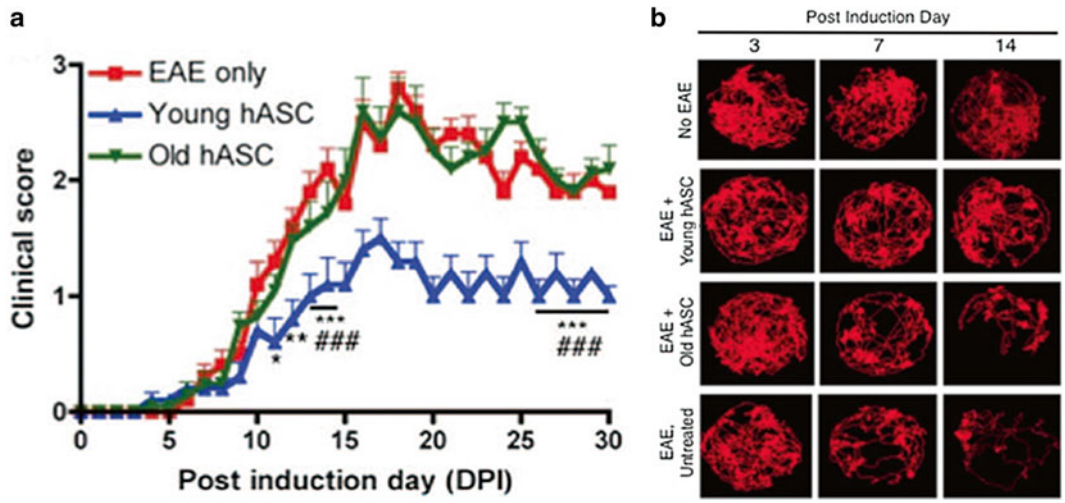

Fig. 4 Clinical scoring over the disease course of the EAE model. Adapted by permission from AlphaMed Press: SCTM. B.A. Scruggs et al. [19]. (**a**) Clinical scoring is a method used by researchers to assess the pathological progression affecting the hind region of the EAE model throughout the course of the disease. (**b**) Track visualization generated by EthoVision XT7 of a research animal from multiple treatment groups that were video recorded over a 5 min period in a cylindrical arena

3.3.1 Clinical Scoring

1. Remove mice out of the housing cage to open area (e.g., biosafety hood).
2. Allow the mice to walk around freely.
3. Observe the tail and gait of each mouse.
4. Suspend each mouse by holding the base of the tail to confirm scoring category (*see* **Note 16**).
5. Record score.

3.3.2 Motor Function Testing Using Noldus EthoVision XT7

1. Set up arena: Place white paper on a flat surface, place the cylinder on top of the paper (*see* **Note 17**).
2. Position a ring stand with an arm holding the webcam overlooking the center of the circular arena at desired height.
3. Access live feed from the webcam on a computer with installed software.
4. Place animal in the arena.
5. Start recording.
6. Stop recording after a desired time interval.
7. Acquire video in the EthoVision XT7 software.
8. Analyze spatial parameters and produce a video tracking image output.

3.3.3 Postmortem Histological Analyses

Several methods are used to analyze harvested tissues, especially CNS tissues. Depending on the preferred method of analysis, tissues can be prepared in different fixatives in order to achieve the best results. Antibody detection is a widely used method for various methods of analysis.

For cell, protein, and/or transcription factor identification and/or quantification using flow cytometry.

1. Harvest tissue.
2. Homogenize the fresh tissue.
3. Process the homogenized tissue by staining with desired antibodies with or without permeabilization and fixation (*see* **Note 18**).
4. Run sample on a flow cytometer to identify cell populations within the tissue samples.

For RNA/DNA or protein quantification using techniques such as qPCRs or Western blot, respectively, tissues are collected and flash-frozen in liquid nitrogen to save until time of processing.

1. Harvest tissue.
2. Collect tissue in a microcentrifuge, 15 mL, or 50 mL tube.
3. Submerge the tube in liquid nitrogen, and transfer it to –80 °C immediately.

4. When the tissue sample is ready to be analyzed, thaw it.
5. Homogenize the tissue sample using a handheld homogenizer with plastic pestles.
6. Process the tissue according to the manufacturer's protocol for extraction of the component, e.g., RNA, DNA, or protein, of interest.

For histological examination using immunohistochemistry, different methods are used to fix tissues in order to embed on a microscope slide. Technique for snap freezing tissues for cryomold-embedded sections:

1. Harvest tissue.
2. Collect the tissue in a tube containing 4 % paraformaldehyde for 24–48 h in 4 °C for fixation.
3. Remove the fixed tissue and transfer to a 30 % sucrose solution in ddH_2O for cryopreservation.
4. When the tissue sinks to the bottom of the tube, remove the tissue.
5. Place the tissue in a cryo-mold.
6. Completely cover the tissue in cryo-embedding compound.
7. Place the mold with the tissue on a platform in a container.
8. Add ethanol to the container until the platform is completely submerged in ethanol and the mold is partially submerged in ethanol (*see* **Note 19**).
9. Place the container in a larger container that can withstand subzero temperatures.
10. Fill the large container with liquid nitrogen until the smaller container is partially submerged.
11. When the tissue in the mold is completely frozen, remove the mold, and wrap in aluminum.
12. Store the frozen mold at –80 °C until sectioning.

Spinal cord processing for formalin-fixed paraffin-embedded sections

1. Remove the entire spinal column and store in 10 % neutral buffered formalin.
2. Allow the tissue to fix for at least 48 h.
3. Remove the spinal cord from the vertebral column using forceps and scissors.
4. Isolate the desired spinal cord section.
5. Place the spinal cord section in a tissue cassette.
6. Submerge the cassette in 10 % neutral buffered formalin.
7. Store at room temperature until sectioning.
8. Tissues are paraffin-embedded then cut with microtome into 5 μm thick sections and prepared on microscope slides.

For IHC on paraffin-embedded sections on a glass microscope slide (*see* **Note 20**):

1. Deparaffinize sections on a heating bed for at least 30 min.
2. Stepwise, rehydrate tissue samples with high to low dilutions of ethanol, then water.
3. Use either a heat-mediated or an enzyme-mediated antigen retrieval method.
4. Wash the sections with phosphate- or Tris-buffered saline-based solutions.
5. Block the sections for 1 h with blocking solution containing serum from the secondary antibody's host and/or bovine serum albumin.
6. Dilute primary antibody in blocking solution.
7. Apply primary antibody either overnight at 4 °C or at room temperature for 1 h in a humidified chamber.
8. Wash the sections.
9. Apply secondary antibody diluted in blocking solution for 1 h at room temperature in a humidified chamber.
10. Wash the sections.
11. For detection of chemiluminescence, apply a chromogenic substrate, counterstain, dehydrate, mount with mounting solution and apply a coverslip. Let dry and visualize under a high resolution microscope.
12. For fluorescence detection, apply mounting solution containing nuclear stain and a coverslip. Let dry and visualize using a deconvolution microscopy (*see* **Note 21**).

4 Notes

1. To test whether product is completely emulsified, add 1 drop of MOG/CFA emulsion to a beaker of water. If drop does not disperse in water, emulsion is complete.
2. Due to pressure from micro-emulsifying needle, hold thumbs firmly on blunt ends of disposable syringes while filling. Do not fill syringe completely. Air pressure will cause blunt end to eject from syringe.
3. Prior to use, warm CEM in a water bath at 37 °C for at least 20 min.
4. A density of 100 cells/cm^2 is ideal for a 140 × 20 mm cell culture dish.
5. Upon plating, a heterogeneous population of cells may be observed. After a few days of culturing in CEM, extraneous cells will deplete leaving a homogenous population of MSCs.

6. BSA protects cells during digestion. $CaCl_2$ is a cofactor to collagenase to assist in digestion.
7. For best results, securely prop the conical tube at 45° angle by taping it to a wedge-shaped object in the incubator shaker.
8. Digestion of the fat tissue is for a total of 1 h, which includes mincing and incubation period.
9. Be sure not to aspirate near SVF. Leave a thin liquid layer on top of the SVF layer to ensure SVF layer remains intact.
10. Density of 5,000 cells/cm^2 is ideal in a T225 flask.
11. Tilt cell culture dish/flask at 30° angle where CEM collects at a corner. Aspirate at corner so that the aspirator tip will not come into contact with the cell cultures.
12. Resuspend pellet in a minimal volume of CEM for ideal concentration for cell counting.
13. Increasing concentration of FBS is optional.
14. Ideal concentration for freezing is 1–2 million cells/mL.
15. Store suspended cells on ice until 30 min prior to injection, then keep at room temperature. At the time of injection, resuspend the cells in HBSS with a micropipette, collect in a 1 mL syringe, and assemble with a needle.
16. During the early stages of pathology, mice are capable of extending hind limbs in a full, even spread. As symptoms progress, legs spread unevenly and/or adduct while mouse is suspended.
17. EthoVision XT7 software detects animal by contrast to background. White paper provides contrast to dark-colored animals.
18. Kits from manufacturers provide the necessary buffers and reagents along with detailed methods depending on the preferred method of analysis.
19. Be sure mold is immobile on the platform.
20. Optimization of protocol must be conducted for each antibody.
21. When using fluorescently labeled antibodies, always process slides away from direct light. Light will cause depletion of the fluorescence molecules.

References

1. Goldenberg M (2012) Multiple sclerosis review. Pharm Therapeut 37:175–184
2. Ascherio A, Munger KL, Lünemann JD (2012) The initiation and prevention of multiple sclerosis. Nat Rev Neurol 8:602–612
3. Batoulis H, Addicks K, Kuerten S (2010) Emerging concepts in autoimmune encephalomyelitis beyond the CD4/T(H)1 paradigm. Ann Anat 192:179–193
4. Lassmann H, van Horssen J (2011) The molecular basis of neurodegeneration in multiple sclerosis. FEBS Lett 585:3715–3723
5. Lassmann H, van Horssen J, Mahad D (2012) Progressive multiple sclerosis: pathology and pathogenesis. Nat Rev Neurol 8:647–656
6. Uccelli A, Laroni A, Freedman MS (2012) Mesenchymal stem cells as treatment for MS – progress to date. Mult Scler 19:515–519

7. Karussis D, Karageorgiou C, Vaknin-Dembinsky A, Gowda-Kurkalli B, Gomori JM, Kassis I et al (2010) Safety and immunological effects of mesenchymal stem cell transplantation in patients with multiple sclerosis and amyotrophic lateral sclerosis. Arch Neurol 67:1187–1194
8. Connick P, Kolappan M, Crawley C, Webber DJ, Patani R, Michell AW et al (2012) Autologous mesenchymal stem cells for the treatment of secondary progressive multiple sclerosis: an open-label phase 2a proof-of-concept study. Lancet Neurol 11:150–156
9. Payne NL, Sun G, McDonald C, Layton D, Moussa L, Emerson-Webber A et al (2012) Distinct immunomodulatory and migratory mechanisms underpin the therapeutic potential of human mesenchymal stem cells in autoimmune demyelination. Cell Transplant 22: 1409–1425
10. Foust KD, Wang X, McGovern VL, Braun L, Bevan AK, Haidet AM et al (2010) Rescue of the spinal muscular atrophy phenotype in a mouse model by early postnatal delivery of SMN. Nat Biotechnol 28:271–274
11. Krampera M, Cosmi L, Angeli R, Pasini A, Liotta F, Andreini A et al (2006) Role for interferon-gamma in the immuno-modulatory activity of human bone marrow mesenchymal stem cells. Stem Cells 24:386–398
12. Freedman MS, Bar-Or A, Atkins HL, Karussis D, Frassoni F, Lazarus H et al (2010) The therapeutic potential of mesenchymal stem cell transplantation as a treatment for multiple sclerosis: consensus report of the International MSCT Study Group. Mult Scler 16:503–510
13. Kassis I, Grigoriadis N, Gowda-Kurkalli B, Mizrachi-Kol R, Ben-Hur T, Slavin S et al (2008) Neuroprotection and immunomodulation with mesenchymal stem cells in chronic experimental autoimmune encephalomyelitis. Arch Neurol 65:753–761
14. Bai L, Lennon DP, Eaton V, Maier K, Caplan AI, Miller SD et al (2009) Human bone marrow-derived mesenchymal stem cells induce Th2-polarized immune response and promote endogenous repair in animal models of multiple sclerosis. Glia 57:1192–1203
15. Zappia E, Casazza S, Pedemonte E, Benvenuto F, Bonanni I, Gerdoni E et al (2005) Mesenchymal stem cells ameliorate experimental autoimmune encephalomyelitis inducing T-cell anergy. Blood 106:1755–1761
16. Constantin G, Marconi S, Rossi B, Angiari S, Calderan L, Anghileri E et al (2009) Adipose-derived mesenchymal stem cells ameliorate chronic experimental auto-immune encephalomyelitis. Stem Cells 27:2624–2635
17. Morando S, Vigo T, Esposito M, Casazza S, Novi G, Principato MC et al (2012) The therapeutic effect of mesenchymal stem cell transplantation in experimental autoimmune encephalomyelitis is mediated by peripheral and central mechanisms. Stem Cell Res Ther 3:3
18. Bernard CC, Carnegie PR (1975) Experimental autoimmune encephalo-myelitis in mice: immunologic response to mouse spinal cord and myelin basic proteins. J Immunol 114: 1537–1540
19. Scruggs BA, Semon JA, Zhang X, Zhang S, Bowles AC, Pandey AC et al (2013) Age of donor reduces the ability of human adipose-derived stem cells to alleviate symptoms in the experimental autoimmune encephalo-myelitis mouse model. Stem Cells Transl Med 2: 797–807
20. Scruggs BA, Bowles AC, Zhang X, Semon JA, Kyzar EJ, Myers L et al (2013) High-throughput screening of stem cell therapy for globoid cell leukodystrophy using automated neuro-phenotyping of twitcher mice. Behav Brain Res 236:35–47

Chapter 26

Analysis of the Neuroregenerative Activities of Mesenchymal Stem Cells in Functional Recovery after Rat Spinal Cord Injury

Akihito Yamamoto, Kohki Matsubara, Fumiya Kano, and Kiyoshi Sakai

Abstract

Spinal cord injury (SCI) involves concurrent, interacting pathological processes, and requires a multifaceted therapeutic strategy. Stem cell-based transplantation holds great promise as such an approach. We have reported that stem cells derived from human dental pulp have remarkable neuroregenerative activity, and that when transplanted into animal models of SCI, these cells promote functional recovery by inhibiting massive SCI-induced apoptosis, preserving neural fibers and myelin, regenerating transected axons, and replacing damaged cells by differentiating into oligodendrocytes. Here, we introduce some details of our experimental procedures, which may serve as a guide for designing experiments to evaluate the therapeutic benefits of various types of stem cells.

Key words Spinal cord injury, Mesenchymal stem cells, Dental pulp stem cells, Apoptosis, Preservation of neural fiber and myelin, Axonal regeneration, Differentiation into oligodendrocyte lineages

1 Introduction

Stem cell-based transplants offer a promising, multifaceted therapeutic strategy for SCI. Over the last decade, a variety of cell types, including human neural stem cells, embryonic stem cell derivatives, and adult bone marrow stromal cells (BMSCs), have been transplanted into the injured SC of rats or mice to evaluate the cells' neuroregenerative activities. These preclinical studies have shown that engrafted stem cells promote significant functional recovery after SCI, not only through cell replacement and cell-autonomous activities but also through paracrine and trophic effects [1]. Thus, these cells' effects must be investigated against a variety of pathogeneses to evaluate their therapeutic benefits for SCI.

Humans have two sets of teeth during their lifetime: 20 deciduous teeth and 32 permanent teeth. The center of each tooth

Bruno Christ et al. (eds.), *Animal Models for Stem Cell Therapy*, Methods in Molecular Biology, vol. 1213,
DOI 10.1007/978-1-4939-1453-1_26,

contains a pulp chamber filled with soft connective tissue called dental pulp [2]. Self-renewing stem cells are found in the perivascular niche of the dental pulp, and include human adult dental pulp stem cells (DPSCs) and stem cells from human exfoliated deciduous teeth (SHEDs) [3]. These cells are thought to originate from the embryonic cranial neural crest, and they simultaneously express early markers for both mesenchymal and neuroectodermal stem/progenitor cells [4–6]. Three independent groups recently transplanted DPSCs or SHEDs into mice or rats with acute, subacute, or chronic SCI, resulting in marked recovery of hindlimb locomotor function [6–8]. Here, we describe the details of our experimental procedures for evaluating the multifaceted neuroregenerative activities of pulp stem cells.

2 Materials

2.1 Reagents

1. Collagenase type I (Wako).
2. Dispase (Wako).
3. Dulbecco's modified Eagle medium (DMEM).
4. Fetal calf serum (FCS).
5. Phosphate-buffered saline (PBS).
6. Bovine serum albumin (BSA).
7. 4 % paraformaldehyde (PFA).
8. Human bone marrow mesenchymal stem cells (hBMSC; Lonza).
9. Human skin fibroblast lines (hFbs; Lonza).
10. Antibodies to detect a pattern of cell surface markers for mesenchymal stem cells (MSCs): $CD105^+$, $CD73^+$, $CD90^+$, $CD34^-$, $CD45^-$, $CD11b^-$, and $HLA\text{-}DR^-$ (mouse IgG, 1:200; BD Biosciences).
11. Neural lineage markers: anti-GFAP (mouse IgG, 1:500; Millipore), anti-βIII-tubulin (mouse IgG, 1:1,000; R&D Systems), anti-NeuN (mouse IgG, 1:100; Millipore), anti-CNPase (mouse IgG, 1:500; Millipore), anti-nestin (rabbit IgG, 1:500; Millipore), anti-DCX (guinea pig IgG, 1:500; Millipore), anti-APC (rabbit IgG, 1:300; Abcam), anti-MBP (rabbit IgG, 1:500; Abcam), and anti-A2B5 mAb (mouse IgG, 1:500; Millipore).
12. Pierce BCA Protein Assay Kit (Takara Bio Inc.).
13. Pentobarbital (Somnopentyl, Kyoritsu Seiyaku Corporation).
14. Fibrin glue matrix (Beriplast P Combi-Set, CSL Behring).
15. Cyclosporine (Novartis).
16. Sodium ampicillin.

17. RNA extraction reagent (Isogen 2, Nippon Gene Co.).
18. RT-PCR kit (Superscript III reverse transcriptase for RT-PCR, Life Technologies).
19. qPCR kit (Thunderbird SYBR qPCR Mix, Toyobo).
20. Rat primers:
    GAPDH forward (5′-AACTTTGGCATCGTGGAAGG-3′),
    GAPDH reverse (5′-CGGATACATTGGGGGTAGGA-3′);
    IL-6 forward (5′-TTGCCTTCTTGGGACTGATG-3′),
    IL-6 reverse (5′-ACTGGTCTGTTGTGGGTGGT-3′);
    IL-1β forward (5′-CAGGATGAGGACCCAAGCAC-3′),
    IL-1β reverse (5′-TCAGACAGCACGAGGCATTT-3′);
    TNF-α forward (5′-CTCGAGTGACAAGCCCGTAG-3′),
    TNF-αreverse(5′-CCTTGAAGAGAACCTGGGAGTAG-3′);
    iNOS forward (5′-GGCAGGATGAGAAGCTGAGG-3′),
    iNOS reverse (5′-CCGCATTAGCACAGAAGCAA-3′);
    IL-10 forward (5′-GCCTGCTCTTACTGGCTGGA-3′),
    IL-10 reverse (5′-TCTGGCTGACTGGGAAGTGG-3′);
    TGF-β1 forward (5′-CCGCAACAACGCAATCTATG-3′),
    TGF-β1 reverse (5′-GCACTGCTTCCCGAATGTCT-3′).
21. OCT compound.
22. Triton X-100.
23. FluoroMyelin green dye (Life Technologies).
24. TUNEL assay kit (In Situ Cell Death Detection Kit, Roche).
25. NeuroTrace [lysine-fixable dextran biotin, 10,000 MW, (BDA-10000); Invitrogen].
26. Diaminobenzidine (DAB Tablet, Wako).
27. 10 μg/mL poly-L-lysine (PLL), 300 ng/mL extracellular chondroitin sulfate proteoglycan mixture (CSPG), or 400 ng/mL myelin associated glycoprotein/Fc chimera (MAG).

2.2 Equipment

1. Infinite Horizon Impactor (IH Impactor; Precision Systems and Instrumentation, Lexington, KY).
2. Glass pipette.
3. Surgical blade.
4. Surgical microscope.
5. Silicone tube.
6. Heating pad.
7. 10 μL Hamilton syringe.
8. Stereotaxic instruments (SR-5R, Narishige Group).
9. Micromanipulator (SM-15, Narishige Group).

10. Auto injector (Legato130, KD Scientific)
11. iPRECIO SMP-200 pump (Primetech Co.).
12. Cryostat.
13. Flow cytometer.
14. 48-well tissue culture plates.

3 Methods

All procedures should be conducted at room temperature unless otherwise specified.

3.1 Isolation and Characterization of Dental Pulp Stem Cells

1. To prepare dental pulp stem cells (*see* **Note 1**), separate the crown and root of the tooth, isolate the dental pulp, and digest it in a solution of 3 mg/mL collagenase type I and 4 mg/mL dispase for 1 h at 37 °C. Plate single-cell suspensions (1×10^4 to 2×10^4 cells/mL) on culture dishes in DMEM supplemented with 10 % fetal calf serum, and incubate at 37 °C in 5 % CO_2 (*see* **Note 2**).
2. To confirm surface markers for mesenchymal stem cells, incubate 1×10^6 cells with primary mAbs conjugated with fluorescent dye at 4 °C for 30 min. Wash the cells twice with PBS containing 0.1 % BSA, and evaluate cell fluorescence by flow cytometry. Typically, more than 95 % of the pulp stem cells are $CD105^+$, $CD73^+$, $CD90^+$, $CD34^-$, $CD45^-$, $CD11b^-$, and $HLA\text{-}DR^-$.
3. To express intracellular neural lineage markers, the cells should be fixed with 4 % (w/v) PFA for 5 min and permeabilized with 0.1 % (v/v) Triton X-100 in PBS for 5 min. Block the cells with 10 % (v/v) goat serum for 30 min. Apply primary antibodies to stain neural lineage markers, followed by the appropriate fluorescent-conjugated secondary antibodies and analyze by flow cytometry. Typically, more than 95 % of the pulp stem cells are $nestin^+$ (neural stem cells), $doublecortin^+$ (DCX; neuronal progenitor cells), $\beta III\text{-}tubulin^+$ (early neuronal cells), $NeuN^+$ (mature neurons), $GFAP^+$ (neural stem cells and astrocytes), $S\text{-}100^+$ (Schwann cells), $A2B5^+$ and $CNPase^+$ (oligodendrocyte progenitor cells), or $adenomatous\ polyposis\ coli\ (APC)^-$ and $myelin\ basic\ protein\ (MBP)^-$ (mature oligodendrocytes).

3.2 Preparation of Conditioned Medium (CM)

1. At passages 3–9, wash SHEDs, BMSCs, or hFbs at 70–80 % confluency with PBS and replace the culture medium with serum-free DMEM. After incubating for 48 h, collect and centrifuge the medium for 4–5 min at $440 \times g$. Collect the supernatant and centrifuge it for 1 min at 4 °C at $17{,}400 \times g$.
2. Use the supernatant for assays or to measure protein concentration using the BCA protein assay kit. Adjust the CM protein concentrations to 3 μg/mL with DMEM.

3.3 Animal Models and Surgical Procedures

1. Animals: We used adult female rats weighing 200–230 g (8–9 weeks old) to generate our SCI model. SCI interferes with bladder discharge, and male rats, having a longer urethra, frequently develop urinary tract infections. Thus, it is advisable to use female rats.
2. Anesthesia and laminectomy: After anesthetizing the rat (*see* **Note 3**), peel the cutaneous and muscle tissues off both sides of the spine. Remove the spinous process, vertebral lamina, and transverse process to completely expose the 9th–11th thoracic vertebral levels. A heating pad can be used to maintain the rat's body temperature at 37 °C during the surgery.
3. Surgery for complete transection: Transect the whole SC using a surgical blade (*see* **Note 4**). The severed ends of the SC will typically retract about 1–2 mm. Lift the rostral and caudal stumps to confirm complete transection, then bind and seal both stumps with fibrin glue matrix (*see* **Note 5**).
4. Contusion-type SCI: Contusion-type SCI can be generated using a commercially available SC-injury device (IH Impactor). Expose the dura mater, and use a force of 200 kdyn to induce injury (*see* **Note 6**).
5. Stem cell transplantation: Use a glass pipette with a tip diameter of 50–70 μm to draw up cells (1×10^6) (*see* **Note 7**). Inject 2.5×10^5 cells in PBS (2.5 μL; injection rate, 0.8 μL/min) at each of two injection sites, one at the rostral stump and one at the caudal stump of the SC. Our injection sites were 2 mm from the lesion and 0.5 mm lateral to the midline, at a depth of 1.5 mm (*see* **Note 8**). Finally, fill the 1- to 2-mm gap in the severed SC with cells (1×10^5) in fibrin glue.
6. Surgical procedure for administering CM: Immediately after the SC contusion, perform a Th12 partial laminectomy. Insert a thin silicone tube intrathecally using a surgical microscope (*see* **Note 9**). Connect the tube to an iPRECIO SMP-200 pump filled with CM. Anchor the tube to the spinous process, and place the pump under the skin on the animal's axilla.
7. Maintenance: Administer 10 mg/kg cyclosporine daily, beginning the day prior to surgery and continuing through the course of the experiment. After performing the surgery, keep the animal in a temperature- and humidity-controlled environment until it is awake. Verify sensation and paralysis in the hind limbs when the rat awakens from surgery, and exclude rats with hind limb movement. Administer an antibiotic (sodium ampicillin, 10 mg/kg body weight) by daily injection for 3 days. Manually express the bladder twice daily until normal voiding reflexes return (*see* **Notes 10–12**).

3.4 Evaluation of Functional and Pathological Recovery After SCI

1. Behavioral examination: Assess hind limb neurobehavior and locomotor recovery with the BBB locomotor rating scale, which evaluates joint movement, stepping ability, coordination, and trunk stability. The BBB scale runs from 0 to 21, with 21 points signifying no locomotor difficulty. Only animals with a BBB score of 0 on the day after surgery, indicating complete hind-end paralysis, should be included in the study. Analyze scores by repeated measures ANOVA with Tukey's multiple comparison tests at each time point (*see* **Note 13**).
2. Real-time quantitative PCR inflammatory response: Isolate total RNA with Isogen according to the manufacturer's instructions, and quantify the isolated RNA by spectrophotometer. Confirm the RNA's integrity on 1 % agarose gels. For RT reactions, use Superscript III Reverse Transcriptase and 0.5 μg of total RNA in a 25 μL total reaction volume. For real-time qPCR, we used SYBR Green qPCR Mix and a real-time PCR system. Primers were designed using the Primer 3 software.
3. Immunohistochemical analysis of apoptosis, axonal and myelin preservation, and neural-lineage differentiation of engrafted stem cells: Under anesthesia, transcardially perfuse the animal with 4 % PFA in 0.1 M PBS. Isolate the SC, embed it in OCT compound, and cut 20-μm sections in the sagittal or transverse plane on a cryostat. Permeabilize SC sections with 0.1 % (v/v) Triton X-100 in PBS for 20 min, block with 5 % (v/v) BSA for 30 min, and stain with the following primary antibodies: anti-Human Nuclei (mouse IgG, 1:100), anti-Neurofilament M (rabbit IgG, 1:300, Millipore), and anti-5-HT (rabbit IgG, 1:500, Sigma). Stain myelin with FluoroMyelin green dye according to the manufacturer's instructions. Analyze the apoptotic cell death by TUNEL assay. Calculate the average number of TUNEL-positive cells per section from the total value obtained by counting serial sagittal sections through the lesion site of each animal (*see* **Note 14**).
4. Axonal regeneration by anterograde neuronal tracing: Trace neurons by injecting biotinylated dextran amine at four sites in the hind limb area of the sensorimotor cortex at a 1.2-mm depth, following the rat brain atlas. After 2 weeks, prepare sagittal SC cryosections (20 μm thick) and process the sections by diaminobenzidine (DAB) staining with the ABC reaction protocol.
5. Neurite outgrowth assays: Coat 48-well tissue culture plates with 10 μg/mL poly-L-lysine (PLL), followed by 300 ng/mL extracellular chondroitin sulfate proteoglycan mixture (CSPG) or 400 ng/mL myelin associated glycoprotein/Fc chimera

(MAG). Leave the plates at 37 °C for 4 h. Next, seed rat cerebellar granule neurons (CGNs) onto 48-well tissue culture plates (1.5×10^5 cells/well) coated with PLL, PLL/CSPG, or PLL/MAG, and culture at 37 °C in 5 % CO_2 with SHED-CM. After a 24 h incubation, fix the cells with 4 % PFA/PBS and visualize neurites by staining with anti-neuron-specific β-tubulin (*see* **Note 15**). Perform each experiment at least three times. Obtain images with 20 or more cells per field. Randomly count and measure at least 100 cells.

4 Notes

1. We isolated SHEDs from human deciduous teeth (from individuals 6–12 years old), and DPSCs from adult third molars (extracted from individuals 18–30 years old; for clinical purposes).
2. In our experiments we also used mesenchymal stem cells from three human bone marrow lines (hBMSCs, from individuals 20–22 years old) and three human skin fibroblast lines (hFbs, 36–40 years old) at passage 5.
3. We used a mixture of 100–150 mg/kg xylazine and 60–90 mg/kg ketamine.
4. We used Feather surgical blade stainless steel no. 11.
5. Maintain hemostatic treatment after transecting the SC to keep a clear surgical field.
6. In the contused SCI model, avoid breaking the arachnoid membrane, since this can cause administered CM to leak.
7. We used a pipette mounted on a 10 μL Hamilton syringe and attached to a micromanipulator.
8. When injecting the cell transplants, indwell the needle tip in the SC for a few minutes after injection to avoid graft cell leakage.
9. To avoid neural damage while inserting the silicone tube into the subarachnoid space, conduct the entire tubing operation under a stereomicroscope.
10. Urinary support must be provided every 12 h. Compress the bladder gently and continuously. Avoid excessive pressure, which may cause the bladder to burst.
11. Place SCI rats in a fresh cage every 3 days to avoid infection through the excretory tract.
12. In our study, the rats remained under postoperative care for 8 weeks.

13. In our study, the animals were evaluated in 4-min sessions by two observers who were blinded to the animals' treatment.
14. In our experiments, we examined three animals per group.
15. We defined cell processes as neurites when they were longer than the diameter of the cell body, and we evaluated neurite length by manually tracing them using ImageJ software and referencing a known length.

References

1. Sharp J, Keirstead HS (2007) Therapeutic applications of oligodendrocyte precursors derived from human embryonic stem cells. Curr Opin Biotechnol 18:434–440
2. Nanci A, Ten Cate AR (2003) In Ten Cate's oral histology: development, structure, and function. 6th ed. Mosby, St. Louis, MO; London. http://www.elsevier.ca/ISBN/9780323078467/Ten-Cates-Oral-Histology
3. Gronthos S, Brahim J, Li W, Fisher LW, Cherman N, Boyde A et al (2002) Stem cell properties of human dental pulp stem cells. J Dent Res 81:531–535
4. Gronthos S, Mankani M, Brahim J, Robey PG, Shi S (2000) Postnatal human dental pulp stem cells (DPSCs) in vitro and in vivo. Proc Natl Acad Sci U S A 97:13625–13630
5. Miura M, Gronthos S, Zhao M, Lu B, Fisher LW, Robey PG et al (2003) SHED: stem cells from human exfoliated deciduous teeth. Proc Natl Acad Sci U S A 100:5807–5812
6. Sakai K, Yamamoto A, Matsubara K, Nakamura S, Naruse M, Yamagata M et al (2012) Human dental pulp-derived stem cells promote locomotor recovery after complete transection of the rat spinal cord by multiple neuro-regenerative mechanisms. J Clin Invest 122:80–90
7. de Almeida FM, Marques SA, Ramalho Bdos S, Rodrigues RF, Cadilhe DV, Furtado D et al (2011) Human dental pulp cells: a new source of cell therapy in a mouse model of compressive spinal cord injury. J Neurotrauma 28:1939–1949
8. Taghipour Z, Karbalaie K, Kiani A, Niapour A, Bahramian H, Nasr-Esfahani MH et al (2012) Transplantation of undifferentiated and induced human exfoliated deciduous teeth-derived stem cells promote functional recovery of rat spinal cord contusion injury model. Stem Cells Dev 21:1794–1802

Part VI

Immunemodulation by Stem Cells

Chapter 27

Therapeutic Application of Mesenchymal Stromal Cells in Murine Models of Inflammatory Bowel Disease

Elena Gonzalez-Rey and Mario Delgado

Abstract

Mesenchymal stromal cells (MSCs) are currently under investigation for the treatment of inflammatory bowel disease (IBD), including Crohn's disease. The models of colitis induced by intrarectal infusion of 2,4,6-trinitrobenzene sulfonic acid (TNBS) or by oral administration of dextran sulfate sodium (DSS) in susceptible mouse strains have been commonly used as preclinical tools to demonstrate the efficiency of treatments with MSCs isolated from various sources. Both models are being and will be critical to improve MSC-based therapies in human IBD by assaying new pathways, therapeutic regimes and tissue targeting strategies. Here, we describe our experiences in the treatment of acute and chronic TNBS- and DSS-induced colitis with MSCs.

Key words Crohn's disease, Ulcerative colitis, Colitis, Dextran sulfate sodium, 2,4,6-Trinitrobenzene sulfonic acid, Mesenchymal stromal cells

1 Introduction

Inflammatory bowel disease (IBD), including Crohn's disease and ulcerative colitis, is a family of chronic, idiopathic, relapsing, and tissue destructive diseases characterized by dysfunction of mucosal T cells and altered cellular inflammation that ultimately leads to damage of the distal small intestine and the colonic mucosa [1]. In both Crohn's disease and experimental colitis, activated T helper 1 cells promote an exaggerated macrophage and neutrophil infiltration and activation, giving rise to a transmural inflamed intestinal mucosa, characterized by prolonged and uncontrolled production of inflammatory cytokines, free radicals, and chemokines that participate in colonic tissue destruction [2, 3].

Based on their potent anti-inflammatory and immunomodulatory activities [4], mesenchymal stromal cells (MSCs) derived from different sources have been proven therapeutically effective in the treatment of IBD in various experimental models [5–12].

Bruno Christ et al. (eds.), *Animal Models for Stem Cell Therapy*, Methods in Molecular Biology, vol. 1213,
DOI 10.1007/978-1-4939-1453-1_27,

Moreover, MSCs are currently under investigation for the treatment of human Crohn's disease ([13], *see* www.trial.gov).

Because they reflect many clinical, immunological and histopathological features of those seen in human IBD, the models of colitis induced by 2,4,6-trinitrobenzene sulfonic acid (TNBS) or by dextran sulfate sodium (DSS) in mice have been widely used as preclinical models to investigate new therapeutic approaches in IBD, including MSC-based therapies [2, 5–12, 14, 15]. Moreover, both models are simple to induce, highly reproducible, and not expensive, which makes them two of the most commonly used models of IBD to study various aspects of IBD such as pathogenesis, genetic predisposition to IBD, and immune mechanisms [2]. In the DSS model, colitis is induced by addition of DSS to drinking water, and intestinal inflammation results from the impairment of the intestinal epithelial cell barrier function by DSS, subsequent exposition of the submucosa to various luminal antigens (bacteria and food) and activation of the inflammatory cells involved in the innate immunity. In the TNBS model, colitis is induced after the rectal instillation of a TNBS–ethanol mixture, in which ethanol acts by disrupting the epithelial barrier integrity and TNBS acts as a haptenizing agent of autologous colonic proteins that initiate a T helper 1-driven inflammatory response in the colonic mucosa. Depending on the concentration, the duration, and frequency of DSS or TNBS administration, the animals may develop acute, chronic, or relapsing-remitting colitis. Clinical manifestations of DSS- and TNBS-induced colitis include marked and sustained weight loss, bloody diarrhea, rectal prolapse, pancolitis accompanied by piloerection and anemia, and eventually death. Here, we describe how to induce acute and chronic colitis with TNBS and DSS and how to treat colitis with MSCs.

2 Materials

2.1 TNBS-Induced Colitis

1. 2,4,6-trinitrobenzene sulfonic acid (TNBS, Sigma) (*see* **Note 1**).
2. Male 6-week-old Balb/c mice, weighing 19–21 g (*see* **Note 2**).
3. Inhalable anesthesia: halothane or isofluorane.
4. 3.5 French polyurethane catheter (*see* **Note 3**).
5. Ethanol, 50 % in distilled water.
6. 1 mL disposable syringe.
7. 20G needle.

2.2 DSS-Induced Colitis

1. Dextran sulfate acid (DSS, molecular weight 36,000–50,000 Da; MP Biomedicals) (*see* **Note 4**).
2. Male 6-week-old C57Bl/6 mice, weighting 19–21 g (*see* **Note 5**).

2.3 Analysis of Colitis

1. Phosphate-buffered saline (PBS): 2 mM KH_2PO_4, 8.1 mM Na_2HPO_4, 130 mM NaCl, 2.6 mM KCl, pH 7.0. Stored at 4 °C, it will be good for 4 weeks.
2. 10 % PBS-buffered formalin: 3.7 % formaldehyde diluted in PBS. Stored at 4 °C, it will be good for 2 months.
3. 10 mL disposable syringe.
4. 22G needle.
5. Scissors.
6. Forceps.
7. Petri dish.
8. Dissecting microscope.
9. 10 mL tube.

3 Methods

3.1 Induction of Acute Colitis with TNBS

1. Weigh and mark each mouse (*see* **Note 6**).
2. Prepare fresh TNBS–ethanol mixture (*see* **Note 7**). Add 900 μL 50 % ethanol to each TNBS stock solution (100 μL) and maintain the tube protected from light on ice. Each mouse will receive 3 mg TNBS in 100 μL 50 % ethanol (*see* **Note 8**). Each tube of TNBS stock solution will allow the induction of colitis in ten mice.
3. Fill a 1 mL disposable syringe attached to a 3.5 French, 15 cm, polyurethane catheter with TNBS–ethanol mixture.
4. Lightly anesthetize Balb/c or SJL mice in a plexiglas chamber containing inhalable anesthetic (*see* **Note 9**).
5. Once the breathing frequency of the animal significantly decreases, hold the mouse by the tail, insert the catheter into the rectum 1 cm and inject 20 μL of TNBS–ethanol mixture.
6. Insert the catheter carefully to a total of 4–5 cm (mark in catheter will help in this step) in the colon (*see* **Note 10**). Slowly inject additional 80 μL of TNBS–ethanol mixture and remove the catheter carefully.
7. Keep the mouse in a vertical position, head down by holding it by the tail for at least 30 s to allow uniform distribution of the TNBS–ethanol mixture in the colon.
8. Put the mouse back in the cage (*see* **Note 11**).
9. Include in each experiment a control group by injecting 50 % ethanol instead of TNBS–ethanol mixture and follow the **steps 1–8**.

3.2 Induction of Chronic Colitis with TNBS

1. Administer TNBS weekly at increasing doses: 0.8 mg per mouse at day 0, 1 mg per mouse at day 7, 1.2 mg per mouse at day 14, and 1.5 mg per mouse at day 21.
2. Follow the steps described in Subheading 3.1 with the exception of **step 2** (*see* **Note 12**).

3.3 Induction of Colitis with DSS

1. Weigh and mark each mouse. Put the mouse back in the cage.
2. Replace drinking water in the mouse cage with DSS solution (5 % DSS for acute colitis and 3 % DSS for chronic relapsing-remitting colitis) (*see* **Note 13**). Drinking will be ad libitum.
3. Change DSS solution every 4 days (*see* **Note 14**).
4. To study acute colitis, sacrifice the mouse on day 7.
5. To study chronic relapsing-remitting colitis, replace 3 % DSS solution in the mouse cage with drinking water on day 8, and replace the drinking water with 3 % DSS solution again on day 15. Replace the 3 % DSS solution on day 22 with drinking water and maintain it until day 28.
6. Use animals hydrated with normal water as naïve controls.

3.4 Treatment with Mesenchymal Stromal Cells (MSCs)

1. Dissolve 10^7 MSCs in 2 mL PBS (solution to treat ten mice), keep them on ice and use them immediately.
2. Take 200 μL of MSC suspension with a 1 mL syringe, without needle.
3. Insert a 20G needle in the syringe and inject slowly the cells in the right side of the peritoneal cavity of the mouse (*see* **Note 15**).

3.5 Analysis of Colitis

Analysis of colitis should be determined in a blinded fashion by one or two observers that do not know the identity of the different experimental groups.

1. Weigh each mouse every day after the induction of colitis (both TNBS and DSS).
2. Determine colitis score and disease activity daily in each animal following the scores described in Tables 1 and 2, respectively.
3. At the end of each model (8–10 days after acute TNBS-induced colitis, 7 days after acute DSS-induced colitis, 28 days after chronic TNBS-induced colitis, and 28 days after relapsing-remitting DSS-induced colitis), sacrifice the animals by excess of isofluorane or CO_2 inhalation. Immobilize the mouse with tapes in a dissection plate, apply 70 % ethanol on the abdominal skin and open the abdominal cavity by layers with scissors. Determine macroscopically the colonic damage following the score described in Table 3.
4. After the macroscopic analysis, carefully dissect/tease the colon from the surrounding mesentery (*see* **Note 16**). Then, transect the colon at the levels of colon–cecal margin and of rectum and move it to a petri dish.

Table 1
Colitis score (scale 0–4)

Score	Observation
0	Normal stool appearance
1	Slight decrease in stool consistency
2	Moderate decrease in stool consistency
3	Moderate decrease in stool consistency and presence of blood in stools
4	Severe watery diarrhea and moderate/severe blooding in stools

Table 2
Clinical disease activity (scale 0–4)

Observation	Score
Weight loss:	
0 %	0
1–10 %	0.5
11–15 %	1
16–20 %	1.5
>20 %	2
Diarrhea:	
Normal stool	0
Soft stool and minimal wet anal fur/tail	0.5
Diarrhea and moderate to severe wet anal fur/tail	1
Frank rectal bleeding:	
Absent	0
Present but minimal	0.5
Moderate/severe	1

5. Clear the stool content of the colon by flushing ice-cold PBS through a 10 mL syringe with a 22G needle (*see* **Note 17**).
6. Weigh the cleaned colon and determine its length with a precision rule (*see* **Note 18**).
7. Confirm macroscopically the colon damage score (*see* Table 3) with a dissecting microscope.

Table 3
Macroscopic colonic damage score (scale 0–8)

Observation	Score
Ulceration:	
Normal appearance	0
Focal hyperemia, no ulcers	1
Ulceration without hyperaemia or bowel wall thickening	2
Ulceration with inflammation at 1 site	3
Two or more sites of ulceration and inflammation	4
Major sites of damage extending >1 cm along length of colon	5
Adhesions:	
No adhesions	0
Minor adhesions, colon can be easily separated from the other tissues	1
Major adhesions	2
Thickness:	
Maximal bowel wall thickness, in millimeters, measured with a caliper	0.5–1

Table 4
Histopathological score (scale 0–4)

Score	Observation
0	No evidence of inflammation
1	Low leukocyte infiltration (<10 % of section), no structural damage
2	Moderate leukocyte infiltration restricted to the mucosal layer (10–25 % of section), crypt elongation, partial loss of goblet cells, bowel wall thickening, no ulcerations
3	Severe leukocyte infiltration beyond the mucosal layer (25–50 % of section), crypt elongation, bowel wall thickening, superficial ulcerations
4	Transmural leukocyte infiltration seen in >50 % of section, distorted crypts, marked loss of goblet cells, bowel wall thickening, extensive ulcerations

8. Fix the colon with 10 % PBS-buffered formalin in a 10 mL tube for at least 8 h at room temperature. Transfer colon tissue to a histology laboratory for paraffin embedding, sectioning, and staining with hematoxylin and eosin. Determine in a blinded fashion the histological score of colitis as determined in Table 4.

4 Notes

1. Wear gloves and handle with care because TNBS is hazardous and contact with skin should be avoided. Following the manufacturer's instruction, dissolve TNBS reagent at 300 mg/mL in 50 % ethanol. Make aliquots of 100 μL in 1.5 mL tubes protected from light with aluminum foil and store the TNBS stock solution at −20 °C (good for up to 4–5 months).
2. Differences in mice strain susceptibility to TNBS-induced colitis are known. Balb/c and SJL mice are susceptible, whereas C57Bl/6 and DBA/2 mice are resistant. We suggest using at least ten mice per experimental group, due to the variability in the severity of this model. Weight prior injection should be uniform between animals, preferably in a range of 19–21 g. Animals weighing less or more than this range could be more susceptible or resistant to colitis, respectively.
3. Attach 15 cm of the catheter to the needle of a 1 mL disposable insulin syringe and fix with lab parafilm. Make a mark at 5 cm from the tip. We also recommend applying surgical lubricant to the end of the catheter to facilitate rectal insertion.
4. For each drinking bottle and cage, dissolve 15 g (for 5 % DSS) or 9 g (for 3 % DSS) of DSS in 300 mL of distilled water and filter with a 0.45 μm cellulose acetate filter. Besides the dose of DSS administered, the severity of colitis will depend on the molecular weight of DSS used in a certain mouse strain. We recommend using DSS with a molecular weight around 40,000 Da in C57Bl/6 mice in order to obtain uniform and consistent results in severity and incidence. The optimal dose and molecular weight of DSS will vary between laboratories and will have to be determined individually.
5. Different mice strains show different susceptibility to DSS-induced colitis. C57Bl/6 and NOD/Ltj mice are the susceptible strains more widely used in this model. We suggest using at least ten mice per experimental group, due to the variability in the severity of this model. Weight prior injection should be uniform between animals, preferably in a range of 19–21 g. Animals weighing less or more than this range could be more susceptible or resistant to colitis, respectively.
6. Mark each animal with a numerical code. We recommend to label the tail of each mouse with a line code using a marker pen and remark when necessary. Avoid methods that cause stress or pain to the animals.
7. TNBS is unstable at room temperature and light sensitive. Therefore, a fresh TNBS–ethanol solution protected from light should be prepared in every experiment and maintained on ice.

8. The severity of the disease will depend on the dose of TNBS and on the percentage of ethanol used. Moreover, severity and incidence of the disease depend on the microbiota of each mouse and it will be affected by the exposition to pathogens and the conditions in each animal facility. Therefore, optimal doses of TNBS and ethanol should be determined individually by each experimenter.
9. Care must be taken to avoid overexposure to inhalable anesthetic, since a prolonged anesthesia will increase contact of TNBS with intestinal mucosa.
10. Although the catheter is very flexible, care must be taken to avoid perforation of the intestine upon catheter advancement. Check signs of colon perforation such as immediate rectal bleeding, hunching position, and inability to ambulate hind legs. If this occurs, sacrifice the animal.
11. We do not recommend to put each animal in an individual cage. Although this could facilitate the analysis of signs of colitis in individual animals, it could disturb established social relations between animals and generate stress conditions that could affect the inflammatory response. We recommend cages containing 5–10 animals. We also recommend monitoring food intake in each experimental group to determine whether weight loss is in part due to changes in food consumption.
12. On day 0, add 3.9 mL 50 % ethanol to each TNBS stock solution (100 μL). On day 8, add 2.9 mL 50 % ethanol to each TNBS stock solution (100 μL). On day 16, add 2.4 mL 50 % ethanol to each TNBS stock solution (100 μL). On day 22, add 1.9 mL 50 % ethanol to each TNBS stock solution (100 μL). By injecting 100 μL of each solution, each mouse will receive 0.8, 1, 1.2, and 1.5 mg TNBS dissolved in 50 % ethanol at each time point.
13. The varying responses to DSS appear to be dependent on not only DSS (concentration, molecular weight, duration of DSS exposure, manufacturer, and batch) but also genetic (strain and gender) and microbiological (microbiological state and intestinal flora) factors of the animals. Stress states in the animals also modify results in DSS-induced colitis. Optimal conditions should be set up individually in each animal facility.
14. Differences in the DSS susceptibility do not correlate normally with differences in the consumption of DSS-supplemented water. However, we recommend monitoring DSS consumption in the different experimental groups.
15. A big calibre in the needle used and a low infusion speed will avoid lysing cells during the injection procedure. Other pathways of administration of MSCs, such as intravenous or subcutaneous, have also been proven effective in experimental colitis.

However, differences in efficiency have been reported by different laboratories using these pathways [8]. Optimal pathway and dose of injection should be individually determined for each type of MSC.

16. Care must be taken during this process to not damage or perforate the colon. Remove all the tissue adherences with help of scissors and forceps.
17. In order to keep the colon orientation and to discriminate distal from proximal colon in further histological analysis, we recommend tying the distal end of the colon with 3-0 suture.
18. Inflammation causes shortening of the colon and increases its weight.

References

1. Fiocchi C (1998) Inflammatory bowel disease: etiology and pathogenesis. Gastroenterology 115:182–205
2. Strober W, Fuss IJ, Blumberg RS (2002) The immunology of mucosal models of inflammation. Annu Rev Immunol 20:495–549
3. Bouma G, Strober W (2003) The immunological and genetic basis of inflammatory bowel disease. Nat Rev Immunol 3:521–533
4. Ucelli A, Moreta L, Pistoia V (2008) Mesenchymal stem cells in Elath and disease. Nat Rev Immunol 8:726–736
5. Gonzalez-Rey E, Anderson P, Gonzalez MA et al (2009) Human adult stem cells derived from adipose tissue protect against experimental colitis and sepsis. Gut 58:929–939
6. Gonzalez MA, Gonzalez-Rey E, Rico L et al (2009) Adipose-derived mesenchymal stem cells alleviate experimental colitis by inhibiting inflammatory and autoimmune responses. Gastroenterology 136:978–989
7. Zhang Q, Shi S, Liu Y et al (2009) Mesenchymal stem cells derived from human gingival are capable of immunomodulatory functions and ameliorate inflammation-related tissue destruction in experimental colitis. J Immunol 183: 7787–7798
8. Castelo-Branco MT, Soares ID, Lopes DV et al (2012) Intraperitoneal but not intravenous cryopreserved mesenchymal stromal cells home to the inflamed colon and ameliorate experimental colitis. PLoS One 7: e33360
9. Kim HS, Shin TH, Lee BC et al (2013) Human umbilical cord blood mesenchymal stem cells reduce colitis in mice by activating NOD2 signaling to COX2. Gastroenterology 145: 1392–1403
10. Zani A, Cananzi M, Fascetti-Leon F et al (2014) Amniotic fluid stem cells improve survival and enhance repair of damaged intestine in necrotising enterocolitis via a COX-2 dependent mechanism. Gut 63:300–309
11. Anderson P, Souza-Moreira L, Morell M et al (2013) Adipose-derived mesenchymal stromal cells induce immunomodulatory macrophages which protect from experimental colitis and sepsis. Gut 62:1131–1141
12. Parolini O, Souza-Moreira L, O'Valle F et al (2014) Therapeutic effect of human amniotic membrane-derived cells in experimental arthritis and other inflammatory disorders. Arthritis Rheumatol. 66:327–339
13. Duijvestein M, Vos AC, Roelofs H et al (2010) Autologous bone marrow derived mesenchymal stromal cell treatment for refractory luminal Crohn's disease: results of a phase I study. Gut 59:1662–1669
14. Duijvestein M, Wildenberg ME, Welling MM et al (2011) Pretreatment with interferon-γ enhances the therapeutic activity of mesenchymal stromal cells in animal models of colitis. Stem Cells 29:1549–1558
15. Ko IK, Kim BG, Awadallah A et al (2010) Targeting improves MSC treatment of inflammatory bowel disease. Mol Ther 18:1365–1372

Chapter 28

Mesenchymal Stem Cells Attenuate Rat Graft-Versus-Host Disease

Masayuki Fujino, Ping Zhu, Yusuke Kitazawa, Ji-Mei Chen, Jian Zhuang, and Xiao-Kang Li

Abstract

Mesenchymal stem cells (MSCs) derived from bone marrow are feasible for the exertion of a powerful immunoregulatory effect and thus shall hold a curative potency in T lymphocyte-dependent pathologies. This current article is intended to describe the method to investigate that MSCs might take advantage of regulation in graft-versus-host disease (GvHD), a major etiology of attack rate and lethality post allogeneic hematopoietic stem cell transplantation (HSCT). MSCs were isolated from Lewis rat bone morrow and cultured for 4 weeks. The purification of enriched conventional MSCs and macrophages was achieved by autoMACS. Using the limiting dilution method, MSCs were cloned and then expanded until more than 6 months. The cultured MSCs showed a typical spindle-shaped morphology and immunophenotypes, lack of CD45 and CD11b/c expression. MSCs are also known for their ability to differentiate into adipocytes. MSCs, like macrophages, exhibit the immunomodulatory propensity to inhibit T lymphocyte proliferation. Following the adoptive transfer, MSCs regulate systemic Lewis to (Lewis × DA) F1 rat GvHD. Meanwhile, the cloned MSCs surprisingly enhanced T cell proliferation in vitro and yielded no clinical benefit in regard to the incidence or severity of GvHD. This is in contradistinction to the immunosuppressive activities of MSCs as conventionally described. Hence, this rat GvHD model treated with MSCs has shown intriguing differences in the regulatory effects of lymphocyte proliferation and GvHD repression between short-term cultured conventional MSCs and cloned MSCs.

Key words Allo-rejection, Cell-based therapy, Graft-versus-host disease, Hematopoietic stem cell transplantation, Mesenchymal stem cell

1 Introduction

One of the most efficient treatments for many hematological malignancies and for primary immunodeficiencies is allogeneic hematopoietic stem cell transplantation (HSCT) [1–4]. HSCT resorts to the ablation of the hematopoietic division by high dosage of chemotherapeutic agent and irradiation, and the rearrangement of a new hematopoietic system supplied by the donor hematopoietic stem cells [5, 6]. Yet, the grafting also includes mature T lymphocytes that are able to elicit graft-versus-host disease

Bruno Christ et al. (eds.), *Animal Models for Stem Cell Therapy*, Methods in Molecular Biology, vol. 1213,
DOI 10.1007/978-1-4939-1453-1_28,

(GvHD), a life imminent complication of allogeneic HSCT [7]. The contaminating donor T lymphocytes are robustly activated following alloantigen recognition presented by the recipient antigen presenting cells (APCs), and invade target organs, where they exert cytotoxicity [8, 9]. Consequently, the main aims of HSCT are to regulate alloresponsiveness by donor allogeneic T lymphocytes without eliciting GvHD, and to minimize the effects of graft-versus-leukemia and graft-versus-infection.

Mesenchymal stem cells (MSCs) exist in bone marrow (BM) as a non-hematopoietic cell cluster, and are marked by their capability of self-regeneration and differentiate into mesenchymal tissues, such as bone, cartilage, or adipose tissue [10–13]. MSCs might exert a massive immunosuppressive potency in vitro and in vivo, and hence may have curative feasibility in T lymphocyte-dependent pathologies [4, 14]. Recently, MSCs have attracted a great deal of attention as a novel curative approach in organ transplantation due to their immunomodulatory properties [15–18]. Cell-based immunoregulatory therapy has been encouraged in recent years with the identification of intrinsic suppressor cells capable of abrogating the lymphocyte effector functions [19]. The vast majority of reports has shown that MSCs are able to prevent the activation of T lymphocyte proliferation and secretion of cytokines. For instance, interleukin-2 and interferon-γ produced by mixed lymphocyte reactions (MLRs) [18, 20–22], mitogens [21, 23], and receptor engagement [24, 25]. In an in vitro study, the soluble factors discharged from MSCs may be the major mechanism of immunoregulation [18, 26]; but, cell contact-dependent modes of suppression may also coexist [27, 28]. Independent of the mechanism of action, the efficacy of MSC transplantation in severe acute GvHD in clinical trials demonstrates the potency of these cells as immunosuppressive agents [14, 28]. These immunosuppressive properties of MSCs open attractive possibilities in the field of solid organ transplant or HSCT. This study demonstrates that MSCs could be used to control GvHD, a major cause of morbidity and mortality after allogeneic HSCT [29].

2 Materials

2.1 Animals

Adult (4–6 weeks of age) male Lewis ($RT1^l$), DA ($RT1^a$), and (Lewis × DA) F1 rats (Shizuoka Laboratory Animal Center, Shizuoka, Japan) were specific pathogen-free animals.

2.2 Isolation and Culture of MSCs from Adult Rat Bone Marrow

1. DMEM medium: 1.0 g/L glucose without L-glutamine and phenol red (*see* **Note 1**).
2. MSC culture medium: DMEM medium containing 10 % FBS, 1 % L-alanyl-glutamine, and 1 % antibiotic–antimycotic mixed solution (cf. 6).

3. 150 mm cell culture dish (Becton, Dickinson and Company; BD, Franklin Lakes, NJ).
4. Fetal bovine serum (FBS).
5. L-alanyl-glutamine (GlutaMAX™, Life Technologies Japan Ltd. Tokyo, Japan) (*see* **Note 2**).
6. Antibiotic-antimycotic mixed solution: 100×, penicillin, streptomycin, amphotericin B (Nacalai Tesque, Tokyo, Japan).
7. Trypsin–EDTA: 5.0 g/L trypsin, 5.3 mM EDTA solution (*see* **Note 3**).
8. Phase contrast microscope (Olympus, Tokyo, Japan).
9. Ether.
10. Scissors (B-52; Natsume Seisakusho Co., Ltd. Tokyo, Japan).
11. Forceps (ME-2; Natsume Seisakusho Co., Ltd.).
12. 1 mL syringe.
13. 70 % ethanol (ethanol–H_2O (7:3, vol/vol)).
14. 60 mm petri dish (BD).
15. 25G needle.
16. 200 μm mesh nylon filter (Tokyo Screen Co. Ltd., Tokyo, Japan).
17. Phosphate-buffered saline (PBS).
18. Hemacytometer.

2.3 MSC Purification and Cloning

1. Phycoerythrin (PE)-conjugated anti-rat CD11b (OX-42, Serotec, Oxford, UK) and CD45 (OX-1, BD) monoclonal antibodies (mAb).
2. Anti-PE MicroBeads (Miltenyi Biotec, K.K. Tokyo, Japan).
3. AutoMACS system (magnetic activated cell sorter; Miltenyi Biotec).
4. 96-well culture plate, flat bottom.

2.4 Adipocyte Differentiation of Cultured MSCs

1. Adipocyte differentiation supplement: insulin, transferrin, selenious acid, and dexamethasone (DS Pharma Biomedical Co., Ltd., Osaka, Japan).
2. 10 % Neutral Buffered Formalin (Sigma-Aldrich, St. Louis, MO): 100 mL/L 37–40 % formaldehyde, 900 mL/L distilled or deionized water, 4.0 g/L sodium phosphate, monobasic, 6.5 g/L sodium phosphate, dibasic (anhydrous).
3. Isopropanol.
4. Oil Red O (Muto Pure Chemicals Co., Ltd., Tokyo, Japan).

2.5 Flow Cytometric Analysis

1. PE-conjugated anti-rat CD11b (OX-42, Serotec), CD90 (OX-7, Serotec), CD45 (OX-1, BD), CD54 (1A29, BD), RT1B

(OX-6, BD), RT1A (OX-18, BD), CD80 (3H5, BD), and CD86 (24F, BD) mAbs.

2. FACScan (fluorescence-activated cell sorter; BD) and CellQuest software (BD).
3. PBS with 1 % FBS.

2.6 T Cell Purification and APC Preparation

1. Cell strainers (70 μm; BD).
2. Ficoll Isopaque (Lympholyte Rat, Cedarlane Lab. Ltd., Ontario, Canada).
3. GIT medium (Nihon Pharmaceutical Co., Ltd., Tokyo, Japan) (*see* **Note 4**).
4. PanT MicroBeads (Miltenyi Biotec).
5. 10× PBS.
6. Anti-rat CD11b/c MicroBeads (Miltenyi Biotec).

2.7 Proliferation Assays

1. Flat bottom 96-well white plate (Corning International K.K., Tokyo, Japan).
2. Concanavalin A (ConA, Sigma-Aldrich, St. Louis, MO).
3. 2-mercaptoethanol.
4. Anti-rat CD3e (G4.18, BD) and CD28 (JJ319, BD) mAbs.
5. Cell proliferation ELISA kits (Roche Diagnostics GmbH, Penzberg, Germany).
6. Chemiluminescence reader (Wallac ARVOTM SX; PerkinElmer, Inc., Wellesley, MA) and Wallac1420 manager software (PerkinElmer).

2.8 Total Lymph Node (LN) Lymphocyte Purification and Assay of Systemic GvH Reactivity

1. 200 μm mesh nylon filter (Tokyo Screen Co. Ltd).
2. Small animal irradiator (CP-160, Faxitron X-ray, Wheeling, VA).
3. Body weight scale for small animals (KN-665-GX; Natsume Seisakusho Co. Ltd.).

3 Methods

All rats were maintained under standard conditions and fed rodent food and water, in accordance with the guidelines of the Animal Use and Care Committee of the National Research Institute for Child Health and Development, Tokyo, Japan.

3.1 Isolation and Culture of MSCs from Adult Rat Bone Marrow

1. Place the femurs from the rats in a petri dish (on ice) containing MSC culture medium.
2. Flush the femurs with this medium using a 25G needle. Mix the suspension well by pipetting and filter through a 200 μm mesh nylon filter to remove bits of bone, etc. and collect the solution in a 50 mL tube (*see* **Note 5**).

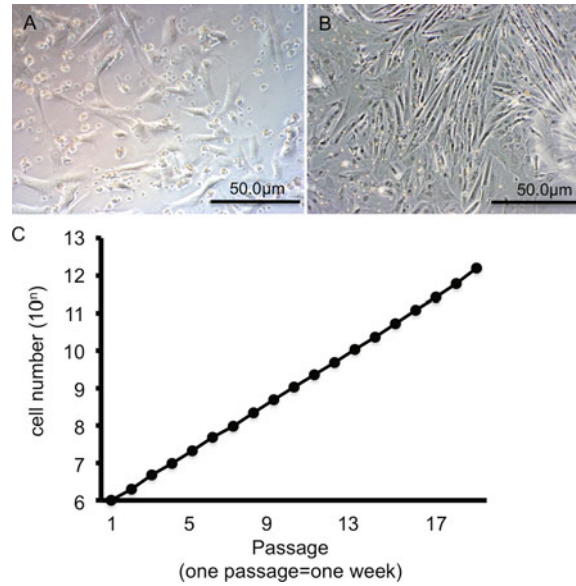

Fig. 1 MSC morphology and proliferation. Established, confluent MSCs in the culture displayed a typical homogeneous fibroblast-like pattern. Phase contrast view of conventional MSCs cultured after sorting at 4 weeks (**a**) and cloned MSCs at 6 months (**b**). (**c**) Growth curve of bone marrow (BM)-derived cloned MSCs. The total expansion over 18 passages was extrapolated to be in the range of 10^{12} cells. Scale bars: 50 μm (**a** and **b**). Figures are modified from data of ref. 29, with permission

3. Determine the cell number and culture all cells in 150 mm cell culture dishes (2 dish/rat; $1 \sim 2 \times 10^6$ cells/dish) in MSC culture medium. Change half of the culture medium every week.
4. On the day 14, trypsinize adherent cells, harvest, and then plate into five new 150 mm dishes ($1 \sim 2 \times 10^6$ cells/dish).
5. On day 28, trypsinize all adherent cells, and harvest for cell sorting. Assess the morphology of the adherent cells by phase contrast microscopy (Fig. 1a) (*see* **Note 6**).

3.2 MSC Purification and Cloning

1. The above suspended 4 weeks cultured adherent bone morrow-derived cells were undergone the isolation of the purified conventional MSCs and macrophages. In detail, stain 5×10^5 cells with 2 μL of PE-conjugated anti-rat CD11b and CD45 mAbs and incubate for 30 min at 4 °C. Thereafter stain the cells with anti-PE microbeads and incubated for 30 min at 4 °C.
2. Sort the cells with an autoMACS system using the negative selection protocol according to manufactures protocol.
3. Verify the negative fraction representing the enriched MSCs fraction, and the positive fraction representing enriched macrophages by Flow Cytometry using anti-rat CD45 and CD11b

mAbs as described in Subheading 3.4. More than 98 % purity of the MSC and 85 % purity of the macrophage populations were obtained routinely (Fig. 1).

4. To obtain cloned MSCs use the limiting dilution method as follows. Suspend the enriched MSCs to 5 cells/mL and plate 100 μL (0.5 cell)/well in 96-well plates. Select the wells containing single cells for subsequent culture, and passage for up to more than 6 months (Fig. 1b, c).

3.3 Adipocyte Differentiation of Cultured MSCs

1. Culture MSCs in 6-well plates (1×10^5 cells/well) with MSC culture medium until they reach confluence.
2. For differentiation, induce MSCs to differentiate into adipocytes in MSC culture medium with adipocyte differentiation supplement. Plate cells (1×10^5 cells/well) in 6-well plates for 21 days, and then switch to fresh medium for 3–4 days.
3. Visualize induced adipocytes. Fix the cells by 10 % formaldehyde buffer for 10 min followed by three times washing with PBS.
4. After washing with 60 % isopropanol for 1 min, stain the cells with Oil Red O for 10–20 min (Fig. 2a, b).

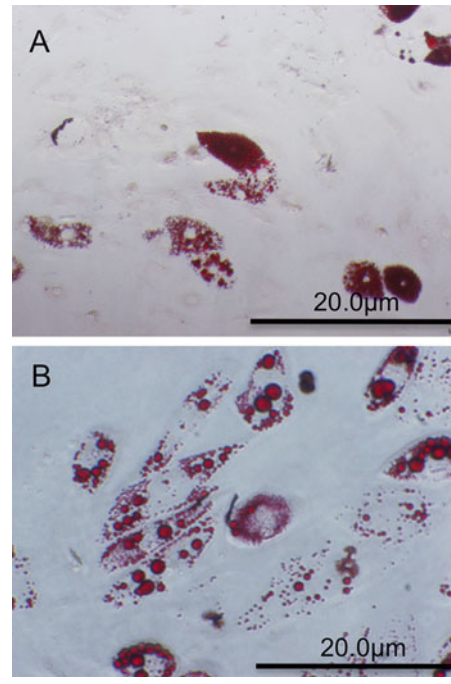

Fig. 2 Adipogenic differentiation potential of MSCs. Both conventional MSCs (**a**) and cloned MSCs (**b**) formed lipid-filled adipocytes detected by Oil Red O staining. Data are consistent with the outcomes from similar experiments. Scale bars: 20 μm (**a** and **b**). Figures are modified from data of ref. 29, with permission

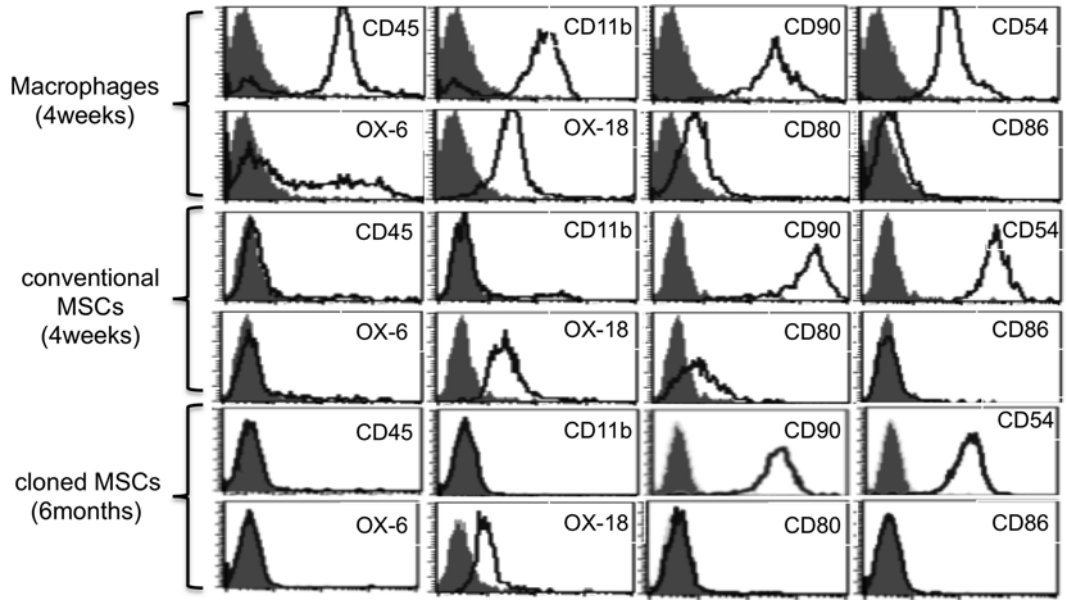

Fig. 3 Characterization of MSCs and macrophages by flow cytometry. The cells were labeled with PE-conjugated antibodies and examined by flow cytometry. Histograms demonstrating the expression of surface molecules were plotted against the control (anti-IgG). The immunophenotypical profile of the macrophages revealed higher CD45, CD11b, CD90, CD54, OX-6, and OX-18, and lower CD80 and CD86 expression. Both MSCs expressed higher CD90, CD54, OX-18, lower CD80, but no CD45, CD11b, OX-6, and CD86. Figures are reproduced from a previous report [29], with permission

3.4 Flow Cytometric Analysis

1. Collect and suspend MSCs in PBS (1×10^5 cell/tube) and then incubate at 4 °C for 20 min with an optimal concentration of PE-conjugated anti-rat CD11b, CD90, CD45, CD54, RT1B, RT1A, CD80, and CD86 mAbs diluted with PBS containing 1 % FBS.
2. Wash the cell pellet twice with 1 mL of PBS with 1 % FBS. Centrifuge at $360 \times g$ for 5 min at 4 °C.
3. Perform flow cytometric analysis using a FACScan cytometer. Data acquisition and analysis were performed using the CellQuest software (Fig. 3).

3.5 T-Cell Purification

1. Harvest spleens from naive Lewis rats and prepare single cell suspensions by passing the tissue through cell strainers as follows.
2. Place the spleen from the rats in a petri dish (on ice) containing GIT medium.
3. Homogenize the spleen between the frosted ends of slides and pass through a sterile cell strainer and collect in a 50 mL tube. Bring the volume to 50 mL with medium and then centrifuge at $360 \times g$ for 5 min at 4 °C.

4. Wash the cell pellet with 50 mL of serum-free DMEM. Centrifuge at 360 × *g* for 5 min at 4 °C.
5. Overlay the cell suspension with Ficoll Isopaque and centrifuge at 1,300 × *g* for 25 min at 24 °C.
6. Harvest the cells of the interface layer and wash twice with PBS.
7. Lyse erythrocytes by hypotonic shock as follows. The pelleted cells are loosened by flicking the base of the tube and add 9 mL of distilled water, cap the tube, and mix by inversion for 12 s.
8. Add 1 mL of 10× PBS, cap the tube, mix by inversion, and wash the remaining cells with GIT medium.
9. Determine the cell number and stain all cells with PanT MicroBeads at 4 °C for 30 min, and sort on autoMACS using the positive selection protocol according the manufacturer's instructions.
10. Verify the enriched PanT cells population by FACScan as described above. More than 95 % purity of the PanT cells population was routinely obtained using an anti-CD3 mAb for evaluation.

3.6 Preparation of APC

1. Prepare DA spleen cells as described in **steps 1–7** in Subheading 3.5.
2. Determine the cell number, stain cells with anti-rat CD11b/c MicroBeads at 4 °C for 30 min, and sort on autoMACS applying the positive selection protocol according manufacturer's instructions.
3. Rinse with 60 % isopropanol followed by distilled water.

3.7 Proliferation Assays

1. Mix enriched PanT cells (1×10^5) from Subheading 3.5 with Lewis enriched MSCs (1×10^3–1×10^5) and culture with DA spleen CD11b/c$^+$ cells (APCs, 1×10^4) from Subheading 3.6 in a flat bottom 96-well white plate at a final volume of 200 μL/well of the GIT medium containing 50 μM 2-mercaptoethanol in a humidified atmosphere at 37 °C for 5 days.
2. To evaluate and assess the response to mitogenic stimulations, culture purified PanT cells at 37 °C for 3 days with ConA at 2 μg/mL or anti-CD3e, anti-CD28 mAbs at 1 μg/mL, and various numbers (1×10^3–1×10^5) of Lewis enriched MSCs.
3. Measure the proliferation of T cells using the cell proliferation ELISA kits (Fig. 4) according to manufacturer's protocol. The chemiluminescence measurement is carried out in a microplate reader and the data are processed using the Wallac1420 manager software.

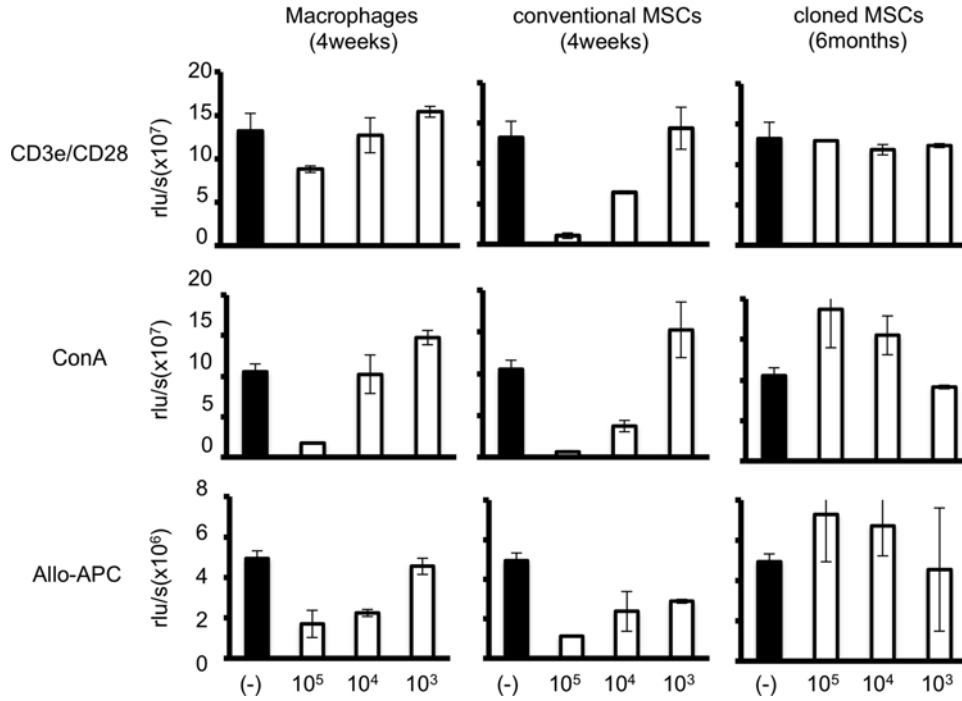

Fig. 4 Immunoregulatory potency of MSCs in vitro. Conventional MSCs have regulatory activity inhibiting T cell proliferation previously induced by various stimuli, but cloned MSCs do not. MSCs, like macrophages, can inhibit T cell proliferation induced by anti-CD3e/CD28 mAb, ConA, and allogeneic stimulator cells in a dose-dependent manner. In contrast, the cloned MSCs enhanced the T cell proliferation stimulated by ConA and alloantigen (allo-APC). Data are representative of those obtained from three independent experiments. rlu/s, relative light units/second. Figures are reproduced from a previous report [29], with permission

3.8 Total LN Lymphocyte Purification

1. For the preparation of purified LN cells, harvest naive Lewis rat LNs and put them in a petri dish (on ice) containing PBS.
2. Grind LNs gently with frosted objective slides in PBS.
3. Filter the cells through a 200 μm mesh nylon filter for single cell suspension preparation.
4. After washing with PBS, overlay cells with Ficoll Isopaque and centrifuge at $1.300 \times g$ for 25 min at 24 °C.
5. Harvest the cells in the interface layer and wash twice with PBS.
6. Lyse erythrocytes by hypotonic shock as described in **steps 6** and **7** under Subheading 3.5.

3.9 Assay of Systemic GvH Reactivity

1. Fill total LN single cell suspensions in PBS (1×10^7 cells/500 μL) in a 1 mL syringe with a 23G needle and inject intravenously into 4 weeks old Lewis × DA F1 rats via tail veins after whole body 6Gy γ-irradiation on day 2.
2. Also fill MSCs in PBS (1×10^7 cells/500 μL) in a 1 mL syringe with a 23G needle and administer to the host rat via tail vein injections at day 1 and day 6 (Fig. 5a) (*see* **Note 7**).

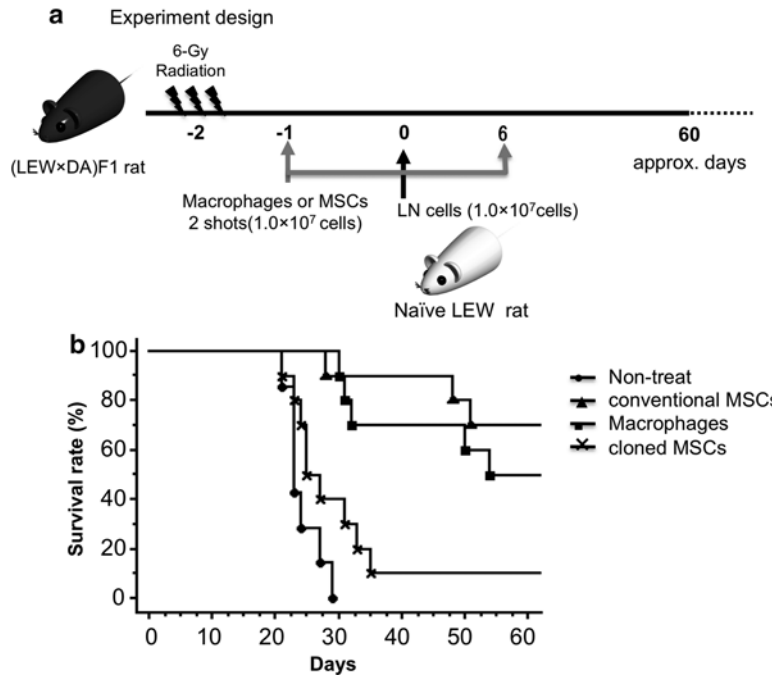

Fig. 5 Treatment with conventional MSCs, but not cloned MSCs, suppressed GvH reactions. (**a**) Experiment design. (**b**) Transfer of the naive Lewis LN T cells (1×10^7) to (Lewis × DA) F1 rat led to the host's weight loss and final lethality in a 6-Gy-irradiated rat GvHD model (*circles*). Nonetheless, the groups of conventional MSC-treated (*triangles*) and macrophage-treated (*squares*) host rats significantly suppressed the GvH reaction. Conversely, there were no protective effects in the cloned MSCs treatment group (*cross*). Figures are reproduced from a previous report [29], with permission

3. Weigh the rats on alternate days during the active phase of the GvHD.
4. Animals undergoing typical GvHD will show rapid weight loss and commonly described signs of the disease, including ruffled fur, reddening of the skin, a hunched posture, and ultimately death (Fig. 5b and Table 1).

4 Notes

1. DMEM with phenol red can also be used.
2. We used GlutaMAX™ instead of L-glutamine. The MSCs were cultured 1 week without any medium replacement. During this period, toxic ammonia buildup is intrinsically harmful. GlutaMAX™ prevents ammonia buildup even during long-term culture.

Table 1
MSCs treatment suppressed systemic GvHD[a]

Group	*n*	Survival (days)	Mean ± SD	*p*-value
Control (no-treat)	7	21, 23 × 3, 24, 27, 29	24.3 ± 2.7	
Conventional MSCs	10	28, 48, 51, >60 × 7	55.6 ± 10.4	$p = 0.0001$
Macrophages	10	30, 31, 32, 50, 54, >60 × 5	49.7 ± 13.3	$p = 0.0001$
Cloned MSCs	10	21, 23, 24, 25 × 2, 27, 31, 33, 35, >60	30.4 ± 11.3	$p = 0.4277$

[a]Systemic GvHD were performed transferring 1.0×10^7 naïve Lewis LN cells to (Lewis × DA) F1 rats after 6Gy radiation. The *p*-value was compared with control (no-treat) group rat and determined by the Kaplan–Meier's test. This table is reproduced from a previous report [29], with permission

3. Trypsin–EDTA solution can detach the MSCs from the culture dish, whereas TrypLE™ Express (Life Technologies Japan Ltd.) is able to provide much better MSC viability than Trypsin–EDTA. MSCs exhibit large cell sizes and a relatively strong resistance to physical stress, while MSCs are highly susceptible to side effects of certain chemical compounds such as Trypsin–EDTA.
4. GIT medium is serum-free and can be replaced by RPMI1640 with 10 %FBS.
5. All of the solutions used for femur flushing should be used for the following culture, do not discard the solution that might contain the unidentified factor(s) that could be helpful for the following culture.
6. It was of pivotal importance to keep the confluence of the cells in culture between 30 and 70 %. A higher confluence might induce differentiation of MSCs and lead to morphological changes and low proliferation.
7. The MSC administration should be slow and cautious to avoid MSCs stuck in the pulmonary capillary plexus caused by the large size of MSCs.

Acknowledgement

This study was supported by research grants from the Ministry of Education, Culture, Sports, Science and Technology of Japan (Grants-in-Aid 20390349, 21659310, 2109739) and the National Center for Child Health and Development (22-10). National Natural Science Foundation of China (81370230), the Major International (Regional) Joint Research Project (2008 DFA31140, 2010 DFA32660).

References

1. Becker AJ, Mc CE, Till JE (1963) Cytological demonstration of the clonal nature of spleen colonies derived from transplanted mouse marrow cells. Nature 197:452–454
2. Kitazawa Y, Fujino M, Li XK et al (2009) Superagonist CD28 antibody preferentially expanded Foxp3-expressing nTreg cells and prevented graft-versus-host diseases. Cell Transplant 18(5):627–637
3. Kitazawa Y, Li XK, Liu Z et al (2010) Prevention of graft-versus-host diseases by in vivo supCD-28mAb-expanded antigen-specific nTreg cells. Cell Transplant 19(6):765–774
4. Weissman IL (2000) Translating stem and progenitor cell biology to the clinic: barriers and opportunities. Science 287(5457):1442–1446
5. Thomas E, Storb R, Clift RA et al (1975) Bone-marrow transplantation (first of two parts). N Engl J Med 292(16):832–843
6. Thomas ED, Storb R, Clift RA et al (1975) Bone-marrow transplantation (second of two parts). N Engl J Med 292(17):895–902
7. Blazar BR, Korngold R, Vallera DA (1997) Recent advances in graft-versus-host disease (GVHD) prevention. Immunol Rev 157: 79–109
8. Billingham RE (1966) The biology of graft-versus-host reactions. Harvey Lect 62:21–78
9. Sackstein R (2006) A revision of Billingham's tenets: the central role of lymphocyte migration in acute graft-versus-host disease. Biol Blood Marrow Transplant 12(1 Suppl 1):2–8
10. Bianco P, Gehron Robey P (2000) Marrow stromal stem cells. J Clin Invest 105(12): 1663–1668
11. Deans RJ, Moseley AB (2000) Mesenchymal stem cells: biology and potential clinical uses. Exp Hematol 28(8):875–884
12. Minguell JJ, Erices A, Conget P (2001) Mesenchymal stem cells. Exp Biol Med (Maywood) 226(6):507–520
13. Prockop DJ (1997) Marrow stromal cells as stem cells for nonhematopoietic tissues. Science 276(5309):71–74
14. Le Blanc K, Rasmusson I, Sundberg B et al (2004) Treatment of severe acute graft-versus-host disease with third party haploidentical mesenchymal stem cells. Lancet 363(9419):1439–1441
15. Le Blanc K, Frassoni F, Ball L et al (2008) Mesenchymal stem cells for treatment of steroid-resistant, severe, acute graft-versus-host disease: a phase II study. Lancet 371(9624):1579–1586
16. Li H, Guo ZK, Li XS et al (2007) Functional and phenotypic alteration of intrasplenic lymphocytes affected by mesenchymal stem cells in a murine allosplenocyte transfusion model. Cell Transplant 16(1):85–95
17. Popp FC, Eggenhofer E, Renner P et al (2009) Mesenchymal stem cells can affect solid organ allograft survival. Transplantation 87(9 Suppl): S57–S62
18. Tse WT, Pendleton JD, Beyer WM et al (2003) Suppression of allogeneic T-cell proliferation by human marrow stromal cells: implications in transplantation. Transplantation 75(3): 389–397
19. Bluestone JA, Thomson AW, Shevach EM et al (2007) What does the future hold for cell-based tolerogenic therapy? Nat Rev Immunol 7(8):650–654
20. Bartholomew A, Sturgeon C, Siatskas M et al (2002) Mesenchymal stem cells suppress lymphocyte proliferation in vitro and prolong skin graft survival in vivo. Exp Hematol 30(1): 42–48
21. Le Blanc K, Tammik L, Sundberg B et al (2003) Mesenchymal stem cells inhibit and stimulate mixed lymphocyte cultures and mitogenic responses independently of the major histocompatibility complex. Scand J Immunol 57(1):11–20
22. Potian JA, Aviv H, Ponzio NM et al (2003) Veto-like activity of mesenchymal stem cells: functional discrimination between cellular responses to alloantigens and recall antigens. J Immunol (Baltimore, MD: 1950) 171(7): 3426–3434
23. Di Nicola M, Carlo-Stella C, Magni M et al (2002) Human bone marrow stromal cells suppress T-lymphocyte proliferation induced by cellular or nonspecific mitogenic stimuli. Blood 99(10):3838–3843
24. Aggarwal S, Pittenger MF (2005) Human mesenchymal stem cells modulate allogeneic immune cell responses. Blood 105(4): 1815–1822
25. Krampera M, Glennie S, Dyson J et al (2003) Bone marrow mesenchymal stem cells inhibit the response of naive and memory antigen-specific T cells to their cognate peptide. Blood 101(9):3722–3729
26. Klyushnenkova E, Mosca JD, Zernetkina V et al (2005) T cell responses to allogeneic human mesenchymal stem cells: immunogenicity, tolerance, and suppression. J Biomed Sci 12(1):47–57
27. Augello A, Tasso R, Negrini SM et al (2005) Bone marrow mesenchymal progenitor cells inhibit lymphocyte proliferation by activation

of the programmed death 1 pathway. Eur J Immunol 35(5):1482–1490

28. Ringden O, Uzunel M, Rasmusson I et al (2006) Mesenchymal stem cells for treatment of therapy-resistant graft-versus-host disease. Transplantation 81(10):1390–1397

29. Kitazawa Y, Li XK, Xie L et al (2012) Bone marrow-derived conventional, but not cloned, mesenchymal stem cells suppress lymphocyte proliferation and prevent graft-versus-host disease in rats. Cell Transplant 21(2–3): 581–590

Chapter 29

Assessment of Anti-donor T Cell Proliferation and Cytotoxic T Lymphocyte-Mediated Lympholysis in Living Donor Kidney Transplant Patients

Aruna Rakha, Marta Todeschini, and Federica Casiraghi

Abstract

Organ transplant recipients are at risk of allograft rejection, and remain dependent on lifelong immunosuppressive agents, with the attendant risks of infections, cancers, and drug toxicities. Mesenchymal stromal cells (MSCs) have emerged as an alternative to the current pharmacologic immunosuppressive therapy as these cells are immune privileged and possess immunomodulatory properties. However, clinical data are incomplete regarding the efficacy of MSC therapy to control alloimmune response of the transplant recipients. Coordinated efforts should now be directed towards assays for monitoring anti-donor T cell response of MSC-treated patients to establish the pro-tolerogenic potential of MSC-based therapy.

Here, we describe two useful tools to monitor MSC-mediated immunomodulation: the assessment of T cell proliferation by carboxyfluorescein succinimidyl ester (CFSE) dilution assay and the evaluation of cytotoxic T lymphocyte (CTL)-mediated lysis of ^{51}Cr-labeled target cells (cell-mediated lympholysis; CML) following mixed lymphocyte cultures of peripheral blood mononuclear cells (PBMCs) from kidney donors and transplant recipients.

Key words T cell proliferation, CFSE, Cytotoxic T cell-mediated lympholysis, ^{51}Cr release assay, Immunomonitoring, Kidney transplant recipients, Mesenchymal stromal cells

1 Introduction

Mesenchymal stromal cells (MSCs) are being explored as an alternative to current pharmacologic immunosuppressive drugs in the field of organ transplantation [1, 2] as they have potent immunomodulatory effects on various cell types, regulating both adaptive [3, 4] and innate immune responses [5, 6]. In vitro and in vivo studies in experimental models of solid organ transplantation depict the suppression of the immune response of T cells, dendritic cells, and macrophages in the presence of MSCs, eventually leading to induction/expansion of regulatory T cells and thus maintaining transplant tolerance [1]. On the other hand, in certain conditions, MSCs have been shown to acquire a pro-inflammatory phenotype

Bruno Christ et al. (eds.), *Animal Models for Stem Cell Therapy*, Methods in Molecular Biology, vol. 1213,
DOI 10.1007/978-1-4939-1453-1_29,

that could be a barrier to transplant tolerance induction [2, 7–9]. The translation of MSC therapy from bench to bedside has been successful in terms of MSC administration being safe, without any infusion-related toxicity [7, 10–13]. However, the data are incomplete and inconsistencies exist in both preclinical and clinical trials regarding the efficacy of MSC therapy. Along with the need of extensive preclinical investigations to dissect the mechanism of action of MSCs in vivo and their behavior in a pro-inflammatory environment, monitoring the interplay of immune cells in MSC-treated patients is crucial to establish the pro-tolerogenic potential of this cell-based therapy [6].

The setting of living donor kidney transplantation gives the unique opportunity to collect PBMCs also from the kidney donor, allowing the evaluation of the specific anti-donor T cell responses in transplant recipients before and after MSC infusion. These evaluations have the potential to provide valuable information on the in vivo impact of MSC treatment on host immune response against donor alloantigens.

The function of donor-reactive T cells is assessed in mixed-lymphocyte reactions, in which host PBMCs are cocultured with irradiated PBMCs from the living donor. The read-outs can be measurement of cytokine release by ELISA or ELISPOT and T cell proliferation. ELISA and ELISPOT assays are relatively easy and fast, and the relating protocols are standardized and well described. More informative, however, is the assessment of T cell proliferation by carboxyfluorescein succinimidyl ester (CFSE) dilution assay as well as the evaluation of cytotoxic T lymphocyte (CTL)-mediated lysis of ^{51}Cr-labeled donor cells (cell-mediated lympholysis; CML). These tools are more complex, prone to several variables requiring well defined procedures for their application to be in place.

CFSE dilution assay is a widely used assay for measuring the proliferation capacity of lymphocytes. CFSE is an intracellular fluorescent dye that is equally distributed over daughter cells following each cell division, and this progressive halving of fluorescence can be monitored through flow cytometry. CFSE passively diffuses into the cells and intracellular esterases then cleave their acetate groups to yield highly fluorescent, amine-reactive carboxyfluorescein succinimidyl ester that further reacts with intracellular amines, forming fluorescent conjugates that are retained inside the cells. With the division of cells, this fluorescence is reduced to half, which makes it possible to track the cells in different stages of division. CFSE-labeled cells from patients are cocultured in mixed-lymphocyte cultures with irradiated donor cells in order to see a donor-specific response.

The classical tool to detect cytotoxic activity of CTL is the ^{51}Cr release assay. In this assay, recipient T cells, previously stimulated in mixed-lymphocyte cultures, are cultured with ^{51}Cr-labeled donor

and third party cells for a short period and the amount of lysis is determined by measuring ^{51}Cr released in the supernatant.

Here, we describe detailed methods for the assessment of T cell proliferation by CFSE dilution assay and for CTL-mediated lysis.

2 Materials

Peripheral blood mononuclear cells (either freshly isolated or thawed after liquid N_2 freezing) from kidney transplant patients (before and at different time points after transplant/MSC infusion), from living kidney donor, and from third party subjects (healthy volunteers) (*see* **Notes 1–3**).

2.1 CFSE Dilution Assay

1. CFSE: CellTrace™ CFSE Cell Proliferation Kit (Molecular Probes™); 5 mM stock solution, 2 μm working solution.
2. Complete medium: (prewarmed until mentioned to be cold) RPMI-1640, 20 % human serum (male, AB), 2 mM L-glutamine, 100 U/mL penicillin/streptomycin, 12.5 μM β-mercaptoethanol
3. Serum-free medium: Neat RPMI-1640, 2 mM EDTA.
4. FACS solution: 1× PBS, 2 % human serum (male, AB), 2 mM EDTA.
5. Changing complete medium: Complete medium, 20 U/mL recombinant IL-2. (IL-2 is optional depending upon experimental requirements)
6. Dimethylsulfoxide (DMSO).
7. Antibodies for staining CD4 and CD8 surface markers (CD4-APC, clone RPA-T4, CD8-PECy7, clone SK1), and 7-AAD for dead cell analysis.
8. Antibodies for proliferation (control): anti-human CD3 (clone OKT3), anti-human CD28 (clone CD28.6).
9. Flow cytometer and FlowJo software.

2.2 Cytotoxic T Lymphocyte-Mediated Lympholysis

1. Tissue-culture sterile disposable: 24-well plates, 96-well round bottom plates, T25 flasks, 15 and 50 mL conical tubes.
2. Complete medium: RPMI-1640, 20 % human serum (male, AB), 2 mM L-glutamine, 100 U/mL penicillin/streptomycin, 12.5 μM β-mercaptoethanol.
3. Phytohemagglutinin (PHA) and recombinant IL-2, 2 μg/μL and 10 U/μL stock solution, respectively.
4. ^{51}Cr sodium chromate, specific activity 15.79 GBq/mg.
5. Triton X-100, to be diluted in 1× PBS.
6. Trypan blue.
7. Radioactive safety cabinet and gamma counter.

3 Methods

For both CFSE dilution assay and CTL-mediated lympholysis, PBMCs isolated from kidney transplant patients are used as responder cells in mixed lymphocyte culture (MLC) against irradiated stimulator cells (4,000 RAD; *see* **Note 4**). Stimulator cells are PBMCs from the kidney transplant patients themselves (control combination, optional), from the kidney donor (anti-donor reactivity), and from a third party subject (anti-third party reactivity) (*see* **Note 5**).

3.1 CFSE Dilution Assay

3.1.1 Cell Preparation

1. Resuspend the responder cells in serum-free medium at a density of $4–5 \times 10^6$ per mL to be stained by CFSE dye.
2. Resuspend irradiated (4,000 RAD) stimulator cells (donor and third party cells) at a cell density of 3.5×10^6 per mL.

3.1.2 CFSE Preparation

1. Prepare the primary 5 mM stock of CFSE by resuspending one vial of dye (50 μg) in 18 μL of dimethylsulfoxide (DMSO) and stock solution stored at −20 °C.
2. Prepare a fresh 2 μm working solution before each staining procedure by diluting the stock solution in serum-free medium.

3.1.3 CFSE Staining

1. Dilute the responder cell suspension with working solution of CFSE in the ratio 1:1 for final concentration of CFSE to be 1 μm, immediately mix by gentle vortexing to ensure that the CFSE is dispersed evenly throughout the suspension.
2. Incubate the suspension at 37 °C for 10–12 min.
3. Stop the reaction by adding 5× volume of ice-cold complete medium for quenching and washing off the excess CFSE.
4. Centrifuge the cells at $450 \times g$ for 10 min, and repeat the washing step for a total of two washings.
5. Resuspend the cells in complete medium at a density of 3.5×10^6 per mL.

3.1.4 Coculture Setup for Proliferation Assay

1. Label the round bottom 96-well culture plate with appropriate conditions. Each condition should be performed in triplicates.
2. Pipette 75 μL (~250,000 cells) of irradiated stimulator donor cell suspension and third party cell suspension (controls) in the respective wells.
3. Add 75 μL (~250,000 cells) of responder cell suspension in all the wells with stimulators or third party controls.
4. Add 150 μL (~500,000 cells) of responder cell suspension in 3 wells having plate-bound anti-human CD3 (4 μg/mL), soluble anti-human CD28 (2 μg/mL), and recombinant IL-2 (20 U/mL). This serves as a control to get proliferation peaks.

5. Add 150 μL (~500,000 cells) of responder cell suspension in 3 wells having no stimulus (neither antibodies nor the stimulator cells). This condition is done to set the negative peak while analyzing proliferation.
6. Incubate at 37 °C, 5 % CO_2 in a humidified chamber for 6 days, change the medium every 2 days with "changing complete medium" (*see* Subheading 2.1, **step 5**).
7. On the seventh day, harvest the cells, wash with FACS solution and stain for CD4, CD8 surface markers and 7-AAD for dead cell analysis.
8. Resuspend in 150 μL of FACs solution.
9. Analyze by flow cytometry in respective channels for CFSE, CD4, CD8, and 7-AAD.

3.1.5 Flow Cytometry

1. Perform the gating of cells according to 7-AAD staining in PerCP channel to exclude dead cells (Fig. 1a).
2. Gate the live cells on the basis of CD4 and CD8 staining (Fig. 1b).
3. Set the negative peak by analyzing the responder cells without any stimulus (Fig. 1c).
4. Analyze the $CD8^+$ T and $CD4^+$ T cells for proliferation in FITC channel for CFSE diffusion in the cells (Fig. 1d, e, respectively).
5. Apply compensation and analyze using FlowJo software.

3.1.6 FlowJo Analysis

$CD4^+$ T and $CD8^+$ T cell subsets are further analyzed for proliferation on the basis of number of divisions each subset has undergone by using the FlowJo platform.

1. On a particular T cell subset ($CD4^+$ or $CD8^+$), plot CFSE-FITC on the *X*-axis and histogram on *Y*-axis. The software calculates the number of peaks attained indicating average of cells in each division.
2. Perform statistical analysis on the number of divisions that each set of cells has undergone from kidney transplant patients at the different time intervals.
3. Plot a line graph to compare the proliferation index of the patients post MSC infusion as compared to before infusion and with patients without MSC infusion.

3.2 Cytotoxic T Lymphocyte-Mediated Lympholysis (^{51}Cr Release Assay)

Be careful when handling radioactive substances and follow the laws of the state regarding personal and environmental protection.

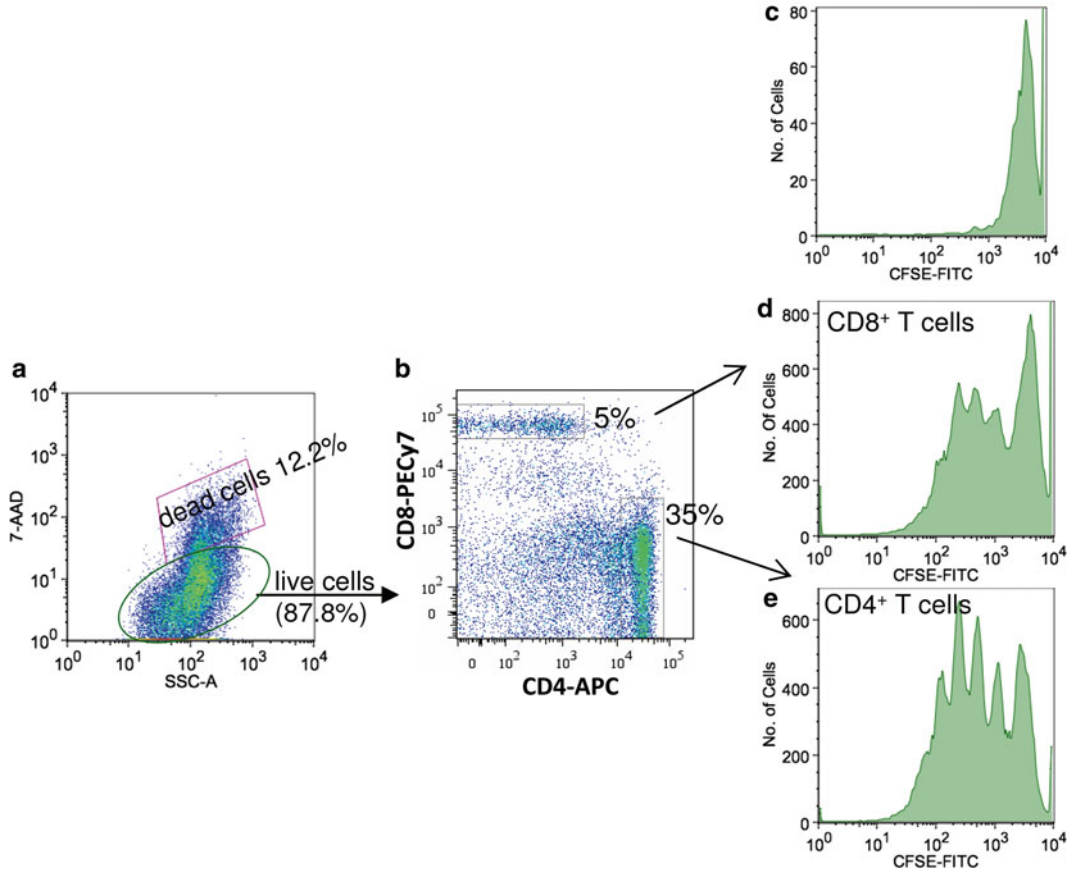

Fig. 1 (**a**) Cells gated according to expression of 7-AAD to exclude dead cells from the analysis. (**b**) Cells gated according to differential expression of CD4 and CD8 antigens. (**c**) Representative histogram indicating the negative peak representing CFSE fluorescence of unstimulated cells. (**d**) Representative CFSE profiles of gated $CD8^+$ T cells stimulated for 6 days in MLR. (**e**) Representative CFSE profiles of gated $CD4^+$ T cells stimulated for 6 days in MLR

3.2.1 Preparation of Effector Cells

1. Prepare responder and irradiated stimulator (donor, third party) PBMC suspensions at a cell density of 2×10^6 cells/mL in complete medium.
2. Mix 1 mL of responder cell suspension with 1 mL of stimulator cell suspension (donor, third party) in a 24-well plate, each condition should be performed in duplicates.
3. Incubate the mixed lymphocyte cultures at 5 % CO_2, 37 °C in a humidified chamber for 6 days.
4. Harvest the cells by gentle pipetting in a sterile 15 mL conical tube (pooling the duplicates). Centrifuge at $450 \times g$ for 10 min. Resuspend in complete medium (500 μL) and count live cells (Trypan blue).
5. Resuspend the cells (effector cells) in complete medium at a cell density of 5×10^6 cells/mL.

3.2.2 Preparation of Target Cells

1. Incubate 3×10^6 non-irradiated PBMCs from the kidney donor and third party (and from kidney transplant recipient, optional) in 10 mL complete medium supplemented with human recombinant IL-2 at a final concentration of 5 U/mL and PHA at a final concentration of 2 μg/mL in T25 flasks. Keep the flasks in vertical position in an atmosphere with 95 % humidity and 5 % CO_2 at 37 °C for 5 days.
2. On the fifth day, transfer the cells in a 50 mL conical tube, add some fresh complete medium and centrifuge at $450 \times g$ for 10 min.
3. Resuspend target cells in 1 mL complete medium, transfer in a well of a 24-well plate and add 1.25 MBq/well ^{51}Cr sodium chromate. Incubate overnight at 5 % CO_2, 37 °C.
4. Harvest ^{51}Cr-labeled target cells in a 50 mL conical tube, add fresh medium and centrifuge at $450 \times g$, 10 min.
5. Discard the supernatant in a controlled manner and count the live cells (Trypan blue). Resuspend the target cells in complete medium at the final cell density of 50,000/mL.

3.2.3 Cell-Mediated Lympholysis

1. In a 96-well plate, mix effector cells with target cells in ratios of 100:1, 50:1, 25:1, 12.5:1, 6.25:1. Mix the cells in the following manner: add 100 μL of target cell suspension (5,000 ^{51}Cr-labeled cells) to respective wells (Fig. 2a). Add 100 μL, 50 μL, 25 μL, 6.2 μL of effector cell suspension to perform 100:1, 50:1, 25:1, 12.5:1, 6.25:1 effector–target cell ratio combination. Adjust final volume to 200 μL by adding complete medium. As controls, incubate 100 μL of target cell suspension with 100 μL complete medium (spontaneous release) and with 100 μL Triton X-100 4 % for the evaluation of maximum ^{51}Cr release (Fig. 2b). Each condition should be performed in triplicates (Fig. 2a). Incubate plates at 5 % CO_2, 37 °C in a humidified chamber for 4 h.
2. At the end of incubation period, centrifuge the plates at $100 \times g$ for 3 min. Collect carefully 125 μL of supernatant from each well and measure the radioactivity.
3. Calculate % of lysis with the following formula:

$$\%\ \text{specific lysis} = \frac{\text{Experimental release}(\text{cpm}) - \text{Spontaneous release}(\text{cpm})}{\text{Maximum release}(\text{cpm}) - \text{Spontaneous release}(\text{cpm})} \times 100$$

Experimental, spontaneous and maximum release values are the mean of the respective triplicates (an example of specific lysis percentages in respect to decreasing effector–target cell ratios obtained in a MLC with PBMCs from healthy volunteers are shown in Fig. 3).

The test should be considered technically successful when the spontaneous release is less than 10–15 % of the maximum release.

a

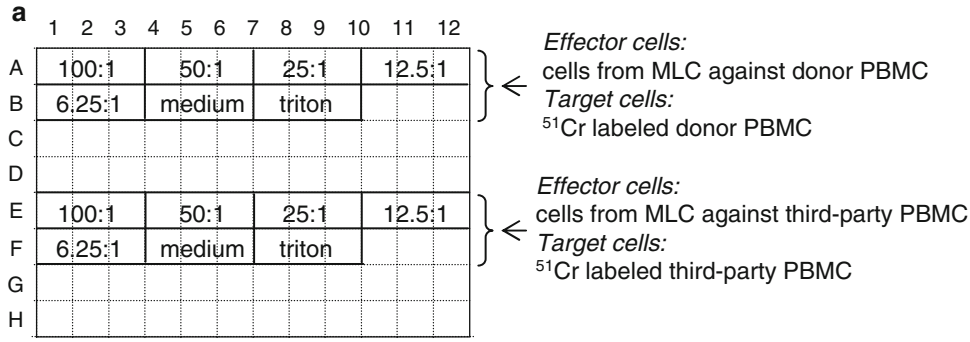

b

Effector:Target ratio	Target cell suspension (μl)	Effector cell suspension (μl)	Complete Medium (μl)
100:1	100	100	0
50:1	100	50	50
25:1	100	25	75
12.5:1	100	12.5	87.5
6.25:1	100	6.25	93.75
Spontaneous release	100	0	100
Maximum lysis	100	0	50 + 50 μl Triton 4%

Fig. 2 (**a**) An example of sample distribution through a 96-well plate for CTL-mediated lympholysis assay. Effector and target cell source are detailed on the *right*. (**b**) Volume of target and effector cell suspension as well as complete medium to be dispensed for achievement of the different effector–target ratios. *MLC* mixed lymphocyte cultures

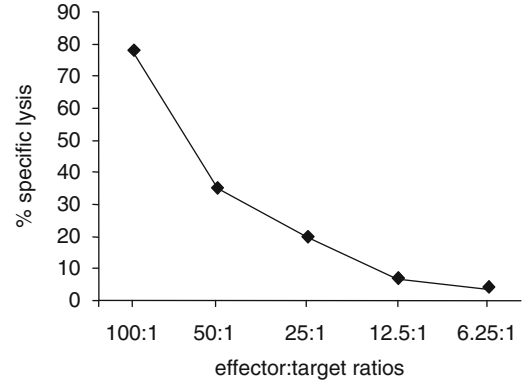

Fig. 3 An example of % of specific lysis (*Y*-axis) in respect to the decreasing effector–target ratios (on *X*-axis). These results have been achieved after performing a CML test with PBMCs from healthy volunteers

4 Notes

1. Peripheral blood mononuclear cells (PBMCs) are isolated from peripheral blood by density gradient centrifugation using standardized protocols. We usually obtain $40–60 \times 10^6$ PBMCs from 50 mL heparinized blood by density gradient centrifugation on Ficoll-Paque PLUS.
2. The analysis of T cell response to third party cells is usually run in parallel in each assay to assess whether any hypo-/unresponsiveness against donor cells is specific (down-regulation of anti-donor T cell response and normal anti-third party response) or if it reflects a state of generalized hypo-/unresponsiveness (both anti-donor and anti-third party T cell responses are down-regulated). Choose third party subjects, to the extent possible, such that the HLA mismatches are the same as those between the donor and the recipient.
3. To avoid any reproducibility/variability issues, it is more appropriate to perform a single assay involving PBMCs collected before and at different time points post transplant from a kidney transplant recipient. This allows a more accurate evaluation of the anti-donor response before and after transplantation/MSCs infusion.
4. Cell irradiation can be performed by X-radiation (4,000 RAD). Commonly used sources are ^{137}Cs or ^{60}Co. If a radiation source is not available, stimulator cells can be inactivated by treatment with mytomycin C. This treatment is performed in the following manner. To a 2 mL (5×10^6 cells) cell suspension add 0.2 mL of mitomycin C (0.25 mg/mL). The mixture is then incubated for 20 min at 5 % CO_2, 37 °C. Following the incubation, the cells are washed three times in culture medium. It is important to note that up to 50 % of the cells may be lost in this procedure.
5. After PBMC thawing, revive responder cells in complete medium for at least an hour at 37 °C, 5 % CO_2 before adding stimulator cells.

Acknowledgements

We greatly acknowledge Prof. Giuseppe Remuzzi and Dr. Norberto Perico for their suggestions and helpful discussion. This study has been partially supported by grants from Fondazione ART per la Ricerca sui Trapianti (Milan, Italy).

References

1. Casiraghi F, Perico N, Remuzzi G (2013) Mesenchymal stromal cells to promote solid organ transplantation tolerance. Curr Opin Organ Transplant 18:51–58
2. English K, Wood KJ (2013) Mesenchymal stromal cells in transplantation rejection and tolerance. Cold Spring Harb Perspect Med 3:a015560
3. Duffy MM, Ritter T, Ceredig R et al (2011) Mesenchymal stem cell effects on T-cell effector pathways. Stem Cell Res Ther 2:34
4. English K (2013) Mechanisms of mesenchymal stromal cell immunomodulation. Immunol Cell Biol 91:19–26
5. Le Blanc K, Mougiakakos D (2012) Multipotent mesenchymal stromal cells and the innate immune system. Nat Rev Immunol 12:383–396
6. Krampera M, Galipeau J, Shi Y et al (2013) Immunological characterization of multipotent mesenchymal stromal cells—the International Society for Cellular Therapy (ISCT) working proposal. Cytotherapy 15:1054–1061
7. Perico N, Casiraghi F, Introna M et al (2011) Autologous mesenchymal stromal cells and kidney transplantation: a pilot study of safety and clinical feasibility. Clin J Am Soc Nephrol 6:412–422
8. Casiraghi F, Azzollini N, Todeschini M et al (2012) Localization of mesenchymal stromal cells dictates their immune or proinflammatory effects in kidney transplantation. Am J Transplant 12:2373–2383
9. Koch M, Lehnhardt A, Hu X et al (2013) Isogeneic MSC application in a rat model of acute renal allograft rejection modulates immune response but does not prolong allograft survival. Transpl Immunol. doi:10.1016/j.trim.2013.08.004
10. Tan J, Wu W, Xu X et al (2012) Induction therapy with autologous mesenchymal stem cells in living-related kidney transplants: a randomized controlled trial. JAMA 307: 1169–1177
11. Reinders ME, de Fijter JW, Roelofs H et al (2013) Autologous bone marrow-derived mesenchymal stromal cells for the treatment of allograft rejection after renal transplantation: results of a phase I study. Stem Cells Transl Med 2:107–111
12. Perico N, Casiraghi F, Gotti E et al (2013) Mesenchymal stromal cells and kidney transplantation: pretransplant infusion protects from graft dysfunction while fostering immunoregulation. Transpl Int 26:867–878
13. Peng Y, Ke M, Xu L et al (2013) Donor-derived mesenchymal stem cells combined with low-dose tacrolimus prevent acute rejection after renal transplantation: a clinical pilot study. Transplantation 95:161–168

Chapter 30

Modulation of Autoimmune Diseases by iPS Cells

Fengyang Lei, Rizwanul Haque, Xiaofang Xiong, and Jianxun Song

Abstract

Autoimmune disease is typically caused by the activated self-reacted immune cells. The mainstream treatment to autoimmune disorders is composed of different mechanisms of immunosuppression. In recent years, a new subtype of T cells called regulatory T (Treg) cells have been identified to maintain the immune homeostasis in terms of suppressing the activated immune components.

According to this discovery, it is suggested that treating autoimmune patients by supplementing Treg cells would be a good choice. However, due to their natural scarcity, it is difficult to isolate a desired number of Treg for this therapeutical approach. Here, we report that by using stem cells, especially the induced pluripotent stem (iPS) cells, we are able to generate a significant amount of Treg cells for the autoimmune prevention and treatment.

Key words iPS cells, Treg cells, Notch signaling, Differentiation, Autoimmune and immunosuppression

1 Introduction

There is a special group of T cells existing in human and mouse immune systems called regulatory T (Treg) cells. The general function of Treg cells is to suppress the activated immune system through different mechanisms such as direct contact or cytokine-mediated immune suppression. Although this Treg-mediated immunosuppression is malicious in timorous condition, on the flip side, it plays an important role in controlling autoimmunity, for example, rheumatoid arthritis and systemic lupus erythematosus. This unique immunosuppressive property of Treg cells renders them good candidates for treating different types of autoimmune diseases. However, due to the nature of the scarcity of Treg cells in humans, it is difficult to collect adequate numbers of active Treg cells in the clinical setting. To find a new approach to generate a large number of Treg cells becomes the hotspot of current research in immunology and stem cell biology. Previous studies have shown that embryonic stem cells are able to differentiate into T cells in a controlled condition and ectopic expression of Treg promoter

Bruno Christ et al. (eds.), *Animal Models for Stem Cell Therapy*, Methods in Molecular Biology, vol. 1213,
DOI 10.1007/978-1-4939-1453-1_30,

FoxP3 is able to convert naïve T cells into Treg cells. Therefore, under these circumstances, it is hypothesized that stem cells, especially embryonic stem cells are able to generate Treg cells by introducing both T cell differentiation signals and Treg-inducing signals. For testing this hypothesis, we used induced pluripotent stem (iPS) cells as a model system to bypass the ethic and technique difficulties in using embryonic stem cells. Meanwhile, using iPS cells as a model system could further help to design a stem cell-originated, personalized immunotherapy to autoimmune patients.

In this chapter, the generation and following characterization of Treg cells from iPS cells will be described in a chronological format. After reading this chapter, readers should have an initial impression about how to generate Treg cells from iPS cells.

2 Materials

2.1 Cells and Mice

1. iPS-MEF-Ng-20D-17 cell line: generated from mouse embryonic fibroblasts by retroviral transduction of Oct3/4 Sox2, Klf4, and c-Myc [1] (*see* **Note 1**). iPS cells are routinely maintained on irradiated SNL76/7 feeder cells with conditioned 15 % FBS-supplemented DMEM.
2. OP9-DL1 cell line (*see* **Note 2**) and OP9-DL1 I-A^b cell line: OP9-DL1 I-A^b cell line is generated by introducing MHC-II molecule I-A^b (*see* **Note 3**) into OP9-DL1 cells through a retroviral transduction [2]. OP9-DL1 and OP9-DL1 I-A^b cell lines are routinely maintained in 20 % FBS-supplemented α-MEM medium.
3. SNL76/7 cell line (ATCC): maintained in 10 % FBS-supplemented DMEM. Before using as iPS feeder cells, SNL76/7 cell are irradiated with a dose of 5,000 Rads in the ^{60}Co irradiator, the irradiated SNL76/7 cells are designated as irSNL76/7 cells [3].
4. 4–12 weeks of age C57/BL6, B6.129S7-*Rag1*^{tm1Mom} (Rag1-deficient), and DBA/1 mice (Jackson Laboratory).
5. Plat-E packaging cells (*see* **Note 4**).

2.2 Cell Culture

1. 6- and 24-well culture plate (BD).
2. 100 mm culture dish (BD).
3. 70 μm cell strainer (BD).
4. Syringes (1 mL and 10 mL, BD).
5. Needles (27G$^{1/2}$ and 18G1$^{1/2}$, BD).
6. Plastic pipettes (5 mL, 10 mL, 25 mL, 50 mL; BD).
7. 0.22 μM bottle-top filter (Corning).
8. 0.4 μm filter (Millipore).

9. Dulbecco's Modified Eagle Medium (DMEM, Invitrogen).
10. α-Minimal Essential Medium (α-MEM, Invitrogen): one pack of α-MEM powder and 2.2 g $NaHCO_3$ in 1 L ddH_2O. Filtration of prepared medium through a 0.22 μM filter is required for sterilization purpose. FBS, antibiotics, and cytokines are added according to different protocols.
11. Phosphate-buffered saline (PBS): 137 mmol/L NaCl, 2.7 mmol/L KCl, 10 mmol/L $Na_2HPO_4 \cdot 2H_2O$, 2 mmol/L KH_2PO_4, pH 7.4, autoclave before use.
12. 100× Penicillin and Streptomycin Mix (10,000 U/mL, Invitrogen).
13. Fetal bovine serum (FBS, heat-inactivated, HyClone).
14. Flt-3ligand (Flt-3L, PeproTech).
15. Interleukin 7 (IL-7, PeproTech).
16. Neutral Formalin buffer (Decal Chemical).
17. Gelatin (Sigma-Aldrich).
18. Brefeldin A (Invitrogen).
19. Formaldehyde solution (Sigma-Aldrich).
20. Fc blocker 24G2 (BD).
21. Permeabilizing kit (BioLegend).
22. [^{3}H]-labeled thymidine.

2.3 Retroviral Transduction

1. GeneJamma transfection reagent (Stratagene).
2. 5 μg/mL polybrene (Sigma-Aldrich).
3. MoFlo cell sorter.

2.4 Collagen-Induced Arthritis (CIA)

1. Complete Freund's Adjuvant (CFA, Chondrex).
2. Chicken Collagen Type II (Chondrex).

2.5 Immunoblot

1. RIPA lysis buffer (G-Biosciences).
2. Bio-Rad D_C Protein Assay (Bio-Rad).
3. Western Blot NuPAGE system (Invitrogen).
4. ECL immunodetection system (Amersham Pharmacia Biotech).

2.6 Histology and Immunofluorescence

1. Formical-4 buffer (Decal Chemical).
2. 3 % hydrogen peroxide (VWR).
3. DAPI reagent (Enzo Life Sciences).
4. Hematoxylin and eosin (HE) or Safranin O–Fast Green (Sigma-Aldrich).
5. Xylene (Sigma-Aldrich).
6. Ethanol (VWR).
7. Blocking buffer: 3 % BSA in PBS.
8. Easy-Titer IgG assay kit.

Table 1
Antibodies

Name	Clone	Company
CD3	2C11	BD Pharmingen
CD28	37.51	BD Pharmingen
CD3	17A2	BioLegend
CD4	GK1.5	BioLegend
CD8	6A242	Santa Cruz
CD25	3C7	BioLegend
CD44	1M7	BioLegend
CD69	H1.2F3	BioLegend
CD117	2B8	BioLegend
CD127	A7R34	BioLegend
CTLA-4	UC10-4B9	BioLegend
FoxP3	150D	BioLegend
TCR-β	H57597	BioLegend
IL-2	JES6-5H4	BD Pharmingen
IL-10	JES5-16E3	BioLegend
IFN-γ	XMG1.2	BD Pharmingen
LAP (TGF-β1)	TW7-16B4	BioLegend

2.7 Antibodies

Antibodies used are listed in Table 1.

3 Methods

3.1 Retroviral Transduction: Generation of Retroviral Construct

1. Construct MSCV-IRES-DsRED (MiDR) vector from MSCV-IRES-GFP vector by substituting the GFP gene by the DsRED gene (*see* **Note 5**).
2. Subclone FoxP3 and Bcl-xl genes into the MiDR vector to make a FoxP3-Bcl-xl-MiDR construct.

3.2 Retroviral Transduction and Cell Sorting (Fig. 1) (See Note 6)

1. Use Plat-E packaging cells to generate a pseudovirus that will be used for the following transduction.
2. Seed 3×10^6 Plat-E cells on a 100 mm culture dish 1 day prior to transfection with the retroviral construct.
3. On day 0, transfect Plat-E cells with FoxP3-Bcl-xl-MiDR plasmid by using GeneJamma transfection reagent.

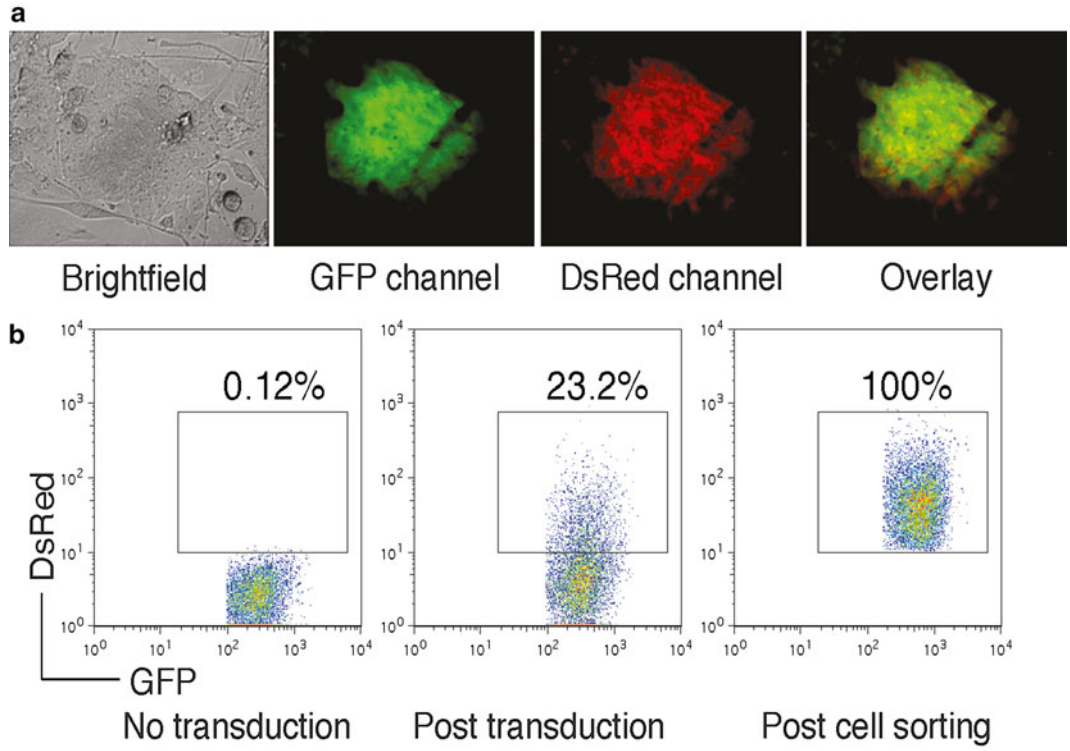

Fig. 1 (**a**) FoxP3-transduced iPS cells were visualized by fluorescence microscopy. (**b**) GFP⁺ iPS cells (*left*) were transduced with the retroviral construct, and GFP⁺ DsRed⁺ iPS cells (*middle*) were analyzed by flow cytometry and sorted by a high-speed cell sorter (*right*)

4. On day 1, seed 1×10^6 iPS cells into one well of a 0.1 % gelatin-pre-coated 24-well plate.
5. On day 2, collect pseudovirus-containing supernatant from Plat-E culture and pass it through a 0.4 μm filter to exclude potential contaminants.
6. Perform transduction at 32 °C and centrifugation at $500 \times g$ for 1 h in the presence of 5 μg/mL polybrene.
7. After centrifuge-based transduction, place cells in 32 °C, 5 % CO_2 incubator overnight.
8. On day 3, repeat the day 2 transduction procedure as described above. Meanwhile, pre-coat a 6-well plate with irSNL76/7 feeder cells for future use.
9. On day 4, trypsinize transduced iPS cells, centrifuge at $400 \times g$ for 5 min and seed on pre-coated irSNL76/7 feeder cells.
10. At confluency, trypsinize cells, centrifuge at $400 \times g$ for 5 min and process for cell sorting. GFP and DsRED double positive cells will be sorted by a MoFlo cell sorter. Culture sorted cells on irSNL76/7 feeder cells for future use (*see* **Note 7**).

3.3 Coculture with OP9-DL1/I-Ab Cells

3.3.1 In Vitro Coculture System

1. On day 0, seed 5×10^4 gene-transduced iPS cells (FoxP3/iPS) on a 100 mm culture dish containing a confluent OP9-DL1/I-Ab cell monolayer in 20 % FBS α-MEM medium.
2. On day 3, change culture medium.
3. On day 5, trypsinize cells and centrifuge at $400 \times g$ for 5 min before incubating on a fresh 100 mm culture dish for 30 min in a 37 °C incubator.
4. Collect and count floating cells, and transfer 5×10^5 cells to a fresh culture dish containing a confluent OP9-DL1/I-A^b cell monolayer in 20 % FBS-supplemented α-MEM medium. Add cytokine mFlt-3L (final concentration: 5 ng/mL) to the culture.
5. On day 8, gently pipette down loosely attached cells.
6. Wash the OP9-DL1/I-A^b feeding layer with 10 mL PBS one more time to get the maximal recovery of partially differentiated iPS cells.
7. After harvesting cells from the coculture, centrifuge cells at $400 \times g$ for 5 min and resuspend in 20 % FBS-supplemented α-MEM medium supplemented with Flt-3L (5 ng/mL) and IL-7 (1 ng/mL).
8. At the end, transfer cells into a 6-well culture plate coated with confluent OP9-DL1/I-A^b cells. Usually iPS cells recovered from one 100 mm culture dish will be transferred into one well of the 6-well plate.
9. From day 10, change culture medium every other day (20 % FBS-supplemented α-MEM medium supplemented with Flt-3L, 5 ng/mL, and IL-7, 1 ng/mL).
10. Culture plates coated with feeder OP9-DL1/MIAb cells will be changed every 4–6 days depending on the growth of the feeder cells.

3.3.2 In Vitro Differentiation of FoxP3/iPS Cells

1. At different days of coculture with OP9-DL1/I-A^b cells, take live cell pictures under a conventional light microscope.
2. Calculate cell recovery rates based on the number of cells harvested from the culture.
3. Analyze surface marker changes by flow cytometry (Fig. 2).
4. On different days of coculture, remove cells by trypsinization and wash with cold PBS before proceeding to cell surface staining.
5. Before staining with different fluorochrome-conjugated antibodies, block cells by Fc blocker 24G2 at 4 °C for 20 min.
6. Stain cells with fluorochrome-conjugated antibodies after Fc blocking.
7. After 20 min of staining at 4 °C, wash the cells three times in cold PBS before flow cytometric examination.

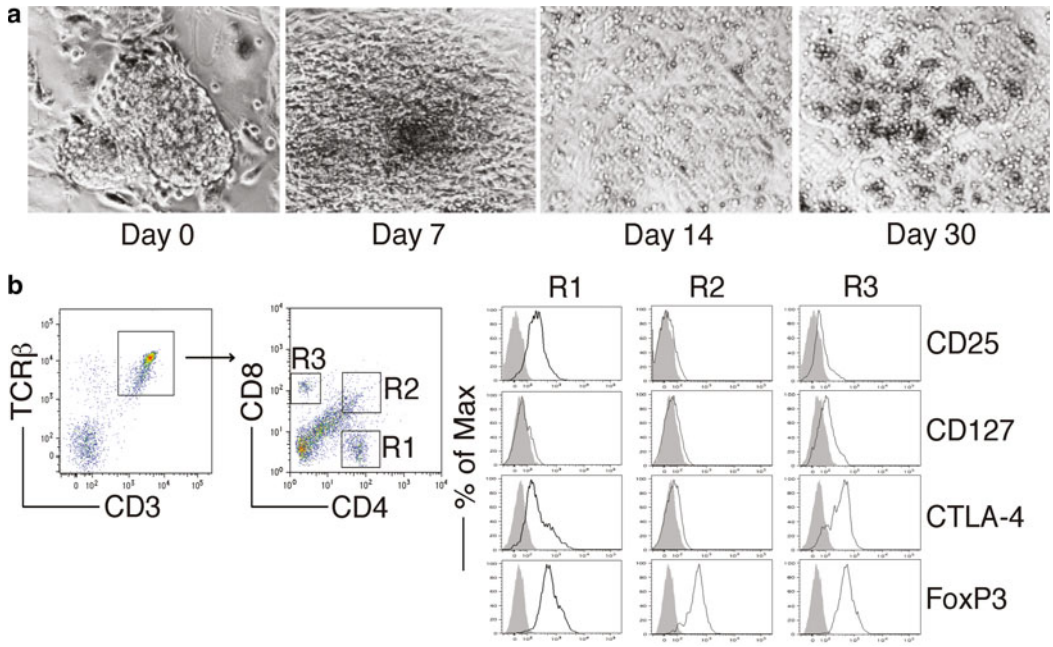

Fig. 2 FoxP3-transduced iPS cells were cocultured on OP9-DL1/M I-A^b cells in the presence of murine recombinant Flt3L and IL-7. (**a**) Morphology of Treg cell differentiation on days 0, 7, 14, and 30. (**b**) Flow cytometric analysis for the protein expression of iPS cell-derived cells on day 30. $CD3^+$ $TCR\alpha\beta^+$ cells were gated as indicated, and analyzed for the expression of CD4 and CD8, with CD25, CD127, CTLA-4, and FoxP3 expression shown for cells gated as $CD4^+$ cells (R1), $CD4^+CD8^+$ cells (R2), and $CD8^+$ cells (R3) (*dark lines*; *shaded areas* indicate isotype controls)

3.3.3 Functional Analysis of In Vitro Differentiated FoxP3/iPS Cells (Fig. 3)

1. One day before activation assay, pre-coat a 24-well plate with anti-CD3 (final concentration: 4 μg/mL in PBS) at 4 °C overnight.
2. On day 45 of coculture, harvest FoxP3/iPS cell-derived T cells from the culture and wash with cold PBS before stimulating with plate-coated anti-CD3 and soluble anti-CD28 antibodies (final concentration: 4 μg/mL).
3. Incubate plate in 37 °C, 5 % CO_2 incubator for 40 h and then add Brefeldin A to the culture for another 4 h.
4. At the end of coculture, harvest cells, wash, and block by Fc blocker as described above. Stain blocked cells for surface markers such as CD3, CD4, CD8, and TCRβ chain by using fluorochrome-conjugated antibodies.
5. After cell surface staining, fix cells by using 4 % formaldehyde, and permeabilize by using BioLegend's Permeabilizing kit.
6. After permeabilization, stain intracellular molecules like TGF-β, IL-10, IL-2, and IFN-γ by using fluorochrome-conjugated antibodies.
7. Before final flow cytometric examination, wash the cells three times in cold PBS to exclude excessive antibodies.

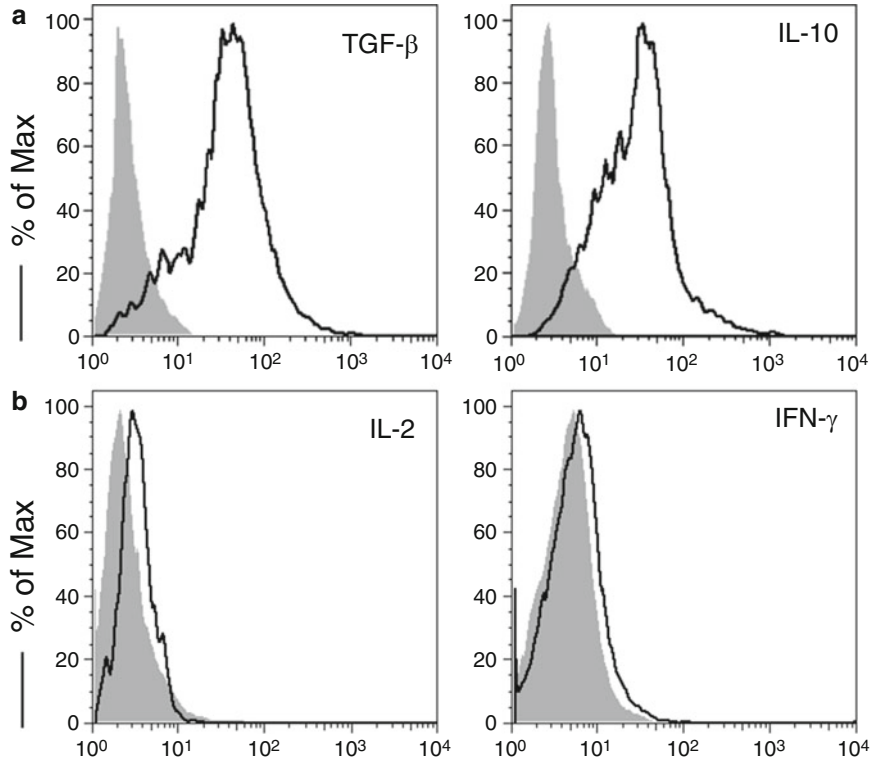

Fig. 3 Murine iPS cell-derived Treg cells were stimulated with plate-coated anti-CD3/anti-CD28 mAbs. Intracellular cytokine production was analyzed by flow cytometry after gating on live $CD4^+$ $CD25^+$ cells (dark *lines*; *shaded areas* indicate isotype controls). (**a**) Intracellular TGF-β and IL-10. (**b**) Intracellular IL-2 and IFN-γ

3.3.4 Immunosuppression Analysis of In Vitro Differentiated FoxP3/iPS Cells (Fig. 4)

1. One day before activation assay, pre-coat a 24-well plate with anti-CD3 (final concentration: 4 μg/mL in PBS) at 4 °C overnight.
2. On day 45 of coculture, harvest FoxP3/iPS cell-derived T cells from culture and wash with cold PBS before stimulating with plate-coated anti-CD3 and soluble anti-CD28 antibodies (final concentration: 4 μg/mL).
3. Harvest naïve CD4 T cells from C57BL/6 mice and mix with in vitro differentiated FoxP3/iPS cells in a 1:1 ratio before the co-stimulatory activation assay.
4. Incubate the mixed population in 37 °C, 5 % CO_2 incubator for 48 h. Add [^{3}H]-labeled thymidine 12 h after the incubation.
5. At the end of coculture, harvest culture supernatant to determine IL-2 and IFN-γ concentrations by ELISA.
6. Later on, harvest cells to check the thymidine incorporation rate.

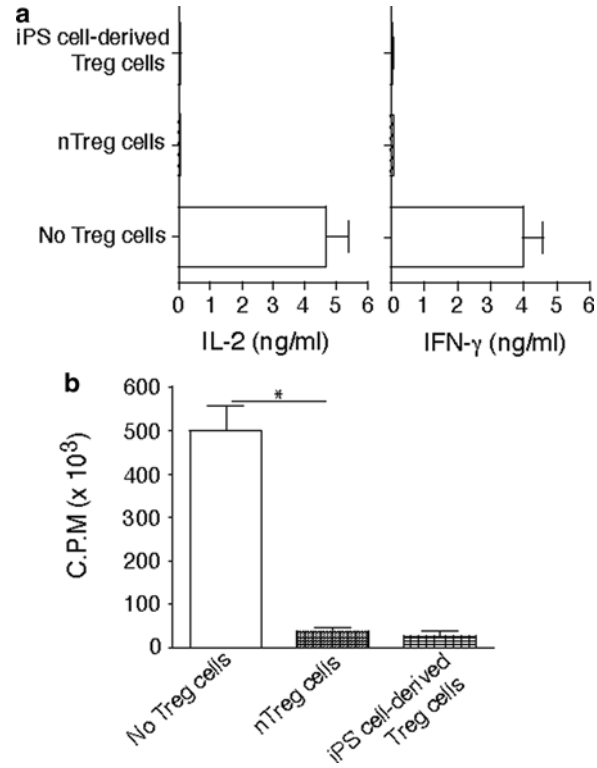

Fig. 4 Murine iPS cell-derived Treg cells were cocultured with naive $CD4^+$ T cells from C57BL/6 mice (Tregs/T cells = 1:1) in the presence of anti-CD3/anti-CD28 mAbs for 2 days. A group of $CD4^+$ T cells stimulated with $CD4^+$ $CD25^+$ Treg cells from C57BL/6 mice as the positive control and a group of $CD4^+$ T cells stimulated without Treg cells as the negative control. Cytokine production was analyzed by ELISA, and proliferation was determined by [^{3}H] thymidine incorporation. (**a**) IL-2 and IFN-γ. (**b**) Thymidine incorporation during the last 12 h. *$P < 0.05$, one-way ANOVA tests

3.4 Adoptive Transfer

FoxP3-Bcl-xl-MiDR-transduced and in vitro-induced iPS (FoxP3/iPS) cells are prepared as described above.

1. After 7 days of in vitro coculture, FoxP3/iPS cells are trypsinized, centrifuged at 400 × *g* for 5 min and resuspended in fresh medium.
2. 30 min incubation on a fresh culture dish in a 37 °C incubator is required to eliminate differentiated cells and remnant feeder cells.
3. At the end of incubation, collect floating cells and centrifuge at 400 × *g* for 5 min.
4. Wash cell pellet in cold PBS three times, and pass cells through a 70 μm nylon strainer in between of two washes to exclude cell clumps (2 × filtration).
5. After wash, count and resuspend cells in cold PBS at a concentration of 1.5×10^7 cells/mL (*see* **Note 8**).

6. Maintain cells on ice before injection.
7. For adoptive transfer, 4–6 weeks old male C57BL/6J mice are used. Before *i.v.* injection through the tail vein, place mice under an infrared light to dilate their tail veins.

3.5 Collagen-Induced Arthritis (CIA)

Fifteen days prior to the adoptive transfer of FoxP3/iPS cells, collagen-induced arthritis (CIA) shall be induced in the recipient male C57BL/6 J mice.

Animal handlings and experimental protocols have to be in accordance with the national regulations and guidelines.

1. Prepare Chicken type-II collagen (CII) according to the manufacturer's protocol. Before CIA, all reagents shall be maintained on ice (*see* **Note 9**).
2. On day 0, CIA is induced in male C57BL/6J mice by one intradermal immunization at two sides in the base and slightly above the tail with chicken CII in CFA.
3. CIA development is monitored by visual inspection as joint swelling and immobility.

3.6 Immunoblot

1. For checking the protein expression level in FoxP3/iPS cells, lyse live cells in RIPA buffer for 30 min to break cell structure and release intracellular proteins.
2. Protein concentration is determined by using Bio-Rad protein assay kit, and equal amounts of protein (30–50 μg) are used for subsequent immunoblotting.
3. All immunoblots are conducted by using a commercial immunoblot kit (Invitrogen's Nu-PAGE system) and all immunoblots are developed with the ECL immunodetection system.

3.7 Histology and Immunofluorescence (Fig. 5)

At day 60 of the CIA experiment, mice will be sacrificed for checking the arthritis development.

1. Amputate hind feet, fix them in Neutral Formalin buffer, and further decalcify in Formical-4 solution.
2. Decalcified samples are prepared as removal of excessive tissue and embedded in paraffin. Make 4 μm sections and stain with HE or Safranin O–Fast Green as described before [4].
3. Perform immunofluorescent staining on the sections after deparaffinization and rehydration by using xylene and ethanol.
4. Block endogenous peroxidase activity by 3 % hydrogen peroxide for 30 min after antibody retrieval.
5. Block nonspecific binding in blocking buffer at room temperature in a moist chamber for 60 min.
6. Add fluorochrome-labeled antibodies in blocking buffer and apply prepared solution onto the slides.

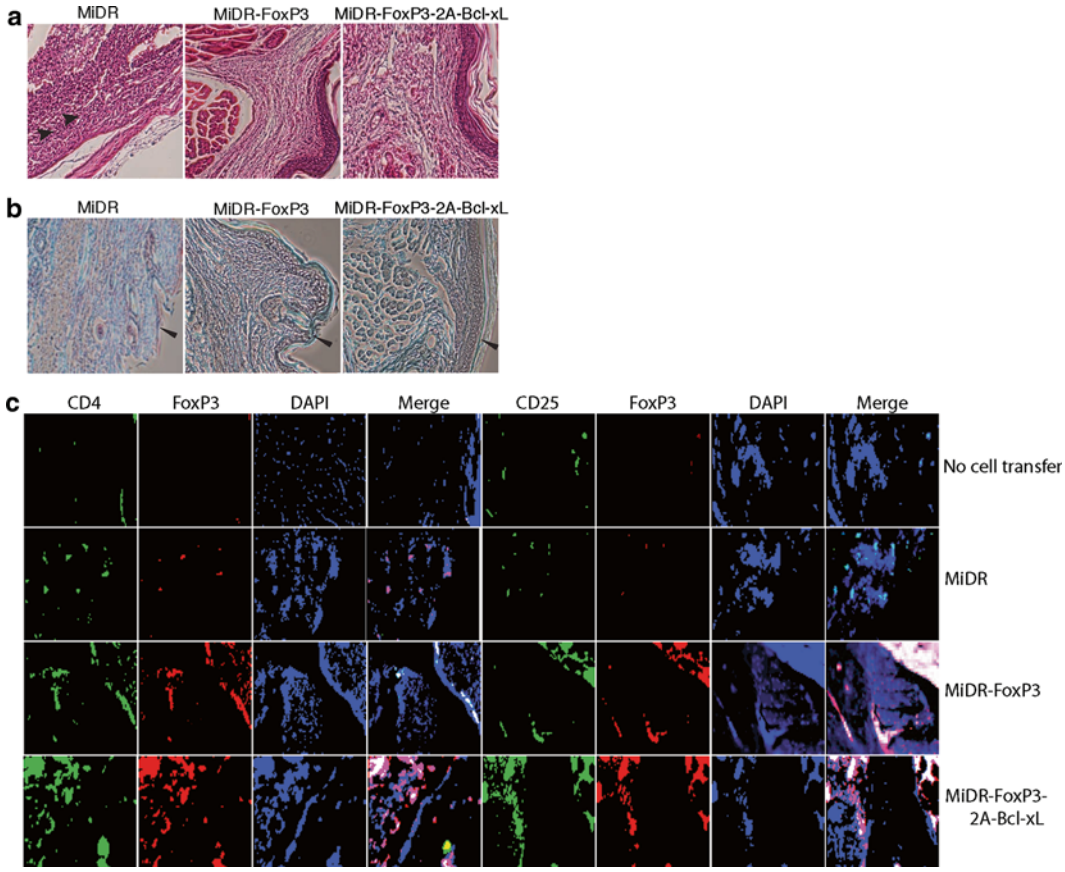

Fig. 5 Murine iPS cells were transduced with retroviral constructs: vector (MiDR), FoxP3 (MiDR-FoxP3), or FoxP3 with Bcl-xL (MiDR-Bcl-xL-2A-FoxP3), and cocultured on OP9-DL1/MIAb cells. On day 7, DsRed-positive (DsRed$^+$) T cells were sorted and prepared for adoptive cell transfer. Collagen-induced arthritis (CIA) was induced in male C57BL/6 mice by one (day 0) intradermal immunization at two sites in the base and slightly above of the tail with chicken type II collagen in complete Freund's adjuvant. On day 15 after the immunization, mice received transduced DsRed$^+$ cells (2.5×10^6/mouse). On day 60 of immunization, hind foot paws were amputated, fixed, and decalcified. The tissues were embedded in paraffin, sectioned, and stained. (**a**) Hematoxylin and eosin (HE) staining. (**b**) Safranin O–Fast Green staining. Infiltrations of polymorphonuclear (PMN) cells (*arrow heads*) in HE staining and massive destruction of cartilage (*leftward arrow heads*) in Safranin O–Fast Green staining are indicated. (**c**) Immunofluorescent staining. There were iPS cell-derived Treg cells (*red*) infiltrating in joints from mice receiving iPS cell-derived Treg cells, but not in tissues from mice receiving vector control-transduced iPS cells or without cell transfer (*green*: CD4 or CD25, *red*: FoxP3, *blue*: DAPI).

7. Incubate the slides at room temperature in a dark moist chamber for 60 min.
8. At the end of incubation, wash the slides in PBS five times before applying DAPI-containing antifade reagent.
9. Evaluate immunofluorescence under fluorescent microscope later.

3.8 Antibody Detection

1. On day 60 of CIA development, sacrifice mice and collect blood from different groups of mice by heart puncture.
2. Collect serum from whole blood from different groups of mice by centrifugation at 1,000 × *g* for 10 min.
3. Total IgG levels are determined by the Easy-Titer IgG assay kit in accordance with the recommendations of the manufacturer.
4. The levels of anti-CII IgG in different blood samples are measured by ELISA as described previously [4].

4 Notes

1. iPS-MEF-Ng-20D-17 cell line is a kind gift from Dr. Shinya Yamanaka at the Kyoto University through the RIKEN cell bank via a completed material transfer agreement (MTA).
2. OP9-DL1 cell line is a kind gift from Dr. J.C. Zuniga-Pflucker [5] at the University of Toronto via a completed material transfer agreement (MTA).
3. MHC-II molecule I-A^b construct is obtained from Dr. Pin Wang at the University of Southern California via a completed material transfer agreement (MTA).
4. Plat-E cells are constructed based on the 293T cell line to permanently express retroviral packaging signals *env* and *gag-pol*, proteins [6].
5. The detailed instruction about retroviral vector, gene fragment manipulation, and construct assembly belongs to the scope of molecular biology. Mastering those molecular biology skills is required to perform this section of work.
6. Usually the retroviral transduction efficiency to induced pluripotent stem cells is low. Adding VSV-G glycoprotein-mediated pseudotyping can increase the transduction efficiency.
7. For cell sorting, cells need to be passed through a cell strainer several times to prevent cell clogging.
8. For adoptive transfer, cells need to be serum-free and clump-free to prevent lung embolism and allergic response in recipient mice. To remove serum, multiple PBS wash is mandatory, and to remove cell clump, pass cells multiple times through cell strainers.
9. When preparing CII in CFA, make sure complete emulsification is achieved otherwise the arthritis induction could be significantly compromised.

Acknowledgements

This project was funded, in part, under grants with the Grant Number K18CA151798 from the National Institutes of Health and the Barsumian Trust to J.S.

References

1. Okita K, Ichisaka T, Yamanaka S (2007) Generation of germline-competent induced pluripotent stem cells. Nature 448:313–317
2. Dai B, Wang P (2009) In vitro differentiation of adult bone marrow progenitors into antigen-specific CD4 helper T cells using engineered stromal cells expressing a notch ligand and a major histocompatibility complex class II protein. Stem Cells Dev 18:235–245
3. Lei F, Zhao B, Haque R, Xiong X, Budgeon L, Christensen ND, Wu Y, Song J (2011) In vivo programming of tumor antigen-specific T lymphocytes from pluripotent stem cells to promote cancer immunosurveillance. Cancer Res 71: 4742–4747
4. Haque R, Lei F, Xiong X, Wu Y, Song J (2010) FoxP3 and Bcl-xL cooperatively promote regulatory T cell persistence and prevention of arthritis development. Arthritis Res Ther 12:R66
5. Schmitt TM, Zuniga-Pflucker JC (2002) Induction of T cell development from hematopoietic progenitor cells by delta-like-1 in vitro. Immunity 17:749–756
6. Morita S, Kojima T, Kitamura T (2000) Plat-E: an efficient and stable system for transient packaging of retroviruses. Gene Ther 7:1063–1066

Chapter 31

A Chimeric Mouse Model to Study Immunopathogenesis of HCV Infection

Moses T. Bility, Anthony Curtis, and Lishan Su

Abstract

Several human hepatotropic pathogens including chronic hepatitis C virus (HCV) have narrow species restriction, thus hindering research and therapeutics development against these pathogens. Developing a rodent model that accurately recapitulates hepatotropic pathogens infection, human immune response, chronic hepatitis, and associated immunopathogenesis is essential for research and therapeutics development. Here, we describe the recently developed AFC8 humanized liver- and immune system-mouse model for studying chronic hepatitis C virus and associated human immune response, chronic hepatitis, and liver fibrosis.

Key words Humanized mice, Chronic hepatitis C virus, Liver immunopathogenesis

1 Introduction

Several human pathogens with significant global health impact, including hepatitis C virus (HCV), hepatitis B virus (HBV), malaria and human immunodeficiency virus (HIV) have narrow host species restriction to humans and other higher primates. Recent advancements in stem cell biology and regenerative medicine have enabled the development of several human–murine chimeric animal models containing lymphoid cells or hepatocytes to overcome host species barriers to studying these pathogens in rodents [1–3]. The Alb-uPA transgenic mouse on an immunodeficient background contains the mouse urokinase-type plasminogen activator (uPA) gene under the control of an Alb enhancer/promoter, which allows for high levels of human adult hepatocyte repopulation. However, these human–murine chimeric liver mouse models lack human immune cells, making it impossible to study chronic hepatitis virus-induced chronic liver inflammation and associated fibrosis [1, 4]. Furthermore, homozygous Alb-uPA transgenic animals are unhealthy and die in the absence of hepatocyte transplantation due to hypofibrinogenemia and associated liver damage [1, 5, 6].

Bruno Christ et al. (eds.), *Animal Models for Stem Cell Therapy*, Methods in Molecular Biology, vol. 1213,
DOI 10.1007/978-1-4939-1453-1_31,

Alb-uPA transgenic immunodeficient mice transplanted with human adult hepatocytes can be infected with HCV, resulting in high levels of virus replication [1]. Additionally, another recently developed human–murine chimeric liver mouse model, the fumarylacetoacetate hydrolase (Fah)-Balb/c-Rag2−/− gamma c−/− mouse allows human adult hepatocytes engraftment and repopulation following liver damage and HCV replication following infection [4, 7, 8].

The development of small animal models that facilitate the elucidation of the mechanisms, by which chronic hepatitis viruses impair human host immune response and promote immunopathology, is a major barrier in biomedical research. To overcome this barrier, we recently developed a humanized mouse model with both human immune system and liver cells. The humanized liver- and immune system-mouse model was developed by transplanting human progenitor liver cells (HPC) and CD34+ hematopoietic stem cells (HSC) into immunodeficient AFC8 mice and inducing Caspase 8-mediated murine-specific hepatocytes apoptosis to promote human hepatocytes regeneration. Caspase 8-mediated murine-specific apoptosis was induced using the AFC8 transgene [9] (Fig. 1). The AFC8 model's construct is a ligand (FKBP) inducible Caspase 8 transgene, under transcriptional regulation by the albumin enhancer/promoter, thus enabling murine liver-specific damage [9] (Fig. 1). The AFC8 construct was used to create the AFC8 mice model in the Balb/c-Rag2−/− gamma c−/− mouse [9]. The Balb/c-Rag2−/− gamma c−/− mouse is a robust

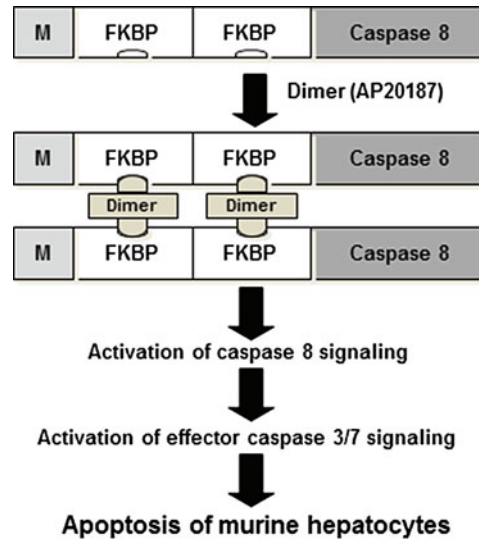

Fig. 1 Murine specific apoptotic signaling induces temporal liver-specific damage in AFC8 immunodeficient mice. The structure of the AFC8 transgene and the mechanism of Caspase-mediated murine hepatocyte apoptosis following ligand (AP20187) activation

immunodeficient mouse model, devoid of functional T, B, and NK cells, and supports development of a functional human immune system following intra-hepatic injection of CD34+ human hematopoietic stem cells [2, 3, 10]. To construct the humanized liver- and immune system-mouse model we co-transplanted human liver progenitor cells (HPC) and CD34+ human hematopoietic stem cells (HSC) into AFC8 transgenic mice and treated them with the FKBP dimerizer (AP20187) to induce human hepatocytes repopulation (Fig. 2). The AFC8-DKO mouse model allows the development of both human liver and immune cells, thereby generating the HSC/Hep humanized mouse model (Fig. 2) [9]. The HSC/Hep mouse model supported HCV infection and generated a human T cell response to HCV. Additionally, HCV infection induced chronic liver inflammation and fibrosis, which correlated with activation of human hepatic stellate cells and expression of human fibrogenic genes [9] (Fig. 3). Furthermore, unpublished results suggest that the HSC/Hep mouse model supports HBV infection and associated immunopathogenesis.

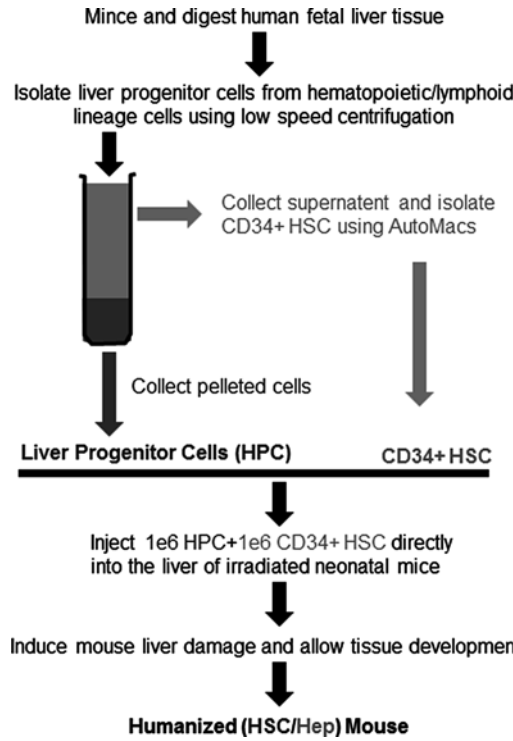

Fig. 2 Liver and immune system humanization in the AFC8 immunodeficient mouse. Overview of hematopoietic stem cell and liver progenitor cell isolation, transplantation, and development of AFC8 humanized HSC/Hep mouse model

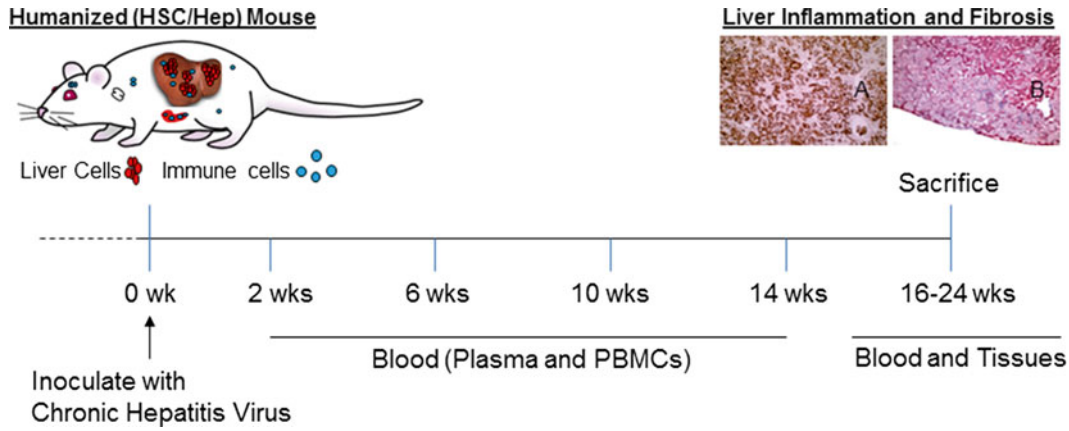

Fig. 3 Chronic hepatitis virus infection, immune response, and liver immunopathogenesis in the humanized mouse model. Timeline for chronic hepatitis virus infection, human immune response, and liver fibrosis analysis in the humanized mouse model. Blood is collected via tail bleeding for longitudinal analysis of plasma and PBMCs. Blood and tissues (liver, spleen, lymph nodes, bone marrow, and other internal organs) are collected at approximately 16 weeks post inoculation (WPI) for analysis; note extensive liver infiltration of human leukocytes (human CD45+, *brown* cells—**a**) and associated liver fibrosis (*blue* stain—**b**)

2 Materials

All experiments using live rodents and human tissues must conform to appropriate National and Institutional Guidelines; appropriate biosafety measure commensurate with the infectious pathogen under investigation should be employed.

2.1 Progenitor Liver Cells and Hematopoietic Stem Cells

1. 15–18 weeks gestation period-human fetal liver obtained from Advanced Bioscience Resources, CA (*see* **Note 1**).
2. Liver Digestion Medium (Gibco).
3. Ficoll.
4. Human CD34 Indirect MicroBead Kit.
5. Manual or automated cell separators.
6. Running Buffer for cell separator.
7. Rinsing Solution for cell separator.
8. Cell Wash Buffer: make fresh using complete Iscove's Modified Dulbecco's Medium (IMDM) with 2.5 μL DNase at 5 mg/mL added per 50 mL.
9. Antibody mix for CD34+ HSC yield and purity: Add 2 μL anti-human CD34 FITC, 2 μL anti-human CD45 PE, and 0.5 μL 7-AAD in 50 μL 2 % Fetal Bovine Serum (FBS)/PBS per sample prior to staining.
10. Antibody mix for human immune repopulation: Add 2 μL anti-human CD45 FITC, 2 μL anti-mouse CD45 PE, and 0.5 μL 7-AAD in 50 μL 2 % FBS/PBS per sample prior to staining.

11. Media: Make fresh using IMDM supplemented with 10 % of FBS, Penicillin–Streptomycin (Pen-Strep), l-glutamine.
12. Trypan Blue.
13. Hemocytometer.
14. Multicolor Flow Cytometer.

2.2 Transplantation of Progenitor Liver and Hematopoietic Stem Cells

1. 2–5-day-old newborn AFC8 mice (Balb/c-Rag2−/− gamma c−/− mice, expressing active Caspase 8 fused with FK506 binding domain under control of the albumin promoter).
2. X-ray irradiators.
3. Microscope lamps.
4. 0.5 cc insulin syringes with 27-gauge needles.
5. Sulfamethoxazole–trimethoprim.
6. ACK lysis buffer.
7. AP20187 (Induces FKBP/Caspase 8 dimerization and mouse hepatocyte damage and human liver cells repopulation) (Ariad Pharmaceuticals).
8. Avertin.

3 Methods

3.1 Liver Digestion

1. Warm up wash buffer in 37 °C water bath and add 2.5 μL DNase for every 50 mL of liver digestion medium to create the liver digestion solution; make 100 mL per liver to be digested. Pour entire fetal liver into a 10 cm dish and mince parenchymal tissue (about 1–2 mm^3) with scalpels; discard the connective tissue. Alternatively, the tissue can be dissociated using automated tissue dissociators and following manufacturer's recommended protocol.
2. Transfer the minced tissue into a 50 mL tube and wash the dish with 10 mL liver digestion solution; add wash to the same tube. Fill the tube with liver digestion solution to 40 mL total volume and wrap the tube cap with Parafilm (*see* **Note 2**).
3. Shake the tube for 5–10 s and place in a 37 °C water bath for 30 min. Shake the tube every 5 min for the duration of the incubation step. The larger tissue pieces will settle to the bottom; remove the liquid portion and filter through a 70 μm filter into a new 50 mL tube and store on ice. Add 35 mL of liver digestion solution to the tube containing larger tissue pieces and repeat digest; filter into a new 50 mL tube.
4. Spin the two tubes with liver cells at 252 × *g* for 10 min at 4 °C and decant the supernatant. Resuspend the cells with 40 mL wash buffer and combine to one 50 mL tube.

3.2 Liver Progenitor Cells (HPC) Purification

1. Spin the suspension down at $18 \times g$ at 4 °C for 5 min and remove the supernatant. Transfer to a new 50 mL tube and store on ice; this is for CD34+ HSC separation.
2. Resuspend the pellet with 14 mL wash buffer and transfer to a 15 mL conical tube. Spin the suspension down at $18 \times g$ for 5 min at 4 °C and transfer the supernatant to a new tube on ice; this is for CD34+ HSC separation.
3. Resuspend the pellet with 14 mL wash buffer and repeat wash procedure including supernatant collection for CD34+ HSC separation. The pellet should appear white or yellow (not red) in color (*see* **Note 3**). The light colored pellet contains liver progenitor cells. Resuspend the pellet containing liver progenitor cells with 10 mL wash buffer and transfer into a 15 mL tube. Store tube containing liver progenitor cells on ice until the transplantation step; limit storage to 12 h. Count cells using a hemocytometer after trypan blue staining.

3.3 CD34+ Cell Purification

1. Combine previously collected supernatants "for HSC purification." Centrifuge the collected supernatants containing CD34+ HSC at $469 \times g$ for 5 min at 4 °C; combine pellets and resuspend in 35 mL of wash buffer.
2. Fill a 15 mL pipette with 14 mL of Ficoll and eject only 11 mL very slowly at constant flow at the bottom of the tube under the cell suspension without disturbing the interface (*see* **Note 4**). Carefully spin the tube at $1{,}880 \times g$ for 30 min at room temperature (24 °C). Remove the cells at the interface without disturbing the Ficoll. Transfer the collected cells into a 50 mL tube and add 40 mL of wash buffer.
3. Centrifuge the suspension at $469 \times g$ at 4 °C for 5 min and discard the supernatant; resuspend the pellet in 10 mL wash buffer. Centrifuge the suspension at $469 \times g$ at 4 °C for 5 min and discard the supernatant without disturbing the pellet.
4. Resuspend the cells in 400 μL of wash buffer for every 1×10^8 cells counted using a hemocytometer and trypan blue. Add 100 μL of the FcR Blocking reagent (Human CD34 Indirect MicroBead Kit) for every 1×10^8 cells and mix well. Add 100 μL of the CD34-Hapten-Antibody reagent (Human CD34 Indirect MicroBead Kit) for every 1×10^8 cells and mix well. Incubate cells on ice for 30 min. Add 40 mL of wash buffer to the cells. Centrifuge the cell suspension at $469 \times g$ for 5 min at 4 °C; discard the supernatant. Resuspend the cells in 400 μL of wash buffer for every 1×10^8 cells. Add 100 μL of the Anti-Hapten MicroBeads reagent (Human CD34 Indirect MicroBead Kit) for every 1×10^8 cells; mix well and incubate on ice for 30 min.

5. Resuspend the cells with 40 mL of wash buffer and spin down the cell suspension at 469 × *g* for 5 min at 4 °C and remove the supernatant. Resuspend the pellet in 3 mL of wash buffer and transfer to a 15 mL tube. Repeat wash-resuspension procedures and transfer the residual cells into the same 15 mL tube and put the tube on ice.
6. Sort the cell suspension using an autoMACS® cell separator machine and combine positive fractions (CD34+ HSC) (if more than one fraction). Centrifuge the negative and positive fractions separately at 469 × *g* at 4 °C for 5 min and resuspend each fraction in 10 mL wash buffer and store on ice. Determine CD34+ cells purity and yield by staining aliquots of positive and negative fraction cells using CD34+, CD45+ antibodies and 7AAD+ (dead) stain and integrated flow cytometry cell counter system; use human CD34+ HSC or a human CD34+ cell line and isotype antibodies as controls.

3.4 Transplantation

1. Centrifuge CD34+ HSC at 469 × *g* for 5 min at 4 °C and resuspend with wash buffer to 1×10^6 cells per mL. Centrifuge the liver progenitor cells (HPC) at 18 × *g* for 5 min at 4 °C and resuspend with wash buffer to 1×10^6 cells per mL. Store cells overnight at 4 °C or proceed to transplantation.
2. Prior to transplantation, centrifuge CD34+ HSC at 469 × *g* and HPC at 18 × *g* for 5 min at 4 °C; resuspend each cell type with wash buffer to 0.5–1×10^6 cells/17.5 μL. Mix approximately 0.5–1×10^6 HSC and 0.5–1×10^6 liver progenitor cells (35 μL total volume) for each mouse to be injected; keep cells on ice (*see* **Note 5**).
3. Irradiate 2–5-day-old newborn AFC8 mice in sterilized paper bags with a single dose of 200 rad using Xrad or other irradiators. Prepare an ice bucket wrapped with autoclaved aluminum foil in the hood. Prepare the warming light for mouse recovery from cold-induced anesthesia. Place a single pup on the foil in the ice bucket and allow the animal to cool for approximately 1 min to induce a mild anesthesia (*see* **Note 6**).
4. Resuspend the cells immediately prior to injection and load the syringe (0.5 cc insulin syringe with 27-gauge needle) with the cell suspension at a volume of 30 μL per mouse. Remove the cooled pup, place on foil, and restrain the pup by placing your index finger between its front legs and your thumb between its hind legs, while applying gentle pressure down and outward, just enough to pull the skin tight without injuring the animal. Vertically position the needle slightly to the left of the right lobe and angle slightly towards the right lobe; push the needle in about halfway then deposit the cells into the right lobe at the rate of 2 s per injection volume. The liver should be visible as a dark region located cranially to the stomach; the

stomach is the white color organ in the abdominal region. Release the pressure immediately with your fingers and immediately remove the needle; place the transplanted animal in a cage with the mother. Repeat transplantation steps for the remaining animals.

5. House transplanted animals in a pathogen-free facility and microisolator cages. Feed animals with autoclaved or irradiated food and maintain on acidified autoclaved water with or without sulfamethoxazole–trimethoprim (7.8 mL SMZ per 250 mL of drinking water) on alternate weeks for the duration of the animals' life (*see* **Note 7**).

3.5 Human Liver and Immune System Reconstitution

1. Wean animals at 3 weeks old and house at ≤ 5 humanized animals per cage; maintain autoclaved/irradiated food and acidified autoclaved water with or without sulfamethoxazole–trimethoprim (7.8 mL SMZ per 250 mL of drinking water) on alternate weeks for the duration of the animals' life.
2. Administer AP20187 at a dose of 5 μg/g body weight to AFC8-humanized mice and appropriate control mice via intraperitoneal injection at 4 weeks post transplantation; repeat injections once a week for 4 weeks.
3. At 12 weeks post transplantation, warm up humanized and control mice with a heat-lamp and bleed by making a single 5 mm cut (nick) on a tail vein with a sterile scalpel. Collect 100 μL of blood in 1.5 mL sterile Eppendorf tubes containing 100 μL of 20 mM PBS/EDTA and place on ice; samples can be kept on ice for up to 12 h. Centrifuge the collected blood–PBS/EDTA solution at 469 × *g* for 5 min at 4 °C. Collect the top portion (plasma) for analysis of human liver reconstitution (human albumin ELISA) and the bottom portion (PBMCs) for analysis of human immune reconstitution (FACs analysis).
4. Resuspend the bottom portion (PBMCs) in 1× ACK lysis buffer, incubate for 5 min. Centrifuge cells at 469 × *g* for 5 min at 4 °C and resuspend in 2 % FBS/PBS containing human CD45, mouse CD45 and 7AAD antibody mixture. Examine human immune reconstitution (% human CD45+ cells/Total CD45+ cells) using flow cytometry analysis. To measure human liver reconstitution, perform human albumin ELISA using plasma and human albumin ELISA kit, following the manufacturer's procedures.

3.6 Virus Inoculation

1. Administer a sub-lethal dose of Avertin (225–240 mg/kg) via intraperitoneal injection to humanized and control mice at 12 weeks post transplantation.
2. Inoculate anesthetized humanized or control animals via retro-orbital injection with 75–100 μL of human clinical isolates of HCV at 1–5 × 10^7 genome copies/mL or control (PBS, uninfected patients sera, heat inactivated inoculum, etc.) [9] (*see* **Note 8**).

3.7 Analysis of Infection, Immune Response, and Liver Disease

1. For longitudinal analysis of infection, liver disease, and immune response, bleed animals and analyze viral load, immune response, and liver damage/fibrosis at approximately every 4 weeks following initial bleeding at 2 weeks post inoculation.
2. Monitor animals weekly and sacrifice at approximately 16 weeks post inoculation. Sacrifice animals by administering 800 μL of Avertin to animals. Collect 500 μL of blood (serum) and 500 μL blood plus 500 μL 20 mM EDTA (plasma and PBMCs) via retro-orbital bleeding.
3. Perform cervical dislocation and collect animal tissues (spleen, lymph nodes, liver, etc.) immediately for DNA, RNA and protein analysis. For cell analysis, place tissues in IMDM medium and keep on ice. For histology and immunohistochemistry fix tissue in formalin and process as paraffin embedded slides. Examine human hepatocyte repopulation in humanized or control tissue at sacrifice point by staining formalin-fixed, paraffin-embedded slides with anti-human albumin antibody or anti-human hepatocyte (HepPar1) antibody. Additionally, examine human hepatocyte differentiation using real-time gene expression analysis of liver RNA. Examine viral load by measuring virus nucleic acids in the serum and liver using established quantitative RT-PCR methods [11].
4. Isolate leukocytes from the spleen, liver, and lymph nodes using standard leukocyte isolation protocols. Determine the frequency, activation state, and number of various human immune cells in the various tissues using standard flow cytometry protocols. Examine anti-HCV T cell immune response by measuring T cell activation and/or expansion following antigen stimulation using standard T cell assays.
5. Examine chronic liver inflammation (hepatitis) by staining paraffin-embedded, formalin-fixed liver slides with antibodies against human immune cells (human CD45+, human CD3+, human CD68+, etc.) [9]. Examine liver fibrosis by staining the liver with either Sirius red/fast green or Masson's trichrome stains.

4 Notes

1. Human tissues should be handled using BSL2-recommended protocols and should be collected and used in accordance with all institutional and governmental ethics guidelines.
2. Parafilm seal prevents contamination of the sample.
3. If the pellet is red, repeat washing step until the pellet appears yellowish or white.
4. Use extreme caution when ejecting the Ficoll so as not to disturb the interface or create bubbles.

5. The cell suspension must be prepared at approximately 35 μL volume per mouse, as injecting animals above this volume will result in injury to the animals.
6. Take caution when handling pups in order to prevent contact with unsterilized ice/surfaces.
7. Failure to keep humanized animals under sterile conditions will result in lower human reconstitution and illness due to opportunistic infections.
8. Unpublished results demonstrate that human clinical isolates of HBV at ~1×10^7 genome copies/mL also infects HSC/Hep humanized mice.

Competing Financial Interests

The authors declare competing financial interests. The University of North Carolina at Chapel Hill has applied for patents covering parts of the method, with L.S. as a coinventor. The University of North Carolina at Chapel Hill manages the invention in accordance with its conflict of interest policies.

References

1. Mercer DF, Schiller DE, Elliott JF, Douglas DN, Hao C, Rinfret A, Addison WR, Fischer KP, Churchill TA, Lakey JR, Tyrrell DL, Kneteman NM (2001) Hepatitis C virus replication in mice with chimeric human livers. Nat Med 7:927–933
2. Shultz LD, Ishikawa F, Greiner DL (2007) Humanized mice in translational biomedical research. Nat Rev Immunol 7:118–130
3. Willinger T, Rongvaux A, Strowig T, Manz MG, Flavell RA (2011) Improving human hemato-lymphoid-system mice by cytokine knock-in gene replacement. Trends Immunol 32:321–327
4. Bissig KD, Wieland SF, Tran P, Isogawa M, Le TT, Chisari FV, Verma IM (2010) Human liver chimeric mice provide a model for hepatitis B and C virus infection and treatment. J Clin Invest 120:924–930
5. Meuleman P, Leroux-Roels G (2008) The human liver-uPA-SCID mouse: a model for the evaluation of antiviral compounds against HBV and HCV. Antiviral Res 80:231–238
6. Meuleman P, Libbrecht L, De Vos R, de Hemptinne B, Gevaert K, Vandekerckhove J, Roskams T, Leroux-Roels G (2005) Morphological and biochemical characterization of a human liver in a uPA-SCID mouse chimera. Hepatology 41:847–856
7. Azuma H, Paulk N, Ranade A, Dorrell C, Al-Dhalimy M, Ellis E, Strom S, Kay MA, Finegold M, Grompe M (2007) Robust expansion of human hepatocytes in Fah−/−/Rag2−/−/Il2rg−/− mice. Nat Biotechnol 25:903–910
8. Bissig KD, Le TT, Woods NB, Verma IM (2007) Repopulation of adult and neonatal mice with human hepatocytes: a chimeric animal model. Proc Natl Acad Sci U S A 104:20507–20511
9. Washburn ML, Bility MT, Zhang L, Kovalev GI, Buntzman A, Frelinger JA, Barry W, Ploss A, Rice CM, Su L (2011) A humanized mouse model to study hepatitis C virus infection, immune response, and liver disease. Gastroenterology 140:1334–1344
10. Traggiai E, Chicha L, Mazzucchelli L, Bronz L, Piffaretti JC, Lanzavecchia A, Manz MG (2004) Development of a human adaptive immune system in cord blood cell-transplanted mice. Science 304:104–107
11. Lindenbach BD, Meuleman P, Ploss A, Vanwolleghem T, Syder AJ, McKeating JA, Lanford RE, Feinstone SM, Major ME, Leroux-Roels G, Rice CM (2006) Cell culture-grown hepatitis C virus is infectious in vivo and can be recultured in vitro. Proc Natl Acad Sci U S A 103:3805–3809

Index

Bruno Christ et al. (eds.), *Animal Models for Stem Cell Therapy*, Methods in Molecular Biology, vol. 1213,
DOI 10.1007/978-1-4939-1453-1, © Springer Science+Business Media New York 2014

D

E

F

G

H

O

P

Q

R

S

T

U

V

X

Z